frontiers | Research Topics

Advances in the research of diabetic retinopathy, volume II

Edited by
Mohd Imtiaz Nawaz and Rajashekhar Gangaraju

Published in
Frontiers in Endocrinology
Frontiers in Public Health

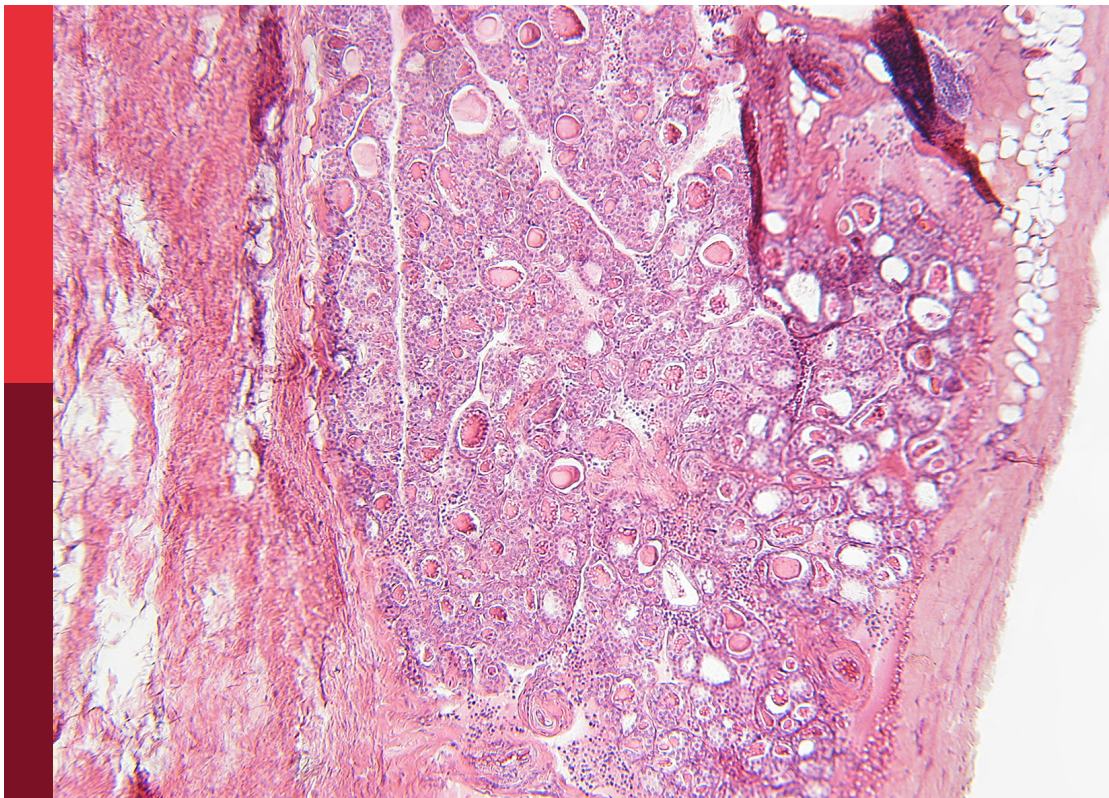

ISSN 1664-8714
ISBN 978-2-8325-3553-0
DOI 10.3389/978-2-8325-3553-0

About Frontiers

Frontiers is more than just an open access publisher of scholarly articles: it is a pioneering approach to the world of academia, radically improving the way scholarly research is managed. The grand vision of Frontiers is a world where all people have an equal opportunity to seek, share and generate knowledge. Frontiers provides immediate and permanent online open access to all its publications, but this alone is not enough to realize our grand goals.

Frontiers journal series

The Frontiers journal series is a multi-tier and interdisciplinary set of open-access, online journals, promising a paradigm shift from the current review, selection and dissemination processes in academic publishing. All Frontiers journals are driven by researchers for researchers; therefore, they constitute a service to the scholarly community. At the same time, the *Frontiers journal series* operates on a revolutionary invention, the tiered publishing system, initially addressing specific communities of scholars, and gradually climbing up to broader public understanding, thus serving the interests of the lay society, too.

Dedication to quality

Each Frontiers article is a landmark of the highest quality, thanks to genuinely collaborative interactions between authors and review editors, who include some of the world's best academicians. Research must be certified by peers before entering a stream of knowledge that may eventually reach the public - and shape society; therefore, Frontiers only applies the most rigorous and unbiased reviews. Frontiers revolutionizes research publishing by freely delivering the most outstanding research, evaluated with no bias from both the academic and social point of view. By applying the most advanced information technologies, Frontiers is catapulting scholarly publishing into a new generation.

What are Frontiers Research Topics?

Frontiers Research Topics are very popular trademarks of the *Frontiers journals series*: they are collections of at least ten articles, all centered on a particular subject. With their unique mix of varied contributions from Original Research to Review Articles, Frontiers Research Topics unify the most influential researchers, the latest key findings and historical advances in a hot research area.

Find out more on how to host your own Frontiers Research Topic or contribute to one as an author by contacting the Frontiers editorial office: frontiersin.org/about/contact

Advances in the research of diabetic retinopathy, volume II

Topic editors

Mohd Imtiaz Nawaz — King Saud University, Saudi Arabia

Rajashekhar Gangaraju — University of Tennessee Health Science Center (UTHSC), United States

Citation

Nawaz, M. I., Gangaraju, R., eds. (2023). *Advances in the research of diabetic retinopathy, volume II*. Lausanne: Frontiers Media SA.

doi: 10.3389/978-2-8325-3553-0

Table of contents

frontiers | Frontiers in Endocrinology

TYPE Editorial
PUBLISHED 08 September 2023
DOI 10.3389/fendo.2023.1281490

OPEN ACCESS

EDITED AND REVIEWED BY
Åke Sjöholm,
Gävle Hospital, Sweden

*CORRESPONDENCE
Mohd Imtiaz Nawaz
mnawaz@ksu.edu.sa

RECEIVED 22 August 2023
ACCEPTED 24 August 2023
PUBLISHED 08 September 2023

CITATION
Nawaz MI (2023) Editorial: Advances in the research of diabetic retinopathy, volume II. *Front. Endocrinol.* 14:1281490. doi: 10.3389/fendo.2023.1281490

Editorial: Advances in the research of diabetic retinopathy, volume II

Mohd Imtiaz Nawaz[1,2]*

[1]Department of Ophthalmology, College of Medicine, King Saud University, Riyadh, Saudi Arabia, [2]Dr. Nasser Al-Rashid Research Chair in Ophthalmology, Abdulaziz University Hospital, Riyadh, Saudi Arabia

KEYWORDS

diabetic retinopathy (DR), pathological complication, scanning swept source optical coherence tomography angiography (SS-OCTA), artificial intelligence (AI), risk predictive model, adjuvant effect

Editorial on the Research Topic
Advances in the research of diabetic retinopathy, volume II

Diabetic retinopathy (DR) is a progressive disease of the retina. Diabetic retinopathy occurs because of long-term accumulated functional and structural impairments in the diabetic retina. The global prevalence of any DR form among diabetic patients is estimated to be around 27.0% (1). It takes several years before any clinical signs of DR appear in a diabetic patient, making it difficult to properly evaluate and diagnose the patient at an early stage of the disease. Diabetic retinopathy is a multifactorial disease arising from the complex interplay between dysregulated biochemical and metabolic pathways. Diabetic retinopathy begins as non-proliferative retinal abnormalities and progresses to proliferative diabetic retinopathy (PDR), characterized by a persistent low grade of inflammation and neovascularization (2, 3). The implication of several inflammatory pathways and angiogenesis processes complicates the pathology through the initiation of retinal neovascularization, vitreous hemorrhage, and/or tractional retinal detachment, which are hallmark features of PDR (4).

Clinically, the use of photocoagulation and vitrectomy remains the standard of care for treating severe complications of PDR. However, these treatments are either destructive or their successful implementation approaches are limited. Additional PDR treatment strategies involve surgical procedures to remove a thin epiretinal membrane from the surface of the retina, which further allows the retina to remodel and reattach. Despite dramatic developments, vitreoretinal surgery for epiretinal membranes is often dissatisfying both anatomically and functionally (5, 6).

The discovery of the role of the potential angiogenic modulator vascular endothelial growth factor (VEGF) in PDR has led to the development of anti-VEGF agents as therapies. However, limitations to anti-VEGF interventions exist that include a short duration of action, the presence of adverse side effects, and a poor response in a significant percentage of patients (7, 8). Furthermore, various pro-inflammatory and angiogenic factors other than VEGF may play a role in PDR (reviewed in (2, 9)), causing resistance to anti-VEGF interventions.

This observation, therefore, suggests that PDR-associated pathogenesis is multifactorial and that factors beyond VEGF may be playing a role in the initiation and progression of the disease. Thus, more theoretical, or clinical insight into the pathogenesis of diabetic retinopathy is warranted. More profound knowledge could help in developing novel approaches to target dysregulated molecular pathways, or increasing target affinity, and shortening treatment durability for the management of PDR.

Given the success of the first edition of the Research Topic *Advances in the Research of Diabetic Retinopathy* (10), and the continuing advancement in the field, we aimed to launch *Volume II* of the edition. The aim of *Volume II* was to seek more research articles exploring new paradigms toward understating the pathological mechanisms that are involved in early retinal vascular damage in patients with diabetic retinopathy. To meet this demand, *Volume II* of the edition was also overwhelmed by the publication of many exciting articles, including original research as well as reviews. Articles addressing or discussing new therapeutic implications for the early management of diabetic retinopathy were given equal space.

The editor of this topic strongly believes that articles published in *volume II* of the Research Topic could have added some knowledge to improve our understanding of the pathogenesis associated with diabetic retinopathy.

Likewise, the work by Su et al. reported that a genetically higher hip circumference is associated with a lower risk of DR. Serum levels of acylcarnitine 8:0 (Jin et al.) and cellular communication network factor-1 (Xiang et al.) can serve as predictive biomarkers for DR identification at an early stage of the disease. Using a confocal scanning laser ophthalmoscope, Song et al. demonstrated that the retinal branch arterial tortuosity may be a direct and specific indicator for early detection or assessment of DR severity. Recent scientific advancements in the use of scanning swept-source optical coherence tomography angiography (SS-OCTA) devices (Zeng et al., Qi et al., Xu et al., Lin et al., and Li et al.) could be an important clinical tool in assessing the early diabetes-induced changes in choroidal or retinal capillaries in DR patients. Furthermore, using OCT, Yao et al. showed preclinical DR may be more severe in diabetic nephropathy (DN) individuals in regard to microvascular and microstructural impairments. Similarly, Xiaodong et al. demonstrated that peripheral blood inflammatory biomarkers and OCT retinal macular imaging indexes have important value for risk prediction and diagnosis of DN in combination with DR. Hsieh et al. showed partial inner segment-outer segment layers are predictive of better response, whereas the presence of epiretinal membrane is a significant predictor of poor response to anti-VEGF treatment in eyes with diabetic macular edema.

Nevertheless, the use of artificial intelligence, or machine learning, and risk nomogram prediction models has been finding its place as a training aid system for assessing the degree of DR pathogenesis in type 2 diabetic patients. Accordingly, using fundus images from real-world diabetics, Qian et al. discussed the AI-based system for high diagnostic accuracy for the detection of DR. Wang et al. developed a predictive risk nomogram using retinal vascular geometry parameters and clinical information with no blood test requirements to facilitate risk stratification and early detection of DR. Independent common or potential predictors were tested to establish and validate a predictive model for DR (Yang et al., Wang et al.). Such a quick screening model can assist clinicians and researchers, based on a minimal amount of clinical data, to quickly determine if a diabetic patient is prone to developing DR.

Among the review topics discussing advancements in PDR treatment strategies, Lin et al. discussed targeted retinal photocoagulation, an emerging laser technology, in combination with anti-VEGF for the management of retinal diseases. A network meta-analysis review article by Wang et al. concluded that there are no distensible effects of intraoperative intravitreal conbercept (IVC) on PDR, but preoperative, except for very long intervals, is an effective adjuvant to par-plana vitrectomy for treating PDR. The analysis was indeed confirmed in an original article by Yang et al. showing that an IVC treatment that was administered 7 days preoperatively was associated with better effectiveness and a lower vitreous VEGF concentration than its administration at other time points.

A growing piece of evidence suggests that various pro-inflammatory and angiogenic factors, other than VEGF may play a role in the progression of pathogenesis associated with PDR. Accordingly, a review by Xu et al. highlights the therapeutic roles of pigment epithelium-derived factors and their receptors in the diagnosis and management of retinal diseases, including PDR. Lastly, two review articles report the significance of oral Chinese patent medicines in improving visual acuity and fundus lesions in non-PDR (Liu et al.) and PDR (Huai et al.) patients. However, the relevant clinical trials on the use of many such Chinese medicines are few, and more high-quality clinical trials await to determine their effectiveness and safety. Towards this, a study by Kim et al. suggests that a 60% edible ethanolic and catechin 7-O-b-Dapiofuranoside extract of *Ulmus davidiana* could be a potential therapeutic agent for reducing vascular leakage by preventing pericyte apoptosis in DR.

In conclusion, *Volume II* of the Research Topic brings new insights and novel data toward understanding the early retinal vascular damage or pathological mechanism involved in the initiation and progression of diabetic retinopathy. The pool of data obtained using an ultrawide SS-OCTA device or predictive nomogram model provides a wealth of knowledge regarding the early assessment or pathological grading of DR. A few research articles dedicated to understanding the role of potential biomarkers could open new therapeutic avenues for the early management of diabetic retinopathy. Nevertheless, the adjuvant effects of conbercept or oral Chinese medicine could be a game changer for the management of diabetic retinopathy.

The editor of this Research Topic strongly feels that this set of articles could be a benchmark and may add some clinical knowledge in the field of diabetic retinopathy. Last but not least, the editor invites more interdisciplinary research towards early assessment and development of treatment strategies for the management of diabetic retinopathy.

Author contributions

MN: Conceptualization, Writing – original draft, Writing – review & editing.

Funding

This work was supported by the Nasser Al-Rasheed Research Chair in Ophthalmology (Abu El-Asrar A.M.), Department of Ophthalmology, College of Medicine, King Saud University, Riyadh, Saudi Arabia.

Acknowledgments

The author would like to thank the hundreds of researchers and scientists who contributed to this Research Topic. The success of this Research Topic would not be completed without the experts in the field, so the author would also like to thank all the reviewers. Lastly, the author extends a sincere thanks to the topic editor Professor Rajashekhar Gangaraju from the University of Tennessee Health Science Center (UTHSC) Memphis, who equally participated in the success of this Research Topic.

Conflict of interest

The author declares that the research was conducted in the absence of any commercial or financial relationships that could be construed as a potential conflict of interest.

The author(s) declared that they were an editorial board member of Frontiers, at the time of submission. This had no impact on the peer review process and the final decision.

Publisher's note

References

1. Thomas RL, Halim S, Gurudas S, Sivaprasad S, Owens DR. IDF Diabetes Atlas: A review of studies utilising retinal photography on the global prevalence of diabetes related retinopathy between 2015 and 2018. *Diabetes Res Clin Pract* (2019) 157:107840. doi: 10.1016/j.diabres.2019.107840

2. Semeraro F, Cancarini A, Dell'omo R, Rezzola S, Romano MR, Costagliola C, et al. Diabetic retinopathy: vascular and inflammatory disease. *J Diabetes Res* (2015) 2015:582060. doi: 10.1155/2015/582060

3. Capitao M, Soares R. Angiogenesis and inflammation crosstalk in diabetic retinopathy. *J Cell Biochem* (2016) 117(11):2443–53. doi: 10.1002/jcb.25575

4. Nawaz IM, Rezzola S, Cancarini A, Russo A, Costagliola C, Semeraro F, et al. Human vitreous in proliferative diabetic retinopathy: Characterization and translational implications. *Prog Retin Eye Res* (2019) 72:100756. doi: 10.1016/j.preteyeres.2019.03.002

5. Charteris DG, Sethi CS, Lewis GP, Fisher SK. Proliferative vitreoretinopathy-developments in adjunctive treatment and retinal pathology. *Eye (Lond)* (2002) 16 (4):369–74. doi: 10.1038/sj.eye.6700194

6. Pastor JC, de la Rua ER, Martin F. Proliferative vitreoretinopathy: risk factors and pathobiology. *Prog Retin Eye Res* (2002) 21(1):127–44. doi: 10.1016/S1350-9462(01)00023-4

7. Kieran MW, Kalluri R, Cho YJ. The VEGF pathway in cancer and disease: responses, resistance, and the path forward. *Cold Spring Harb Perspect Med* (2012) 2 (12):a006593. doi: 10.1101/cshperspect.a006593

8. van Wijngaarden P, Qureshi SH. Inhibitors of vascular endothelial growth factor (VEGF) in the management of neovascular age-related macular degeneration: a review of current practice. *Clin Exp Optometry* (2008) 91(5):427–37. doi: 10.1111/j.1444-0938.2008.00305.x

9. Urias EA, Urias GA, Monickaraj F, Mcguire P, Das A. Novel therapeutic targets in diabetic macular edema: Beyond VEGF. *Vision Res* (2017) 139:221–7. doi: 10.1016/j.visres.2017.06.015

10. Chakrabarti S, Lanza M, Siddiqui K. Editorial: Advances in the research of diabetic retinopathy. *Front Endocrinol (Lausanne)* (2022) 13:1038056. doi: 10.3389/fendo.2022.1038056

frontiers | Frontiers in Endocrinology

TYPE Original Research
PUBLISHED 06 October 2022
DOI 10.3389/fendo.2022.972339

OPEN ACCESS

EDITED BY
Rajashekhar Gangaraju,
University of Tennessee Health Science Center (UTHSC), United States

REVIEWED BY
Mengmeng Tong,
Gemeente Eindhoven, Netherlands
Jan Kubicek,
VSB-Technical University of Ostrava, Czechia

*CORRESPONDENCE
Shanshan Zhu
zhushanshan@nbu.edu.cn
Shuo Chen
chenshuo@bmie.neu.edu.cn

SPECIALTY SECTION
This article was submitted to Clinical Diabetes, a section of the journal Frontiers in Endocrinology

RECEIVED 18 June 2022
ACCEPTED 20 September 2022
PUBLISHED 06 October 2022

CITATION
Song Y, Zhou Z, Liu H, Du R, Zhou Y, Zhu S and Chen S (2022) Tortuosity of branch retinal artery is more associated with the genesis and progress of diabetic retinopathy. *Front. Endocrinol.* 13:972339. doi: 10.3389/fendo.2022.972339

Tortuosity of branch retinal artery is more associated with the genesis and progress of diabetic retinopathy

Yunfeng Song[1], Zheng Zhou[2], Henan Liu[3], Runyu Du[4], Yaoyao Zhou[2], Shanshan Zhu[5]* and Shuo Chen[1,6]*

[1]College of Medicine and Biological Information Engineering, Northeastern University, Shenyang, China, [2]School of Innovation and Entrepreneurship, Liaoning Institute of Science and Technology, Benxi, China, [3]Department of Ophthalmology, Shengjing Hospital, China Medical University, Shenyang, China, [4]Department of Endocrinology, Shengjing Hospital, China Medical University, Shenyang, China, [5]Research Institute for Medical and Biological Engineering, Ningbo University, Ningbo, China, [6]Key Laboratory of Intelligent Computing in Medical Image, Ministry of Education, Shenyang, China

Objective: The purpose of this study is to investigate the potential of using the tortuosity of branch retinal artery as a more promising indicator for early detection and accurate assessment of diabetic retinopathy (DR).

Design and method: The diagnoses, consisting of whether DR or not as well as DR severity, were given by ophthalmologists upon the assessment of those fundus images from 495 diabetic patients. Meanwhile, benefiting from those good contrast and high optical resolution fundus images taken by confocal scanning laser ophthalmoscope, the branch arteries, branch veins, main arteries and main veins in retina can be segmented independently, and the tortuosity values of them were further extracted to investigate their potential correlations with DR genesis and progress based on one-way ANOVA test.

Results: For both two comparisons, i.e., between non-DR group and DR group as well as among groups with different DR severity levels, larger tortuosity increments were always observed in retinal arteries and the increments in branch retinal vessels were even larger. Furthermore, it was newly found that branch arterial tortuosity was significantly associated with both DR genesis ($p=0.030$) and DR progress ($p<0.001$).

Conclusion: Based on this cohort study of 495 diabetic patients without DR and with different DR severity, the branch arterial tortuosity has been found to be more closely associated with DR genesis as well as DR progress. Therefore, the branch arterial tortuosity is expected to be a more direct and specific indicator for early detection of DR as well as accurate assessment of DR severity, which can further guide timely and rational management of DR to prevent from visual impairment or even blindness resulting from DR.

KEYWORDS

diabetic retinopathy, vascular tortuosity, branch retinal vessels, fundus imaging, retinal vessel analysis

Introduction

Diabetic retinopathy (DR) is a common microvascular complication of diabetes (1, 2). The number of DR patients worldwide is approximately 95 million (3), and is estimated to reach 156 million by 2045 (4). The local hypoxia caused by hyperglycemia can induce elevated vascular permeability, intraretinal vascular leakage and neovascularization, eventually leading to vision impairment or even blindness (5). However, it is reported that 90% of such vision impairment or blindness can be prevented by the early diagnosis and rational intervention (6, 7). Currently, fundus imaging has been suggested as a regular examination for DR screening at least once a year (8). However, at its early stage, the DR patients rarely suffer from self-perceived vision impairment and the clinical symptoms are often unnoticeable on fundus images, thus its early and accurate diagnosis is still challenging and relies heavily on clinicians' experience.

Because retinal microvascular damage induced by high-glucose level is typically recognized as the major cause of DR, the retinal microvascular parameters, such as caliber, fractal dimension and tortuosity (9, 10), have demonstrated to be important indicators to quantitatively associate with the early diagnose of DR (11, 12). Among those retinal microvascular parameters, the changes of retinal microvascular tortuosity has been reported to occur earlier than others (13), and is an important hallmark of retinal ischemia that is closely associated with the genesis and progress of DR (14). Numerous studies have been implemented to investigate the correlation between the retinal vascular tortuosity and DR in diabetic patients. Mustafa *et al.* obtained the global tortuosity from 4 DR patients and 16 diabetic patients without DR in DRIVE (15) and STARE databases (16, 17), and higher global tortuosity was observed in DR patients. Moreover, Lee et al. found that increased global tortuosity was also associated with higher level of DR severity, which was investigated on 121 diabetic patients with different levels of DR severity (18). Besides, Sasongko et al. calculated the tortuosity values of retinal arteries and veins separately based on the color fundus photographs of 144 diabetic patients with different levels of DR severity and 80 diabetic patients without DR; only arterial tortuosity showed statistically significant increase between DR group versus non-DR group as well as between mild DR group versus moderate DR group (19, 20). In the above previous studies, the investigations were mainly focused on the tortuosity of main retinal vessels in the absence of branch retinal vessels, due to the relative low contrast of color fundus images and the lack of proper method for branch retinal vessel extraction. However, the abnormalities of branch retinal vessels, causing extracellular matrix protein synthesis and capillary basement membrane thickening, have been proved to be the major pathological basis underlying abnormal main blood vessels in diabetic patients (21, 22). In addition, anomalous angiogenesis can be induced by the nutrient matrix leaked from abnormal retinal vessels, which leads to the acceleration of DR progress (23). Therefore, we infer that branch retinal vessels might have higher correlation with both DR genesis and progress compared to main retinal vessels, in which the tortuosity only from the branch retinal vessels might serve as a more conducive indicator for early diagnosis and accurate assessment of DR. However, to the best of our knowledge, there has been no effort in the literature related to investigating correlation between tortuosity of branch retinal vessels and DR.

In this study, fundus images with good contrast and high optical resolution (~15μm) were taken by confocal scanning laser ophthalmoscope from 495 diabetic patients without DR and with different DR severity levels. Benefiting from those good contrast and high optical resolution fundus images, the branch arteries, branch veins, main arteries and main veins in retina can be segmented separately, and the tortuosity values of them were further extracted to investigate their potential correlations with DR genesis and progress based on statistical analysis, i.e. one-way ANOVA test. According to the results, the tortuosity of branch arteries showed much larger increment from patients without DR to patients with DR as well as from patients with low level DR severity to patients with high level DR severity. Interestingly, it is newly found that branch arteriolar tortuosity was statistically correlated with both DR genesis ($p=0.030$) and progress ($p<0.001$). Therefore, it is expected that the tortuosity of branch retinal arteries can serve as a more promising indicator for the early detection and accurate assessment of DR, which can be helpful for guiding rational management of diabetic retinopathy.

Materials and methods

Study participants and fundus image collection

In this study, a total of 495 patients with type 2 diabetes were recruited from the Endocrinology Department of Shengjing Hospital in China. A pair of fundus images from each patients, i.e., green channel fundus image with 520nm laser and infrared channel fundus image with 780nm laser, were taken by a non-mydriatic confocal scanning laser ophthalmoscope (EasyScan, i-Optics Inc., Netherlands) with 45° field of view. With the employment of confocal optical setup, stray light from the lens and viscous body can be prevented, allowing high optical resolution (~15μm) and good contrast. The green channel fundus image was chosen for further diagnosis and analysis, because of its optimal blood vessel contrast, as show in Figure 1A. The fundus image of right eye was preferably chosen for further image processing and analysis; if the fundus

10.3389/fendo.2022.972339

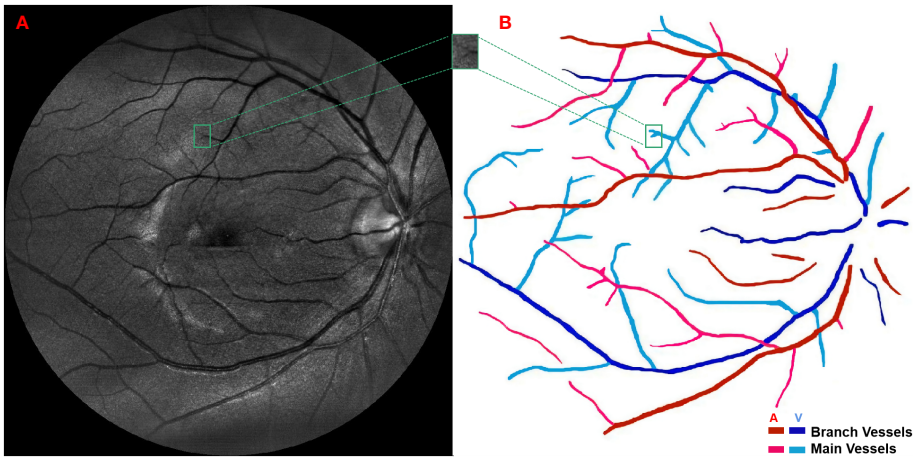

FIGURE 1
(A) A green channel fundus image taken by confocal scanning laser ophthalmoscope and **(B)** the extraction of main arteries, main veins, branch arteries and branch veins.

image of right eye suffered from low quality (e.g. containing incomplete, blurred regions and/or more than two ungradable vessels), the fundus image of left eye would be chosen instead. The diagnoses, consisting of whether DR or not as well as the DR severity, were given by the ophthalmologists upon the assessment of green channel fundus image following an international clinical DR severity scales (24). More specifically, all patients can be divided into DR and non-DR groups according to whether at least one microaneurysm or hemorrhage can be observed or not; and patients in DR group can be further subdivided into groups with different levels of DR severity, i.e., V1 group (mild non-proliferative DR), V2 group (moderate non-proliferative DR) and V3 group (severe non-proliferative DR and proliferative DR). The patients' detailed characteristics were listed in Table 1. This study has been approved by the medical ethics committee of Shengjing Hospital of China Medical University, and the signed consent forms were obtained from all participants.

Vascular segmentation, tortuosity extraction and statistical analysis

The green channel fundus images obtained by confocal scanning laser ophthalmoscope were used as the input of Retinal Health Information and Notification System (RHINO) software (25, 26) to extract and differentiate arterial and venous retinal vessels. More specifically, a local normalization was first performed on the original retinal images to alleviate varying contrast problem caused by non-uniform illumination; then, the rotating multiscale second-order Gaussian derivative filters (27) were employed to enhance the retinal vessels and further segment them with proper thresholds; finally, the features of the segmented retinal vessels were extracted, including the mean, standard deviation, median, minimum and maximum of the intensities inside circular regions and the intensity values along the center line of each retinal vessels, and inputted into a logistic regression classifier to differentiate retinal arteries and veins. Those extracted retinal vessels were

TABLE 1 The detailed characteristics of patients in different groups.

Characteristics	Non-DR group (n = 122)	DR group		
		V1 (n = 200)	V2 (n = 139)	V3 (n = 34)
Sex (male/female)	69/53	120/80	80/59	19/15
Age (years)	49.1 ± 15.20	48.5 ± 11.40	56.4 ± 11.50	55.5 ± 10.60
HbA1c (%)	8.9 ± 2.40	8.9 ± 2.30	8.8 ± 2.10	8.61 ± 2.14
Fasting blood sugar (mmol/L)	9.3 ± 3.50	9.3 ± 3.30	9.3 ± 3.70	9.4 ± 4.26
Body mass index (kg/m²)	26.00 ± 4.00	26.0 ± 3.90	25.1 ± 3.10	25.0 ± 2.80

Data are mean ± SD unless otherwise indicated.

further segmented into main and branch retinal vessels by a semi-automatic method based on region growing according to the following criterion: only the largest vessels originated from the retinal vessels in optic disk were defined as main retinal vessels while the others were defined as branch retinal vessels, as demonstrated in Figure 1B. The outcomes of vessel segmentation and classification were assessed by ophthalmologists and corrected when necessary. Furthermore, the overall tortuosity values of the above four retinal vessel types, i.e., the main artery, main vein, branch artery and branch vein, were calculated based on a published method developed by Bekkers et al. (28) More specifically, the planar retinal vessels were lifted to 3D functions with an additional orientation dimension by convoluting with a specially designed anisotropic cake-wavelet, curvature and confidence values of each location were then extracted by locally fitting exponential curves, and the overall tortuosity of each type of retinal vessels can be derived by the weighted average of the curvatures with confidences as weights (29–31).

The overall tortuosity values of four different retinal vessel types from each patient were served as the independent inputs of the statistical analysis to investigate their potential correlations with DR genesis and progress, respectively. The one-way ANOVA test was implemented to analyze the overall tortuosity values between DR group and non-DR group and the overall tortuosity values among groups with different levels of DR severity, i.e., V1, V2 and V3 groups, and $p < 0.05$ was considered as statistically significant. The above statistical analyses were conducted by SPSS version 26.0.

Results

The average overall tortuosity values of main arteries, main veins, branch arteries and branch veins between DR group and non-DR group are listed and plotted in Table 2 and Figure 2, respectively. According to Table 2 and Figure 2, it can be found that the average overall tortuosity of DR group are always larger than those of non-DR group in all types of retinal vessels, which is consistent with the findings of larger global tortuosity in DR patients in other studies (17, 19); furthermore, larger increments of average overall tortuosity are always observed in retinal arteries, and the increments in branch retinal vessels are even larger than those in main retinal vessels; moreover, the statistically significant difference is only observed in branch retinal arteries ($p=0.030$).

The average overall tortuosity values of main arteries, main veins, branch arteries and branch veins among groups with different levels of DR severity (i.e., V1, V2 and V3) are listed and plotted in Table 3 and Figure 3, respectively. According to Table 3 and Figure 3, it can be found that the average overall tortuosity values of all types of retinal vessels increase with higher level of DR severity, which is consistent with the findings of larger global tortuosity in patients with higher level of DR severity in other studies (19, 26), and the increments from V2 to V3 are even larger than those from V1 to V2; furthermore, larger increments of average overall tortuosity are always observed in retinal arteries, and the increments in branch retinal vessels are even larger than those in main retinal vessels; moreover, statistically significant differences are observed in both branch retinal arteries ($p<0.001$) and branch retinal veins ($p=0.049$), however, the branch retinal arteries yield much larger statistically significant difference.

Discussions

Although several previous studies have already investigated the association between retinal vascular tortuosity and diabetic retinopathy, they mainly focused on the global tortuosity of main retinal vessels in the absence of branch retinal vessels, due to the relative low contrast of color fundus images and the lack of proper method for branch retinal vessel extraction. To the best of our knowledge, this study is for the first time that the correlation between the tortuosity of branch retinal vessels and diabetic retinopathy is comprehensively investigated, benefiting from the high contrast fundus images acquired by confocal scanning laser ophthalmoscope and proper branch retinal vessel extraction method. According to the results from 495 diabetic patients, it has been newly found that the tortuosity of branch retinal artery should be more associated with the genesis and progress of diabetic retinopathy, thus the tortuosity of branch retinal artery is expected to serve as a more promising indicator for the early detection and accurate assessment of diabetic retinopathy. More specifically, for both two comparative experiments, i.e., between non-DR group and DR group as well as among different levels of DR severity, larger tortuosity increments were always observed in branch retinal

TABLE 2 Comparison of the average overall tortuosity values between DR group and non-DR group.

	Average overall tortuosity ($\times 10^4$)			F value	p value
	Non-DR group	DR group	Difference		
Main artery	10.27 ± 4.16	10.69 ± 4.41	0.42	0.027	0.868
Main vein	11.92 ± 3.53	12.18 ± 3.79	0.26	0.003	0.985
Branch artery	9.31 ± 4.72	10.15 ± 5.73	0.84	4.746	0.030*
Branch vein	10.42 ± 4.31	10.73 ± 4.41	0.31	3.210	0.074

*refers to with statistically significant difference.

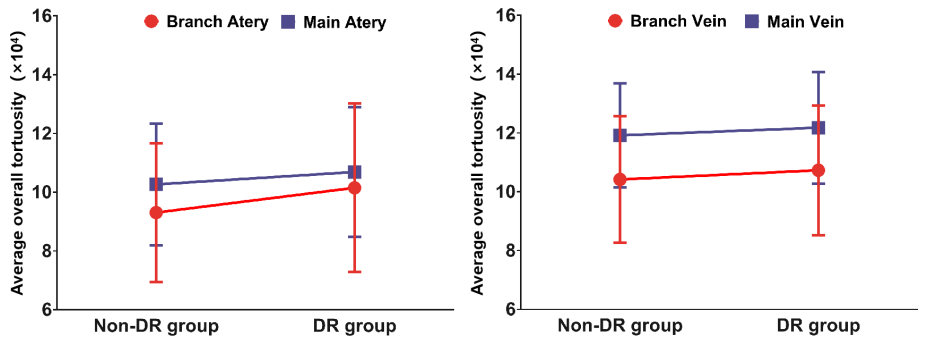

FIGURE 2
The relationship between retinal vascular tortuosity and DR genesis.

vessels, compared to main retinal vessels; furthermore, statistically significant differences were observed in the tortuosity values of branch retinal arteries for both those two comparative experiments. Thus, the branch arterial tortuosity should be more closely associated with DR genesis as well as DR progress. The potential underlying mechanisms are interpreted as follows.

DR group versus non-DR group

The larger increment of average overall tortuosity in retinal arteries can be attributed to the fact that blood pressure in arteries is typically higher than that in veins, thus the arterial vascular walls are expected to suffer greater damage due to greater hemodynamic insult. Another reason might be that the arterial occlusion is one of the key pathogenic factors for venous occlusion (32) and commonly occurs earlier, thus such earlier vascular occlusion in retinal artery caused by hyperglycemia is supposed to induce more abnormality in retinal arterial tortuosity. The larger increments of average overall tortuosity in branch retinal vessels can be attributed to the fact that branch vessels with small sizes are more sensitive to hyperglycemia and the subsequent hypoxia-ischemia (33). Based on the joint action of the above two aspects, the largest increment of the average overall tortuosity from non-DR group to DR group is supposed to be found in branch retinal arteries, which further lead to the statistically significant difference between the average overall tortuosity values of those two groups. Therefore, the branch arterial tortuosity is expected to be a more direct and specific indicator for identifying DR.

Groups with different DR severity levels

The larger increments in arterial and branch vessels can be attributed to the similar facts as discussed above, i.e., higher blood pressure in arteries and vulnerability of branch vessels. The sharper increments of average overall tortuosity from V2 to V3 in branch retinal vessels might be due to the additional vigorous neovascularization (34), which is an unique feature in V3 diabetic retinopathy (35). The underlying mechanism is as follows: hyperglycemia first induces hypoxia-ischemia and further leads to the over-expression of vascular endothelial growth factor (VEGF) (36, 37), i.e., a hypoxia-inducible cytokine to promote neovascularization (38–40), neo-vessels then branch off from pre-existing branch vessels, bend slowly and even cluster in balls (tufts), leading to elevated tortuosity of branch vessels (41), thus the increased tortuosity of branch retinal vessels may signal pathogenic neovascularization induced by hyperglycemia. Recently, Lee et al. have experimentally proved the close relationship between the global tortuosity of retinal vessels and neovascularization in a

TABLE 3 Comparison of the average overall tortuosity values among groups with different levels of DR severity.

	Average overall tortuosity (×10⁴)				F value	p value
	V1 group	V2 group	V3 group	Difference (V3 - V1)		
Main artery	10.50 ± 4.38	10.84 ± 4.66	11.28 ± 3.41	0.78	0.573	0.565
Main vein	12.17 ± 3.98	12.18 ± 3.63	12.28 ± 3.38	0.11	0.011	0.989
Branch artery	9.48 ± 5.11	10.18 ± 5.52	13.96 ± 8.26	4.48	9.271	<0.001*
Branch vein	10.35 ± 3.90	10.88 ± 4.61	12.31 ± 5.90	1.96	3.041	0.049*

*refers to with statistically significant difference.

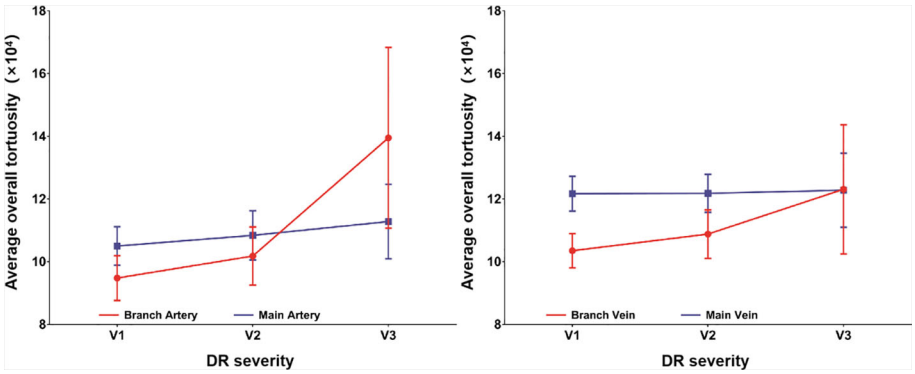

FIGURE 3
The relationship between retinal vascular tortuosity and DR progress.

rat model, in which larger global tortuosity of retinal vessels was observed in rats with more vigorous retinal neovascularization (33). Interestingly, the average overall tortuosity values of branch retinal vessels are close or even much higher than those of main retinal vessels in V3 group, which can be an indirect evidence for the occurrence of hyperglycemia based retinal vascular distortion even during neovascularization. Therefore, the branch vascular tortuosity, especially the branch arterial tortuosity, is expected to be a more direct and specific indicator for assessing DR severity.

Conclusion

In this study, good contrast and high optical resolution retinal photographs taken by confocal scanning laser ophthalmoscope were used to obtain the overall tortuosity values of main arteries, main veins, branch arteries and branch veins, respectively. Based on the statistical analysis of overall tortuosity, the branch arterial tortuosity should be more closely associated with DR genesis as well as DR progress, and is also expected to be a more direct and specific indicator for early detection of DR as well as accurate assessment of DR severity, which can further guide timely and rational management of DR to prevent from visual impairment or even blindness resulting from DR.

Data availability statement

The raw data supporting the conclusions of this article will be made available by the authors, without undue reservation.

Ethics statement

The studies involving human participants were reviewed and approved by The medical ethics committee of Shengjing Hospital of China Medical University. The patients/participants provided their written informed consent to participate in this study.

Author contributions

YS, SC and SZ contributed to conception and design of the study. HL and RD collected the data. YS, ZZ and YZ performed the data processing and analysis. YS wrote the first draft of the manuscript. All authors contributed to manuscript revision, read, and approved the submitted version

Funding

This study was supported by National Natural Science Foundation of China (61605025), Fundamental Research Funds for the Central Universities (N2119002) and National Training Program of Innovation and Entrepreneurship for Undergraduates (D202110161215451139).

Conflict of interest

The authors declare that the research was conducted in the absence of any commercial or financial relationships that could be construed as a potential conflict of interest.

Publisher's note

References

1. Mollazadegan K, Ludvigsson JF. Diabetes: Microvascular complications in T1DM and coeliac disease. *Nat Rev Endocrinol* (2015) 11(6):320–2. doi: 10.1038/nrendo.2015.52

2. Forbes JM, Cooper ME. Mechanisms of diabetic complications. *Physiol Rev* (2013) 93(1):137–88. doi: 10.1152/physrev.00045.2011

3. Tilahun M, Gobena T, Dereje D, Welde M, Yideg G. Prevalence of diabetic retinopathy and its associated factors among diabetic patients at debre markos referral hospital, Northwest Ethiopia, 2019: Hospital-based cross-sectional study. *Diabetes Metab Syndr Obes* (2020) 13:2179–87. doi: 10.2147/DMSO.S260694

4. Teo ZL, Tham YC, Yu M, Chee ML, Rim TH, Cheung N, et al. Global prevalence of diabetic retinopathy and projection of burden through 2045 systematic review and meta-analysis. *Ophthalmology* (2021) 128(11):1580–91. doi: 10.1016/j.ophtha.2021.04.027

5. Kollias AN, Ulbig MW. Diabetic retinopathy: Early diagnosis and effective treatment. *Dtsch Arztebl Int* (2010) 107(5):75–83. doi: 10.3238/arztebl.2010.0075

6. Safi H, Safi S, Hafezi-Moghadam A, Ahmadieh H. Early detection of diabetic retinopathy. *Surv Ophthalmol* (2018) 63(5):601–8. doi: 10.1016/j.survophthal.2018.04.003

7. Heng LZ, Comyn O, Peto T, Tadros C, Ng E, Sivaprasad S, et al. Diabetic retinopathy: Pathogenesis, clinical grading, management and future developments. *Diabetes Med* (2013) 30(6):640–50. doi: 10.1111/dme.12089

8. World Health Organization *Regional Office Europe*. (2020). Available at: https://apps.who.int/iris/handle/10665/336660

9. Nguyen TT, Wang JJ, Wong TY. Retinal vascular changes in pre-diabetes and prehypertension: New findings and their research and clinical implications. *Diabetes Care* (2007) 30(10):2708–15. doi: 10.2337/dc07-0732

10. Grauslund J, Hodgson L, Kawasaki R, Green A, Sjolie AK, Wong TY. Retinal vessel calibre and micro- and macrovascular complications in type 1 diabetes. *Diabetologia* (2009) 52(10):2213–7. doi: 10.1007/s00125-009-1459-8

11. Frank RN. Diabetic retinopathy and systemic factors. *Middle East Afr J Ophthalmol* (2015) 22(2):151–6. doi: 10.4103/0974-9233.154388

12. Crawford TN, Alfaro DV3rd, Kerrison JB, Jablon EP. Diabetic retinopathy and angiogenesis. *Curr Diabetes Rev* (2009) 5(1):8–13. doi: 10.2174/157339909787314149

13. Malek J, Azar AT, Tourki R. Impact of retinal vascular tortuosity on retinal circulation. *Neural Computing Applications* (2015) 26(1):25–40. doi: 10.1007/s00521-014-1657-2

14. Wei YH, Gong JS, Xu ZH, Thimmulappa RK, Mitchell KL, Welsbie DS, et al. Nrf2 in ischemic neurons promotes retinal vascular regeneration through regulation of semaphorin 6A. *P Natl Acad Sci USA* (2015) 112(50):E6927–36. doi: 10.1073/pnas.1512683112

15. Staal J, Abramoff MD, Niemeijer M, Viergever MA, van Ginneken B. Ridge-based vessel segmentation in color images of the retina. *IEEE Trans Med Imaging* (2004) 23(4):501–9. doi: 10.1109/TMI.2004.825627

16. Hoover A, Goldbaum M. Locating the optic nerve in a retinal image using the fuzzy convergence of the blood vessels. *IEEE Trans Med Imaging* (2003) 22 (8):951–8. doi: 10.1109/Tmi.2003.815900

17. Mustafa NBA, Zaki WMDW, Hussain A, Hamzah JC. A study of retinal vascular tortuosity in diabetic retinopathy. 2016 international conference on advances in electrical, electronic and systems engineering (ICAEES) (Putrajaya Malaysia: IEEE) (2016) 636–41. doi: 10.1109/ICAEES.2016.7888124

18. Lee H, Lee M, Chung H, Kim HC. Quantification of retinal vessel tortuosity in diabetic retinopathy using optical coherence tomography angiography. *Retina-the J Retinal Vitreous Diseases* (2018) 38(5):976–85. doi: 10.1097/Iae.0000000000001618

19. Sasongko MB, Wong TY, Nguyen TT, Cheung CY, Shaw JE, Wang JJ. Retinal vascular tortuosity in persons with diabetes and diabetic retinopathy. *Diabetologia* (2011) 54(9):2409–16. doi: 10.1007/s00125-011-2200-y

20. Sasongko MB, Wong TY, Donaghue KC, Cheung N, Jenkins AJ, Benitez-Aguirre P, et al. Retinal arteriolar tortuosity is associated with retinopathy and early kidney dysfunction in type 1 diabetes. *Am J Ophthalmology* (2012) 153(1):176–83. doi: 10.1016/j.ajo.2011.06.005

21. Gartner V, Eigentler TK. Pathogenesis of diabetic macro- and microangiopathy. *Clin Nephrol* (2008) 70(1):1–9. doi: 10.5414/cnp70001

22. Chawla A, Chawla R, Jaggi S. Microvasular and macrovascular complications in diabetes mellitus: Distinct or continuum? *Indian J Endocrinol Metab* (2016) 20(4):546–51. doi: 10.4103/2230-8210.183480

23. Miller JW, Le Couter J, Strauss EC, Ferrara N. Vascular endothelial growth factor a in intraocular vascular disease. *Ophthalmology* (2013) 120(1):106–14. doi: 10.1016/j.ophtha.2012.07.038

24. Wilkinson CP, Ferris FL, Klein RE, Lee PP, Agardh CD, Davis M, et al. Proposed international clinical diabetic retinopathy and diabetic macular edema disease severity scales. *Ophthalmology* (2003) 110(9):1677–82. doi: 10.1016/S0161-6420(03)00475-5

25. Dashtbozorg B, Zhang J, Abbasi-Sureshjani S, Huang F, Romeny BMTH. Retinal health information and notification system (RHINO). *Proc SPIE - Prog Biomed Optics Imaging* (2017) 10134:1013437. doi: 10.1117/12.2253839

26. Zhu SS, Liu HA, Du RY, Annick DS, Chen S, Qian W. Tortuosity of retinal main and branching arterioles, venules in patients with type 2 diabetes and diabetic retinopathy in China. *IEEE Access* (2020) 8:6201–8. doi: 10.1109/Access.2019.2963748

27. Zhang J, Dashtbozorg B, Bekkers E, Pluim JPW, Duits R, Romeny BMT. Robust retinal vessel segmentation via locally adaptive derivative frames in orientation scores. *IEEE Trans Med Imaging* (2016) 35(No.12):2631–44. doi: 10.1109/tmi.2016.2587062

28. Bekkers EJ, Zhang J, Duits R, ter Haar Romeny BM. Curvature based biomarkers for diabetic retinopathy *via* exponential curve fits in SE (2). *Proc Ophthalmic Med Image Anal Second Int Workshop* (2015 2017) 2(2015):113–20. doi: 10.17077/omia.1034

29. Duits R, Franken E. Left-invariant parabolic evolutions on Se(2) and contour enhancement *Via* invertible orientation scores part I: Linear left-invariant diffusion equations on Se(2). *Q Appl Mathematics* (2010) 68(2):255–92. doi: 10.1090/S0033-569x-10-01172-0

30. Duits R, Janssen MHJ, Hannink J, Sanguinetti GR. Locally adaptive frames in the roto-translation group and their applications in medical imaging. *J Math Imaging Vision* (2016) 56(3):367–402. doi: 10.1007/s10851-016-0641-0

31. Duits R, Felsberg M, Granlund G, Romeny B. Image analysis and reconstruction using a wavelet transform constructed from a reducible representation of the euclidean motion group. *Int J Comput Vision* (2006) 72 (1):79–102. doi: 10.1007/s11263-006-8894-5

32. Bertelsen M, Linneberg A, Rosenberg T, Christoffersen N, Vorum H, Gade E, et al. Comorbidity in patients with branch retinal vein occlusion: Case-control study. *BMJ* (2012) 345:e7885. doi: 10.1136/bmj.e7885

33. Lee SHS, Chang H, Kim JH, Kim HJ, Choi JS, Chung S, et al. Inhibition of mTOR *via* an AAV-delivered shRNA tested in a rat OIR model as a potential antiangiogenic gene therapy. *Invest Ophthalmol Visual Science* (2020) 61(2):1552–5783. doi: 10.1167/iovs.61.2.45

34. Jackson ZS, Dajnowiec D, Gotlieb AI, Langille BL. Partial off-loading of longitudinal tension induces arterial tortuosity. *Arterioscler Thromb Vasc Biol* (2005) 25(5):957–62. doi: 10.1161/01.ATV.0000161277.46464.11

35. Zhang Q, Wang D, Kundumani-Sridharan V, Gadiparthi L, Johnson DA, Tigyi GJ, et al. PLD1-dependent PKCgamma activation downstream to src is essential for the development of pathologic retinal neovascularization. *Blood* (2010) 116(8):1377–85. doi: 10.1182/blood-2010-02-271478

36. Zhang L, Zhang ST, Yin YC, Xing S, Li WN, Fu XQ. Hypoglycemic effect and mechanism of isoquercitrin as an inhibitor of dipeptidyl peptidase-4 in type 2 diabetic mice. *Rsc Advances* (2018) 8(27):14967–74. doi: 10.1039/c8ra00675j

37. Gariano RF, Gardner TW. Retinal angiogenesis in development and disease. *Nature* (2005) 438(7070):960–6. doi: 10.1038/nature04482

38. Azad AD, Chen EM, Hinkle J, Rayess N, Wu D, Eliott D, et al. Anti-vascular endothelial growth factor and panretinal photocoagulation use after protocol s for proliferative diabetic retinopathy. *Ophthalmol Retina* (2021) 5(2):151–9. doi: 10.1016/j.oret.2020.07.018

39. Ding J, Cheung CY, Ikram MK, Zheng YF, Cheng CY, Lamoureux EL, et al. Early retinal arteriolar changes and peripheral neuropathy in diabetes. *Diabetes Care* (2012) 35(5):1098–104. doi: 10.2337/dc11-1341

40. Liao M, Wang X, Yu J, Meng X, Liu Y, Dong X, et al. Characteristics and outcomes of vitrectomy for proliferative diabetic retinopathy in young versus senior patients. *BMC Ophthalmol* (2020) 20(1):416. doi: 10.1186/s12886-020-01688-3

41. Sidman RL, Li J, Lawrence M, Hu W, Musso GF, Giordano RJ, et al. The peptidomimetic vasotide targets two retinal VEGF receptors and reduces pathological angiogenesis in murine and nonhuman primate models of retinal disease. *Sci Transl Med* (2015) 7(309):309ra165. doi: 10.1126/scitranslmed.aac4882

frontiers | Frontiers in Endocrinology

TYPE Original Research
PUBLISHED 27 October 2022
DOI 10.3389/fendo.2022.977428

OPEN ACCESS

EDITED BY
Mohd Imtiaz Nawaz,
Department of Ophthalmology, King Saud University, Saudi Arabia

REVIEWED BY
Tingting Yue,
School of Public Health, Central South University, China
Xiangqing Hou,
University of Macau, China

*CORRESPONDENCE
Guangyun Mao
mgy@wmu.edu.cn
Chao Zheng
chao_zheng@zju.edu.cn

†These authors have contributed equally to this work and share first authorship

SPECIALTY SECTION
This article was submitted to Clinical Diabetes, a section of the journal Frontiers in Endocrinology

RECEIVED 24 June 2022
ACCEPTED 17 October 2022
PUBLISHED 27 October 2022

CITATION
Jin D, Zhao S, Li H, Xia Z, Che M, Huang R, Lai M, Wang Y, Zhang Z, Wang H, Zuo J, Zheng C and Mao G (2022) Plasma acylcarnitine and diabetic retinopathy: A study from Eastern China.
Front. Endocrinol. 13:977428.
doi: 10.3389/fendo.2022.977428

Plasma acylcarnitine and diabetic retinopathy: A study from Eastern China

Dongzhen Jin[1†], Shuzhen Zhao[1†], Huihui Li[1], Zhezheng Xia[1], Mingzhu Che[1], Ruogu Huang[1], Mengyuan Lai[1], Yanan Wang[1], Zejie Zhang[1], Hui Wang[1], Jingjing Zuo[2,3], Chao Zheng[4*] and Guangyun Mao[1,2,3*]

[1]Division of Epidemiology and Health Statistics, Department of Preventive Medicine, School of Public Health and Management, Wenzhou Medical University, Wenzhou, China, [2]Eye Hospital and School of Ophthalmology and Optometry, Wenzhou Medical University, Wenzhou, China, [3]National Clinical Research Center for Ocular Diseases, Wenzhou Medical University, Wenzhou, China, [4]The Second Affiliated Hospital of Zhejiang University School of Medicine, Hangzhou, China

Background and purpose: Acylcarnitines (ACars) are important for insulin resistance and type 2 diabetes (T2D). However, their roles in diabetic retinopathy (DR) remain controversial. In this study, we aimed to investigate the association of ACars with DR and their values in DR detection.

Methods: This was a two-center case-control study based on the propensity score matching approach between August 2017 to June 2018 in Eastern China. Multivariable logistic regression models were applied to estimate the association of plasma ACars with DR. Differential ACars were screened by models of least absolute shrinkage and selection operator, elastic net, and weighted quantile sum regression, and their roles in DR identification were further evaluated by the area under the receiver operating curve (AUC).

Results: Eight of twenty plasma ACars (8:0, 12:0, 12:1, 14:1, 16:2, 18:0, 18:2 and 18:3) were associated with DR, while only ACar 8:0 was selected by three variable selection methods. As compared to those with the 1st tertile of ACar 8:0, the adjusted odds ratio (OR) and 95% confidence interval (CI) of DR were 0.22 (0.08, 0.59) and 0.12 (0.04, 0.36) for subjects in the 2nd and 3rd tertiles, respectively (P for trend < 0.001). Consistent associations were also observed in both restricted cubic spline regression models and subgroup analyses. AUC (95% CI) were 0.74 (0.66, 0.82) for ACar 8:0 alone and 0.77 (0.70, 0.85) for ACar 8:0 combined with covariates.

Conclusions: Our findings suggest higher ACar 8:0 is significantly associated with a decreased risk of DR, which provides a unique window for early identification of DR.

KEYWORDS

plasma acylcarnitines, type 2 diabetes, diabetic retinopathy, propensity score matching, Acylcarnitine 8:0

Introduction

Diabetes mellitus (DM) is spiraling out of control and leads to a variety of important diseases (1). The number of diabetic retinopathy (DR), a chronic eye disease caused by DM, has also increased rapidly over the past few decades and is expected to rise from 93 million in 2012 to 224 million in 2040 (2). Due to the insidious onset of DR, almost all patients are diagnosed at a moderate or advanced stage (3), which not only leads to a decrease in clinical efficacy but also results in a huge waste of limited healthcare budgets. Therefore, it is critical to identify potential biomarkers to prevent and screen for DR.

It is reported that strict glycemic control cannot completely prevent the development from DM to DR (4), while disorders of lipid metabolism may play a key role in the pathogenesis of DR (5). A recent study revealed that carnitine metabolites were altered in patients with DR compared to those without DR (6), which provides a unique window for early identification of DR through novel lipid biomarkers. Acylcarnitine (ACar) is one of the acetyl derivatives of L-carnitine which plays a key role in the β-oxidation of long-chain fatty acids through the inner mitochondrial membrane (7, 8). Therefore, the accumulation of ACar is regarded as a response to the dysregulation of fatty acid oxidation (9). Available evidence shows that the level of specific ACars is different in patients with obesity, insulin resistance, metabolic syndrome, and diabetes compared to healthy participants (10–13). However, studies on the relationship between ACar and DR are scarce. An untargeted metabolomics study *via* high-resolution mass spectrometry found that plasma levels of deoxynivalenol in patients with diabetic retinopathy were higher than in diabetic controls (6). Another more intensive study from northern China found that multiple ACars (C2, C14DC, C16, C18:1OH, C18:1) were negatively associated with risk of retinopathy in patients with type 2 diabetes (14). However, the evidence based on population remains limited and the relationship of ACars with DR is controversial. In addition, an important question on whether ACars can serve as appropriate biomarkers for DR identification is not yet fully answered, either.

In this study, we aim to clarify the relationship between DR and plasma ACars, as well as to assess the role of plasma ACars in distinguishing DR from type 2 diabetes mellitus. These may be helpful to further elucidate the pathogenesis of DR and provide new insights into the possibility of new treatment development.

Materials and methods

Research subjects

This was a two-center case-control study, which is a propensity score matching (PSM) based lipidomics study conducted in China between August 2017 and June 2018. Detailed information on this study design and participants can be found in our previous works (15–17). In brief, a total of 195 patients with type 2 diabetes (T2D) patients (83 with DR and 112 without DR) aged over 35 years and free from type 1 diabetes, cardiovascular diseases, cerebrovascular diseases, hyperkalemia, cancers, infectious diseases, or other chronic systemic diseases were recruited from two affiliated hospitals of Wenzhou Medical University and Anhui Medical University. To adjust for potential effects of possible confounders and improve the comparability of the results to some extent, the PSM approach was applied, in which T2D patients with DR (case) and those without DR (control) were matched at a ratio of 1:1 by age, sex, body mass index (BMI), blood pressure (BP) and glycated hemoglobin A1c (HbA1c) (Supplementary Figure 1). Finally, a total of 69 pairs of cases and controls were included in this study. The cases included 58 with non-proliferative diabetic retinopathy (NPDR: 6 mild, 27 moderate, and 25 severe) and 11 with proliferative diabetic retinopathy (PDR).

Definition of DM and DR

T2D was defined as self-reported doctor diagnosis of diabetes, use of insulin or oral hypoglycemic medication, or according to the standard criteria recommended by the World Health Organization (WHO): venous plasma glucose concentration ≥ 11.1 mmol/L (1 mmol/L = 18 g/L) or fasting plasma glucose concentration > 7.0 mmol/L or the 2h glucose concentration ≥ 11.1 mmol/L in oral glucose tolerance test (OGTT) (18). The determination of DR was independently assessed by two experienced ophthalmologists strictly following the clinical diagnostic and image screening guidelines (19). The stages of DR were further graded as mild non-proliferative DR (NPDR), moderate NPDR, severe NPDR, and proliferative DR (PDR) by the same ophthalmologists. The details on the DR diagnosis can be found in the Supplementary Materials of this manuscript.

Demographic and clinical variables

Demographic variables including age, gender, duration of diabetes, smoking habits, alcohol consumption, occupation, and education were obtained by using a standardized questionnaire. This procedure was carried out by two systematically trained researchers strictly following the standard operation procedures (SOP) and quality control protocols specially prepared for this study. Besides, all participants also received anthropometric measurements such as weight, height, and blood pressure. Body mass index (BMI) was calculated using a formula as BMI = weight (kg)/height $(m)^2$. After at least 8 hours of fasting, the blood of each participant was collected, separated into serum and plasma, and stored at -86°C strictly following the

SOP for future assessment. An automated biochemical analyzer (Roche, Cobas c311) was used to obtain clinical features including fasting plasma glucose (FPG), HbA1c, and routine lipid profiles such as low-density lipoprotein cholesterol (LDL-C), high-density lipoprotein cholesterol (HDL-C), total cholesterol (TC), and triglyceride (TG).

Determination of plasma ACars levels

Plasma ACars were carefully profiled by an experienced, professional technician from the central laboratory of Shanghai ProfLeader Biotech Co., China. The details of metabolomics methods used can also be found in the Supplementary Materials. In short, the thawed plasma samples were added with internal standard, methanol and methyl tert-butyl ether (MTBE), etc., and then vortex shaken, ice-water ultrasonic bath, rested, centrifuged, and dried before the assessment by ultra-performance liquid chromatography-electrospray ionization-tandem mass spectrometry (UPLC-ESI-MS/MS) system. To avoid or decrease potential information bias as much as possible, all the following procedures associated with the determinations were finished strictly following the SOP by a single technician, and professional quality control measures were also applied. Samples from the cases and controls were processed in a random manner, and the technician was also blind to the categories of these samples. Plasma fractions were separated by the UPLC-ESI-MS/MS and identified by their retention times compared with those internal standards and expressed as peak areas.

In addition, the quantitative analyses of the screened plasma ACars were performed under the same conditions as above, and their intensities were calculated by plotting the peak area of the corresponding substance against the concentration of the standard (μmol/L) using a linear calibration curve.

Sample size estimation

To ensure that the sample size was sufficient to meet statistical requirements and to ensure the reliability of our findings, we estimated the sample size using G*Power (http://stats.idre.ucla.edu/other/gpower/). With type I error as 0.05, effect size equals to 0.8, a total sample size of 60 will be needed to achieve a power of 0.8 at the allocation ratio of 1 (Supplementary Figure 2).

Statistical analysis

Considering that missing data may lead to some bias and affect the credibility of findings to some extent, multiple imputations were performed for all covariates with a missing proportion of less than 20%. Demographic and clinical characteristics of cases and controls were compared by Chi-square test (categorical variables) and Student's t-test or Mann-Whitney U tests (continuous variables), respectively. Due to the skewed distributions of plasma ACars, we improved their normality first by log-transforming and normalizing them to Z scores. The Pearson correlation coefficients were used to describe the relationship between any two plasma ACars.

To comprehensively examine the association of plasma ACars with DR, the adjusted odds ratio (OR) and 95% confidence intervals (CI) were first estimated based on increases in each interquartile range (IQR) of ACars, depending on a multiple logistic regression model with adjusting for age, sex, BMI, smoking habits, alcohol consumption, education, duration of diabetes, TG, FPG, systolic blood pressure (SBP) and study center. In addition, considering that the relationship between ACars and DR may vary depending on their acyl chain length and unsaturation degree, ACars were classified into two categories, medium and long chains (defined as having carbon chains of 7 to 14, and ≥16, respectively), and further analyzed based on carbon atom and double bond numbers.

To thoroughly assess the potential role of ACars in the detection of DR, some commonly used feature selection approaches including least absolute shrinkage and selection operator (LASSO), elastic net (ENET), and weighted quantile sum (WQS) regression models were applied to detect potential biomarkers of DR from plasma ACars. Concentrations of the screened ACars were further determined based on UPLC-ESI-MS/MS platform. The relationship between potential biomarkers and DR was described in two ways: with concentrations as continuous variables [scaled to interquartile range (IQR)] and as categorical variables (tertiles). Meanwhile, linear trend tests were also performed. Restricted cubic spline (RCS) regression models with three knots of 5%, 50%, and 95% were additionally performed to further deeply investigate the potential dose-response relationships between detected biomarkers and the odds of DR. In addition, subgroup analyses and sensitivity analyses were also applied to test reliability and stability of the association.

To evaluate the role of screened plasma ACars in DR identification, we compared the performance of these potential biomarkers within models constructed from traditional indicators such as smoking habits, alcohol consumption, education, SBP, TG, FPG, and duration of diabetes by area under receiver operating characteristic (ROC) curves (AUC), sensitivity, specificity, positive predictive value (PPV), and negative predictive value (NPV). The comparisons of AUCs were additionally conducted by Delong's tests.

All statistical analyses were conducted using Stata/MP 15.1 for windows (Copyright 1985-2017 Stata Corp LLC, College Station, Texas 77845, USA) and R version 4.0.4 for Windows (R Foundation for Statistical Computing, Vienna, Austria). The R

package gWQS were used for WQS analyses (20). Two-tailed *P* values ≤ 0.05 were regarded as statistically significant.

Results

Characteristics of study participants

Characteristics of 138 participants were presented in Table 1. In addition to age, sex, BMI, BP, and HbA1c matched under PSM, fasting HDL, LDL, FPG, TG, TC, and lifestyle factors including smoking habits, alcohol consumption, occupation, and education status in the cases and controls were also balanced and comparable. However, patients with DR were more likely to have longer durations of diabetes than those without DR.

Distributions of plasma ACars

In the present study, we detected a panel of 20 plasma ACars that span the full range of total carbon atomic number (C8-C26) and unsaturation degree (n[C=C]=0–4) (Supplementary Table 1). The distribution of these ACars levels were shown in Supplementary Figure 3. The cases would like to have lower levels of ACars (8:0, 11:1, 12:0, 14:1, 16:0, 16:1, 16:2, 18:1, and

TABLE 1 Demographic and clinical characteristics between DM and DR subjects.

Variables	DM (n=69)	DR (n=69)	*P* values
Age, years	54.0 (49.0, 65.0)	57.0 (51.0, 65.0)	0.107
Gender (%)			0.863
Male	40 (58.0)	39 (56.5)	
Female	29 (42.0)	30 (43.5)	
BMI, kg/m2	24.10 (22.07, 26.61)	24.14 (22.49, 26.78)	0.609
DBP, mmHg	79 (75, 87)	77 (70, 81)	0.126
SBP, mmHg	126 (119, 140)	134 (121, 146)	0.077
FPG, mmol/L	8.12 (6.59, 10.80)	8.50 (6.31, 10.89)	0.893
HbA1c, %	9.94 ± 2.08	9.68 ± 1.92	0.433
HDL, mmol/L	1.02 (0.81, 1.35)	1.09 (0.86, 1.24)	0.946
LDL, mmol/L	2.62 ± 0.97	2.52 ± 1.06	0.562
TG, mmol/L	1.56 (1.03, 1.92)	1.41 (1.00, 1.93)	0.488
TC, mmol/L	4.72 ± 1.14	4.54 ± 1.39	0.424
Duration of diabetes, years	8.92 ± 6.21	12.43 ± 6.83	0.002
Education (%)			0.283
Junior high school or below	53 (76.8)	58 (84.1)	
High school or above	16 (23.2)	11 (15.9)	
Occupation (%)			0.390
Manual workers	31 (44.9)	36 (52.2)	
Mental workers	21 (30.4)	14 (20.3)	
Both	17 (24.6)	19 (27.5)	
Smoking habits (%)			0.700
Nonsmoker	41 (59.4)	38 (55.1)	
Current smoker	22 (31.9)	22 (31.9)	
Former smoker	6 (8.7)	9 (13.0)	
Alcohol consumption (%)			0.160
Nondrinkers	36 (52.2)	32 (46.4)	
Current drinkers	29 (42.0)	26 (37.7)	
Former drinkers	4 (5.8)	11 (15.9)	
Center (%)			0.106
Wenzhou	41 (59.4)	50 (72.5)	
Anhui	28 (40.6)	19 (27.5)	

Data are presented as mean ± SD for normal distributed variables, median (1st quartile, 3rd quartile) for skewed distributed variables, number (%) for categorical variables. When comparing differences between groups, the Chi-square test is used for categorical variables, the Student's t-test for normally distributed variables, and t Mann-Whitney U tests for skewed variables.
DM, type 2 diabetes (T2D) without diabetic retinopathy; DR, T2D with diabetic retinopathy.

26:1) than the controls ($P < 0.05$). Except for two pairs of ACars (13:0 & 20:1, 13:0 & 26:1), the correlation coefficients among other ACars showed significant positive relationships between any two of them ($r > 0$, $P \leq 0.05$) (Supplementary Figure 4).

Plasma ACars profiles and DR

Based on multivariable logistic regression analyses, significant differences between the cases and controls were observed in 6 kinds of plasma ACars (8:0, 11:1, 12:0, 14:1, 16:1, and 16:2) after adjusting for age, gender, BMI, smoking habits, alcohol consumption, education, duration of diabetes, TG, FPG, SBP, and the study center (Figure 1). Meanwhile, restricted cubic spline (RCS) model-based results also revealed apparent non-linear dose-response relationships between the 6 plasma ACars and DR (all $P_{\text{for nonlinearity}} > 0.05$) (Supplementary Figure 5). In addition, a moderately low risk was observed for those with increased medium-chain ACars, whereas no association was found between long-chain ACars and DR (Figure 1). Similar results were also detected in the association between ACars and DR when they were stratified by different carbon atom numbers and double bonds. We found that ACars with lower carbon atomic numbers ($C \leq 16$) were negatively associated with the odds of DR, regardless of whether the total ACars were adjusted or not (Figures 2A, B, green filled). However, interestingly, the association between ACars with higher carbon atom number (C18) and the likelihood of DR changed from no significant ($P > 0.05$) (Figure 2A, green unfilled) to significantly positive ($P \leq 0.05$) (Figure 2B, red filled) after adjusting for total ACars.

Association of ACar 8:0 with DR and its role in the identification of DR

To avoid or greatly decrease bias induced by potential collinearity and overfitting before constructing reasonable multiple regression models, several commonly used approaches containing LASSO, ENET and WQS regression models were respectively conducted to screen valuable ACars. Among all 20 detected plasma ACars, only ACar 8:0 was selected by LASSO and ENET and had the highest weight in the WQS model (Supplementary Table 2). To accurately clarify the relationship between plasma ACar 8:0 and DR, its actual concentration was determined by a calibration curve (Supplementary Figure 6). As was shown in Table 2, with per IQR increase of ACar 8:0, the adjusted likelihood of DR significantly decreased by 70% (OR: 0.30, 95% CI: 0.17 - 0.55). Similar results were also observed when evaluating the association *via* a quantile regression model: comparing to subjects with the lowest tertile plasma ACar 8:0, the adjusted odds of DR decreased by 78% (OR: 0.22, 95% CI: 0.08 - 0.59) and 88% (OR: 0.12, 95% CI: 0.04 - 0.36) for those in the 2nd and 3rd tertile of ACar 8:0, respectively. An apparent linear trend of ACar 8:0 with DR was additionally detected ($P_{\text{for trend}} < 0.001$). And results based on further sensitivity analyses (Supplementary

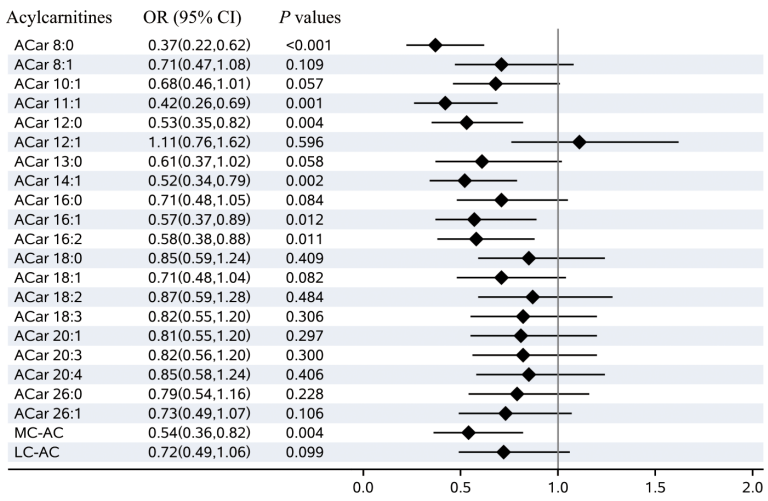

FIGURE 1
Plasma acylcarnitines and the risks of diabetic retinopathy. Notes: Odds ratio (OR) of developing diabetic retinopathy per SD increase in each plasma acylcarnitines were calculated by the logistic regression model, after adjusting for age, sex, BMI, smoking habits, alcohol consumption, education, duration of diabetes, TG, FPG, SBP, and center. OR, odds ratio; CI, confidence interval; MC-AC, medium-chain acylcarnitines; LC-AC, long-chain acylcarnitines..

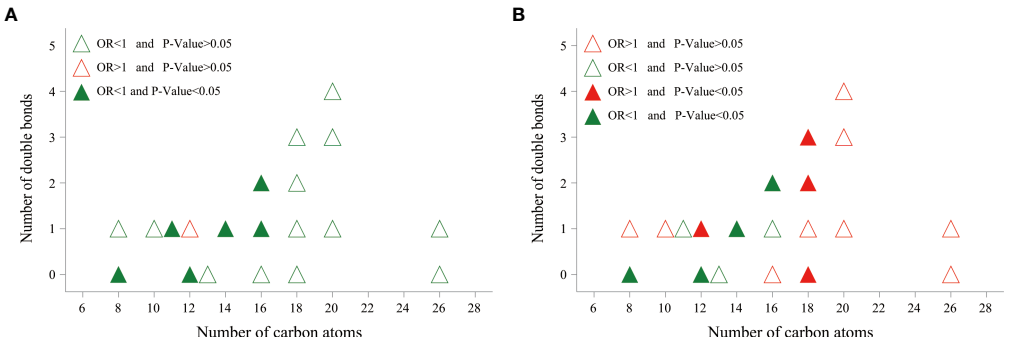

FIGURE 2
The relationship between DR risk and total number of carbon atoms and degree of saturation of various acylcarnitines. Odds ratio (OR) of developing DR per SD increase in each plasma acylcarnitines was calculated by logistic regression model, after adjusting for age, sex, BMI, smoking habits, alcohol consumption, education, duration of diabetes, TG, FPG, SBP, and center. **(A)** Acylcarnitines were log-transformed, and standardized before logistic regression analysis. **(B)** Acylcarnitines were divided by total acylcarnitine concentration, log-transformed, and standardized before logistic regression analysis. OR, odds ratio.

TABLE 2 Association between ACar 8:0 and the presence of DR.

ACar 8:0 (μmol/L)	N	Cases (%)	Model 1 [a]		Model 2 [b]		Model 3 [c]	
			OR (95%CI)	*P* values	OR (95%CI)	*P* values	OR (95%CI)	*P* values
Per IQR=0.012	138	69(50.00)	0.33(0.20,0.55)	<0.001	0.30(0.17,0.54)	<0.001	0.30(0.17,0.55)	<0.001
Tertiles								
T_1 (0.002~)	46	35(76.09)	1.00(1.00,1.00)	Ref.	1.00(1.00,1.00)	Ref.	1.00(1.00,1.00)	Ref.
T_2 (0.014~)	46	20(43.48)	0.24(0.10,0.59)	0.002	0.21(0.08,0.55)	0.002	0.22(0.08,0.59)	0.003
T_3 (0.021~0.097)	46	14(30.43)	0.14(0.06,0.35)	<0.001	0.11(0.04,0.33)	<0.001	0.12(0.04,0.36)	<0.001
$P_{fortrend}$				<0.001		<0.001		<0.001

[a]Unadjusted for potential confounders; [b]Adjusted for age, sex, BMI, smoking habits, alcohol consumption, education, TG, FPG, SBP, and center; [c]Adjusted for age, sex, BMI, smoking habits, alcohol consumption, education, TG, FPG, SBP, center, duration of diabetes.
DR, type 2 diabetic patients with diabetic retinopathy; n, numbers of subjects in each stratum; Case (%), numbers with DR and percentage; OR, odds ratio; CI, confidence interval; T1, T2, and T3, the 1st, 2nd, and 3rd tertiles of Acar 8:0, respectively, ACar, acylcarnitine.

Table 4) as well as RCS model (Figure 3) were highly consistent. None of the other variables, including age, gender, blood pressure, and regions showed significant effect modification on the association between plasma ACar 8:0 and the risk of DR (P for interaction > 0.05 for all these stratified variables) (Supplementary Figure 7). And patients with increasing levels of DR did not have decreasingly lower ACar 8:0 levels (Supplementary Figure 8).

We further explored the potential role of ACar 8:0 as a biomarker for early DR identification. Based on ROC curve analyses, with removing matching factors from the reference model, combining ACar 8:0 with the reference (Ref) model increased the area under the curve (AUC) from 0.67 (0.58, 0.76) (Ref) to 0.77 (0.70, 0.85) (Ref + ACar 8:0) (P = 0.011) (Supplementary Table 5; Supplementary Figure 9). Meanwhile, the sensitivity, specificity, positive predictive value (PPV), and negative predictive value (NPV) of the combined model were 82.61%, 65.22%, 70.37%, and 78.95%, respectively (Supplementary Table 5).

Discussion

In this PSM-based case-control study, we found that four plasma ACars (8:0, 12:0, 14:1 and 16:2), mainly medium-chain ACars, were inversely associated with the risk of DR, while four other ACars (12:1, 18:0, 18:2 and 18:3), predominantly long-chain ACars, were positively associated with DR after adjusting for total ACars. Particularly, the magnitude of the association between ACar 8:0 and DR was substantial, with high ACar 8:0 levels associated with an approximately 80% lower odds ratio of DR across tertiles in the categorical analysis. And the association did not seem to differ by age, gender, BMI, blood pressure, and variation in regions. In addition, ACars 8:0 might also can serve

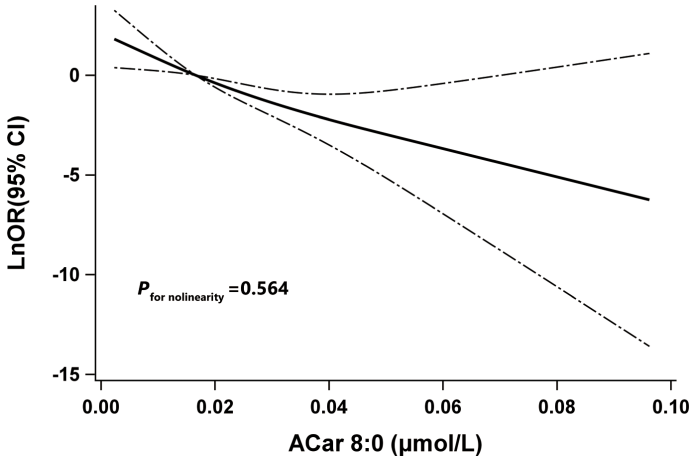

FIGURE 3
The restricted cubic spline for the association between Acar 8:0 and odds ratio (natural log-transformed) of DR. Notes: Knots were located at the 5th, 50th, and 95th percentiles of Acar 8:0.The solid line indicates LnOR and dashed lines indicate 95% CI. Adjusted confounders were age, sex, BMI, smoking habits, alcohol consumption, education, duration of diabetes, TG, FPG, SBP, and center. P for nonlinearity was used to test for linearity. DR, type 2 diabetic patients with diabetic retinopathy; LnOR, natural log-transformed odds ratios; CI, confidence interval, ACar, acylcarnitine.

as an ideal biomarker for DR identification though its alteration was not significantly observed amongst different stages of DR.

Available evidence suggests that ACars are associated with β-oxidative dysfunction, mitochondrial stress, and insulin resistance (9), and a panel of ACars, especially those with long chains, are significantly associated with increased risks of type 2 diabetes (21, 22). However, studies on the relationship between ACars and DR remain scarce and controversial. Wang et al. (14) found that individuals with DR were more likely to had higher levels of plasma Acars than those without DR. However, an untargeted metabolomics study showed that increased levels of ACars were related to the higher risk of DR (6). This was in line with supportive evidence from another study that patients with PDR had higher levels of ACars in vitreous compared with non-diabetic controls (23). Our current findings suggest that there may be potential beneficial (inverse) associations between medium-chain ACars and DR, but positive associations between long-chain ACars and DR. Although the discrepant findings of these studies might be ascribed to the differences in study design, study population, biosample type, and methodology associated with exposure estimation, the greatest differences may arise from the complex inter-relationships and metabolic effects of different ACars. Notably, in our study, after adjusting for the total ACars level, the odds ratio between majority of long-chain ACars and DR changed from less than 1 to greater than 1. Therefore, the negative association of long-chain ACars and DR in the previous study (14) should be interpreted with caution. In contrast, the inverse association between medium-chain ACars and the risk of DR is robust with or without correction of the total ACar level. The precise mechanisms of how ACars may influence DR risk are unknown, but there is evidence suggesting that incomplete oxidation of fatty acids was a major contributor to the pathway.

Biologically, ACars are mainly divided into short, medium and long chains according to the length of the carbon chain. Except for short-chain ACars, which are mainly derived from alternative energy sources, i.e., branched-chain amino acids (24), medium- and long-chains are predominantly originated from acylated derivatives of L-carnitine after β-oxidation of fatty acids (FAO) in mitochondria and peroxisomes (25). A previous study has reported that peroxisomal FAO is directly related to energy production (26). Because of this functional difference, the majority of medium- and long-chain ACars can be produced by mitochondrial FAO (27). As shown in Supplementary Figure 10, when FAO does not proceed completely (fewer cycles), it will inevitably lead to a reduction in the levels of medium-chain ACars, while long-chain ACars may produce a buildup (27). Therefore, the accumulations of long-chain ACars in plasma are often used to suggest defective FAO. Although there is no direct evidence that long-chain ACars are harmful to DR, a previous study has suggested that the inability of patients to regulate the oxidation of long-chain fatty acids will make them more susceptible to oxidative stress (28), which further increases the risk of developing DR (29). Therefore, this may be a potential interpretation of why high levels of long-chain ACars in plasma are associated with DR, while medium-chain ACars showed negative associations.

Furthermore, our findings highly suggest that ACar 8:0 may serve as a potential biomarker in distinguishing DR from T2D. Depending on the evidence from other studies (30), it shows that

plasma ACar 8:0 appears to have unique biological functions and can be used in clinical practice to detect diseases caused by impaired energy metabolism, particularly those caused by defects in mitochondrial medium -chain metabolism. Although extrapolating from possible mechanisms, such a result may suggest that T2D patients without DR can complete more cycles of FAO as compared to those with DR, further biochemical and clinical research is needed to examine a causal role of FAO in glycemic outcomes, particularly in diabetes complications.

The strengths of this study can be summarized as follows. First, the cases and controls are all enrolled in the endocrinology departments of comprehensive hospitals. Among participants, no one has obvious ocular symptoms, which may avoid some potential factors due to eye diseases in our findings. Second, the cases and controls are matched by the PSM approach, which has been widely accepted as an optimal strategy to effectively adjust for some known or unknown confounding bias in observational studies and can achieve class-balanced data. Third, the study population was enrolled from the departments of endocrinology in two top general hospitals in Zhejiang and Anhui, China. The two provinces cover a population of over 150 million residents, which may be beneficial to largely improve the credibility of our findings. In addition, LASSO, ENET, and WQS regression models are simultaneously used to screen the desirable profile of plasma ACars, which can not only avoid potential multicollinearity in the following multiple regression models but also efficiently and reasonably assess the effects of several ACars at the same time.

Inevitably, this study also has limitations. First, our findings are mainly based on a case-control study, which cannot exactly interpret possible causal relationships and mechanisms between ACars and DR. Although our results need to be additionally confirmed by longitudinal studies, their credibility has been demonstrated to a large extent depending on the results of sensitivity analyses. Second, although our sample size may be relatively small, it does not necessarily equal inadequacy. As is shown in Supplementary Figure 1, a total sample size over 60 will lead to power over 0.8 and the current sample size is sufficient to meet statistical requirements since the associated power has achieved 0.998, which ensures that our findings are credible. Third, diet patterns may partly affect the modification of plasma ACar. Third, data related to the red meat diet was not collected in the present study, but changes in the subjects' daily diet should not significantly affect the ACars concentrations measured in fasted blood samples, which could be used as a marker for long-term *in vivo* ACars levels (31). Fourth, as the PSM approach was applied, matched factors were not used in the construction of the identification model, but the model also performed well when it contained only ACar 8:0. Fifth, participants were limited to those who were from Zhejiang and Anhui, which might restrict the generalization of our findings, but these two places are representative of the areas in eastern China and the findings are consistent between the two areas.

Conclusions

Plasma ACar 8:0 is significantly associated with decreased risks of DR in T2D patients and plays an important role in distinguishing DR patients from T2D subjects. Our findings may be helpful for the secondary prevention of DR in clinical practice and provide new insights into the mechanisms of DR as well as the possibility of new treatment target development.

Data availability statement

The raw data supporting the conclusions of this article will be made available by the authors, without undue reservation.

Ethics statement

The studies involving human participants were reviewed and approved by Ethics Committee of the Eye hospital of Wenzhou medical university (Number: KYK (2017) 46). The patients/participants provided their written informed consent to participate in this study.

Author contributions

DJ and SZ conducted the study design, data management, data analysis and manuscript draft. HL, RH, JZ, and ML performed the quality control, data cleaning and analysis. ZX MC, YW, ZZ, and HW contributed to the epidemiological investigation, sample handling, data management and analysis. GM and CZ designed the study, thoroughly reviewed and edited the manuscript. All authors contributed to the manuscript revision, and approved the final version of manuscript. The corresponding authors had full access to all the data in the study and had final responsibility for the decision to submit for publication.

Funding

This study was supported by the National key research plan (2020YFC2008201), National Nature Science Foundation of China (82070833), Zhejiang Basic Public Welfare Research Project (LGF19H260011), Natural Science Foundation of Zhejiang Province (LZ19H020001) and the Scientific and technological innovation activity (new talent) plan for college students in Zhejiang Province (2021R413062). Part of this work was also funded by Zhejiang Provincial Key Research & Development Program (2021C03070).

Acknowledgments

We sincerely thank all participants who participated in this study and the team members from Wenzhou Medical University, Anhui Medical University, and Zhejiang University School of Medicine who assisted in the collection of samples. We are also grateful for the dedication and hard work of Shanghai ProfLeader Biotech Co., Ltd, for their careful assay of all the plasma samples.

Conflict of interest

The authors declare that the research was conducted in the absence of any commercial or financial relationships that could be construed as a potential conflict of interest.

Publisher's note

Supplementary material

The Supplementary Material for this article can be found online at: https://www.frontiersin.org/articles/10.3389/fendo.2022.977428/full#supplementary-material

References

1. IDF. *Diabetes is spiralling out of control: International diabetes federation* (2022). Available at: https://www.idf.org/.

2. Yau JW, Rogers SL, Kawasaki R, Lamoureux EL, Kowalski JW, Bek T, et al. Global prevalence and major risk factors of diabetic retinopathy. *Diabetes Care* (2012) 35(3):556–64. doi: 10.2337/dc11-1909

3. Guo Y, Guo C, Ha W, Ding Z. Carnosine improves diabetic retinopathy *via* the Mapk/Erk pathway. *Exp Ther Med* (2019) 17(4):2641–7. doi: 10.3892/etm.2019.7223

4. Cheung N, Mitchell P, Wong TY. Diabetic retinopathy. *Lancet* (2010) 376 (9735):124–36. doi: 10.1016/s0140-6736(09)62124-3

5. Crosby-Nwaobi R, Chatziralli I, Sergentanis T, Dew T, Forbes A, Sivaprasad S. Cross talk between lipid metabolism and inflammatory markers in patients with diabetic retinopathy. *J Diabetes Res* (2015) 2015:191382. doi: 10.1155/2015/191382

6. Sumarriva K, Uppal K, Ma C, Herren DJ, Wang Y, Chocron IM, et al. Arginine and carnitine metabolites are altered in diabetic retinopathy. *Invest Ophthalmol Vis Sci* (2019) 60(8):3119–26. doi: 10.1167/iovs.19-27321

7. Steiber A, Kerner J, Hoppel CL. Carnitine: A nutritional, biosynthetic, and functional perspective. *Mol Aspects Med* (2004) 25(5-6):455–73. doi: 10.1016/j.mam.2004.06.006

8. Bieber LL. Carnitine. *Annu Rev Biochem* (1988) 57:261–83. doi: 10.1146/annurev.bi.57.070188.001401

9. Koves TR, Ussher JR, Noland RC, Slentz D, Mosedale M, Ilkayeva O, et al. Mitochondrial overload and incomplete fatty acid oxidation contribute to skeletal muscle insulin resistance. *Cell Metab* (2008) 7(1):45–56. doi: 10.1016/j.cmet.2007.10.013

10. Mihalik SJ, Goodpaster BH, Kelley DE, Chace DH, Vockley J, Toledo FG, et al. Increased levels of plasma acylcarnitines in obesity and type 2 diabetes and identification of a marker of glucolipotoxicity. *Obes (Silver Spring)* (2010) 18 (9):1695–700. doi: 10.1038/oby.2009.510

11. Mihalik SJ, Michaliszyn SF, de las Heras J, Bacha F, Lee S, Chace DH, et al. Metabolomic profiling of fatty acid and amino acid metabolism in youth with obesity and type 2 diabetes: Evidence for enhanced mitochondrial oxidation. *Diabetes Care* (2012) 35(3):605–11. doi: 10.2337/dc11-1577

12. Bene J, Márton M, Mohás M, Bagosi Z, Bujtor Z, Oroszlán T, et al. Similarities in serum acylcarnitine patterns in type 1 and type 2 diabetes mellitus and in metabolic syndrome. *Ann Nutr Metab* (2013) 62(1):80–5. doi: 10.1159/000345759

13. Adams SH, Hoppel CL, Lok KH, Zhao L, Wong SW, Minkler PE, et al. Plasma acylcarnitine profiles suggest incomplete long-chain fatty acid beta-oxidation and altered tricarboxylic acid cycle activity in type 2 diabetic African-American women. *J Nutr* (2009) 139(6):1073–81. doi: 10.3945/jn.108.103754

14. Wang WY, Liu X, Gao XQ, Li X, Fang ZZ. Relationship between acylcarnitine and the risk of retinopathy in type 2 diabetes mellitus. *Front Endocrinol (Lausanne)* (2022) 13:834205. doi: 10.3389/fendo.2022.834205

15. Zhao S, Jin D, Wang S, Xu Y, Li H, Chang Y, et al. Serum Ω-6/Ω-3 polyunsaturated fatty acids ratio and diabetic retinopathy: A propensity score matching based case-control study in China. *EClinicalMedicine* (2021) 39:101089–. doi: 10.1016/j.eclinm.2021.101089

16. Li JS, Wang T, Zuo JJ, Guo CN, Peng F, Zhao SZ, et al. Association of n-6 pufas with the risk of diabetic retinopathy in diabetic patients. *Endocr Connect* (2020) 9(12):1191–201. doi: 10.1530/ec-20-0370

17. Zuo J, Lan Y, Hu H, Hou X, Li J, Wang T, et al. Metabolomics-based multidimensional network biomarkers for diabetic retinopathy identification in patients with type 2 diabetes mellitus. *BMJ Open Diabetes Res Care* (2021) 9(1): e001443. doi: 10.1136/bmjdrc-2020-001443

18. Society CD. Guidelines for the prevention and control of type 2 diabetes in China (2017 edition). *Chin J Pract Internal Med* (2018) 10(1):4–67. doi: 10.19538/j.nk2018040108

19. Wilkinson CP, Ferris FL, Klein RE3rd, Lee PP, Agardh CD, Davis M, et al. Proposed international clinical diabetic retinopathy and diabetic macular edema disease severity scales. *Ophthalmology* (2003) 110(9):1677–82. doi: 10.1016/s0161-6420(03)00475-5

20. Renzetti S, Gennings C, Curtin PC. gWQS: An R Package for Linear and Generalized Weighted Quantile Sum (Wqs) Regression. (2020). Available at: https://cran.r-project.org/web/packages/gWQS/vignettes/gwqs-vignette.pdf.

21. Guasch-Ferré M, Ruiz-Canela M, Li J, Zheng Y, Bulló M, Wang DD, et al. Plasma acylcarnitines and risk of type 2 diabetes in a Mediterranean population at high cardiovascular risk. *J Clin Endocrinol Metab* (2019) 104(5):1508–19. doi: 10.1210/jc.2018-01000

22. Sun L, Liang L, Gao X, Zhang H, Yao P, Hu Y, et al. Early prediction of developing type 2 diabetes by plasma acylcarnitines: A population-based study. *Diabetes Care* (2016) 39(9):1563–70. doi: 10.2337/dc16-0232

23. Paris LP, Johnson CH, Aguilar E, Usui Y, Cho K, Hoang LT, et al. Global metabolomics reveals metabolic dysregulation in ischemic retinopathy. *Metabolomics* (2016) 12:15. doi: 10.1007/s11306-015-0877-5

24. Zhang S, Zeng X, Ren M, Mao X, Qiao S. Novel metabolic and physiological functions of branched chain amino acids: A review. *J Anim Sci Biotechnol* (2017) 8:10. doi: 10.1186/s40104-016-0139-z

25. Schooneman MG, Vaz FM, Houten SM, Soeters MR. Acylcarnitines: Reflecting or inflicting insulin resistance? *Diabetes* (2013) 62(1):1–8. doi: 10.2337/db12-0466

26. Demarquoy J, Le Borgne F. Crosstalk between mitochondria and peroxisomes. *World J Biol Chem* (2015) 6(4):301–9. doi: 10.4331/wjbc.v6.i4.301

27. McCann MR, George de la Rosa MV, Rosania GR, Stringer KA. L-carnitine and acylcarnitines: Mitochondrial biomarkers for precision medicine. *Metabolites* (2021) 11(1):51. doi: 10.3390/metabo11010051

28. Schneider J, Han WH, Matthew R, Sauvé Y, Lemieux H. Age and sex as confounding factors in the relationship between cardiac mitochondrial function and type 2 diabetes in the Nile grass rat. *PloS One* (2020) 15(2):e0228710. doi: 10.1371/journal.pone.0228710

29. Kowluru RA, Chan P-S. Oxidative stress and diabetic retinopathy. *Exp Diabetes Res* (2007) 2007:43603. doi: 10.1155/2007/43603

30. Van Hove JL, Zhang W, Kahler SG, Roe CR, Chen YT, Terada N, et al. Medium-chain acyl-coa dehydrogenase (Mcad) deficiency: Diagnosis by acylcarnitine analysis in blood. *Am J Hum Genet* (1993) 52(5):958–66.

31. Rebouche CJ. Kinetics, pharmacokinetics, and regulation of l-carnitine and acetyl-L-Carnitine metabolism. *Ann New York Acad Sci* (2004) 1033(1):30–41. doi: 10.1196/annals.1320.003

frontiers | Frontiers in Public Health

TYPE Original Research
PUBLISHED 07 November 2022
DOI 10.3389/fpubh.2022.1025271

OPEN ACCESS

EDITED BY
Mohd Imtiaz Nawaz,
King Saud University, Saudi Arabia

REVIEWED BY
Gilbert Yong San Lim,
SingHealth, Singapore
Anwar P. P. Abdul Majeed,
Xi'an Jiaotong-Liverpool University, China

*CORRESPONDENCE
Qu Yi
yiqucn@sdu.edu.cn

SPECIALTY SECTION
This article was submitted to Clinical Diabetes, a section of the journal Frontiers in Public Health

RECEIVED 22 August 2022
ACCEPTED 18 October 2022
PUBLISHED 07 November 2022

CITATION
Qian X, Jingying H, Xian S, Yuqing Z, Lili W, Baorui C, Wei G, Yefeng Z, Qiang Z, Chunyan C, Cheng B, Kai M and Yi Q (2022) The effectiveness of artificial intelligence-based automated grading and training system in education of manual detection of diabetic retinopathy.
Front. Public Health 10:1025271.
doi: 10.3389/fpubh.2022.1025271

The effectiveness of artificial intelligence-based automated grading and training system in education of manual detection of diabetic retinopathy

Xu Qian[1,2,3], Han Jingying[4], Song Xian[1], Zhao Yuqing[1], Wu Lili[1], Chu Baorui[1], Guo Wei[5], Zheng Yefeng[6], Zhang Qiang[6], Chu Chunyan[6], Bian Cheng[6], Ma Kai[6] and Qu Yi[1,2,3]*

[1]Department of Geriatrics, Qilu Hospital of Shandong University, Jinan, China, [2]Key Laboratory of Cardiovascular Proteomics of Shandong Province, Jinan, China, [3]Jinan Clinical Research Center for Geriatric Medicine (202132001), Jinan, China, [4]School of Basic Medical Sciences, Shandong University, Jinan, China, [5]Lunan Eye Hospital, Linyi, China, [6]Tencent Healthcare, Shenzhen, China

Background: The purpose of this study is to develop an artificial intelligence (AI)-based automated diabetic retinopathy (DR) grading and training system from a real-world diabetic dataset of China, and in particular, to investigate its effectiveness as a learning tool of DR manual grading for medical students.

Methods: We developed an automated DR grading and training system equipped with an AI-driven diagnosis algorithm to highlight highly prognostic related regions in the input image. Less experienced prospective physicians received pre- and post-training tests by the AI diagnosis platform. Then, changes in the diagnostic accuracy of the participants were evaluated.

Results: We randomly selected 8,063 cases diagnosed with DR and 7,925 with non-DR fundus images from type 2 diabetes patients. The automated DR grading system we developed achieved accuracy, sensitivity/specificity, and AUC values of 0.965, 0.965/0.966, and 0.980 for moderate or worse DR (95 percent CI: 0.976–0.984). When the graders received assistance from the output of the AI system, the metrics were enhanced in varying degrees. The automated DR grading system helped to improve the accuracy of human graders, i.e., junior residents and medical students, from 0.947 and 0.915 to 0.978 and 0.954, respectively.

Conclusion: The AI-based systemdemonstrated high diagnostic accuracy for the detection of DR on fundus images from real-world diabetics, and could be utilized as a training aid system for trainees lacking formal instruction on DR management.

KEYWORDS

medical image education, artificial intelligence, diabetic retinopathy, medical students, diagnosis

Introduction

Diabetic Retinopathy (DR) is the leading cause of blindness and visual impairment in the working-age population worldwide (1). Numerous studies have shown that early detection and timely treatment of DR could prevent severe vision loss in more than 90% of diabetics (2, 3). However, due to a severe shortage of retinal specialists, a large proportion of patients in underdeveloped countries were unable to receive annual eye examinations recommended by the protocol (4, 5). In the face of a rapidly rising global diabetes incidence (6), a new approach to diabetes management is urgently needed. It has been confirmed that after receiving training in fundus photographic reading, non-ophthalmologists were highly sensitive as ophthalmologists in detecting DR (7). The training for non-ophthalmological readers seems to be an important step toward their integration into diabetic eye screening.

Accurate clinical staging of DR is a proven prerequisite for choosing the most appropriate personalized treatment. The Early Treatment Diabetic Retinopathy Study (ETDRS) based on color fundus photography is now the gold standard of DR grading (8). Nevertheless, the training procedure of image identification is of great implementation complexity because of individual variations of real-life cases encountered. In order to acquire skills to establish diagnosis in daily clinical practice, the trainees need to learn from a considerable number of images to extract image features. But training opportunities might be compressed due to limitations of resources, staff and finance (9). Furthermore, even highly qualified instructors might be subjective as well as have intra- and inter-reader diagnostic variations (10). Traditional ophthalmology courses often fail to provide a fairly large number of standardized cases for training purposes.

In recent years, artificial intelligence (AI) has shown obvious advantages in diagnosis and prediction of major eye diseases particularly those involving image analysis (11–13). Recent advances in automated retinal image screening systems using AI have demonstrated that specialist-level accuracy was can be achieved inDR assessment (10, 14). The implementations of big data and AI technologies in educational environments have also demonstrated significant potential for enhancing the efficiency of instruction (15). The essential information extracted from big data can help to shorten training periods and improve the learning curve of students. However, AI' s potential as an examination system and/or a robot teacher offering personalized education for medical students and traineesrequires further evaluation.

In this study, we developed an AI-based automated DR grading system equipped with an AI-driven diagnosis algorithm, and validated its role as an instructional and learning tool in training non-ophthalmic physicians in DR manual grading.

Materials and methods

The AI-based automated DR grading and training system

The study protocol was approved by the institutional review board of Qilu Hospital of Shandong University (QLHSDU) and conducted in accordance with the Declaration of Helsinki.

Dataset

78,000 anonymized color fundus images were primarily collected from consecutive patients with diabetes over 40 years old in the diabetes clinic of QLHSDU from January 1st, 2016 to January 14th, 2019. The mean age was 60.82 years (SD 11.34), and 58.44% of the participants were male. Macula-centered fundus images were captured using a Canon CR-2 fundus camera (45° field-of-view) with JPEG compression format (resolution in 18 megapixels). Participants' informed consents were exempted by the institutional review board of QLHSDU because the study was retrospective in nature that used completely anonymized data.

All the collected images were preprocessed by an image quality filter and reviewed by three experienced senior ophthalmologists. Images with severe blur, under-exposure, over exposure or severe cataract, out of focus, and fractional images without optic disc were graded as "poor quality", as it was impossible to make reasonable diagnosis of DR. Among all the 78,000 images, 19,245 (24.67%) were excluded due to image quality issues, leaving 58,755 with a conclusive DR severity grading in total. 8,063 cases of all the obtained 58,755 images were diagnosed as DR, so we randomly selected 7,925 non-DR fundus images from the remaining dataset in order to balance the data distribution and avoid data overfitting. The DR images were classified into four categories according to the International Clinical Diabetic Retinopathy (ICDR) severity scale (16), and each category was randomly chosen at a ratio of 4:1 to divide the images into a training set and a validation set, to guarantee that there was a similar distribution of data between the training set and the validation set. Of the total 15,988 images, 13,222 images were randomly assigned to the training dataset and the remaining 2,766 images were held for validation.

Algorithm development

In this study, the underlying AI algorithm of the automated DR grading system was developed by Tencent Healthcare, where deep convolutional neural networks were initially pre-trained on

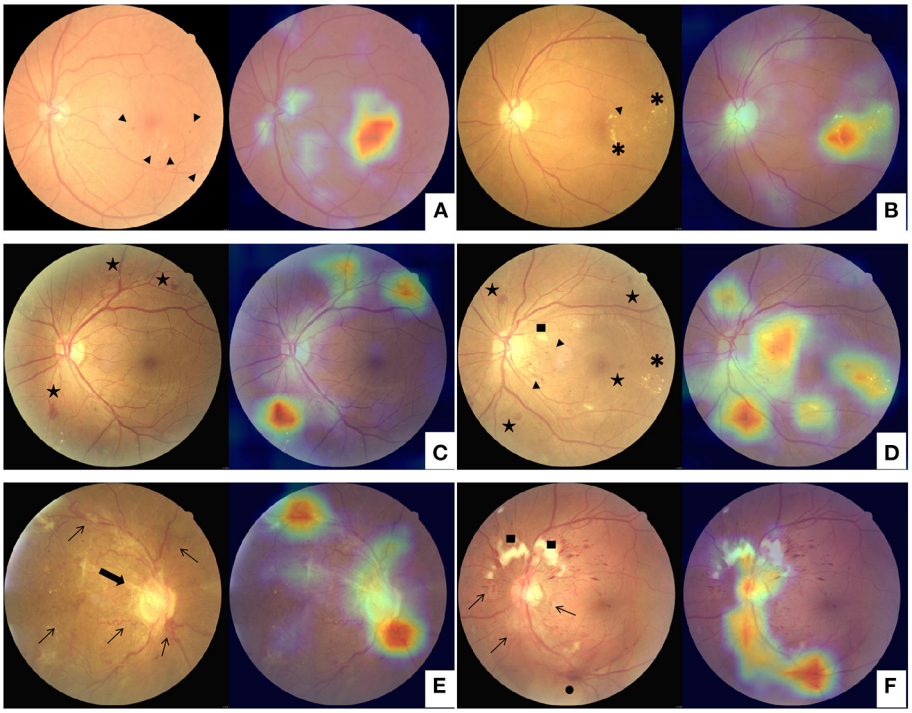

FIGURE 1
Examples of class activation mapping of lesion on the fundus images with mild diabetic retinopathy **(A,B)**, moderate and severe diabetic retinopathy **(C,D)**, and proliferative diabetic retinopathy **(E,F)** by automated grading system. The augmented image includes the original fundus images (Left) and one highlighted image that indicates the location of the lesions (Right). Arrowhead: microangiomas; Asterisk: hard exudates; Pentagram: intraretinal hemorrhages; Square: cotton-wool spot; Arrowhead: tail; Thin arrows: neovascularization; Thick arrow: fibrovascular proliferation; Black dot: vitreous hemorrhage.

a large volume of fundus images collected from several Chinese hospitals for the 5-stage DR classification task according to the ICDR severity scale. The network models were further fine-tuned with the collected real-world training dataset in this study to accommodate data and annotation variations.

The AI framework consisted of a standard ResNet-50 image classification network and an auxiliary graph convolutional network that integrated the prior class-dependency into the classification task. The prior class-dependency was represented by an adjacency matrix to reflect the correlations of adjacent DR stages. And the values of the adjacency matrix were updated simultaneously within the network training process. The learned prior information was used as residual information in the inference stage to re-rank the original results of the classification network and could potentially boost the performance of the algorithm. More details of the network design were introduced in the previous work (17).

For both training and validation datasets, we cropped the images to the size of 512 × 512 and applied the standard normalization to uniform the pixel values to the range (−1, 1). The Stochastic Gradient Descent (SGD) was utilized as the optimizer and the learning rate was set to 0.0001. Augmentation of the data including random scaling, rotation, horizontal flip, and vertical flip was involved to enlarge the size of the training set.

The network generated DR-stage probabilities for each input image, including none, mild, moderate, severe, and proliferative DR. The category with the highest probability value served as the network prediction. We noted that the annotation used a different fundus range from the ICDR scale, which was susceptible to misclassification in moderate DR and severe DR images. As a result, the modified 4-stage DR classification, including Non-DR, Mild DR, Moderate and Severe DR, and PDR, was implemented to prevent underestimating the prevalence of diabetic retinopathy. While the network models were trained for the multi-stage DR classification, we also analyzed the model performance on a binary classification task, i.e., referable DR vs. non-referable DR, where referable DR was defined as moderate DR or worse.

In addition to the DR stage prediction, a heatmap image was also generated by the network model using the Classification Activation Mapping (CAM) technique, similar to highlighting the highly prognostic related regions in the input image (18). The heatmap visualization identified image regions of retinal hemorrhage, exudate, neovascularization, venous beading and looping, etc., which were typical clinical findings associated

10.3389/fpubh.2022.1025271

TABLE 1 15-item questionnaire.

No.	Question
	One-choice questions (A, strongly agree; B, agree; C, neutral; D, disagree; E, strongly disagree)
Basic understanding	
1	I think current development of ophthalmic AI is good
2	I regularly encounter AI systems in my clinical practice
3	I regularly encounter AI systems in my training and education
Domain-based impact evaluation	
4	AI-based automated grading and training system improved my training and education
5	AI-based automated grading and training system is more effective and motivate
6	AI-based automated grading and training system challenged me to do my best
7	AI-based automated grading and training system promoted the learning of essential concepts or skills
8	AI-based automated grading and training system increased reading of the textbook by the students
9	AI-based automated grading and training system is beneficial to help me to develop critical and creative thinking
Respondent's attitude	
10	There is currently sufficient training in AI in my clinical training curriculum
11	More training in AI should be made available for medical students in the education of ophthalmology
12	I will be willing to incorporate AI-based automated grading and training system into my clinical training curriculum
13	I will recommend AI-based automated grading and training system to other students
14	I believed that AI teaching in ophthalmology will replace ophthalmology practice
15	I believed that AI teaching in ophthalmology will replace traditional ophthalmology courses

with DR (Figure 1). Based on the visualization output, the human graderscould substantiate the validity of the deep learning models and promote the clinical adoption of the AI-based automated grading system. Furthermore, the model and parameters were adjusted to point out the site of lesions more precisely to make the algorithm proper for education. The negative images determined by the algorithm would not present any heatmap to avoid confusion. The predicted lesion sites would be highlighted in positive images to guide the participants.

All graders except the two retinal specialists (conducting DR assessment over 20 years) were masked from the annotation results of each other. Three senior ophthalmologists were involved in annotating the training dataset. The reference standard was built up when all the three senior graders draw the same conclusion on the training dataset, and the discordant findings were adjudicated by the two retinal specialists.

Trainees' evaluations

To mimic the performance of less experienced human graders, two graders who volunteered to participate in the experiment were recruited: a junior ophthalmology trainee in the first year of residency and a medical student who has completed basic medicine courses. After reviewing the traditional lecture of DR before the trial began and being briefed about the annotation protocol, they diagnosed and evaluated 200 images of validation datasets loaded randomly.To evaluate the capability of the training course, 1 month later, the graders were given the extra training course comprising 200 AI-augmented color fundus photos with heatmap images that indicate the location of lesions. After that, they were required to re-annotate the whole validation dataset with the same protocol and made diagnosis.

Then, 120 students in their final year of medical school training who had entered the clinical rotation were recruited from the Medical School at Shandong University to learn diagnosis and grading of DR through this AI-based learning module. After completing the module, participants' evaluations of this system were measured by a 15-item questionnaire rated on five-point Likert-type scales (ranging from "strongly agree" to "strongly disagree") (Table 1). Using the Questionnaire Star APP (a professional questionnaire survey app in China, easy to edit and distribute survey questionnaires), the questionnaire was devised from the previous studies in other subjects of medical education (19–21). Information of the questionnaire consisted of three parts, which included: basic understanding (three items), domain-based impact evaluation (six items) and respondent's attitude (six items).

Statistical analysis

The accuracy, sensitivity and specificity metrics of the algorithm's outputs and manual grading results were calculated and then compared with the reference standard using StatsModels version 0.6.1 (Python). To evaluate the discriminatory ability of this automated DR grading system, the area under the receiver operating characteristic curve (AUC) was also calculated. The 95% confidence intervals (CIs) were offered meanwhile. After online survey collection, internal reliability of the survey questions was measured by calculating Cronbach's alpha. Descriptive statistics and analysis were carried out using SPSS version 24 (SPSS, Inc., Chicago, IL, USA).

TABLE 2 Confusion matrix for adjudicated reference standard and automatic DR grade system output according to modified protocol based on ICDR grading system.

Reference standard	Automated DR grading system				
	Non-DR	Mild DR	Moderate and Severe DR	PDR	Total
Non-DR	1435	19	4	4	1462
Mild DR	27	534	59	5	625
Moderate and Severe DR	1	19	554	17	591
PDR	3	1	3	81	88
Total	1466	573	620	107	2766

DR, diabetic retinopathy; ICDR, international clinical diabetic retinopathy; PDR, proliferative diabetic retinopathy.

TABLE 3 Two graders with/without artificial intelligence assistance verse automatic grading system on referable diabetic retinopathy detection.

	Automatic grading system	Junior resident		Medical student	
		w/o AI asst	With AI asst	w/o AI asst	With AI asst
SEN	0.965	0.910	0.972	0.838	0.976
SPE	0.966	0.993	0.994	0.921	0.946
AUC	0.980 (0.976–0.984)	0.952 (0.941–0.962)	0.982 (0.975–0.989)	0.880 (0.864–0.895)	0.961 (0.954–0.969)
ACC	0.965	0.973	0.987	0.901	0.965
PPV	0.901	0.976	0.974	0.775	0.901
FP	0.035	0.007	0.009	0.079	0.035
NPV	0.988	0.971	0.991	0.946	0.988
FN	0.035	0.090	0.028	0.162	0.035

AI, artificial intelligence; SEN, sensitivity; SPE, specificity; AUC, area under curve; ACC, accuracy; PPV, positive predictive palue; FP, false positive; NPV, negative predictive value; FN, false negative; w/o: without, asst, assistance.

Results

A comparison of the 4-stage DR diagnosis distribution between the automated grading results and the reference standard on the validation dataset was summarized in Table 2.

Table 3 demonstrated that the overall accuracy, sensitivity/specificity and AUC of the grading system for referable DR were 0.965, 0.965/0.966 and 0.980 (95% CI: 0.976–0.984), respectively. The grading system also achieved higher positive predictive value (PPV)/negative predictive value (NPV) of 0.901/0.988, and lower false positive (FP)/false negative (FN) of 0.035/0.035, than that of previous report for referable DR (22). Similar results were demonstrated when we examined other levels of DR according to ICDR grading system (Supplementary Table 1).

Both human graders achieved decent pre-training scores of the grading system for referable DR on the validation dataset (Table 3). However, the score improved in varying degrees when the graders were assisted with the AI system's output. The accuracy of human graders, i.e., junior resident and medical student, was improved from 0.973 and 0.901 to 0.987 and 0.965, respectively. The post-training AUC of the junior resident and medical student for referable DR were 0.982 and 0.961, respectively. Most notably, for the junior resident, the grading sensitivity showed remarkable improvement with AI support (0.910 vs. 0.972). While for the medical student, the improvement was even more pronounced (0.838 vs. 0.976).

As presented in Tables 4, 5, similar results were demonstrated when they grade any levels of DR according to ICDR grading system. In comparing the pre- and post-training scores of different degrees of DR, we identified a significantly higher gained sensitivity of mild DR in the junior resident (0.766 vs. 0.928) and medical student (0.714 vs. 0.838). Moreover, the automated DR grading system increased the graders' sensitivity without reducing the specificity, which was consistent with previous report (23).

As shown in Figure 2, of the 120 respondents, 103 students responded to the online survey (response rate 85.83%; 50.49% female). Overall, there was high internal reliability of the survey questions (Cronbach's alpha 0.93). The percentage of respondents who regularly encounter AI systems in their clinical practice and training and education was almost 50%. Over 70% of the trainees agreed that AI respondents were satisfied, helpful and effective. The percentage of respondents who

TABLE 4 Manual detection of diabetic retinopathy based on ICDR grading system by the junior resident.

	Junior resident							
	w/o AI asst				with AI asst			
	Non-DR	Mild DR	Moderate and Severe DR	PDR	Non-DR	Mild DR	Moderate and Severe DR	PDR
SEN	0.949	0.766	0.905	0.830	0.967	0.928	0.968	0.909
SPE	0.886	0.945	0.992	0.997	0.969	0.974	0.993	0.996
AUC	0.917 (0.907–0.928)	0.856 (0.838–0.873)	0.949 (0.937–0.961)	0.913 (0.874–0.953)	0.968 (0.961–0.975)	0.951 (0.941–0.962)	0.980 (0.973–0.988)	0.953 (0.923–0.983)
ACC	0.919	0.905	0.974	0.992	0.968	0.964	0.987	0.994
ACC*			0.947				0.978	

AI, artificial intelligence; DR, diabetic retinopathy; ICDR, international clinical diabetic retinopathy; PDR, proliferative diabetic retinopathy; SEN, sensitivity; SPE, specificity; AUC, area under curve; ACC, accuracy; w/o, without, asst, assistance. ACC* represents the overall accuracy for all evaluated images.

TABLE 5 Manual detection of diabetic retinopathy based on ICDR grading system by the medical student.

	Medical student							
	w/o AI asst				with AI asst			
	Non-DR	Mild DR	Moderate and Severe DR	PDR	Non-DR	Mild DR	Moderate and Severe DR	PDR
SEN	0.900	0.714	0.811	0.636	0.920	0.838	0.954	0.898
SPE	0.925	0.920	0.918	0.993	0.989	0.950	0.949	0.992
AUC	0.913 (0.902–0.923)	0.817 (0.798–0.835)	0.864 (0.847–0.881)	0.814 (0.764–0.865)	0.954 (0.947–0.962)	0.894 (0.879–0.909)	0.952 (0.942–0.961)	0.945 (0.913–0.977)
ACC	0.912	0.873	0.895	0.981	0.952	0.925	0.950	0.989
ACC*		0.915				0.954		

AI, artificial intelligence; DR, diabetic retinopathy; ICDR, international clinical diabetic retinopathy; PDR, proliferative diabetic retinopathy; SEN, sensitivity, SPE, specificity; AUC, area under curve; ACC, accuracy; w/o, without; asst, assistance. ACC* represents the overall accuracy for all evaluated images.

supported more formal AI training was 80 %, while only 14.56% reported sufficient AI training in their current curricula. The AI-based system motivated initiative of trainees, but couldn't replace the traditional ophthalmology practice and courses (18.45%, 19.42%).

Discussion

In this study, we finetuned an automated DR grading and training system on a real-world diabetic dataset of China and evaluated the diagnostic accuracy as well as its assistance to human graders.

The involved automated grading system achieved high diagnostic accuracy (0.965) and AUC (0.980) for the detection of vision-threatening referral DR on the validation dataset. The PPV of the automated DR grading system achieved 0.901 on referable DR differentiation, which showed high consistency of the grading system with the reference standard. Compared with previous studies (22), high sensitivity (0.965) and NPV (0.988), and more excellent performance on avoiding FN (only 0.035 on grading referable DR) of this system were demonstrated. False positive instances were mainly caused by misclassifying the mild DR as referable DR, while false negative cases were mainly due to the misclassification of referable DR as mild DR. Intra-retinal microvascular abnormalities were identified as the main source of misclassification (24), which was optimized in the training datasets (both laboratory and real-world clinic workflow). False positive cases are mainly due to mild DR being misclassified as referable DR, and false negative cases are mainly due to refeOur automated DR grading system showed great potential as an efficient and low-cost assistant to human graders to detect referral DR patients who need closer follow-up with retinal doctors.

The AI-based DR grading system also revealed its capability to be an effective tool for quantitative assessment of trainees'

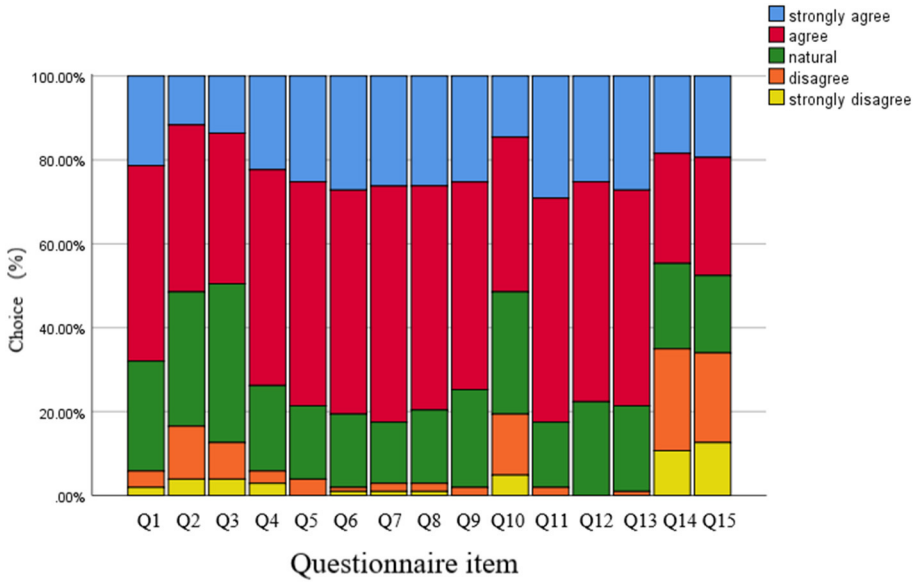

FIGURE 2
Results of the student evaluation questionnaires regarding the artificial intelligence based grading system. Each survey question used a five-point scale. For details of the questionnaire, see the Table 1.

diagnostic accuracy on fundus images collected from real-world clinics. In conventional DR courses, students are generally taught several foundational knowledge such as fundus anatomy, pathology, grading standards, and representative images of lesions, which are essential for the identification and diagnosis of the disease. Before AI-assisted learning, the two volunteer graders in this study achieved high accuracy as well as high sensitivity and specificity on referable DR and each level of DR independently, which indicated that traditional lectures played a key role in the process of understanding how to diagnose and grade the disease correctly. The integration of theoretical knowledge and clinical practice, however, is the most difficult and crucial aspect yet for medical students. On the other hand, the AI-based DR diagnostic system improved the grading ability of the two trainees, and the medical student with AI assistance even outperformed the junior resident without it. Previous studies have proven that topics that are visually intensive, detail-oriented, and difficult to conceptualize are particularly well-suited for computer-based presentation (25). The grading system provided a large number of fundus images which were collected from the real-world diabetic clinic and generated lesion-emphasized heatmap which can establish linkage between fundamental knowledge and real-life practice. Thermograms generated by AI highlighted the different lesions in real fundus photographs, strengthening students' understanding of pathological characteristics. After grading, the system could give the correct answer immediately, helping students to improve their learning efficiency. The timely monitoring and specific feedback provided by the system allowed students to identify learning goals and knowledge gaps, summarize and analyze their conceptual misunderstandings. Therefore, with training, students can improve the accuracy of their diagnosis by studying a limited number of patients. Our research also revealed that this module significantly considerably improved the students' sensitivity to mild DR detection (e.g., 97% for referable DR, respectively), which was crucial for screening of DR. We thus assumed that this additional course could to some extent compensate for the lack of background knowledge.

Regarding the trainees' classification mistakes, there were two potential causes. First off, due to technological limitations, we were only able to provide a heatmap rather than an arrowhead that points directly to a lesion. In fundus photographs that show multiple lesions at the same time, inexperienced medical students may find it difficult to distinguish between these different lesions. Second, persistent, intentional practice, frequent reinforcement, and expert teacher leadership were required to develop the trainees' ability to classify. Since, repeated practice in a controlled environment is very important in simulation-based education (26), even with more efficient instruments, constant work is still necessary for a successful education. Regarding teacher support, AI can only be used for low-level supervision, so that they cannot completely replace human teachers who can provide additional supervision, intensive training, coaching, and on-going support for students. The teacher's explanation of the clinical analytical thinking processes is critical to the development of students' clinical reasoning ability.

Moreover, the young generation of medical professionals grow up in the era of the internet (27), and there is almost no obstacle for them to use this AI-based system. According to the questionnaire, majority of medical students were more attentive and active during the training process. There is optimism that it will improve their learning of essential concepts or skills and facilitate high diagnostic accuracy with limited learning cases by using this system (28). In common with other surveys, majority of medical students reported their appetite for formal AI training in ophthalmic clinical curricula (29, 30). Although previous research has shown that eLearning is comparable to, and possibly superior to, traditional learning in terms of knowledge, skills, attitudes and satisfaction (31), the current medical school curriculum has not yet fully adapted to these educational needs. Medical students should have sufficient knowledge and experience of artificial intelligence, including its strengths and weaknesses, which is a crucial obligation for future doctors. However, only a small percentage of the population has ever received AI training, and a substantial portion of medical students lack a basic knowledge of these techniques. Although the application of ophthalmic AI goes quickly, AI training of medical trainees in ophthalmology was insufficient. We recommend that the AI-based education system should be integral to the improvement in ophthalmic medical education, especially in diagnosis and grading of DR.

The medical student and the junior resident represent the average diagnosis level of Chinese rural doctors. As we know, regular follow-up with early detection and treatment of vision-threatening DR enables a lower rate of vision loss, making DR no longer the leading cause of blindness among working-age adults in some regions of the world (32). Unfortunately, there are no more than 6,000 specialized doctors in retina diseases in China with uneven distribution around the country (4), screening for DR by ophthalmologists will not be immediately possible. In the longer term, training of the primary care physicians is an effective way to resolve this contradiction. Very little, if any, clinical experience and insufficient training in DR management contribute to lower diagnostic accuracy on DR (33). Thus, ophthalmic education is essential not only for future ophthalmologists but also for non-ophthalmic practitioners in the outpatient clinic. Application of the AI-based training system represents a possible solution to the increasing demand for DR grading education. Advanced technology has enabled learners in resource-limited settings to connect to other individuals, faculty, and even other curricula (34). Compared to traditional education, the automated DR grading and training system would potentially improve rural doctors' ability of DR grading even in limited resource settings.

Beyond the aforementioned key strengths of this study, some limitations must also be considered. First of all, diabetic macular edema (DME) was not involved in this study. This was because we choose optical coherence tomography (OCT) instead of fundus images to determine the presence of DME in the daily clinic, which might make DME underappreciated herein. Secondly, the automated DR grading system might overlook retinal diseases other than DR which might influence the FP rate. The involved images were collected from diabetic clinics, which may excludeother retinal diseases, e.g., age-related macular degeneration myopic maculopathy, retinal vessel occlusion, relatively infrequent or unintentionally (35). Last but not least, the sample size was relatively small, which might affect the validity of the study, the results require to be validated with larger sample size. Given that AI has yet not been widely implemented in clinical practice, there may be legitimate concerns about its instructional use. In order for optimal efficacy, AI-based teaching and learning systems should be rigorously evaluated through expert opinion and multi-institutional studies.

Conclusion

In summary, the proposed AI-based automated DR grading achieved high diagnostic accuracy for the detection of referral DR and each level of DR according to the modified protocol of ICDR grading system. It can aid the human graders to improve their diagnostic accuracy and sensitivity especially to those lacking didactic training on DR management. Furthermore, it can be used as assistant training system for medical students to experience the real scenarios which makes the traditional lectures properly illustrated. To give the system the essential curriculum knowledge for contextually driven education, further refinement of the system is necessary. Given the explosive recent growth of DM, and the lack of proven models for DR screening, the AI-based DR diagnostic system may be potential for establishment of appropriate primary care system of diabetes and as great importance in aiding medical education.

Data availability statement

The original contributions presented in the study are included in the article/Supplementary materials, further inquiries can be directed to the corresponding author.

Ethics statement

The studies involving human participants were reviewed and approved by the Institutional Review Board of Qilu Hospital of Shandong University (QLHSDU). The patients/participants provided their written informed consent to participate in this study.

Author contributions

QY was responsible for concept and design, supervised the project, guarantors of this work, had full access to all of the data in the study, take responsibility for the integrity of the data, and the accuracy of the data analysis. XQ and HJ wrote the original manuscript draft and were responsible for statistical analysis. XQ mainly takes charge of writing and researching, in the final version of the article, and is tagged as the only first author. All authors contributed to the article and approved the submitted version.

Funding

Publication of this article was sponsored by the Undergraduate Education and Teaching Reform and Research Project of Shandong University Cheeloo College of Medicine (Grant No. qlyxy-202012) and Education and Teaching Reform Project of Shandong University (Grant No. 2021Y139).

Acknowledgments

The authors express their sincere gratitude to the patients who participated in the trial.

Conflict of interest

The authors declare that the research was conducted in the absence of any commercial or financial relationships that could be construed as a potential conflict of interest.

Publisher's note

Supplementary material

The Supplementary Material for this article can be found online at: https://www.frontiersin.org/articles/10.3389/fpubh.2022.1025271/full#supplementary-material

References

1. Thomas RL, Halim S, Gurudas S, Sivaprasad S, Owens DR. Idf Diabetes atlas: a review of studies utilising retinal photography on the global prevalence of diabetes related retinopathy between 2015 and 2018. *Diabetes Res Clin Pract.* (2019) 157:107840. doi: 10.1016/j.diabres.2019.107840

2. Early Photocoagulation for Diabetic Retinopathy. Etdrs report number 9. early treatment diabetic retinopathy study research group. *Ophthalmology.* (1991) 98:766-85. doi: 10.1016/S0161-6420(13)38011-7

3. Yonekawa Y, Modi YS, Kim LA, Skondra D, Kim JE, Wykoff CC. American society of retina specialists clinical practice guidelines on the management of nonproliferative and proliferative diabetic retinopathy without diabetic macular edema. *J Vitreoretinal Dis.* (2020) 4:125–35. doi: 10.1177/2474126419893829

4. Song P, Yu J, Chan KY, Theodoratou E, Rudan I. Prevalence, risk factors and burden of diabetic retinopathy in china: a systematic review and meta-analysis. *J Glob Health.* (2018) 8:010803. doi: 10.7189/jogh.08.010803

5. Gange WS, Xu BY, Lung K, Toy BC, Seabury SA. Rates of eye care and diabetic eye disease among insured patients with newly diagnosed type 2 diabetes. *Ophthalmol Retina.* (2021) 5:160–8. doi: 10.1016/j.oret.2020.07.004

6. Saeedi P, Petersohn I, Salpea P, Malanda B, Karuranga S, Unwin N, et al. Global and regional diabetes prevalence estimates for 2019 and projections for 2030 and 2045: results from the international diabetes federation diabetes atlas, 9(Th) edition. *Diabetes Res Clin Pract.* (2019) 157:107843. doi: 10.1016/j.diabres.2019.107843

7. Liu Y, Rajamanickam VP, Parikh RS, Loomis SJ, Kloek CE, Kim LA, et al. Diabetic retinopathy assessment variability among eye care providers in an urban teleophthalmology program. *Telemed J E Health.* (2019) 25:301–8. doi: 10.1089/tmj.2018.0019

8. Early Treatment Diabetic Retinopathy Study Research G. grading diabetic retinopathy from stereoscopic color fundus photographs - an extension of the modified airlie house classification: etdrs report number 10. *Ophthalmology.* (2020) 127:S99–S119. doi: 10.1016/j.ophtha.2020.01.030

9. Succar T, Grigg J, Beaver HA, Lee AG, A. Systematic review of best practices in teaching ophthalmology to medical students. *Surv Ophthalmol.* (2016) 61:83–94. doi: 10.1016/j.survophthal.2015.09.001

10. Gulshan V, Peng L, Coram M, Stumpe MC, Wu D, Narayanaswamy A, et al. Development and validation of a deep learning algorithm for detection of diabetic retinopathy in retinal fundus photographs. *JAMA.* (2016) 316:2402–10. doi: 10.1001/jama.2016.17216

11. Heydon P, Egan C, Bolter L, Chambers R, Anderson J, Aldington S, et al. Prospective evaluation of an artificial intelligence-enabled algorithm for automated diabetic retinopathy screening of 30 000 patients. *Br J Ophthalmol.* (2021) 105:723–8. doi: 10.1136/bjophthalmol-2020-316594

12. Grassmann F, Mengelkamp J, Brandl C, Harsch S, Zimmermann ME, Linkohr B, et al. A Deep learning algorithm for prediction of age-related eye disease study severity scale for age-related macular degeneration from color fundus photography. *Ophthalmology.* (2018) 125:1410–20. doi: 10.1016/j.ophtha.2018.02.037

13. Liu H, Li L, Wormstone IM, Qiao C, Zhang C, Liu P, et al. Development and validation of a deep learning system to detect glaucomatous optic neuropathy using fundus photographs. *JAMA Ophthalmol.* (2019) 137:1353–60. doi: 10.1001/jamaophthalmol.2019.3501

14. Krause J, Gulshan V, Rahimy E, Karth P, Widner K, Corrado GS, et al. Grader variability and the importance of reference standards for evaluating machine learning models for diabetic retinopathy. *Ophthalmology.* (2018) 125:1264–72. doi: 10.1016/j.ophtha.2018.01.034

15. Luan H, Geczy P, Lai H, Gobert J, Yang SJH, Ogata H, et al. Challenges and future directions of big data and artificial intelligence in education. *Front Psychol.* (2020) 11:580820. doi: 10.3389/fpsyg.2020.580820

16. Haneda S, Yamashita H. International clinical diabetic retinopathy disease severity scale. *Nihon Rinsho Jap.J Clin Med.* (2010) 68:228–35. Available online at: https://www.ncbi.nlm.nih.gov/pubmed/21661159

17. Liu SGL, Ma K, Zheng Y. *Green: A Graph Residual Re-Ranking Network for Grading Diabetic Retinopathy*. Cham: Springer (2020).

18. Van der Heijden AA, Abramoff MD, Verbraak F, van Hecke MV, Liem A, Nijpels G. Validation of automated screening for referable diabetic retinopathy with the Idx-Dr device in the hoorn diabetes care system. *Acta ophthalmologica.* (2018) 96:63–8. doi: 10.1111/aos.13613

19. Huang Z, Li M, Zhou Y, Ao Y, Xin W, Jia Y, et al. Modified team-based learning in an ophthalmology clerkship in China. *PLoS One.* (2016) 11:e0154250. doi: 10.1371/journal.pone.0154250

20. Valikodath NG, Cole E, Ting DSW, Campbell JP, Pasquale LR, Chiang MF, et al. Impact of artificial intelligence on medical education in ophthalmology. *Transl Vis Sci Technol.* (2021) 10:14. doi: 10.1167/tvst.10.7.14

21. Blease C, Kharko A, Bernstein M, Bradley C, Houston M, Walsh I, et al. Machine learning in medical education: a survey of the experiences and opinions of medical students in Ireland. *BMJ Health Care Inform.* (2022) 29:100480. doi: 10.1136/bmjhci-2021-100480

22. De Fauw J, Ledsam JR, Romera-Paredes B, Nikolov S, Tomasev N, Blackwell S, et al. Clinically applicable deep learning for diagnosis and referral in retinal disease. *Nat Med.* (2018) 24:1342–50. doi: 10.1038/s41591-018-0107-6

23. Sayres R, Taly A, Rahimy E, Blumer K, Coz D, Hammel N, et al. Using a deep learning algorithm and integrated gradients explanation to assist grading for diabetic retinopathy. *Ophthalmology.* (2019) 126:552–64. doi: 10.1016/j.ophtha.2018.11.016

24. Li Z, Keel S, Liu C, He Y, Meng W, Scheetz J, et al. An automated grading system for detection of vision-threatening referable diabetic retinopathy on the basis of color fundus photographs. *Diabetes Care.* (2018) 41:2509–16. doi: 10.2337/dc18-0147

25. Greenhalgh T. Computer assisted learning in undergraduate medical education. *BMJ.* (2001) 322:40–4. doi: 10.1136/bmj.322.7277.40

26. Wang Z, Liu Q, Wang H. Medical simulation-based education improves medicos' clinical skills. *J Biomed Res.* (2013) 27:81–4. doi: 10.7555/JBR.27.20120131

27. Sit C, Srinivasan R, Amlani A, Muthuswamy K, Azam A, Monzon L, et al. Attitudes and perceptions of UK medical students towards artificial intelligence and radiology: a multicentre survey. *Insights Imaging.* (2020) 11:14. doi: 10.1186/s13244-019-0830-7

28. Tran AQ, Nguyen LH, Nguyen HSA, Nguyen CT, Vu LG, Zhang M, et al. Determinants of intention to use artificial intelligence-based diagnosis support system among prospective physicians. *Front Public Health.* (2021) 9:755644. doi: 10.3389/fpubh.2021.755644

29. Zhao G, Fan M, Yuan Y, Zhao F, Huang H. The comparison of teaching efficiency between virtual reality and traditional education in medical education: a systematic review and meta-analysis. *Ann Transl Med.* (2021) 9:252. doi: 10.21037/atm-20-2785

30. Wu D, Xiang Y, Wu X, Yu T, Huang X, Zou Y, et al. Artificial intelligence-tutoring problem-based learning in ophthalmology clerkship. *Ann Transl Med.* (2020) 8:700. doi: 10.21037/atm.2019.12.15

31. Rasmussen K, Belisario JM, Wark PA, Molina JA, Loong SL, Cotic Z, et al. Offline elearning for undergraduates in health professions: a systematic review of the impact on knowledge, skills, attitudes and satisfaction. *J Glob Health.* (2014) 4:010405. doi: 10.7189/jogh.04.010405

32. Groeneveld Y, Tavenier D, Blom JW, Polak BCP. Incidence of sight-threatening diabetic retinopathy in people with type 2 diabetes mellitus and numbers needed to screen: a systematic review. *Diabet Med.* (2019) 36:1199–208. doi: 10.1111/dme.13908

33. McKenna M, Chen T, McAneney H, Vazquez Membrillo MA, Jin L, Xiao W, et al. Accuracy of trained rural ophthalmologists versus non-medical image graders in the diagnosis of diabetic retinopathy in rural China. *Br J Ophthalmol.* (2018) 102:1471–6. doi: 10.1136/bjophthalmol-2018-312440

34. O'Donovan J, Maruthappu M. Distant peer-tutoring of clinical skills, using tablets with instructional videos and skype: a pilot study in the Uk and Malaysia. *Med Teach.* (2015) 37:463–9. doi: 10.3109/0142159X.2014.956063

35. Choi RY, Coyner AS, Kalpathy-Cramer J, Chiang MF, Campbell JP. Introduction to machine learning, neural networks, and deep learning. *Transl Vis Sci Technol.* (2020) 9:14.

frontiers | Frontiers in Endocrinology

TYPE Original Research
PUBLISHED 21 November 2022
DOI 10.3389/fendo.2022.1033611

OPEN ACCESS

EDITED BY
Mohd Imtiaz Nawaz,
Department of Ophthalmology, King Saud University, Saudi Arabia

REVIEWED BY
Jeena Gupta,
Lovely Professional University, India
Linsha Yang,
First Hospital of Qinhuangdao, China

*CORRESPONDENCE
Xiyuan Zhou
2668895079@qq.com;
zhouxiyuan2002@aliyun.com

SPECIALTY SECTION
This article was submitted to Clinical Diabetes, a section of the journal Frontiers in Endocrinology

RECEIVED 31 August 2022
ACCEPTED 27 October 2022
PUBLISHED 21 November 2022

CITATION
Wang M, Zhou X, Liu DN, Chen J, Zheng Z and Ling S (2022) Development and validation of a predictive risk model based on retinal geometry for an early assessment of diabetic retinopathy.
Front. Endocrinol. 13:1033611.
doi: 10.3389/fendo.2022.1033611

Development and validation of a predictive risk model based on retinal geometry for an early assessment of diabetic retinopathy

Minglan Wang[1], Xiyuan Zhou[1]*, Dan Ning Liu[1], Jieru Chen[2], Zheng Zheng[1] and Saiguang Ling[3]

[1]Department of Ophthalmology, Second Affiliated Hospital of Chongqing Medical University, Chongqing, China, [2]School of Computer Science and Engineering, Faculty of Engineering, University of New South Wales, Sydney, NSW, Australia, [3]Institute of EVision Computing, EVision technology (Beijing) co. LTD, Beijing, China

Aims: This study aimed to develop and validate a risk nomogram prediction model based on the retinal geometry of diabetic retinopathy (DR) in patients with type 2 diabetes mellitus (T2DM) and to investigate its clinical application value.

Methods: In this study, we collected the clinical data of 410 patients with T2DM in the Second Affiliated Hospital of Chongqing Medical University between October 2020 and March 2022. Firstly, the patients were randomly divided into a development cohort and a validation cohort in a ratio of 7:3. Then, the modeling factors were selected using the least absolute shrinkage and selection operator (LASSO). Subsequently, a nomogram prediction model was built with these identified risk factors. Two other models were constructed with only retinal vascular traits or only clinical traits to confirm the performance advantage of this nomogram model. Finally, the model performances were assessed using the area under the receiver operating characteristic curve (AUC), calibration plot, and decision curve analysis (DCA).

Results: Five predictive variables for DR among patients with T2DM were selected by LASSO regression from 33 variables, including fractal dimension, arterial tortuosity, venular caliber, duration of diabetes mellitus (DM), and insulin dosage ($P< 0.05$). A predictive nomogram model based on these selected clinical and retinal vascular factors presented good discrimination with an AUC of 0.909 in the training cohort and 0.876 in the validation cohort. By comparing the models, the retinal vascular parameters were proven to have a predictive value and could improve diagnostic sensitivity and specificity when combined with clinical characteristics. The calibration curve displayed high consistency

between predicted and actual probability in both training and validation cohorts. The DCA demonstrated that this nomogram model led to net benefits in a wide range of threshold probability and could be adapted for clinical decision-making.

Conclusion: This study presented a predictive nomogram that might facilitate the risk stratification and early detection of DR among patients with T2DM.

KEYWORDS

nomogram, prediction model, retinal geometry, diabetic retinopathy, T2DM

Introduction

It is estimated that more than 600 million individuals will be reported with diabetes mellitus (DM) worldwide by 2040 (1); 85% of these individuals will have type 2 diabetes mellitus (T2DM) (2), and more than one-fifth will suffer from diabetic retinopathy (DR) (3). DR is one of the vascular-incompetent complications of DM, resulting from chronic hyperglycemia. It is the leading cause of preventable blindness in the working population (4). This severe sight-threatening complication is characterized by irreversible visual loss and progressive retinal circulation damage, manifested as patches of retinal non-perfusion and neovascularization, pathologically (5, 6).

Although the pathogenesis of DR is not completely clear to date, several risk factors have been confirmed, including increased hemoglobin A1c (HbA1c) level, chronic hyperglycemia, and duration of DM (4, 7). However, these traditional risk factors cannot explain the risk variation of DR completely (8). Identifying additional risk factors beyond these conventional and recognized factors is of significant importance to the early detection and better management of DR, especially the risk factors related to retinal vascular incompetence.

In the last decade, the retinal vascular geometry (the retinal vascular morphology) of DR has gained prominence in emerging studies. The retinal vascular tree is the only site lacking autonomic innervation (9), spreading across the whole retina and modifying itself to fit local metabolism. The retinal vascular morphology is the key measure of local perfusion and metabolism status, indirectly reflecting the retinal function. Chronic high blood sugar contributes to abnormal serum, disrupting the balance of self-regulation of retinal vessels and leading to a higher risk of incident DR. Although a mature treatment plan for DR has been applied clinically according to correlative clinical guidelines, predicting the probability of incident DR precisely, screening high-risk individuals efficiently in the early phase, and determining the timing of medical intervention accurately are still issues demanding for solutions at present.

A nomogram is a useful tool to predict the accurate probability of clinical events, especially adverse outcomes, aiding to meet the drive for individualized medicine (10). It can transform a complicated calculation formula into a scoring system (11), intuitively showing the numerical correlation between a specific event and risk factors. This study aimed to develop a predictive nomogram model to screen the risk of DR among patients with T2DM. Early detection and identification of high-risk populations may facilitate early treatment and a better prognosis.

Methods

Research participants

We collected and analyzed the data of 410 patients with T2DM in the Second Affiliated Hospital of Chongqing Medical University between October 2020 and March 2022. The inclusion criteria included 1) T2DM with or without DR, diagnosed according to relevant criteria (fasting plasma glucose ≥ 7.0 mmol/L or 2-h plasma glucose ≥ 11.1 mmol/L or HbA1c ≥ 6.5%) (12); 2) no other retinopathy; and 3) complete clinical data. The exclusion criteria included 1) other co-occurring retinopathy-like retinal vascular occlusion, age-related macular degeneration, and so forth; 2) axial length >25 mm; 3) incomplete data; 4) previous interventions (retinal laser photocoagulation, intravitreal injection, and vitrectomy); and 5) blurred digital fundus image.

After the aforementioned screening, a total of 410 participants were recruited in this study and randomly divided into a training cohort (n = 292) and a validation cohort (n = 118) in a ratio of 7:3 using R software. Many variables showed statistically significant differences between DR and non-

diabetic retinopathy (NDR), such as hypertension, serum creatinine level, and duration of DM. These nonhomogeneous variables were potential factors for modeling. More details are presented in Table 1.

Retinal vascular geometry measurement

The retinal vascular traits were measured with the optic-centered fundus images, and the required digital images were obtained using a high-resolution TOPCON TRC-NW8 digital retinal camera (Topcon Optical Company, Tokyo, Japan) at a 45° angle after pupil dilation. All study participants underwent fundus fluorescein angiography (FFA) to determine their retinal status. These photos were classified as DR and NDR by two experienced professors (XZ and DL) according to the Early Treatment Diabetic Retinopathy Study and the result of the FFA (13).

To ensure the accuracy of the measurements, two researchers measured the retinal vessel characteristics independently (SL and

TABLE 1 Characteristics of the patients in the NDR and DR.

Characteristics	NDR (n = 182)		DR (n = 228)		P
	Mean	SD/Percentage	Mean	SD/Percentage	
Age (years)	62.12	0.0968	64.2000	10.7480	0.132
Gender (Female)	93	51.1%	123.0000	53.90%	0.566
Duration (years)	6.058	3.4002	9.1180	4.5801	<0.001*
Oral drug only (yes)	122	67%	90.0000	39.50%	<0.001*
Insulin dose (IU)	9.786	16.3549	20.6080	20.9781	<0.001*
BMI (kg/m^2)	24.2318	3.312	24.7295	3.7429	0.072
Systolic blood pressure (mmHg)	131.2	16.821	139.2500	19.2050	0.038
Diastolic blood pressure (mmHg)	81.82	13.45	80.5100	13.4190	0.198
Hypertension (yes)	93	51.1%	149.0000	65.40%	0.004
Smoking history (yes)	57	31.3%	57.0000	25.00%	0.156
Mean branch angle (°)	54.2921	0.7497	53.2071	10.1054	0.032
Fractal dimension	1.5584	0.0358	1.5131	0.0531	<0.001*
Arterial tortuosity	0.6039	0.1274	0.7402	0.4000	<0.001*
Venular tortuosity	0.819	0.138	0.8776	0.1991	0.002
Arterial caliber (μm)	48.5279	3.2934	48.4769	4.2410	0.487
Venular caliber (μm)	68.3851	5.2224	73.6248	7.0740	<0.001*
AVR	0.7137	0.5277	0.6629	0.6782	0.002
HbA1c (%)	8.5129	1.8219	8.7895	2.1703	0.419
eGFR (ml/min/1.73 m^2)	98.402	21.4759	82.9920	28.5300	<0.001*
Creatinine (μmol/L)	9.1145	2.9815	10.3861	5.1095	0.001
Fasting plasma glucose (mmol/L)	9.1145	2.9815	10.3861	5.1095	0.181
A/G	1.5884	0.3739	1.4424	0.3039	<0.001*
Triglyceride (mmol/L)	1.8976	1.1818	2.0131	1.9573	0.084
TC (mmol/L)	4.4555	1.0263	4.5810	1.1400	0.206
HDL (mmol/L)	1.1520	0.3579	1.1328	0.3038	0.946
LDL (mmol/L)	2.3223	0.7051	2.4768	0.8359	0.112
ApoA1 (mmol/L)	1.6296	5.2539	1.2940	0.2700	0.055
ApoB (mmol/L)	0.8775	0.2597	0.8213	0.2510	0.027
ApoE (mmol/L)	46.1534	24.7181	40.8618	17.8197	<0.001*
Lipoprotein (mmol/L)	220.1080	267.0026	255.8300	267.1131	0.043
NEFA (mmol/L)	1.1201	9.5043	0.3629	0.2405	0.004
Urinary albumin-to-creatinine ratio	4.1964	15.3784	50.4970	156.3525	<0.001*
Albuminuria (mmol/L)	31.2920	112.3517	301.3360	1026.3131	<0.001*

AVR, arteriole-to-venule ratio; BMI, body mass index; HbA1c, hemoglobin A1c; HDL, high-density lipoprotein; LDL, low-density lipoprotein; TC, total cholesterol; A/C, albumin-to-globulin ratio; eGFR, estimated glomerular filtration rate; SD, standard deviation.
Continuous variables are presented as mean and SD, and categorical variables are presented as mean and percentage. P-values were compared by independent t-test, Mann–Whitney U test, or chi-square test as appropriate. *P < 0. 001.

ZZ) using digital fundus image analysis software EVisionAI. This software was based on bionic human vision and deep learning system and could automatically recognize and segment retinal features. If different consequences were obtained from the two experts, another measurement was required. The right fundus image was collected. The left fundus image was an alternative if the poor image led to a blurred view of the retinal vessel.

First, the digital images were uploaded to the software, and the position of the optic disc and fovea was located automatically. Then, the software automatically sketched the map of the retinal geometry. At the same time, the vessels were classified as venule and arteriole. The operator edited the incorrectly labeled vessels. Furthermore, the vascular traits were quantified using a built-in computerized algorithm.

The vascular traits in this study included vascular caliber, tortuosity, fractal dimension, arteriole-to-venule ratio (AVR), and mean branch angle. The arterial diameter was defined as the average diameter of all visible arteries in the fundus image; the venular diameter was also measured similarly. The AVR was defined as the ratio of the arterial diameter to the venous diameter in the same image measured in an aforementioned manner. The vascular tortuosity was measured as the mean value of the tangent slope at every point on the pathway of tortuous vessels. The fractal dimension was measured on the basis of self-similarity, reflecting how the branching pattern filled the space, describing the complexity of the retinal vascular tree effectively. In a word, the more complex the vascular texture, the larger the fractal dimension value was. The mean branch angle is the average measurement of all of the branching angles within the area of two disc diameters away from the optic disc boundary.

Observation indexes

The clinical data including age, sex, duration of DM, smoking history, HbA1c, fasting plasma glucose, insulin dosage, hypertension, and so forth were collected. The retinal vascular parameters were measured, including mean vascular caliber, AVR, mean vascular tortuosity, fractal dimension, and mean branch angle. Two researchers (MW and XZ) checked the collected data independently to ensure completeness and reliability.

Statistical analysis

The statistical analysis was performed on IBM SPSS version 23 software and R software (version 4.2.1). All continuous variables were checked for normality. The categorical variables were displayed as counts and percentages and analyzed using the χ^2 test. The continuous variables were displayed as means ± standard deviation and analyzed using the t-test or Mann–Whitney U test. The independent predictors for DR among patients with T2DM were identified by the least absolute shrinkage and selection operator (LASSO) regression. Before selection, all of the feature values were standardized using the Z-score to remove dimension divergence among the observational data. The discrimination, calibration, and clinical application value of the prediction models were validated in both training and validation cohorts with areas under the receiver operating characteristic curve (AUCs), calibration plots, and decision curve analysis (DCA) curves. A P value < 0.05 indicated statistically significant differences. The details were presented in Figure 1.

Results

General characteristics of the participants

A total of 410 patients with T2DM, including 292 in the training cohort and 118 in the validation cohort, participated in this study. In the training cohort, 160 patients developed DR, accounting for 54.79%. In the validation cohort, 68 patients developed DR, accounting for 57.63%. No significant differences were observed in sex, age, and Body Mass Index (BMI) between DR and NDR ($P > 0.05$), indicating comparability between the two groups. More details are presented in Table 1.

Predictors selection

The LASSO regression analysis can select the independent risk factors for the linear regression models by shrinking the regression coefficients of variables toward zero. Supposing the regression coefficient is zero, the corresponding variable is excluded from the model. The remaining factors with non-zero regression coefficients are called independent risk factors having a closer association with the outcome event. In this study, 33 variables were introduced, and five variables with non-zero regression coefficients remained (Figure 2). The features selected in the LASSO analysis were fractal dimension, venular caliber, arterial tortuosity, insulin dosage, and duration of T2DM.

Development of models

A nomogram model was developed for DR risk prediction with these selected features using the multivariable logistic regression analysis (Figure 3). The probability of incident DR was calculated using the following equation:

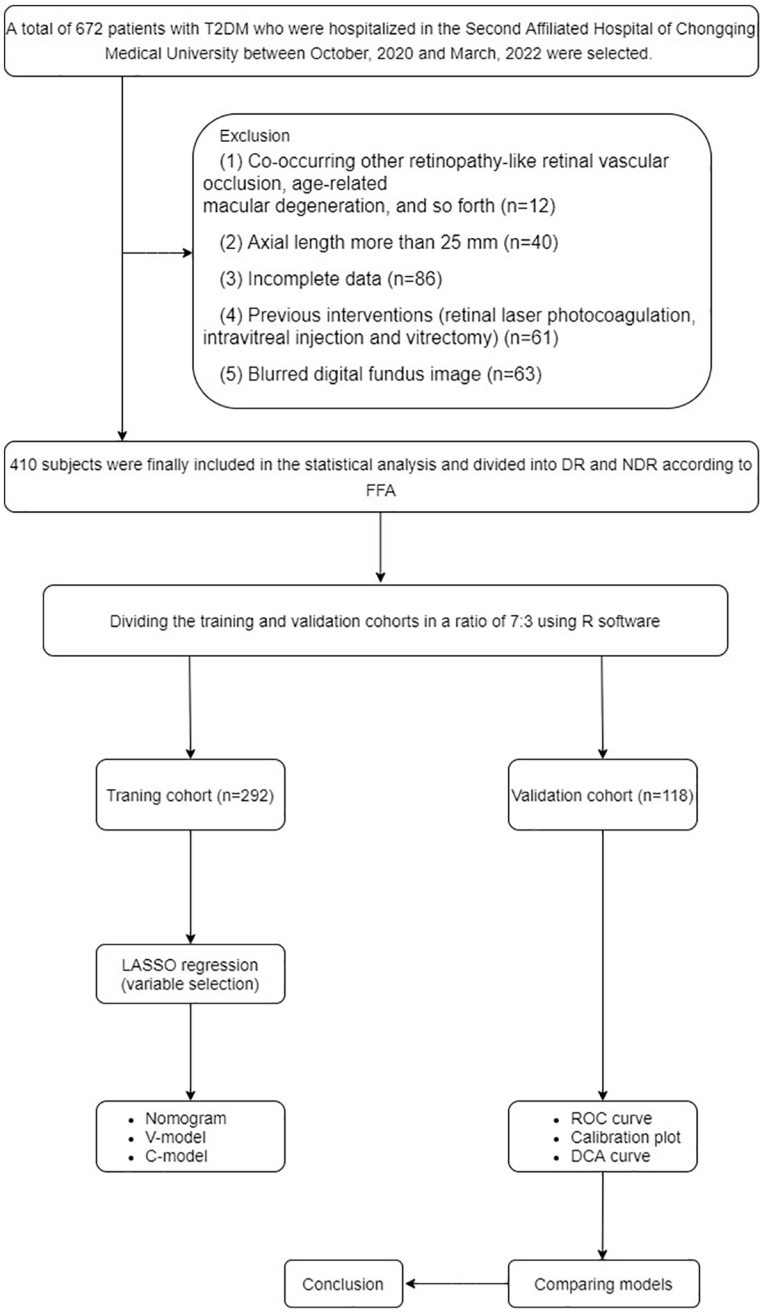

FIGURE 1
Flow diagram of the analysis.

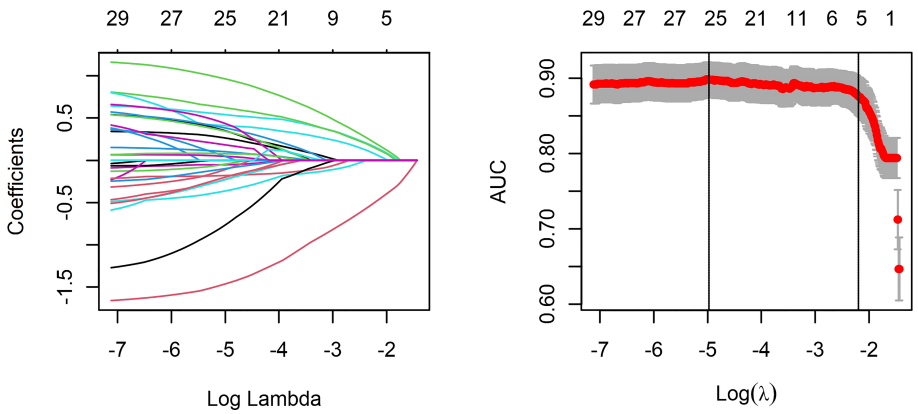

FIGURE 2
Least absolute shrinkage and selection operator (LASSO) regression and variable selection. All features were normalized by Z-score to remove the dimension divergence among the observational variables. In the cross-validated error plot, 25 variables with non-zero coefficients were selected at minimum cross-validated error, while five variables with non-zero coefficient remained at minimum cross-validation error within 1 standard error of the minimum.

$$\text{logist}(P) = 31.4591 - 28.7245 \times \text{fractal dimension} + 0.1022 \times \text{venular caliber} + 5.8777 \times \text{arterial tortuosity} + 0.0304 \times \text{insulin dosage} + 0.1881 \times \text{duration of T2DM}$$

Additionally, two models were constructed to confirm the performance advantage of the nomogram. The clinical model (C-Model) was built by a previous study (14) with clinical signatures (age, HbA1c, triglyceride, albuminuria, and duration of DM). The selected retinal vascular traits (fractal dimension, venular caliber, and arterial tortuosity) were used to establish the vascular geometry model (V-Model). According to the receiver operating characteristic (ROC) curves, the performance of the V-Model was better than that of the C-Model in both training and validation cohorts (Figure 4). This indicated that the retinal vascular signatures exhibited more predictive value than that of the clinical data. However, the predictive nomogram model displayed the highest AUC among these three (0.909 in the training cohort and 0.876 in the validation cohort). Accordingly, the retinal vascular traits combined with the clinical data of patients could improve the specificity and sensitivity of diagnosis.

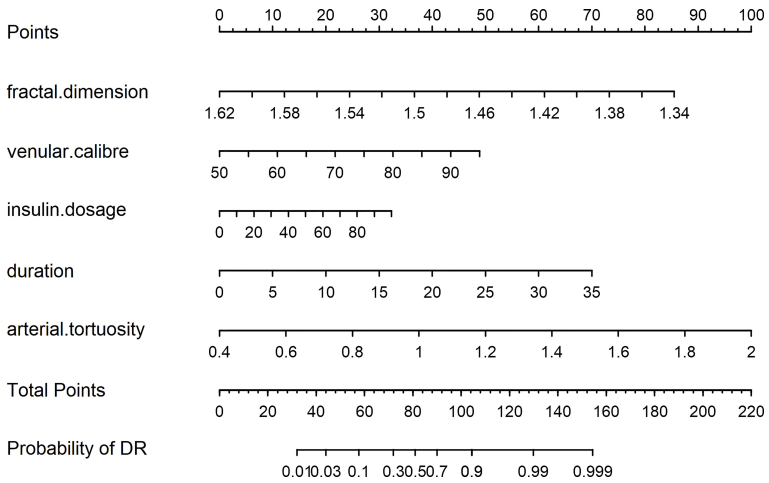

FIGURE 3
The nomogram model.

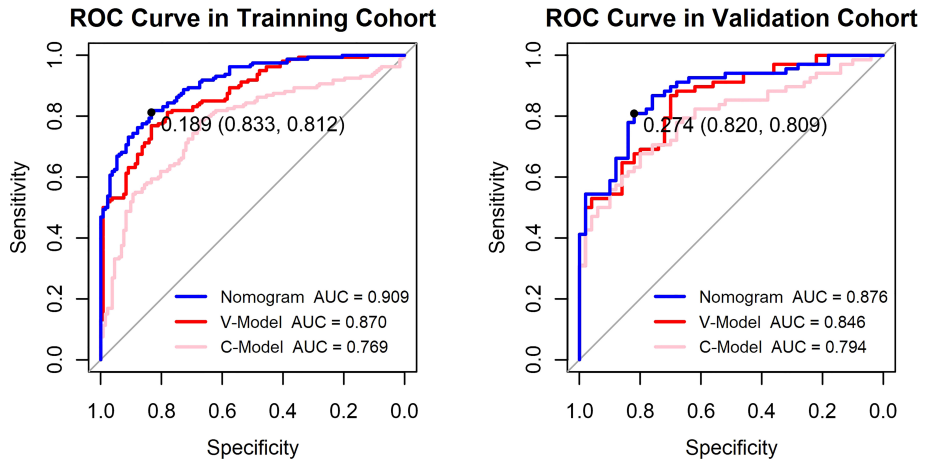

FIGURE 4
Receiver operating characteristic (ROC) curves of the constructed models. The y-axis means the true-positive rate of the risk prediction. The x-axis means the false-positive rate of the risk prediction. The blue line represents the performance of the nomogram. The cutoff value and area under the receiver operating characteristic curve (AUC) are presented in the picture as well.

Validation of the models

Calibration

The calibration curve of the established models evaluated the consistency between actual and predicted probabilities. In this study, it presented remarkable coherence in the three models in both training and validation cohorts (Figure 5). However, the P values of the Hosmer–Lemeshow test of the C-Model in both training and validation cohorts (0.263 and 0.374, respectively) were lower than those of the other two models. This illustrated that the V-Model and the nomogram model performed with higher calibration and better fitting.

Clinical use of the prediction nomogram

The results of the DCA for the models are presented in Figure 6. The DCA curves were drawn on the basis that the retinopathy prevalence of newly diagnosed diabetes was 30.6% in China (15). The horizontal line represented that none of the patients was living with DR, and all of them were treatment-free. The other oblique line was drawn on the assumption that all of the patients with T2DM had DR and received clinical intervention. The clinical net benefit was calculated using the following formula: net benefit = (true positive + false negative) – (false positive + true negative). For the C-Model, only if the threshold probability was larger than 13% in the validation cohort and in a relatively narrow range in the training cohort, the net benefit of patients was higher than that of the other two extreme curves (horizontal and oblique lines). However, according to the DCA curves, the net benefit of the nomogram and the V-Model was non-zero and much higher than that of the C-Model in a wide range of threshold probability. Moreover, among the established models, the nomogram model gained the highest net benefit in a wide range of threshold probability in both training and validation cohorts. This distinct difference indicated the performance advantage of this nomogram with good clinical safety. Furthermore, the cutoff value (18.9%) of the nomogram model according to the ROC curve of the training cohort was within the range of threshold probability in both DCA curves, showing good clinical usefulness as well. Given that 18.9% is defined as the threshold probability for screening DR and taking medical intervention, the net clinical benefit in the training and validation cohorts was 73.82% and 72.19%, respectively. That is, 73 and 72 of every 100 patients with T2DM who were found to have DR using this nomogram model in the training and validation cohorts would gain clinical benefits, respectively.

Visualization application of diabetic retinopathy

In a patient with T2DM, the relevant information of risk factors was obtained as follows: fractal dimension, 1.53; venular

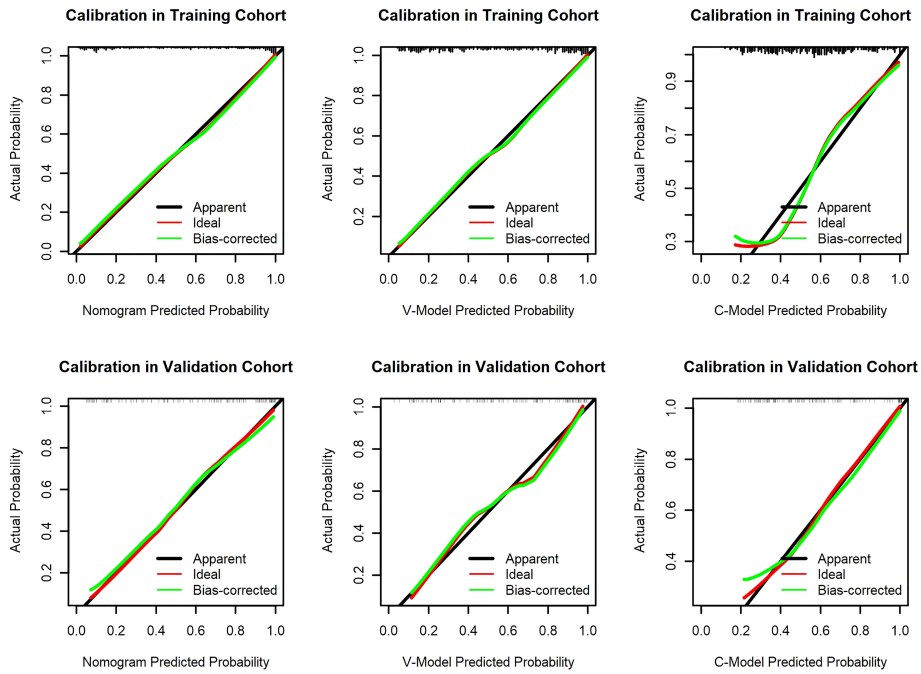

FIGURE 5
Calibration curves of the constructed models. The y-axis means the actual diagnosed diabetic retinopathy (DR). The x-axis meant the predicted risk of DR. The green lines represent the performance of the training cohort and validation cohort, which indicate a closer fit to the red line. This represents a better prediction.

caliber, 65 μm; arterial tortuosity, 0.0007; insulin dosage, 30 IU/day; and duration of DM, 10 years. According to the predictive nomogram (Figure 3), the risk of DR for this patient was approximately 30%, much higher than the cutoff value (18.9%). According to the DCA curve, the medical intervention was supposed to be taken to reduce the risk of incident DR. Meanwhile, a web page was built for screening based on this nomogram model (http://116.205.175.141:4949).

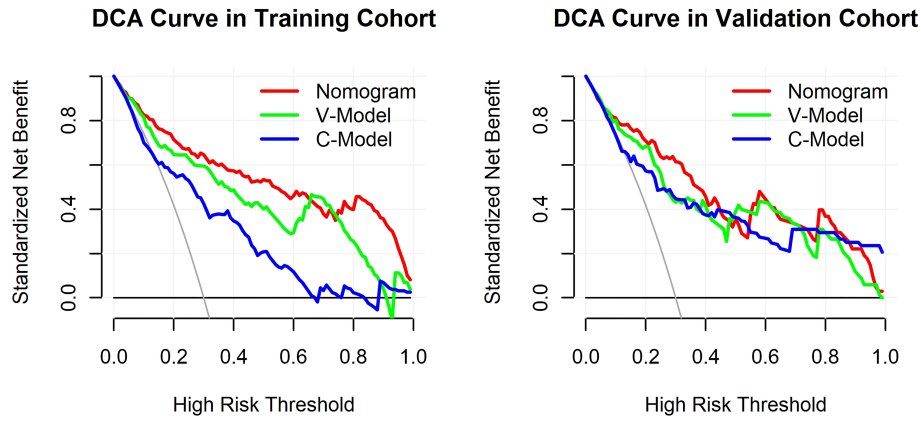

FIGURE 6
Decision curve analysis (DCA) for the constructed models. The y-axis measured the standardized net benefit. The horizontal line represented that none of the patients has diabetic retinopathy (DR) and all of them were treatment-free. The other oblique line is drawn on the assumption that all of the type 2 diabetes mellitus (T2DM) patients have DR and received clinical intervention.

Discussion

Currently, the nomogram has drawn increasing attention as a predictive tool in diagnosis and prognosis because it can quantify the individual probability of a clinical event with several significant variables (10). It meets our need for early detection with a mathematical model and facilitates individualized medicine (16). Furthermore, the scoring system presents the probability of a clinical outcome clearly and intuitively, promoting the doctor–patient communication and better clinical decision-making (17). In this study, we developed a nomogram using retinal vascular geometry parameters and basic clinical information with no blood test required. Therefore, it may play a key role in screening DR because of its convenience.

A total of 55.61% of the enrolled patients with T2DM had DR. This prediction nomogram model indicated that a smaller fractal dimension, larger venular caliber, increased arterial tortuosity, longer duration of DM, and larger insulin dosage were the key risk factors determining the incident DR for T2DM. Although 14 clinical indicators showed significant differences ($P< 0.05$) between the DR and NDR groups, only two variables were selected by the LASSO method. The circulation information gained from biological samples, such as blood and urine, was affected by multiple potential comorbidities and personal lifestyles. Whether the accessible circulation information reliably reflected the retinal status and local concentration of any specific factor was worth considering. To assess disease status, it would be optimal to measure indicators directly in the tissues influenced by the disease of interest (18). However, the biopsy of retinal tissue *in vivo* is unrealistic. The evaluation of altered retinal vascular morphology can be a viable alternative. Furthermore, the C-Model showed limited prediction accuracy, while the V-Model displayed favorable predictive performance. However, the predictive value of clinical data could not be ignored as well. In this study, the predictive nomogram developed with retinal vascular factors and clinical factors presented satisfactory predictive capability and better performance than those of the V-Model and C-Model.

The individual risk probability of DR could be obtained by introducing specific indicators of patients into this nomogram. The relatively good discrimination and calibration suggested that this prediction nomogram model could be adapted clinically. Additionally, it would help in risk stratification, leading to better management of patients with and without DR. For individuals at high risk, a closer follow-up was required. This study developed a relatively reliable predictive tool to evaluate the risk of DR in patients with T2DM. Yet, more efforts should be taken to improve the model in terms of accuracy and applicability.

Duration of disease and insulin dosage

The duration of DM and insulin dosage were risk factors for T2DM. The result implied that longer duration and larger insulin dosages had a close association with incident DR. They should be considered as a pair of risk variables in analyzing the association with DR. Insulin is indispensable for normal protein, fat, and carbohydrate metabolism. Patients with T2DM are initially treated with antiglycemic drugs such as biguanide. However, over time, most of them show a decrease in insulin production; hence, insulin supplementation is required to control chronic high blood sugar levels. Abundant resources greatly satisfy the needs of human beings and influence people's behavior and lifestyle. An unhealthy lifestyle is the main reason for the shift in the therapeutic regimen for patients with T2DM (19), starting with glucose-lowering medicines, followed by low-dose insulin, and then increasing the insulin dosage. Over time, the function of islet cells is impaired with insufficient insulin secretion, leading to a growing demand for exogenous insulin dosage (20).

In our study, the mean duration of the disease course was approximately 6 years in NDR and 9 years in DR in both training and validation cohorts. The use of mean insulin dosage in DR was much more than that in NDR in both cohorts. Thus, we could infer that the insulin dosage was roughly parallel with the duration of T2DM. Long-term hyperglycemia can damage the vascular system insidiously, including the retinal vascular tree. Studies also showed that a longer duration of DM led to a higher prevalence of DR (21, 22). Based on this perception, the duration of DM may be a more vital factor to the risk of retinopathy. Meanwhile, the regression coefficient of the duration of DM was larger than that of insulin dosage, suggesting that the duration was a more important one contributing to incident DR. The patients with a longer duration of T2DM and a larger dosage of insulin were more likely to suffer from DR.

Retinal geometry

Previous researchers reported an optimal circulation that drove blood flow with the least energy and completely met the metabolic demands of local tissues (23). Any deviation from this optimal vascular structure would result in reduced circulatory efficiency. The primary functions of the retinal vascular tree were nourishing the retinal tissue and removing local wastes. As a result, the retinal vascular needed to modify itself continuously to accommodate the changing demand for metabolism and blood pressure. Therefore, the peripheral metabolic environment and perfusion demands were of paramount importance to determine the ultimate retinal vascular architecture, especially in metabolic diseases, such as diabetes.

Vascular tortuosity

The normal retinal vascular is gently curved or roughly straight. A tortuous vascular may result from increasing vascular endothelial growth factor (VEGF) levels in response to an incomplete retinal vessel wall caused by hypoxia or ischemia (24). Except traditional neovascularization, tortuosity is considered as another form of angiogenesis with an increased VEGF level (25) because it must elongate enough to accommodate its tortuous changes. This appears to be consistent with the conventional view of the retinopathy signs of venular beading. Yet, in this study, both arterial and venular vascular showed a statistically significant difference between NDR and DR in terms of tortuosity. The coefficient of venular tortuosity shrunk to zero in the LASSO analysis, implying a less predictive value in this study than that of arterial tortuosity.

The hyperglycemia-mediated retinal vascular injury started with the loss of endothelial cells and surrounding pericytes, resulting in autoregulation dysfunction (26). The chronic high blood sugar level undermined the basement membrane of the vessel wall. The collagen fibers of the basement membrane functioned against the irregular longitudinal traction and transmural pressure with its axial strain, maintaining the morphological stability of the retinal vasculature (27). The increased vascular tortuosity indicated a decrease in endothelial cells and pericytes (28), thus being relatively more fragile and vulnerable to hemorrhage. This was parallel with well-recognized features of retinopathy in diabetes. We inferred that patients with tortuous retinal vessels suffered from more severe retinopathy and were more likely to be observed with hemorrhage spots under a funduscope. Moreover, neovascularization might appear much earlier than less tortuous retinal vasculature.

Vascular caliber

The biological mechanism of the changes in the retinal vessel caliber in patients with DR is unclear. The widening venule may reflect increased volumetric blood flow related to hyperglycemia and retinal hypoxia. The uncontrollable blood sugar and tissue hypoxia would finally result in accumulative lactic acidosis and autoregulatory endothelial dysfunction (29). The retinal vascular caliber largely depends on retinal perfusion and vascular autoregulation. Blunt vasomotion caused by impaired endothelial cells may play a role in this. Furthermore, retinal perfusion is regulated by the demands of local metabolism. A smaller vascular caliber has been reported in patients undergoing panretinal photocoagulation (30). The reduced demand of the metabolism secondary to the damage of the ischemic retinal area was assumed to be responsible for narrowed retinal blood vessel with improved oxygenation and lower volumetric blood flow. Furthermore, a close connection was reported between the gradually increased venular caliber and higher HbA1c level (31), as well as the severity of retinopathy (32), which reflected poor blood glucose control indirectly.

In this study, a significant difference in the venular caliber was observed between DR and NDR, while no obvious difference was found in the arterial caliber. The observed result was consistent with the findings of population-based studies (32, 33). In elderly patients without DM, both arteriolar and venular calibers decreased with age, and the narrowing retinal vascular was proven to be associated with hypertension and cardiovascular risk (34, 35). It was assumed that the adverse effect of hyperglycemia was underestimated, and poor control of blood sugar level might exert a greater influence on vascular architecture than blood pressure (36, 37).

Fractal dimension

The fractal dimension is a relatively simple method used for evaluating the complexity of the retinal vascular tree. It is not associated with macrovascular disease and has a closer association with microvascular disease (38). As DR progresses, further non-perfusion patches formed with occlusive microvasculature and the complexity of retinal vascular pattern reduces with a decrease in fractal dimension (39, 40).

Generally, the retinal vascular fractal dimension decreases in vessel-involving diseases, including DR, which is in agreement with the findings of our study. However, increased fractal dimension in DR was also reported in previous studies. The disorganized morphology of neovascularization may be responsible for this. In this study, among the five selected variables, fractal dimension had the largest absolute value of the coefficient with a P value<0.0001, indicating that the fractal dimension had the greatest impact on the predictive probability. This was parallel with the point that fractal analysis was a potential predictive factor for diagnosing DR (41).

Currently, the preventive measures for retinopathy in T2DM are limited to blood sugar control and a healthy lifestyle. Limited therapeutic measures can slow down the progression of DR but can never cure it completely. In clinical practice, identifying patients with DR early and precisely determining the timing for intervention are worth considering. Meanwhile, the retinal vascular geometry is closely related to tissue metabolism, reflecting retina status directly. This study developed and validated a prediction nomogram model based on retinal vascular indicators for retinopathy in T2DM and assessed its

clinical usefulness. In our study, the DCA curve suggested that the observed net clinical benefit of the nomogram was much higher than that of reference lines in a wide range of threshold probability. Considering the cutoff value (18.9%) as the threshold probability of the DCA curve, no clinical interventions should be taken for patients with probabilities lower than 18.9%. However, if the probability of DR is more than 18.9%, further examination can be arranged and a close follow-up is required. Based on this perception, this prediction model facilitates risk stratification and clinical decision-making in patients with T2DM.

Conclusion

In conclusion, the five identified independent risk variables for DR in T2DM in our study were fractal dimension, venular caliber, arterial tortuosity, duration of DM, and insulin dosage. Additionally, we developed a personalized nomogram model and a further web page, making it more convenient for clinical application. This predictive nomogram presented a wide range of probability thresholds, indicating good clinical application. This can facilitate early detection and risk stratification of developing DR.

Limitations

This study still had some limitations. First, the enrolled population was relatively small. All of the recruited participants were hospitalized patients mainly distributed in surrounding communities. No biochemical factors were introduced in this nomogram model. Further studies are supposed to be conducted to confirm the contribution of biochemical risk factors in the diagnosis of DR. Therefore, extending the range of participants might make the nomogram model more representative. Also, the duration of DM is an arbitrary variable because most patients were not aware of it when they were initially in such a state. Furthermore, no patient could remember the exact date even the month of diagnosis precisely. Third, the venular diameter was the only variable influenced by magnification in this model. These magnification differences caused by refractive error were unavoidable among individuals, leading to slight differences in the measurement of vascular diameter. Therefore, prospective studies should be implemented further to confirm the diagnostic value of the retinal vascular caliber.

Data availability statement

The raw data supporting the conclusions of this article will be made available by the authors, without undue reservation.

Ethics statement

The studies involving human participants were reviewed and approved by Medical Ethics Committee of the Second Affiliated Hospital of Chongqing Medical University. The patients/participants provided their written informed consent to participate in this study.

Author contributions

Study conception and design: MW and XZ; retinal traits measurement: SL and ZZ; data collection and data analysis: MW and XZ; original manuscript writing: MW; manuscript revising: XZ, DL, and ZZ; web page design and construction: JC. All authors contributed to the article and approved the final manuscript.

Funding

This study was supported by National Natural Science Foundation of China (No.82070976) and Future Medical Youth Innovation Team Development Support Program of Chongqing Medical University.

Acknowledgments

We thank all the patients who allowed their data to be used for this study. We gratefully thank the doctors and nurses of orthopedics and internal medicine at Second Affiliated Hospital of Chongqing Medical University for the help in this study.

Conflict of interest

Author SL is employed by EVision technology Beijing co.LTD, China.

The remaining authors declare that the research was conducted in the absence of any commercial or financial relationships that could be construed as a potential conflict of interest.

Publisher's note

References

1. Unnikrishnan R, Pradeepa R, Joshi SR, Mohan V. Type 2 diabetes: Demystifying the global epidemic. *Diabetes* (2017) 66:1432–42. doi: 10.2337/db16-0766

2. Forouhi NG, Wareham NJ. Epidemiology of diabetes. *Medicine (Abingdon)* (2014) 42(12):698–702. doi: 10.1016/j.mpmed.2014.09.007

3. Teo ZL, Tham YC, Yu M, Chee ML, Rim TH, Cheung N, et al. Global prevalence of diabetic retinopathy and projection of burden through 2045: Systematic review and meta-analysis. *Ophthalmology* (2021) 128:1580–91. doi: 10.1016/j.ophtha.2021.04.027

4. Cheung N, Mitchell P, Wong TY. Diabetic retinopathy. *Lancet* (2010) 376:124–36. doi: 10.1016/S0140-6736(09)62124-3

5. Gariano RF, Gardner TW. Retinal angiogenesis in development and disease. *Nature* (2005) 438:960–6. doi: 10.1038/nature04482

6. Kusuhara S, Fukushima Y, Ogura S, Inoue N, Uemura A. Pathophysiology of diabetic retinopathy: The old and the new. *dmj* (2018) 42:364–76. doi: 10.4093/dmj.2018.0182

7. Atchison E, Barkmeier A. The role of systemic risk factors in diabetic retinopathy. *Curr Ophthalmol Rep* (2016) 4:84–9. doi: 10.1007/s40135-016-0098-8

8. Hirsch IB, Brownlee M. Beyond hemoglobin A1c–need for additional markers of risk for diabetic microvascular complications. *JAMA* (2010) 303:2291–2. doi: 10.1001/jama.2010.785

9. Denninghoff KR, Smith MH, Hillman L. Retinal imaging techniques in diabetes. *Diabetes Technol Ther* (2000) 2:111–3. doi: 10.1089/152091599316810

10. Balachandran VP, Gonen M, Smith JJ, Dematteo RP. Nomograms in oncology: more than meets the eye. *Lancet Oncol* (2015) 16:e173–80. doi: 10.1016/S1470-2045(14)71116-7

11. Martinez-Pagan P, Roschier L. Nomography: A renewed pedagogical tool to sciences and engineering high-education studies. *Heliyon* (2022) 8:e09731. doi: 10.1016/j.heliyon.2022.e09731

12. International Expert, C. International expert committee report on the role of the A1C assay in the diagnosis of diabetes. *Diabetes Care* (2009) 32:1327–34. doi: 10.2337/dc09-9033

13. Told R, Baratsits M, Garhöfer G, Schmetterer L. Early treatment diabetic retinopathy study (ETDRS) visual acuity. *Ophthalmologe* (2013) 110:960–5. doi: 10.1007/s00347-013-2813-2

14. Chen X, Xie Q, Zhang X, Lv Q, Liu X, Rao H. Nomogram prediction model for diabetic retinopathy development in type 2 diabetes mellitus patients: A retrospective cohort study. *J Diabetes Res* (2021) 2021:3825155. doi: 10.1155/2021/3825155

15. Ruta LM, Magliano DJ, Lemesurier R, Taylor HR, Zimmet PZ, Shaw JE, et al. Prevalence of diabetic retinopathy in type 2 diabetes in developing and developed countries. *Diabetes Med* (2013) 30:387–98. doi: 10.1111/dme.12119

16. Kattan MW, Marasco J. What is a real nomogram? *Semin Oncol* (2010) 37:23–6. doi: 10.1053/j.seminoncol.2009.12.003

17. Wang H, Zhang L, Liu Z, Wang X, Geng S, Li J, et al. Predicting medication nonadherence risk in a Chinese inflammatory rheumatic disease population: Development and assessment of a new predictive nomogram. *Patient Prefer Adherence* (2018) 12:1757–65. doi: 10.2147/PPA.S159293

18. Marcovecchio ML. Importance of identifying novel biomarkers of microvascular damage in type 1 diabetes. *Mol Diagn Ther* (2020) 24:507–15. doi: 10.1007/s40291-020-00483-6

19. Wilke T, Picker N, Mueller S, Geier S, Foersch J, Aberle J, et al. Real-world insulin therapy in German type 2 diabetes mellitus patients: patient characteristics, treatment patterns, and insulin dosage. *Diabetes Metab Syndr Obes* (2019) 12:1225–37. doi: 10.2147/DMSO.S214288

20. Lei C, Zhang Y, Zhang M. The association between different hypoglycemic regimens and postoperative diabetic macular edema after vitrectomy in the Japanese patients with proliferative diabetic retinopathy. *Front Endocrinol (Lausanne)* (2022) 13:764254. doi: 10.3389/fendo.2022.764254

21. Jenchitr W, Samaiporn S, Lertmeemongkolchai P, Chongwiriyanurak T Anujaree P, Chayaboon D, et al. Prevalence of diabetic retinopathy in relation to duration of diabetes mellitus in community hospitals of lampang. *J Med Assoc Thai* (2004) 87:1321–6.

22. Wan Nazaimoon WM, Letchuman R, Noraini N, Ropilah AR, Zainal M, Ismail , IS, et al, et al. Systolic hypertension and duration of diabetes mellitus are important determinants of retinopathy and microalbuminuria in young diabetics. *Diabetes Res Clin Pract* (1999) 46:213–21. doi: 10.1016/S0168-8227(99)00095-9

23. Murray CD. The physiological principle of minimum work: I. the vascular system and the cost of blood volume. *Proc Natl Acad Sci USA* (1926) 12:207–14. doi: 10.1073/pnas.12.3.207

24. Curtis TM, Gardiner TA, Stitt AW. Microvascular lesions of diabetic retinopathy: clues towards understanding pathogenesis? *Eye (Lond)* (2009) 23:1496–508. doi: 10.1038/eye.2009.108

25. Jorgensen CM, Hardarson SH, Bek T. The oxygen saturation in retinal vessels from diabetic patients depends on the severity and type of vision-threatening retinopathy. *Acta Ophthalmol* (2014) 92:34–9. doi: 10.1111/aos.12283

26. Stehouwer CDA. Microvascular dysfunction and hyperglycemia: A vicious cycle with widespread consequences. *Diabetes* (2018) 67:1729–41. doi: 10.2337/dbi17-0044

27. Jackson ZS, Dajnowiec D, Gotlieb AI, Langille BL. Partial off-loading of longitudinal tension induces arterial tortuosity. *Arterioscler Thromb Vasc Biol* (2005) 25:957–62. doi: 10.1161/01.ATV.0000161277.46464.11

28. Tsuji-Tamura K, Ogawa M. Morphology regulation in vascular endothelial cells. *Inflammation Regener* (2018) 38:25. doi: 10.1186/s41232-018-0083-8

29. Stefansson E, Olafsdottir OB, Eliasdottir TS, Vehmeijer W, Einarsdottir A. B, Bek T, et al. Retinal oximetry: Metabolic imaging for diseases of the retina and brain. *Prog Retin Eye Res* (2019) 70:1–22. doi: 10.1016/j.preteyeres.2019.04.001

30. Torp TL, Kawasaki R, Wong TY, Peto T, Grauslund J. Temporal changes in retinal vascular parameters associated with successful panretinal photocoagulation in proliferative diabetic retinopathy: A prospective clinical interventional study. *Acta Ophthalmol* (2018) 96:405–10. doi: 10.1111/aos.13617

31. Liew G, Benitez-Aguirre P, Craig ME, Jenkins AJ, Hodgson LAB, Kifley A, et al. Progressive retinal vasodilation in patients with type 1 diabetes: A longitudinal study of retinal vascular geometry. *Invest Ophthalmol Vis Sci* (2017) 58:2503–9. doi: 10.1167/iovs.16-21015

32. Yang X, Deng Y, Gu H, Ren X, Lim A, Snellingen T, et al. Relationship of retinal vascular calibre and diabetic retinopathy in Chinese patients with type 2 diabetes mellitus: The desheng diabetic eye study. *Br J Ophthalmol* (2016) 100:1359–65. doi: 10.1136/bjophthalmol-2014-306078

33. Frydkjaer-Olsen U, Soegaard Hansen R, Simó R, Cunha-Vaz J, Peto T Grauslund J. Correlation between retinal vessel calibre and neurodegeneration in patients with type 2 diabetes mellitus in the European consortium for the early treatment of diabetic retinopathy (EUROCONDOR). *Ophthalmic Res* (2016) 56:10–6. doi: 10.1159/000444396

34. Ho H, Cheung CY, Sabanayagam C, Yip W, Ikram MK, Ong PG, et al. Retinopathy signs improved prediction and reclassification of cardiovascular disease risk in diabetes: A prospective cohort study. *Sci Rep* (2017) 7:41492. doi: 10.1038/srep41492

35. Grunwald JE, Pistilli M, Ying GS, Maguire MG, Daniel E, Whittock-Martin R , et al. Progression of retinopathy and incidence of cardiovascular disease: findings from the chronic renal insufficiency cohort study. *Br J Ophthalmol* (2021) 105:246–52. doi: 10.1136/bjophthalmol-2019-315333

36. Paneni F, Cosentino F, Passerini J, Volpe M. Is there any memory effect of blood pressure lowering in diabetes? *Int J Cardiol* (2011) 151:384–5. doi: 10.1016/j.ijcard.2011.06.114

37. Grunwald JE, Pistilli M, Ying GS, Daniel E, Maguire M, Xie D, et al. Association between progression of retinopathy and concurrent progression of kidney disease: Findings from the chronic renal insufficiency cohort (CRIC) study. *JAMA Ophthalmol* (2019) 137:767–74. doi: 10.1001/jamaophthalmol.2019.1052

38. Grauslund J, Green A, Kawasaki R, Hodgson L, Sjølie AK, Wong TY. Retinal vascular fractals and microvascular and macrovascular complications in type 1 diabetes. *Ophthalmology* (2010) 117:1400–5. doi: 10.1016/j.ophtha.2009.10.047

39. Leontidis G, Al-Diri B, Wigdahl J, Hunter A. Evaluation of geometric features as biomarkers of diabetic retinopathy for characterizing the retinal vascular changes during the progression of diabetes. *Annu Int Conf IEEE Eng Med Biol Soc* (2015) 2015:5255–9. doi: 10.1109/EMBC.2015.7319577

40. Popovic N, Radunovic M, Badnjar J, Popovic T. Fractal dimension and lacunarity analysis of retinal microvascular morphology in hypertension and diabetes. *Microvasc Res* (2018) 118:36–43. doi: 10.1016/j.mvr.2018.02.006

41. Colomer A, Naranjo V, Janvier T, Mossi JM. Evaluation of fractal dimension effectiveness for damage detection in retinal background. *J Comput Appl Mathematics* (2018) 337:341–53. doi: 10.1016/j.cam.2018.01.005

frontiers | Frontiers in Endocrinology

TYPE Original Research
PUBLISHED 05 January 2023
DOI 10.3389/fendo.2022.1099302

OPEN ACCESS

EDITED BY
Mohd Imtiaz Nawaz,
Department of Ophthalmology, King Saud University, Saudi Arabia

REVIEWED BY
Yan Wang,
University of Pittsburgh, United States
Ruiheng Zhang,
Beijing Tongren Hospital, Capital Medical University, China

*CORRESPONDENCE
Qin Zhang
zhangqin@medmail.com.cn
Xiaomei Xu
xiaomeixu@stu.cqmu.edu.cn

†These authors have contributed equally to this work and share first authorship

SPECIALTY SECTION
This article was submitted to Clinical Diabetes, a section of the journal Frontiers in Endocrinology

RECEIVED 15 November 2022
ACCEPTED 19 December 2022
PUBLISHED 05 January 2023

CITATION
Yang Y, Tan J, He Y, Huang H, Wang T, Gong J, Liu Y, Zhang Q and Xu X (2023) Predictive model for diabetic retinopathy under limited medical resources: A multicenter diagnostic study. *Front. Endocrinol.* 13:1099302. doi: 10.3389/fendo.2022.1099302

Predictive model for diabetic retinopathy under limited medical resources: A multicenter diagnostic study

Yanzhi Yang[1†], Juntao Tan[2†], Yuxin He[3], Huanhuan Huang[4], Tingting Wang[5], Jun Gong[6], Yunyu Liu[7], Qin Zhang[1*] and Xiaomei Xu[8,9*]

[1]Department of Endocrinology and Metabolism, Chengdu First People's Hospital, Chengdu, China, [2]Operation Management Office, Affiliated Banan Hospital of Chongqing Medical University, Chongqing, China, [3]Department of Medical Administration, Affiliated Banan Hospital of Chongqing Medical University, Chongqing, China, [4]Department of Nursing, the First Affiliated Hospital of Chongqing Medical University, Chongqing, China, [5]College of Medical Informatics, Chongqing Medical University, Chongqing, China, [6]Department of Information Center, The University Town Hospital of Chongqing Medical University, Chongqing, China, [7]Medical Records Department, the Second Affiliated Hospital of Chongqing Medical University, Chongqing, China, [8]Department of Infectious Diseases, The First Affiliated Hospital of Chongqing Medical University, Chongqing, China, [9]Department of Gastroenterology, Chengdu Fifth People's hospital, Chengdu, China

Background: Comprehensive eye examinations for diabetic retinopathy is poorly implemented in medically underserved areas. There is a critical need for a widely available and economical tool to aid patient selection for priority retinal screening. We investigated the possibility of a predictive model for retinopathy identification using simple parameters.

Methods: Clinical data were retrospectively collected from 4, 159 patients with diabetes admitted to five tertiary hospitals. Independent predictors were identified by univariate analysis and least absolute shrinkage and selection operator (LASSO) regression, and a nomogram was developed based on a multivariate logistic regression model. The validity and clinical practicality of this nomogram were assessed using concordance index (C-index), area under the receiver operating characteristic curve (AUROC), calibration curves, decision curve analysis (DCA), and clinical impact curves (CIC).

Results: The predictive factors in the multivariate model included the duration of diabetes, history of hypertension, and cardiovascular disease. The three-variable model displayed medium prediction ability with an AUROC of 0.722 (95%CI 0.696-0.748) in the training set, 0.715 (95%CI 0.670-0.754) in the internal set, and 0.703 (95%CI 0.552-0.853) in the external dataset. DCA showed that the threshold probability of DR in diabetic patients was 17-55% according to the nomogram, and CIC also showed that the nomogram could be applied clinically if the risk threshold exceeded 30%. An operation interface on a webpage (https://cqmuxss.shinyapps.io/dr_tjj/) was built to improve the clinical utility of the nomogram.

10.3389/fendo.2022.1099302

Conclusions: The predictive model developed based on a minimal amount of clinical data available to diabetic patients with restricted medical resources could help primary healthcare practitioners promptly identify potential retinopathy.

KEYWORDS

diabetes mellitus, diabetic retinopathy, predictive model, medically underserved settings, webpage

1 Introduction

In China, the number of people with diabetes mellitus (DM) has increased significantly over the last four decades. The prevalence of DM has increased more than 15-fold, from 0.67% (1) in 1980 to 11.2% (2)in recent population studies. Diabetic retinopathy (DR) is a common chronic complication of DM and a leading cause of irreversible visual impairment in working-age adults (3).

The fact that patients with DR (including diabetic macular edema) may be asymptomatic in the early stages provides strong evidence for conventional retinal screening. The guidelines recommend that patients with type 1 or type 2 diabetes should undergo an initial comprehensive eye examination within 5 years after the onset of diabetes or at the time of diagnosis, respectively (4, 5). However, the capacity for early DR testing is insufficient, and there are few national programs for DR screening in China (6),especially given the high incidence of DM. The causes are numerous and include a lack of effective screening tools, scarcity of eye care professionals, and a multidisciplinary strategy from picture capture to DR diagnosis. In addition, regional economic imbalances and disparities in lifestyle make it challenging to replicate the DR management approaches in China. This is particularly problematic in restricted medical resource settings, where the annual screening rates for DR are significantly lower than the national average (7, 8).

Several molecular and biochemical pathways are involved in the incidence and development of DR, but the interactions between various mechanisms remain to be fully elucidated (9). Clinical studies have identified a number of risk factors for DR, including demographic characteristics such as age (10–12), duration of diabetes (10, 11, 13–17), obesity (10), and pregnancy status in diabetic women of childbearing age (18), comorbidities or complications such as hypertension (10, 12, 16), dyslipidemia (10, 12, 13), cardiovascular disease(CVD) (11, 12) and diabetic nephropathy (10, 12, 17, 19), and other laboratory parameters such as glycated hemoglobin (10, 11, 13, 15–17, 19), glycemic variability (20, 21), and susceptibility genes (22). However, the aforementioned risk factors derived from population-based studies can only account for 9% of DR progression (23). Laboratory biomarkers are difficult to obtain in healthcare resource-limited settings, and the rate of self-monitoring of blood glucose (SMBG) adherence in Chinese diabetic individuals has not reached an optimal level (24).

Considerable research effort has recently focused on developing predictive models for DR using machine learning algorithms (10, 12, 13, 16, 19, 21), but these models cannot be applied well in low-medical-resource settings. Nearly 510 million Chinese people (36.1% of the total population) live in rural areas (25), and 72.5% of patients do not comply with structured SMBG (24), not to mention consecutive follow-up records or regular laboratory tests. Medical providers in this primary health care (PHC) setting require a simple screening tool for quickly identifying patients at high risk of DR in a single visit and appropriately referring them to retinal specialist ophthalmologists.

This study aimed to provide a direct diagnostic paradigm for PHC clinicians and to develop an online application based on the nomogram so that patients at risk of DR without access to routine eye examinations could be prioritized for retinal screening.

2 Methods

2.1 Data source

Clinical data were obtained from five tertiary hospitals in southwest China, including five in Chongqing (hospitals A-D) and one in Chengdu (hospital E). In this multicenter retrospective study, 4,159 of 32,168 diabetic patients with clinical consultation records met the quality standards for the final analysis. These patients were randomly divided into a training set with 2,610 samples and an internal validation set with 1,119 samples from hospitals A-D. A total of 430 samples from hospital E were used for external validation. The study adhered to the principles of the Declaration of Helsinki and the Transparent Reporting of a Multivariable Prediction Model for Individual Prognosis or Diagnosis Guidelines (26). Clinical research ethics approval was obtained from the Ethics

Committee of the Affiliated Banan Hospital of Chongqing Medical University. Individual patient-level consent was not required because the study only used fully de-identified collected data.

2.2 Diagnostic criteria

DM was diagnosed according to the 1999 World Health Organization criteria, consistent with the standards of medical care for type 2 diabetes in China (2019) (5). According to these guidelines (4, 5), the diagnosis of DR was determined based on fundus photography, examination using dilated funduscopy on ophthalmologist consultation, or prior medical records. Clinical diagnosis (CVD, hypertension, DR) and symptoms in our database are recorded using the ICD-10 code system. ICD-10 codes related to our study are given in Table S1.

2.3 Inclusion and exclusion criteria

The inclusion criteria for this study were diabetes patients admitted between July 2010 and June 2022 with laboratory parameters and ocular variables. Exclusion criteria were as follows: (i) age <18 years, (ii) data on diabetes duration and body matrix index (BMI) not available, and (iii) variables with >30% missing values. The detailed selection process is shown in Supplementary Figure S1.

2.4 Data collection

On the basis of previous studies, 42 variables routinely tested or recorded were collected, which included age, duration of diabetes, body mass index (BMI), systolic blood pressure (SBP), diastolic blood pressure (DBP), gender, smoking and alcohol consumption status, previous diagnosis of hypertension, cardiovascular disease (CVD) and stroke, antihypertensive drug therapy, lipid-lowering treatment (statins, fenofibrate), antiplatelet therapy, antidiabetic drugs [insulin, thiazolidinediones (TZD), alpha-glucosidase inhibitors (AGI), sulfonylurea (SU), dipeptidyl peptidase-4 inhibitor (DPP-4i), GLP-1 receptor agonists (GLP-1RAs), metformin (Met), sodium-glucose cotransporter-2 inhibitors (SGLT2-i)], glycated hemoglobin (HbA_1c), fasting blood glucose (FBG), estimated glomerular filtration rate (eGFR), serum levels of creatinine (SCR), uric acid (SUA), albumin (ALB), total bilirubin (TBIL), alkaline phosphatase (AKP), aspartate aminotransferase (AST), alanine aminotransferase (ALT), total cholesterol (TC), triglycerides (TG), low-density lipoprotein cholesterol (LDL-C), neutrophil percentage (NP), neutrophil-to-lymphocyte ratio (NLR), platelet-to-lymphocyte ratio (PLR), lymphocyte to monocyte ratio (LMR), Systemic immune-inflammation index (SII; platelet count × neutrophil-to-lymphocyte ratio), and neutrophil percentage-to-albumin ratio (NPAR). eGFR was calculated using equations from the Modification of Diet in Renal Disease (MDRD), according to current recommendations (5). NLR, PLR, LMR, SII, and NPAR have been used to evaluate systemic inflammation, and these novel markers were recently found to be related to DR based on results from the National Health and Nutrition Examination Survey (NHANES) (27–29).

2.5 Statistical analysis

Statistical analysis was performed using SPSS 22.0 and R software (version 4.0.2, Vienna, Austria). Normally distributed variables were expressed as the mean ± standard deviation and compared by t-test between two groups. The median (interquartile range, [IQR]) was used to express variables without normal distributions, and the Mann-Whitney U test was used to compare them. Qualitative data were reported as percentages and compared using the χ^2 test. Independent risk factors were selected using least absolute shrinkage and selection operator (LASSO) regression and multivariate logistic regression (30). A nomogram for identifying DR occurrence was constructed using covariates selected by multivariate regression, and discriminatory ability was assessed by measuring the area under the receiver operating characteristic curve (AUROC) (31). Calibration curves were used to evaluate calibration of the nomogram (32). Decision curve analysis and clinical impact curves were used to assess the clinical applicability of the nomogram (33). Multiple interpolation was used to fill in missing values that did not exceed 30% for continuous variables. All statistical analyses were two-sided, and statistical significance was set at $P < 0.05$.

3 Results

3.1 Patient characteristics

Table 1 summarizes the clinical characteristics of patients in the training and internal validation sets. The two groups did not show significant differences in age, sex, history of smoking or alcohol consumption, hypertension, CVD, stroke, antihypertensive drugs, lipid-lowering treatment (statins, fenofibrate), antiplatelet therapy, antidiabetic drugs (insulin, TZD, AGI, SU, DPP-4i, GLP-1 Ras, Met, SGLT2-i), duration, BMI, SBP, DBP, or most laboratory parameters ($P > 0.05$).

3.2 Selection of predictors for DR in the training set

Patients in the training set were divided into DR and non-DR groups. Univariate analysis revealed that the following

10.3389/fendo.2022.1099302

TABLE 1 Demographic and clinical characteristics of the training and internal validation sets.

Variables	Training set (n = 2610)	Internal validation set (n = 1119)	P value
Age (IQR, years)	63.00 (54.00,70.00)	64.00 (54.00,71.50)	0.563
Sex			0.923
Female	1317 (50.46)	562 (50.22)	
Male	1293 (49.54)	557 (49.78)	
Smoking (yes, n, %)	819 (31.38)	346 (30.92)	0.811
Alcohol (yes, n, %)	706 (27.05)	287 (25.65)	0.397
DR (yes, n, %)	455 (17.43)	169 (15.10)	0.087
Hypertension (yes, n,%)	1005 (38.51)	396 (35.39)	0.078
CVD (yes, n, %)	363 (13.91)	141 (12.60)	0.309
Stroke (yes, n, %)	176 (6.74)	64 (5.72)	0.274
Antihypertensive drug (yes, n, %)	1260 (48.28)	519 (46.38)	0.305
Statins (yes, n, %)	1345 (51.53)	592 (52.90)	0.464
Fenofibrate (yes, n, %)	190 (7.28)	75 (6.70)	0.576
Antiplatelet drug (yes, n, %)	1493 (57.20)	622 (55.59)	0.380
Antidiabetic drug			
Insulin (yes, n, %)	2003 (76.74)	864 (77.21)	0.788
TZD (yes, n, %)	117 (4.48)	52 (4.65)	0.893
AGI (yes, n, %)	872 (33.41)	341 (30.47)	0.086
SU (yes, n, %)	985 (37.74)	423 (37.80)	1.000
DPP-4i (yes, n, %)	57 (2.18)	31 (2.77)	0.335
GLP-1RAs (yes, n, %)	74 (2.84)	31 (2.77)	0.999
Met (yes, n, %)	952 (36.48)	425 (37.98)	0.403
SGLT2-i (yes, n, %)	115 (4.41)	60 (5.36)	0.238
Duration (IQR, years)	9.00 (4.00,14.00)	8.00 (4.00,13.00)	0.128
BMI (IQR, kg/m^2)	24.20 (22.00,26.70)	24.20 (21.70,26.70)	0.495
SBP (IQR, mmHg)	136.00 (124.00,150.00)	136.00 (123.50,149.00)	0.953
DBP (IQR, mmHg)	79.00 (71.00,87.00)	79.00 (70.00,86.00)	0.408
NP (IQR)	64.50 (57.18,72.30)	64.00 (57.25,71.95)	0.773
NLR (IQR)	2.39 (1.70,3.62)	2.31 (1.70,3.49)	0.610
PLR (IQR)	110.89 (83.71,150.00)	110.24 (81.70,150.00)	0.523
LMR (IQR)	4.62 (3.30,6.37)	4.80 (3.42,6.41)	0.224
SII (IQR)	435.30 (288.25,704.11)	430.61 (276.31,687.38)	0.475
NPAR (IQR)	15.60 (13.50,18.20)	15.50 (13.60,18.10)	0.814
TBIL (IQR, umol/l)	10.70 (8.10,14.30)	10.60 (8.00,14.20)	0.622
ALP (IQR, IU/L)	77.00 (63.00,95.53)	78.00 (63.00,95.00)	0.699
AST (IQR, IU/L)	20.00 (16.00,26.00)	19.00 (16.00,24.90)	0.023

(Continued)

TABLE 1 Continued

Variables	Training set (n = 2610)	Internal validation set (n = 1119)	P value
ALT (IQR, IU/L)	19.65 (14.00,29.73)	19.00 (13.40,27.70)	0.008
TC (IQR, mmol/l)	4.58 (3.85,5.34)	4.59 (3.80,5.43)	0.314
TG (IQR, mmol/l)	1.55 (1.06,2.38)	1.57 (1.10,2.29)	0.686
LDL-C (IQR, mmol/L)	2.56 (1.97,3.19)	2.61 (2.01,3.25)	0.217
Cr (IQR, umol/l)	63.40 (51.70,79.20)	64.10 (52.15,81.10)	0.254
URAC (IQR, umol/l)	315.25 (255.78,381.33)	311.10 (257.30,387.30)	0.991
Alb (IQR,g/L)	41.10 (38.10,43.90)	40.90 (37.90,44.05)	0.990
HbA_1c (IQR, %)	8.90 (7.40,11.10)	9.10 (7.40,11.40)	0.258
FBG (IQR, mmol/l)	9.61 (6.81,14.30)	9.50 (6.69,13.98)	0.396
eGFR (IQR, ml/min/1.73m^2)	99.45 (79.74,116.89)	97.87 (77.95,116.20)	0.302

DR, diabetic retinopathy; CVD, cardiovascular disease; TZD, thiazolidinediones; AGI, alpha-glucosidase inhibitors; SU, sulfonylurea; DPP-4i, dipeptidyl peptidase-4 inhibitor; GLP-1RAs, GLP-1 receptor agonists; Met, metformin; SGLT2-i, sodium-glucose cotransporter-2 inhibitors; BMI, body mass index; SBP, systolic blood pressure; DBP, diastolic blood pressure; NP, neutrophil percentage; NLR, neutrophil-to-lymphocyte ratio; PLR, platelet-to-lymphocyte ratio; LMR, lymphocyte to monocyte ratio; SII, systemic immune-inflammation index; NPAR, neutrophil percentage-to-albumin ratio; TBIL, total bilirubin; ALP, alkaline phosphatase; AST, aspartate aminotransferase; ALT, alanine aminotransferase; TC, total cholesterol; TG, triglycerides; LDL-C, low-density lipoprotein cholesterol; Cr, serum levels of creatinine; URAC, uric acid; Alb, albumin; HbA1c, glycated hemoglobin; FBG, fasting blood glucose; eGFR, estimated glomerular filtration rate; IQR, interquartile range.

variables were significantly associated with DR: age, sex, hypertension, CVD, stroke, antihypertensive drugs, statins, antiplatelet drugs, antidiabetic drugs (insulin, TZD, AGI, DPP-4i, GLP-1 RAs, Met), duration, BMI, SBP, SII, TBIL, TC, Cr, LDL-C, Alb, HbA1c, FBG, and eGFR (Table 2).

Indicators with statistical differences in univariate analysis were further by LASSO regression and multivariate logistic regression analysis (Figure 1, Table 3). In LASSO regression, ten-fold crossover method was used to verify the adjusted parameters λ. Figure 1 shows the process of LASSO screening for optimal parameters. In the solution path diagram of λ and variables, as λ keeps increasing, the impact of the shrinkage penalty grows, the compression of the model gets stronger, and the fewer variables are selected. Each line represents the change of coefficients of different variables, and the different number of predictors selected according to λ and the coefficients corresponding to the selected variables are shown in Figure 1A. Figure 1B shows the logarithmic value of λ in the horizontal coordinate, the error value in the vertical coordinate, and the number of predictive variables for different values of λ in the upper part of the figure, and the two dashed lines indicate lambda.min and lambda.1se, respectively. The model chose lambda.1se corresponding to a λ value of 0.03027783 and selected three predictors (hypertension, CVD, duration). The importance of each variable in predicting DR can be assessed using the odds ratios provided by multivariate logistic regression model (Table 3).

3.3 Nomogram construction and performance

To visualize the diagnostic model, we developed a nomogram that provides a convenient and personalized presentation tool for predicting the probability of DR (Figure 2A). Points were assigned for all risk factors, first by drawing a line upward from the corresponding value to the "Points" line to get the points for each factor, then the points for all factors were added to obtain the total points and a vertical line was drawn to the "Total point" row to determine DR occurrence. One patient from our study was shown as an example (presented in red). The distinct area of rectangles represented the difference of the relative proportion of patients in each subgroup (Figure 2B).

In the training set, the area under the AUROC curve was 0.722 (95% CI:0.696-0.748), which showed that the diagnostic model had good discriminatory ability (Figure 3). The calibration curve (bootstraps=1000) suggested that the predicted probability was highly consistent with the actual probability (Figure 4). The AUROC curves of the nomogram were 0.712 (95% CI:0.670-0.754) and 0.703 (95% CI:0.552-0.853) in the internal validation and external validation sets, respectively (Supplementary Figures S2, S3). Table 4 lists the detailed performance metrics of the three datasets.

Based on the original model, we combined other risk factors previously reported in the literature, including SBP, HbA1c, LDL-C, and all three. The performance of these models were

10.3389/fendo.2022.1099302

TABLE 2 Univariate analysis of variables associated with DR.

Variables	Total (N=2610)	DR group (N=455)	Non-DR group (N=2155)	P value
Age	63.00 (54.00,70.00)	65.00 (57.00,71.50)	63.00 (53.00,70.00)	<0.001
Sex				0.031
Female	1317 (50.46)	251 (55.16)	1066 (49.47)	
Male	1293 (49.54)	204 (44.84)	1089 (50.53)	
Smoking (yes, n, %)	819 (31.38)	152 (33.41)	667 (30.95)	0.332
Alcohol (yes, n, %)	706 (27.05)	129 (28.35)	577 (26.77)	0.529
Hypertension (yes, n, %)	1005 (38.51)	286 (62.86)	719 (33.36)	<0.001
CVD (yes, n, %)	363 (13.91)	128 (28.13)	235 (10.90)	<0.001
Stroke (yes, n, %)	176 (6.74)	55 (12.09)	121 (5.61)	<0.001
Antihypertensive drug (yes, n, %)	1260 (48.28)	291 (63.96)	969 (44.97)	<0.001
Statins (yes, n, %)	1345 (51.53)	280 (61.54)	1065 (49.42)	<0.001
Fenofibrate (yes, n, %)	190 (7.28)	30 (6.59)	160 (7.42)	0.602
Antiplatelet drug (yes, n, %)	1493 (57.20)	331 (72.75)	1162 (53.92)	<0.001
Antidiabetic drug				
Insulin (yes, n, %)	2003 (76.74)	377 (82.86)	1626 (75.45)	0.001
TZD (yes, n, %)	117 (4.48)	35 (7.69)	82 (3.81)	<0.001
AGI (yes, n, %)	872 (33.41)	186 (40.88)	686 (31.83)	<0.001
SU (yes, n, %)	985 (37.74)	170 (37.36)	815 (37.82)	0.897
DPP4-i (yes, n, %)	57 (2.18)	19 (4.18)	38 (1.76)	0.003
GLP-1 RAs (yes, n, %)	74 (2.84)	24 (5.27)	50 (2.32)	0.001
Met (yes, n, %)	952 (36.48)	186 (40.88)	766 (35.55)	0.036
SGLT2-i (yes, n, %)	115 (4.41)	22 (4.84)	93 (4.32)	0.715
Duration (IQR, years)	9.00 (4.00,14.00)	12.00 (7.50,20.00)	8.00 (4.00,12.00)	<0.001
BMI (IQR, kg/m^2)	24.20 (22.00,26.70)	24.70 (22.40,27.20)	24.20 (21.80,26.60)	<0.001
SBP (IQR, mmHg)	136.00 (124.00,150.00)	138.00 (126.00,152.00)	135.00 (123.00,148.00)	0.015
DBP (IQR, mmHg)	79.00 (71.00,87.00)	78.00 (71.00,86.00)	79.00 (72.00,87.00)	0.213
NP (IQR)	64.50 (57.18,72.30)	64.30 (56.80,70.60)	64.50 (57.25,72.50)	0.280
NLR (IQR)	2.39 (1.70,3.62)	2.39 (1.71,3.36)	2.40 (1.70,3.68)	0.636
PLR (IQR)	110.89 (83.71,150.00)	107.00 (84.30,143.44)	111.45 (83.50,150.59)	0.191
LMR (IQR)	4.62 (3.30,6.37)	4.43 (3.40,5.97)	4.66 (3.27,6.46)	0.230
SII (IQR)	435.30 (288.25,704.11)	422.38 (278.28,644.7)	440.53 (290.38,724.03)	0.048
NPAR (IQR)	15.60 (13.50,18.20)	15.70 (13.80,18.20)	15.50 (13.50,18.10)	0.234
TBIL (IQR, umol/l)	10.70 (8.10,14.30)	9.60 (7.50,12.50)	10.90 (8.30,14.70)	<0.001
ALP (IQR, IU/L)	77.00 (63.00,95.53)	75.00 (63.00,93.00)	78.00 (63.60,96.15)	0.056
AST (IQR, IU/L)	20.00 (16.00,26.00)	20.00 (16.00,26.00)	20.00 (16.00,26.00)	0.556
ALT (IQR, IU/L)	19.65 (14.00,29.73)	21.00 (14.55,30.00)	19.10 (14.00,29.50)	0.211
TC (IQR, mmol/l)	4.58 (3.85,5.34)	4.29 (3.61,4.97)	4.63 (3.90,5.43)	<0.001

(Continued)

TABLE 2 Continued

Variables	Total (N=2610)	DR group (N=455)	Non-DR group (N=2155)	P value
TG (IQR, mmol/l)	1.55 (1.06,2.38)	1.49 (1.03,2.20)	1.56 (1.07,2.42)	0.087
LDL-C (IQR, mmol/L)	2.56 (1.97,3.19)	2.29 (1.77,2.90)	2.61 (2.00,3.25)	<0.001
Cr (IQR, umol/l)	63.40 (51.70,79.20)	66.20 (52.60,84.25)	63.00 (51.40,78.15)	0.009
URAC (IQR, umol/l)	315.25 (255.78,381.33)	323.80 (264.95,387.65)	313.40 (254.45,379.30)	0.056
Alb (IQR,g/L)	41.10 (38.10,43.90)	40.30 (37.60,43.00)	41.20 (38.30,44.10)	<0.001
HbA_1c (IQR, %)	8.90 (7.40,11.10)	8.50 (7.30,10.50)	9.00 (7.40,11.20)	0.008
FBG (IQR, mmol/l)	9.61 (6.81,14.30)	9.07 (6.62,13.29)	9.77 (6.85,14.48)	0.026
eGFR (IQR, ml/min/1.73m^2)	99.45 (79.74,116.89)	93.92 (75.60,107.16)	100.89 (81.91,118.77)	<0.001

DR, diabetic retinopathy; CVD, cardiovascular disease; TZD, thiazolidinediones; AGI, alpha-glucosidase inhibitors; SU, sulfonylurea; DPP-4i, dipeptidyl peptidase-4 inhibitor; GLP-1RAs, GLP-1 receptor agonists; Met, metformin; SGLT2-i, sodium-glucose cotransporter-2 inhibitors; BMI, body mass index; SBP, systolic blood pressure; DBP, diastolic blood pressure; NP, neutrophil percentage; NLR, neutrophil-to-lymphocyte ratio; PLR, platelet-to-lymphocyte ratio; LMR, lymphocyte to monocyte ratio; SII, systemic immune-inflammation index; NPAR, neutrophil percentage-to-albumin ratio; TBIL, total bilirubin; ALP, alkaline phosphatase; AST, aspartate aminotransferase; ALT, alanine aminotransferase; TC, total cholesterol; TG, triglycerides; LDL-C, low-density lipoprotein cholesterol; Cr, serum levels of creatinine; URAC, uric acid; Alb, albumin; HbA1c, glycated hemoglobin; FBG, fasting blood glucose; eGFR, estimated glomerular filtration rate; IQR, interquartile range.

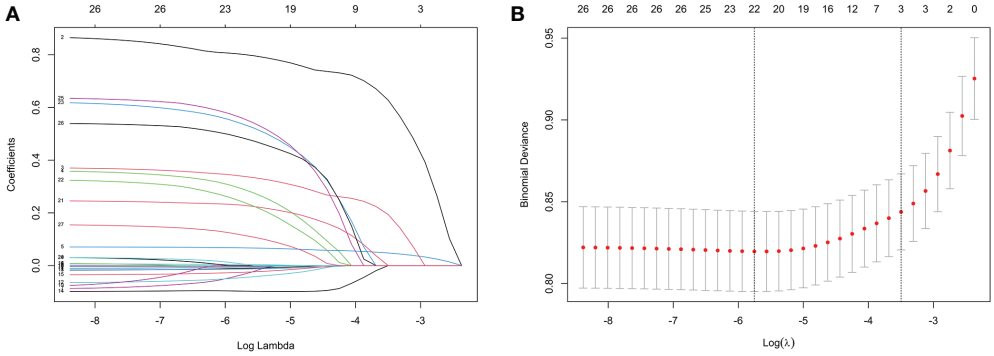

FIGURE 1
Features selection by LASSO. **(A)** LASSO coefficients profiles (y-axis) of the 26 features. The upper x-axis is the average numbers of predictors and the lower x-axis is the log(λ). **(B)** 10-fold cross-validation for tuning parameter selection in the LASSO model.

compared using Delong test (Table 5). Logistic regression trained to detect DR in our model had an AUC of 0.722 (95% CI 0.696-0.748), non-inferior to the original model combined with SBP (AUC 0.723, 95% CI 0.698-0.749), LDL-C (AUC 0.726, 95% CI 0.700-0.752), HbA1c (AUC 0.721, 95% CI 0.695-0.747), and all three variables (AUC 0.726, 95% CI 0.700-0.752) (P=0.605, 0.247, 0.107, 0.286, respectively).

3.4 Clinical utility of the nomogram

The decision curves showed that the threshold probability of DR in diabetic patients was 17-55% according to the nomogram (Figure 5), and that applying this nomogram to identify DR would provide greater benefit than an all-treatment regimen or an all-no-treatment regimen. In addition, further clinical impact curves were created to assess the nomogram's clinical impact and provide a more intuitive understanding of its significance (Figure 6). The clinical impact curves depicted the estimated number of diabetic patients with DR at each risk threshold as well as the actual number of patients presenting with DR. When the risk threshold exceeded 30%, the estimated number of patients was closer to the actual number of patients.

3.5 Construction of web app to easily access the nomogram

Finally, we developed a user-friendly interface on a web link (https://cqmuxss.shinyapps.io/dr_tjj/) to calculate the precise

TABLE 3 Results of multivariate logistic regression model.

Variables	β	SE	OR(95%CI)	P value
Hypertension	0.969	0.116	2.635(2.099,3.308)	<0.001
CVD	0.435	0.141	1.545(1.172,2.037)	0.002
Duration	0.070	0.007	1.073(1.058,1.087)	<0.001

CVD: cardiovascular disease; SE: Standard Error; OR: odds ratio; CI: Confidence Interval.

probability of concomitant DR in patients with diabetes. For the same example in Figure 2B, the likelihood of DR was 0.653 (95% CI:0.579-0.721) when a patient had both hypertension and CAD and the duration of diabetes was 30 years (Figure 2C).

4 Discussion

We found that 21.7% (455/2610) of patients had some degree of DR, and this percentage was in consistent with the report by Song (8), who described an 18.7% prevalence in patients with a similar duration and also from southwest China. Given that the current study comprised a hospitalized-based population with relatively severe conditions, including long-term diabetes (median duration, 9 years) and poor management of blood glucose (median glycosylated hemoglobin, 8.9%) on admission, the high prevalence of DR revealed by our data is not surprising.

Our study demonstrated that an easy-to-use diagnostic model can identify underlying DR with a high NPV (97.7% on an external validation dataset), high specificity (94.1%), and qualified sensitivity (57.1%). When the common predictors (HbA1c, lipids, and SBP) proposed in previous studies were considered, our original model's output remained non-inferior to that of complex equations with a greater number of risk variables.

Previous studies reported that common risk factors for DR included both duration of DM and age at visit (10, 11); however, designing a prompt referral for DR screening should take into account the length of DM as a crucial determinant (4, 13). A longer duration may represent a longer period of hyperglycemia-induced retinal toxicity, which is believed to be associated with both vascular and neural retinal death. Recent studies have shown that there is a significant interaction between the patient's age and the duration of DM, based on sensitivity analysis (11). In contrast, age was observed to be a protective factor for DR due to a state of low retinal perfusion in elderly patients (19). A nationwide population-based cohort study also showed a reduced prevalence of DR in individuals with diabetes

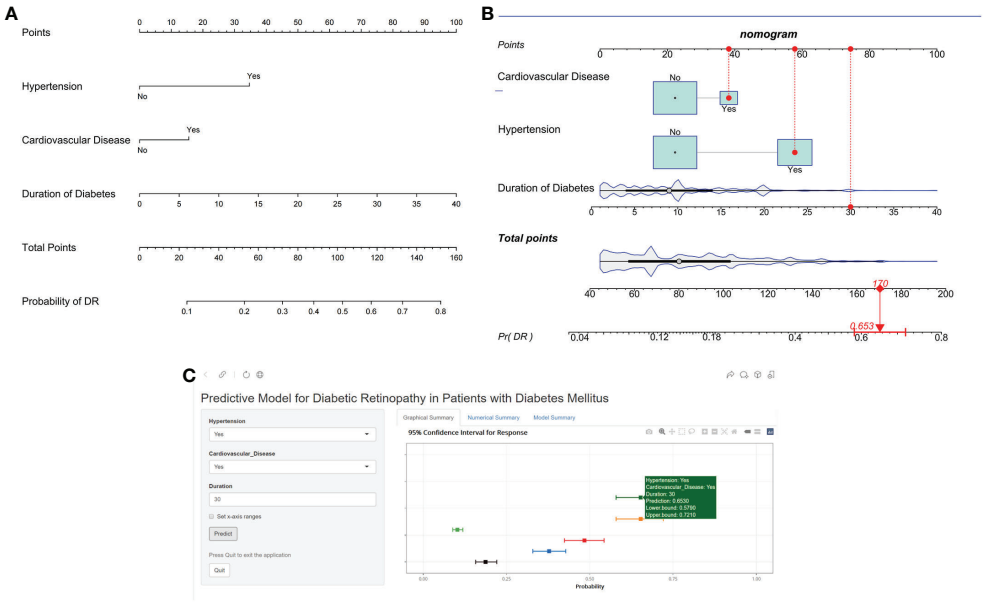

FIGURE 2
Nomogram identifying retinopathy in patients with DM. **(A)** Risk nomogram for identifying retinopathy in patients with DM. **(B)** One patient from our study is shown as an example (presented in red). **(C)** An example of Nomogram to identifying retinopathy in patients with DM Via a Link.

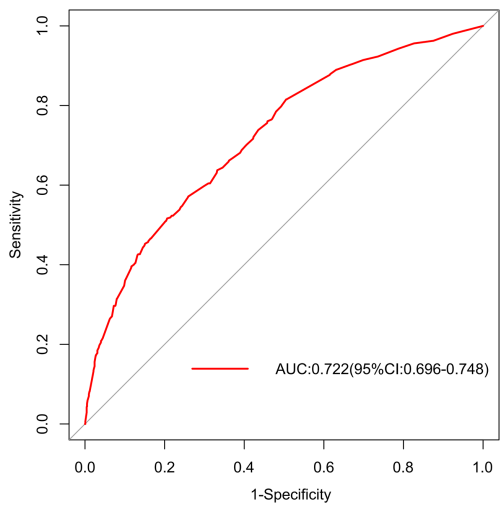

FIGURE 3
AUROC in training set.

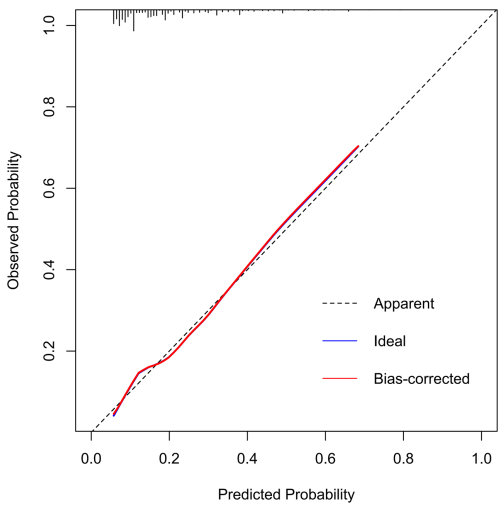

FIGURE 4
Calibration curve of the DR incidence risk nomogram prediction in training set.

of less than 5 years duration, and regular screening had no impact on detection rates among young patients (< 45 years) (34). Patients with a younger age of onset have a longer duration of diabetes, and there is an interaction between the patient's age at visit, age at onset, and duration of diabetes. Consequently, studying the effect of one of these factors on DR requires adjusting for the other two variables. Our findings suggest that age was only subordinate in determining the prevalence of DR, compared to the duration of diabetes, which was a predominant predictor.

Earlier studies revealed that glycated hemoglobin (10, 11, 13, 15–17, 19) or glycemic variability (20, 21) could be predictors for DR, but structured glycemic detection adherence was highly correlated with social support (24). Local experience-based studies from China, India, and Brazil have indicated that the routine use of SMBG was frequently challenging, mainly because of the out-of-pocket expenditures associated with glucose monitoring (35). In comparison to our simple model, mandatory inclusion of hemoglobin A1c did not substantially increase the AUROC. A previous study suggested that glucose variability was linked to the development and progression of DR (20), but no significant relationships were found after adjusting for hemoglobin A1c (36), making this association less relevant. Glycemic records from continuous glucose monitoring systems were not collected in our study, as this novel technology is not available in most cases with limited medical resources.

The relationship between elevated blood lipid profiles and DR development of DR was complex. Previous studies on the correlation between conventional serum lipid levels (TG, TC, HDL-C, and LDL-C) and DR have shown conflicting results (10, 13, 19, 37). Similarly, the current focus on the role of lipoprotein (a) in the pathogenesis of DR remains controversial (38, 39).A recent study focused on the relationship between

TABLE 4 Detailed performance metrics for the three datasets.

Models	AUC (95%CI)	Sensitivity (95%CI)	Specificity (95%CI)	PPV (95%CI)	NPV (95%CI)
Training set	0.722	0.571	0.741	0.317	0.891
	0.696-0.748	0.526-0.617	0.722-0.79	0.286-0.349	0.877-0.906
Internal validation set	0.712	0.509	0.806	0.319	0.902
	0.670-0.754	0.434-0.584	0.781-0.831	0.263-0.374	0.882-0.922
External validation set	0.703	0.571	0.941	0.333	0.977
	0.553-0.853	0.360-0.783	0.919-0.964	0.179-0.487	0.962-0.992

AUC, area under the curve; PPV, positive predictive value; NPV, negative predictive value; CI, Confidence Interval.

TABLE 5 Model performance statistics in training dataset.

Models	AUC (95%CI)	Sensitivity (95%CI)	Specificity (95%CI)	PPV (95%CI)	NPV (95%CI)	P value
Model	0.722	0.571	0.741	0.317	0.891	/
	0.696-0.748	0.526-0.617	0.722-0.790	0.286-0.349	0.877-0.906	
Model+SBP	0.723	0.670	0.643	0.284	0.902	0.605
	0.698-0.749	0.627-0.714	0.622-0.663	0.257-0.311	0.887-0.917	
Model+LDL-C	0.726	0.765	0.557	0.267	0.918	0.247
	0.700-0.752	0.726-0.804	0.536-0.578	0.243-0.291	0.903-0.933	
Model+HbA1c	0.721	0.563	0.752	0.324	0.891	0.107
	0.695-0.747	0.517-0.608	0.734-0.770	0.291-0.356	0.876-0.905	
Model+SBP+HbA1c+LDL-C	0.726	0.776	0.550	0.267	0.921	0.286
	0.700-0.752	0.738-0.814	0.529-0.571	0.243-0.291	0.906-0.936	

SBP, systolic blood pressure; LDL-C, low-density lipoprotein cholesterol; HbA1c, glycated hemoglobin; AUC, area under the curve; PPV, positive predictive value; NPV, negative predictive value; CI, Confidence Interval.
Symbol "/" means that "Model" is used as the reference object for AUC comparison.

apolipoproteins and DR (40); however, these novel laboratory parameters have not yet been widely used in clinical practice. Our data support previous evidence that customary serum lipid levels were not strongly or consistently related to DR. Traditional lipid measures are unstable laboratory markers, and their serum levels are significantly altered by diets and lipid-lowering agents, which might be a possible explanation for this finding.

Increased blood pressure can lead to additional damage to the retinal vessels by hyperperfusion, shearing forces, and increased edema formation. Hypertension, mainly SBP, was previously identified as the most common modifiable risk factor for DR (4, 16); however, these variables did not present a steady correlation in other studies (13, 19). The association between poorly controlled hypertension and DR has not recently been observed in the Chinese population compared to this relationship in Malays and Indians (41). SBP was found to be a risk factor for DR in univariate analysis but was not included in the LASSO model in our study. A cross tabulation was created to assess whether antihypertensive drugs affected DR onset, with the chi-square test result revealing the independent of the two variables (P = 0.361, Supplementary Table S2), even though SBP was slightly lower in the medicated group than in the non-medicated group (141mmHg and 146mmHg, respectively, P = 0.026). Extensive background treatment with antihypertensive drugs in diabetic patients (86.4%, 868/1005, Supplementary Table S2) may remarkably alter blood pressure values within a single visit. On the other hand, SBP was 132mmHg, 135mmHg, 138mmHg in the short-duration (< 5 years), medium-duration (5-10 years), and long-duration (≥10 years) group, respectively

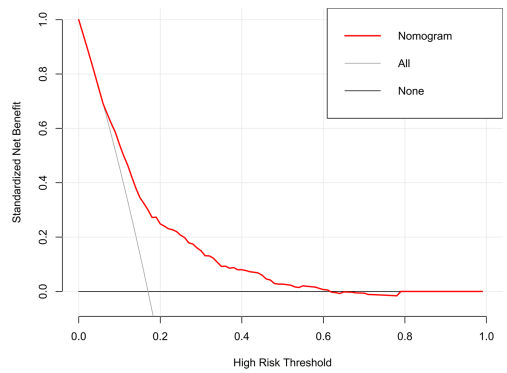

FIGURE 5
Decision curve analysis of the nomogram.

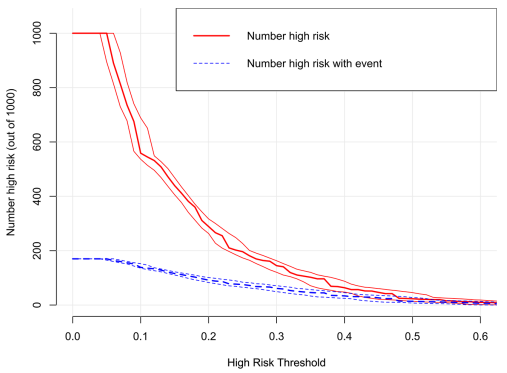

FIGURE 6
Clinical impact curve of the nomogram.

(F=19.387, P < 0.001, Supplementary Table S3). Therefore, the length of diabetes might be a potential confounding variable in the SBP-DR correlation observed in univariate analysis, and comorbid hypertension was identified as a predictor of high importance.

Several studies have shown a correlation between DR and CVD, but most have concluded that DR is a predictor of CVD (42, 43). Multivariate logistic regression results based on the type 1 diabetes population revealed that patients with DR were more likely to develop CVD (42). Similarly, diabetic retinal vascular disease was recently found to predict CVD morbidity and mortality in patients with type 2 diabetes (43). In addition, according to univariate analysis, diabetic patients with a history of CVD had a 60% greater chance of developing sight-threatening DR than those without a history of CVD (11). Our study results are in accordance with those of previous reports. Although further research remains to be conducted to properly comprehend the relationship between DR and CVD, our findings confirmed the continuum of diabetic vascular disease, showing that microangiopathy and macroangiopathy appeared to be interrelated rather than distinct conditions. Another important implication is that comorbid CVD may prompt PHC to identify a subset of patients with diabetes for priority eye examinations.

Some antidiabetic drugs are thought to be associated with an increased risk of DR. TZD can cause fluid retention and peripheral edema in patients with diabetes (5), and systematic fluid retention may emerge as diabetic macular edema. However, the ACCORD Eye Study group reported no consistent evidence of DR progression in patients receiving TZD, suggesting that this correlation requires further study (44). For GLP-1 RAs, worsening of retinopathy has been considered a new potential side effect of this treatment. An unexpected increase in retinopathy was found in SUSTAIN-6, and a nonsignificantly higher rate of DR was found in LEADER and REWIND (45). However, poor outcomes, such as blindness or the need for numerous procedures, which damage a person's quality of life and raise expenditures, were not adequately described, and definitions of ocular events varied widely among these studies. The first answer to these issues may come from a trial that is currently underway (FOCUS trial; NCT03811561), which will examine the long-term impact of semaglutide on diabetic eye complications (up to 5 years). Data from our study showed that TZD and DPP-4i were risk factors, whereas GLP-1 RAs were protective factors in the univariate analysis. However, all of them failed to enter the LASSO regression, not ruling out a false-positive result due to the low usage rate of these three drugs (4.48%, 2.18%, and 2.84%, respectively). AGI or Met alone cannot usually manage blood glucose in diabetic patients with a median length of 9 years, and positive results in univariate analysis could include the effect of other drugs. The use of insulin tended to be highly correlated with duration, which may explain why the risk effect was not found in the LASSO regression.

In 2020, the annual per capita disposable income of rural households in China was approximately 17,132 yuan, which is approximately one-third of the income of urban households (25). Previous findings revealed that only 10% of DR patients in rural China were properly diagnosed and treated, nearly 70% of DM subjects had never received an eye exam (46), and over 70% of participants considered financial cost as the leading barrier to routine retinal screening (47). Significant variations in the development and severity of DR have been found in clinical studies of patients with DM, but the variations have not been fully elucidated by known risk factors (23). Thus, it is important to minimize the number of variables in diagnostic tools as much as possible in medically underserved settings. The population with limited access to ophthalmologic care may benefit from our diagnostic model, which was developed based on restricted medical resources and would not incur additional expenditures. The easy-to-use web calculator will help PHC practitioners quickly identify at-risk individuals for DR and make prompt referrals.

The strengths of the current study include the use of a large sample from multicenter electronic medical records of diabetic individuals with or without DR. However, our study was subject to some limitations. First, our study had a cross-sectional design. Compared to cohort studies, cross-sectional studies provide weaker evidence, and the interpretation of these findings should be considered with caution. Second, the current dataset had an incomplete recording of UACR with 58.74% missing values and HbA1c with 14.6% missing values. We could not account for the effect of albuminuria on DR, even though multiple imputations were used to address missing HbA1c values. Therefore, further studies with complete data for all pertinent covariates would be useful. In addition, the efficacy of our model for indetifying referral DR needs to be validated in community patients, but this requires complete medical records both in the community and the hospital. Finally, it is not clear whether our findings based on patients with type 2 diabetes (2584/2610) are applicable to patients with type 1 diabetes, while few data on type 1 diabetes suggest that the retinal risk factors were generally similar (16).

5 Conclusions

Our study suggests that a simple predictive model could provide added value as an automated screening tool to triage patients for priority retinal examination. Obtaining information on the duration of diabetes, history of hypertension, and CVD requires no additional medical costs and is convenient. Further validation studies on the proposed model are required. Moreover, this model cannot replace standard DR screening but could be more reasonable as a timely warning tool, and a more effective option is to promote a nationwide DR examination program for all diabetic patients.

Data availability statement

The raw data supporting the conclusions of this article will be made available by the authors, without undue reservation.

Ethics statement

The Ethics Committee of the Affiliated Banan Hospital of Chongqing Medical University approved the study. Written informed consent for participation was not required for this study due to its retrospective design, and the study was undertaken in accordance with national legislation and institutional requirements.

Author contributions

YY and JT designed the research. YY, JT, HH, JG, and YL collected and organized data. YY, JT, YH, and TW analyzed the data. YY and JT drafted the manuscript. QZ and XX contributed to the critical revision of the manuscript. All authors contributed to the manuscript and approved the submitted version.

Funding

This study was funded by Project of Banan District Science and Technology Bureau of Chongqing Municipality.

Acknowledgments

We would like to thank all the participants of this project and investigators for collecting the data. We would like to thank Editage (www.editage.com) for English language editing.

Conflict of interest

The authors declare that the research was conducted in the absence of any commercial or financial relationships that could be construed as a potential conflict of interest.

Publisher's note

All claims expressed in this article are solely those of the authors and do not necessarily represent those of their affiliated organizations, or those of the publisher, the editors and the reviewers. Any product that may be evaluated in this article, or claim that may be made by its manufacturer, is not guaranteed or endorsed by the publisher.

Supplementary material

The Supplementary Material for this article can be found online at: https://www.frontiersin.org/articles/10.3389/fendo.2022.1099302/full#supplementary-material

References

1. Zhong XL. Diabetes mellitus survey in China. *Chin Med J* (1982) 95(6):423–30.

2. Li Y, Teng D, Shi X, Qin G, Qin Y, Quan H, et al. Prevalence of diabetes recorded in mainland China using 2018 diagnostic criteria from the American diabetes association: national cross sectional study. *BMJ (Clinical Res ed)* (2020) 369:m997. doi: 10.1136/bmj.m997

3. Yang QH, Zhang Y, Zhang XM, Li XR. Prevalence of diabetic retinopathy, proliferative diabetic retinopathy and non-proliferative diabetic retinopathy in Asian T2DM patients: a systematic review and meta-analysis. *Int J ophthalmology.* (2019) 12(2):302–11. doi: 10.18240/ijo.2019.02.19

4. Committee ADAPP. 12. Retinopathy, neuropathy, and foot care: Standards of medical care in diabetes–2022. *Diabetes Care* (2021) 45(Supplement_1):S185–S94. doi: 10.2337/dc22-S012

5. Jia W, Weng J, Zhu D, Ji L, Lu J, Zhou Z, et al. Standards of medical care for type 2 diabetes in China 2019. *Diabetes/metabolism Res Rev* (2019) 35(6):e3158. doi: 10.1002/dmrr.3158

6. Zhang Y, Shi J, Peng Y, Zhao Z, Zheng Q, Wang Z, et al. Artificial intelligence-enabled screening for diabetic retinopathy: a real-world, multicenter and prospective study. *BMJ Open Diabetes Res Care* (2020) 8(1):e001596. doi: 10.1136/bmjdrc-2020-001596

7. Huang XM, Yang BF, Zheng WL, Liu Q, Xiao F, Ouyang PW, et al. Cost-effectiveness of artificial intelligence screening for diabetic retinopathy in rural China. *BMC Health Serv Res* (2022) 22(1):260. doi: 10.1186/s12913-022-07655-6

8. Song P, Yu J, Chan KY, Theodoratou E, Rudan I. Prevalence, risk factors and burden of diabetic retinopathy in China: a systematic review and meta-analysis. *J Global Health* (2018) 8(1):010803. doi: 10.7189/jogh.08.010803

9. Oshitari T. The pathogenesis and therapeutic approaches of diabetic neuropathy in the retina. *Int J Mol Sci* (2021) 22(16):9050. doi: 10.3390/ijms22169050

10. Zhao Y, Li X, Li S, Dong M, Yu H, Zhang M, et al. Using machine learning techniques to develop risk prediction models for the risk of incident diabetic retinopathy among patients with type 2 diabetes mellitus: A cohort study. *Front endocrinology.* (2022) 13:876559. doi: 10.3389/fendo.2022.876559

11. Nugawela MD, Gurudas S, Prevost AT, Mathur R, Robson J, Sathish T, et al. Development and validation of predictive risk models for sight threatening diabetic retinopathy in patients with type 2 diabetes to be applied as triage tools in resource limited settings. *EClinicalMedicine.* (2022) 51:101578. doi: 10.1016/j.eclinm.2022.101578

12. Basu S, Sussman JB, Berkowitz SA, Hayward RA, Yudkin JS. Development and validation of risk equations for complications of type 2 diabetes (RECODe) using individual participant data from randomised trials. *Lancet Diabetes endocrinology.* (2017) 5(10):788–98. doi: 10.1016/S2213-8587(17)30221-8

13. Syriga M, Ioannou Z, Pitsas C, Dagalaki I, Karampelas M. Diabetic retinopathy in Greece: prevalence and risk factors studied in the medical retina clinic of a Greek tertiary hospital. *Int ophthalmology.* (2022) 42(6):1679–87. doi: 10.1007/s10792-021-02162-9

14. García-Fiñana M, Hughes DM, Cheyne CP, Broadbent DM, Wang A, Komárek A, et al. Personalized risk-based screening for diabetic retinopathy: A multivariate approach versus the use of stratification rules. *Diabetes Obes Metab* (2019) 21(3):560–8. doi: 10.1111/dom.13552

15. Kang EY, Lo FS, Wang JP, Yeh LK, Wu AL, Tseng YJ, et al. Nomogram for prediction of non-proliferative diabetic retinopathy in juvenile-onset type 1 diabetes: a cohort study in an Asian population. *Sci Rep* (2018) 8(1):12164. doi: 10.1038/s41598-018-30521-7

16. Schreur V, Ng H, Nijpels G, Stefánsson E, Tack CJ, Klevering BJ, et al. Validation of a model for the prediction of retinopathy in persons with type 1 diabetes. *Br J ophthalmology.* (2021) 105(9):1286–8. doi: 10.1136/bjophthalmol-2018-313539

17. Boonsaen T, Choksakunwong S, Lertwattanarak R. Prevalence of and factors associated with diabetic retinopathy in patients with diabetes mellitus at siriraj hospital - thailand's largest national tertiary referral center. *Diabetes Metab syndrome Obes Targets Ther* (2021) 14:4945–57. doi: 10.2147/DMSO.S346719

18. Widyaputri F, Rogers SL, Kandasamy R, Shub A, Symons RCA, Lim LL. Global estimates of diabetic retinopathy prevalence and progression in pregnant women with preexisting diabetes: A systematic review and meta-analysis. *JAMA ophthalmology.* (2022) 140(5):486–94. doi: 10.1001/jamaophthalmol.2022.0050

19. Li W, Song Y, Chen K, Ying J, Zheng Z, Qiao S, et al. Predictive model and risk analysis for diabetic retinopathy using machine learning: a retrospective cohort study in China. *BMJ Open* (2021) 11(11):e050989. doi: 10.1136/bmjopen-2021-050989

20. Lu J, Ma X, Zhou J, Zhang L, Mo Y, Ying L, et al. Association of time in range, as assessed by continuous glucose monitoring, with diabetic retinopathy in type 2 diabetes. *Diabetes Care* (2018) 41(11):2370–6. doi: 10.2337/dc18-1131

21. Hsing SC, Lin C, Chen JT, Chen YH, Fang WH. Glycemic gap as a useful surrogate marker for glucose variability and progression of diabetic retinopathy. *J personalized Med* (2021) 11(8):799. doi: 10.3390/jpm11080799

22. Jin L, Wang T, Jiang S, Chen M, Zhang R, Hu C, et al. The association of a genetic variant in SCAF8-CNKSR3 with diabetic kidney disease and diabetic retinopathy in a Chinese population. *J Diabetes Res* (2017) 2017:6542689. doi: 10.1155/2017/6542689

23. Antonetti DA, Silva PS, Stitt AW. Current understanding of the molecular and cellular pathology of diabetic retinopathy. *Nat Rev Endocrinology.* (2021) 17 (4):195–206. doi: 10.1038/s41574-020-00451-4

24. Wang X, Luo JF, Qi L, Long Q, Guo J, Wang HH. Adherence to self-monitoring of blood glucose in Chinese patients with type 2 diabetes: current status and influential factors based on electronic questionnaires. *Patient preference adherence.* (2019) 13:1269–82. doi: 10.2147/PPA.S211668

25. National Bureau of Statistics of China. *China Statistical yearbook 2021*. Beijing: China statistical Publishing House (2021).

26. Collins GS, Reitsma JB, Altman DG, Moons KG. Transparent reporting of a multivariable prediction model for individual prognosis or diagnosis (TRIPOD): the TRIPOD statement. *BMC Med* (2015) 13(1):1-10. doi: 10.1186/s12916-014-0241-z

27. Wang H, Guo Z, Xu Y. Association of monocyte-lymphocyte ratio and proliferative diabetic retinopathy in the U.S. population with type 2 diabetes. *J Trans Med* (2022) 20(1):219. 10.1186/s12967-022-03425-4

28. He X, Qi S, Zhang X, Pan J. The relationship between the neutrophil-to-lymphocyte ratio and diabetic retinopathy in adults from the united states: results from the national health and nutrition examination survey. *BMC ophthalmology.* (2022) 22(1):346. doi: 10.1186/s12886-022-02571-z

29. He X, Dai F, Zhang X, Pan J. The neutrophil percentage-to-albumin ratio is related to the occurrence of diabetic retinopathy. *J Clin Lab analysis.* (2022) 36(4): e24334. doi: 10.1002/jcla.24334

30. Robert T. Regression shrinkage and selection via the lasso. *J R Stat Soc Ser B (Methodological)* (1996) 58(1):267-288. doi: 10.1111/j.2517-6161.1996.tb02080.x

31. Hanley JA, McNeil BJ. A method of comparing the areas under receiver operating characteristic curves derived from the same cases. *Radiology.* (1983) 148 (3):839–943. doi: 10.1148/radiology.148.3.6878708

32. Austin PC, Harrell FE, Klaveren Dv. Graphical calibration curves and the integrated calibration index (ICI) for survival models. *Stat Med* (2020) 39 (21):2714–42. doi: 10.1002/sim.8570

33. Fitzgerald M, Saville BR, Lewis RJ. Decision curve analysis. *JAMA.* (2015) 313(4):409–10. doi: 10.1001/jama.2015.37

34. Chung YC, Xu T, Tung TH, Chen M, Chen PE. Early screening for diabetic retinopathy in newly diagnosed type 2 diabetes and its effectiveness in terms of morbidity and clinical treatment: A nationwide population-based cohort. *Front Public Health* (2022) 10:771862. doi: 10.3389/fpubh.2022.771862

35. Pleus S, Freckmann G, Schauer S, Heinemann L, Ziegler R, Ji L, et al. Self-monitoring of blood glucose as an integral part in the management of people with type 2 diabetes mellitus. *Diabetes Ther research Treat Educ Diabetes related Disord* (2022) 13(5):829–46. doi: 10.1007/s13300-022-01254-8

36. Wakasugi S, Mita T, Katakami N, Okada Y, Yoshii H, Osonoi T, et al. Associations between continuous glucose monitoring-derived metrics and diabetic retinopathy and albuminuria in patients with type 2 diabetes. *BMJ Open Diabetes Res Care* (2021) 9(1):e001923. doi: 10.1136/bmjdrc-2020-001923

37. Sasongko MB, Wong TY, Nguyen TT, Kawasaki R, Jenkins A, Shaw J, et al. Serum apolipoprotein AI and b are stronger biomarkers of diabetic retinopathy than traditional lipids. *Diabetes Care* (2011) 34(2):474–9. doi: 10.2337/dc10-0793

38. Singh SS, Rashid M, Lieverse AG, Kronenberg F, Lamina C, Mulder MT, et al. Lipoprotein(a) plasma levels are not associated with incident microvascular complications in type 2 diabetes mellitus. *Diabetologia.* (2020) 63(6):1248–57. doi: 10.1007/s00125-020-05120-9

39. Yun JS, Lim TS, Cha SA, Ahn YB, Song KH, Choi JA, et al. Lipoprotein(a) predicts the development of diabetic retinopathy in people with type 2 diabetes mellitus. *J Clin lipidology.* (2016) 10(2):426–33. doi: 10.1016/j.jacl.2015.12.030

40. Zhang X, Nie Y, Gong Z, Zhu M, Qiu B, Wang Q. Plasma apolipoproteins predicting the occurrence and severity of diabetic retinopathy in patients with type 2 diabetes mellitus. *Front endocrinology.* (2022) 13:915575. doi: 10.3389/fendo.2022.915575

41. Liu L, Quang ND, Banu R, Kumar H, Tham YC, Cheng CY, et al. Hypertension, blood pressure control and diabetic retinopathy in a large population-based study. *PLoS One* (2020) 15(3):e0229665. doi: 10.1371/journal.pone.0229665

42. Melo LGN, Morales PH, Drummond KRG, Santos DC, Pizarro MH, Barros BSV, et al. Diabetic retinopathy may indicate an increased risk of cardiovascular disease in patients with type 1 diabetes-a nested case-control study in Brazil. *Front endocrinology.* (2019) 10:689. doi: 10.3389/fendo.2019.00689

43. Barrot J, Real J, Vlacho B, Romero-Aroca P, Simó R, Mauricio D, et al. Diabetic retinopathy as a predictor of cardiovascular morbidity and mortality in subjects with type 2 diabetes. *Front Med* (2022) 9:945245. doi: 10.3389/fmed.2022.945245

44. Gower EW, Lovato JF, Ambrosius WT, Chew EY, Danis RP, Davis MD, et al. Lack of longitudinal association between thiazolidinediones and incidence and progression of diabetic eye disease: The ACCORD eye study. *Am J ophthalmology.* (2018) 187:138–47. doi: 10.1016/j.ajo.2017.12.007

45. Marchand L, Luyton C, Bernard A. Glucagon-like peptide-1 (GLP-1) receptor agonists in type 2 diabetes and long-term complications: FOCUS on retinopathy. *Diabetic Med J Br Diabetic Assoc* (2021) 38(1):e14390. doi: 10.1111/dme.14390

46. Wang D, Ding X, He M, Yan L, Kuang J, Geng Q, et al. Use of eye care services among diabetic patients in urban and rural China. *Ophthalmology.* (2010) 117(9):1755–62. doi: 10.1016/j.ophtha.2010.01.019

47. Chen T, Jin L, Zhu W, Wang C, Zhang G, Wang X, et al. Knowledge, attitudes and eye health-seeking behaviours in a population-based sample of people with diabetes in rural China. *Br J ophthalmology.* (2021) 105(6):806–11. doi: 10.1136/bjophthalmol-2020-316105

frontiers | Frontiers in Endocrinology

TYPE Original Research
PUBLISHED 17 January 2023
DOI 10.3389/fendo.2022.1087965

OPEN ACCESS

EDITED BY
Mohd Imtiaz Nawaz,
Department of Ophthalmology, College of Medicine, King Saud University, Saudi Arabia

REVIEWED BY
Jeena Gupta,
Lovely Professional University, India
Kei Hang Katie Chan,
City University of Hong Kong, Hong Kong SAR, China

*CORRESPONDENCE
Fagang Jiang
fgjiang@hotmail.com
Xinghua Wang
xinghua_wang@hust.edu.cn

†These authors have contributed equally to this work and share first authorship

SPECIALTY SECTION
This article was submitted to Clinical Diabetes, a section of the journal Frontiers in Endocrinology

RECEIVED 02 November 2022
ACCEPTED 28 December 2022
PUBLISHED 17 January 2023

CITATION
Su Z, Wu Z, Liang X, Xie M, Xie J, Li H, Wang X and Jiang F (2023) Diabetic retinopathy risk in patients with unhealthy lifestyle: A Mendelian randomization study. *Front. Endocrinol.* 13:1087965. doi: 10.3389/fendo.2022.1087965

Diabetic retinopathy risk in patients with unhealthy lifestyle: A Mendelian randomization study

Zixuan Su[1†], Zhixin Wu[2†], Xueqing Liang[3], Meng Xie[1], Jia Xie[1], Huiqing Li[2], Xinghua Wang[1*] and Fagang Jiang[1*]

[1]Department of Ophthalmology, Union Hospital, Tongji Medical College, Huazhong University of Science and Technology, Wuhan, China, [2]Department of Endocrinology, Union Hospital, Tongji Medical College, Huazhong University of Science and Technology, Wuhan, China, [3]Department of Biostatistics, School of Public Health, Southern Medical University, Guangzhou, China

Purpose: This study aimed to investigate the causal association between unhealthy lifestyle factors and diabetic retinopathy (DR) risk and to determine better interventions targeting these modifiable unhealthy factors.

Design: Two-sample Mendelian randomization (MR) analysis was performed in this study. The inverse variance-weighted method was used as the primary method.

Method: Our study included 687 single-nucleotide polymorphisms associated with unhealthy lifestyle factors as instrumental variables. Aggregated data on individual-level genetic information were obtained from the corresponding studies and consortia. A total of 292,622,3 cases and 739,241,18 variants from four large consortia (MRC Integrative Epidemiology Unit [MRC-IEU], Genetic Investigation of Anthropometric Traits [GIANT], GWAS & Sequencing Consortium of Alcohol and Nicotine Use [GSCAN], and Neale Lab) were included.

Result: In the MR analysis, a higher body mass index (BMI) (odds ratio [OR], 95% confidence interval [CI] = 1.42, 1.30–1.54; $P < 0.001$] and cigarettes per day (OR, 95% CI = 1.16, 1.05–1.28; $P = 0.003$) were genetically predicted to be causally associated with an increased risk of DR, while patients with higher hip circumference (HC) had a lower risk of DR (OR, 95% CI = 0.85, 0.76–0.95; $P = 0.004$). In the analysis of subtypes of DR, the results of BMI and HC were similar to those of DR, whereas cigarettes per day were only related to proliferative DR (PDR) (OR, 95% CI = 1.18, 1.04–1.33; $P = 0.009$). In the MR-PRESSO analysis, a higher waist-to-hip ratio (WHR) was a risk factor for DR and PDR (OR, 95% CI = 1.24, 1.02–1.50, $P = 0.041$; OR, 95% CI = 1.32, 1.01–1.73, $P = 0.049$) after removing the outliers. Furthermore, no pleiotropy was observed in these exposures.

Conclusion: Our findings suggest that higher BMI, WHR, and smoking are likely to be causal factors in the development of DR, whereas genetically higher HC is associated with a lower risk of DR, providing insights into a better understanding of the etiology and prevention of DR.

KEYWORDS

Mendelian randomization, diabetic retinopathy, unhealthy lifestyle factors, obesity, smoking, alcohol intake

1 Introduction

Diabetic retinopathy (DR), a common microvascular complication of diabetes mellitus (DM), remains a leading cause of acquired vision loss in adults of working age and is associated with an increased risk of life-threatening systemic vascular complications (1). Moreover, 35% of individuals with diabetes experience DR, and 10% are in the stage of vision threatening (2). To confront the growing threat,revealing the risk factors of DR is an essential part of implementing interventions for prevention.

Considering unhealthy lifestyle a modifiable factor, mounting observational epidemiological studies have focused on the association between unhealthy lifestyle and DR. However, based on the current studies, the results of some unhealthy lifestyle factors are controversial and inconsistent (3–7). According to a meta-analysis of prospective cohort studies, obesity was a risk factor for non-proliferative DR (5). However, another meta-analysis failed to find any correlation between obesity and DR risk (7). Regarding alcohol intake, different meta-analyses also present controversial results. Chen et al. demonstrated no significant association between alcohol intake and DR (6) whereas Zhu et al. found protective effects in the wine group (3). Due to potential methodological limitations in observational studies, the causal association between such factors and DR can be confused by reverse causality or ethnicity, sex, and age.

Mendelian randomization (MR) analysis utilizes genetic predictors as instrumental variables (IVs) to investigate the causal association between risk factors and diseases (8). Because genetic variants are randomly distributed at conception, each IV is considered an alternative to randomized controlled trials and can avoid various bias commonly presented in traditional observational studies (9). However, most previous MR studies have focused on modified factors and diabetes, and we did not find any study concern about unhealthy lifestyle factors and DR. In addition, the influence of these factors on the different types of DR is uncertain. Thus, based on publicly available data, we performed MR analysis to assess the causal associations between unhealthy lifestyle factors (including smoking, alcohol intake, and obesity) and the risk of DR, including its subtypes.

2 Materials and methods

2.1 Genetic variants associated with unhealthy lifestyle

In this study, smoking, alcohol intake, and obesity were selected as typical examples of unhealthy lifestyle habits. We selected body mass index (BMI) (ukb-a-248), waist circumference (ieu-a-67), hip circumference (HC, ieu-a-55), and waist-to-hip ratio (WHR, ieu-a-79) as indicators of obesity. Single nucleotide variants (single-nucleotide polymorphisms [SNPs]) for BMI were retrieved from the Neale Lab consortium, and the rest were retrieved from a published meta-analysis of genome-wide association studies (GWAS) datasets summarized by Shungin (10) (datasets: ukb-a-248, ieu-a-79, ieu-a-55, ieu-a-67). The SNPs for smoking were obtained from another published meta-analysis of GWAS datasets summarized by Liu (11) and the MRC Integrative Epidemiology Unit (MRC-IEU) consortium (datasets: ieu-b-24, ieu-b-25, ukb-b-20261), including three phenotypes measured by the heaviness of smoking: age of smoking initiation, cigarettes per day, and ever smoked. For alcohol intake, we selected the SNPs of alcoholic drinks per week and alcohol intake frequency from a published meta-analysis of GWAS datasets summarized by Liu (11) and the GWAS & Sequencing Consortium of Alcohol and Nicotine use consortium (datasets: ieu-b-73, ukb-b-5779). All SNPs associated with exposures that reached the GWAS threshold of statistical significance ($P < 5 \times 10^{-8}$) were extracted as IVs. To ensure that they were entirely independent, linkage disequilibrium analysis was performed using a threshold of $r^2 < 0.001$. Additionally, we extracted the summary data and effects of each SNP and calculated the effect sizes and standard errors using the MR-Base platform (12). Details of the data sources are provided in Table 1.

2.2 GWAS summary data on diabetic retinopathy

Published GWAS summary data on DR were retrieved from the MRC-IEU (14,584 cases and 176,010 controls, European ancestry) (https://gwas.mrcieu.ac.uk/) (13). To evaluate potential heterogeneity in the causal effects, we further stratified the DR type for background DR (BDR) and PDR. BDR is an early stage of DR known as non-PDR. We used GWAS summary data of 2026 BDR cases and 8681 PDR cases from the MRC-IEU with 204,208 common controls (Table 1). For each selected SNP, we retrieved summary data (the effects on DR, effect sizes, standard errors, and effect alleles) for the MRC-IEU using the MR-Base platform (12, 14).

2.3 Statistical analyses

We used a two-sample MR approach to examine the potential causal association between unhealthy lifestyle and DR incidence. The MR method must satisfy three assumptions: (i) the IVs need to be robustly related to the exposures; (ii) the instruments influence the outcome only through the exposures of interest; and (iii) the IVs are independent of any confounders of the exposure–outcome association (Figure 1) (15). A flowchart of the statistical analyses is shown in Figure 2.

In the MR analyses, the inverse-variance weighted (IVW) model was the main method used in this study. The MR-Egger regression and weighted median (WM) models were also used to test the coherence of the causal estimates. The IVW method treated each SNP as a valid natural experiment, assessing the causal effects of each

Abbreviations: AGEs, advanced glycation end-products; BMI, body mass index; BDR, background diabetic retinopathy; CI, confidence interval; DM, diabetes mellitus; DR, diabetic retinopathy; GIANT, Genetic Investigation of ANthropometric Traits; GWAS, genome-wide association studies; GSCAN, GWAS & Sequencing Consortium of Alcohol and Nicotine use; HC, hip circumference; IDF, International Diabetes Federation; IVs, instrumental variables; IVW, inverse-variance weighted; LD, linkage disequilibrium; MR, Mendelian randomization; MRC-IEU, MRC Integrative Epidemiology Unit; MR-PRESSO, MR Pleiotropy Residual Sum and Outlier; NPDR, non-proliferative diabetic retinopathy; OR, odds ratio; PDR, proliferative diabetic retinopathy; SNPs, single-nucleotide polymorphisms; WC, waist circumference; WHR, waist-to-hip ratio; WM, weighted median.

TABLE 1 Details of studies included in Mendelian randomization analyses.

Consortium	Phenotype	First author	Sample size	Year	Note
MRC-IEU	Diabetic retinopathy	NA	14,584	2021	https://gwas.mrcieu.ac.uk/datasets/finn-b-DM_RETINOPATHY_EXMORE/
	Background diabetic retinopathy		2,026		https://gwas.mrcieu.ac.uk/datasets/finn-b-DM_BCKGRND_RETINA/
	Proliferative diabetic retinopathy		8,681		https://gwas.mrcieu.ac.uk/datasets/finn-b-DM_RETINA_PROLIF/
GSCAN	Cigarettes per day	Liu M (11)	337,334	2019	https://www.nature.com/articles/s41588-018-0307-5
	Age Of Smoking Initiation		341,427		
	Alcoholic drinks per week		335,394		
MRC-IEU	Ever smoked	Ben Elsworth	461,066	2018	https://gwas.mrcieu.ac.uk/datasets/ukb-b-20261/
	Alcohol intake frequency		462,346		https://gwas.mrcieu.ac.uk/datasets/ukb-b-5779/
Neale Lab	Body mass index	Neale	336,107	2017	http://www.nealelab.is/blog/2017/9/11/details-and-considerations-of-the-uk-biobank-gwas
GIANT	Waist-to-hip ratio	Shungin D (10)	210,082	2015	https://www.nature.com/articles/nature14132
	Hip circumference		211,114		
	Waist circumference		231,353		

MRC-IEU, MRC Integrative Epidemiology Unit; GSCAN, GWAS & Sequencing Consortium of Alcohol and Nicotine use; GIANT, Genetic Investigation of ANthropometric Traits.

SNP on the outcome, and used the outcome as weights for meta-analysis to evaluate the combined causal effect. The IVW (fixed-effect) method provides an unbiased estimate in the absence of horizontal pleiotropy or when horizontal pleiotropy is balanced (16). If heterogeneity was present, the multiplicative random-effects IVW model was used and provided valid estimates under the assumption of balanced pleiotropy (17, 18).

In sensitivity analyses, the MR-Egger-intercept test was used to determine pleiotropy. We also applied the MR pleiotropy residual sum and outlier (MR-PRESSO) method to identify outlying SNPs and examine whether the causal effect would change after removing these outliers (19). Cochran's Q statistic was used to determine the heterogeneity test between individual genetic variants (20). Leave-one-out analysis was performed to evaluate whether MR estimates were driven or biased by a single SNP and to calculate the meta-effect of the remaining SNPs. The asymmetry in funnel plots may indicate that the second assumption is violated by horizontal pleiotropy.

The results were shown as odds ratios (ORs) with their corresponding 95% confidence intervals (CIs). Because we included analyses of nine exposures with three outcomes, using a conservative approach, a Bonferroni-corrected P value < 0.05 divided by 27 (i.e., $1.852e^{-3}$) was considered a significant causal association to adjust for multiple testing. A P-value between 0.05 and $1.852e^{-3}$ was considered suggestive of a potential association. All statistical analyses were performed in R (version 4.1.0) using the R package "Two sample MR" (version 0.5.6) and "MR- PRESSO" (version 1.0) (12).

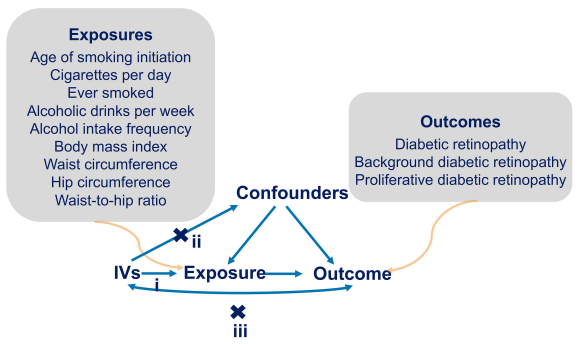

FIGURE 1
Diagram of MR assumptions. i): represents the IVs need to be related with the exposures robustly. ii): represents the IVs influence the outcome only through the exposures of interest. iii): represents the IVs are independent of any confounders of the exposure-outcome relation. Arrows interpret the causal relationships among variables.

3 Results

3.1 Mendelian randomization analysis

3.1.1 Overview of the results

An overview of the MR analysis results is shown in Figure 3. More specific results from the MR analyses are summarized in Figure 4, Table 2, and Tables S2, S3. Detailed information on each SNP is provided in Table S1.

3.1.2 Results of DR

The IVW method indicated an over 40% increased risk of DR incidence per standard deviation (SD) increase in BMI (OR = 1.42; 95% CI, 1.30–1.54; $P < 0.001$*) and an approximately 20% increase in the risk of cigarettes per day (OR = 1.16; 95% CI, 1.05–1.28; $P = 0.003$*). Interestingly, higher HC decreased 15% lower risk in DR incidence per SD (OR = 0.85; 95% CI, 0.76–0.95; $P = 0.004$*). A forest plot of SNPs associated with cigarettes per day, BMI, and HC is presented in Figure S1. The results obtained using the WM method

10.3389/fendo.2022.1087965

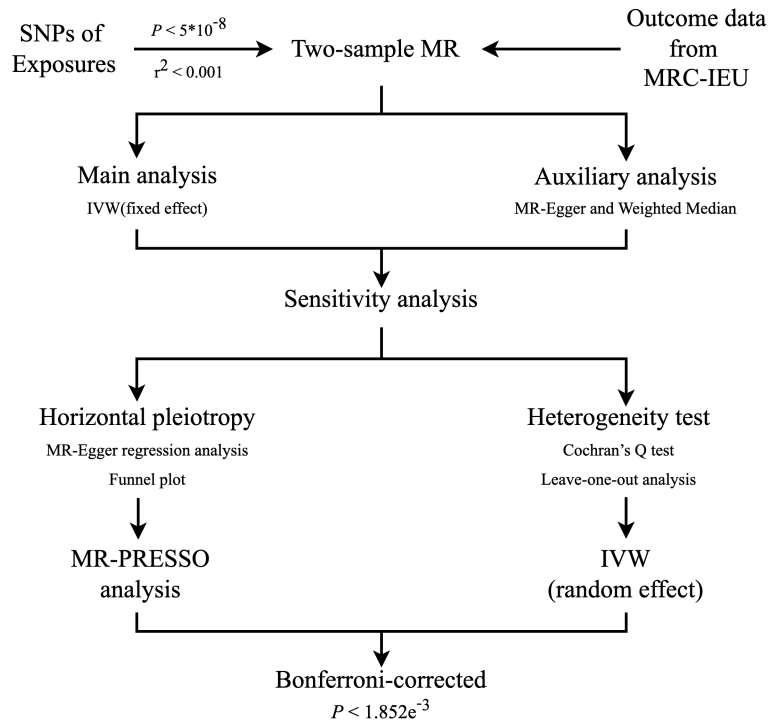

FIGURE 2
Flowchart of the statistical analyses, outlining the different analyses performed at each stage of the study. SNP, single-nucleotide polymorphism; MR, Mendelian randomization; MRC-IEU, MRC Integrative Epidemiology Unit; IVW, inverse-variance weighted.

were similar to those obtained using the IVW method (Table 2). In the MR-Egger model, BMI also showed a significant causal effect. However, the MR-Egger model showed a consistent effect direction in cigarettes per day, and HC was not statistically significant (Table 2). We did not observe any association between alcohol intake and DR (Figure 4). We further proceeded with Bonferroni correction, which indicated significant causal effects between BMI and DR risk (P = $9.389e^{-16}$).

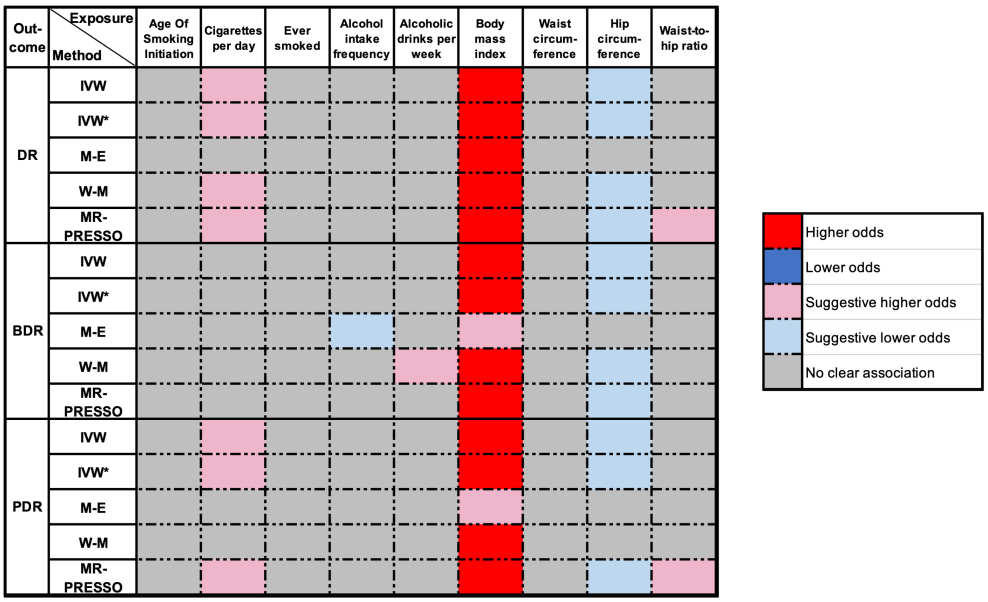

FIGURE 3
Overview of the main results of MR analyze. DR, diabetic retinopathy; BDR, background diabetic retinopathy; PDR, proliferative diabetic retinopathy; IVW, inverse-variance weighted (fixed-effect); IVW*, Inverse variance weighted (multiplicative random-effects); MR, Mendelian randomization; M-E, MR Egger; W-M, weighted median; MR-PRESSO, MR Pleiotropy Residual Sum and Outlier. P-value < $1.852e^{-03}$ was regarded as a significant causal association, the P-value between 0.05 and $1.852e^{-03}$ was considered suggestive of a potential association.

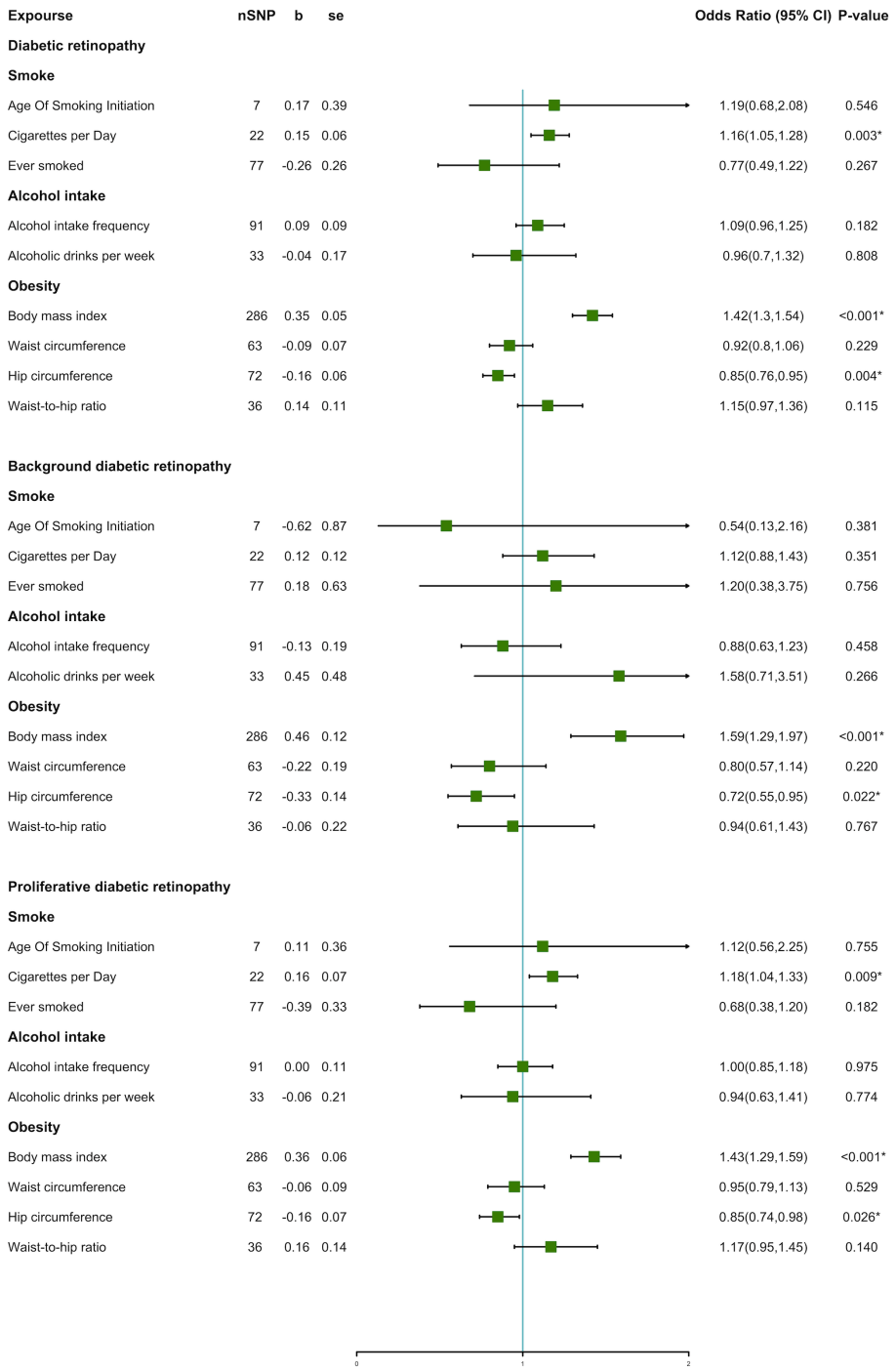

FIGURE 4
Forest plot of unhealthy lifestyle factors associated with the risk of DR and its subtypes.

3.1.3 Results of DR subtypes

In DR subtypes, a genetically predicted higher BMI increased the risk of BDR (OR = 1.59; 95% CI, 1.29–1.97; $P < 0.001$*) and PDR (OR = 1.43; 95% CI, 1.29–1.59; $P < 0.001$*). In the WM method and MR-Egger model, BMI also indicated an analogous causal effect. Higher HC was a protective factor in BDR (OR = 0.72; 95% CI, 0.55–0.95; $P = 0.022$*) and PDR (OR = 0.85; 95% CI, 0.74–0.98; $P = 0.026$*). The result of cigarettes per day indicated an increased risk of PDR (OR = 1.18; 95% CI, 1.04–1.33; $P = 0.009$*). The forest plot of SNPs associated with the above exposures and the risks of BDR and PDR are presented in Figure S2. The HC in the BDR using the WM method was also significant. The results of the MR-Egger model and other results of the WM method are presented in Tables S2, S3. We did not find causality in the other factors with BDR and PDR. After Bonferroni correction, a higher BMI still had a significant causal

TABLE 2 Mendelian randomization estimates of the associations between unhealthy lifestyle and risk of DR.

Exposure	IVW method (fixed-effect)		MR-Egger		Weighted median method	
	OR (95% CI)	*P*-value	OR (95% CI)	*P*-value	OR (95% CI)	*P*-value
Smoking						
Age Of Smoking Initiation	1.19(0.68,2.08)	0.546	0.43(0.04,5.00)	0.532	1.17(0.54,2.55)	0.691
Cigarettes per day	1.16(1.05,1.28)	0.003*	1.15(0.93,1.42)	0.221	1.20(1.04,1.38)	0.010*
Ever smoked	0.77(0.49,1.22)	0.267	0.24(0.02,2.73)	0.251	0.61(0.30,1.25)	0.177
Alcohol intake						
Alcohol intake frequency	1.09(0.96,1.25)	0.182	0.73(0.43,1.23)	0.242	1.05(0.85,1.29)	0.681
Alcoholic drinks per week	0.96(0.7,1.32)	0.808	0.93(0.43,2.00)	0.854	0.92(0.56,1.50)	0.729
Obesity						
Body mass index	1.42(1.3,1.54)	<0.001*	1.65 (1.25,2.18)	0.0005*	1.40 (1.22,1.61)	<0.001*
Waist circumference	0.92(0.8,1.06)	0.229	0.96(0.50,1.84)	0.904	0.93(0.76,1.15)	0.508
Hip circumference	0.85(0.76,0.95)	0.004*	0.94(0.62,1.43)	0.775	0.83(0.70,0.98)	0.033*
Waist-to-hip ratio	1.15(0.97,1.36)	0.115	0.99(0.36,2.70)	0.990	1.18(0.92,1.52)	0.192

IVW, inverse-variance weighted; OR, odds ratio; CI, confidence interval.

association with BDR and PDR risks (BDR, $P = 1.687e^{-5;}$ PDR, $P = 4.085e^{-11}$).

3.2 Sensitivity analyses

3.2.1 Sensitivity analyses of DR

We assessed heterogeneity using Cochran's Q test and horizontal pleiotropy from the MR-Egger regression analysis. There was no evidence of directional pleiotropy using MR-Egger regression (Table 3). Cochran's Q test for BMI was statistically significant ($P <$ 0.05). Hence, we used a multiplicative random-effects model to re-estimate the MR effect of BMI. The results showed a causal association and positive correlation between BMI and DR risk ($P = 4.24e^{-13}$*).

3.2.2 Sensitivity analyses of DR subtypes

In DR subtypes, the heterogeneity analysis showed a similar result for BMI ($P < 0.05$). The results of multiplicative random effects showed that BMI was a causal risk factor for BDR ($P = 1.06e^{-04}$) and PDR ($P = 6.05e^{-09}$). Directional pleiotropy was found in alcohol

TABLE 3 Sensitivity test of Mendelian randomization analyze of the associations between unhealthy lifestyle and risk of DR.

Exposure	MR-Egger regression analysis		Cochran's Q test		IVW method (multiplicative random-effects)	
	Intercept	*P-value*	*Q statistic*	*P-value*	OR (95% CI)	*P-value*
Smoke						
Age Of Smoking Initiation	0.023	0.432	9.79	0.081	1.19(0.55,2.55)	0.659
Cigarettes per day	0.001	0.888	30.92	0.056	1.16(1.03,1.31)	0.013*
Ever smoked	0.008	0.335	92.89	0.079	0.77(0.46,1.28)	0.318
Alcohol intake						
Alcohol intake frequency	0.010	0.112	147.44	<0.001*	1.09(0.92,1.30)	0.304
Alcoholic drinks per week	0.001	0.927	34.24	0.315	0.96(0.69,1.34)	0.814
Obesity						
Body mass index	-0.003	0.251	348.61	0.005*	1.42 (1.29,1.56)	<0.001*
Waist circumference	-0.001	0.886	66.64	0.289	0.92(0.79,1.06)	0.246
Hip circumference	-0.003	0.622	72.67	0.390	0.85(0.76,0.95)	0.005*
Waist-to-hip ratio	0.004	0.776	52.13	0.024*	1.15(0.93,1.41)	0.197

IVW, inverse-variance weighted; MR, Mendelian randomization.

intake frequency in PDR ($P = 0.024$*) using MR-Egger regression. No evidence of directional pleiotropy was found in the other exposures (Tables S4, S5).

3.2.3 MR-PRESSO analysis

We applied MR-PRESSO to recognize outlying SNPs that might cause horizontal pleiotropy effects. Several outliers were identified during the MR-PRESSO analysis. After removing these outliers, we found that a higher WHR indicated a higher risk of DR (OR = 1.24; 95% CI, 1.02–1.50; $P = 0.041$) and PDR (OR = 1.32; 95% CI, 1.01–1.73; $P = 0.049$). In the remaining cases, the results remained consistent with the original results after the removal of these outliers. The corrected results of the MR-PRESSO analysis are listed in Table S6.

3.2.4 Leave-one-out analysis and funnel plot

The leave-one-out analysis suggested that the risk estimates of cigarettes per day, BMI, and HC for DR, BDR, and PDR generally remained consistent after eliminating each single SNP at a time (Figures S3, S4, Table S7). In addition, the points were roughly symmetrical on both sides of the vertical line in funnel plot, which meant no horizontal pleiotropy in the SNPs for shown exposures (Figures S5, S6).

4 Discussion

The present study demonstrated a causal association among cigarettes per day, BMI, and WHR and an increased risk of DR, whereas HC was found to have a lower risk of DR. In subgroup analyses, we found that higher BMI increased the risk of all types of DR, especially BDR. Cigarettes per day was only associated with PDR. Additionally, HC decreased the risks of BDR and PDR. These results were contrary to those of several previous conventional observational studies (3–7). A possible explanation is that the small sample sizes and confounders might interfere with the results of traditional observational epidemiological studies. Here, MR analysis demonstrated an unbiased estimation of whether certain risk factors played a causal role in diseases, using data from published large-scale GWAS data, which made our results more reliable and convincing.

The mechanisms underlying the associations among cigarette smoking, BMI, HC, WHR, and DR remain unclear. In smoking patients, nicotine causes a vasoconstrictive effect. This reduces the blood flow of the retina and makes it difficult for the retinal blood vessels to autoregulate hyperoxia (21, 22). Additionally, smoking may increase carboxyhemoglobin levels (23), thereby reducing the retinal oxygen delivery and oxygen-carrying capacity of the blood. Moreover, mainstream cigarette smoke contains certain components (24) that can interact with plasma and extracellular matrix proteins. This leads to the formation of covalent adducts similar to advanced glycation end products (25, 26) and involved in diabetic end-organ complications.

For obesity, a higher BMI is often associated with dyslipidemia – a disease that may be responsible for the development of DR (27). Moreover, obese individuals with hyperleptinemia (28) are more likely to have higher blood pressure and oxidative stress levels which consequently, are possibly correlated with an increased risk of DR. Additionally, higher levels of the vascular endothelial growth factor found in obese individuals (29) were related to the pathogenesis of PDR (30). For WHR, abdominal obesity played a role in insulin resistance (31) and inflammation (32). Both of these have an association with the pathogenesis of DR (33–35). For HC, the protective effects of a higher HC might result from a larger muscle mass in the gluteofemoral region (36). Different fat deposits exhibit different metabolic properties; lower body fat could somewhat reverse the impact of abdominal fat and protect against insulin resistance (37). As suggested by previous research, for a certain amount of abdominal fat, higher peripheral fat accumulation in the hips and thighs might relate to a better metabolic state (38–42). Additionally, a larger HC might reduce the risk of DR by the contribution of active lipoprotein lipase and the low turnover of fatty acid in gluteofemoral adipose tissues.

The present study has several strengths. First, very few studies have comprehensively investigated the association between unhealthy lifestyles and DR incidence. To the best of our knowledge, our study is the first to investigate the potential causal association between unhealthy lifestyles and the risk of DR employing the MR approach and a large GWASs data. Second, due to the use of MR analysis, our findings were less likely to cause confounding and reverse causality, when compared to those of conventional observational studies. Third, the accuracy of our findings might be higher as we applied analysis of subtypes stratified by clinical classification to investigate the consistency of the pooled effects. Finally, the sample overlap only could account for up to 6.94%, and the exposure and outcome data were obtained from different databases, thereby reducing the bias of the estimate in the direction of observational association. These strengths of MR analysis, as a result, might increase the reliability of our findings.

However, certain limitations were found in our study. The SNPs were obtained from five large European populations-based consortia, which, therefore, might affect the generalization of our findings in other populations and regions. Otherwise, our study only performed MR analysis with summarized statistics. This could only allow us to make a preliminary conclusion on the causal association between unhealthy lifestyles and DR but fail to further investigate this association in terms of age, sex, type of diabetes, and DR severity. Additionally, it is hardly possible to remove all pleiotropy in our studies, especially the correlated horizontal pleiotropy. Consequently, some undetected confounders between exposures and outcomes may bias our results. Therefore, our findings should be cautiously interpreted and confirmed through further studies.

In conclusion, we demonstrate that smoking, BMI, and WHR are risk factors for DR. For future studies, informed by the work reported here, individual-level data and basic science approaches are required to investigate the further mechanism underlying the association between cigarette intake and obesity and DR development. In addition, due to the contrary results of WHR and HC, more emphasis should be placed on how different fat distributions relate to DR, which can disclose the underlying association between obesity and DR and strengthen the understanding of obesity. For clinical practice and public health strategies, the present study highlights the

importance of lifestyle management in patients with diabetes and provides a reference for the future refined identification of high-risk individuals for DR. Health education can be strengthened to suggest avoiding unhealthy lifestyles. In addition, more frequent ocular examinations may be essential in patients with diabetes with such risk factors.

Data availability statement

The original contributions presented in the study are included in the article/Supplementary Material. Further inquiries can be directed to the corresponding authors.

Author contributions

FJ and XW were responsible for the concept and design of the study, interpretation of data, and drafting and writing of the article. ZS and ZW were contributed equally to the manuscript as joint first authors. The other authors were responsible for interpretation of data and revision of the intellectual content. All authors contributed to the article and approved the submitted version.

Funding

This work was supported by the National Natural Science Foundation of China (No.81900912). The funding organization had no role in the design or conduct of this study.

Acknowledgments

The authors acknowledge the efforts of the consortia in providing high-quality GWAS resources for researchers. Data and materials are available from the corresponding GWAS consortium. The authors would like to thank the editors and the reviewers for their valuable comments and suggestions to improve the quality of the paper.

Conflict of interest

The authors declare that the research was conducted in the absence of any commercial or financial relationships that could be construed as a potential conflict of interest.

Publisher's note

Supplementary material

The Supplementary Material for this article can be found online at: https://www.frontiersin.org/articles/10.3389/fendo.2022.1087965/full#supplementary-material

References

1. Cheung N, Mitchell P, Wong TY. Diabetic retinopathy. *Lancet (London England).* (2010) 376(9735):124–36. doi: 10.1016/S0140-6736(09)62124-3

2. Yau JW, Rogers SL, Kawasaki R, Lamoureux EL, Kowalski JW, Bek T, et al. Global prevalence and major risk factors of diabetic retinopathy. *Diabetes Care* (2012) 35(3):556–64. doi: 10.2337/dc11-1909

3. Zhu W, Meng YF, Wu Y, Xu M, Lu J. Association of alcohol intake with risk of diabetic retinopathy: a meta-analysis of observational studies. *Sci Rep* (2017) 7(1):4. doi: 10.1038/s41598-017-00034-w

4. Cai X, Chen Y, Yang W, Gao X, Han X, Ji L. The association of smoking and risk of diabetic retinopathy in patients with type 1 and type 2 diabetes: a meta-analysis. *Endocrine* (2018) 62(2):299–306. doi: 10.1007/s12020-018-1697-y

5. Zhu W, Wu Y, Meng YF, Xing Q, Tao JJ, Lu J. Association of obesity and risk of diabetic retinopathy in diabetes patients: A meta-analysis of prospective cohort studies. *Medicine* (2018) 97(32):e11807. doi: 10.1097/MD.0000000000011807

6. Chen C, Sun Z, Xu W, Tan J, Li D, Wu Y, et al. Associations between alcohol intake and diabetic retinopathy risk: a systematic review and meta-analysis. *BMC Endocr Disord* (2020) 20(1):106. doi: 10.1186/s12902-020-00588-3

7. Zhou Y, Zhang Y, Shi K, Wang C. Body mass index and risk of diabetic retinopathy: A meta-analysis and systematic review. *Med (Baltimore).* (2017) 96(22):e6754. doi: 10.1097/MD.0000000000006754

8. Davey Smith G, Ebrahim S. What can mendelian randomisation tell us about modifiable behavioural and environmental exposures? *BMJ (Clinical Res ed)* (2005) 330 (7499):1076–9. doi: 10.1136/bmj.330.7499.1076

9. Su Z, Jiang Y, Li C, Zhong R, Wang R, Wen Y, et al. Relationship between lung function and lung cancer risk: a pooled analysis of cohorts plus mendelian randomization study. *J Cancer Res Clin Oncol* (2021) 147(10):2837–49. doi: 10.1007/s00432-021-03619-1

10. Shungin D, Winkler TW, Croteau-Chonka DC, Ferreira T, Locke AE, Mägi R, et al. New genetic loci link adipose and insulin biology to body fat distribution. *Nature* (2015) 518(7538):187–96. doi: 10.1038/nature14132

11. Liu M, Jiang Y, Wedow R, Li Y, Brazel DM, Chen F, et al. Association studies of up to 1.2 million individuals yield new insights into the genetic etiology of tobacco and alcohol use. *Nat Genet* (2019) 51(2):237–44.

12. Hemani G, Zheng J, Elsworth B, Wade KH, Haberland V, Baird D, et al. The MR-base platform supports systematic causal inference across the human phenome. *eLife* (2018) 7:e34408. doi: 10.7554/eLife.34408

13. Wang Y, McKay JD, Rafnar T, Wang Z, Timofeeva MN, Broderick P, et al. Rare variants of large effect in BRCA2 and CHEK2 affect risk of lung cancer. *Nat Genet* (2014) 46(7):736–41. doi: 10.1038/ng.3002

14. Elsworth B, Lyon M, Alexander T, Liu Y, Matthews P, Hallett J, et al. The MRC IEU OpenGWAS data infrastructure. *bioRxiv* (2020). doi: 10.1101/2020.08.10.244293

15. Boef AGC, Dekkers OM, le Cessie S. Mendelian randomization studies: a review of the approaches used and the quality of reporting. *Int J Epidemiol.* (2015) 44(2):496–511. doi: 10.1093/ije/dyv071

16. Hemani G, Bowden J, Davey Smith G. Evaluating the potential role of pleiotropy in mendelian randomization studies. *Hum Mol Genet* (2018) 27(R2):R195–r208. doi: 10.1093/hmg/ddy163

17. Bowden J, Spiller W, Del Greco MF, Sheehan N, Thompson J, Minelli C, et al. Improving the visualization, interpretation and analysis of two-sample summary data mendelian randomization *via* the radial plot and radial regression. *Int J Epidemiol* (2018) 47(4):1264–78. doi: 10.1093/ije/dyy101

18. Bowden J, Holmes MV. Meta-analysis and mendelian randomization: A review. *Res Synth Methods* (2019) 10(4):486–96. doi: 10.1002/jrsm.1346

19. Verbanck M, Chen C-Y, Neale B, Do R. Detection of widespread horizontal pleiotropy in causal relationships inferred from mendelian randomization between complex traits and diseases. *Nat Genet* (2018) 50(5):693–8. doi: 10.1038/s41588-018-0099-7

20. Greco M FD, Minelli C, Sheehan NA, Thompson JR. Detecting pleiotropy in mendelian randomisation studies with summary data and a continuous outcome. *Stat Med* (2015) 34(21):2926–40. doi: 10.1002/sim.6522

21. Morgado PB, Chen HC, Patel V, Herbert L, Kohner EM. The acute effect of smoking on retinal blood flow in subjects with and without diabetes. *Ophthalmology* (1994) 101(7):1220–6. doi: 10.1016/S0161-6420(94)31185-7

22. Costa F, Soares R. Nicotine: a pro-angiogenic factor. *Life Sci* (2009) 84(23-24):785–90. doi: 10.1016/j.lfs.2009.03.002

23. Leone A. Biochemical markers of cardiovascular damage from tobacco smoke. *Curr Pharm Des* (2005) 11(17):2199–208. doi: 10.2174/1381612054367391

24. Nicholl ID, Bucala R. Advanced glycation endproducts and cigarette smoking. *Cell Mol Biol (Noisy-le-Grand France).* (1998) 44(7):1025–33.

25. Brownlee M, Vlassara H, Cerami A. Nonenzymatic glycosylation and the pathogenesis of diabetic complications. *Ann Internal Med* (1984) 101(4):527–37. doi: 10.7326/0003-4819-101-4-527

26. Wautier JL, Guillausseau PJ. Advanced glycation end products, their receptors and diabetic angiopathy. *Diabetes Metab* (2001) 27(5 Pt 1):535–42.

27. Chew EY, Davis MD, Danis RP, Lovato JF, Perdue LH, Greven C, et al. The effects of medical management on the progression of diabetic retinopathy in persons with type 2 diabetes: the action to control cardiovascular risk in diabetes (ACCORD) eye study. *Ophthalmology* (2014) 121(12):2443–51. doi: 10.1016/j.ophtha.2014.07.019

28. Considine RV, Sinha MK, Heiman ML, Kriauciunas A, Stephens TW, Nyce MR, et al. Serum immunoreactive-leptin concentrations in normal-weight and obese humans. *New Engl J Med* (1996) 334(5):292–5. doi: 10.1056/NEJM199602013340503

29. Miyazawa-Hoshimoto S, Takahashi K, Bujo H, Hashimoto N, Saito Y. Elevated serum vascular endothelial growth factor is associated with visceral fat accumulation in human obese subjects. *Diabetologia* (2003) 46(11):1483–8. doi: 10.1007/s00125-003-1221-6

30. Aiello LP, Avery RL, Arrigg PG, Keyt BA, Jampel HD, Shah ST, et al. Vascular endothelial growth factor in ocular fluid of patients with diabetic retinopathy and other retinal disorders. *New Engl J Med* (1994) 331(22):1480–7. doi: 10.1056/NEJM199412013312203

31. Fujimoto WY, Abbate SL, Kahn SE, Hokanson JE, Brunzell JD. The visceral adiposity syndrome in Japanese-American men. *Obes Res* (1994) 2(4):364–71. doi: 10.1002/j.1550-8528.1994.tb00076.x

32. Panagiotakos DB, Pitsavos C, Yannakoulia M, Chrysohoou C, Stefanadis C. The implication of obesity and central fat on markers of chronic inflammation: The ATTICA study. *Atherosclerosis* (2005) 183(2):308–15. doi: 10.1016/j.atherosclerosis.2005.03.010

33. Anan F, Takayuki M, Takahashi N, Nakagawa M, Eshima N, Saikawa T, et al. Diabetic retinopathy is associated with insulin resistance and cardiovascular autonomic dysfunction in type 2 diabetic patients. *Hypertens Res* (2009) 32(4):299–305. doi: 10.1038/hr.2009.8

34. Maneschi F, Mashiter K, Kohner EM. Insulin resistance and insulin deficiency in diabetic retinopathy of non-insulin-dependent diabetes. *Diabetes* (1983) 32(1):82–7. doi: 10.2337/diab.32.1.82

35. Chaturvedi N, Sjoelie AK, Porta M, Aldington SJ, Fuller JH, Songini M, et al. Markers of insulin resistance are strong risk factors for retinopathy incidence in type 1 diabetes. *Diabetes Care* (2001) 24(2):284–9. doi: 10.2337/diacare.24.2.284

36. Manolopoulos KN, Karpe F, Frayn KN. Gluteofemoral body fat as a determinant of metabolic health. *Int J Obes (Lond).* (2010) 34(6):949–59. doi: 10.1038/ijo.2009.286

37. Snijder MB, Dekker JM, Visser M, Bouter LM, Stehouwer CD, Kostense PJ, et al. Associations of hip and thigh circumferences independent of waist circumference with the incidence of type 2 diabetes: the hoorn study. *Am J Clin Nutr* (2003) 77(5):1192–7. doi: 10.1093/ajcn/77.5.1192

38. Williams MJ, Hunter GR, Kekes-Szabo T, Snyder S, Treuth MS. Regional fat distribution in women and risk of cardiovascular disease. *Am J Clin Nutr* (1997) 65 (3):855–60. doi: 10.1093/ajcn/65.3.855

39. Van Pelt RE, Evans EM, Schechtman KB, Ehsani AA, Kohrt WM. Contributions of total and regional fat mass to risk for cardiovascular disease in older women. *Am J Physiol Endocrinol Metab* (2002) 282(5):E1023–8. doi: 10.1152/ajpendo.00467.2001

40. Tankó LB, Bagger YZ, Alexandersen P, Larsen PJ, Christiansen C. Peripheral adiposity exhibits an independent dominant antiatherogenic effect in elderly women. *Circulation* (2003) 107(12):1626–31. doi: 10.1161/01.CIR.0000057974.74060.68

41. Ferreira I, Snijder MB, Twisk JW, van Mechelen W, Kemper HC, Seidell JC, et al. Central fat mass versus peripheral fat and lean mass: opposite (adverse versus favorable) associations with arterial stiffness? the Amsterdam growth and health longitudinal study. *J Clin Endocrinol Metab* (2004) 89(6):2632–9. doi: 10.1210/jc.2003-031619

42. Snijder MB, Dekker JM, Visser M, Bouter LM, Stehouwer CD, Yudkin JS, et al. Trunk fat and leg fat have independent and opposite associations with fasting and postload glucose levels: the hoorn study. *Diabetes Care* (2004) 27(2):372–7. doi: 10.2337/diacare.27.2.372

frontiers | Frontiers in Endocrinology

TYPE Original Research
PUBLISHED 19 January 2023
DOI 10.3389/fendo.2022.1036625

OPEN ACCESS

EDITED BY
Mohd Imtiaz Nawaz,
Department of Ophthalmology, King Saud University, Saudi Arabia

REVIEWED BY
Haoyu Chen,
The Chinese University of Hong Kong, China
Honghua Yu,
Guangdong Provincial People's Hospital, China
Li Zhang,
Zhejiang University, China

*CORRESPONDENCE
Jianqiao Li
18560087118@163.com

†These authors have contributed equally to this work

SPECIALTY SECTION
This article was submitted to Clinical Diabetes, a section of the journal Frontiers in Endocrinology

RECEIVED 04 September 2022
ACCEPTED 20 December 2022
PUBLISHED 19 January 2023

CITATION
Xu F, Li Z, Yang X, Gao Y, Li Z, Li G, Wang S, Ning X and Li J (2023) Assessment of choroidal structural changes in patients with pre- and early-stage clinical diabetic retinopathy using wide-field SS-OCTA. *Front. Endocrinol.* 13:1036625. doi: 10.3389/fendo.2022.1036625

Assessment of choroidal structural changes in patients with pre- and early-stage clinical diabetic retinopathy using wide-field SS-OCTA

Fabao Xu[1,2,3†], Zhiwen Li[1†], Xueying Yang[1], Yang Gao[2,3,4], Zhiwei Li[5], Guihua Li[6], Shaopeng Wang[6], Xiaolin Ning[2,3,4] and Jianqiao Li[1,2,3*]

[1]Department of Ophthalmology, Qilu Hospital, Shandong University, Jinan, China, [2]Shandong Key Laboratory: Magnetic Field-free Medicine & Functional Imaging, Jinan, China, [3]Research Institute of Shandong University: Magnetic Field-free Medicine & Functional Imaging, Jinan, China, [4]School of Physics, Beihang University, Beijing, China, [5]Jinan Aier Eye Hospital, Jinan, China, [6]Zibo Central Hospital, Binzhou Medical University, Zibo, Shandong, China

Purpose: To investigate the micro-vascular changes in choroidal structures in patients with pre- and early-stage clinical diabetic retinopathy (DR) using wide-field Swept-Source Optical Coherence Tomography Angiography (SS-OCTA).

Method: This observational cross-sectional study included 131 eyes of 68 subjects that were divided into healthy controls (group 1, n = 46), pre-DR (group 2, n = 43), early-stage DR (group 3, n = 42) cohorts. All participants that underwent SS-OCTA examination were inpatients in the department of Ophthalmology and the department of Endocrinology, Qilu Hospital, Shandong University, and Department of Ophthalmology, Aier Eye Hospital, Jinan, from July 11, 2021 to March 17, 2022. The choroidal vascularity index (CVI), choroidal thickness (ChT) and central macular thickness (CMT) in the whole area (diameter of 12 mm) and concentric rings with different ranges (0–3, 3–6, 6–9, and 9–12 mm) were recorded and analyzed from the OCTA image.

Result: Compared with healthy eyes, decreases in CVI and ChT were found in the eyes of patients with pre-or early-stage DR. The changes were more significant in the peripheral choroid, with the most prominent abnormalities in the 9-12mm area ($P < 0.001$). However, there was no obvious difference in the average CMT value. Furthermore, CVI and ChT were significantly correlated with the duration of diabetes in the range of 6–9 and 9–12 mm (Ps < 0.05; Correlation coefficient = -0.549, -0.395, respectively), with the strongest correlation (Ps < 0.01; Correlation coefficient = -0.597, -0.413, respectively) observed at 9–12 mm.

10.3389/fendo.2022.1036625

Conclusion: The CVI and ChT values of diabetic patients are significantly lower than in healthy controls, especially in patients with early-stage DR. In addition, the peripheral choroidal capillaries are more susceptible to early DM-induced injury than in the central area.

KEYWORDS

diabetes mellitus, diabetic retinopathy, wide-field optical coherence tomographic angiography, choroidal vascular changes, choroidal vascularity index (CVI)

Introduction

Current evidence suggests that the annual prevalence of diabetes mellitus (DM) has increased in recent years (1, 2). According to the latest Diabetes Atlas (10th edition) released by the International Diabetes Federation (IDF) in 2021, about 537 million adults aged 20-79 suffer from DM worldwide (https://diabetesatlas.org/). Diabetic retinopathy (DR) is widely acknowledged as one of DM's most serious ocular complications and the most common cause of blindness (3–6). Given the lack of obvious symptoms in early-stage disease, patients are often diagnosed in the vision-threatening stage of DR, when irreversible damage to visual acuity (VA) has already occurred. Therefore, effective early screening and intervention are essential to prevent severe vision loss secondary to DR. An increasing body of evidence suggests that a sustained hyperglycemic environment can cause vascular endothelial cell dysfunction and narrowing of the choroidal and retinal capillaries (7, 8). As the permeability of the inner retinal blood barrier increases, retinal exudates hemorrhage and edema occur, leading to irreversible damage to the retinal photoreceptors (9, 10). There are reportedly no retinal capillaries in the fovea within a diameter of 0.5 mm, and the choroidal circulation is the only blood supply for this area. In addition, the ellipsoid zone of the outer retina is supplied by choroidal circulation (11–13). Accordingly, the assessment of choroidal capillaries parameters can potentially detect retinal damage in early-stage disease and reveal the pathological mechanism of DR. Since Saracco and colleagues first put forward the conception of diabetic choroidopathy in 1982, clinical studies on choroids have constantly been emerging, and our understanding of diabetic choroidopathy has gradually deepened (14–16). As a new biological measurement tool, the choroidal vascularity index (CVI) has been documented to provide a more stable and objective assessment of choroidal conditions by measuring the ratio of the choroidal vessels to tissue composition (17). Current evidence suggests that CVI and choroidal thickness (ChT) enable quantitative analysis of the morphological and structural changes of choroidal circulation abnormalities and can be used as early assessment indicators for many chorioretinal diseases (8, 18, 19).

Optical coherence tomographic angiography (OCTA) can effectively assist in investigating the quantitative characteristics of changes in choroidal microvascular circulation and is the main imaging modality for the early detection and evaluation of diabetic choroidopathy (20–22). Given that the traditional OCTA (3 mm × 3 mm or 6 mm ×6 mm) has a limited visual field, the pathological features of the peripheral retina of DM patients cannot be obtained (22–24). Wide-field swept source (SS)-OCTA represents a new non-invasive instrument suitable for various follow-up applications. Importantly, with a scanning scope enlarged to 12×12 mm, wide-field SS-OCTA enables more comprehensive observation of diseases (25, 26). In this study, we sought to measure CVI and the thickness of the retina and choroid with wide-field SS-OCTA to better understand vascular abnormalities in early-stage DM patients and promote the early detection and treatment of diabetic retinopathy.

Methods

This retrospective observational study was conducted as per the tenets of the Declaration of Helsinki and approved by the Medical Research and Ethics Committee of Qilu Hospital and Shierming Hospital. Written informed consent was obtained from subjects after explaining the purpose of the study and informing them of the details and any potential risks involved in the study. The study included 46 eyes of healthy controls and 85 eyes of patients with DM. All subjects were treated in the Department of Ophthalmology and Department of endocrinology, Qilu Hospital, Shandong University, and Department of Ophthalmology, Aier Eye Hospital, Jinan, from July 11, 2021 to March 17, 2022.

In this study, we first shortlisted patients with type 2 DM and the healthy control group subjects were matched for age, gender and refractive error distribution. Subjects were divided into the following three groups according to ophthalmoscopy and fundus photography (Patients were grouped according to the eye with more advanced lesions): Group 1, healthy subjects without diabetes;

Group 2, pre-DR patients (Diabetes patients without DR); Group 3, diabetic patients with early-stage DR (DR patients with only microaneurysm). The exclusion criteria were as follows: (1) age ≥ 18 years old; (2) Subjects with serious systemic diseases (tumor, stroke, dementia, etc.); (3) Subjects with diabetic macular edema; (4) History of ocular trauma and other vitreoretinal surgery; (5) Subjects with glaucoma, high myopia (spherical equivalent >= −6.00D), and other ocular conditions that may affect the choroidal and retinal capillaries; (6) Ocular media opacity; (7) Images of low quality (quality index < 6).

The three groups of subjects underwent standardized examinations. Ophthalmic examinations included best-corrected visual acuity (BCVA) and slit lamp bio-microscopy. Demographic data of age, gender, and duration were recorded for all participants. The fasting venous blood samples from all participants were analyzed for biochemical testing of serum glycated hemoglobin (HbA1C).

For OCTA examination, all patients were imaged using a commercial wide-field instrument (VG200, SVision Imaging, Ltd., Luoyang, China) with a 1,050 nm wavelength sweeping laser. All examinations were performed by an experienced ophthalmologist. The SS-OCTA scan was executed with a scanning speed of 200,000 A-scans per second and a wavelength-sweeping laser with a central wavelength of 1050nm. The axial resolution was 5 μm, the lateral resolution was 15 μm, and the scan depth was 3 mm. This equipment possessed eye-tracking technology involving an integrated confocal scanning laser ophthalmoscope to reduce eye-motion artifacts. Choroidal and retinal parameters acquired from wide-field SS-OCTA (including CVI, CT and CMT) were separately calculated in each annular region with built-in software of VG200, SVision Imaging (version 1.32.9.). We measured and automatically calculated the total choroidal area (TCA) and luminal area (LA) of the subjects under the calibration of a retinal specialist (Jianqiao Li). Choroidal vascular index (CVI) is defined as the ratio or proportion of the LA within the TCA (Shown in Figure 1), the ChT is defined as the vertical distance between the outer margin of the RPE-Bruch's complex to the inner border of the choroidoscleral junction, and the CMT is defined as the mean distance in the central 12000-μm diameter area between the vitreoretinal interface and the outer margin of the RPE-Bruch's complex. Besides, we also calculated the differentials of capillaries between different retinochoroid zones and the whole area (the values were calculated as $Circle_{x\text{-}y}$ - average values, and the mean values of each group were shown in Table 1). All measurements were performed by the same ophthalmologist.

Statistical analysis

All statistical analyses in this study were conducted using SPSS software (version 19.0 SPSS, Inc, Chicago, IL, USA). The Kolmogorov-Smirnov test was used for normality testing. Normally-distributed variables were expressed as the mean and standard deviation (SD), and non-parametric variables as the median and interquartile range (IQR). A paired-sample t-test was used to compare the number of patients enrolled, mean ages, durations, VA, Glucose, and Hemoglobin A1C between DM patients and healthy controls. Differences between the healthy controls, pre-DR, and early-stage DR groups were evaluated by generalized estimating equations (GEEs) for binocular data. The correlations between duration and choroidal characteristics were also calculated. A P-value < 0.05 was statistically significant.

Results

General clinical characteristics

A total of 131 eyes from 68 patients were included in the study, with no significant difference in age, sex composition or BCVA among groups (P_s> 0.05). Significant differences were found between the pre-and early-stage DR groups in the duration of DM (9.02 ± 6.09 *vs*. 27.09 ± 13.51 (months)), blood glucose (9.05 ± 7.34 *vs*. 9.61 ± 8.47 (mmol/L)), and glycated hemoglobin (6.31 ± 4.25 *vs*. 8.62 ± 3.49 (%) (Table 1).

Characteristics of the choroid

The choroidal parameter values in each zone for the three groups are shown in Table 2 and Figure 2. Although the mean CVI was lower in patients with pre- and early-stage DR than in healthy controls, a significant difference was only found for patients with early-stage DR (p = 0.013). During subgroup analyses, after stratifying by region, the differences in CVI values in the 9–12 mm range between the pre-DR group and the early-stage DR group decreased significantly compared to the control group (p = 0.016, p < 0.001, respectively). Moreover, ChT values were significantly reduced in the pre-DR group and the early-stage DR group in the 0–3 mm (p = 0.016, p = 0.002, respectively) and 9–12 mm ranges (p = 0.016, p = 0.002, respectively) and the early-stage DR group in the 6-9 mm range (p = 0.015). In addition, no changes were observed in any region except for a significant decrease in CMT in the 9–12 mm region of the early-stage DR group (p = 0.034).

The different parameters in different ranges and the whole area are shown in Table 3 and Figure 3. Compared to each region of the control group, the changes in CVI values were significantly increased in the 0–3 mm, 6–9 mm, and 9–12 mm regions of the pre-DR patients (p = 0.008, p = 0.027, p = 0.032, respectively), and the CVI values were significantly increased in early-stage DR patients in the 0–3 mm and 9–12 mm regions(p = 0.007, p = 0.03, respectively). Besides, the ChT of early-stage DR patients was significantly decreased compared with healthy subjects in 3–6 mm and 9–12 mm zones (p = 0.042, p < 0.001, respectively). Finally, only the CMT in the 9–12 mm zone in the early-stage DR group

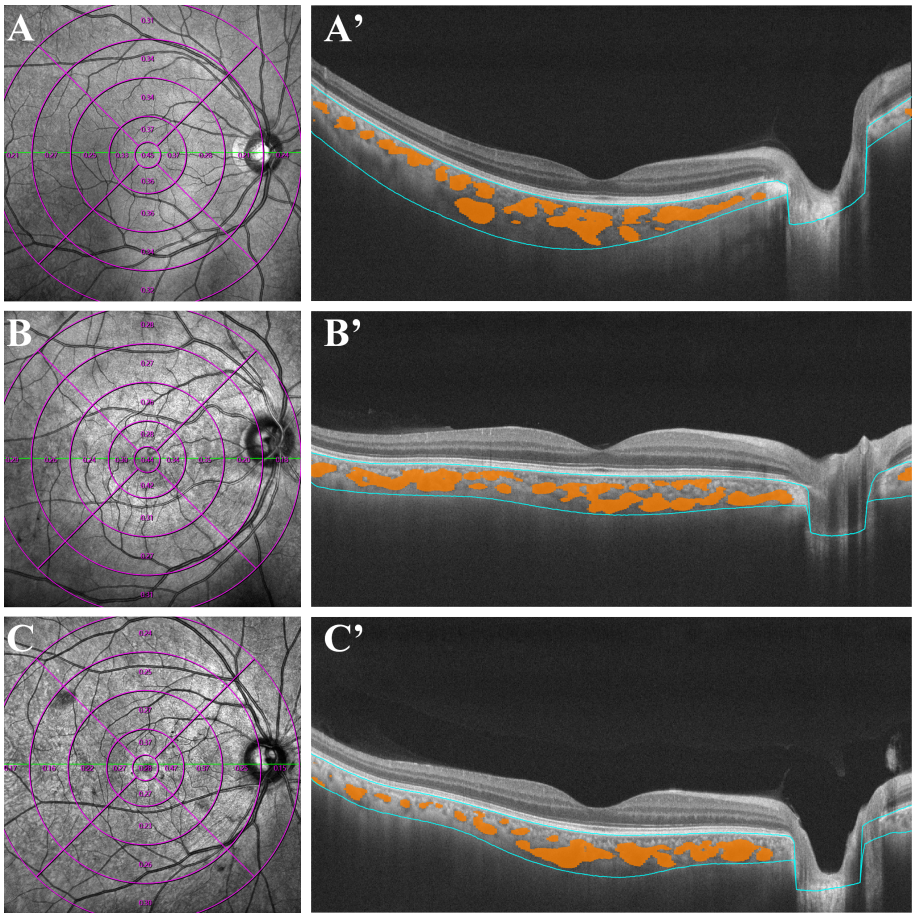

FIGURE 1
Examples of quantitative measurements of CVI using Wide-field OCTA in patients with early-stage DR (C, C'), diabetes mellitus without DR (B, B') and normal control subjects (A, A'). The left column consists of en face infrared (12 ×12 mm) images. The right column represent the optical coherence tomography of the retina and choroid across the fovea, yellow marks represent the choroidal lumen, and the blue lines indicate the upper and lower bounds of the choroid. CVI, choroidal vascularity index; OCTA, optical coherence tomographic angiography.

decreased significantly compared with the healthy control group ($p = 0.014$).

The results of correlation analysis between the duration of DM and choroidal parameters are shown in Table 4. The disease duration in patients with DM was negatively correlated with ChT ($p = 0.047$, correlation coefficient= -0.395; $p = 0.006$, correlation coefficient= -0.549, respectively) and CVI ($p = 0.038$, correlation coefficient= -0.413; $p = 0.004$, correlation coefficient= -0.597, respectively) in 6–9 mm and 9–12mm ranges. Finally, the mean ChT negatively correlated with disease duration ($p = 0.032$, correlation coefficient= -0.420).

Discussion

In this cross-sectional study, wide-field SS-OCTA examinations were performed on three groups (healthy subjects and patients with pre and early-stage DR). To investigate the early changes of choroidal vascular structure in the hyperglycemia environment and to clarify the pathological features of diabetic retinopathy, we assessed CVI, CMT, and ChT of the retinal and choroidal capillaries based on a 12 × 12 mm field of view, as well as the correlations between DM duration and retinochoroid parameters. The CVI and ChT values of DR patients were significantly lower than the healthy control group, and the CVI and ChT values in peripheral areas of DM patients decreased more significantly than those in central regions. However, the CMT outside the 9-12 mm range did not decrease significantly in most areas in DR patients.

Moreover, there was a significant decrease in CVI between the two DM groups and the control group ($p = 0.035$), suggesting that the choroidal perfusion might decrease in DM patients even before the onset of macroscopic retinochoroid lesions. Tan et al. reported that the CVI of the DM group was significantly lower than the control group, while the CVI of the

TABLE 1 Comparison of different retinal and choroidal zones' capillaries changes ($Circle_{x-y}$ - Average ChT, CVI and CMT) in patients with early-stage diabetic retinopathy, DM without DR and non-diabetic individuals from the control group.

	Location	Normal control	DM without DR	p values	Early-stage DR	P values
ChT	Average thickness	287.48 ± 73.67	281.49 ± 50.65	N/A	270.41 ± 86.42	N/A
	Circle 0-3	38.16 ± 23.16	35.21 ± 25.18	p = 0.751	39.05 ± 30.05	p = 0.862
	Circle 3-6	26.47 ± 25.61	22.34 ± 23.82	p = 0.659	35.01 ± 31.28	p = 0.042*
	Circle 6-9	3.32 ± 20.45	-3.62 ± 22.09	p = 0.264	-5.68 ± 28.31	p = 0.083
	Circle 9-12	-20.21 ± 22.08	-26.30 ± 28.57	p = 0.182	-34.89 ± 27.65	p < 0.001*
CVI	Average CVI	0.292 ± 0.068	0.271 ± 0.064	N/A	0.240 ± 0.059	N/A
	Circle 0-3	0.052 ± 0.064	0.068 ± 0.071	p = 0.008*	0.069 ± 0.065	p = 0.007*
	Circle 3-6	0.028 ± 0.055	0.031 ± 0.059	p = 0.530	0.029 ± 0.059	p = 0.865
	Circle 6-9	-0.007 ± 0.061	0.006 ± 0.058	p = 0.027*	-0.009 ± 0.068	p = 0.721
	Circle 9-12	-0.019 ± 0.065	-0.031 ± 0.074	p = 0.032*	-0.038 ± 0.051	p = 0.003*
CMT	Average thickness	264.32 ± 9.45	261.09 ± 13.92	N/A	262.34 ± 10.56	N/A
	Circle 0-3	57.32 ± 11.59	52.08 ± 13.87	p = 0.772	59.66 ± 14.94	p = 0.914
	Circle 3-6	32.08 ± 12.07	28.04 ± 14.84	p = 0.801	26.47 ± 13.78	p = 0.710
	Circle 6-9	4.28 ± 11.67	2.51 ± 12.76	p = 0.482	2.69 ± 17.05	p = 0.517
	Circle 9-12	-9.88 ± 11.20	-11.29 ± 13.27	p = 0.207	-18.64 ± 19.57	p = 0.014*

Values were calculated as $Circle_{x-y}$ - average values and shown as means ± SDs (). DM, diabetes mellitus; DR, diabetic retinopathy; ChT, Choroidal thickness; CVI, Choroidal Vascularity Index; CMT, central macular thickness. Statistical differences were analyzed between the groups of patients with DM and the normal control, $p < 0.05$ indicates a statistically significant difference, annotated with *. NA, not applicable.

TABLE 2 Demographic data of DM patients and healthy controls.

	Normal control	DM without DR	p values	Early-stage DR	P values
Patients (Female)	23 (12)	22 (12)	0.961	23(11)	1.000
Age	55.25 ± 9.65	57.34 ± 10.14	0.812	56.08 ± 12.07	0.873
Eyes	46	43	0.818	42	0.780
Duration of DM (months)	N/A	9.02 ± 6.09	N/A	27.09 ± 13.51	N/A
Spherical equivalent (diopters)	+0.67 ± 0.39	+0.52 ± 0.43	0.783	+0.58 ± 0.46	0.826
VA (letters)	82.09 ± 3.05	82.24 ± 2.02	0.971	82.43 ± 2.07	0.964
GLU (mmol/L)	N/A	9.05 ± 7.34	N/A	9.61 ± 8.47	N/A
HbA1c (%)	N/A	6.31 ± 4.25	N/A	8.62 ± 3.49	N/A

Values are presented as the means ± standard deviations at baseline in different groups. DM, diabetes mellitus; DR, diabetic retinopathy; VA, Visual acuity; in Early Treatment Diabetic Retinopathy Study (ETDRS) units; GLU, Glucose; HbA1c, Hemoglobin A1C. Statistical differences were analyzed between the patients with DM and the normal control, $p < 0.05$ indicates statistically significant difference. NA, not applicable.

DR group was lower than the non-DR group, indicating that the choroidal capillaries in diabetic patients decreased significantly (27), consistent with the present study findings. Another study by Foo, V. H. et al. substantiated that the CVI of Haller's layer in the eyes of pre-DR patients was significantly lower than in healthy controls, suggesting that early diabetic choroidal damages could affect larger choroidal capillaries much earlier (28). Unlike the past studies, the scanning range of wide-field SS-OCTA was expanded to 12 × 12mm with the fovea of the macula as the center in the present study, which

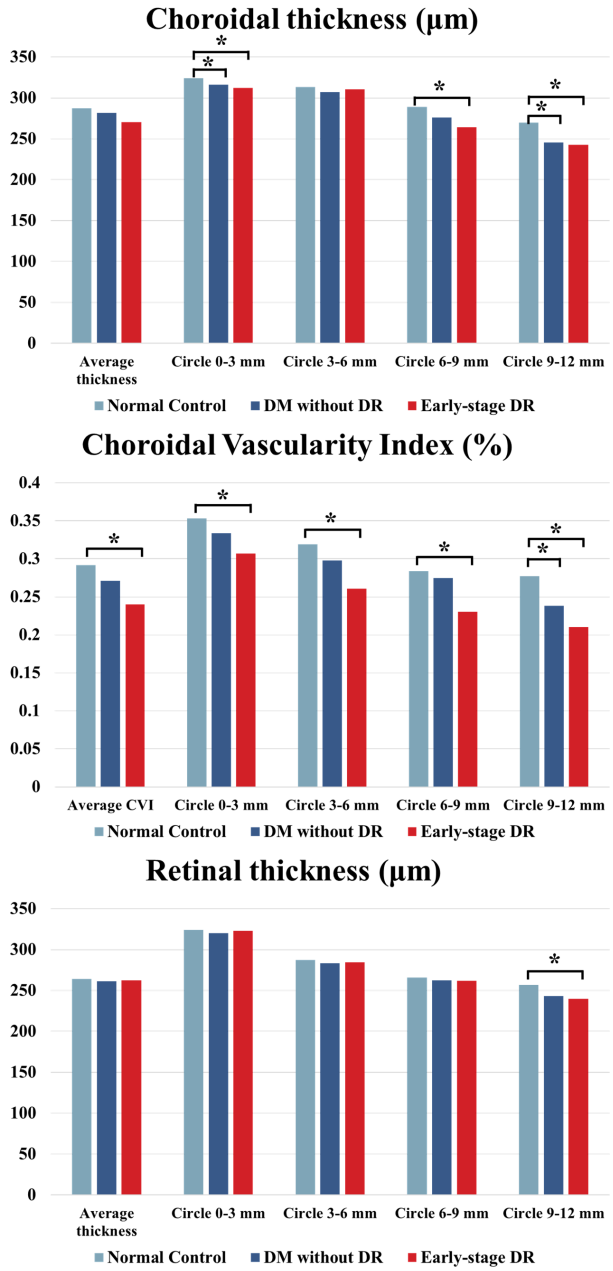

FIGURE 2
ChT, CVI and CMT comparison of patients with early-stage DR, diabetes mellitus without ophthalmoscopic signs of DR and normal control subjects of the control group. * indicates a statistically significant difference ($p < 0.05$).

enables observation of the microcirculation of the peripheral retinochoroid capillaries.

To further explore the structural changes of choroidal capillaries in different areas, the wide-field OCTA images of the three groups were divided into four concentric circles according to the distance from the fovea. The decreases in CVI values within the 9–12 mm circle region were most significant in four concentric circles of the early-stage DR and pre-DR groups, suggesting that the choroidal circulation of peripheral retinochoroid areas was more sensitive to blood

10.3389/fendo.2022.1036625

TABLE 3 Optical coherence tomographical findings in patients with early-stage diabetic retinopathy, diabetes mellitus without DR and normal control group.

	Location	Normal control	DM without DR	p values	Early-stage DR	p values
ChT	Average thickness	287.48 ± 73.67	281.49 ± 50.65	p = 0.654	270.41 ± 86.42	p = 0.210
	Circle 0-3	324.26 ± 92.07	316.25 ± 71.63	p = 0.016*	312.35 ± 120.31	p = 0.002*
	Circle 3-6	313.27 ± 84.78	306.83 ± 62.24	p = 0.542	310.50 ± 107.11	p = 0.784
	Circle 6-9	289.05 ± 77.48	276.24 ± 51.58	p = 0.461	264.28 ± 84.03	p = 0.015*
	Circle 9-12	269.88 ± 65.64	245.37 ± 45.65	p = 0.008*	242.76 ± 75.93	p < 0.001*
CVI	Average CVI	0.292 ± 0.068	0.271 ± 0.064	p = 0.178	0.240 ± 0.059	p = 0.013*
	Circle 0-3	0.353 ± 0.120	0.334 ± 0.100	p = 0.097	0.307 ± 0.099	p = 0.020*
	Circle 3-6	0.319 ± 0.081	0.298 ± 0.080	p = 0.086	0.261 ± 0.075	p = 0.008*
	Circle 6-9	0.284 ± 0.063	0.275 ± 0.062	p = 0.310	0.230 ± 0.056	p = 0.007*
	Circle 9-12	0.277 ± 0.065	0.238 ± 0.062	p = 0.016*	0.210 ± 0.060	p < 0.001*
CMT	Average thickness	264.32 ± 9.45	261.09 ± 13.92	p = 0.863	262.34 ± 10.56	p = 0.716
	Circle 0-3	324.03 ± 14.26	320.01 ± 14.56	p = 0.841	323.05 ± 12.16	p = 0.890
	Circle 3-6	287.31 ± 11.28	283.17 ± 15.16	p = 0.806	284.64 ± 15.08	p = 0.773
	Circle 6-9	265.95 ± 10.16	262.47 ± 12.05	p = 0.754	261.87 ± 17.29	p = 0.681
	Circle 9-12	256.64 ± 10.08	243.12 ± 15.19	p = 0.069	240.08 ± 23.57	p = 0.034*

Values are showed as means ± SDs. DM, diabetes mellitus; DR, diabetic retinopathy; ChT, Choroidal thickness; CVI, Choroidal Vascularity Index; CMT, central macular thickness. Statistical differences were analyzed between the groups of patients with DM and the normal control, $p < 0.05$ indicates statistically significant difference, annotated with *.

glucose changes than the central areas. It is reasonable to speculate that disease progression may begin in peripheral areas, and the choroidal capillaries may be the most seriously affected area. Indeed, the scanning range of OCTA devices was limited to 6 × 6mm in most previous studies, and the wide-field OCTA adopted in our study makes up SS-OCTA makes up for the narrow visual field of traditional OCTA.

An increasing body of evidence suggests that ChT can quantify the structural changes of the choroid. Nonetheless, no consensus has been reached on the changes in ChT in DM patients (29, 30). Querques, G. et al. indicated that ChT of DR patients might decrease (31); however, Kim, J.T. et al. found that the choroidal thickness decreased in the early stages of DR but increased in the stage of severe NPDR or PDR (32). DM is a metabolic disease affecting the retinal and choroidal vasculature. Although the principal changes in diabetic eyes occur in the retinal vasculature, additional changes have been paid more and more attention in recent years. Histologic studies showed increased tortuosity, and the formation of sinuslike structures between the choroidal lobules, what's more, in some advanced cases, luminal narrowing of the capillaries, capillary dropout, and focal scarring were also observed (33). In our study, the ChT between the DR group in the range of 0–3/6–9/9–12 mm decreased significantly (P<0.05) compared with the control group. In addition, the decrease in ChT was more significant in the peripheral area. However, there was no significant difference in CMT between DM patients without DR and healthy control, while only a slight decrease was observed in the peripheral areas of early-stage DR patients. However, the positive result was somewhat accidental in the analysis of CMT. Although there was no significant change in retinal thickness, the choroidal thickness decreased significantly. It can be concluded that CMT is insensitive in the early stage of DR and poorly reflects early damage to the retinal capillaries. Accordingly, choroidal parameters may be more sensitive indicators for patients with pre- and early-stage DR.

In addition, correlation analysis between CVI, ChT and the duration of DR showed a significant negative correlation between CVI and ChT at 6–9 mm and 9–12mm (P<0.05), and a significant correlation was observed at 9–12 mm (P<0.01). A longer DR duration was associated with lower choroidal CVI and ChT values. During the early diagnosis of DR, peripheral CVI and ChT can be used as evaluation indexes, indicating choroidal damage in DM patients without visible pathological

10.3389/fendo.2022.1036625

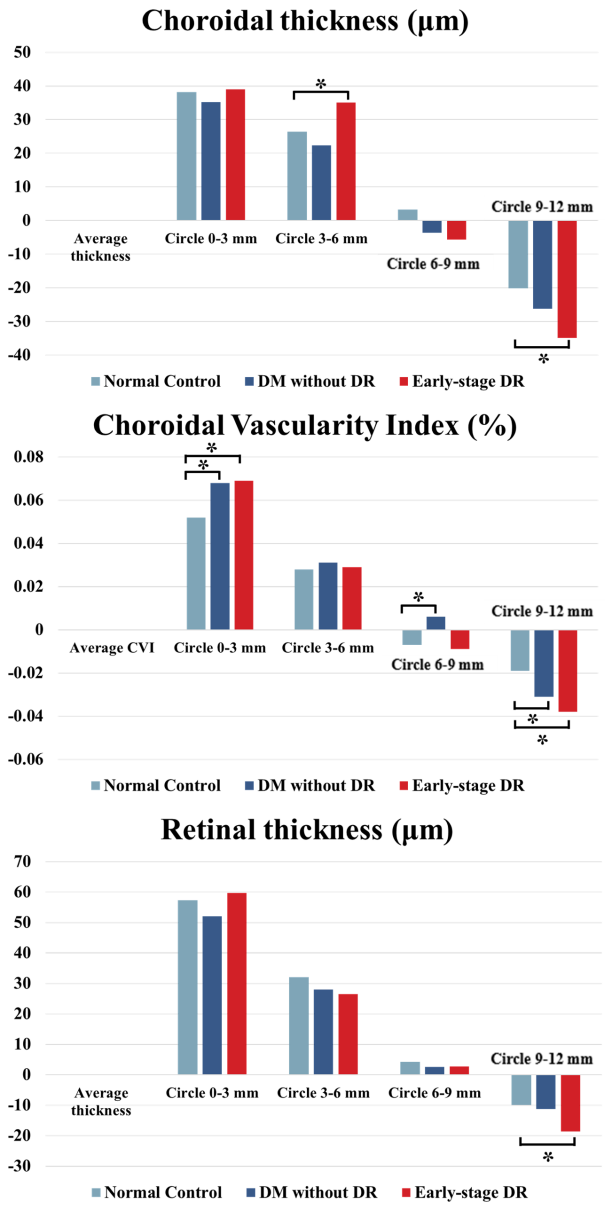

FIGURE 3
ChT, CVI and CMT changes in different fundus zones (Circle$_{x-y}$ *vs.* Average density) in patients with early-stage DR, diabetes mellitus without ophthalmoscopic signs of DR and non-diabetic subjects of the control group. * indicates a statistically significant difference ($p < 0.05$).

retina changes more sensitively. Therefore, wide-field SS-OCTA is a more sensitive and effective tool to evaluate disease progression in DM patients.

Some limitations and shortcomings were present in the current research. First of all, the sample size was small. Indeed, a larger sample size is required in future studies to obtain more reliable and robust results. Besides, patients with proliferative DR should be enrolled to study the relationship between CVI changes and the different stages of DR. Moreover, the cross-section areas studied in the present study do not enable dynamic evaluation of the choroid changes with disease progression. Further longitudinal prospective research is warranted to confirm current results. Finally, hypertension and functional impairment are common in patients with diabetes (34, 35), which may have an

TABLE 4 The correlations between duration and choroidal characteristics in patients with diabetes mellitus.

	Characteristic	Mean values	Correlation coefficient	p values
ChT	Average thickness	276.32 ± 65.29	-0.420	p = 0.032*
	Circle 0-3	313.89 ± 92.05	-0.134	p = 0.236
	Circle 3-6	308.06 ± 88.04	-0.189	p = 0.125
	Circle 6-9	269.96 ± 74.23	-0.395	p = 0.047*
	Circle 9-12	243.86 ± 61.98	-0.549	p = 0.006*
CVI	Average CVI	0.257 ± 0.063	-0.178	p = 0.146
	Circle 0-3	0.321 ± 0.097	-0.057	p = 0.463
	Circle 3-6	0.282 ± 0.083	-0.128	p = 0.216
	Circle 6-9	0.254 ± 0.057	-0.413	p = 0.038*
	Circle 9-12	0.225 ± 0.063	-0.597	p = 0.004*

Values are shown as means ± SDs. ChT, Choroidal thickness; CVI, Choroidal Vascularity Index; $p < 0.05$ indicates a statistically significant difference, annotated with *.

impact on choroidal blood flow, but we did not make a detailed analysis due to the lack of relevant data.

In conclusion, we comprehensively used wide-field SS-OCTA to explore the characteristics of choroidal microcirculation structure in DM patients. The results showed that CVI and ChT decreased significantly, especially in the peripheral area (9-12 mm) in the pre-and early-stage DR groups, which indicates that monitoring of choroidal microcirculation parameters is essential for early diagnosis of DR.

Data availability statement

The raw data supporting the conclusions of this article will be made available by the authors, without undue reservation.

Ethics statement

The studies involving human participants were reviewed and approved by Medical Research and Ethics Committee of Qilu Hospital. The patients/participants provided their written informed consent to participate in this study.

Author contributions

(I) Conception and design: ZnL, FX and JL. (II) Administrative support: SW and JL. (III) Provision of study materials or patients: FX, ZnL and XY. (IV) Collection and assembly of data: ZnL, XY, ZiL and GL. (V) Data analysis and interpretation: FX and ZnL. All authors contributed to the article and approved the submitted version.

Conflict of interest

The authors declare that the research was conducted in the absence of any commercial or financial relationships that could be construed as a potential conflict of interest.

Publisher's note

All claims expressed in this article are solely those of the authors and do not necessarily represent those of their affiliated organizations, or those of the publisher, the editors and the reviewers. Any product that may be evaluated in this article, or claim that may be made by its manufacturer, is not guaranteed or endorsed by the publisher.

References

1. Collaboration NCDRF. Worldwide trends in diabetes since 1980: a pooled analysis of 751 population-based studies with 4.4 million participants. *Lancet* (2016) 387(10027):1513–30. doi: 10.1016/S0140-6736(16)00618-8

2. Danaei G, Finucane MM, Lu Y, Singh GM, Cowan MJ, Paciorek CJ, et al. National, regional, and global trends in fasting plasma glucose and diabetes prevalence since 1980: systematic analysis of health examination surveys and

epidemiological studies with 370 country-years and 2.7 million participants. *Lancet* (2011) 378(9785):31–40. doi: 10.1016/S0140-6736(11)60679-X

3. Wong TY, Cheung CM, Larsen M, Sharma S, Simo R. Diabetic retinopathy. *Nat Rev Dis Primers* (2016) 2:16012. doi: 10.1038/nrdp.2016.12

4. Kastelan S, Oreskovic I, Biscan F, Kastelan H, Gverovic Antunica A. Inflammatory and angiogenic biomarkers in diabetic retinopathy. *Biochem Med (Zagreb)* (2020) 30(3):30502. doi: 10.11613/BM.2020.030502

5. Zhang Y, Xu F, Lin Z, Wang J, Huang C, Wei M, et al. Prediction of visual acuity after anti-VEGF therapy in diabetic macular edema by machine learning. *J Diabetes Res* (2022) 2022:5779210. doi: 10.1155/2022/5779210

6. Rubsam A, Parikh S, Fort PE. Role of inflammation in diabetic retinopathy. *Int J Mol Sci* (2018) 19(4). doi: 10.3390/ijms19040942

7. Nguyen TT, Wong TY. Retinal vascular changes and diabetic retinopathy. *Curr Diabetes Rep* (2009) 9(4):277–83. doi: 10.1007/s11892-009-0043-4

8. Durbin MK, An L, Shemonski ND, Soares M, Santos T, Lopes M, et al. Quantification of retinal microvascular density in optical coherence tomographic angiography images in diabetic retinopathy. *JAMA Ophthalmol* (2017) 135(4):370–6. doi: 10.1001/jamaophthalmol.2017.0080

9. Mendrinos E, Stangos AN, Pournaras CJ. Diabetic retinopathy. *BMJ Clin Evid* (2007) 2007.

10. Wang XN, Li ST, Li W, Hua YJ, Wu Q. The thickness and volume of the choroid, outer retinal layers and retinal pigment epithelium layer changes in patients with diabetic retinopathy. *Int J Ophthalmol* (2018) 11(12):1957–62. doi: 10.18240/ijo.2018.12.14

11. Alves CH, Fernandes R, Santiago AR, Ambrosio AF. Microglia contribution to the regulation of the retinal and choroidal vasculature in age-related macular degeneration. *Cells* (2020) . doi: 10.3390/cells9051217

12. Lu ES, Cui Y, Le R, Zhu Y, Wang JC, Lains I, et al. Detection of neovascularisation in the vitreoretinal interface slab using widefield swept-source optical coherence tomography angiography in diabetic retinopathy. *Br J Ophthalmol Apr* (2022) 106(4):534–9. doi: 10.1136/bjophthalmol-2020-317983

13. Bandello F, Corbelli E, Carnevali A, Pierro L, Querques G. Optical coherence tomography angiography of diabetic retinopathy. *Dev Ophthalmol* (2016) 56:107–12. doi: 10.1159/000442801

14. Saracco JB, Gastaud P, Ridings B, Ubaud CA. [Preliminary study on diabetic choroidopathy]. *Bull Soc Ophtalmol Fr* (1982) 82(3):451–4. Etude preliminaire sur la choroidopathie diabetique.

15. Lutty GA. Diabetic choroidopathy. *Vision Res Oct* (2017) 139:161–7. doi: 10.1016/j.visres.2017.04.011

16. Wang JC, Lains I, Providencia J, Armstrong GW, Santos AR, Gil P, et al. Diabetic choroidopathy: Choroidal vascular density and volume in diabetic retinopathy with swept-source optical coherence tomography. *Am J Ophthalmol* (2017) 184:75–83. doi: 10.1016/j.ajo.2017.09.030

17. Kim M, Ha MJ, Choi SY, Park YH. Choroidal vascularity index in type-2 diabetes analyzed by swept-source optical coherence tomography. *Sci Rep* (2018) 8 (1):70. doi: 10.1038/s41598-017-18511-7

18. Hamadneh T, Aftab S, Sherali N, Vetrivel Suresh R, Tsouklidis N, An M. Choroidal changes in diabetic patients with different stages of diabetic retinopathy. *Cureus* (2020) 12(10):e10871. doi: 10.7759/cureus.10871

19. Hormel TT, Hwang TS, Bailey ST, Wilson DJ, Huang D, Jia Y. Artificial intelligence in OCT angiography. *Prog Retin Eye Res* (2021) 85:100965. doi: 10.1016/j.preteyeres.2021.100965

20. Hormel TT, Jia Y, Jian Y, Hwang TS, Bailey ST, Pennesi ME, et al. Plexus-specific retinal vascular anatomy and pathologies as seen by projection-resolved optical coherence tomographic angiography. *Prog Retin Eye Res* (2021) 80:100878. doi: 10.1016/j.preteyeres.2020.100878

21. Safi H, Safi S, Hafezi-Moghadam A, Ahmadieh H. Early detection of diabetic retinopathy. *Surv Ophthalmol* (2018) 63(5):601–8. doi: 10.1016/j.survophthal.2018.04.003

22. Simonett JM, Scarinci F, Picconi F, Giorno P, De Geronimo D, Di Renzo A, et al. Early microvascular retinal changes in optical coherence tomography angiography in patients with type 1 diabetes mellitus. *Acta Ophthalmol* (2017) 95(8):e751–5. doi: 10.1111/aos.13404

23. Ting DSW, Tan GSW, Agrawal R, Yanagi Y, Sie NM, Wong CW, et al. Optical coherence tomographic angiography in type 2 diabetes and diabetic retinopathy. *JAMA Ophthalmol* (2017) 135(4):306–12. doi: 10.1001/jamaophthalmol.2016.5877

24. Soares M, Neves C, Marques IP, Pires I, Schwartz C, Costa MA, et al. Comparison of diabetic retinopathy classification using fluorescein angiography and optical coherence tomography angiography. *Br J Ophthalmol* (2017) 101 (1):62–8. doi: 10.1136/bjophthalmol-2016-309424

25. Pichi F, Smith SD, Abboud EB, Neri P, Woodstock E, Hay S, et al. Wide-field optical coherence tomography angiography for the detection of proliferative diabetic retinopathy. *Graefes Arch Clin Exp Ophthalmol* (2020) 258(9):1901–9. doi: 10.1007/s00417-020-04773-x

26. Qian Y, Yang J, Liang A, Zhao C, Gao F, Zhang M. Widefield swept-source optical coherence tomography angiography assessment of choroidal changes in vogt-Koyanagi-Harada disease. *Front Med (Lausanne)* (2021) 8:698644. doi: 10.3389/fmed.2021.698644

27. Tan KA, Laude A, Yip V, Loo E, Wong EP, Agrawal R. Choroidal vascularity index - a novel optical coherence tomography parameter for disease monitoring in diabetes mellitus? *Acta Ophthalmol* (2016) 94(7):e612–6. doi: 10.1111/aos.13044

28. Foo VHX, Gupta P, Nguyen QD, Chong CCY, Agrawal R, Cheng CY, et al. Decrease in choroidal vascularity index of haller's layer in diabetic eyes precedes retinopathy. *BMJ Open Diabetes Res Care* (2020) 8(1). doi: 10.1136/bmjdrc-2020-001295

29. Lains I, Talcott KE, Santos AR, Marques JH, Gil P, Gil J, et al. Choroidal thickness in diabetic retinopathy assessed with swept-source optical coherence tomography. *Retina* (2018) 38(1):173–82. doi: 10.1097/IAE.0000000000001516

30. Tavares Ferreira J, Vicente A, Proenca R, Santos BO, Cunha JP, Alves M, et al. Choroidal thickness in diabetic patients without diabetic retinopathy. *Retina* (2018) 38(4):795–804. doi: 10.1097/IAE.0000000000001582

31. Querques G, Lattanzio R, Querques L, Del Turco C, Forte R, Pierro L, et al. Enhanced depth imaging optical coherence tomography in type 2 diabetes. *Invest Ophthalmol Vis Sci* (2012) 53(10):6017–24. doi: 10.1167/iovs.12-9692

32. Kim JT, Lee DH, Joe SG, Kim JG, Yoon YH. Changes in choroidal thickness in relation to the severity of retinopathy and macular edema in type 2 diabetic patients. *Invest Ophthalmol Vis Sci* (2013) 54(5):3378–84. doi: 10.1167/iovs.12-11503

33. Hidayat AA, Fine BS. Diabetic choroidopathy. light and electron microscopic observations of seven cases. *Ophthalmology* (1985) 92(4):512–22. doi: 10.1016/S0161-6420(85)34013-7

34. Peng Q, Hu Y, Huang M, Wu Y, Zhong P, Dong X, et al. Retinal neurovascular impairment in patients with essential hypertension: An optical coherence tomography angiography study. *Invest Ophthalmol Vis Sci* (2020) 61 (8):42. doi: 10.1167/iovs.61.8.42

35. Zeng X, Hu Y, Chen Y, Lin Z, Liang Y, Liu B, et al. Retinal neurovascular impairment in non-diabetic and non-dialytic chronic kidney disease patients. *Front Neurosci* (2021) 15:703898. doi: 10.3389/fnins.2021.703898

frontiers | Frontiers in Endocrinology

TYPE Original Research
PUBLISHED 09 February 2023
DOI 10.3389/fendo.2023.1049326

OPEN ACCESS

EDITED BY
Mohd Imtiaz Nawaz,
Department of Ophthalmology, King Saud University, Saudi Arabia

REVIEWED BY
Yuye Ling,
Shanghai Jiao Tong University, China
Cuixia Dai,
Shanghai Institute of Technology, China
Chi-Xin Du,
Zhejiang University, China

*CORRESPONDENCE
Meixiao Shen
smx77@sohu.com
Chenxiao Wang
chenxiao@eye.ac.cn

†These authors have contributed equally to this work and share first authorship

SPECIALTY SECTION
This article was submitted to Clinical Diabetes, a section of the journal Frontiers in Endocrinology

RECEIVED 20 September 2022
ACCEPTED 24 January 2023
PUBLISHED 09 February 2023

CITATION
Lin Z, Yu H, Shi C, Chen H, Lin G, Shen M and Wang C (2023) Acute hyperglycemia compromises the responses of choroidal vessels using swept-source optical coherence tomography during dark and light adaptations.
Front. Endocrinol. 14:1049326.
doi: 10.3389/fendo.2023.1049326

Acute hyperglycemia compromises the responses of choroidal vessels using swept-source optical coherence tomography during dark and light adaptations

Zhiyang Lin[1†], Huankai Yu[1,2†], Ce Shi[1], Hongling Chen[1], Guangqing Lin[1], Meixiao Shen[1,2*] and Chenxiao Wang[1*]

[1]Eye Hospital and School of Ophthalmology and Optometry, Wenzhou Medical University, Wenzhou, China, [2]Oujiang Laboratory (Zhejiang Lab for Regenerative Medicine, Vision and Brain Health), Eye Hospital, Wenzhou Medical University, Wenzhou, Zhejiang, China

Purpose: To clarify the effects of acute hyperglycemia on the responses of choroidal structural components and vascularity index during light modulation in healthy participants using techniques including image binarization and artificial intelligence (AI) segmentation based on swept-source optical coherence tomography (SS-OCT).

Methods: Twenty-four eyes of 24 healthy participants were imaged at different stages after ambient light, 40 min of dark adaptation, and 5 min of light adaptation in two imaging sessions: control and after receiving 75 g of oral glucose solution. The choroidal structural parameters, including luminal volume (LV), stromal volume (SV), total choroidal volume (TCV), and choroidal vascularity index (CVI) within a 6 mm area were determined using a custom algorithm based on image binarization and AI segmentation of SS-OCT. These measurements were compared among the conditions after adjusting for axial length, age to identify the differences.

Results: In the dark, CVI decreased (-0.36 ± 0.09%) significantly in acute hyperglycemia compared to the control condition. During the transition to ambient light, there was an increasing trend in the choroidal parameters compared with the control experiment. However, only TCV (0.38 ± 0.17 mm^3) and LV (0.27 ± 0.10 mm^3) showed a significant increase at the time point of 5 min after ambient light.

Conclusion: Analysis of choroidal structural parameters and CVI based on SS-OCT images is a potentially powerful method to objectively reflect subtle changes in neurovascular coupling between the choroid and photoreceptor during dark adaptation.

KEYWORDS

hyperglycemia, choroid, choroidal vascularity index (CVI), swept-source optical coherence tomography (SSOCT), dark and light adaptation

Introduction

Rod and cone photoreceptor cells are the most prevalent cells in the retina, and their highest oxygen demand occurs in the dark (1, 2). Accumulating evidence suggests that hyperglycemia is associated with suppression of photoreceptor metabolism and increased consumption of oxygen and glucose (3). As the major blood supply system for photoreceptor cells, the vascular responses of the choroid may be compromised while modulating light adaptation and glucose. A confocal laser Doppler flowmeter study demonstrated decreased choroidal blood flow during dark adaptation in normal human eyes (4). Fuchsjäger-Mayrl et al. also found that choroidal blood flow decreased during dark adaptation and increased during light adaptation (5). Using OCT, Alagoz et al. showed that subfoveal choroidal thickness increased during dark adaptation and decreased during light adaptation (6).In addition, Kwan et al. found that hyperglycemia leads to a complete reversal of dark/light adaptation trends in the vessel density of the inner retinal capillary plexus (7). However, it is unclear whether acute hyperglycemia affects any of the choroidal changes that occur during dark adaptation and transition to light. Determining the effects of acute hyperglycemia on the choroid may improve our understanding of the mechanisms of retinal diseases, including diabetic retinopathy (DR), and help identify novel biomarkers for early diagnosis and treatment.

The advent of SS-OCT allows for more precise, non-invasive imaging of the choroid *in vivo* than SD-OCT (8, 9). The techniques used in the previous studies assess only changes in the choroidal thickness, which includes both lumina and stroma, and it is not clear whether the change is caused by LA or SA. Furthermore, it lacks repeatability, and changes in refractive errors vary significantly with age, sex, and axial length (10). Agrawal et al. first proposed the Niblack image binarization technique (10) to differentiate lumina and stroma and defined the luminal area (LA), stromal area (SA), total choriodal area (TCA), and choroidal vascularity index (CVI) as quantitative parameters to assess choroidal structures through EDI-OCT scans (10). This method has been validated with good reproducibility and also applied in research in many diseases, such as DR (11), central serous chorioretinopathy (CSC) (12), age-related macular degeneration (AMD) (13). Recently, our group developed an AI segmentation combined with Niblack's automatic local threshold to obtain choroid volume parameters (14). Therefore, choroidal structural parameters, including luminal volume (LV), stromal volume (SV), total choroidal volume (TCV), and CVI, defined as the ratio of LV to TCV, may be potential quantitative indicators for characterizing the choroidal response while modulating light adaptation and blood glucose.

In this study, we sought to clarify the effects of acute hyperglycemia on the responses of choroidal structural components and the vascularity index during dark adaptation and transition to ambient light in healthy participants using techniques such as image binarization and AI segmentation based on SS-OCT.

Materials and methods

Twenty-four healthy young adults were recruited from the students and work staff of theWenzhou Medical University. This prospective cross-sectional study was conducted at the Affiliated Eye Hospital of the Wenzhou Medical University. This study was conducted in accordance with the tenets of the Declaration of Helsinki and approved by the Ethics Committee of Wenzhou Medical University (Approval ID. 2022-142-K-111-01). Written informed consent was obtained from all the participants before the examination. Inclusion criteria: All the participants underwent basic ophthalmic examinations performed by experienced ophthalmologists (ZL and HY). The axial length (AL) was measured using Lenstar LS 900 (Haag Streit, Koeniz, Switzerland). BCVA was determined using subjective refraction. All participants were imaged during their working hours (from 8:00 AM to 12:00 AM), and participants with a BCVA of 20/20 or better in the right eye were recruited. The exclusion criteria were ocular diseases affecting best-corrected visual acuity (BCVA) and retinal morphology, systematic diseases, history of ocular surgery and trauma, and relevant ocular treatment.

OCT image acquisition

Only the right eyes of the participants were imaged using SS-OCT (VG200 S, SVision Imaging, Henan, China), as described in detail in our previous studies (8, 9). Briefly, this SS-OCT device had a central wavelength of 1050 nm, axial resolution of 6.3 μm, lateral resolution of 13 μm, speed of 200,000 A-scans/s, and scan depth of 3 mm (8, 9). For the acquisition of SS-OCT structural images, 18 radial scan lines centered on the fovea were obtained. Each scan consisted of 2048 A-lines, had an image width of 12 mm, and was performed at intervals of 10°. Every structural scan was repeated for 16 B-scans to reduce the noise and improve the signal-to-noise ratio. Each layer of the retina and choroid boundaries could be clearly visualized in a single SS-OCT structural image. The total acquisition duration was approximately 3 seconds (Figure 1A).

All the images were visually checked by two experienced ophthalmologists (ZL and HY), and only images with quality scores ≥ 8 and without signs of extensive eye movement and image artifacts were selected for further image analysis.

Imaging protocol

In the control experiment, all participants were instructed to look at a distance for 10 min before the first SS-OCT scan. All the participants underwent OCT imaging of the choroid at ambient level. Subsequently, all the participants underwent dark adaptation by staying in a completely dark room (0 cd/m^2) and wearing a thick eye patch over the right eye for 45 min (15). Each participant was instructed to undergo OCT by moving the eye patch and scanning the choroid around the macula. During imaging, the internal fixation light in the SS-OCT system was turned off to ensure that the eye was still dark adapted (16). The room light was turned on to ambient levels (200 cd/m^2), and participants were instructed to obtain choroid SS-OCT images at three time points (30 s, 2 min, and 5 min) (Figure 2).

In the glucose experiment, baseline blood glucose levels were measured at the same time the next day. Each participant was given 10 min to consume a standard 75 g oral glucose tolerance test solution

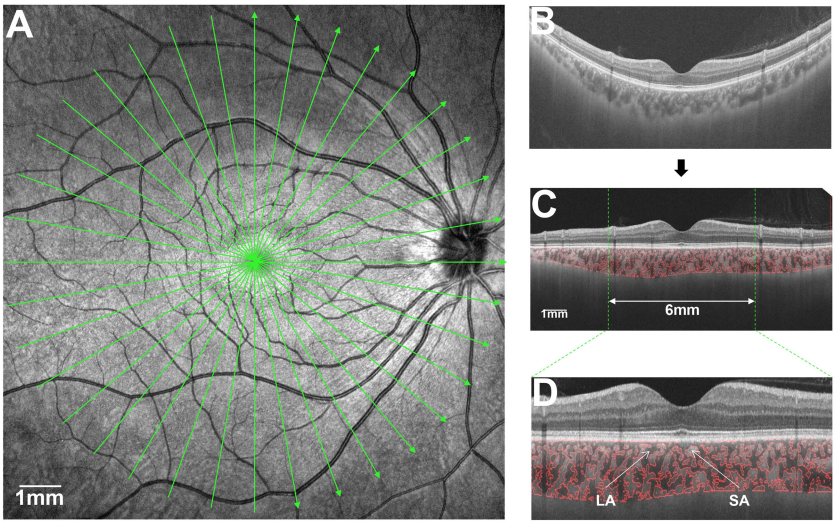

FIGURE 1
Illustration of choroidal analysis. **(A)**, scan range of choroid within 12 mm with 18 radial lines; **(B)**, Raw images of the choroid; **(C)**, Choroidal vascular and stroma image is flattened; **(D)**, Magnified Choroidal vascular and stroma imagein 6 mm.

(17). The participants then underwent dark adaptation and OCT imaging, as described above, and the blood glucose level was measured again after dark adaptation.

The same procedure was used in both the experiments. Before the study, all subjects were instructed not to consume any alcohol (18) or caffeinated drinks (19), refrain from performing workouts for 24 hours (20), and not to consume any food or drinks other than water for 8 hours prior to the experiment.

Image analysis

A custom algorithm based on image binarization and AI segmentation of SS-OCT (14) was used to obtain the choroidal structural parameters and vascularity index, which has been described in detail in our previous studies (9, 21). Briefly, the upper and lower boundaries of the choroid were automatically detected using an algorithm based on the deep learning network implemented in MATLAB 2017a (Mathworks, Inc., Natick, MA, USA). Subsequently, using the Niblack's automatic local threshold technique, the choroidal luminal area and stroma were divided (12, 22). Bennett's formula was used to adjust the magnification of the OCT imaging system camera (23). Before the volumetric measurements of the choroid, the foveal center was manually marked by an experienced ophthalmologist (ZL), and the images were flattened by the reflection of the retinal pigment epithelium to reduce the image tilt angle, which affected the calculation of the anatomical parameters of the choroid. After the reconstruction, the LV, SV, and TCV in the range of 0 – 3 mm, 3 – 6 mm, 0 - 6 mm around the macula were separated and the CVI was derived by calculating the ratio of LV to TCV (Figures 1B–D).

Statistical analysis

All statistical tests were performed using the R software (version 4.1.1). The choroidal structural parameters were compared at each time point in both the control and hyperglycemic conditions using mixed-effects linear regression models to adjust for axial length, age. The paired-samples T test was used to test the changes in choroidal structural parameters after dark adaptation and transition to ambient light. Statistical significance was set at $P < 0.05$. All choroidal structural parameters and the vascularity index are presented as the mean ± standard error.

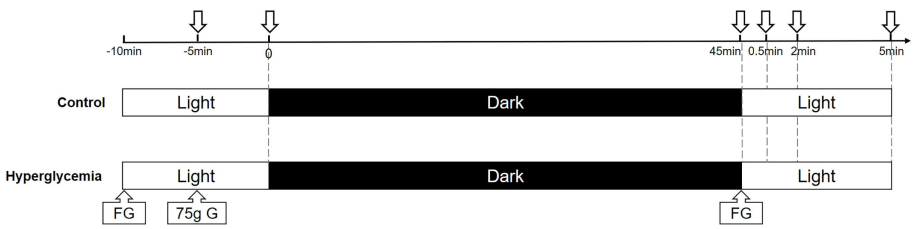

FIGURE 2
A schematic of dark and light adaptation image acquisition. Images were acquired at baseline in ambient light, after 45 min of dark adaptation, and at several time points (30 s, 2 min, 5 min) after transitioning from dark to ambient light in the control and hyperglycemia conditions. FG, finger blood sugar; G, glucose.

Results

Twenty-four right eyes from 24 healthy participants (9 men and 15 women) with a mean age of 25.29 ± 1.91 years were enrolled in this study. At baseline in the control condition experiment, the mean TCV was 26.08 ± 1.30 mm^3. The mean luminal and stromal volumes were 15.34 ± 0.78 mm^3 and 10.74 ± 0.54 mm^3, respectively, which yielded a mean CVI of 58.77 ± 0.29% (Table 1). There was no significant difference in any measurement of the choroidal structural parameters and CVI between the two experiments in the control condition and hyperglycemia at baseline (all $P > 0.05$). Blood sugar levels increased significantly after consumption of the glucose solution ($P < 0.001$) in the hyperglycemia experiment. The basic information of the enrolled participants was shown in (Table 1).

After adjusting for axial length, age, we compared the parameters of the structural choroid in hyperglycemia to those in control conditions. After dark adaptation in the control condition, there was a decreasing trend in the choroidal structural parameters, including LV, SV, and TCV, and an increasing trend of CVI compared to the baseline; in the hyperglycemia condition, all choroidal structural parameters and CVI showed a tendency to decrease (Figure 3). However, only the difference in CVI from light to dark adaptation reached significance between the hyperglycemic and control conditions ($P < 0.001$, Figure 3, Table 2).

With the transition to ambient light, hyperglycemia causes an increase in LV, SV, TCV, and CVI. In the control condition, there was no significant change in any of the choroidal structural parameters and CVI, although it appeared that there was a decreasing trend in the volumes of stroma and lumina, and total choroid described by LV, SV, and TCV at the time point of 5 min of ambient light. In hyperglycemia, LV, SV, TCV, and CVI increased compared to those in the dark. However, only the differences in LV ($P = 0.013$, Figure 4) and TCV ($P = 0.034$, Figure 4) between hyperglycemia and control groups reached significance at the time point of 5 min of ambient light (Table 2). We found similar results in 0– 3 mm and 3 – 6 mm regions (Supplement Tables 1, 2).

TABLE 1 Participants' characteristics.

Characteristic	Value
Number of females, n (%)	15 (62.5)
Age (years)	25.29 ± 1.91
SE (Diopter, D)	-4.41 ± 2.22
AL (mm)	25.47 ± 1.16
Blood glucose, mmol/L	
Pre-oral glucose tolerance test	5.03 ± 0.34
Post-oral glucose tolerance test	7.70 ± 1.48
Change	2.67 ± 1.49*
Choroidal parameters at baseline	Control vs. Hyperglycemia
LV (mm^3)	15.34 ± 0.72 vs. 15.32 ± 0.66
SV (mm^3)	10.74 ± 0.50 vs. 10.72 ± 0.46
TCV (mm^3)	26.08 ± 1.21 vs. 26.04 ± 1.11
CVI (%)	58.77 ± 0.27 vs. 58.81 ± 0.28

*: $P<0.05$.

Discussion

Since Agrawal et al. first proposed the Niblack image binarization technique for EDI-OCT images, the choroid can be differentiated into luminal and stromal components (10, 14). Through the acquisition of more detailed information on the choroidal structures using the deep-learning-based automatic segmentation and modified image binarization technique, our study demonstrated the effect of acute hyperglycemia on the choroidal components and CVI while modulating light adaptation in healthy participants. Under hyperglycemia in the dark, LV and TCV showed a decreasing trend, and CVI decreased compared to the control, although only CVI reached significance. This suggests that an eye with hyperglycemia was likely to exhibit a decreased range of reaction in lumina and a smaller reaction in stroma during darkness, likely underlying the observed decrease in CVI.

In darkness, the metabolic needs of the photoreceptors reach their peak (1, 2) in the absence of autoregulation of the choroidal vasculature. The photoreceptors residing in the zone where both the choroidal and retinal circulations provide oxygen support (24). F Scarinci et al. found that macular photoreceptor disruption in patients with diabetic retinopathy corresponds to areas of capillary non-perfusion at deep capillary plexus (DCP) using OCT/OCTA. This demonstrates that DCP ischemia contributes to disruption of the photoreceptor layers (25). As shown in another study (7), in the dark, there was a decrease in DCP in hyperglycemia. Previous studies had shown that photoreceptor metabolism induced physiological hypoxia in the retina (26) and this episode induced retinal glial cells to express the hypoxia-inducible vascular endothelial growth factor (VEGF) (27, 28).Furthermore, Saint-Geniez M et al. found that VEGF signaling was involved in the maintenance of the choriocapillaris, which might affect choroidal blood flow change (29).Therefore, during dark adaptation, photoreceptors were exposed to a relatively hypoxia environment due to metabolic demands. We speculated that VEGF secreted by retinal glial cells was received by choriocapillaris, resulting in increased in choroidal blood flow in normal subjects to meet the oxygen consumption of photoreceptors. Thus, the finding of significantly decreased CVI with hyperglycemia in the dark may further lead to relative photoreceptor hypoxia, which requires further validation of this concept.With transition to ambient light, LV, TCV, and CVI increased in hyperglycemia compared to the control, and only the increased LV and TCV reached a significant change. There were no significant differences in CVI between the hyperglycemia and control conditions. This suggests that hyperglycemia mainly causes vasodilatation of choroidal lumina during transition to ambient light. Several studies have shown that hyperglycemia decreases blood flow in the choroid (30, 31). Based on this evidence, we speculated that during hyperglycemia, choroidal LV increases in the face of overall decreased flow, which could indicate a reactive vasodilator response at the choroidal lumina in response to the overall decreased flow. This needs to be validated in future studies.

To the best of our knowledge, this is the first study to explore the effects of acute hyperglycemia on choroidal structural components and

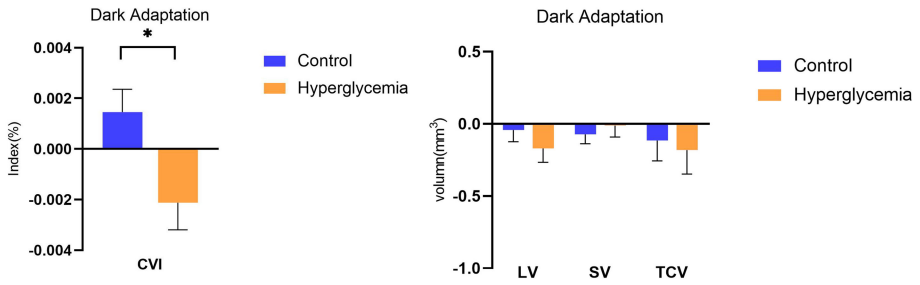

FIGURE 3
Difference in choroidal parameters between the glucose condition and control during dark adaption. Asterisks represent a significant difference between hyperglycemia and control (P < 0.05). CVI, choroidal vascular index; SV, stromal volume; TCV, total choroidal volume; LV, luminal volume.

TABLE 2 Mean differences in choroidal parameters change between glucose and control conditions during light modulation.

		Light Adaption		
	Dark Adaption	30 secs	2 min	5 min
Parameter				
TCV (mm^3)	-0.07 ± 0.15	0.18 ± 0.14	0.25 ± 0.17	0.38 ± 0.17*
P value	0.655	0.197	0.161	0.034
LV (mm^3)	-0.13 ± 0.08	0.12 ± 0.08	0.20 ± 0.10	0.27 ± 0.10*
P value	0.135	0.137	0.069	0.013
SV (mm^3)	0.06 ± 0.08	0.06 ± 0.08	0.05 ± 0.08	0.11 ± 0.08
P value	0.443	0.435	0.556	0.187
CVI (%)	-0.36 ± 0.09*	-0.09 ± 0.33	-0.14 ± 0.33	-0.11 ± 0.33
P value	<0.001	0.453	0.099	0.230

Mean difference (glucose – control) ± SE.
TCV, total choroidal volume; LV, luminal volume; SV, stromal volume; CVI, choroidal vascularity index.
*: P<0.05.

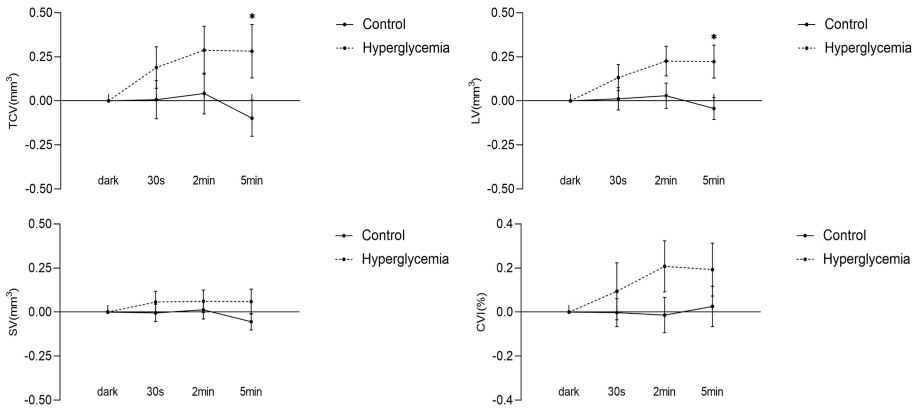

FIGURE 4
Difference in choroidal parameters between the glucose condition and control during light adaption. Asterisks represent a significant difference between hyperglycemia and control (P < 0.05). CVI, choroidal vascular index; SV, stromal volume; TCV, total choroidal volume; LV, luminal volume.

vascularity index while modulating light adaptation and glucose levels in healthy subjects. Current evidence suggests that acute hyperglycemia affects the response of the choroid vessels during dark/light adaptation. These findings could have important implications for DR. Changes in the underlying choroidal vasculature may contribute to the pathophysiology of DR. Choroidal vascular degeneration, choroidal aneurysms, choriocapillaris dropout, choroidal neovascularization, blood flow change, and increased tortuosity and narrowing of the

vessels were evident in previous histopathological and animal studies in diabetic (32, 33). A previous study by our group demonstrated that choroidal thickness decreased in the eyes with no DR and in the eyes with mild to moderate NPDR (34). In addition to the choroidal thickness, CVI also decreases at the early stage of DR (11, 35, 36). Damian et al. showed that an increase in RPE thickness, which points to compromised function of the outer retinal layers, was associated with CVI in the eyes with DR (37). Based on these research evidences, we assume that the decreased changes in choroidal vascularity with hyperglycemia in the dark observed in the current study, may leave photoreceptor cells extremely vulnerable to ischemia in disease states such as DR, where the choroidal vessels are already pathologically compromised. Our results suggest that hyperglycemia, especially at night, may exacerbate these metabolic deficits. This hypothesis needs to be verified in future studies through exploring the effects of acute hyperglycemia on CVI and its association with dark adaptometry function in patients with DR.

This study had several limitations. First, it might be considered a limitation that the study did not include different age group or non-myopic population and a lack of flicker stimuli. However, the main purpose of the current study was to investigate the effect of acute hyperglycemia on choroidal structural components and vascularity index while modulating light adaptation in heathy subjects. We used the same group of normal individuals to compare the changes under the two conditions. So, the main results might not be influenced by the sample selection. Nevertheless, because of the limited range of healthy population, the effect of aging (38) or elongation of axial length could not be evaluated. More participants are necessary to explore the effects of aging, elongation of axial length on the response of choroidal structural components and vascularity index. Future studies using a built-in flicker stimulus based on a larger sample size could also provide better insight into the choroidal vascular response to flicker stimulation. Second, this study was also limited by the algorithm used to analyze the choroidal capillaries, which has not yet been investigated. Finally, blood pressure, intraocular pressure, and other physiological variables that could affect the choroidal structures and CVI were not measured in this study. Nevertheless, our study mainly focused on the response of choroidal components, including the lumina and stroma, during dark and light adaptations. We also adjusted for some main factors, including axial length and age, which are known to affect the parameters of choroidal structure components.

In summary, we found that acute hyperglycemia caused a significant decrease in CVI in the dark, which may leave photoreceptors more susceptible to ischemia, especially in disease states where choroid vascularity is compromised. During the transition to ambient light, there was a significant increase in choroidal lumen volume compared with that in the control experiment. These findings suggest that glucose compromises choroidal vascularity. Additional studies are necessary to explore how these findings translate to individuals with diabetes. Analysis of choroidal structural parameters and CVI based on SS-OCT images may be a potentially powerful method to objectively reflect subtle changes in the neurovascular coupling between the choroid and photoreceptor during dark adaptation. Further studies with a longitudinal study design are needed to test choroidal vascular changes in individuals likely to experience a wide range of glucose fluctuations and in patients with diabetes.

Data availability statement

The raw data supporting the conclusions of this article will be made available by the authors, without undue reservation.

Ethics statement

The studies involving human participants were reviewed and approved by the Ethics Committee of Wenzhou Medical University. The patients/participants provided their written informed consent to participate in this study.

Author contributions

ZL, HY, CS, MS, and CW contributed to the study design. ZL and HY contributed to the data collection. ZL, HY, CS, HC and GL contributed to the data analysis and interpretation. ZL, HY, CS, MS, and CW contributed to the manuscript preparation. ZL and HY contributed equally to this work and share first authorship. All authors contributed to the article and approved the submitted version.

Funding

This research was supported by Zhejiang Provincial Natural Science Foundation of China under Grant No. LGF22H120016 and Key R&D Program Projects in Zhejiang Province (2021C03053) and National Natural Science Foundation of China (Grant No. 82171016).

Acknowledgments

The authors thank all the subjects who took part in the study. We would like to thank Editage (www.editage.com) for English language editing.

Conflict of interest

The authors declare that the research was conducted in the absence of any commercial or financial relationships that could be construed as a potential conflict of interest.

Publisher's note

Supplementary material

The Supplementary Material for this article can be found online at: https://www.frontiersin.org/articles/10.3389/fendo.2023.1049326/full#supplementary-material

References

1. Linsenmeier RA, Goldstick TK, Blum RS, Enroth-Cugell C. Estimation of retinal oxygen transients from measurements made in the vitreous humor. *Exp Eye Res* (1981) 32:369–79. doi: 10.1016/s0014-4835(81)80016-4

2. Nickla DL, Wallman J. The multifunctional choroid. *Prog Retinal Eye Res* (2010) 29:144–68. doi: 10.1016/j.preteyeres.2009.12.002

3. Rowan S, Jiang S, Korem T, Szymanski J, Chang ML, Szelog J, et al. Involvement of a gut-retina axis in protection against dietary glycemia-induced age-related macular degeneration. *Proc Natl Acad Sci U S A* (2017) 114:E4472–e4481. doi: 10.1073/pnas.1702302114

4. Longo A, Geiser M, Riva CE. Subfoveal choroidal blood flow in response to light-dark exposure. *Invest Ophthalmol Visual Sci* (2000) 41:2678–83.

5. Fuchsjäger-Mayrl G, Polska E, Malec M, Schmetterer L. Unilateral light-dark transitions affect choroidal blood flow in both eyes. *Vision Res* (2001) 41:2919–24. doi: 10.1016/s0042-6989(01)00171-7

6. Alagöz C, Pekel G, Alagöz N, Sayın N, Yüksel K, Yıldırım Y, et al. Choroidal thickness, photoreceptor thickness, and retinal vascular caliber alterations in dark adaptation. *Curr Eye Res* (2016) 41:1608–13. doi: 10.3109/02713683.2015.1135961

7. Kwan CC, Lee HE, Schwartz G, Fawzi AA. Acute hyperglycemia reverses neurovascular coupling during dark to light adaptation in healthy subjects on optical coherence tomography angiography. *Invest Ophthalmol Visual Sci* (2020) 61:38. doi: 10.1167/iovs.61.4.38

8. Wu H, Xie Z, Wang P, Liu M, Wang Y, Zhu J, et al. Differences in retinal and choroidal vasculature and perfusion related to axial length in pediatric anisomyopes. *Invest Ophthalmol Visual Sci* (2021) 62:40. doi: 10.1167/iovs.62.9.40

9. Wu H, Zhang G, Shen M, Xu R, Wang P, Guan Z, et al. Assessment of choroidal vascularity and choriocapillaris blood perfusion in anisomyopic adults by SS-OCT/OCTA. *Invest Ophthalmol Visual Sci* (2021) 62:8. doi: 10.1167/iovs.62.1.8

10. Agrawal R, Gupta P, Tan KA, Cheung CM, Wong TY, Cheng CY. Choroidal vascularity index as a measure of vascular status of the choroid: Measurements in healthy eyes from a population-based study. *Sci Rep* (2016) 6:21090. doi: 10.1038/srep21090

11. Kim M, Ha MJ, Choi SY, Park YH. Choroidal vascularity index in type-2 diabetes analyzed by swept-source optical coherence tomography. *Sci Rep* (2018) 8:70. doi: 10.1038/s41598-017-18511-7

12. Agrawal R, Chhablani J, Tan KA, Shah S, Sarvaiya C, Banker A. CHOROIDAL VASCULARITY INDEX IN CENTRAL SEROUS CHORIORETINOPATHY. *Retina* (2016) 36:1646–51. doi: 10.1097/iae.0000000000001040

13. Invernizzi A, Benatti E, Cozzi M, Erba S, Vaishnavi S, Vupparaboina KK, et al. Choroidal structural changes correlate with neovascular activity in neovascular age related macular degeneration. *Invest Ophthalmol Visual Sci* (2018) 59:3836–41. doi: 10.1167/iovs.18-23960

14. Zheng G, Jiang Y, Shi C, Miao H, Yu X, Wang Y, et al. Deep learning algorithms to segment and quantify the choroidal thickness and vasculature in swept-source optical coherence tomography images. *J Innov Opt Heal Sci* (2021) 14(01):2140002. doi: 10.1142/s1793545821400022

15. Lamb TD, Pugh ENJr. Dark adaptation and the retinoid cycle of vision. *Prog Retinal Eye Res* (2004) 23:307–80. doi: 10.1016/j.preteyeres.2004.03.001

16. Tomasso L, Benatti L, Carnevali A, Mazzaferro A, Baldin G, Querques L, et al. Photobleaching by spectralis fixation target. *JAMA Ophthalmol* (2016) 134:1060–2. doi: 10.1001/jamaophthalmol.2016.2283

17. Klefter ON, Vilsbøll T, Knop FK, Larsen M. Retinal vascular and structural dynamics during acute hyperglycaemia. *Acta Ophthalmol* (2015) 93:697–705. doi: 10.1111/aos.12797

18. Kang HM, Woo YJ, Koh HJ, Lee CS, Lee SC. The effect of consumption of ethanol on subfoveal choroidal thickness in acute phase. *Br J Ophthalmol* (2016) 100:383–8. doi: 10.1136/bjophthalmol-2015-306969

19. Vural AD, Kara N, Sayin N, Pirhan D, Ersan HB. Choroidal thickness changes after a single administration of coffee in healthy subjects. *Retina* (2014) 34:1223–8. doi: 10.1097/iae.0000000000000043

20. Sayin N, Kara N, Pekel G, Altinkaynak H. Choroidal thickness changes after dynamic exercise as measured by spectral-domain optical coherence tomography. *Indian J Ophthalmol* (2015) 63:445–50. doi: 10.4103/0301-4738.159884

21. Chen S, Zheng G, Yu X, Jiang Y, Lin Z, Lin G, et al. Impact of penetration and image analysis in optical coherence tomography on the measurement of choroidal vascularity parameters. *Retina* (2022) 42:1965–74. doi: 10.1097/iae.0000000000003547

22. Sonoda S, Sakamoto T, Yamashita T, Uchino E, Kawano H, Yoshihara N, et al. Luminal and stromal areas of choroid determined by binarization method of optical coherence tomographic images. *Am J Ophthalmol* (2015) 159:1123–1131.e1121. doi: 10.1016/j.ajo.2015.03.005

23. Ye J, Shen M, Huang S, Fan Y, Yao A, Pan C, et al. Visual acuity in pathological myopia is correlated with the photoreceptor myoid and ellipsoid zone thickness and affected by choroid thickness. *Invest Ophthalmol Visual Sci* (2019) 60:1714–23. doi: 10.1167/iovs.18-26086

24. Nesper PL, Lee HE, Fayed AE, Schwartz GW, Yu F, Fawzi AA. Hemodynamic response of the three macular capillary plexuses in dark adaptation and flicker stimulation using optical coherence tomography angiography. *Invest Ophthalmol Visual Sci* (2019) 60:694–703. doi: 10.1167/iovs.18-25478

25. Scarinci F, Nesper PL, Fawzi AA. Deep retinal capillary nonperfusion is associated with photoreceptor disruption in diabetic macular ischemia. *Am J Ophthalmol* (2016) 168:129–38. doi: 10.1016/j.ajo.2016.05.002

26. Stone J, Itin A, Alon T, Pe'er J, Gnessin H, Chan-Ling T, et al. Development of retinal vasculature is mediated by hypoxia-induced vascular endothelial growth factor (VEGF) expression by neuroglia. *J Neurosci: Off J Soc Neurosci* (1995) 15:4738–47. doi: 10.1523/jneurosci.15-07-04738.1995

27. Shweiki D, Itin A, Soffer D, Keshet E. Vascular endothelial growth factor induced by hypoxia may mediate hypoxia-initiated angiogenesis. *Nature* (1992) 359:843–5. doi: 10.1038/359843a0

28. Stone J, Maslim J, Valter-Kocsi K, Mervin K, Bowers F, Chu Y, et al. Mechanisms of photoreceptor death and survival in mammalian retina. *Prog Retinal Eye Res* (1999) 18:689–735. doi: 10.1016/s1350-9462(98)00032-9

29. Saint-Geniez M, Maldonado AE, D'Amore PA. VEGF expression and receptor activation in the choroid during development and in the adult. *Invest Ophthalmol Visual Sci* (2006) 47:3135–42. doi: 10.1167/iovs.05-1229

30. Braun RD, Wienczewski CA, Abbas A. Erythrocyte flow in choriocapillaris of normal and diabetic rats. *Microvasc Res* (2009) 77:247–55. doi: 10.1016/j.mvr.2009.02.003

31. Muir ER, Rentería RC, Duong TQ. Reduced ocular blood flow as an early indicator of diabetic retinopathy in a mouse model of diabetes. *Invest Ophthalmol Visual Sci* (2012) 53:6488–94. doi: 10.1167/iovs.12-9758

32. Hidayat AA, Fine BS. Diabetic choroidopathy. light and electron microscopic observations of seven cases. *Ophthalmology* (1985) 92:512–22. doi: 10.1016/S0161-6420(85)34013-7

33. Lutty GA, McLeod DS. Phosphatase enzyme histochemistry for studying vascular hierarchy, pathology, and endothelial cell dysfunction in retina and choroid. *Vision Res* (2005) 45:3504–11. doi: 10.1016/j.visres.2005.08.022

34. Chen Q, Tan F, Wu Y, Zhuang X, Wu C, Zhou Y, et al. Characteristics of retinal structural and microvascular alterations in early type 2 diabetic patients. *Invest Ophthalmol Visual Sci* (2018) 59:2110–8. doi: 10.1167/iovs.17-23193

35. Gupta C, Tan R, Mishra C, Khandelwal N, Raman R, Kim R, et al. Choroidal structural analysis in eyes with diabetic retinopathy and diabetic macular edema-a novel OCT based imaging biomarker. *PloS One* (2018) 13:e0207435. doi: 10.1371/journal.pone.0207435

36. Kim M, Choi SY, Park Y-H. Quantitative analysis of retinal and choroidal microvascular changes in patients with diabetes. *Sci Rep-Uk* (2018) 8:12146. doi: 10.1038/s41598-018-30699-w

37. Damian I, Roman G, Nicoară SD. Analysis of the choroid and its relationship with the outer retina in patients with diabetes mellitus using binarization techniques based on spectral-domain optical coherence tomography. *J Clin Med* (2021) 10(2):210. doi: 10.3390/jcm10020210

38. Zhou H, Dai Y, Shi Y, Russell JF, Lyu C, Noorikolouri J, et al. Age-related changes in choroidal thickness and the volume of vessels and stroma using swept-source OCT and fully automated algorithms. *Ophthalmol Retina* (2020) 4:204–15. doi: 10.1016/j.oret.2019.09.012

frontiers | Frontiers in Endocrinology

TYPE Original Research
PUBLISHED 20 February 2023
DOI 10.3389/fendo.2023.1111360

OPEN ACCESS

EDITED BY
Mohd Imtiaz Nawaz,
Department of Ophthalmology, King Saud University, Saudi Arabia

REVIEWED BY
Salvatore Di Lauro,
Hospital Clínico Universitario de Valladolid, Spain
Kai Shi,
First Affiliated Hospital of Chongqing Medical University, China
Li Kaiming,
The Affiliated Hospital of Southwest Medical University, China

*CORRESPONDENCE
Jie Zhong
zhongjie@med.uestc.edu.cn
Jie Li
lijieyk@med.uestc.edu.cn

†These authors have contributed equally to this work and share first authorship

SPECIALTY SECTION
This article was submitted to Clinical Diabetes, a section of the journal Frontiers in Endocrinology

RECEIVED 29 November 2022
ACCEPTED 06 February 2023
PUBLISHED 20 February 2023

CITATION
Li M, Mao M, Wei D, Liu M, Liu X, Leng H, Wang Y, Chen S, Zhang R, Zeng Y, Wang M, Li J and Zhong J (2023) Different scan areas affect the detection rates of diabetic retinopathy lesions by high-speed ultra-widefield swept-source optical coherence tomography angiography. *Front. Endocrinol.* 14:1111360. doi: 10.3389/fendo.2023.1111360

Different scan areas affect the detection rates of diabetic retinopathy lesions by high-speed ultra-widefield swept-source optical coherence tomography angiography

Mengyu Li[1,2,3†], Mingzhu Mao[1,2,4†], Dingyang Wei[1,2,4], Miao Liu[1,2,3], Xinyue Liu[1,2,3], Hongmei Leng[1,2,4], Yiya Wang[1,2,4], Sizhu Chen[1,2,3], Ruifan Zhang[1,2], Yong Zeng[1,2], Min Wang[5], Jie Li[1,2*] and Jie Zhong[1,2*]

[1]Department of Ophthalmology, Sichuan Provincial People's Hospital, University of Electronic Science and Technology of China, Chengdu, China, [2]Department of Ophthalmology, Chinese Academy of Sciences Sichuan Translational Medicine Research Hospital, Chengdu, China, [3]Eye School, Chengdu University of Traditional Chinese Medicine, Chengdu, China, [4]School of Medicine, University of Electronic Science and Technology of China, Chengdu, China, [5]Department of Ophthalmology, Dayi Shaoxiang Hospital, Chengdu, China

Introduction: The study aimed to determine the effect of the scanning area used for high-speed ultra-widefield swept-source optical coherence tomography angiography (SS-OCTA) on the detection rate of diabetic retinopathy (DR) lesions.

Methods: This prospective, observational study involved diabetic patients between October 2021 and April 2022. The participants underwent a comprehensive ophthalmic examination and high-speed ultra-widefield SS-OCTA using a 24 mm × 20 mm scanning protocol. A central area denoted as "12 mm × 12 mm-central" was extracted from the 24 mm × 20 mm image, and the remaining area was denoted as "12 mm~24mm-annulus." The rates of detection of DR lesions using the two scanning areas were recorded and compared.

Results: In total, 172 eyes (41 eyes with diabetes mellitus without DR, 40 eyes with mild to moderate non-proliferative diabetic retinopathy (NPDR), 51 eyes with severe NPDR, and 40 eyes with proliferative diabetic retinopathy (PDR) from 101 participants were included. The detection rates of microaneurysms (MAs), intraretinal microvascular abnormalities (IRMAs), and neovascularization (NV) for the 12 mm × 12 mm central and 24 mm × 20 mm images were comparable ($p > 0.05$). The detection rate of NPAs for the 24 mm × 20 mm image was 64.5%, which was significantly higher than that for the 12 mm × 12 mm central image (52.3%, $p < 0.05$). The average ischemic index (ISI) was 15.26% for the 12 mm~24mm-annulus, which was significantly higher than that for the 12 mm ×

12 mm central image (5.62%). Six eyes had NV and 10 eyes had IRMAs that only existed in the 12 mm~24mm-annulus area.

Conclusions: The newly developed high-speed ultra-widefield SS-OCTA can capture a 24 mm × 20 mm retinal vascular image during a single scan, which improves the accuracy of detecting the degree of retinal ischemia and detection rate of NV and IRMAs.

KEYWORDS

diabetic retinopathy, microaneurysms, intraretinal microvascular abnormalities, retinal neovascularization, swept-source optical coherence tomography angiography, capillary non-perfusion areas

1 Introduction

Diabetic retinopathy (DR), one of the most common microvascular complications of diabetes, is among the main causes of vision loss among the working-age population globally. Several meta-analyses have predicted that the global prevalence of diabetes will be 600–700 million people in the next two decades (1, 2). Another study reported an estimated prevalence of 34.6% for all forms of DR and 7.0% for proliferative DR (PDR) (3). PDR is the leading cause of vision loss and preventable blindness in the working-age population.

Within the past decade, several novel imaging technologies have been developed for screening and diagnosing DR. These include laser scanning fundus imaging and swept-source optical coherence tomography angiography (SS-OCTA). As a noninvasive alternative, SS-OCTA has been used in examinations for retinal neovascular diseases including DR. Previous studies have demonstrated that OCTA can detect vascular lesions in DR, such as microaneurysms (MAs), intraretinal microvascular abnormalities (IRMAs), neovascularization (NV), capillary non-perfusion areas (NPAs), hard exudates (HEs), and diabetic macular edema (DME) (4–6).

However, most of the commonly used commercial SS-OCTA devices used in previous studies had a scan area of 12 mm × 12 mm or less centered on the fovea by a single scan. Due to the limitation of the range of observation, clinically significant information outside the scan area may not be captured. Several studies have reported that the imaging area can be increased by stitching images together after multiple scans or adding dioptric lenses to expand the field of view (FOV) (7–10). However, these scanning protocols or techniques required longer durations of acquisition and may introduce more artifacts (8, 10).

The recently developed TowardPi high-speed ultra-widefield SS-OCTA systems have an A-scan rate of 400 kHz (BMizar), which can capture an area of 24 mm × 20 mm (about 120° FOV) in a single scan. In this study, we used the latest high-speed ultra-widefield SS-OCTA to obtain a 24 mm × 20 mm retinal blood flow image and compared its detection of DR lesions detection with a relatively narrower 12 mm × 12 mm image.

2 Methods

2.1 Participants

This prospective observational study involved patients with DR or diabetes mellitus recruited from the ophthalmic outpatient department of Sichuan Provincial People's Hospital from October 2021 to April 2022. A total of 172 eyes from 101 participants were included; the participants were 56.50 ± 10.58 (25–86) years old. The durations of diabetes (since diagnosis) among the participants ranged from 1 month to 32 years (Table 1). This study was approved by the Ethics Committee of Sichuan Provincial People's Hospital. Informed consent was obtained from the patients before the examination. All procedures were conducted following the guidelines of the Declaration of Helsinki.

2.2 Inclusion and exclusion criteria

The inclusion criterion was diabetes mellitus diagnosed with or without DR. The exclusion criteria were as follows: uncooperative patients with extremely poor visual acuity or inability to fix the bulbus oculi and severe opacity of the refractive media; vitreoretinopathy caused by other eye diseases; complications other than hypertension, dyslipidemia, and abnormal renal function; intraocular surgery other than for cataracts; poor images, including images with a system built-in automatic quality score below 6/10 (5), images with severe motion artifacts preventing accurate analysis, and blurry images (11); and opacities of the refractive media affecting more than 30% of OCTA images (Supplementary SFig. 1) (12).

2.3 Examination procedure

All patients underwent a comprehensive ophthalmic examination, including best-corrected visual acuity, intraocular pressure, computerized optometry, fundus photography, ocular biometry, and high-speed ultra-widefield OCTA. We used TowardPi high-speed

TABLE 1 Demographic characteristics of participants.

Participants (eyes)	101 (172)
Mean ± SD age, y	56.50 ± 10.58
Males/Females	55/46
Type of diabetes (participants)	
Type 1	1
Type 2	100
Mean ± SD duration of diabetes, y	9.66 ± 6.97
Groups, the severity of DR eyes	
No DR in DM patients	41
Mild and Moderate NPDR	40
Severe NPDR	51
PDR	40
Right eyes/Left eyes	87/85
DME eyes	63

DM, diabetes mellitus; DR, diabetic retinopathy; NPDR, non-proliferative diabetic retinopathy; PDR, proliferative diabetic retinopathy; DME, diabetic macular edema.

ultra-widefield SS-OCTA systems (BM-400K BMizar, TowardPi Medical Technology; Beijing, China) to examine the patients. The instrument used a swept frequency laser with a center wavelength of 1,060 nm and a scanning speed of 400,000 times/s. With patient cooperation and no tracking, a single image was obtained in 15 seconds with a scan depth of 6 mm and a FOV of 120° resulting in a maximum fundus imaging area of 24 mm × 20 mm.

The participants were instructed to look at the inner marker light, and a 24 mm × 20 mm SS-OCTA image was obtained with the fovea as the center. Image quality was automatically rated on a scale of 1 to 10 by built-in software. If the image quality is poor (<6/10), the process was repeated and new images were obtained when the image quality was poor; images with better quality were selected for the analysis. For each participant, SS-OCTA was performed using the 24 mm × 20 mm scanning mode, and 76 eyes from 38 patients were also scanned using 12 mm × 12 mm scanning mode at the same time.

2.4 Image analysis

The images were annotated by two experienced ophthalmologists. Disagreements between them were openly adjudicated by an independent senior retina specialist (ZL) who had more than 30 years of working experience in diagnosing and treating DR. All lesions were identified based on their characteristics on high-speed ultra-widefield SS-OCTA images, as in previous reports (6, 10, 13). MAs were defined as moderate or hyperreflective spots, and they had various morphologic patterns, including fusiform, saccular, curved, and rarely coiled shapes, in the SS-OCTA images (14). Adjacent to the NPAs, the IRMAs appeared as tortuous, dilated, and annular abnormal microvessels in the retina. After segmentation error correction, the NVs were observed as extraretinal vessels present on the vitreoretinal interface slab. The NPAs were defined as absence of capillary beds between a terminal arteriole and a proximal venule or larger vessel (15), and potential NPAs with areas less than 0.2 mm^2 were not delineated (16). The hard exudates appeared on the B-scan as bright hyperreflective lesions with posterior shadows (10).

Each 24 mm × 20 mm SS-OCTA image was marked with a 12 mm × 12 mm square centered on the macula with the built-in tool and divided into 12 mm × 12 mm-central and 12 mm~24mm-annulus areas (Figure 1). The presence or absence of MAs, IRMAs, NV, NPAs, HEs, and DME was marked in each area (Figure 2). The

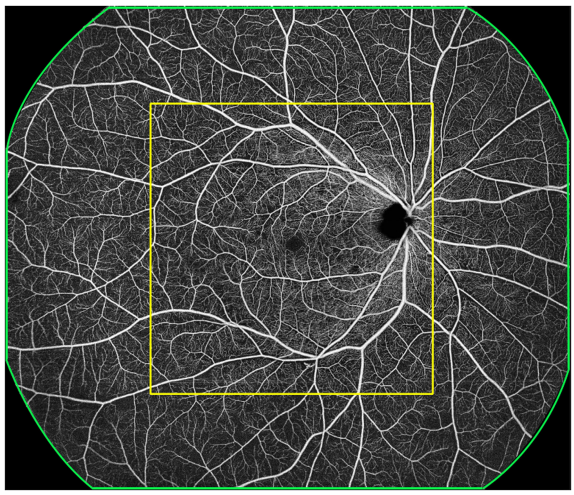

FIGURE 1
A representative OCTA image. The green outline represents the 24 mm × 20 mm scanning area, with the imaging centered on the fovea. The yellow outline represents the 12 mm × 12 mm scanning area, with the imaging centered on the fovea; this was termed the 12 mm × 12 mm central. The area outside the yellow outline and within the green outline was termed 12 mm~24mm-annulus.

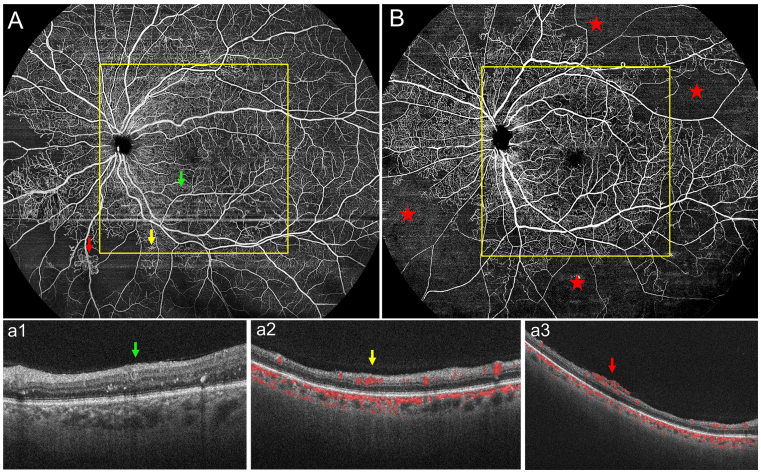

FIGURE 2
(A) Representative 24 mm × 20 mm OCTA image of one eye with PDR. Representative DR lesions are marked with green arrows for microaneurysms (MAs) with corresponding B-scans (a1); yellow arrows for intraretinal microvascular abnormalities (IRMAs) with corresponding B-scans (a2); and red arrows for neovascularization (NV) with corresponding B-scans (a3). **(B)** In another representative 24 mm × 20 mm OCTA image, the red stars represent non-perfusion areas (NPAs); most of the NPAs were seen in the 12 mm~24mm-annulus. PDR, proliferative diabetic retinopathy.

dimensions of the NPAs (mm^2) were also recorded (16). The ischemic Index (ISI) was calculated by dividing NPAs by the corresponding retinal area (17). To evaluate the accuracy of the 12 mm × 12 mm-central scanning area, which was obtained partially from an area of 24 mm × 20 mm, 76 eyes were selected for both the 12 mm × 12 mm and 24 mm × 20 mm high-speed ultra-widefield SS-OCTA scans.

In this study, severity of DR was graded using the Optos ultra-widefield retinal image (Optos PLC; Scotland, United Kingdom) of all participants (18, 19), according to the International Clinical Diabetic Retinopathy Severity Scale (20). Based on the lesion characteristics, we classified DR into DM without DR, mild to moderate non-proliferative diabetic retinopathy (NPDR), severe NPDR, and proliferative diabetic retinopathy (PDR).

2.5 Data analysis

Statistical analysis was performed using SPSS version 26.0 (IBM, Armonk, New York). The data were expressed as mean ± standard deviation. The non-normally distributed data were analyzed using nonparametric tests. The chi-squared test was used to compare the rates of detection of the DR features in different modes. Two-tailed p-values of < 0.05 denoted statistical significance.

3 Results

3.1 Demographics

In total, 172 eyes (41 eyes with DM without DR, 40 eyes with mild to moderate NPDR, 51 eyes with severe NPDR, and 40 eyes with PDR) from 101 participants were included in the study. The average age of the participants was 56.50 ± 10.58 years, and the average duration since the diagnosis of diabetes was 9.66 ± 6.97 years. A total of 63 participants had DME (Table 1).

3.2 Detection rates of DR lesions in different areas of a 24 mm × 20 mm high-speed ultra-widefield SS-OCTA image

The detection rates (the number of eyes found divided by the total number of eyes examined) of MAs, IRMAs, and NV were 66.9%, 44.2%, and 19.2% for the 12 mm × 12 mm-central images and 74.4%, 51.2%, and 23.3% for the 24 mm × 20-mm images, respectively ($p > 0.05$). The detection rate of NPAs was 64.5% for the 24 mm × 20 mm image, which was higher than that for the 12 mm × 12 mm-central image (52.3%) ($p < 0.05$). The two scan protocols had identical detection rates for HE and DME ($p = 1.00$, Table 2).

3.3 Distribution of nonperfusion areas and ischemic index in different retinal zones

NPAs were present in 111 eyes. The average dimension of the NPAs was 8.09 ± 13.58 mm^2 in the 12 mm × 12 mm-central image, with an average ISI of 5.62 ± 9.43%. The average dimension of the NPAs was 45.86 ± 58.69 mm^2 in a 12 mm~24mm-annulus image, with an average ISI of 15.26 ± 19.52% ($p < 0.05$, Table 3).

4 Discussion

In our study, we compared the detection rates and distributions of DR lesions in SS-OCTA images with fields of 24 mm × 20 mm

TABLE 2 DR lesion detection rates of 12 mm × 12 mm central and 24 mm × 20 mm OCTA images.

	Eyes with DR Lesions present in different scan areas (n/N Eyes, %)		
DR lesions	12 mm × 12 mm central	24 mm×20 mm	p-value
MAs	115/172 (66.9%)	128/172 (74.4%)	.155
IRMAs	76/172 (44.2%)	88/172 (51.2%)	.235
NV	33/172 (19.2%)	40/172 (23.3%)	.429
NPAs	90/172 (52.3%)	111/172 (64.5%)	.029
HE	110/172 (64.0%)	110/172 (64.0%)	1.000
DME	63/172 (36.6%)	63/172 (36.6%)	1.000

MAs, microaneurysms; IRMAs, intraretinal microvascular abnormalities; NV, neovascularization; NPAs, non-perfusion areas; HE, Hard exudates; DME, diabetic macular edema; p-value. The difference was statistically significant (p<.05).

(FOV 120°) and 12 mm × 12 mm (FOV 50°). With the increase in FOV, more IRMAs and NV were detected by the ultra-widefield SS-OCTA. The retinal ischemia was more severe in the mid-peripheral retina than in the posterior area. In addition, there was no loss of details of the posterior DR lesions in the 24 mm × 20 mm scanning mode relative to the 12 mm × 12 mm scanning mode.

Within the last decade, SS-OCTA has been gradually used to detect and research vascular changes in DR. Most previous studies used SS-OCTA with a scanning area of 12 mm × 12 mm (FOV 50°) (21–24). Higher FOV (90°) can be achieved using the montage technique. The montage technique allows a higher FOV. However, it has certain limitations, such as misalignment, motion artifacts, and longer processing times (25). Another simple technique for increasing the scan length for OCTA is an extended field imaging technique. However, it leads to a decrease in image resolution and missing retinal vascular information (26). In this study, we used the newly developed and commercialized high-speed ultra-widefield SS-OCTA systems. Its 24 mm × 20 mm scanning mode (444.6 mm^2) provides a 208.7% larger scanning area than the 12 mm × 12 mm scanning mode (144 mm^2) and facilitated a wider retinal field (approximately 120° FOV). According to the recommendation of the International Widefield Imaging Study Group, the FOV of the OCTA system in our study can be categorized as ultra-widefield (approximately 110–220°, anterior edge of vortex vein ampulla, and beyond to pars plana) (27).

We evaluated the presence or absence of DR lesions including MAs, IRMAs, NV, NPAs, HE, and DME. The larger scanning area did not increase the detection rate of MAs, IRMAs, and NV ($p > 0.05$, Table 2). However, the detection rate of the NPAs, an indicator of retinal ischemia, increased with the expansion of the scanning area ($p < 0.05$, Table 2). We quantified the NPAs and evaluated the ISI for different areas. The average ISI for the 12 mm × 24 mm-annulus image was 15.26 ± 19.52%, which was significantly higher than that for the 12 mm × 12 mm-central image (5.62% ± 9.43%) (Table 3). These results suggested that ischemia was more severe in the peripheral region than in the posterior pole within the 24 mm × 20 mm area (Figure 2B). Fan et al. (17) proposed that ISI increases with an increase in the distance from the foveal center. Wang et al. (7) used an OCTA montage image composed of five 12 mm × 12 mm OCTA images for analysis and reported that the capillary non-perfusion of the 50–100° FOV sector in DR was more prominent in the peripheral regions of the retina compared to that of the central FOV sectors. These findings were similar to our results. However, the authors were aware of the several limitations of their study: the 12 mm × 12 mm scans only provide a lateral resolution of 24 μm; the automated montage feature failed at times due to the disparate overlap of the 12 mm × 12 mm scans requiring time-consuming manual correction; and the image distortion may have affected the measurements of peripheral capillary nonperfusion (7). In our study, a single scanning could provide a 24 mm × 20 mm image (FOV 120°) with a transverse resolution of 10 μm and an axial optical resolution of 3.8 μm, which enabled us to observe the capillary non-perfusion areas more accurately. The display of the ischemic area was more comprehensive and intuitive with a wider SS-OCTA image. Theoretically, these non-invasive wider SS-OCTA images could be quickly and repeatedly acquired from the patients for follow-up of the change in capillary drop-out in clinical practice.

Besides NPAs, IRMAs and NV were vital considerations for DR management. It is important to distinguish between IRMAs and retinal NV to determine disease severity and prognosis and make treatment decisions. SS-OCTA can show frontal and cross-sectional analyses, while B-scans help to differentiate IRMA from NV (28, 29). Similar to the methods used by Lee et al. (30) and Cho et al. (31), we differentiated IRMA from NV by analyzing B-scans (Figures 2: a2, a3). In this study, there were no statistically significant differences between the detection

TABLE 3 ISIs for 12 mm × 12 mm central and 12 mm~24mm-annulus imaging.

	Different scan areas		
DR lesions	12 mm × 12 mm central	12 mm~24mm-annulus	p-value
NPAs area (mm^2)	8.09 ± 13.58	45.86 ± 58.69	.000
Average ISI (%)	5.62 ± 9.43	15.26 ± 19.52	.000

Data were presented as means ± standard deviations; NPAs, non-perfusion areas; ISI =ischemic index (ISI =NPAs/retinal area); p-value. The difference was statistically significant (p<.05); 12 mm × 12 mm central retinal area is 144 mm^2, and 12 mm~24mm-annulus retinal area is 300.6 mm^2.

rates of IRMAs and NV in the 12 mm × 12 mm-central and 24 mm × 20 mm SS-OCTA images. These results were similar to the findings of previous studies. However, we observed more IRMAs and NV within the 24 mm × 20 mm area than within the 12 mm × 12 mm-central area. (Figure 3). Of the total of 40 eyes with PDR and 51 eyes with severe NPDR, 6 eyes had NV and 10 eyes had IRMAs that were only observed within the 12 mm~24mm-annulus area. Compared with the 12 mm × 12 mm-central area, more severe lesions were observed in 16 eyes within the 24 mm × 20 mm area due to an increase in the FOV. With the detection of more regions of NV, 6 eyes that were originally diagnosed with severe NPDR based on 12 mm × 12 mm-central images were diagnosed with PDR. Therefore, a wider scanning field for SS-OCTA can facilitate more accurate determination of DR progression and timely interventions and guide clinical diagnosis and treatment. However, prospective studies with larger sample sizes are needed to test this hypothesis.

Additionally, since this is a newly developed SS-OCTA device, we also investigated differences in the lesion detection rate using the 24 mm× 20 mm and 12 mm × 12 mm scan modes. Seventy-six eyes from 38 patients were scanned using the two modes. We compared the 12 mm × 12 mm SS-OCTA images extracted from the 24 mm × 20 mm scanning mode with the image obtained by the 12 mm × 12 mm scanning mode. There were no statistical differences between the detection rates for all the lesions (Table 4), and we found that the 24 mm × 20 mm scanning mode did not lose the information within the 12 mm × 12 mm area during DR lesion detection (Figure 4); instead, it provided more information in the mid-peripheral retina. However, the 12 mm × 12 mm scan mode has an advantage of a relatively short scan time.

OCTA can non-invasively reveal the structures of multiple layers of the vascular plexus, including the superficial capillary plexus (SCP), intermediate capillary plexus, deep capillary plexus (DCP), and peripapillary radial plexus (PRP) (32, 33). Some previous studies reported that the DCP was more susceptible to ischemia and significantly related to the progression of DR than the SCP (34, 35). However, we did not analyze the distribution of the NPAs in each capillary plexus in this study, since the automatic

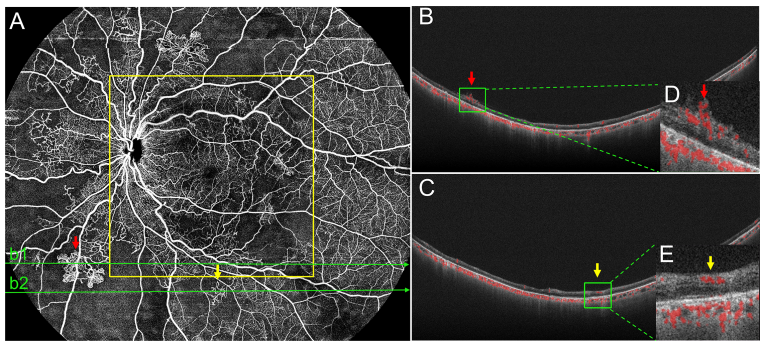

FIGURE 3
Representative OCTA image of PDR. **(A)** In the 24 mm ×20 mm image, the red arrows mark the neovascularization (NV), and a corresponding BScan image (b1) is provided **(B, D)**. Yellow arrows mark intraretinal microvascular abnormalities (IRMAs) and a corresponding B-Scanimage (b2) is provided **(C, E)**. Structurally, IRMAs were defined as new vessels formed within the retinal layers whereas, retinal NV breached the internal limiting membrane. In this eye, both NV and IRMAs were outside the 12 mm ×12 mm area (yellow outline), but they were accurately detected using the 24 mm ×20 mm scanning mode. PDR, proliferative diabetic retinopathy.

TABLE 4 Comparison of 12 mm×12 mm central and A-single-scan 12 mm×12 mm OCTA images.

	The same areas for different scanning protocols		
DR lesions	12 mm×12 mm central (eyes)	A-single-scan 12 mm×12 mm (eyes)	p-value
MAs	60/76 (78.9%)	63/76 (82.0%)	0.68
IRMA	46/76 (60.5%)	46/76 (60.5%)	1.00
NV	19/76 (25.0%)	19/76 (25.0%)	1.00
NPAs	52/76 (68.4%)	52/76 (68.4%)	1.00
HE	51/76 (67.1%)	51/76 (67.1%)	1.00
DME	35/76 (46.1%)	35/76 (46.1%)	1.00

MAs, microaneurysms; IRMA, intraretinal microvascular abnormalities; NV, neovascularization; NPAs, nonperfusion areas; HE, hard exudates; DME, diabetic macular edema; p-value. The difference was statistically significant (p<.05).

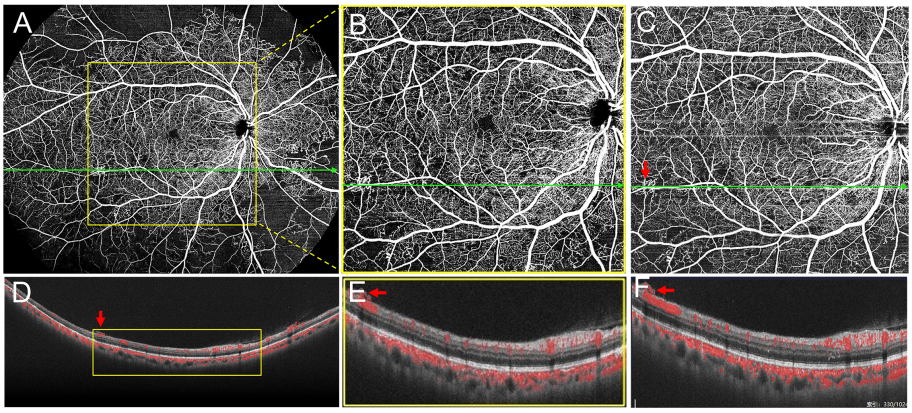

FIGURE 4
Scans of the same eye using two different protocols. **(A)** The 24 mm ×20 mm scanning mode. **(B)** The 12 mm ×12 mm image was extracted from the yellow outline area in **(A)**. **(C)** Image obtained using the 12 mm × 12 mm scanning mode. **(D–F)** B-Scan images acquired with corresponding scan lines in **(A)**, **(B)**, and **(C)**, respectively. As shown in **(D–F)**, both 24 mm ×20 mm and 12 mm ×12 mm scanning modes show the neovascularization breaking through the internal limiting membrane (red arrows).

stratification of the DCP and SCP in the peripheral retina is not as accurate as that in the macular area. Meanwhile, the manual correction of the entire B-scan images is very time-consuming. This limitation needs to be addressed in further studies.

Our study had several other limitations. This was a single-center study involving a relatively small sample. Similar to the previously reported SS-OCTA, TowardPi high-speed ultra-widefield SS-OCTA was influenced by the turbidity of the refractive medium and artifacts. For the 24 mm × 20 mm scanning mode, some optical occlusion or artifacts may be produced in patients with longer and thicker eyelashes, small eyelid fissures, and poor tear film function, which can affect the observation of DR lesions. In addition, patients with macular disease and DME have poor fixation, which may lead to more projection and motion artifacts and affect image quality. These issues need to be considered in future studies.

Despite our limitations, our data suggest the high-speed ultra-widefield SS-OCTA used in this study can obtain a 24 mm × 20 mm OCTA fundus image in a single scan. The high-speed ultra-widefield SS-OCTA can more accurately reveal the degree of retinal ischemia and also detect more NV and IRMAs lesions using the 24 mm × 20 mm compared with the 12 mm × 12 mm scanning area.

Data availability statement

The raw data supporting the conclusions of this article will be made available by the authors, without undue reservation.

Ethics statement

The studies involving human participants were reviewed and approved by Ethics Committee of Sichuan Provincial People's Hospital. The patients/participants provided their written informed consent to participate in this study.

Author contributions

JZ, JL, MYL, and MM had full access to the data in the study and take responsibility for the integrity of the data and the accuracy of the data analysis. JZ and JL conceived and designed the research. MYL, MM, DW, ML, XL, HL, YW, SC, RZ, YZ, and MW acquired and analyzed the data. MM and MYL reviewed and graded the images. JL, JZ, MYL, and MM wrote the draft of the manuscript. JZ and JL critically reviewed and extensively revised the manuscript. MM and MYL performed the statistical analyses. JZ, JL, YZ, and RZ acquired funding. JZ and JL supervised the study. All authors contributed to the article and approved the submitted version.

Funding

This study was supported in part by the Sichuan Province Science and Technology Support Program (grant number 2021ZYD0108); Health and Family Planning Commission of Sichuan Province (grant number 19ZD012); Science and Technology Project of The Health Planning Committee of Sichuan (grant number 21PJ077); Clinical and Translational Research Fund of Sichuan Provincial People's Hospital (General Project) (grant number 2020LY04); Sichuan Provincial People's Hospital (grant number 2021QN13); The Science & Technology Department of Sichuan Province (grant numbers 2017YSKY0001 and 2021YJ0234); and Natural Science Foundation of Sichuan Province (grant number 2023NSFSC0592).

Acknowledgments

The authors thank Chen Bin, Xue Zhou, and Weilin Wang for technical assistance.

Conflict of interest

The authors declare that the research was conducted in the absence of any commercial or financial relationships that could be construed as a potential conflict of interest.

Publisher's note

All claims expressed in this article are solely those of the authors and do not necessarily represent those of their affiliated organizations, or those of the publisher, the editors and the reviewers. Any product that may be evaluated in this article, or claim that may be made by its manufacturer, is not guaranteed or endorsed by the publisher.

Supplementary material

The Supplementary Material for this article can be found online at: https://www.frontiersin.org/articles/10.3389/fendo.2023.1111360/full#supplementary-material

References

1. Barth T, Helbig H. [Diabetic retinopathy]. *Klinische Monatsblatter fur Augenheilkunde* (2021) 238:1143–59. doi: 10.1055/a-1545-9927

2. Yau JW, Rogers SL, Kawasaki R, Lamoureux EL, Kowalski JW, Bek T, et al. Global prevalence and major risk factors of diabetic retinopathy. *Diabetes Care* (2012) 35:556–64. doi: 10.2337/dc11-1909

3. Safi H, Safi S, Hafezi-Moghadam A, Ahmadieh H. Early detection of diabetic retinopathy. *Surv Ophthalmol* (2018) 63(5):601–8. doi: 10.1016/j.survophthal.2018.04.003

4. Ra H, Park JH, Baek JU, Baek J. Relationships among retinal nonperfusion, neovascularization, and vascular endothelial growth factor levels in quiescent proliferative diabetic retinopathy. *J Clin Med* (2020) 9(5):1–11. doi: 10.3390/jcm9051462

5. Enders C, Baeuerle F, Lang GE, Dreyhaupt J, Lang GK, Loidl M, et al. Comparison between findings in optical coherence tomography angiography and in fluorescein angiography in patients with diabetic retinopathy. *Ophthalmologica* (2020) 243:21–6. doi: 10.1159/000499114

6. Cui Y, Zhu Y, Wang JC, Lu Y, Zeng R, Katz R, et al. Comparison of widefield swept-source optical coherence tomography angiography with ultra-widefield colour fundus photography and fluorescein angiography for detection of lesions in diabetic retinopathy. *Br J Ophthalmol* (2021) 105(4):577–81. doi: 10.1136/bjophthalmol-2020-316245

7. Wang F, Saraf SS, Zhang Q, Wang RK, Rezaei KA. Ultra-widefield protocol enhances automated classification of diabetic retinopathy severity with oct angiography. *Ophthalmol Retina* (2020) 4:415–24. doi: 10.1016/j.oret.2019.10.018

8. Mishra DK, Shanmugam MP, Ramanjulu R, Sagar P. Comparison of standard and "Innovative wide-field" optical coherence tomography images in assessment of vitreoretinal interface in proliferative diabetic retinopathy: A pilot study. *Indian J Ophthalmol* (2021) 69:99–102. doi: 10.4103/ijo.IJO_289_20

9. Sawada O, Ichiyama Y, Obata S, Ito Y, Kakinoki M, Sawada T, et al. Comparison between wide-angle oct angiography and ultra-wide field fluorescein angiography for detecting non-perfusion areas and retinal neovascularization in eyes with diabetic retinopathy. *Graefe's Arch Clin Exp Ophthalmol = Albrecht von Graefes Archiv fur klinische und experimentelle Ophthalmol* (2018) 256:1275–80. doi: 10.1007/s00417-018-3992-y

10. Zhu Y, Cui Y, Wang JC, Lu Y, Zeng R, Katz R, et al. Different scan protocols affect the detection rates of diabetic retinopathy lesions by wide-field swept-source optical coherence tomography angiography. *Am J Ophthalmol* (2020) 215:72–80. doi: 10.1016/j.ajo.2020.03.004

11. Tang FY, Chan EO, Sun Z, Wong R, Lok J, Szeto S, et al. Clinically relevant factors associated with quantitative optical coherence tomography angiography metrics in deep capillary plexus in patients with diabetes. *Eye Vis (Lond)* (2020) 7:7. doi: 10.1186/s40662-019-0173-y

12. Li J, Wei D, Mao M, Li M, Liu S, Li F, et al. Ultra-widefield color fundus photography combined with high-speed ultra-widefield swept-source optical coherence tomography angiography for non-invasive detection of lesions in diabetic retinopathy. *Front Public Health* (2022) 10:1047608. doi: 10.3389/fpubh.2022.1047608

13. Khalid H, Schwartz R, Nicholson L, Huemer J, El-Bradey MH, Sim DA, et al. Widefield optical coherence tomography angiography for early detection and objective evaluation of proliferative diabetic retinopathy. *Br J Ophthalmol* (2021) 105:118–23. doi: 10.1136/bjophthalmol-2019-315365

14. Schreur V, Domanian A, Liefers B, Venhuizen FG, Klevering BJ, Hoyng CB, et al. Morphological and topographical appearance of microaneurysms on optical coherence tomography angiography. *Br J Ophthalmol* (2018) 2018:1–6. doi: 10.1136/bjophthalmol-2018-312258

15. Couturier A, Rey PA, Erginay A, Lavia C, Bonnin S, Dupas B, et al. Widefield oct-angiography and fluorescein angiography assessments of nonperfusion in diabetic retinopathy and edema treated with anti-vascular endothelial growth factor. *Ophthalmology* (2019) 126:1685–94. doi: 10.1016/j.ophtha.2019.06.022

16. Wang K, Ghasemi Falavarjani K, Nittala MG, Sagong M, Wykoff CC, van Hemert J, et al. Ultra-Wide-Field fluorescein angiography-guided normalization of ischemic index calculation in eyes with retinal vein occlusion. *Invest Ophthalmol Vis Sci* (2018) 59(8):3278–85. doi: 10.1167/iovs.18-23796

17. Fan W, Nittala MG, Velaga SB, Hirano T, Wykoff CC, Ip M, et al. Distribution of nonperfusion and neovascularization on ultrawide-field fluorescein angiography in proliferative diabetic retinopathy (recovery study): Report 1. *Am J Ophthalmol* (2019) 206:154–60. doi: 10.1016/j.ajo.2019.04.023

18. Silva PS, Cavallerano JD, Sun JK, Noble J, Aiello LM, Aiello LP. Nonmydriatic ultrawide field retinal imaging compared with dilated standard 7-field 35-mm photography and retinal specialist examination for evaluation of diabetic retinopathy. *Am J Ophthalmol* (2012) 154(3):549–59.e2. doi: 10.1016/j.ajo.2012.03.019

19. Price LD, Au S, Chong NV. Optomap ultrawide field imaging identifies additional retinal abnormalities in patients with diabetic retinopathy. *Clin Ophthalmol* (2015) 9:527–31. doi: 10.2147/opth.S79448

20. Wilkinson CP, Ferris FL3rd, Klein RE, Lee PP, Agardh CD, Davis M, et al. Proposed international clinical diabetic retinopathy and diabetic macular edema disease severity scales. *Ophthalmology* (2003) 110:1677–82. doi: 10.1016/s0161-6420(03)00475-5

21. Zhang Q, Rezaei KA, Saraf SS, Chu Z, Wang F, Wang RK. Ultra-wide optical coherence tomography angiography in diabetic retinopathy. *Quant Imaging Med Surg* (2018) 8:743–53. doi: 10.21037/qims.2018.09.02

22. Schaal KB, Munk MR, Wyssmueller I, Berger LE, Zinkernagel MS, Wolf S. Vascular abnormalities in diabetic retinopathy assessed with swept-source optical coherence tomography angiography widefield imaging. *Retina* (2019) 39:79–87. doi: 10.1097/iae.0000000000001938

23. Motulsky EH, Liu G, Shi Y, Zheng F, Flynn HWJr., Gregori G, et al. Widefield swept-source optical coherence tomography angiography of proliferative diabetic retinopathy. *Ophthalmic Surg Lasers Imaging Retina* (2019) 50:474–84. doi: 10.3928/23258160-20190806-01

24. Russell JF, Al-Khersan H, Shi Y, Scott NL, Hinkle JW, Fan KC, et al. Retinal nonperfusion in proliferative diabetic retinopathy before and after panretinal photocoagulation assessed by widefield oct angiography. *Am J Ophthalmol* (2020) 213:177–85. doi: 10.1016/j.ajo.2020.01.024

25. Pichi F, Smith SD, Abboud EB, Neri P, Woodstock E, Hay S, et al. Wide-field optical coherence tomography angiography for the detection of proliferative diabetic retinopathy. *Graefes Arch Clin Exp Ophthalmol* (2020) 258:1901–9. doi: 10.1007/s00417-020-04773-x

26. Kimura M, Nozaki M, Yoshida M, Ogura Y. Wide-field optical coherence tomography angiography using extended field imaging technique to evaluate the nonperfusion area in retinal vein occlusion. *Clin Ophthalmol* (2016) 10:1291–5. doi: 10.2147/opth.S108630

27. Choudhry N, Duker JS, Freund KB, Kiss S, Querques G, Rosen R, et al. Classification and guidelines for widefield imaging: recommendations from the international widefield imaging study group. *Ophthalmol Retina* (2019) 3:843–9. doi: 10.1016/j.oret.2019.05.007

28. de Carlo TE, Bonini Filho MA, Baumal CR, Reichel E, Rogers A, Witkin AJ, et al. Evaluation of preretinal neovascularization in proliferative diabetic retinopathy using optical coherence tomography angiography. *Ophthalmic Surg Lasers Imaging Retina* (2016) 47:115–9. doi: 10.3928/23258160-20160126-03

29. Arya M, Sorour O, Chaudhri J, Alibhai Y, Waheed NK, Duker JS, et al. Distinguishing intraretinal microvascular abnormalities from retinal neovascularization using optical coherence tomography angiography. *Retina* (2020) 40:1686–95. doi: 10.1097/iae.0000000000002671

30. Lee CS, Lee AY, Sim DA, Keane PA, Mehta H, Zarranz-Ventura J, et al. Reevaluating the definition of intraretinal microvascular abnormalities and neovascularization elsewhere in diabetic retinopathy using optical coherence tomography and fluorescein angiography. *Am J Ophthalmol* (2015) 159(1):101–10 e1. doi: 10.1016/j.ajo.2014.09.041

31. Cho H, Alwassia AA, Regiatieri CV, Zhang JY, Baumal C, Waheed N, et al. Retinal neovascularization secondary to proliferative diabetic retinopathy characterized by spectral domain optical coherence tomography. *Retina* (2013) 33:542–7. doi: 10.1097/IAE.0b013e3182753b6f

32. Battista M, Borrelli E, Sacconi R, Bandello F, Querques G. Optical coherence tomography angiography in diabetes: a review. *Eur J Ophthalmol* (2020) 30:411–6. doi: 10.1177/1120672119899901

33. Millas SC, Di Lauro S, Mira DG, López Galvez MI. Optic coherence tomography angiography in diabetic retinopathy. In: Di Lauro S, Millas SC, Mira DJG, editors. *Eye diseases - recent advances, new perspectives and therapeutic options*. Rijeka: IntechOpen (2022). p. 1–11.

34. Sun Z, Tang F, Wong R, Lok J, Szeto SKH, Chan JCK, et al. Oct Angiography metrics predict progression of diabetic retinopathy and development of diabetic macular edema: a prospective study. *Ophthalmology* (2019) 126:1675–84. doi: 10.1016/j.ophtha.2019.06.016

35. Yu DY, Cringle SJ, Su EN, Yu PK, Jerums G, Cooper ME. Pathogenesis and intervention strategies in diabetic retinopathy. *Clin Exp Ophthalmol* (2001) 29:164–6. doi: 10.1046/j.1442-9071.2001.00409.x

frontiers | Frontiers in Endocrinology

TYPE Review
PUBLISHED 22 February 2023
DOI 10.3389/fendo.2023.1098165

OPEN ACCESS

EDITED BY
Mohd Imtiaz Nawaz,
Department of Ophthalmology, King Saud University, Saudi Arabia

REVIEWED BY
Suyan Li,
The Affiliated Xuzhou Municipal Hospital of Xuzhou Medical University, China
Xiaohui Zhang,
Xi'an Jiaotong University, China
Lian Ping,
Zhongshan Ophthalmic Center, Sun Yat-sen University, China
Wei Chen,
Tianjin Eye Hospital, China

*CORRESPONDENCE
Weiwei Wang
hybweiwei@126.com

SPECIALTY SECTION
This article was submitted to Clinical Diabetes, a section of the journal Frontiers in Endocrinology

RECEIVED 14 November 2022
ACCEPTED 31 January 2023
PUBLISHED 22 February 2023

CITATION
Wang W, Qu C and Yan H (2023) Network meta-analysis of intravitreal conbercept as an adjuvant to vitrectomy for proliferative diabetic retinopathy.
Front. Endocrinol. 14:1098165.
doi: 10.3389/fendo.2023.1098165

Network meta-analysis of intravitreal conbercept as an adjuvant to vitrectomy for proliferative diabetic retinopathy

Weiwei Wang*, Chaoyi Qu and Huanhuan Yan

Shaanxi Eye Hospital, Xi'an People's Hospital (Xi'an Fourth Hospital), Xi'an, China

Purpose: Intravitreal Conbercept (IVC) has been shown to be effective in treating proliferative diabetic retinopathy (PDR) as an adjuvant in pars plana vitrectomy (PPV); however, the best timing of IVC injection remains unknown. This network meta-analysis (NMA) sought to ascertain the comparative efficacy of different timings of IVC injection as an adjuvant to PPV on PDR.

Methods: A comprehensive literature search was conducted in PubMed, EMBASE, and the Cochrane Library to identify relevant studies published before August 11, 2022. According to the mean time of IVC injection before PPV, the strategy was defined as very long interval if it was > 7 days but ≤ 9 days, long interval if it was > 5 days but ≤ 7 days, mid interval if it was > 3 days but ≤ 5 days, and short interval if it was ≤ 3 days, respectively. The strategy was defined as perioperative IVC if IVC was injected both before and at the end of PPV, and the strategy was intraoperative IVC if injected immediately at the end of PPV. The mean difference (MD) and odds ratio (OR) with corresponding 95% confidence interval (CI) for continuous and binary variables, respectively, were computed through network meta-analysis using Stata 14.0 MP.

Results: Eighteen studies involving 1149 patients were included. There was no statistical difference between intraoperative IVC and control in treating PDR. Except for a very long interval, preoperative IVC significantly shortened operation time, and reduced intraoperative bleeding and iatrogenic retinal breaks. Long and short intervals reduced endodiathermy application, and mid and short intervals reduced postoperative vitreous hemorrhage. Moreover, long and mid intervals improved BCVA and central macular thickness. However, very long interval was associated with an increased risk of postoperative vitreous hemorrhage (RR: 3.27, 95%CI: 1.84 to 5.83). Moreover, mid interval was better than intraoperative IVC in shortening operation time (MD: -19.74, 95%CI: -33.31 to -6.17).

Conclusions: There are no discernible effects of intraoperative IVC on PDR, but preoperative IVC, except for very long interval, is an effective adjuvant to PPV for treating PDR.

KEYWORDS

proliferative diabetic retinopathy, vitrectomy, conbercept, intravitreal, network meta-analysis

Introduction

Diabetic retinopathy (DR), the most common diabetic complication, is characterized by damage and abnormalities in retinal blood vessels, which can result in visual impairment and blindness (1). Depending on the severity, DR can be classified into three subtypes: non-proliferative DR, proliferative DR (PDR), and diabetic macular edema (2). PDR is one of the most common causes of blindness in DR patients and is linked to vitreous hemorrhage, traction detachment, and neovascular glaucoma (3–5). DR affected approximately 103 million adults worldwide in 2020, which is expected to reach 160 million by 2045 (6). Therefore, it is critical to treat patients with PDR effectively.

Panretinal photocoagulation (5) and vitrectomy (7) are two traditional treatment options for PDR. Pars plana vitrectomy (PPV) remains the preferred treatment for PDR (8), as it removes long-standing hematoma in the vitreous cavity, blocks the pathways to neovascularization, and restores the stable intraocular structure to the retina (9). However, this procedure may be associated with an increased risk of several complications, such as retinal detachment (RD) and repeated vitreous hemorrhage. These complications can undoubtedly delay patients' vision recovery and increase surgical costs (10). Clinical practitioners are trying to mitigate the possible negative effects of PPV by different approaches.

Vascular endothelial growth factor (VEGF) plays a central role in the development of PDR (11), and it has been demonstrated that intravitreal anti-VEGF decreases the need for repeated vitrectomy and recurrent vitreous hemorrhage (12, 13). As a novel anti-VEGF drug, Conbercept was approved by the China Food and Drug Administration (CFDA) to treat age-related macular degeneration in 2013 (14). Conbercept is a recombinant fusion protein with multiple targets, increased affinity, and the capacity to prevent the growth of new blood vessels (15). Su et al. first evaluated the effect and safety of using Conbercept as an adjuvant to PPV in treating PDR, showing that intravitreal Conbercept (IVC) before PPV effectively accelerates visual recovery and reduces non-clearing vitreous hemorrhage (16). Subsequent meta-analyses also demonstrated the therapeutic efficacy and safety of IVC injection as an adjuvant to PPV in treating PDR.

Nevertheless, the intervals of IVC injection as an adjuvant to PPV varies in clinical practice, such as injection before PPV and immediate injection at the end of PPV. Currently, the impact of the intervals of IVC injection on intraoperative and postoperative outcomes in PDR patients undergoing PPV remains unknown because previous meta-analyses did not differentiate the intervals of IVC injection. Therefore, we conducted this network meta-analysis to evaluate the differences in therapeutic efficacy and safety between different intervals of IVC injection as an adjuvant to PPV in treating patients with PDR.

Subjects and methods

Study design

We conducted an NMA following the Preferred Reporting Items for Systematic Reviews and Meta-analyses guidelines (PRISMA) extension statement for reporting network meta-analysis (17). Since the statistical analysis was done using the published data, ethical approval and the patient's informed consent were unnecessary. We have registered the present network meta-analysis in PROSPERO with registration number CRD42022361537.

Eligibility criteria

The following criteria guided our selection of eligible studies: (a) adult patients received pars plana vitrectomy (PPV) for PDR; (b) PPV combined with intravitreal Conbercept (IVC) compared with PPV without Conbercept or each other; (c) the dose of IVC was limited to 0.5 mg, but there was no restriction on the type of PPV (23G, 25G, and 27G); (d) studies reported at least one of the best corrected visual acuity (BCVA), operation time, central macular thickness, intraoperative bleeding, iatrogenic retinal breaks, endodiathermy application, silicone oil tamponade, and postoperative vitreous hemorrhage (VH); and (e) only RCTs with full texts were considered.

Ineligible studies were excluded based on the following criteria: (a) papers reporting data from the same study, (b) studies without reporting IVC dose, (c) studies combining IVC with other drugs, (d) studies only report a broad time range to conduct IVC, (e) abstracts, letters to the editor, case reports, cell studies, animal studies, and reviews.

Literature retrieval

Two independent authors searched the PubMed, EMBASE, and Cochrane library databases for relevant publications from their inception until August 11, 2022, using a combination of the terms "diabetic retinopathy" and "Conbercept." We also manually searched relevant review articles and the reference lists of all eligible studies to identify additional studies. Supplementary Table 1 shows the detailed search strategies for three targeted databases. Disagreements were resolved through discussions between the two authors until a consensus was reached.

Study selection

In the following three steps, two authors independently selected eligible studies. First, we used the EndNote X9 software to remove duplicate studies. Second, we excluded irrelevant studies after reviewing the title and abstract. Third, ineligible studies were further identified by checking the full texts of the remaining studies. Disagreements between the two authors were resolved through discussions until an agreement was reached.

Data extraction

Two authors extracted the following data independently: first author's name, country, publication year, sample size, the proportion of males, patients' mean age, duration of diabetes, details of comparisons and interventions, and follow-up duration. Only

information from the final follow-up was extracted for the meta-analysis. We filled in missing data by contacting the corresponding author *via* email if necessary. The two authors debated any conflicts until they agreed.

Outcomes of interest

The primary outcomes were the BCVA expressed as a logarithm of the minimal angle of resolution (*LogMAR*) at the final follow-up, the operation time, and the central macular thickness; however, intraoperative bleeding, iatrogenic retinal breaks, endodiathermy application, silicone oil tamponade, and postoperative vitreous hemorrhage were secondary outcomes.

Assessment of risk of bias

Two independent authors used the revised Cochrane risk-of-bias tool for randomized trials (RoB2) to assess the risk of bias (18) from the randomization process, derivation for intended interventions, the missing outcome data, measurement of the outcome, selection of the reported results, and the overall results. Each domain was assigned a rating of low, no information, some concerns, or high risk. The two authors talked things out until they came to an agreement to resolve any disagreements.

Data analysis

The estimates of continuous and binary variables were expressed using mean difference (MD) and risk ratio (RR) with corresponding 95% confidence intervals (CI), respectively. We first assessed transitivity between studies by determining whether there was an insignificant difference in major clinical and methodological characteristics between comparisons (19, 20). Then, we used the design-by-treatment interaction method (21) and the node-splitting method (22) to examine global and local consistency, respectively. Additionally, we also used the node-splitting method (23, 24) to examine the loop-closed inconsistency. We used random network meta-analysis to compare the efficacy of different regimens regardless of statistical heterogeneity (25). Furthermore, the relative rankings of all regimens were determined by estimating ranking probabilities using the surface under the cumulative ranking (SUCRA) (26). Finally, we created a comparison-adjusted funnel plot to investigate the possibility of publication bias (27). STATA 14.0 was used for statistical analysis (StataCorp LP, College Station, Texas, USA) (28). The graphical tools created by Chaimani et al. (29) were used to present all results graphically.

Results

Literature retrieval and selection

Figure 1 shows the flow diagram for retrieving and selecting studies. We identified 362 records from an electronic literature search and excluded 84 duplicates and registered protocols. After reviewing the abstracts, we eliminated 225 studies. Initially, 53 studies were potentially relevant. Among them, 35 studies were excluded after reading the full text. Finally, 18 studies were included in this network meta-analysis.

Study characteristics

All studies (30–45) were performed in China and published between 2015 and 2021. The sample size of the individual study ranged from 31 to 111, with a total of 1149 patients. We defined it as short interval (SI) if the mean time of conducting IVC before PPV was ≤ 3 days, mid interval (MI) if the mean time of conducting IVC before PPV was > 3 days but ≤ 5 days, long interval (LI) if the mean time of conducting IVC before PPV was > 5 days but ≤ 7 days, and very long interval (VLI) if the mean time of conducting IVC before PPV was > 7 days but ≤ 9 days. Moreover, if IVC was conducted both before and at the end of PPV, we defined this strategy as perioperative IVC; however, the strategy was defined as intraoperative IVC if it was conducted immediately at the end of PPV. Overall, seven studies (32–34, 36, 40, 42, 46) compared LI with control, three studies (37, 38, 44) compared MI with control, three studies (35, 43, 47) compared SI with control, two studies (31, 39) compared intraoperative IVC with control, one study (41) compared VLI with SI, one study (45) compared MI with SI, and one study (30) compared MI with intraoperative and perioperative IVC. Detailed baseline characteristics of the included studies are presented in Table 1. We assessed transitivity based on publication year, sample size, male proportion, patients' mean age, diabetes duration, and follow-up duration. The distribution of these six factors is insignificant across comparisons, as shown in Supplemental Table 2, demonstrating transitivity between comparisons.

Risk of bias of eligible studies

Even though all eligible studies were RCTs, only seven studies (31, 32, 34, 36, 37, 39, 45) provided information on the randomization process. There was insufficient data to determine whether results are biased by deviations from the intended intervention and bias in outcome measures. Four studies were rated to be high risk due to incomplete outcome data. All studies were rated to be low risk in selective outcome reporting. Supplementary Figure 1 shows the details of the risk of bias assessment.

Meta-analysis of BCVA

BCVA was reported in fourteen studies (30, 31, 33–37, 39–43, 45, 46), involving a total of 886 patients and seven regimens (Figure 2A). We used an inconsistency model to estimate the relative efficacy of various regimens because inconsistency examination revealed the existence of global inconsistency (Supplementary Figure 2A) and local inconsistency (Supplementary Table 3). As shown in Table 2, EP was associated with better BCVA compared to the control regimen (MD: -0.29, 95%CI: -0.44 to -0.15); however, no statistical difference was found in the remaining comparisons. Nevertheless, according to ranking probabilities based on SUCRA, VLI ranked first (70.6%), followed by LI (69.6%), intraoperative IVC (64.0%), perioperative IVC (53.0%), SI (47.3%), MI (35.4%), and control (10.2%), as shown in Figure 3A.

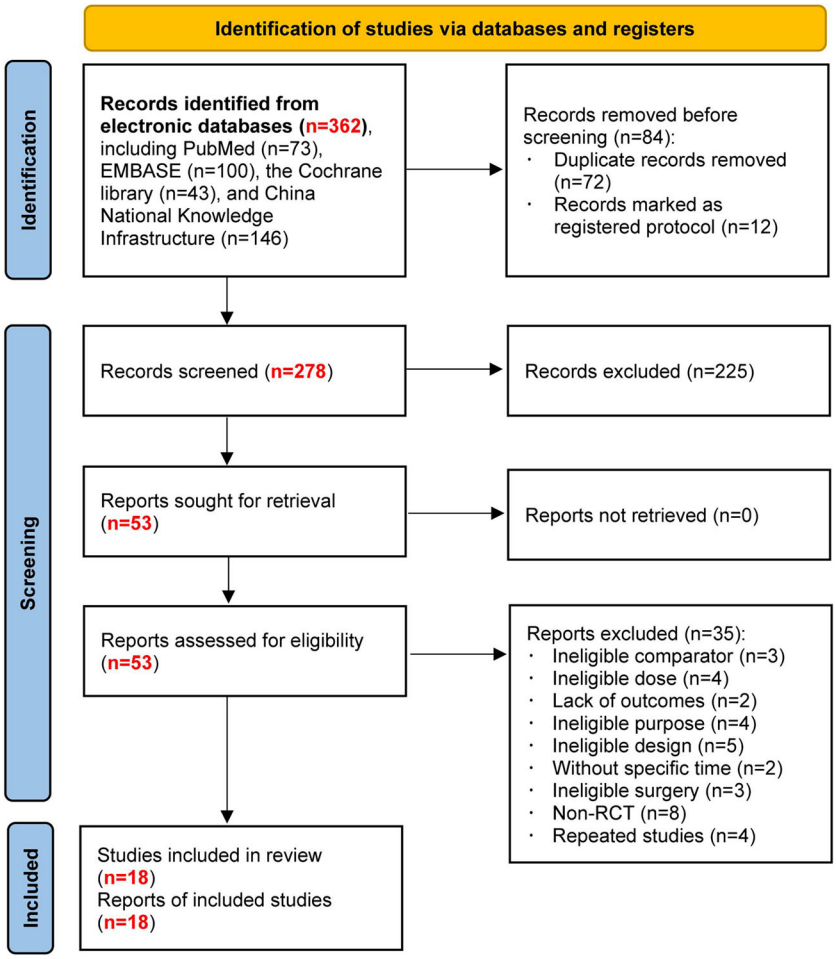

FIGURE 1
Flow diagram of study retrieval and selection.

Meta-analysis of operation time

Operation time was reported in sixteen studies (30, 32–46), involving a total of 1008 patients and seven regimens (Figure 2B). We used a consistency model to estimate the relative efficacy of various regimens because inconsistency examination revealed the absence of global inconsistency (Supplementary Figure 2B) and local inconsistency (Supplementary Table 3). All regimens, except for VLI and intraoperative IVC, were associated with fewer operation times when compared to the control regimen, as shown in Table 2; however, we found no statistical difference in the remaining comparisons. Meanwhile, MI outperformed intraoperative IVC in reducing operation time (MD: -19.74, 95%CI: -33.31 to -6.17). According to ranking probabilities based on SUCRA, MI ranked first (88.2%), followed by SI (79.3%), perioperative IVC (67.2%), LI (52.3%), VLI (29.3%), intraoperative IVC (27.4%), and control (6.3%), as shown in Figure 3B.

Meta-analysis of central macular thickness

Central macular thickness was reported in ten studies (31, 33–40, 43), involving 635 patients and five regimens (Figure 2C). Because inconsistency examination does not apply to this outcome, we used a consistency model to estimate the relative efficacy of various regimens. As shown in Table 2, MI was better than the control regimen in improving central macular thickness (MD: -114.20, 95%CI: -179.93 to -48.48); however, no statistical difference was found in the remaining comparisons. According to ranking probabilities based on SUCRA, MI ranked first (93.4%), followed by intraoperative IVC (66.8%), SI (43.2%), LI (40.7%), and control (5.9%), as shown in Figure 3C.

Meta-analysis of intraoperative bleeding

Intraoperative bleeding was reported in ten studies (31, 36–41, 45), involving 711 patients and six regimens (Figure 2D). Global inconsistency examination is not applicable to this outcome, but the assumption of the presence of local inconsistency was rejected (Supplementary Table 3). Therefore, we used a consistency model to estimate the relative efficacy of various regimens. As shown in Table 2, except for intraoperative IVC, all regimens were associated with fewer intraoperative bleeding when compared to control regimen; however, no statistical difference was found in the remaining comparisons. According to ranking probabilities based on SUCRA, MI ranked first (84.2%), followed by perioperative IVC

10.3389/fendo.2023.1098165

TABLE 1 The baseline characteristics of eligible studies included in this network meta-analysis (n=18).

Study	Groups	Sample size, n	Males, n	Mean age, years	Duration of diabetes, years	Details of procedures	Follow-up duration
Li et al., 2020	Control	20	9	56.0±10.5	14.0±6.8	23G PPV without IVC	n.r.
	LI	20	13	51.1±11.6	10.9±7.7	0.5mg IVC at 7 days before 23G PPV	
Li et al., 2021	Control	38	16	51.9±9.2	10.2±3.3	27G PPV without IVC	6 months
	LI	39	20	52.1±8.5	9.9±2.7	0.5mg IVC at 6-7 days before 27G PPV	
Lin et al., 2018	Control	47	31	58.9±7.8	9.6±2.6	23G PPV without IVC	6 months
	LI	47	29	56.3±9.6	10.4±2.2	0.5mg IVC at 5-7 days before 23G PPV	
Luo et al., 2021	Control	42	22	62.5±3.7	5.0±1.5	23G PPV without IVC	1 month
	SI	42	21	62.1±3.5	6.0±1.6	0.5mg IVC at 3 days before 23G PPV	
Luo et al., 2018	Control	16	7	57.7±11.3	n.r.	23G PPV without IVC	3 months
	LI	15	5	57.0±13.1	n.r.	0.5mg IVC at 7 days before 23G PPV	
Ou et al., 2021	Control	37	14	57.4±11.0	8.89±2.23	23G PPV without IVC	3 months
	MI	38	15	56.7±12.7	8.71±1.98	0.5mg IVC at 5 days before 23G PPV	
Ran et al., 2016	Control	29	15	49.5±5.4	n.r.	23G PPV without IVC	n.r.
	MI	27	13	47.5±3.2	n.r.	0.5mg IVC at 5 days before 23G PPV	
Shang et al, 2018	Control	30	16	55.6±5.9	15.1±1.9	23G PPV without IVC	3 months
	LI	30	18	54.2±6.3	14.4±1.7	0.5mg IVC at 7 days before 23G PPV	
Su et al., 2016	Control	18	n.r.	n.r.	n.r.	23G PPV without IVC	1 month
	LI	18	n.r.	n.r.	n.r.	0.5mg IVC at 7 days before 23G PPV	
Sun et al., 2017	Control	42	23	45.2±8.9	10.03±5.74	25G PPV without IVC	3 months
	SI	41	22	48.7±9.5	9.86±6.07	0.5mg IVC at 3 days before 25G PPV	
Sun et al., 2015	Control	28	18	57.4±3.3	10.0±1.3	23G PPV without IVC	6 months
	MI	28	18	51.2±3.2	10.0±1.4	0.5mg IVC at 3-5 days before 23G PPV	
Yang et al., 2016	Control	53	24	49.6±8.7	15.9±4.8	23G PPV without IVC	3 months
	SI	54	27	48.6±8.2	16.7±4.5	0.5mg IVC at 3 days before 23G PPV	
Zhao et al., 2018	Control	18	22	46.9±12.3	n.r.	23G PPV without IVC	3 months
	LI	18				0.5mg IVC at 7 days before 23G PPV	
Jiang et al., 2020	Control	15	10	53.5±9.6	9.88±8.52	23G PPV without IVC	6 months
	Intraoperative	15	6	55.5±9.9	13.19±8.08	0.5mg IVC at the end of the 23G PPV	
Ren et al., 2019	Control	22	15	46-80	1204±6.05	25G PPV without IVC	6 months
	Intraoperative	23	16	28-69	10.36±4.17	0.5mg IVC at the end of the 25G PPV	

(Continued)

TABLE 1 Continued

Study	Groups	Sample size, n	Males, n	Mean age, years	Duration of diabetes, years	Details of procedures	Follow-up duration
Gao et al., 2020	MI	34	14	50.8±13.5	14.5±5.2	0.5mg IVC at 3-5 days before 23G PPV	6 months
	Intraoperative	35	16	54.0±14.8	12.9±5.2	0.5mg IVC at the end of the 25G PPV	
	Perioperative	29	16	52.6±14.6	12.7±5.2	0.5mg IVC at 3-5 days before and after 23G PPV	
Shi et al., 2020	SI	26	13	52.7±9.0	8.9±5.9	0.5mg IVC at 2-3 days before 25G PPV	6 months
	VLI	21	9	52.1±10.5	10.3±5.9	0.5mg IVC at 7-8 days before 25G PPV	
Wen et al., 2019	Control	30	18	59.0±6.2	6.87±1.69	25G PPV without IVC	3 months
	SI	30	17	61.3±7.1	6.91±1.71	0.5mg IVC at 3 days before 25G PPV	
	MI	30	20	60.7±6.6	6.59±1.61	0.5mg IVC at 5 days before 25G PPV	

PPV, pars plana vitrectomy; IVC, intravitreal conbercept; VLI, very long interval; LI, long interval; MI, mid interval; SI, short interval; n.r., not reported.

(82.7%), intraoperative IVC (57.0%), LI (38.1%), SI (37.0%), and control (1.1%), as shown in Figure 3D.

Meta-analysis of iatrogenic retinal breaks

The data of iatrogenic retinal breaks were reported in ten studies (33–36, 38, 42–46), involving 643 patients and four regimens (Figure 2E). We used a consistency model to estimate the relative efficacy of various regimens because inconsistency examination revealed the absence of global inconsistency (Supplementary Figure 2C) and local inconsistency (Supplementary Table 3). All regimens were associated with fewer iatrogenic retinal breaks when compared to the control regimen, as shown in Table 2; however, no statistical difference was found in the remaining comparisons. According to ranking probabilities based on SUCRA, LI ranked first (72.1%), followed by MI (64.2%), SI (63.5%), and control (0.1%), as shown in Figure 3E.

Meta-analysis of endodiathermy application

Endodiathermy application was reported in eight studies (32, 34, 35, 37, 38, 42, 43, 46), involving a total of 486 patients and four

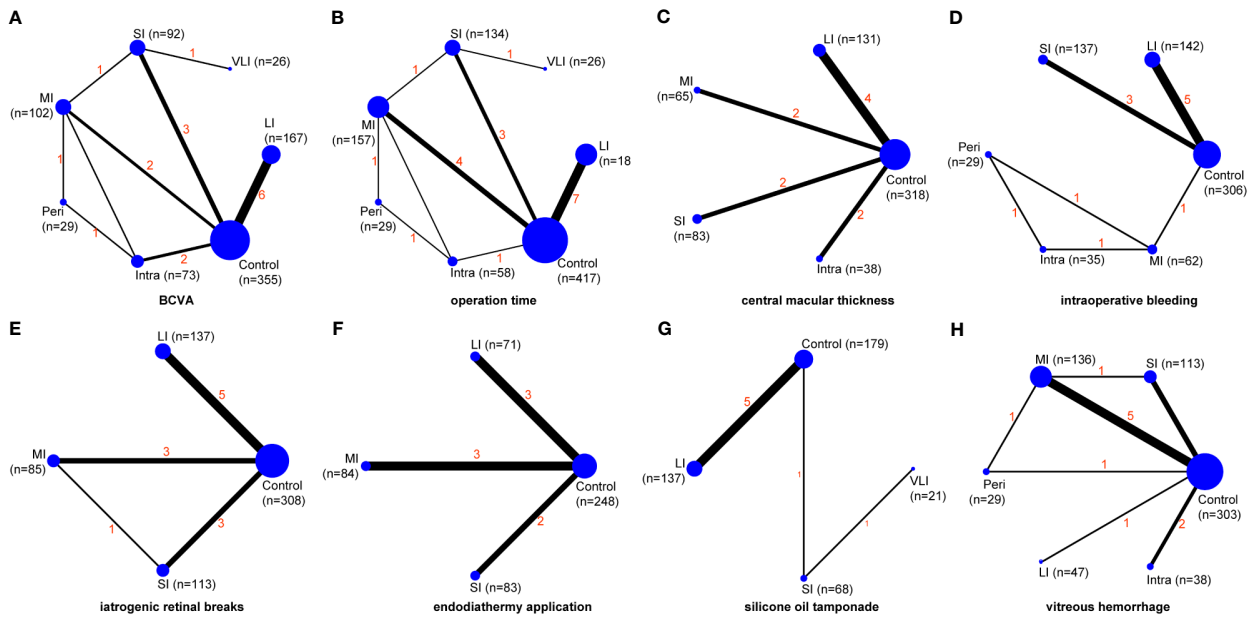

FIGURE 2
Network maps of evidence for all outcomes, including BCVA **(A)**, operation time **(B)**, central macular thickness **(C)**, intraoperative bleeding **(D)**, iatrogenic retinal breaks **(E)**, endodiathermy application **(F)**, silicone oil tamponade **(G)**, and vitreous hemorrhage **(H)**. VLI, very long interval; LI, long interval; MI, mid interval; SI, short interval; Intra, intraoperative; Peri, perioperative; BCVA, best corrected visual acuity.

10.3389/fendo.2023.1098165

TABLE 2 Network meta-analysis of all regimens in terms of all outcomes.

Comparisons	BCVA, LogMAR	Operation time, min	Central macular thickness, μm	Intraoperation bleeding, n	Iatrogenic retinal breaks, n	Endodiathermy application, n	Silicone oil tamponade, n	Vitreous hemorrhage, n
VLI vs Control	-0.38 (-1.04, 0.28)	-1.56 (-29.21, 26.10)	n.a.	n.a.	n.a.	n.a.	**3.27 (1.84,5.83)**	n.a.
VLI vs LI	-0.09 (-0.76, 0.59)	16.91 (-11.91, 45.74)	n.a.	n.a.	n.a.	n.a.	2.33 (0.99,5.49)	n.a.
VLI vs MI	-0.25 (-0.96, 0.46)	26.10 (-2.50, 54.70)	n.a.	n.a.	n.a.	n.a.	n.a.	n.a.
VLI vs SI	-0.19 (-0.77, 0.39)	17.81 (-7.35, 42.97)	n.a.	n.a.	n.a.	n.a.	1.88 (0.70,5.10)	n.a.
VLI vs Intra	-0.11 (-0.81, 0.60)	6.92 (-24.37, 38.21)	n.a.	n.a.	n.a.	n.a.	n.a.	n.a.
VLI vs Peri	-0.16 (-0.95, 0.63)	26.10 (-2.50, 54.70)	n.a.	n.a.	n.a.	n.a.	n.a.	n.a.
Peri vs Control	-0.19 (-0.50, 0.12)	**-21.81 (-42.52, -1.10)**	n.a.	**0.04 (0.00, 0.76)**	n.a.	n.a.	n.a.	0.34 (0.07,1.55)
Peri vs LI	0.07 (0.38, 0.53)	-3.34 (-25.59, 18.92)	n.a.	0.16 (0.01, 3.07)	n.a.	n.a.	n.a.	0.51 (0.05,5.14)
Peri vs MI	-0.09 (-0.43, 0.25)	5.85 (-13.73, 25.43)	n.a.	1.01 (0.38, 2.65)	n.a.	n.a.	n.a.	1.43 (0.29,7.03)
Peri vs SI	-0.03 (-0.56, 0.50)	-2.44 (-25.51, 20.63)	n.a.	0.15 (0.01, 3.10)	n.a.	n.a.	n.a.	0.93 (0.17,4.94)
Peri vs Intra	0.05 (-0.45, 0.56)	-13.33 (-30.06, 6.41)	n.a.	0.60 (0.26, 1.41)	n.a.	n.a.	n.a.	1.09 (0.12,10.02)
MI vs Control	-0.09 (-0.50, 0.32)	**-27.66 (-37.19, -18.13)**	**-114.20 (-179.93, -48.48)**	**0.04 (0.00,0.65)**	**0.28 (0.12, 0.65)**	0.42 (0.17, 1.08)	n.a.	**0.24 (0.10,0.57)**
MI vs LI	0.16 (-0.14, 0.47)	-9.19 (-21.71, 3.34)	-80.65 (-161.67, 0.37)	0.16 (0.01,2.60)	1.12 (0.38, 3.28)	2.04 (0.42, 9.79)	n.a.	0.36 (0.05,2.51)
MI vs SI	0.06 (-0.35, 0.47)	-8.29 (-21.88, 5.30)	-77.54 (-170.22, 15.13)	0.15 (0.01, 2.63)	0.99 (0.31, 3.18)	1.30 (0.35, 4.82)	n.a.	0.65 (0.21,1.96)
MI vs Intra	0.14 (-0.23, 0.52)	**-19.18 (-34.50, -3.85)**	-45.31 (-143.42, 52.81)	0.60 (0.27,1.34)	n.a.	n.a.	n.a.	0.76 (0.12,4.80)
SI vs Control	-0.13 (-0.40, 0.14)	**-19.37 (-30.84, -7.89)**	-36.66 (-101.98, 28.66)	**0.27 (0.13,0.54)**	**0.29 (0.12, 0.68)**	**0.33 (0.13, 0.83)**	1.74 (0.55,5.49)	**0.37 (0.18,0.74)**
SI vs LI	0.10 (-0.24, 0.45)	-0.90 (-14.96, 13.17)	-3.11 (-83.76, 77.55)	1.03 (0.45,2.40)	1.14 (0.38, 3.42)	1.57 (0.33, 7.45)	1.24 (0.74,2.06)	0.55 (0.08,3.59)
SI vs Intra	0.08 (-0.32, 0.49)	-10.89 (-29.49, 7.71)	32.23 (-65.36, 129.83)	4.00 (0.20,78.47)	n.a.	n.a.	n.a.	1.17 (0.20,6.85)

(Continued)

TABLE 2 Continued

Comparisons	BCVA, LogMAR	Operation time, min	Central macular thickness, μm	Intraoperation bleeding, n	Iatrogenic retinal breaks, n	Endodiathermy application, n	Silicone oil tamponade, n	Vitreous hemorrhage, n
Intra vs LI	0.02 (-0.28, 0.32)	9.99 (-7.29, 27.28)	-35.34 (-121.83, 51.15)	0.26 (0.01,4.84)	n.a.	n.a.	n.a.	0.47 (0.04,5.06)
Intra vs Control	0.19 (-0.18, 0.56)	-8.48 (-23.73, 6.77)	-68.89 (-141.48, 3.69)	0.07 (0.00,1.20)	n.a.	n.a.	n.a.	0.31 (0.06,1.58)
LI vs Control	**-0.29 (-0.44, -0.15)**	**-18.47 (-26.61, -10.34)**	-33.55 (-80.87, 13.77)	**0.26 (0.16,0.41)**	**0.25 (0.13, 0.50)**	**0.21 (0.06, 0.73)**	1.40 (0.50,3.94)	0.67 (0.12,3.81)

BCVA, best corrected visual acuity; LogMAR, logarithm of the minimal angle of resolution; VLI, very long interval; LI, long interval; MI, mid interval; SI, short interval; Intra, intraoperative; Peri, perioperative.
Numbers in bold font indicates statistical significance. n.a., not applicable.

regimens (Figure 2F). Because inconsistency examination is not applicable to this outcome, we used a consistency model to estimate the relative efficacy of various regimens. As shown in Table 2, except for MI, SI and LI were associated with fewer endodiathermy applications compared to the control regimen; however, no statistical difference was found in the remaining comparisons. According to ranking probabilities based on SUCRA, LI ranked first (84.0%), followed by SI (64.5%), MI (49.9%), and control (1.6%), as shown in Figure 3F.

Meta-analysis of silicone oil tamponade

Silicone oil tamponade was reported in seven studies (33–36, 41, 42, 46), involving 405 patients and four regimens (Figure 2G). Because inconsistency examination is not applicable to this outcome, we used a consistency model to estimate the relative efficacy of various regimens. As shown in Table 2, VLI was associated with more silicone oil tamponade compared to the control regimen (RR: 3.27, 95%CI, 1.84 to 5.83); however, no statistical difference was found in the remaining comparisons. According to ranking probabilities based on SUCRA, LI ranked first (86.0%), followed by SI (67.4%), VLI (42.1%), and control (4.5%), as shown in Figure 3G.

Meta-analysis of postoperative vitreous hemorrhage

Postoperative vitreous hemorrhage was reported in ten studies (30, 31, 34, 35, 37–39, 43–45), involving a total of 666 patients and six regimens (Figure 2H). We used a consistency model to estimate the relative efficacy of various regimens because inconsistency examination revealed the absence of global inconsistency (Supplementary Figure 2D) and local inconsistency (Supplementary Table 3). MI and SI were associated with fewer postoperative vitreous hemorrhages compared to the control regimen, as shown in Table 2; however, no statistical difference was found in the remaining comparisons. According to ranking probabilities based on SUCRA, MI ranked first (77.9%), followed by intraoperative IVC (62.7%), perioperative IVC (59.4%), SI (57.6%), LI (32.0%), and control (10.3%), as shown in Figure 3H.

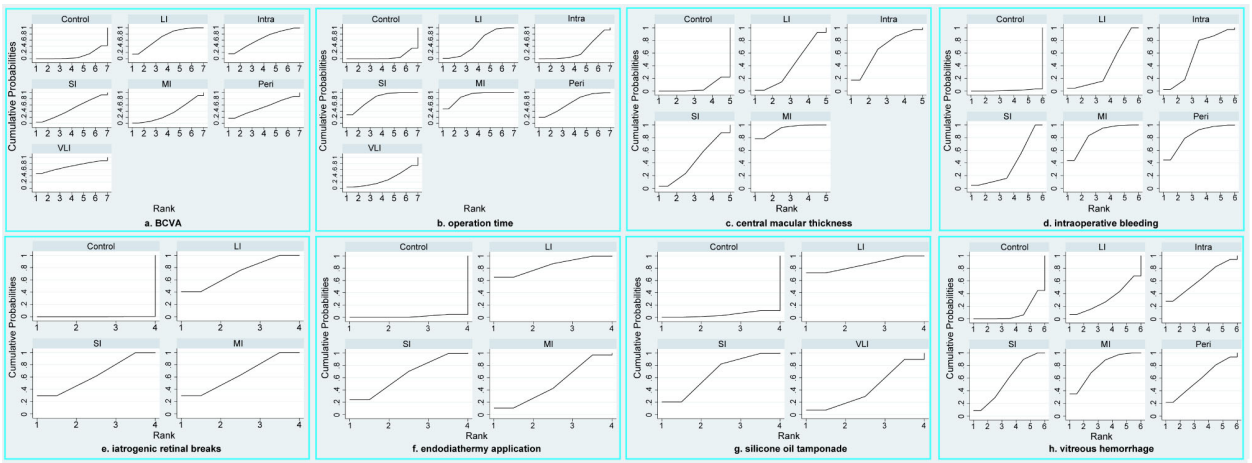

FIGURE 3
SUCRA plots of all outcomes, including BCVA **(A)**, operation time **(B)**, central macular thickness **(C)**, intraoperative bleeding **(D)**, iatrogenic retinal breaks **(E)**, endodiathermy application **(F)**, silicone oil tamponade **(G)**, and vitreous hemorrhage **(H)**. VLI, very long interval; LI, long interval; MI, mid interval; SI, short interval; Intra, intraoperative; Peri, perioperative; BCVA, best corrected visual acuity.

Loop-closed inconsistency

Among eight target outcomes, the evidence maps of four outcomes covered loop-closed. As shown in Supplementary Table 4, loop-closed inconsistency was present for BCVA but not for operation time, iatrogenic retinal breaks, and postoperative vitreous hemorrhage.

Publication bias

As shown in Supplementary Figure 3, all results reject the hypothesis of the existence of a small study effect, as all plots were visually symmetric.

Discussion

As far as we know, this is the first study to ascertain the comparative efficacy of different timings of conducting IVC as an adjuvant to PPV on PDR by introducing the network meta-analysis technique. In the present network meta-analysis, the pooled results showed that the application of IVC in patients with PDR immediately after the PPV does not achieve additional therapeutic benefit. However, the application of IVC in patients with PDR before PPV, especially long and mid intervals, significantly increases the efficacy and safety of PPV.

The current network meta-analysis suggests that clinical practitioners may consider administering Conbercept before PPV to improve intraoperative and postoperative outcomes in patients with PDR. However, overly long interval between administration of IVC and PPV is associated with an increased need for silicone oil tamponade, so clinical workers need to weigh carefully regarding the timing of preoperative application. There is no consensus about the exact reasons for the different treatment responses at different intervals of IVC administration before PPV. Previous studies reveal possible effects of various intervals of performing IVC on clinical outcomes in patients undergoing PPV. Du and colleagues observed an immediate and rapid increase in the concentration when injecting Conbercept to treat hyperglycemic mouse eyes, with a decrease beginning on the seventh day after injection (48). Previous studies also suggested that administration of IVC seven days before PPV benefits achieving the best surgical outcomes (49, 50). This evidence partially explains why very-early preoperative IVC did not produce better surgical outcomes than other strategies. However, the specific reasons for the differences between preoperative, intraoperative, and perioperative IVC remain inconclusive. As a result, future research should investigate the underlying mechanisms by which IVC administration results in different clinical outcomes in PDR patients receiving PPV at different intervals.

To date, three meta-analyses (51–53) have investigated IVC's therapeutic efficacy and safety on PPV for patients with PDR. The meta-analysis by Pranata and Vania (52) concluded that, compared to PPV alone, PPV combined with IVC was associated with greater improvement in BCVA, better intraoperative outcome, and less postoperative vitreous hemorrhage. The efficacy and safety of preoperative IVC as an adjunct to PPV in the treatment of PDR were also assessed in a meta-analysis by Si et al. (53). The results of a combined study of 23 studies (including 11 RCTs, 2 cohort studies, and 10 case-control studies) showed that preoperative IVC significantly shortened the average operation time and decreased the incidences of intraoperative bleeding, iatrogenic retinal breaks, and postoperative vitreous hemorrhage. We should note that two previous meta-analyses integrated the results from studies with different types of designs to estimate the efficacy and safety of IVC, which inevitably introduced bias to pooled results. Following the previous meta-analyses, another meta-analysis (51) with RCTs was performed to evaluate IVC's efficacy in PPV for patients with PDR. The pooled results of eight studies suggested that IVC was associated with less intraoperative bleeding and endodiathermy applications, shorter surgical time, and better BCVA outcomes. Overall, three previous meta-analyses consistently supported IVC's therapeutic efficacy and safety in PPV for patients with PDR. Although the previous meta-analysis noted the preoperative and intraoperative application of IVC, separate analyses were not performed according to the intervals of administering IVC. More importantly, the differences between preoperative and intraoperative IVC were not evaluated.

In contrast to earlier network meta-analyses, the current one only used RCTs to evaluate therapeutic efficacy and safety, greatly reducing the bias introduced by the study design. Furthermore, our network meta-analysis first designed a separate analysis to investigate the role of different intervals of administering IVC in the treatment of PDR and found that intraoperative application of IVC did not add additional benefits to PPV in treating patients with PDR. Finally, the present network meta-analysis also first classified the preoperative application of IVC into four sub-phases, including very long interval, long interval, mid interval, and short interval. It is noted that very long interval was found to have no additional therapeutic benefits to PPV but was associated with more application of silicone oil tamponade.

In addition, compared to previous meta-analyses, the current network meta-analysis also offers the following advantages in terms of methodology: (a) We retrieved all currently available eligible studies by employing a thorough literature retrieval strategy; (b) We could estimate the relative differences of various intervals of preoperative IVC using network meta-analysis; and (c) All the regimens were ranked using the SUCRA method, making it easier to choose the best regimen for clinical use.

Our pooled results should be interpreted with caution due to the following limitations: (a) This network meta-analysis only included a small number of eligible studies with small sample sizes, which may have a significant negative impact on the robustness of all pooled results; (b) Because all studies were conducted in China, results should be cautiously used in other clinical contexts before being further validated; (c) There was inconsistency between direct and indirect evidences which were used to estimate the relative efficacy in improving BCVA of all regimens; therefore, the pooled result of this outcome should be cautiously interpreted; (d) Three types of PPV were used in eligible studies; however, we could not perform subgroup

analysis to eliminate the negative impact of type of PPV on the pooled results because there were limited studies were included in this network meta-analysis; and (e) Only two of the eight outcomes we examined covered all regimens, and it worth noting that there was no statistical difference between mid interval and perioperative IVC in terms of postoperative vitreous hemorrhage although ranking probability suggested more higher ranking for mid interval. SUCRA cannot show whether the difference between treatments is clinically meaningful. Therefore, more studies with larger sample sizes are required to evaluate the difference between different strategies, especially in postoperative vitreous hemorrhage between mid interval and perioperative IVC.

Our findings showed that using intraoperative IVC as an adjuvant to PPV does not achieve additional benefits for treating PDR. But preoperative IVC as an adjuvant to PPV, especially long and mid intervals of injecting IVC before performing PPV, achieves significant intraoperative and postoperative benefits in treating PDR, except for very long interval. However, additional studies are undoubtedly needed to validate our findings further.

Author contributions

WW and CQ carried out the studies, participated in collecting data, and drafted the manuscript. CQ and HY performed the statistical analysis and participated in its design. WW and CQ participated in acquisition, analysis, or interpretation of data and draft the manuscript. All authors contributed to the article and approved the submitted version.

Funding

This study was supported by Shaanxi Science and Technology Project (No. 2022SF-434) and Xi'an Science and Technology Project (No. 21YXYJ0044).

Acknowledgments

We would like to deeply appreciate all authors who performed all eligible studies which have been included in the present network meta-analysis.

Conflict of interest

The authors declare that the research was conducted in the absence of any commercial or financial relationships that could be construed as a potential conflict of interest.

Publisher's note

Supplementary material

The Supplementary Material for this article can be found online at: https://www.frontiersin.org/articles/10.3389/fendo.2023.1098165/full#supplementary-material

SUPPLEMENTARY FIGURE 1
Risk of bias assessment based on traffic light plot **(A)** and summary plot **(B)**.

SUPPLEMENTARY FIGURE 2
Global consistency model test for BCVA **(A)**, operation time **(B)**, iatrogenic retinal breaks **(C)**, and vitreous hemorrhage **(D)**. BCVA; best corrected visual acuity.

SUPPLEMENTARY FIGURE 3
Comparison-adjusted funnel plots of all outcomes.

References

1. Flaxel CJ, Adelman RA, Bailey ST, Fawzi A, Lim JI, Vemulakonda GA, et al. Diabetic retinopathy preferred practice pattern®. *Ophthalmology* (2020) 127:P66–P145. doi: 10.1016/j.ophtha.2019.09.025

2. Wong TY, Cheung CM, Larsen M, Sharma S, Simó R. Diabetic retinopathy. *Nat Rev Dis Primers* (2016) 2:16012. doi: 10.1038/nrdp.2016.12

3. Bressler SB, Qin H, Melia M, Bressler NM, Beck RW, Chan CK, et al. Exploratory analysis of the effect of intravitreal ranibizumab or triamcinolone on worsening of diabetic retinopathy in a randomized clinical trial. *JAMA Ophthalmol* (2013) 131:1033–40. doi: 10.1001/jamaophthalmol.2013.4154

4. Lee R, Wong TY, Sabanayagam C. Epidemiology of diabetic retinopathy, diabetic macular edema and related vision loss. *Eye Vis (Lond)* (2015) 2:17. doi: 10.1186/s40662-015-0026-2

5. D.R.S.R. Group. Preliminary report on effects of photocoagulation therapy. *Am J Ophthalmol* (1976) 81:383–96. doi: 10.1016/0002-9394(76)90292-0

6. Teo ZL, Tham YC, Yu M, Chee ML, Rim TH, Cheung N, et al. Global prevalence of diabetic retinopathy and projection of burden through 2045: Systematic review and meta-analysis. *Ophthalmology* (2021) 128:1580–91. doi: 10.1016/j.ophtha.2021.04.027

7. D.R.V.S.R. Group. Two-years course of visual acuity in severe proliferative diabetic retinopathy with conventional management. diabetic retinopathy vitrectomy study (DRVS) report# 1. *Ophthalmology* (1985) 92:492–502. doi: 10.1016/S0161-6420(85)34002-2

8. Berrocal MH, Acaba-Berrocal L. Early pars plana vitrectomy for proliferative diabetic retinopathy: Update and review of current literature. *Curr Opin Ophthalmol* (2021) 32:203–8. doi: 10.1097/ICU.0000000000000760

9. Karimov M, Akhundova L, Aliyeva T. Pars plana vitrectomy for full-thickness macular holes in patients with proliferative diabetic retinopathy and active fibrovascular proliferation. *Clin Ophthalmol (Auckland NZ)* (2020) 14:4125. doi: 10.2147/OPTH.S280654

10. Liao M, Wang X, Yu J, Meng X, Liu Y, Dong X, et al. Characteristics and outcomes of vitrectomy for proliferative diabetic retinopathy in young versus senior patients. *BMC Ophthalmol* (2020) 20:1–8. doi: 10.1186/s12886-020-01688-3

11. Yang Y, Liu Y, Li Y, Chen Z, Xiong Y, Zhou T, et al. MicroRNA-15b targets VEGF and inhibits angiogenesis in proliferative diabetic retinopathy. *J Clin Endocrinol Metab* (2020) 105:3404–15. doi: 10.1210/clinem/dgaa538

12. Raczyńska D, Lisowska KA, Pietruczuk K, Borucka J, Ślizień M, Raczyńska K, et al. The level of cytokines in the vitreous body of severe proliferative diabetic retinopathy patients undergoing posterior vitrectomy. *Curr Pharm Des* (2018) 24:3276–81. doi: 10.2174/1381612824666180926110704

13. Pakzad-Vaezi K, Albiani DA, Kirker AW, Merkur AB, Kertes PJ, Eng KT, et al. A randomized study comparing the efficacy of bevacizumab and ranibizumab as pre-treatment for pars plana vitrectomy in proliferative diabetic retinopathy. *Ophthalmic Surg Lasers Imaging Retina* (2014) 45:521–4. doi: 10.3928/23258160-20141118-06

14. Zhou J, Liu Z, Chen M, Luo Z-H, Li Y-Q, Qi G-Y, et al. Concentrations of VEGF and PlGF decrease in eyes after intravitreal conbercept injection. *Diabetes Ther* (2018) 9:2393–8. doi: 10.1007/s13300-018-0527-9

15. Wu Z, Zhao J, Lam W, Yang M, Chen L, Huang X, et al. Comparison of clinical outcomes of conbercept versus ranibizumab treatment for retinopathy of prematurity: A multicentral prospective randomised controlled trial. *Br J Ophthalmol* (2022) 106:975. doi: 10.1136/bjophthalmol-2020-318026

16. Su L, Ren X, Wei H, Zhao L, Zhang X, Liu J, et al. Intravitreal conbercept (KH902) for surgical treatment of severe proliferative diabetic retinaopathy. *Retina* (2016) 36:938–43. doi: 10.1097/IAE.0000000000000900

17. Hutton B, Salanti G, Caldwell DM, Chaimani A, Schmid CH, Cameron C, et al. The PRISMA extension statement for reporting of systematic reviews incorporating network meta-analyses of health care interventions: checklist and explanations. *Ann Internal Med* (2015) 162:777–84. doi: 10.7326/M14-2385

18. Sterne JA, Savović J, Page MJ, Elbers RG, Blencowe NS, Boutron I, et al. RoB 2: A revised tool for assessing risk of bias in randomised trials. *BMJ* (2019) 366:l4898. doi: 10.1136/bmj.l4898

19. Cipriani A, Higgins JP, Geddes JR, Salanti G. Conceptual and technical challenges in network meta-analysis. *Ann Internal Med* (2013) 159:130–7. doi: 10.7326/0003-4819-159-2-201307160-00008

20. Salanti G. Indirect and mixed-treatment comparison, network, or multiple-treatments meta-analysis: many names, many benefits, many concerns for the next generation evidence synthesis tool. *Res Synth Methods* (2012) 3:80–97. doi: 10.1002/jrsm.1037

21. Tu YK. Using generalized linear mixed models to evaluate inconsistency within a network meta-analysis. *Value Health* (2015) 18:1120–5. doi: 10.1016/j.jval.2015.10.002

22. Higgins JP, Jackson D, Barrett JK, Lu G, Ades AE, White IR. Consistency and inconsistency in network meta-analysis: Concepts and models for multi-arm studies. *Res Synth Methods* (2012) 3:98–110. doi: 10.1002/jrsm.1044

23. Yu-Kang T. Node-splitting generalized linear mixed models for evaluation of inconsistency in network meta-analysis. *Value Health* (2016) 19:957–63. doi: 10.1016/j.jval.2016.07.005

24. Lu G, Ades AE. Assessing evidence inconsistency in mixed treatment comparisons. *J Am Stat Assoc* (2006) 101:447–59. doi: 10.1198/016214505000001302

25. Lu G, Ades AE. Combination of direct and indirect evidence in mixed treatment comparisons. *Stat Med* (2004) 23:3105–24. doi: 10.1002/sim.1875

26. Mbuagbaw L, Rochwerg B, Jaeschke R, Heels-Andsell D, Alhazzani W, Thabane L, et al. Approaches to interpreting and choosing the best treatments in network meta-analyses. *Systematic Rev* (2017) 6:79. doi: 10.1186/s13643-017-0473-z

27. Sterne JA, Egger M, Smith GD. Systematic reviews in health care: Investigating and dealing with publication and other biases in meta-analysis. *Bmj* (2001) 323:101–5. doi: 10.1136/bmj.323.7304.101

28. White Ian. (2017), NETWORK: Stata module to perform network meta-analysis. Available at: https://EconPapers.repec.org/RePEc:boc:bocode:s458319.

29. Chaimani A, Higgins JP, Mavridis D, Spyridonos P, Salanti G. Graphical tools for network meta-analysis in STATA. *PloS One* (2013) 8:e76654. doi: 10.1371/journal.pone.0076654

30. Gao S, Lin Z, Chen Y, Xu J, Zhang Q, Chen J, et al. Intravitreal conbercept injection as an adjuvant in vitrectomy with silicone oil infusion for severe proliferative diabetic retinopathy. *J ocular Pharmacol Ther* (2020) 36:304–10. doi: 10.1089/jop.2019.0149

31. Jiang T, Gu J, Zhang P, Chen W, Chang Q. The effect of adjunctive intravitreal conbercept at the end of diabetic vitrectomy for the prevention of post-vitrectomy hemorrhage in patients with severe proliferative diabetic retinopathy: a prospective, randomized pilot study. *BMC Ophthalmol* (2020) 20:43. doi: 10.1186/s12886-020-1321-9

32. Li B, Li MD, Ye JJ, Chen Z, Guo ZJ, Di Y. Vascular endothelial growth factor concentration in vitreous humor of patients with severe proliferative diabetic retinopathy after intravitreal injection of conbercept as an adjunctive therapy for vitrectomy. *Chin Med J* (2020), 133:664–9. doi: 10.1097/CM9.0000000000000687

33. Li CS, Zhang QS, Zou JX, Liu X. Effect and safety of PPV assisted by intravitreal injection of conbercept in the treatment of PDR combined with vitreous hemorrhage. *Int Eye Sci* (2021) 21:1597–600. doi: 10.3980/j.issn.1672-5123.2021.9.21

34. Lin SB. Effect of intravitreal injection of conbercept before PPV on complications and visual recovery in patients with PDR. *Int eye Sci* (2018) 18:919–21.

35. Luo J, Liu LL, Zhou L. The effect of conbercept combined with vitrectomy in the treatment of progressive proliferative diabetic retinopathy. *Shanghai Med Pharm J 42* (2021), 42:35–36+59.

36. Luo LH, Duan GP, Zeng Q, Hu R, Li QX. The effect of conbercept combined with vitrectomy in the treatment of proliferative diabetic retinopathy. *J Chin Physician* (2018) 20:742–4. doi: 10.3760/cma.j.issn.1008-1372.2018.05.030

37. Ou Z, Wang Q, Jiang J, Liu X. Intravitreal injection of conbercept combined with PPV in the treatment of proliferative diabetic retinopathy. *Int Eye Sci* (2021) 21:986–90. doi: 10.3980/j.issn.1672-5123.2021.6.09

38. Ran Q, Feng C, Zhou WQ. Effects of conbercept assisted resection of vitreous body in the treatment of diabetic retinopathy. *Chin J Med Guide* (2016) 18:708–709+711. doi: CNKI:SUN:DKYY.0.2016-07-033

39. Ren X, Bu S, Zhang X, Jiang Y, Tan L, Zhang H, et al. Safety and efficacy of intravitreal conbercept injection after vitrectomy for the treatment of proliferative diabetic retinopathy. *Eye (Basingstoke)* (2019) 33:1177–83. doi: 10.1038/s41433-019-0396-0

40. Shang YX, Wang X, Xie SP, Zhang SJ, Wang LF. Clinical observation of parsplana vitrectomy combined with intravitreal conbercept in the treatment of proliferative diabetic retinopathy complicated with macular edema. *Chin J Mod Med* (2018) 28:122–4. doi: 10.3969/j.issn.1005-8982.2018.16.025.

41. Shi SH, Xu F, Li M. Clinical study of conbercept in patients with proliferative diabetic retinopathy undergoing vitrectomy. *Int eye Sci* (2020) 20:852–5. doi: 10.3980/j.issn.1672-5123.2020.5.24

42. Su L, Ren X, Wei H, Zhao L, Zhang X, Liu J, et al. Intravitreal conbercept (Kh902) for surgical treatment of severe proliferative diabetic retinopathy. *Retina (Philadelphia Pa.)* (2016) 36:938–43. doi: 10.1097/IAE.0000000000000900

43. Sun LY, ZHao MS, Li FZ, Yao Q, ZHu ZQ, Yang XG. Clinical curative effect of vitreous cavity injection combined with transconjunctival sutureless vitrectomy on the patients with poliferative diabetic retinopathy. *Xian Dai Sheng Wu Yi Xue Jin Zhan* (2017) 17:4579–82. doi: 10.13241/j.cnki.pmb.2017.23.043

44. Sun M, Li MX. Study of anti-vascular endothelial growth factor medicine for proliferative diabetic retinopathy at perioperative period. *Int Eye Sci* (2015) 15:1772–4. doi: 10.3980/j.issn.1672-5123.2015.10.26

45. Wen XX, Tan DW, Li HJ, Liu YY, Jiang XJ, Fang T. Preoperative medication timing analysis and effect on neovascular membrane vascular endothelial growth factor in patients with proliferative diabetic retinopathy assisted by conbercept. *J Chin Physician* (2019) 21:89–93.

46. Zhao XL, Zhang D, Yang G, Yuan A. Intravitreal conbercept as a pretreatment of vitrectomy for patients with severe proliferative diabetic retinopathy. *Chin J Ophthalmol Otorhinol* (2018) 18:22–5.

47. Yang X, Xu J, Wang R, Mei Y, Lei H, Liu J, et al. A randomized controlled trial of conbercept pretreatment before vitrectomy in proliferative diabetic retinopathy. *J Ophthalmol* (2016) 2016:1–8. doi: 10.1155/2016/2473234

48. Du L, Peng H, Wu Q, Zhu M, Luo D, Ke X, et al. Observation of total VEGF level in hyperglycemic mouse eyes after intravitreal injection of the novel anti-VEGF drug conbercept. *Mol Vis* (2015) 21:185–93.

49. di Lauro R, De Ruggiero P, di Lauro R, di Lauro MT, Romano MR. Intravitreal bevacizumab for surgical treatment of severe proliferative diabetic retinopathy. *Graefes Arch Clin Exp Ophthalmol* (2010) 248:785–91. doi: 10.1007/s00417-010-1303-3

50. Ishikawa K, Honda S, Tsukahara Y, Negi A. Preferable use of intravitreal bevacizumab as a pretreatment of vitrectomy for severe proliferative diabetic retinopathy. *Eye (Lond)* (2009) 23:108–11. doi: 10.1038/sj.eye.6702983

51. Chen GH, Tzekov R, Mao SH, Tong YH, Jiang FZ, Li WS. Intravitreal conbercept as an adjuvant in vitrectomy for proliferative diabetic retinopathy: a meta-analysis of randomised controlled trials. *Eye (Lond)* (2022) 36:619–26. doi: 10.1038/s41433-021-01474-5

52. Pranata R, Vania A. Intravitreal conbercept improves outcome in patients undergoing vitrectomy for proliferative diabetic retinopathy: A systematic review and meta-analysis. *J Evid Based Med* (2020) 13:116–24. doi: 10.1111/jebm.12379

53. Si X, Sun CF, Che Y, Feng WY, Feng YF. A meta-analysis of the effects of intavitreal conbercept as an adjunct before vitrectomy in proliferative diabetic retinopathy. *Chin J Exp Opthalmol* (2020) 38:773–80. doi: 10.3760/cma.j.cn115989-20200715-00498

frontiers | Frontiers in Endocrinology

TYPE Review
PUBLISHED 02 March 2023
DOI 10.3389/fendo.2023.1108394

OPEN ACCESS

EDITED BY
Rajashekhar Gangaraju,
University of Tennessee Health Science Center (UTHSC), United States

REVIEWED BY
Tingting Liu,
Shandong Eye Institute, China
Guiting Lin,
University of California, San Francisco, United States
Haijiang Lin,
Massachusetts Eye & Ear Infirmary and Harvard Medical School, United States

*CORRESPONDENCE
Aijun Deng
dengaijun@hotmail.com

SPECIALTY SECTION
This article was submitted to Clinical Diabetes, a section of the journal Frontiers in Endocrinology

RECEIVED 26 November 2022
ACCEPTED 21 February 2023
PUBLISHED 02 March 2023

CITATION
Lin Z, Deng A, Hou N, Gao L and Zhi X (2023) Advances in targeted retinal photocoagulation in the treatment of diabetic retinopathy.
Front. Endocrinol. 14:1108394.
doi: 10.3389/fendo.2023.1108394

Advances in targeted retinal photocoagulation in the treatment of diabetic retinopathy

Zichun Lin, Aijun Deng*, Ning Hou, Liyu Gao and Xushuang Zhi

Affiliated Hospital of Weifang Medical University, School of Clinical Medicine, Weifang Medical University, Weifang, China

Aim: Targeted retinal photocoagulation (TRP) is an emerging laser technology for retinal targeted therapy. TRP can specifically act on unperfused retinal capillaries and retinal intermediate ischemic areas, reduce damage to tissue perfusion areas and panretinal photocoagulation (PRP) complications or adverse events. In this regard, this review discusses the treatment options, efficacy, and latest progress of TRP for diabetic retinopathy (DR) based on randomized controlled trial (RCT), meta-analysis, case review, and other existing studies.

Methods: In-depth research was conducted on articles about the proposal and development of TRP, its simple application in DR, and combined therapy. In order to review the new progress, application methods, effects, and prospects of TRP in the treatment of DR, the articles related to TRP in the databases of PubMed and Web Of Science since this century were comprehensively analyzed.

Results: TRP is effective in treating DR and may become a substitute for PRP in the future. In addition, the treatment regimen of TRP combined with intravitreal injection of anti-vascular endothelial growth factor (anti-VEGF) drugs can also be used as a new therapeutic approach to expand the treatment regimen for the treatment of DR, and this combination therapy also has effects on other retinal vascular diseases.

Conclusions: With the advancement of technology, TRP has been continuously applied in clinical practice, and its potential benefits have opened up broad prospects for the treatment of DR. The combination therapy of TRP and anti-VEGF is expected to become a new option for patients with DR an retinal diseases.

KEYWORDS

diabetic retinopathy, targeted retinal photocoagulation, retinal vascular disease, retina, laser, treatment

1 Introduction

The effects of laser interaction with retinal tissue have long been mentioned, in the 1940s when German ophthalmologist Meyer-Schwickerath pioneered retinal photocoagulation (1, 2). For more than 40 years, retinal photocoagulation has been used as the standard choice for the treatment of retinal vascular diseases and complications, mainly including proliferative diabetic retinopathy (PDR), diabetic macular edema (DME), retinal vein occlusion (RVO) and retinal tears, etc (Figure 1).

The scope of traditional PRP is mainly distributed in the middle and peripheral part of the retina, 1.5-2 optic disc diameters (DD) posteriorly from the optic disc and 2 DD temporally from the fovea, bounded by the superior and inferior vascular arches; forward to the ampulla of the vortex vein (or equator). Currently, PRP is the gold standard for the treatment of extensive areas of non-perfusion (suggesting severe retinal ischemia) (Diabetic Retinopathy Research Group 1981) (3), as well as the main method for the treatment of severe nonproliferative diabetic retinopathy (NPDR) and PDR. However, due to the photochemical damage of the laser, panretinal laser photocoagulation causes more damage to the ocular tissue, and its side effects include hemorrhage, choroidal detachment, acute angle-closure glaucoma, decreased color vision and contrast sensitivity, night blindness, lens burn (4–6) and permanent retinal scarring resulting in blind spots, etc. The occurrence of these complications is closely related to laser parameters such as increased duration and power and intensive treatment in a single session, which all lead to increased diffusion of thermal energy within the retina and choroid (7).

2 Materials and methods

The databases of PubMed, Web of Science were searched using the following keyword combinations: Targeted Retinal Photocoagulation, TRP, Diabetic Retinopathy, Retinopathy. Related articles discuss the effects of various treatment options of TRP in DR and other common retinopathy through RCT, meta-analysis, case review and other research methods. Inclusion criteria included full text, English and publications from this century. Articles were initially selected by searching for titles and abstracts. The full text of the papers was reviewed and papers with titles or abstracts that did not fit the purpose of this review or did not provide sufficient data for a full evaluation were excluded. To complement the search, citations to relevant articles were also collected, and we got 23 qualified publications (Figure 2). We grouped all obtained studies into application of TRP in DR and other retinopathy (RVO and radiation retinopathy), summarized and analyzed the main research contents of TRP in treating DR in chronological order (Table 1). To try to explore the effects and potential benefits of these treatment schemes.

3 Results

3.1 Progress of TRP

In 2009, Reddy et al. improved on the basis of panretinal laser photocoagulation and designed a peripheral laser strategy assisted by ultra-wide-angle fluorescein angiography (8),to reduce the damage to the retina caused by panretinal laser photocoagulation, which is also the prototype concept of targeted retinal laser photocoagulation.

TRP is a laser technology aimed at the peripheral non-perfusion and ischemic areas of the retina, and the laser area is determined according to the degree and progression of the patient's retinopathy. To ensure coverage of the entire ischemic area and its margins (usually suspected of having high-density or leaking microaneurysms), the laser extends 1-2DD of the laser scan over the peripheral ischemic and non-perfused areas. Compared with panretinal laser photocoagulation, targeted retinal laser photocoagulation is more targeted to the treatment area and has fewer laser points, so it can minimize the amount of laser treatment and reduce the occurrence of ocular adverse events caused by retinal photocoagulation rate.

The value of ultra-wide-angle fluorescein fundus angiography (UWFFA) and ultra-wide-angle swept-frequency optical coherence tomography (WF SS-OCTA) in TRP. Since the key of TRP treatment is to accurately treat the non-perfused and ischemic areas of the retina, accurate positioning of the entire ischemic area of the retina is the primary condition for the successful treatment of targeted lasers. Visualization of the entire retina is fundamental to assess non-perfused areas, vascular leakage,

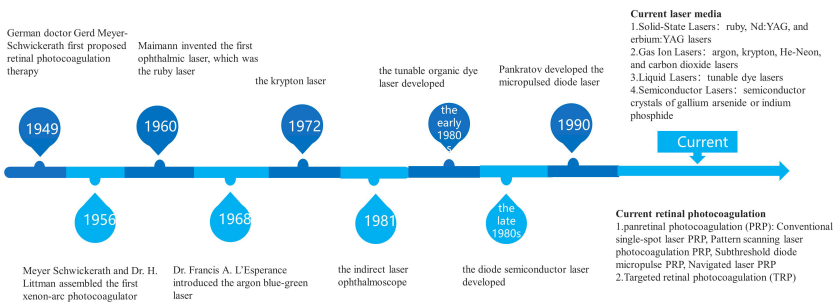

FIGURE 1
Advances in targeted retinal photocoagulation in the treatment of diabetic retinopathy.

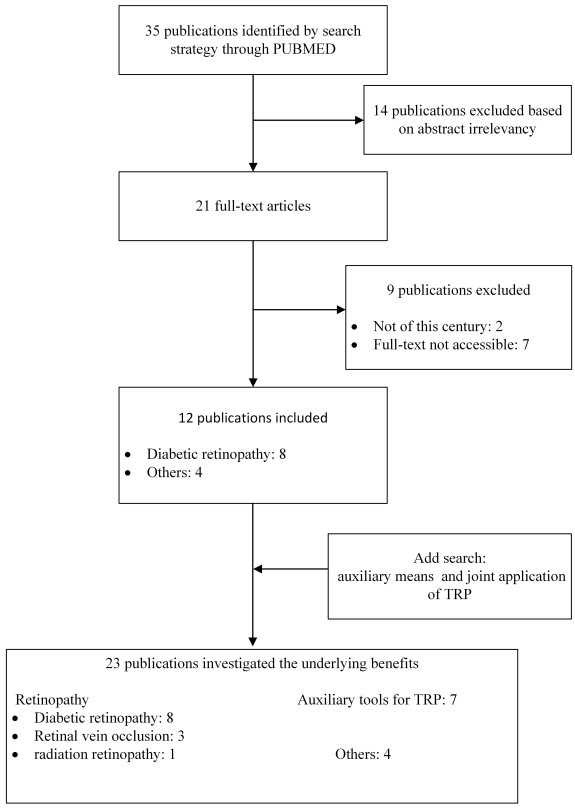

FIGURE 2
Flow diagram of systematic search.

microvascular abnormalities, and neovascularization, and ultra-wide-field (UWF) imaging improves retinal visualization by up to 82% in a single image (15).

Fluorescein angiography (FA) has been used for 50 years in the evaluation of superficial retinal vascular abnormalities in different stages of DR. In order to expand the inspection field, people currently mainly choose to use wide-field (>30° and >200°) and UWF (≥200°) fundus angiography and UWFFA (16). Since UWFFA can capture a 200° area and can view the posterior pole, central peripheral and peripheral fundus, in another study it was confirmed that the capillary non-perfusion (CNP) area detected by UWFFA in patients with DR was 3.9 times that of conventional angiography (17). Thus, UWFFA is an important aid for the successful implementation of targeted lasers.

With the advent of optical coherence tomography angiography (OCTA), it has become possible to obtain highly detailed depth-resolved images of retinal and choroidal microvascular abnormalities. While early OCTA focused on viewing the macular region, WF SS-OCTA significantly increases the field of view (FOV) at the retinal surface, and WF SS-OCTA has been shown to be effective in identifying diabetic retinopathy (18, 19). Two case analyses reported the correspondence and superiority of WF SS-OCTA relative to UWF FA in longitudinal assessment of retinal nonperfusion (RNP) in PDR, with higher detection rates in NP areas after anti-VEGF drug injection treatment (20), and provided important insights into the stability of retinal ischemia after PRP (21). However, there is no clinical report on TRP assisted by WF SS-OCTA.

3.2 Clinical application of TRP

3.2.1 TRP for DR

3.2.1.1 TRP therapy

DR is the main cause of blindness in diabetic patients, and the main pathological change in blindness is neovascularization. At present, the main method for the treatment of retinal neovascularization is retinal photocoagulation. Since this century, the research of TRP has increased year by year. Researchers have comprehensively explored the therapeutic effect and safety of TRP on DR through combined treatment, comparative control and other methods (Table 2). In 2009, the University of California reported two cases of UWFFA-assisted targeted laser treatment of diabetic retinopathy (8). For both patients, 532 nm laser was accurately applied to the ischemic area displayed and clearly demarcated by UWFFA for a total of 1000-1400 times. This treatment technology first entered the public eye as an individualized treatment plan: retinal angiography found that TRP successfully regressed retinal neovascularization in two patients. At 9-month follow-up, the patients' vision was maintained and there was no recurrence of neovascularization and macular edema. In a clinical trial reported in the United Kingdom in 2013 (3), 20 newly treated patients with PDR were treated with TRP alone. The results of the study show that in the short term (12 weeks to 24 weeks), its clinical efficacy and safety are worthy of recognition:76% of patients experienced PDR regression at week 12; patients' vision and visual field did not worsen or even improved; macular thickness was significantly reduced (mean baseline 251 μm, 12.1 μm at 24 weeks); disease progression was slow, and no TRP-related ocular adverse events occurred during the study period.

3.2.1.2 Ultra-wide-angle assisted guidance TRP

The visual field of fluorescein angiography of the standard fundus camera is 30 – 60°. It is necessary to take different images at different times in the study to image the periphery of the retina. This makes it very difficult to accurately delineate retinal capillary non-perfusion and accurately apply photocoagulation within the ischemic boundary. UWFFA is a very useful tool in the diagnosis, staging, management and treatment of DR (22). UWFFA can display more retinal pathology even in eyes judged as normal by 7 standard field (7SF) (16). In 2008, Friberg et al (23). first reported the feasibility of UWFA in 30 eyes of 30 DR patients. Compared with the standard system, they observed that UWFA allowed imaging of a larger area of retinal surface (8.7 ± 1.6 vs 3.4 ± 0.76DD, P<0.001) and retinal ischemia (16.9 ± 15 vs 3.4 ± 4.26 sectors, P<0.05), although the image quality was reduced. Then in 2009, the first case report (8) of TRP and UEFFA mentioned that under UWFFA, the non-perfusion area and its boundary of the patient's retinal capillaries could be identified very accurately, providing a clearer and more discernible field of vision for the application of TRP. UWFFA can initially and accurately locate the

TABLE 1 The historical process of the treatment of PDR with TRP.

Time	Magazine	Type	Ideas	Content	Conclusion
2009 (8)	Semin Ophthalmol.	Case Reports	PRP may excessively damage the retina, so consider using UWFFA and TRP to reduce complications	Two cases of using UWFFA to guide TRP to the NPAs of retinal capillary were reported for the first time	When TRP is used in combination with UWFFA, it can cause the regression of neovascularization in diabetes and minimize the amount of laser treatment applied to the retina
2012 (9)	Clin Ophthalmol.	Clinical Trial	Accurate positioning during laser treatment may help to improve the clinical results of laser treatment	TRP was performed on 54 patients with DME by using navigation laser photocoagulation system Navilas	The laser navigation effect is consistent with the target area in positioning, and the pain associated with treatment is significantly lower than PRP
2013 (10)	Br J Ophthalmol.	Randomized Controlled Trial	In order to reduce the adverse effects of laser treatment, many experts began to use the laser with lighter burn and lower intensity than the original provisions of ETDRS to treat patients	The short-term effects of PRP and TRP on macular thickness were compared	Local laser treatment did not increase the macular thickness or any serious adverse events in the eye in a short time
2013 (3)	Acta Ophthalmol.	Clinical Trial	Compared with PRP, TRP may prevent well-perfused tissue from laser-induced tissue scar formation	TRP of 28 patients with PDR at the initial stage of treatment with WFFA	TRP, a laser technology that only targets the local ischemic retina, can reduce the potential long-term damage associated with the expansion of long-pulse PRP burn
2014 (11)	Invest Ophthalmol Vis Sci.	Randomized Controlled Trial	Find a technology to reduce DME recurrence after intravitreal injection of anti-VEGF drugs to avoid repeated injection	Apply IVB or IVB+TRP to 52 DME patients	TRP for NPAs can effectively maintain the reduced CRT after IVB
2018 (12)	Int Ophthalmol.	Randomized Controlled Trial	ETRP procedure to treat areas of capillary non-perfusion and intermediate ischemic zones posterior to the equator as well as the entire retina anterior to the equator	Apply PRP or ETRP to 234 PDR patients	ETRP is a sensible substitution for CPRP to induce PDR regression.
2018 (13)	Ophthalmology.	Clinical Trial	To test the hypothesis that WFFA eguided TRP significantly reduces the number of required anti-VEGF injections	Apply IVR or IVR+TRP to 29 DME patients	There was no significant evidence that the combination of leizumab and TRP was more effective compared to Leizumab alone.
2021 (14)	Doc Ophthalmol.	Randomized Controlled Trial	Compared with PRP, the leakage area of neovascularization in PRP+IVR is reduced, and more focal TRP is considered to reduce the loss of retinal function	Applying IVR+PRP or IVR+TRP to 28 PDR patients	The reduction level of retinal neovascularization leakage area by two laser modes is similar in one year

PDR, proliferative diabetic retinopathy; TRP, targeted retinal photocoagulation; PRP, panretinal photocoagulation; UWFFA, ultra-wide-angle fluorescein fundus angiography; DME, diabetic macular edema; ETDRS, early treatment of diabetic retiopathy study; WFFA, wide-angle fluorescein fundus angiography; anti-VEGF, anti-vascular endothelial growth factor; IVB, intravitreal bevacizumab; NPAs, non-perfusion areas; CRT, central retinal thickness; ETRP, Extended TRP; CPRP, central panretinal photocoagulation; IVR, intravitreal ranibizumab.

non-perfusion area of retinal capillaries in a 200° field of vision at the early stage of application. In 2013, Muqi et al. (3) evaluated the effect of UWFFA-guided TRP in the eyes of 28 PDR patients. At 12 weeks, 76% of patients had PDR regression, and 37% had complete disease regression at 24 weeks. They found that the thickness of the central retina decreased significantly over time, measured by optical coherence tomography (22). With the gradual maturity of the UWFFA program, as an assistant retinal examination tool, it has been more and more widely used in clinical work. However, the specific use standards for its joint application with TRP still need to be further clarified through large-scale research in the future.

3.2.1.3 Compared with panretinal photocoagulation

The primary difference between targeted retinal laser and panretinal laser photocoagulation is that the narrowing of the laser range results in a significant reduction in the number of laser spots on the retina. In all randomized controlled clinical trials, regardless of whether the targeted laser range is specified as "optos-guided TRP treatment covered the area of capillary non-perfusion from the ora serrata up to 1 DD into perfused retina (10)", "navigated, semi-automatic pattern laser application was conducted based on the treatment plan (9)" or "capillary non -perfusion and intermediate ischemic zones posterior to the equator as well as the entire retina anterior to the equator (12)", the TRP has significantly fewer laser spots (9, 12) or lower power (10). In this regard, the visual analog scale was used to quantify the degree of pain in the treatment of patients, and it was found that the pain of TRP was significantly lower than that of PRP.

For the improvement of visual function, both treatment modalities improved visual acuity and mean visual field defect in the short term (4-12 weeks) but there was no significant difference between the two (10); in the medium and long term (at least 3 months)) The mean best-corrected visual acuity (BCVA) after treatment was significantly decreased, and the difference was not significant (12). DME is a serious complication of DR and one of the main causes of visual loss in DR patients, so central macular thickness (CMT)/central retinal thickness (CRT) is also an important research parameter. CMT decreased in the short term

TABLE 2 Summary of studies targeted retinal photocoagulation for diabetic retinopathy.

Study	Patients	Targeted laser range	Outcomes of interest (primary and secondary)	Follow-up period	Main conclusions
Shantan Reddy et al. (8)	A middle-aged man with NPDR in both eyes and a middle-aged woman with PDR in the left eye	retinal ischemic area	Ultra wide field fluorescein angiography	9 months	TRP successful led to the regression of the retinal neovascularization
Mahiul M K Muqit (3)	Treatment-naive PDR (n=20)	areas of peripheral retinal capillary non-perfusion and intermediate zones of perfused and non-perfused retina	PDR grade; CRT; MD; standard V; ETDRS VA	24 weeks	TRP has a satisfactory short-term safety profile and is a promising treatment option with no deterioration in CRT, VA, or VF in the affected eye after short-term treatment
Mahiul M K Muqit (10)	Treatment-naive PDR (n=24)	area of capillary non-perfusion from the ora serrata up to 1 DD into perfused retina	Primary Outcome Measures: change in CRT on OCT Secondary Outcome Measures: OCT peripapillary NFL thickness; PDR disease regression on optos angiography; VF; VA	12 weeks	high-density 20-ms TRP using 2500 burns did not produce increased macular thickness or any ocular adverse events during the short-term
Marcus Kernt (9)	DME (n=54)	navigated, semi-automatic pattern laser application	visual analog scale directly; Navilas color images	1 months	treatment-related pain following Navilas laser photocoagulation was significantly lower than pain following conventional laser treatment
Homayoun Nikkhah (12).	naïve early or high-risk PDR (n=234)	areas of capillary non-perfusion and intermediate ischemic zones posterior to the equator as well as the entire retina anterior to the equator.	Primary Outcome Measures: early PDR regression, specified as reduction in retinal neovascularization based on WFFA at 3 months. Secondary Outcome Measures: BCVA; CMT changes.	3 months	TRP may be an appropriate alternative to PRP in PDR regression at least through 3 months
David M Brown (13)	DME (n=29)	areas of nonperfused peripheral retina plus a 1edisc area margin	Primary Outcome Measures: mean change in ETDRS BCVA from baseline and number of intravitreal injections administered Secondary Outcome Measures: percentage of patients gaining or losing 15 ETDRS letters or more from baseline, mean change in CRT, mean change in peripheral visualfield as measured by GVF testing, and incidence and severity of adverse events.	36 months	Combination therapy did not reduce treatment burden and improve vision compared with drug injection alone, but may reduce the development and incidence of neovascular complications
Yoshihiro Takamura (11)	DME (n=52)	nonperfused areas (NPAs)	BCVA;CRT	6 months	TRP for NPAs was effective to maintain the reduced CRT after grid/focal photocoagulation and IVB for patients with DME
Luiza Toscano (14)	adult patients with treatment-naive PDR and a BCVA better than 20/800 (n=23)	retinal ischemic areas	Primary Outcome Measures: FLA of active new vessels Secondary Outcome Measures : BCVA;CSFT; Number of Ranibizumab Intravitreal Injections; Electroretinography	48 weeks	PIR+IVR or PRP+IVR are comparable strategies regarding FLA control in PDR and led to similar retinal function impairment

PDR, proliferative diabetic retinopathy; CRT, central retinal thickness; MD, mean deviation; TRP, targeted retinal photocoagulation; VF, visual fields; VA, visual acuity; NFL, nerve fibre layer; PRP, panretinal photocoagulation; UWFFA, ultra-wide-angle fluorescein fundus angiography; DME, diabetic macular edema; ETDRS, early treatment of diabetic retiopathy study; WFFA, wide-angle fluorescein fundus angiography; anti-VEGF, anti-vascular endothelial growth factor; IVB, intravitreal bevacizumab; NPAs, non-perfusion areas; IVR, intravitreal ranibizumab; FLA, fluorescein leakage area; BCVA,best corrected visual acuity.

(4-12 weeks) after PTR treatment, and was not significantly different from PRP; although a clinical trial (NCT01232179) (12) reported that TRP or PRP alone was used to treat patients with early or high-risk PDR after 3 months There is an increase in CMT, and CMT thickening after laser treatment has been demonstrated in many other studies (9, 24–26), but there is no difference in results between the two laser modalities. In terms of safety, there were no serious ocular complications or adverse events immediately after TRP treatment, short-term or even mid-to-long term, and there were no signs of intraretinal hemorrhage, vascular damage or traction retinal detachment in the laser treatment area. There is also no adjustment to the treatment regimen for patients treated with TRP, such as switching to PRP.

Comparing the efficacy and safety of the two laser methods, after analyzing many research parameters such as the number of laser points, visual function, UWF, pain level, prognosis, and

adverse events, there may be no difference in the efficacy of the two on DR. But TRP reduces retinal damage and preserves more healthy retinas due to fewer laser points, which also improves patient comfort. Therefore, TRP may be a future alternative to PRP to some extent (27)

3.2.1.4 Combination therapy of TRP and vitreous anti-VEGF drug injection

With the research on the pathophysiology of retinal vascular diseases, the use of anti-VEGF drugs for the treatment of retinal vascular diseases has become more and more popular. Such drugs can bind tightly to VEGF to reduce vascular permeability and then inhibit the formation of new blood vessels. Anti-VEGF is currently the gold standard treatment for veno-occlusive macular edema, especially BRVO (28). However, the short half-life of the drug causes its concentration in the eye to drop rapidly and the concentration in the vitreous cavity is unstable and the treatment effect is short. Retinal neovascularization and macular swelling are prone to recur after a single injection of anti-VEGF drugs (13). Therefore, frequent intravitreal injections of anti-VEGF drugs are required to control macular edema, which increases the likelihood of adverse events such as endophthalmitis and retinal detachment. Researchers have found in clinical trials that Through the combined application of vitreous drug injection and targeted laser therapy, the use of targeted laser can effectively reduce the frequency of drug injections or improve the prognosis, which may achieve the purpose of reducing the number of patient visits, costs and the risk of adverse events.

Current studies have suggested that anti-VEGF drugs can reduce retinal thickness, improve DME, and improve vision in the treatment of DR, but require repeated injections for optimal results. In this regard, in order to reduce the number of injections of anti-VEGF drugs and reduce the occurrence of adverse events, researchers considered the combined application of TRP and intravitreal injection of anti-VEGF drugs. At present, two controlled clinical trials have been completed in Japan (UMIN000007566) and the United States (NCT01552408), involving a total of 81 DME patients. Visual function and CRT were mainly compared between patients receiving TRP and anti-VEGF drugs in combination with patients receiving anti-VEGF drugs alone. However, the results of the two trials are contradictory: after a 6-month study by the Japanese team, it was found that the average best corrected visual acuity (BCVA) of the combined treatment group improved more significantly, And the CRT of the patients in the injection-only group increased to a higher degree at the 3rd, 4th, and 5th months (11);however, after a 3-year Randomized DAVE Trial, the US team found that the combined treatment group was not better than the single injection group in terms of BCVA, visual field, CRT, and the number of injections, but in In terms of safety, there were 5 new cases of new PDR-related neovascularization in the drug injection group but no endophthalmitis in the combined treatment group (13). The difference in results between the two groups may be related to the inclusion criteria, dosing schedule, and sample size. Compared with the US study, the participants in the Japanese trial were injected with bevacizumab (1.25 mg IV bevacizumab: 0.3 mg IV ranibizumab), which may explain the difference in results between the two groups.

In addition, a controlled clinical trial (NCT03904056) (14) reported by the São Paulo State University research team in 2021 compared the effect of PRP combined with intravitreal injection of ranibizumab (IVR) and TRP combined with IVR in the treatment of PDR. The results showed that there were no significant changes in BCVA and central subfield thickness (CSFT) between the two groups; the fluorescein leakage area of active new vessels (FLA) was significantly reduced in the two groups, but there was no between-group difference. In addition, we checked on the International Clinical Trials Registry website (ClinicalTrials.gov) that the Cairo University research team has initiated a RCT (NCT04674254),to compare the changes of macular area in PDR patients receiving anti-VEGF therapy combined with TRP or PRP therapy, and we will continue to pay attention to this.

Overall, TRP helps to improve DME recurrence after vitreous drug injection, additional laser may help to suppress VEGF production in the ischemic area, and combination therapy of TRP and anti-VEGF drugs may help reduce the frequency of vitreous drug injections, patient treatment costs, number of clinic visits, and adverse events (eg, endophthalmitis, retinal detachment).

3.2.2 TRP of other retinopathy

In addition to DR, the researchers also studied the therapeutic effects of TRP on other retinopathy. We mainly analyzed the effects of TRP on RVO and radiation retinopathy (Table 3). Studies have found that RVO is the second most common retinal vascular disease, and macular edema is a common complication of this disease and the main cause of reduced vision. Therefore, improving macular edema is a key link in the treatment of this disease. The researchers selected patients with RVO and macular edema (ME) who met the treatment criteria to conduct individualized treatment for a single case or controlled clinical trials with different durations of 6 months, 9 months, and 12 months have been carried out successively (28–30, 32).A total of 101 patients were enrolled, and the efficacy and safety of TRP combined with anti-VEGF drug injection and drug injection alone were compared.

First, all patients showed significant improvement in visual function, in terms of BCVA: the mean increase in Early Treatment of Diabetic Retiopathy Study (ETDRS) letters in the RBZ group in the comparative trial with ranibizumab (RBZ) was 25.7 ± 8.2 (95% CI: 21.5–29.9), RBZ + TRP group was 23.38 ± 7.6 (95% CI: 19.3–27.4) (28); in the comparative trial of intravenous bevacizumab (IVB), the BCVA of the IVB+TRP group gradually improved and reached a significant level at 6 months, However, there was no significant improvement in the IVB group (30). In addition, the mean contrast sensitivity and visual field of the patients were significantly improved under both treatment regimens (28), and there were no disease progression or adverse events related to TRP or intravitreal injection, such as infectious ophthalmia, intravitreal hemorrhage, neovascularization, retinal detachment, etc. Second, patients' mean CRT (or CMT) continued significant improvement (28–30). Finally, the combined application of TRP can reduce the

TABLE 3 Summary of studies targeted retinal photocoagulation for retinal vein occlusion and radiation retinopathy.

Study	Patients	Targeted laser range	Outcomes of interest (primary and secondary)	Follow-up period	Main conclusions
Siddhi Goel (28)	treatment naïve BRVO with ME (n=32)	the CNP areas and at the junction of ischemic and nonischemic areas, extending anteriorly up to ora serrata	VA; CSFT; the number of injections required with a minimum follow-up of 9 months	9 months	TRP reduced the number of ranibizumab injections in patients with BRVO macular edema, while maintaining similar benefits to the combination arm in improving BCVA, CSFT, and contrast sensitivity
Soonil Kwon (29)	RVO with recurrent ME (n=30)	areas of retinal non-perfusio outside of the macula, no closer than two disc diameters from the optic nerve head	Primary Outcome Measures: Total Number of Intravitreal Injections Over a 12 Month Period;VA Secondary Outcome Measures: Retinal Ischemia; Foveal Avascular Zone; Adverse Events; Neovascularization of the Iris, Optic Nerve and Elsewhere; Central Foveal Outcome; Aqueous VEGF Levels;VF	12 months	The role of TRP, particularly to NPAs and PMA, warrants further investigation in recalcitrant RVO-associated ME
Yoko Tomomatsu (30)	BRVO with ME (n=38)	NPAs 3000μm away from the centre of the fovea	BCVA;CRT	6 months	RP of NPAs reduced the amount of ME recurrence following IVB compared to IVB alone
Hannah J. Yu (31)	radiation-related ME (n=40)	areas of peripheral retinal ischemia as defined by wide-field angiography	Primary Outcome Measures: BCVA Secondary Outcome Measures: The Mean Number of Intravitreal Injections; Percentage of Subjects With Retinal Hemorrhage; Percentage of Subjects With Intraretinal Exudates on Fundus Examination; Mean Change in Central Mean Thickness Compared to Baseline	104 weeks	Combination therapy did not result in significant visual and anatomical improvement over monthly medical therapy alone, but compared with history, serious complications were prevented

BRVO, retinal vein occlusion; ME, macular edema; TRP, targeted retinal photocoagulation; VA, visual acuity; CSFT, central subfield thickness; VEGF, vascular endothelial growth factor; VF, visual fields; RVO, retinal vein occlusion; BCVA, best corrected visual acuity; CRT, central retinal thickness; RP, retinal photocoagulation; IVB, intravitreal bevacizumab; NPAs, non-perfusion areas.

number of injections as needed: the number of additional injections of bevacizumab in the IVB group was significantly greater than that in the IVB+TRP group (1.58 ± 0.69:0.83 ± 0.62); the RBZ group was also more frequent than the RBZ group. + TRP group (5.76 ± 1.3:4.06 ± 0.99), the above differences were all statistically significant. Therefore, compared with single drug injection, the combination therapy with TRP can achieve similar efficacy or even better prognosis on the basis of Reduce the number of injections, and reduce the development and recurrence of ME caused by RVO.

We also found on the International Clinical Trials Registry website (ClinicalTrials.gov) that the research team at the University of Leipzig has initiated a clinical trial comparing injection of ranibizumab with or without targeted photocoagulation in the treatment of central RVOwith macular edema (NCT04444492), which is expected to be completed in 2024, and the author will continue to pay attention to the progress and results of the trial.

Radiation retinopathy is a common, progressive visual side effect of ophthalmic radiation therapy for intraocular or orbital tumors. It typically presents as late-onset disease of the retinal vasculature between 6 months and 3 years after radiation therapy, with clinical signs of macular edema, cotton wool spots, neovascularization, and/or vitreous hemorrhage, which has a serious impact on the vision of patients (31, 33–36). Therefore, Hannah J Yu et al. (31) also tried to treat the disease with TRP. This randomized controlled clinical trial (NCT0222610) included 40 patients with radioactive ME, and compared the efficacy and tolerance of intraocular injection of RBZ and RBZ+TRP in the treatment of patients with radioactive retinopathy. After 2 years of treatment and follow-up, it was found that the average ETDRS BCVA of patients improved after 1 year, but the effect of combined treatment was not significantly better than that of injection alone. The trial found that additional TRP did not bring significant visual and anatomical improvement to patients, but it may prevent serious complications during treatment. Because there are few clinical trials related to this disease at present, a large number of clinical trials are still needed to confirm the efficacy and safety of TRP for this disease.

4 Conclusions

DR is one of the serious complications of diabetes and one of the four major blindness diseases in Europe and the United States. Although anti-VEGF therapy is widely used in DR and some retinal diseases, retinal laser photocoagulation remains the main treatment option for these diseases (37). Traditional PRP has some side effects due to the damage to eye tissue caused by laser light. With the advancement of technology, TRP has been continuously applied in clinical practice, and its potential benefits have opened up broad prospects for the treatment of DR. The combination therapy of TRP and anti-VEGF is expected to become a new option for patients with DR and some retinal diseases (such as RVO, radiation retinopathy, etc.). It is believed that with the advancement of science and technology, new treatment methods and approaches will surely bring new hope to DR patients.

Author contributions

AD and ZL contributed to conception and design of the study. ZL wrote the first draft of the manuscript. NH, LG and XZ wrote sections of the manuscript. All authors contributed to the article and approved the submitted version.

Funding

Funding from Shandong Provincial Natural Science Foundation, China (No: ZR2020MH173).

Acknowledgments

The authors are grateful to the Weifang Medical University and Affiliated Hospital of Weifang Medical University for the encouragement and support for this work. The authors have no other relevant affiliations or financial involvement with any organization or entity with a financial interest in or financial conflict with the subject matter or materials discussed in the manuscript apart from those disclosed.

Conflict of interest

The authors declare that the research was conducted in the absence of any commercial or financial relationships that could be construed as a potential conflict of interest.

Publisher's note

References

1. The Early Treatment Diabetic Retinopathy Study Research Group. Techniques for scatter and local photocoagulation treatment of diabetic retinopathy: Early treatment diabetic retinopathy study report no. 3. *Int Ophthalmol Clin* (1987) 27:254–64. doi: 10.1097/00004397-198702740-00005

2. Meyer-Schwickerath GR. The history of photocoagulation. *Aust N Z J Ophthalmol* (1989) 17:427–34. doi: 10.1111/j.1442-9071.1989.tb00566.x

3. Muqit MM, Marcellino GR, Henson DB, Young LB, Patton N, Charles SJ, et al. Optos-guided pattern scan laser (Pascal)-targeted retinal photocoagulation in proliferative diabetic retinopathy. *Acta Ophthalmol* (2013) 91:251–8. doi: 10.1111/j.1755-3768.2011.02307.x

4. Fong DS, Girach A, Boney A. Visual side effects of successful scatter laser photocoagulation surgery for proliferative diabetic retinopathy: A literature review. *Retina* (2007) 27:816–24. doi: 10.1097/IAE.0b013e318042d32c

5. Pahor D. Visual field loss after argon laser panretinal photocoagulation in diabetic retinopathy: Full- versus mild-scatter coagulation. *Int Ophthalmol* (1998) 22:313–9. doi: 10.1023/A:1006367029134

6. Henricsson M, Heijl A. The effect of panretinal laser photocoagulation on visual acuity, visual fields and on subjective visual impairment in preproliferative and early proliferative diabetic retinopathy. *Acta Ophthalmol (Copenh)* (1994) 72:570–5. doi: 10.1111/j.1755-3768.1994.tb07181.x

7. Reddy SV, Husain D. Panretinal photocoagulation: A review of complications. *Semin Ophthalmol* (2018) 33:83–8. doi: 10.1080/08820538.2017.1353820

8. Reddy S, Hu A, Schwartz SD. Ultra wide field fluorescein angiography guided targeted retinal photocoagulation (TRP). *Semin Ophthalmol* (2009) 24:9–14. doi: 10.1080/08820530802519899

9. Kernt M, Cheuteu RE, Cserhati S, Seidensticker F, Liegl RG, Lang J, et al. Pain and accuracy of focal laser treatment for diabetic macular edema using a retinal navigated laser (Navilas). *Clin Ophthalmol* (2012) 6:289–96. doi: 10.2147/OPTH.S27859

10. Muqit MM, Young LB, McKenzie R, John B, Marcellino GR, Henson DB, et al. Pilot randomised clinical trial of pascal TargETEd retinal versus variable fluence PANretinal 20 ms laser in diabetic retinopathy: PETER PAN study. *Br J Ophthalmol* (2013) 97:220–7. doi: 10.1136/bjophthalmol-2012-302189

11. Takamura Y, Tomomatsu T, Matsumura T, Arimura S, Gozawa M, Takihara Y, et al. The effect of photocoagulation in ischemic areas to prevent recurrence of diabetic macular edema after intravitreal bevacizumab injection. *Invest Ophthalmol Vis Sci* (2014) 55:4741–6. doi: 10.1167/iovs.14-14682

12. Nikkhah H, Ghazi H, Razzaghi MR, Karimi S, Ramezani A, Soheilian M. Extended targeted retinal photocoagulation versus conventional pan-retinal photocoagulation for proliferative diabetic retinopathy in a randomized clinical trial. *Int Ophthalmol* (2018) 38:313–21. doi: 10.1007/s10792-017-0469-7

13. Brown DM, Ou WC, Wong TP, Kim RY, Croft DE, Wykoff CC, et al. Targeted retinal photocoagulation for diabetic macular edema with peripheral retinal nonperfusion: Three-year randomized DAVE trial. *Ophthalmology* (2018) 125:683–90. doi: 10.1016/j.ophtha.2017.11.026

14. Toscano L, Messias A, Messias K, de Cenco Lopes R, Ribeiro JAS, Scott IU, et al. Proliferative diabetic retinopathy treated with intravitreal ranibizumab and photocoagulation directed at ischemic retinal areas-a randomized study. *Doc Ophthalmol* (2021) 143:313–22. doi: 10.1007/s10633-021-09848-6

15. Oishi A, Hidaka J, Yoshimura N. Quantification of the image obtained with a wide-field scanning ophthalmoscope. *Invest Ophthalmol Vis Sci* (2014) 55:2424–31. doi: 10.1167/iovs.13-13738

16. Rabiolo A, Parravano M, Querques L, Cicinelli MV, Carnevali A, Sacconi R, et al. Ultra-wide-field fluorescein angiography in diabetic retinopathy: a narrative review. *Clin Ophthalmol* (2017) 11:803–7. doi: 10.2147/OPTH.S133637

17. Wessel MM, Aaker GD, Parlitsis G, Cho M, D'Amico DJ, Kiss S. Ultra-wide-field angiography improves the detection and classification of diabetic retinopathy. *Retina* (2012) 32:785–91. doi: 10.1097/IAE.0b013e3182278b64

18. Cui Y, Zhu Y, Wang JC, Lu Y, Zeng R, Katz R, et al. Comparison of widefield swept-source optical coherence tomography angiography with ultra-widefield colour fundus photography and fluorescein angiography for detection of lesions in diabetic retinopathy. *Br J Ophthalmol* (2021) 105:577–81. doi: 10.1136/bjophthalmol-2020-316245

19. Russell JF, Flynn HWJr., Sridhar J, Townsend JH, Shi Y, Fan KC, et al. Distribution of diabetic neovascularization on ultra-widefield fluorescein angiography and on simulated widefield OCT angiography. *Am J Ophthalmol* (2019) 207:110–20. doi: 10.1016/j.ajo.2019.05.031

20. Couturier A, Rey PA, Erginay A, Lavia C, Bonnin S, Dupas B, et al. Widefield OCT-angiography and fluorescein angiography assessments of nonperfusion in diabetic retinopathy and edema treated with anti-vascular endothelial growth factor. *Ophthalmology* (2019) 126:1685–94. doi: 10.1016/j.ophtha.2019.06.022

21. Russell JF, Al-Khersan H, Shi Y, Scott NL, Hinkle JW, Fan KC, et al. Retinal nonperfusion in proliferative diabetic retinopathy before and after panretinal photocoagulation assessed by widefield OCT angiography. *Am J Ophthalmol* (2020) 213:177–85. doi: 10.1016/j.ajo.2020.01.024

22. Ghasemi Falavarjani K, Tsui I, Sadda SR. Ultra-wide-field imaging in diabetic retinopathy. *Vision Res* (2017) 139:187–90. doi: 10.1016/j.visres.2017.02.009

23. Friberg TR, Gupta A, Yu J, Huang L, Suner I, Puliafito CA, et al. Ultrawide angle fluorescein angiographic imaging: a comparison to conventional digital acquisition systems. *Ophthalmic Surg Lasers Imaging* (2008) 39:304–11. doi: 10.3928/15428877-20080701-06

24. Shimura M, Yasuda K, Nakazawa T, Abe T, Shiono T, Iida T, et al. Panretinal photocoagulation induces pro-inflammatory cytokines and macular thickening in high-risk proliferative diabetic retinopathy. *Graefes Arch Clin Exp Ophthalmol* (2009) 247:1617–24. doi: 10.1007/s00417-009-1147-x

25. Soman M, Ganekal S, Nair U, Nair K. Effect of panretinal photocoagulation on macular morphology and thickness in eyes with proliferative diabetic retinopathy without clinically significant macular edema. *Clin Ophthalmol* (2012) 6:2013–7. doi: 10.2147/OPTH.S37340

26. Diabetic Retinopathy Clinical Research N, Brucker AJ, Qin H, Antoszyk AN, Beck RW, Bressler NM, et al. 3rd, observational study of the development of diabetic macular edema following panretinal (scatter) photocoagulation given in 1 or 4 sittings. *Arch Ophthalmol* (2009) 127:132–40. doi: 10.1001/archophthalmol.2008.565

27. Kozak I, Luttrull JK. Modern retinal laser therapy. *Saudi J Ophthalmol* (2015) 29:137–46. doi: 10.1016/j.sjopt.2014.09.001

28. Goel S, Kumar A, Ravani RD, Chandra P, Chandra M, Kumar V. Comparison of ranibizumab alone versus ranibizumab with targeted retinal laser for branch retinal vein occlusion with macular edema. *Indian J Ophthalmol* (2019) 67:1105–8. doi: 10.4103/ijo.IJO_1364_18

29. Kwon S, Wykoff CC, Brown DM, van Hemert J, Fan W, Sadda SR. Changes in retinal ischaemic index correlate with recalcitrant macular oedema in retinal vein occlusion: WAVE study. *Br J Ophthalmol* (2018) 102:1066–71. doi: 10.1136/bjophthalmol-2017-311475

30. Tomomatsu Y, Tomomatsu T, Takamura Y, Gozawa M, Arimura S, Takihara Y, et al. Comparative study of combined bevacizumab/targeted photocoagulation vs bevacizumab alone for macular oedema in ischaemic branch retinal vein occlusions. *Acta Ophthalmol* (2016) 94:e225–30. doi: 10.1111/aos.12721

31. Yu HJ, Fuller D, Anand R, Fuller T, Munoz J, Moore C, et al. Two-year results for ranibizumab for radiation retinopathy (RRR): A randomized, prospective trial. *Graefes Arch Clin Exp Ophthalmol* (2022) 260:47–54. doi: 10.1007/s00417-021-05281-2

32. Singer MA, Tan CS, Surapaneni KR, Sadda SR. Targeted photocoagulation of peripheral ischemia to treat rebound edema. *Clin Ophthalmol* (2015) 9:337–41. doi: 10.2147/OPTH.S75842

33. Gossage DL, Cieslarova B, Ap S, Zheng H, Xin Y, Lal P, et al. Phase 1b study of the safety, pharmacokinetics, and disease-related outcomes of the matrix metalloproteinase-9 inhibitor andecaliximab in patients with rheumatoid arthritis. *Clin Ther* (2018) 40:156–165 e5. doi: 10.1016/j.clinthera.2017.11.011

34. Finger PT, Chin KJ, Duvall G. Palladium-103 for choroidal melanoma study, palladium-103 ophthalmic plaque radiation therapy for choroidal melanoma: 400 treated patients. *Ophthalmology* (2009) 116:790–6, 796.e1. doi: 10.1016/j.ophtha.2008.12.027

35. Krema H, Somani S, Sahgal A, Xu W, Heydarian M, Payne D, et al. Stereotactic radiotherapy for treatment of juxtapapillary choroidal melanoma: 3-year follow-up. *Br J Ophthalmol* (2009) 93:1172–6. doi: 10.1136/bjo.2008.153429

36. Haas A, Pinter O, Papaefthymiou G, Weger M, Berghold A, Schrottner O, et al. Incidence of radiation retinopathy after high-dosage single-fraction gamma knife radiosurgery for choroidal melanoma. *Ophthalmology* (2002) 109:909–13. doi: 10.1016/S0161-6420(02)01011-4

37. Everett LA, Paulus YM. Laser therapy in the treatment of diabetic retinopathy and diabetic macular edema. *Curr Diabetes Rep* (2021) 21:35. doi: 10.1007/s11892-021-01403-6

frontiers | Frontiers in Endocrinology

TYPE Original Research
PUBLISHED 15 March 2023
DOI 10.3389/fendo.2023.1132036

OPEN ACCESS

EDITED BY
Rajashekhar Gangaraju,
University of Tennessee Health Science Center (UTHSC), United States

REVIEWED BY
Alessandro Salatino,
Magna Græcia University, Italy
Lu Hao,
Shanghai University of Traditional Chinese Medicine, China
Di Zhu,
Air Force Medical University, China

*CORRESPONDENCE
De-Liang Liu
ldl2580@gzucm.edu.cn
Shu-Fang Chu
chushufanggzhtcm@163.com
Hui-Lin Li
sztcmlhl@163.com

†These authors have contributed equally to this work

SPECIALTY SECTION
This article was submitted to Clinical Diabetes, a section of the journal Frontiers in Endocrinology

RECEIVED 26 December 2022
ACCEPTED 27 February 2023
PUBLISHED 15 March 2023

CITATION
Wang G-X, Hu X-Y, Zhao H-X, Li H-L, Chu S-F and Liu D-L (2023) Development and validation of a diabetic retinopathy risk prediction model for middle-aged patients with type 2 diabetes mellitus. *Front. Endocrinol.* 14:1132036. doi: 10.3389/fendo.2023.1132036

Development and validation of a diabetic retinopathy risk prediction model for middle-aged patients with type 2 diabetes mellitus

Gao-Xiang Wang[1,2†], Xin-Yu Hu[2,3†], Heng-Xia Zhao[2], Hui-Lin Li[2*], Shu-Fang Chu[2*] and De-Liang Liu[2*]

[1]Department of Endocrinology, Shenzhen Traditional Chinese Medicine Hospital Affiliated to Nanjing University of Chinese Medicine, Shenzhen, Guangdong, China, [2]Department of Endocrinology, Shenzhen Traditional Chinese Medicine Hospital, Shenzhen, Guangdong, China, [3]Department of Endocrinology, The Fourth Clinical Medical College of Guangzhou University of Chinese Medicine, Shenzhen, Guangdong, China

Objectives: The study aims to establish a predictive nomogram of diabetic retinopathy(DR) for the middle-aged population with type 2 diabetes mellitus (T2DM).

Methods: This retrospective study screened 931 patients with T2DM between 30 and 59 years of age from the 2011-2018 National Health and Nutrition Examination Survey database. The development group comprised 704 participants from the 2011-2016 survey, and the validation group included 227 participants from the 2017-2018 survey. The least absolute shrinkage and selection operator regression model was used to determine the best predictive variables. The logistic regression analysis built three models: the full model, the multiple fractional polynomial (MFP) model, and the stepwise (stepAIC) selected model. Then we decided optimal model based on the receiver operating characteristic curve (ROC). ROC, calibration curve, Hosmer-Lemeshow test, and decision curve analysis (DCA) were used to validate and assess the model. An online dynamic nomogram prediction tool was also constructed.

Results: The MFP model was selected to be the final model, including gender, the use of insulin, duration of diabetes, urinary albumin-to-creatinine ratio, and serum phosphorus. The AUC was 0.709 in the development set and 0.704 in the validation set. According to the ROC, calibration curves, and Hosmer-Lemeshow test, the nomogram demonstrated good coherence. The nomogram was clinically helpful, according to DCA.

Conclusion: This study established and validated a predictive model for DR in the mid-life T2DM population, which can assist clinicians quickly determining who is prone to develop DR.

KEYWORDS

prediction model, nomogram, diabetic retinopathy, middle-aged, type 2 diabetes mellitus

Introduction

Diabetic retinopathy (DR) is a usual microvascular complication of type 2 diabetes mellitus (T2DM), one of the major reasons for blindness (1). According to The Global Burden of Disease Study, DR was the only cause of age-standardized vision loss to increase over the past three decades (2). Over 103.12 million adults worldwide were diagnosed with DR in 2020, and with the prevalence of diabetes increasing at an alarming rate, it is estimated that the world DR population will grow by 55.6%(57.4 million) between 2020 and 2045 (3). A prevalence-based cost-of-illness model estimates that Indonesia will spend $8.9 billion on the healthcare of DR in 2025 (4). As DR is often asymptomatic until the later, even more, severe stages, early diagnosis, and intervention are essential and more cost-effective for public health and healthcare costs (5–7).

DR prevalence has been discussed in some studies in different age groups of T2DM. The ADVANCE Collaborative group (8) has reported that the course of diabetes is independently related to the risk of microvascular complications, and diabetes duration has a more significant impact on younger people than on older people. Middleton et al. (9) have found that DR seems more susceptible in people diagnosed with T2DM in middle age (or with a younger present age), and the odds of DR decreased with increasing age at diagnosis. They considered this difference to be caused by reducing insulin-like growth factor 1 and growth hormone with increasing age. DR is more likely to occur in the middle-aged population after diagnosis of T2DM than in the elderly (10), so a more targeted prediction model and intervention strategy are needed.

Several prediction models have been applied to the identification and diagnosis of DR (11–13). However, these prediction models were constructed for almost all age groups. They have shortcomings in predicting the development of DR in different age groups. This will limit their ability to stratify individual patients according to risk level and select the optimal treatment. To our knowledge, there is a lack of predictive models developed separately for the middle-aged population. We suggested that developing a separate DR prediction model for the middle-aged age group and narrowing the prediction model orientation may be more important for applying the model for early identification and prevention of DR. We developed a model predicting the development of DR in middle-aged people with T2DM based on data from the National Health and Nutrition Examination Survey (NHANES), which may provide more personalized screening and treatment options for middle-aged T2DM patients.

Materials and methods

Study design and participants

NHANES is a study program to evaluate US adults' and kids' health and nutritional condition. They sampled about 5,000 nationally representative persons with a multistage, graded, clustered sampling approach every year (14).

We included 39,156 participants in this study from the NHANES 2011 to 2018. According to the guideline from the American Diabetes Association (15), patients with T2DM were defined as follows: (1) participants who a doctor told them that they had diabetes with a diagnosis age ≥30 years; (2) participants who didn't self-report diabetes diagnosis with HbA1c ≥6.5%. We excluded data for participants <30 years (n=20,291) and >59 years (n=7,683) to obtain 11,182 cases in the age group of 30-59 years. Then, participants were separated into two groups depending on whether or not they had data of how old they were first told by a professional that they had diabetes, with data in the first group (n=1,083) and miss data in the second group (n=10,099). The first group excluded participants who were younger than 30 years old when they were first told they had diabetes and those who had no data for DR, resulting in 604 participants. The second group excluded patients with missing glycohemoglobin data and glycohemoglobin<6.5%, resulting in 327 cases. The two data groups were combined to get the final population included in the analysis for this study. The population from 2011 to 2016 was used to establish the development cohort, and the population from 2017 to 2018 was adopted as an external validation cohort. Figure 1 illustrates the detailed selection operation.

Ethics statement

Each participator provided written informed agreement before inclusion in the NHANES database, which was examined and allowed by the National Center for Health Statistics Ethics Review Board. Anonymously processing the data makes it available to the public. The researchers then can transform the data into a form suitable for analysis following privacy-preserving. Based on the study's data usage guidelines, all data will be analyzed statistically, and all studies will comply with all relevant laws and standards.

Potential predictors

We selected some potential predictors which might affect DR progress based on current relevant research and clinical experience (16–18), including age, gender, diabetes duration, HbA1C, use of insulin, use of hypoglycemic pills, hypertension, weak failing kidneys, body mass index (BMI), waist circumference, alkaline phosphatase, alanine aminotransferase (ALT), aspartate aminotransferase (AST), serum calcium, serum phosphorus, serum potassium, serum uric acid, total cholesterol, triglyceride, serum calcium, serum iron, blood urea nitrogen, serum albumin, serum creatinine, urinary albumin-to-creatinine ratio(UACR). The information on hypertension and renal failure came from the questionnaires.

Statistical analysis

R statistical software version 3.6.3 and EmpowerStats version 2.0 were used to conduct the statistical analysis for this study. Data

for normally distributed was displayed as the mean ± standard deviation, and a two independent samples *t*-test was performed to analyze differences between groups. The categorical variables were described with proportion, which was tested using the chi-square test.

In linear regression mode, least absolute shrinkage and selection operator (LASSO) regression analysis is used for shrinkage and variable option. Firstly, we used the development set data and analyzed the data using the LASSO regression method. LASSO regression analysis was used to determine the appropriate and effective risk predictors for T2DM patients with DR, and 7 independent variables were selected according to lambda.min. Then, we built three models based on the logistic regression analysis: the full model, the multiple fractional polynomial (MFP) model, and the stepwise (stepAIC) selected model. We used the odds ratio and *P*-value with 95% confidence interval (CI) to describe the features. At the same time, according to the comparison of the area under the receiver operating characteristic (ROC) curve of each model in the development set and the validation set, the model with the most significant area under the curve (AUC) was selected. The model's consistency was evaluated based on the calibration curve and the Hosmer-Lemeshow test. The clinical effectiveness of the model was assessed using decision curve analysis (DCA). All statistical analyses were two-sided, with an alpha of 0.05 as the significance grade. Finally, according to the model, we established the nomogram and online dynamic nomogram prediction tool.

Results

Baseline characteristics

According to the prespecified exclusion and inclusion criteria, 931 participants were enrolled in our research, including 704 in the development group and 227 in the validation group. Baseline characteristics like demographic, biochemical indexes, physical examination findings, duration of diabetes, and the use of medications are shown in Table 1.

Risk factors in the development group

We included 24 associated characteristic variables in LASSO regression analysis (Figures 2A, B) and selected 7 non-zero potential predictors from the LASSO regression analysis results based on the data of the development group. These predictors included gender, taking insulin now, weak failing kidneys, duration of diabetes, UACR, blood urea nitrogen, and serum phosphorus.

Prediction model development

To construct the prediction model, we performed the following steps. Firstly, we combined all 7 potential predictors selected by LASSO regression analysis into a multivariable model using

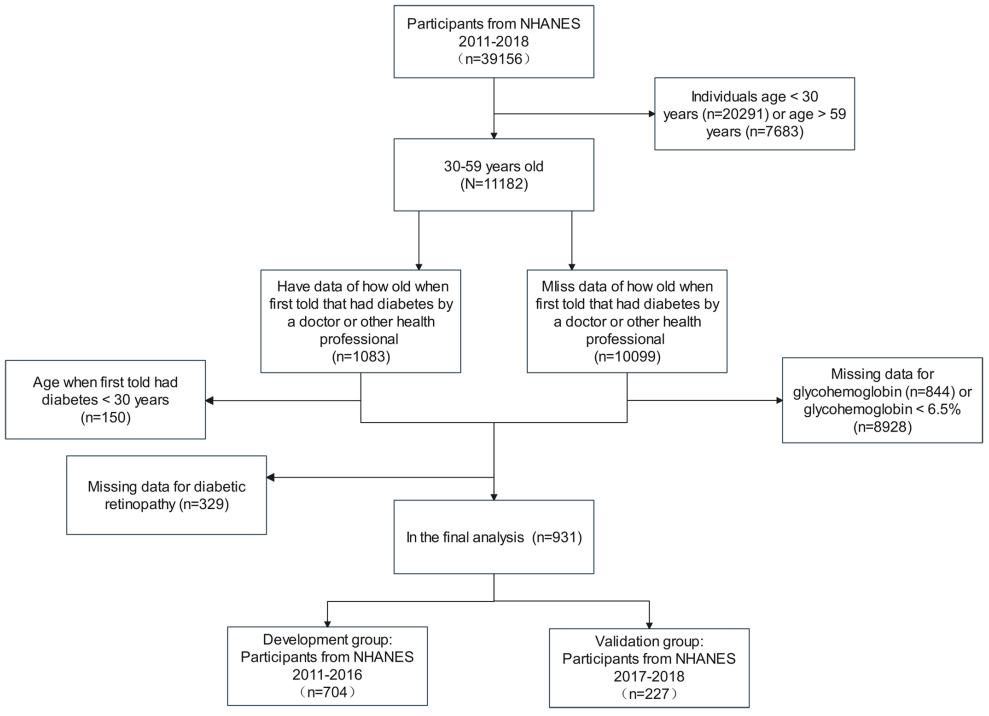

FIGURE 1
Flow chart of the development and validation groups.

10.3389/fendo.2023.1132036

TABLE 1 Characteristics of the study sample.

	Development group (n=704)	Validation group (n=227)	P value
Age (years)	50.12 ± 6.74	50.10 ± 6.74	0.957
Gender (%)			0.591
male	50.41	52.41	
female	49.59	47.59	
Duration of diabetes (years)	6.61 ± 5.44	6.79 ± 5.60	0.653
Glycohemoglobin (%)	7.67 ± 1.96	7.53 ± 1.74	0.346
Taking insulin now(%)			0.621
No	76.81	78.36	
Yes	23.19	21.64	
Take diabetic pills now (%)			0.174
No	28.47	23.96	
Yes	71.53	76.04	
High blood pressure (%)			0.949
No	36.55	36.78	
Yes	63.45	63.22	
Had weak failing kidneys (%)			0.076
No	94.36	97.21	
Yes	5.64	2.79	
Body mass index (kg/m^2)	34.62 ± 8.13	36.03 ± 8.03	0.021
Waist circumference (cm)	113.48 ± 16.96	115.65 ± 16.36	0.084
Alkaline phosphatase (u/L)	73.27 ± 23.27	83.87 ± 29.03	<0.001
Alanine aminotransferase (u/L)	73.27 ± 23.27	83.87 ± 29.03	<0.001
Aspartate aminotransferase (u/L)	28.15 ± 25.90	24.68 ± 17.89	0.054
Serum calcium (mmol/L)	2.35 ± 0.09	2.32 ± 0.11	<0.001
Serum phosphorus (mmol/L)	1.23 ± 0.18	1.14 ± 0.19	<0.001
Serum potassium (mmol/L)	4.03 ± 0.33	4.12 ± 0.41	<0.001
Serum uric acid (umol/L)	329.25 ± 90.31	323.61 ± 84.66	0.395
Total cholesterol (mmol/L)	4.89 ± 1.21	4.83 ± 1.15	0.553
Triglyceride (mmol/L)	2.53 ± 3.00	2.40 ± 2.06	0.554
Serum iron (umol/L)	13.89 ± 5.67	14.89 ± 6.95	0.027
Blood urea nitrogen (mmol/L)	5.11 ± 2.17	5.29 ± 2.15	0.242
Serum albumin (g/L)	41.89 ± 3.42	39.69 ± 3.44	<0.001
Serum creatinine (umol/L)	81.01 ± 65.60	76.17 ± 55.82	0.305
Urinary albumin creatinine ratio (mg/g)	125.75 ± 598.05	166.02 ± 840.45	0.421
Diabetic retinopathy (%)			0.423
No	83.57	81.32	
Yes	16.43	18.68	

Continuous variables are displayed as mean ± standard deviation. Based on a linear regression model, the *P*-value was calculated. The categorical variables were described with proportion, *P*-value was calculated by the chi-square test.

multivariate logistic regression, which built the full model. Then, the stepwise backward regression selection method was used to fit the stepwise model based on Akaike's Information Criterion (AIC). Since the multicollinearity of the predictors, we constructed the multiple fractional polynomial (MFP) model. The details of the three models are shown in Table 2. Finally, ROC curves were plotted for all three models, and the AUC of these models was compared (Figure 3). We chose the MFP model to construct the nomogram according to the results.

Development of nomogram

According to the MFP model, 5 independent predictors were introduced to establish a DR risk nomogram (Figure 4A). To make it more convenient for T2DM patients to predict the progress of DR, we created an online dynamic nomogram tool (http://www.empowerstats.net/pmodel/?m=22793_GaoXiangWangredictionmodelofretinopathyinmiddleagedpatientswithtype2diabetesmellitus). In the online tool, doctors can calculate the risk of DR in middle-aged T2DM patients based on the specific values of each indicator (Figure 4B).

Assessment of predictive nomogram

We applied the ROC curve to test the discrimination of the model (Figures 3A, B). In the development group, the AUC was 0.709(95%CI:0.659-0.759) for the MFP model, 0.680 (95% CI:0.627-0.733) for the stepwise model, and 0.679 (95%CI:0.627-0.732) for the full model (Figure 3A). And in the validation group, the AUC was 0.704(95%CI:0.611-0.798) for the MFP model, 0.667(95% CI:0.567-0.774) for the full model, and 0.666 (95%CI:0.560-0.773) for the stepwise model (Figure 3B).

To check the consistency of this model, calibration curves and the Hosmer-Lemeshow test were used. As shown in Figure 5, the calibration curves of the model in both the development and validation sets were plotted. The horizontal axis stands for the predicted DR risk, the vertical coordinates represent the actual diagnosed DR risk, and the gray diagonal line stands for the perfect prediction of the ideal nomogram. Nomogram performance is shown by the solid line, where the closer to the diagonal gray line suggests greater predictive performance. According to the calibration curves, the nomogram displayed good coherence. In addition, there was no significant difference between the validation and development groups when we used the Hosmer-Lemeshow test to test the model calibration degree. (P=0.42 in the development group, P=0.52 in the validation group).

Figure 6 shows the results of DCA curves for development and validation groups. The dashed line stood for the model, the gray line showed the net benefit when all patients with DR, and the black line represented the net benefit when no patients with DR. The region of the model curve between the "black line" and the "gray line" represented the model's clinical applicability. If the dashed line is above the black and gray lines, we can assume that the dashed value of the period can benefit.

Discussion

Nomogram is a useful and reliable forecasting tool that can produce individual probabilities of endpoint events by combining different variables and quantifying the risk individually (19). In the risk predictor analysis of this study, gender, use of insulin, renal failure, duration of diabetes, UACR, blood urea nitrogen, and serum phosphorus were related to the risk of DR in midlife patients with T2DM. Based on this, we used statistical analysis to screen five of these variables to construct and validate a novel DR risk predictive tool for middle-aged patients with T2DM. The model showed that being male, taking insulin now, longer duration of diabetes, higher UACR, and lower serum phosphorus were critical factors in determining the risk of DR in patients with T2DM, which has the same part of risk factors as those reported in previous studies (10, 20). To make it more convenient for physicians to provide early individualized intervention for middle-aged T2DM patients, we have built an online, free prediction tool. According to Anne et al. (21), the AUC value of 0.7 or higher is considered acceptable or good for model discrimination. Our model presented good

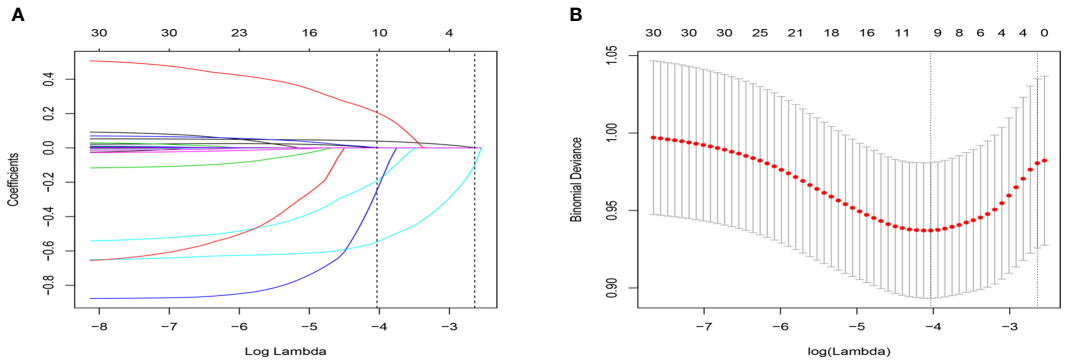

FIGURE 2
Selection of variables using the LASSO regression model. **(A)** The coefficient profile was plotted against the log (lambda) sequence. **(B)** The plot of partial likelihood deviance (binomial deviance) versus log (lambda) was performed.

10.3389/fendo.2023.1132036

discrimination and calibration ability, offering a personalized prediction of DR incidence.

For patients with T2DM, the course of the disease is an unchangeable risk factor. Unlike T1DM, disease duration has a more significant impact on patients with T2DM combined with DR (22). Compared to older T2DM patients, midlife patients have a longer survival time and will be exposed to the increased risk of complications associated with a longer disease course. Elevated blood glucose and lipid metabolism disorders in T2DM patients caused pathological reactions, such as oxidative stress and inflammatory response (23, 24), which were considered an important pathogenesis of DR (25–27), Longer disease duration means a sustained state of inflammation for a longer period, which raises the risk of DR. As reported by Singh et al. (28), DR prevalence was five times higher in patients with a disease duration of >15 years than it was in patients with an illness duration of < 5 years. According to Sun et al. (29), the duration of diabetes is strongly correlated with the risk of DR. In middle-aged patients with T2DM. It is critical to diagnose and intervene in the early stages of DR progression to minimize the risks that come with a longer disease course.

Gender has been discovered in some studies to be relevant to the risk of developing diabetes-related complications (30, 31). Middle-aged men were significantly more likely to have T2DM, indicating that gender factors are involved to some extent in the pathogenesis of T2DM and its complications in the middle-aged population (32, 33). Several studies have revealed sexual dimorphism in fat distribution, inflammatory signaling pathway activation, and T2DM risk (34–37). Middle-aged T2DM patients have demonstrated gender differences in disease progression and

TABLE 2 Logistic regression analysis for risk factors in three models.

Model	Estimate	Std error	Odds ratio	95%CI.low	95%CI.upp	P-value
Model 1						
(Intercept)	-0.6306	0.6663	0.5323	0.1442	1.9648	0.3439
Gender=female	-0.3878	0.2093	0.6786	0.4503	1.0227	0.0639
Taking insulin now=yes	0.7185	0.2347	2.0513	1.2949	3.2495	0.0022
Weak failing kidneys=yes	0.4099	0.3718	1.5066	0.7269	3.1225	0.2703
Duration of diabetes	0.052	0.0172	1.0534	1.0185	1.0895	0.0025
Urinary albumin creatinine ratio	0.0004	0.0002	1.0004	1	1.0007	0.0253
Blood urea nitrogen	0.0367	0.0447	1.0374	0.9505	1.1323	0.4108
Serum phosphorus	-1.2588	0.581	0.284	0.0909	0.887	0.0303
Model 2						
(Intercept)	-0.6154	0.6668	0.5404	0.1463	1.9967	0.356
Gender= female	-0.4129	0.2071	0.6617	0.4409	0.9931	0.0462
Taking insulin now=yes	0.7216	0.2345	2.0577	1.2994	3.2584	0.0021
Weak failing kidneys=yes	0.5119	0.3479	1.6684	0.8437	3.2991	0.1412
Duration of diabetes	0.0533	0.0171	1.0548	1.0199	1.0908	0.0019
Urinary albumin creatinine ratio	0.0004	0.0002	1.0004	1.0001	1.0007	0.0194
Serum phosphorus	-1.1235	0.5558	0.3251	0.1094	0.9665	0.0432
Model 3						
(Intercept)	0.089	0.7097	1.0931	0.272	4.3933	0.9002
Gender=female	-0.4145	0.2061	0.6607	0.4411	0.9896	0.0444
Taking insulin now=yes	0.7175	0.2307	2.0492	1.3039	3.2206	0.0019
Duration of diabetes/10	0.5111	0.1718	1.6672	1.1905	2.3347	0.0029
(Urinary albumin creatinine ratio/100)^-0.5	-0.3199	0.0734	0.7262	0.6288	0.8387	<0.0001
Serum phosphorus	-0.9159	0.5467	0.4001	0.137	1.1683	0.0939

Model 1: Full model:Risk of Diabetic retinopathy=-0.63058 -0.38775*(Gender=female) +0.05199*Duration of diabetes +0.00037*Urinary albumin creatinine ratio +0.40987*(Weak failing kidneys=yes) +0.71848*(Taking insulin now=yes) +0.03673*Blood urea nitrogen-1.25877*Serum phosphorus.
Model 2: Stepwise (stepAIC) selected model: Risk of Diabetic retinopathy=-0.61541 -0.41290*(Gender=female) +0.05331*Duration of diabetes +0.00039*Urinary albumin creatinine ratio +0.51186*(Weak failing kidneys=yes) +0.72158*(Taking insulin now=yes) -1.12349*Serum phosphorus.
Model 3:Multiple Fractional Polynomial mode:Risk of Diabetic retinopathy=0.08903 +0.71746*(Taking insulin now=Yes) +0.51112*(Duration of diabetes/10)-0.31991*((Urinary albumin creatinine ratio/100)^-0.5) -0.91593*Serum phosphorus -0.41447*(Gender= Female).

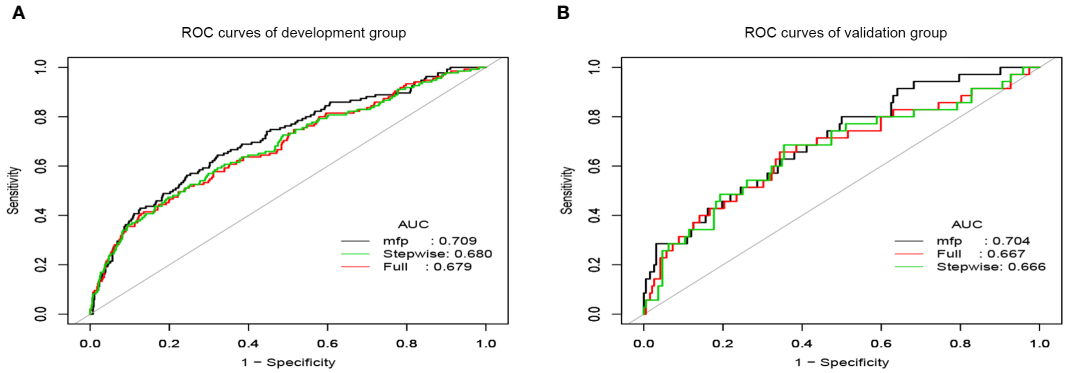

FIGURE 3
The ROC curves of prediction models. **(A)** ROC curves of the development group. **(B)** ROC curves of the validation group.

pathogenesis, and our model suggested that being male is significantly associated with DR in the middle-aged population. Studies based on national databases from the UK and Finland found that the male sex is an independent risk factor for advanced DR in T2DM and a risk predictor for disease progression (38, 39). Maric-Bilkan et al. (40) concluded that age-related differences in hormone levels, glycemic control, duration of diabetes, and ethnic background could explain the reported gender differences in DR risk. Although the pathological mechanisms of gender influence on DR progression are unclear now, the significantly different prevalence between gender implied different individualized care measures. Prevention strategies targeting modifiable risk factors are critical for the middle-aged T2DM population.

Since its first clinical use in 1922, exogenous insulin has become a widely used hypoglycemic drug for many forms of diabetic patients worldwide (41). Our results found that mid-aged T2DM patients on insulin therapy were at greater risk of developing DR. A meta-analysis based on seven cohort studies has shown a significant association between the use of insulin and the risk of DR (42). A systematic review conducted by Song et al. (43) discovered that insulin therapy was remarkably correlated with an increased prevalence of any DR. The correlation between insulin therapy and DR demonstrated in various studies indicated that clinicians need to be more cautious when applying insulin therapy to patients at high risk of developing DR. Besides when dealing with patients on long-term insulin therapy, DR should be detected more carefully.

UACR is a clinically used indicator of renal function and a marker of endothelial dysfunction and may affect the microvasculature of the kidney and retina. Wang et al. (44) found that UACR, in addition to being an important marker of chronic kidney disease, was also closely related to the progression of DR. A 10-year prospective follow-up study confirmed that both UACR and estimated glomerular filtration rate (eGFR) were significant risk factors for DR, but UACR had a more significant association than eGFR (45), which is consistent with our result. The current studies found that high UACR is linked to changes in retinal vascular geometry, that patients with high UACR appear to be potentially predisposed to systemic vascular endothelial cell disease, and glycemic control may not affect the inherent biological risk of developing microvascular complications (46, 47). For this reason, UACR may be a favorable and easily accessible biochemical indicator for predicting DR.

Although the prediction model developed in this research is meaningful for the early prevention and treatment of the middle-

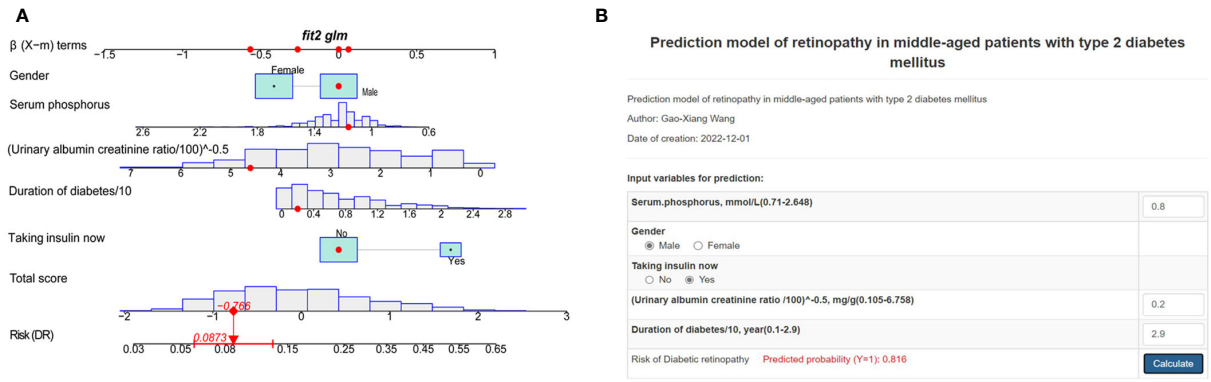

FIGURE 4
Risk nomogram development. **(A)** An example of the dynamic nomogram. **(B)** An example of the online dynamic nomogram tool.

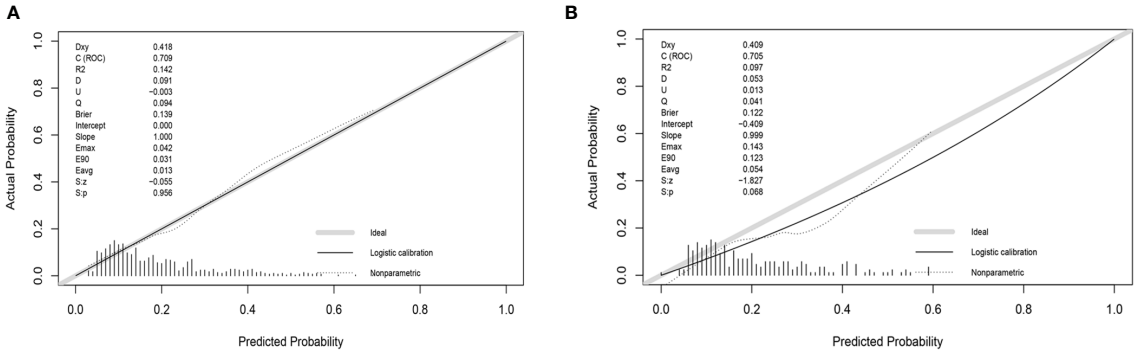

FIGURE 5
Calibration curve of the risk nomogram. **(A)** Calibration curve of development group. **(B)** Calibration curve of validation group.

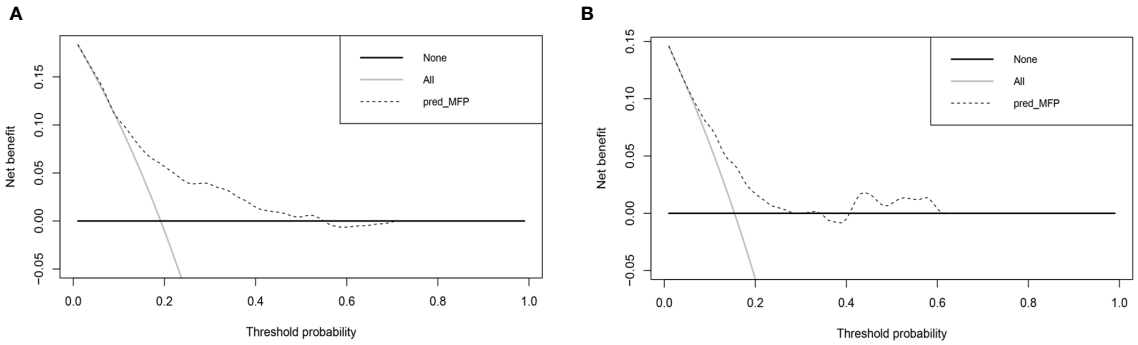

FIGURE 6
Decision curve analysis for the nomogram. **(A)** Decision curve analysis of development group. **(B)** Decision curve analysis of validation group.

aged T2DM population, there are still some limitations. First, the population included in this study was the general middle-aged US population. Due to the differences in lifestyle and eating habits, the DR prediction nomogram may be limited in its generalization to other national people. Second, all patient data in this study were obtained from the NHANES database. Although we used data from different periods for validation, multicenter clinical validation is needed to assess the efficacy of the nomogram. Third, we could not refine our DR study according to whether it was proliferative due to the lack of data limitations of DR staging in the NHANES database data.

The study developed a new web-based nomogram for predicting DR prevalence in middle-aged T2DM patients. After internal and external validation, the nomogram demonstrated good predictive performance. The line chart includes 5 common clinical characteristics of gender, serum phosphorus, UACR, duration of diabetes, and use of insulin. This nomogram enabled early to identify the high-risk groups of DR in middle-aged T2DM patients and helped to develop an aggressive individualized prevention and treatment strategy to reduce the prevalence and slow down the progression of DR. More clinical prospective and multicenter trials are needed to confirm our nomogram.

Data availability statement

This study uses data from a free and open public database, which can be found here: www.cdc.gov/nchs/nhanes/.

Ethics statement

Ethical approval was not provided for this study on human participants because each participator provided written informed agreement before inclusion in the NHANES database, which was examined and allowed by the National Center for Health Statistics Ethics Review Board. Anonymously processing the data makes it available to the public. The researchers then can transform the data into a form suitable for analysis following privacy-preserving. Based on

the study's data usage guidelines, all data will be analyzed statistically, and all studies will comply with all relevant laws and standards. Written informed consent for participation was not required for this study in accordance with the national legislation and the institutional requirements.

Author contributions

G-XW and X-YH contributed equally to this study. All the authors contributed to the article and approved the final version.

Funding

This study was funded by the National Natural Science Foundation of China (No. 82104759); and The Natural Science Foundation of Guangdong Provincial (No. 2019A1515110108).

Conflict of interest

The authors declare that the research was conducted in the absence of any commercial or financial relationships that could be construed as a potential conflict of interest.

Publisher's note

References

1. Lin K, Hsih W, Lin Y, Wen C, Chang T. Update in the epidemiology, risk factors, screening, and treatment of diabetic retinopathy. *J Diabetes Investig* (2021) 12:1322–5. doi: 10.1111/jdi.13480

2. Steinmetz JD, Bourne RRA, Briant PS, Flaxman SR, Taylor HRB, Jonas JB, et al. Causes of blindness and vision impairment in 2020 and trends over 30 years, and prevalence of avoidable blindness in relation to VISION 2020: the right to sight: an analysis for the global burden of disease study. *Lancet Global Health* (2021) 9:e144–60. doi: 10.1016/S2214-109X(20)30489-7

3. Teo ZL, Tham Y-C, Yu M, Chee ML, Rim TH, Cheung N, et al. Global prevalence of diabetic retinopathy and projection of burden through 2045. *Ophthalmology* (2021) 128:1580–91. doi: 10.1016/j.ophtha.2021.04.027

4. Sasongko MB, Wardhana FS, Febryanto GA, Agni AN, Supanji S, Indrayanti SR, et al. The estimated healthcare cost of diabetic retinopathy in Indonesia and its projection for 2025. *Br J Ophthalmol* (2020) 104:487–92. doi: 10.1136/bjophthalmol-2019-313997

5. Wong TY, Sun J, Kawasaki R, Ruamviboonsuk P, Gupta N, Lansingh VC, et al. Guidelines on diabetic eye care. *Ophthalmology* (2018) 125:1608–22. doi: 10.1016/j.ophtha.2018.04.007

6. Vujosevic S, Aldington SJ, Silva P, Hernández C, Scanlon P, Peto T, et al. Screening for diabetic retinopathy: New perspectives and challenges. *Lancet Diabetes Endocrinol* (2020) 8:337–47. doi: 10.1016/S2213-8587(19)30411-5

7. Siegel KR, Ali MK, Zhou X, Ng BP, Jawanda S, Proia K, et al. Cost-effectiveness of interventions to manage diabetes: Has the evidence changed since 2008? *Diabetes Care* (2020) 43:1557–92. doi: 10.2337/dci20-0017

8. for the ADVANCE Collaborative group, Zoungas S, Woodward M, Li Q, ME C, Hamet P, et al. Impact of age, age at diagnosis and duration of diabetes on the risk of macrovascular and microvascular complications and death in type 2 diabetes. *Diabetologia* (2014) 57:2465–74. doi: 10.1007/s00125-014-3369-7

9. Middleton TL, Constantino MI, Molyneaux L, D'Souza M, Twigg SM, Wu T, et al. Young-onset type 2 diabetes and younger current age: Increased susceptibility to retinopathy in contrast to other complications. *Diabetes Med* (2020) 37:991–9. doi: 10.1111/dme.14238

10. Liu Y, Yang J, Tao L, Lv H, Jiang X, Zhang M, et al. Risk factors of diabetic retinopathy and sight-threatening diabetic retinopathy: A cross-sectional study of 13 473 patients with type 2 diabetes mellitus in mainland China. *BMJ Open* (2017) 7: e016280. doi: 10.1136/bmjopen-2017-016280

11. Li J, Guo C, Wang T, Xu Y, Peng F, Zhao S, et al. Interpretable machine learning-derived nomogram model for early detection of diabetic retinopathy in type 2 diabetes mellitus: A widely targeted metabolomics study. *Nutr Diabetes* (2022) 12:36. doi: 10.1038/s41387-022-00216-0

12. Chen X, Xie Q, Zhang X, Lv Q, Liu X, Rao H. Nomogram prediction model for diabetic retinopathy development in type 2 diabetes mellitus patients: A retrospective cohort study. *J Diabetes Res* (2021) 2021:1–8. doi: 10.1155/2021/3825155

13. Shan Y, Wang Q, Zhang Y, Tong X, Pu S, Xu Y, et al. High remnant cholesterol level is relevant to diabetic retinopathy in type 2 diabetes mellitus. *Lipids Health Dis* (2022) 21:12. doi: 10.1186/s12944-021-01621-7

14. Xu Z, McClure S, Appel L. Dietary cholesterol intake and sources among U.S adults: Results from national health and nutrition examination surveys (NHANES), 2001–2014. *Nutrients* (2018) 10:771. doi: 10.3390/nu10060771

15. American Diabetes Association Professional Practice Committee. 2. classification and diagnosis of diabetes: Standards of medical care in diabetes–2022. *Diabetes Care* (2022) 45:S83–96. doi: 10.2337/dc22-S006

16. Yang H, Xia M, Liu Z, Xing Y, Zhao W, Li Y, et al. Nomogram for prediction of diabetic retinopathy in patients with type 2 diabetes mellitus: A retrospective study. *J Diabetes its Complications* (2022) 36:108313. doi: 10.1016/j.jdiacomp.2022.108313

17. Li Y, Li C, Zhao S, Yin Y, Zhang X, Wang K. Nomogram for prediction of diabetic retinopathy among type 2 diabetes population in xinjiang, China. *DMSO* (2022) 15:1077–89. doi: 10.2147/DMSO.S354611

18. Mo R, Shi R, Hu Y, Hu F. Nomogram-based prediction of the risk of diabetic retinopathy: A retrospective study. *J Diabetes Res* (2020) 2020:1–9. doi: 10.1155/2020/7261047

19. Balachandran VP, Gonen M, Smith JJ, DeMatteo RP. Nomograms in oncology: More than meets the eye. *Lancet Oncol* (2015) 16:e173–80. doi: 10.1016/S1470-2045(14)71116-7

20. Yang J, Jiang S. Development and validation of a model that predicts the risk of diabetic retinopathy in type 2 diabetes mellitus patients. *Acta Diabetol* (2022) 60:43–51. doi: 10.1007/s00592-022-01973-1

21. de Hond AAH, Steyerberg EW, van Calster B. Interpreting area under the receiver operating characteristic curve. *Lancet Digit Health* (2022) 4:e853–5. doi: 10.1016/S2589-7500(22)00188-1

22. He M, Long P, Chen T, Li K, Wei D, Zhang Y, et al. ALDH2/SIRT1 contributes to type 1 and type 2 diabetes-induced retinopathy through depressing oxidative stress. *Oxid Med Cell Longev* (2021) 2021:1641717. doi: 10.1155/2021/1641717

23. Kang Q, Yang C. Oxidative stress and diabetic retinopathy: Molecular mechanisms, pathogenetic role and therapeutic implications. *Redox Biol* (2020) 37:101799. doi: 10.1016/j.redox.2020.101799

24. Busik JV. Lipid metabolism dysregulation in diabetic retinopathy. *J Lipid Res* (2021) 62:100017. doi: 10.1194/jlr.TR120000981

25. Catrina S-B, Zheng X. Hypoxia and hypoxia-inducible factors in diabetes and its complications. *Diabetologia* (2021) 64:709–16. doi: 10.1007/s00125-021-05380-z

26. Forrester JV, Kuffova L, Delibegovic M. The role of inflammation in diabetic retinopathy. *Front Immunol* (2020) 11:583687. doi: 10.3389/fimmu.2020.583687

27. Augustine J, Troendle EP, Barabas P, McAleese CA, Friedel T, Stitt AW, et al. The role of lipoxidation in the pathogenesis of diabetic retinopathy. *Front Endocrinol* (2021) 11:621938. doi: 10.3389/fendo.2020.621938

28. Singh HV, Das S, Deka DC, Kalita IR. Prevalence of diabetic retinopathy in self-reported diabetics among various ethnic groups and associated risk factors in north-East India: A hospital-based study. *Indian J Ophthalmol* (2021) 69:3132–7. doi: 10.4103/ijo.IJO_1144_21

29. Sun Q, Jing Y, Zhang B, Gu T, Meng R, Sun J, et al. The risk factors for diabetic retinopathy in a Chinese population: A cross-sectional study. *J Diabetes Res* (2021) 2021:5340453. doi: 10.1155/2021/5340453

30. Peters SAE, Woodward M. Sex differences in the burden and complications of diabetes. *Curr Diabetes Rep* (2018) 18:33. doi: 10.1007/s11892-018-1005-5

31. Huebschmann AG, Huxley RR, Kohrt WM, Zeitler P, Regensteiner JG, Reusch JEB. Sex differences in the burden of type 2 diabetes and cardiovascular risk across the life course. *Diabetologia* (2019) 62:1761–72. doi: 10.1007/s00125-019-4939-5

32. Li J, Ni J, Wu Y, Zhang H, Liu J, Tu J, et al. Sex differences in the prevalence, awareness, treatment, and control of diabetes mellitus among adults aged 45 years and older in rural areas of northern China: A cross-sectional, population-based study. *Front Endocrinol* (2019) 10:147. doi: 10.3389/fendo.2019.00147

33. Sattar N. Gender aspects in type 2 diabetes mellitus and cardiometabolic risk. *Best Pract Res Clin Endocrinol Metab* (2013) 27:501–7. doi: 10.1016/j.beem.2013.05.006

34. Henstridge DC, Abildgaard J, Lindegaard B, Febbraio MA. Metabolic control and sex: A focus on inflammatory-linked mediators. *Br J Pharmacol* (2019) 176:4193–207. doi: 10.1111/bph.14642

35. Winkler TW, Justice AE, Graff M, Barata L, Feitosa MF, Chu S, et al. The influence of age and sex on genetic associations with adult body size and shape: A Large-scale genome-wide interaction study. *PloS Genet* (2015) 11:e1005378. doi: 10.1371/journal.pgen.1005378

36. Pulit SL, Karaderi T, Lindgren CM. Sexual dimorphisms in genetic loci linked to body fat distribution. *Bioscience Rep* (2017) 37:BSR20160184. doi: 10.1042/BSR20160184

37. de Ritter R, de Jong M, Vos RC, van der Kallen CJH, Sep SJS, Woodward M, et al. Sex differences in the risk of vascular disease associated with diabetes. *Biol Sex Differ* (2020) 11:1. doi: 10.1186/s13293-019-0277-z

38. Looker HC, Nyangoma SO, Cromie D, Olson JA, Leese GP, Black M, et al. Diabetic retinopathy at diagnosis of type 2 diabetes in Scotland. *Diabetologia* (2012) 55:2335–42. doi: 10.1007/s00125-012-2596-z

39. Kostev K, Rathmann W. Diabetic retinopathy at diagnosis of type 2 diabetes in the UK: A database analysis. *Diabetologia* (2013) 56:109–11. doi: 10.1007/s00125-012-2742-7

40. Maric-Bilkan C. Sex differences in micro- and macro-vascular complications of diabetes mellitus. *Clin Sci* (2017) 131:833–46. doi: 10.1042/CS20160998

41. Mathieu C, Martens P-J, Vangoitsenhoven R. One hundred years of insulin therapy. *Nat Rev Endocrinol* (2021) 17:715–25. doi: 10.1038/s41574-021-00542-w

42. Zhao C, Wang W, Xu D, Li H, Li M, Wang F. Insulin and risk of diabetic retinopathy in patients with type 2 diabetes mellitus: Data from a meta-analysis of seven cohort studies. *Diagn Pathol* (2014) 9:130. doi: 10.1186/1746-1596-9-130

43. Song P, Yu J, Chan KY, Theodoratou E, Rudan I. Prevalence, risk factors and burden of diabetic retinopathy in China: A systematic review and meta-analysis. *J Global Health* (2018) 8:10803. doi: 10.7189/jogh.08.010803

44. Wang J, Xin X, Luo W, Wang R, Wang X, Si S, et al. Anemia and diabetic kidney disease had joint effect on diabetic retinopathy among patients with type 2 diabetes. *Invest Ophthalmol Vis Sci* (2020) 61:25. doi: 10.1167/iovs.61.14.25

45. Romero-Aroca P, Baget-Bernaldiz M, Navarro-Gil R, Moreno-Ribas A, Valls-Mateu A, Sagarra-Alamo R, et al. Glomerular filtration rate and/or ratio of urine albumin to creatinine as markers for diabetic retinopathy: A ten-year follow-up study. *J Diabetes Res* (2018) 2018:5637130. doi: 10.1155/2018/5637130

46. Benitez-Aguirre PZ, Marcovecchio ML, Chiesa ST, Craig ME, Wong TY, Davis EA, et al. Urinary albumin/creatinine ratio tertiles predict risk of diabetic retinopathy progression: A natural history study from the adolescent cardio-renal intervention trial (AdDIT) observational cohort. *Diabetologia* (2022) 65:872–8. doi: 10.1007/s00125-022-05661-1

47. Benitez-Aguirre PZ, Wong TY, Craig ME, Davis EA, Cotterill A, Couper JJ, et al. The adolescent cardio-renal intervention trial (AdDIT): Retinal vascular geometry and renal function in adolescents with type 1 diabetes. *Diabetologia* (2018) 61:968–76. doi: 10.1007/s00125-017-4538-2

frontiers | Frontiers in Endocrinology

TYPE Original Research
PUBLISHED 17 March 2023
DOI 10.3389/fendo.2023.1144257

OPEN ACCESS

EDITED BY
Mohd Imtiaz Nawaz,
Department of Ophthalmology, King Saud University, Saudi Arabia

REVIEWED BY
Jihong Lin,
Heidelberg University, Germany
Robert Charles Andrew Symons,
University of Melbourne, Australia

*CORRESPONDENCE
Zijing Li
lizj29@mail.sysu.edu.cn

SPECIALTY SECTION
This article was submitted to Clinical Diabetes, a section of the journal Frontiers in Endocrinology

RECEIVED 14 January 2023
ACCEPTED 24 February 2023
PUBLISHED 17 March 2023

CITATION
Yao H and Li Z (2023) Is preclinical diabetic retinopathy in diabetic nephropathy individuals more severe?
Front. Endocrinol. 14:1144257.
doi: 10.3389/fendo.2023.1144257

Is preclinical diabetic retinopathy in diabetic nephropathy individuals more severe?

Hongyan Yao[1] and Zijing Li[2,3]*

[1]Ningbo Eye Hospital, Ningbo University, Ningbo, China, [2]Department of Ophthalmology, Sun Yat-sen Memorial Hospital, Sun Yat-sen University, Guangzhou, China, [3]State Key Laboratory of Ophthalmology, Zhongshan Ophthalmic Center, Sun Yat-Sen University, Guangzhou, China

Purpose: To analyse the retinal vessel density and thickness characteristics of diabetic nephropathy (DN) individuals with preclinical diabetic retinopathy (DR) using optical coherence tomography angiography (OCTA).

Methods: This retrospective case–control study included 88 eyes of 88 type 2 DM patients with preclinical DR [44 non-DN (NDN) and 44 DN]. OCTA images and data were acquired using AngioVue 2.0 of the spectral domain OCT device. The foveal avascular zone (FAZ) area, superficial capillary plexus (SCP) and deep capillary plexus vessel densities, ganglion cell complex (GCC) and full retinal thicknesses, peripapillary capillary density and nerve fibre layer (RNFL) thickness were compared between the NDN and DN groups. The relationship between each renal function parameter and each OCTA parameter was analysed.

Results: SCP vessel density, GCC thickness and full retinal thickness were significantly reduced in DN individuals compared to NDN individuals [(NDN versus DN) SCP vessel density: 46.65 ± 3.84% versus 44.35 ± 5.25%, p=0.030; GCC thickness: 100.79 ± 5.92 μm versus 93.28 ± 8.66 μm, p<0.001; full retinal thickness: whole area: 287.04 ± 13.62 μm versus 277.71 ± 15.10 μm, p=0.005). Within the peripapillary area, capillary density was also significantly reduced in the whole area (50.19 ± 3.10% versus 47.46 ± 5.93%, p=0.016) and some sectors in the DN group, though RNFL thickness was only decreased in some sectors. For all individuals, estimated glomerular filtration rate (eGFR) correlated significantly with most OCTA parameters and then showed a significantly negative correlation with FAZ area (β=−16.43, p=0.039) in multivariate linear regression analysis. In the NDN group, eGFR showed a significantly negative correlation with FAZ area (β=−18.746, p=0.048) and a significantly positive correlation with SCP vessel density (β=0.580, p=0.036).

Conclusion: Preclinical DR may be more severe in DN individuals than in NDN individuals with regard to microvascular and microstructural impairment. Moreover, eGFR may be a good indicator for retinal microvascular impairment.

KEYWORDS

preclinical diabetic retinopathy, diabetic nephropathy, optical coherence tomography angiography, estimated glomerular filtration rate, microstructural impairment

Introduction

Diabetic retinopathy (DR), a common complication of diabetes mellitus (DM), remains the major cause of vision loss in the working-age population worldwide (1). Another common and severe complication of DM is diabetic nephropathy (DN), which may cause life-threatening end-stage renal disease (2). DR and DN are both microvascular DM complications, and they have similar pathophysiological mechanisms. Microvascular endothelial cells are regarded as common targets of hyperglycaemic impairment. Various common pathophysiological processes, including inflammation, oxidative stress and crosstalk between endothelial cells and pericytes/podocytes, exist in both complications (3). Previous clinical studies have suggested that the severity of DR parallels that of DN (4, 5).Zhang even found that DR might predict the renal function prognosis of type 2 DM (T2DM) patients with DN (5). Accordingly, in our routine clinical practice, severe DR, such as PDR and DME, is often detected in T2DM individuals with DN.

However, we also noticed that DN and DR are not consistent in some cases. Some DN individuals with poor renal function lack DR appearance in their fundus. DM patients without DR have been termed preclinical DR individuals in previous studies because reduced vessel density and other subtle microvascular lesions can be observed when using optical coherence tomography angiography (OCTA), a non-invasive cross-sectional real-time imaging technique, despite no obvious DR detected with conventional imaging methods (6, 7). Thus, we sought to determine whether more severe microvascular or microstructural alterations occur in DN than in NDN when using OCTA in preclinical DR individuals, which may help in further understanding the mutual effects and possible mechanisms between DR and DN. Unfortunately, few studies have focused on the retinal characteristics of DN individuals with preclinical DR.

Therefore, the purpose of this study was to analyse the retinal vessel density and thickness characteristics of DN individuals with preclinical DR using OCTA.

Methods

Subjects

This was a retrospective case–control clinical study. The study was conducted according to the principles of the Declaration of Helsinki and was approved by the institutional review board of Sun Yat-sen Memorial Hospital, Sun Yat-sen University (approval number: SYSEC-KY-KS-2021-263). Eighty-eight eyes of 88 T2DM patients with preclinical DR (44 NDN and 44 DN) were recruited from the Endocrinology Department between January 2018 and October 2021. The inclusion criteria included 1) a diagnosis of preclinical DR in the unilateral or bilateral eyes of T2DM patients; 2) age from 40 to 75 years; and 3) eyes with a logMAR best corrected visual acuity (BCVA) not more than 0.1. A random eye was chosen when the bilateral eyes involved preclinical DR. The diagnosis of T2DM, DR and DN were confirmed by an endocrinologist, an ophthalmologist and a nephrologist, respectively, based on criteria by the American Diabetes Association (8–10). The criteria for DN were 1) estimated glomerular filtration rate (eGFR) < 60 ml/min/1.73 m2, 2) urinary albumin to creatinine ratio > 30 mg/g for more than 3 months and 3) renal biopsy evidence in suspected patients. The values of eGFR were calculated using the Xiangya equation, a more accurate equation for eGFR in the Chinese population (11). Urinary albumin to creatinine ratio was tested in one random urine sample. A solid-phase fuorescent immunoassay was used to measure urinary albumin, and the Jafe rate method was applied to measure urinary creatinine (12). The exclusion criteria were as follows: 1) ocular diseases that may cause vision impairment, such as glaucoma, optic neuritis, uveitis and other retinal diseases; 2) spherical equivalent higher than −6 diopters or AL greater than 26 mm; 3) lens opacities affecting OCTA imaging; and 4) history of intraocular surgery.

The demographic and systemic data recorded for each individual included age, sex, body mass index (BMI), waist-to-hip ratio (WHR), haemoglobin A1c (HbAlc) levels, DM duration, DM therapy regimen, renal function (eGFR, blood urea, blood creatinine, blood uric acid, urinary protein and urinary microalbumin) and presence of hypertension. Hypertension was determined as >130/80 mmHg according to 2017 high blood pressure guidelines from the American College of Cardiology (13). Thorough ophthalmic examinations, including logMAR BCVA, intraocular pressure (IOP) (non-contact tonometer, Canon, Inc., Tokyo, Japan), axial length (AL), central anterior chamber depth (CACD), dilated fundus examination, colour fundus photos (Canon, Inc., Tokyo, Japan), OCTA (Optovue, Inc., Fremont, CA, USA) and FFA (if necessary and possible) (Microclear, Inc., Suzhou, China), were assessed in these individuals. AL and CACD were measured using IOLMaster (Carl Zeiss Meditec, Inc., Dublin, USA).

OCTA image collection

OCTA images and data were acquired using AngioVue 2.0 of the spectral domain OCT device. Split-spectrum amplitude-decorrelation angiography was conducted to detect and analyse erythrocyte movement in vessels. An image of the 6 mm × 6 mm macular area and one of the 4.5 × 4.5 mm optic disc area were captured. Images with a scan quality < 6 were excluded. The vessel densities and retinal thickness of the macular and peripapillary capillary plexuses were then automatically exported. The recorded parameters included the foveal avascular zone (FAZ) area, superficial capillary plexus (SCP) and deep capillary plexus (DCP) vessel densities, ganglion cell complex (GCC) and full retinal thicknesses, peripapillary capillary density and nerve fibre layer (RNFL) thickness. Detailed retinal segmentations and divisions were similar to those in our previous work (14).

Statistical analysis

Statistical analyses were performed using SPSS 26.0 (SPSS Inc. Chicago, IL, USA). Independent Student's t tests were employed to

compare normally distributed parameters, and Mann–Whitney tests were applied to compare nonnormally distributed parameters. Categorical variables were analysed using chi-squared tests. The relationship between each renal function parameter (level of eGFR, blood urea, blood creatinine, blood uric acid, urinary protein and urinary microalbumin) and each OCTA parameter (FAZ area, SCP and DCP vessel densities, GCC and full retinal thicknesses, peripapillary capillary density and RNFL thickness) was examined using bivariate correlation analysis in all individuals, the NDN group and the DN group, respectively. A value of $p<0.05$ was considered to be statistically significant. All OCTA parameters with statistical significance would be included in multivariate linear regression analyses adjusted for sex, age and DM duration for each renal function parameter. However, when OCTA parameters of different area (whole area, foveal, parafoveal or perifoveal) involved in the same terms (for example: SCP vessel density), only one representative parameter of this term [for example: SCP vessel density (whole area)] was included in multivariate analyses. Scatter diagrams were created using GraphPad Prism 7.0 (GraphPad Software, San Diego, CA, USA).

Results

Patient characteristics

Eighty-eight eyes of 88 T2DM patients with preclinical DR (44 NDN and 44 DN) were included in this study. Compared to the NDN group, the DN individuals had significantly increased WHR, longer DM duration, lower levels of eGFR, blood urea, blood creatinine, blood uric acid, urinary protein and urinary microalbumin and greater logMAR BCVA. A greater portion of individuals receiving subcutaneous insulin injection and a higher ratio of hypertension were noted in the DN group. No significant difference between the two groups was shown with regard to age, sex, BMI, HbAlc level or other variables. Details are shown in Table 1.

OCTA findings

In the macular area, SCP vessel density was significantly reduced in the DN individuals compared to the NDN individuals (NDN versus DN: whole area: 46.65 ± 3.84% versus 44.35 ± 5.25%, p=0.030). Similar reductions were also observed in para- and perifoveal areas (parafoveal: 48.53 ± 4.54% versus 45.63 ± 7.62%, p=0.044; perifoveal: 47.26 ± 4.19% versus 44.86 ± 5.08%, p=0.025). However, there was no significant difference in FAZ or DCP vessel density between the two groups. Details are shown in Table 2. GCC and full retinal thicknesses were significantly decreased in the DN group (GCC thickness: whole area: 100.79 ± 5.92 μm versus 93.28 ± 8.66 μm, p<0.001; full retinal thickness: whole area: 287.04 ± 13.62 μm versus 277.71 ± 15.10 μm, p=0.005). Details are shown in Table 3.

Within the peripapillary area, capillary density was also significantly reduced in the whole area (50.19 ± 3.10% versus 47.46 ± 5.93%, p=0.016) and some sectors in the DN group, but RNFL thickness was only decreased in some sectors (Table 4).

Representative images of the vessel density and GCC thickness were shown in Figure 1.

TABLE 1 Patient characteristics.

	NDN	DN	p
Patients (n)	44	44	NA
Age (years)	58.86 ± 11.60	59.80 ± 12.55	0.718*
Male:female (n)	30:16	30:16	1.000#
Anthropometrics			
BMI (kg/m^2)	24.87 ± 3.18	29.42 ± 20.43	0.157*
WHR	0.91 ± 0.071	0.96 ± 0.073	**0.004***
HbAlc (%)	8.96 ± 2.88	8.91 ± 1.89	0.930*
DM duration (years)	5.60 ± 5.70	7.07 ± 6.53	0.057
DM therapy regimen			
Oral medication (n, %)	32	14	**<0.001#**
Subcutaneous insulin injection (n, %)	2	10	
Both (n, %)	10	24	
Renal function			
eGFR (mL/min/1.73m^2)	76.98 ± 6.70	65.09 ± 15.74	**<0.001***
Blood urea (mmol/L)	5.42 ± 1.45	8.64 ± 5.19	**<0.001***

(Continued)

TABLE 1 Continued

	NDN	DN	p
Blood creatinine (μmol/L)	76.23 ± 10.01	123.81 ± 89.73	**<0.001***
Blood uric acid (μmol/L)	344.84 ± 121.36	424.95 ± 153.16	**0.014***
Urinary protein (g/L)	0.028 ± 0.027	0.37 ± 0.76	**0.012***
Urinary microalbumin (mg/L)	13.46 ± 3.83	469.81 ± 1089.65	**0.031***
Hypertension (n, %)	16, 36.36	32, 72.73	**<0.001#**
SBP (mmHg)	132.36 ± 13.87	138.18 ± 18.90	0.103*
DBP (mmHg)	79.77 ± 13.66	82.43 ± 15.04	0.388*
Ocular parameters			
BCVA (logMAR)	-0.011 ± 0.097	0.039 ± 0.078	**0.009***
IOP (mmHg)	15.43 ± 2.11	15.59 ± 2.55	0.750*
CACD (mm)	3.17 ± 0.43	3.23 ± 0.29	0.549*
AL (mm)	23.83 ± 1.23	23.62 ± 0.70	0.395*
DR in fellow eye (n, %)	8	6	**0.560#**

NDN, non-diabetic nephropathy; DN, diabetic nephropathy; NA, not available; BMI, body mass index; WHR, waist-to-hip ratio; HbAlc, haemoglobin A1c; DM, diabetes mellitus; eGFR, estimated glomerular filtration rate; SBP, systolic blood pressure; DBP, diastolic blood pressure; BCVA, best corrected visual acuity; IOP, intraocular pressure; CACD, central anterior chamber depth; AL, axial length. *using Student's t test; #using chi-squared test; p value in bold style, p<0.05.

Relationship between renal function and OCTA findings

For all individuals, only the level of eGFR correlated significantly with most of the OCTA parameters (Table 5), whereas there was no relationship between the level of the remaining renal function parameters (blood urea, blood creatinine, blood uric acid, urinary protein and urinary microalbumin) and OCTA parameters. Relationships between the level of eGFR and each representative OCTA parameter are shown

TABLE 2 Vessel density in the macular area.

	NDN	DN	p
FAZ area (mm^2)	0.30 ± 0.11	0.37 ± 0.26	0.198
SCP vessel density			
Whole area (%)	46.65 ± 3.84	44.35 ± 5.25	**0.030**
Foveal (%)	17.23 ± 7.19	15.48 ± 8.24	0.319
Parafoveal (%)	48.53 ± 4.54	45.63 ± 7.62	**0.044**
Temporal (%)	48.41 ± 5.82	46.43 ± 7.52	0.195
Superior (%)	49.06 ± 5.53	46.33 ± 7.88	0.079
Nasal (%)	47.97 ± 5.13	44.34 ± 9.93	**0.046**
Inferior (%)	48.67 ± 5.40	45.42 ± 8.94	0.055
Perifoveal (%)	47.26 ± 4.19	44.86 ± 5.08	**0.025**
Temporal (%)	42.50 ± 5.16	40.01 ± 7.15	0.08
Superior (%)	47.14 ± 4.70	45.34 ± 5.32	0.116
Nasal (%)	51.51 ± 3.86	48.72 ± 5.07	**0.007**
Inferior (%)	47.89 ± 4.27	45.46 ± 4.84	**0.022**
DCP vessel density			
Whole area (%)	46.29 ± 5.53	44.16 ± 7.32	0.148

(Continued)

TABLE 2 Continued

	NDN	DN	p
Foveal (%)	32.86 ± 9.69	29.87 ± 9.82	0.176
Parafoveal (%)	52.13 ± 4.54	50.20 ± 6.93	0.148
Temporal (%)	53.29 ± 5.21	52.40 ± 6.82	0.517
Superior (%)	51.31 ± 5.41	50.43 ± 7.60	0.557
Nasal (%)	53.60 ± 5.33	50.36 ± 9.23	0.061
Inferior (%)	50.33 ± 5.75	47.62 ± 9.02	0.116
Perifoveal (%)	46.83 ± 6.08	44.53 ± 8.13	0.160
Temporal (%)	49.11 ± 6.43	46.12 ± 9.87	0.115
Superior (%)	46.16 ± 6.11	44.95 ± 8.34	0.466
Nasal (%)	46.15 ± 6.98	43.52 ± 8.87	0.149
Inferior (%)	45.87 ± 7.13	43.61 ± 8.16	0.198

NDN, non-diabetic nephropathy; DN, diabetic nephropathy; FAZ, foveal avascular zone; SCP, superficial capillary plexus; DCP, deep capillary plexus; p value in bold style, p<0.05.

in scatter diagrams (Figure 2). In multivariate linear regression analysis adjusted for sex, age and DM duration for eGFR, representative OCTA parameters with statistical significance including FAZ area, SCP and DCP vessel densities (whole area), GCC and full retinal thicknesses (whole area), peripapillary capillary density (whole area) and RNFL thickness (whole area) were included. Finally, the level of eGFR showed a significantly negative correlation with the FAZ area (β=−16.43, p=0.039) and a significantly positive correlation with the RNFL thickness (β=0.169, p=0.025).

TABLE 3 Retinal thickness in the macular area.

	NDN	DN	p
GCC thickness			
Whole area (μm)	100.79 ± 5.92	93.28 ± 8.66	**<0.001**
Foveal (μm)	52.38 ± 9.85	48.23 ± 11.11	0.081
Parafoveal (μm)	107.66 ± 8.67	98.50 ± 12.82	**<0.001**
Temporal (μm)	100.51 ± 7.94	93.52 ± 9.90	**<0.001**
Superior (μm)	110.26 ± 8.67	100.36 ± 14.55	**<0.001**
Nasal (μm)	108.50 ± 9.93	98.91 ± 13.30	**<0.001**
Inferior (μm)	111.38 ± 9.00	101.21 ± 16.43	**<0.001**
Perifoveal (μm)	100.55 ± 5.83	93.45 ± 7.99	**<0.001**
Temporal (μm)	86.29 ± 4.85	82.08 ± 6.20	**0.001**
Superior (μm)	100.47 ± 7.63	93.45 ± 10.38	**<0.001**
Nasal (μm)	117.09 ± 8.41	108.62 ± 11.00	**<0.001**
Inferior (μm)	98.40 ± 6.56	90.17 ± 10.68	**<0.001**
Full retinal thickness			
Whole area (μm)	287.04 ± 13.62	277.71 ± 15.10	**0.005**
Foveal (μm)	250.01 ± 24.65	243.24 ± 23.48	0.212
Parafoveal (μm)	319.53 ± 18.38	307.56 ± 19.54	**0.006**
Temporal (μm)	310.91 ± 18.27	301.17 ± 18.17	**0.019**
Superior (μm)	322.31 ± 18.66	311.89 ± 16.90	**0.011**

(Continued)

TABLE 3 Continued

	NDN	DN	p
Nasal (μm)	324.72 ± 19.38	311.27 ± 21.50	**0.004**
Inferior (μm)	320.23 ± 18.47	305.89 ± 25.84	**0.006**
Perifoveal (μm)	278.74 ± 12.79	270.07 ± 14.76	**0.006**
Temporal (μm)	265.83 ± 13.13	259.97 ± 13.45	0.052
Superior (μm)	281.21 ± 13.81	274.44 ± 14.96	**0.039**
Nasal (μm)	298.62 ± 15.30	287.65 ± 20.88	**0.009**
Inferior (μm)	269.34 ± 12.47	258.46 ± 17.64	**0.002**

NDN, non-diabetic nephropathy; DN, diabetic nephropathy; GCC, ganglion cell complex; p value in bold style, p<0.05.

TABLE 4 Peripapillary capillary density and retinal nerve fibre layer (RNFL) thickness.

	NDN	DN	p
Peripapillary capillary density (%)			
Whole area (%)	50.19 ± 3.10	47.46 ± 5.93	**0.016**
Nasal superior (%)	46.82 ± 3.91	43.96 ± 7.42	**0.042**
Nasal inferior (%)	44.77 ± 4.55	43.08 ± 7.43	0.242
Inferior nasal (%)	47.68 ± 6.33	46.00 ± 7.00	0.277
Inferior temporal (%)	54.93 ± 5.13	51.66 ± 7.42	**0.030**
Temporal inferior (%)	51.27 ± 4.70	47.06 ± 6.95	**0.004**
Temporal superior (%)	54.87 ± 4.40	51.96 ± 6.77	**0.034**
Superior temporal (%)	51.65 ± 4.82	49.82 ± 7.93	0.233
Superior nasal (%)	48.94 ± 5.04	46.07 ± 7.15	**0.049**
Peripapillary RNFL thickness (μm)			
Whole area (μm)	112.14 ± 19.91	103.44 ± 21.46	0.072
Nasal superior (μm)	90.14 ± 13.30	91.73 ± 26.55	0.746
Nasal inferior (μm)	79.91 ± 13.80	82.04 ± 30.96	0.705
Inferior nasal (μm)	127.22 ± 23.74	125.53 ± 38.37	0.821
Inferior temporal (μm)	148.92 ± 26.74	129.91 ± 26.37	**0.003**
Temporal inferior (μm)	84.79 ± 66.18	65.62 ± 14.10	0.082
Temporal superior (μm)	97.08 ± 46.34	79.25 ± 15.19	**0.028**
Superior temporal (μm)	142.89 ± 17.68	131.00 ± 25.71	**0.023**
Superior nasal (μm)	128.04 ± 18.31	120.71 ± 37.78	0.294

NDN, non-diabetic nephropathy; DN, diabetic nephropathy; p value in bold style: p<0.05.

Relationships between renal function parameters and OCTA parameters for the NDN group are shown in Table 6. Representative OCTA parameters with significant correlations were then included in multivariate linear regression analyses adjusted for sex, age and DM duration for each renal function parameter. The multivariate linear regression analysis for eGFR included FAZ area, SCP vessel densities (whole area), DCP vessel densities (foveal), GCC thicknesses (parafoveal) and peripapillary capillary density (whole area), and finally showed that eGFR had a significantly negative correlation with the FAZ area (β=−18.746, p=0.048) and a significantly positive correlation with the SCP vessel density (β=0.580, p=0.036). FAZ area, SCP vessel densities (whole area) and GCC thicknesses (perifoveal) were included in the multivariate linear regression analysis for blood creatinine. The level of blood creatinine showed a significantly negative correlation with the SCP vessel density (β=-1.024, p=0.003) consequently. The multivariate linear regression analysis for urinary protein included SCP and DCP vessel densities (whole area), and finally showed that

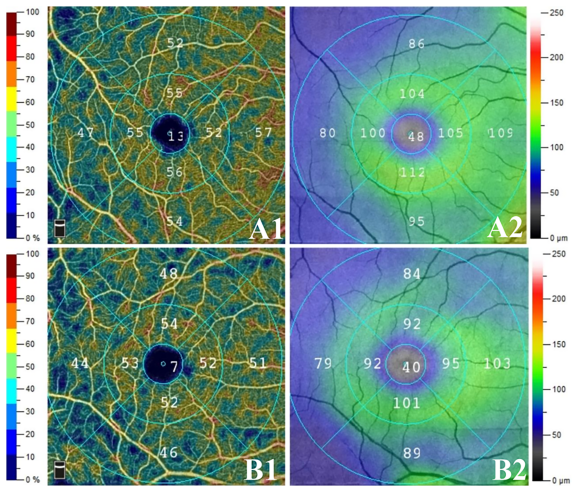

FIGURE 1
Representative images of the vessel density and GCC thickness in two groups. The right eyes of two age-matched male patients with preclinical diabetic retinopathy: **(A)** non- diabetic nephropathy (NDN) group, **(B)** DN group; (1) superficial capillary plexus (SCP) vessel density, (2) ganglion cell complex (GCC) thicknesses. Compared to NDN group, SCP vessel density and GCC thicknesses reduced in DN group. Moreover, more dark blue area was noticed in DN group than in NDN group.

TABLE 5 Correlation analysis between estimated glomerular filtration rate (eGFR) and optical coherence tomography angiography parameters in all individuals.

	eGFR (mL/min/1.73m^2)	
	r	p
FAZ area (mm^2)	-0.290	**0.012**
SCP vessel density		
Whole area (%)	0.304	**0.007**
Foveal (%)	0.241	**0.035**
Parafoveal (%)	0.259	**0.023**
Perifoveal (%)	0.330	**0.003**
DCP vessel density		
Whole area (%)	0.267	**0.019**
Foveal (%)	0.270	**0.017**
Parafoveal (%)	0.198	0.085
Perifoveal (%)	0.286	**0.021**
GCC retinal thickness		
Whole area (μm)	0.341	**0.002**
Foveal (μm)	0.278	**0.014**
Parafoveal (μm)	0.372	**<0.001**
Perifoveal (μm)	0.298	**0.008**
Full retinal thickness		
Whole area (μm)	0.280	**0.013**
Foveal (μm)	0.124	0.279
Parafoveal (μm)	0.285	**0.012**
Perifoveal (μm)	0.268	**0.018**
Peripapillary capillary density (μm)	0.258	**0.026**
Peripapillary RNFL thickness (μm)	0.327	**0.004**

FAZ, foveal avascular zone; SCP, superficial capillary plexus; DCP, deep capillary plexus; GCC, ganglion cell complex; RNFL, retinal nerve fibre layer; r, Pearson correlation coefficient; p value in bold style, p<0.05.

the level of urinary protein had a significantly positive correlation with the SCP vessel density (β=0.004, p=0.002). As for blood urea and urinary microalbumin, only one OCTA parameter was included in previous bivariate correlation analyses respectively. In linear regression analyses adjusted for sex, age and DM duration, a significantly positive correlation between the level of blood urea and the full retinal thickness (β=0.033, p=0.032) was shown, while no significant correlation was noticed between the level of urinary microalbumin and the OCTA parameter.

For the DN group, only the level of blood uric acid correlated positively with the perifoveal GCC thickness (r=0.359, p=0.043) and RNFL thickness (r=0.442, p=0.009). In multivariate linear regression analysis adjusted for sex, age and DM duration, the level of blood uric acid correlated positively with the RNFL thickness (β=2.692, p=0.009).

The corresponding details were summarized in Table 7.

Discussion

Is preclinical DR in DN individuals more severe? According to our present study, the answer may be "yes" when compared to the NDN individuals.

In our study, SCP vessel density rather than DCP vessel density was significantly reduced in DN individuals. Zhuang's study revealed that SCP and DCP vessel densities decrease as chronic kidney disease (CKD) progresses in DM patients but that SCP vessel density reduction is more pronounced (15). Wang's study showed that DN patients had reduced macular vessel density compared to NDN patients, but macular vessel density was not divided into the SCP and DCP (16). Our result was somewhat consistent with these studies. Nevertheless, Zhuang's and Wang's studies included preclinical DR and DR simultaneously, and the percentage of DR in the DN group was obviously higher than that in NDN. Vessel density may therefore be greatly affected by the constitution of DR at different stages. Our study focused specifically on preclinical DR, which may minimize the above effects and for the first time provide a possible answer to the interesting question: Is preclinical DR in DN individuals more severe? As stated in previous studies, capillary impairment is more remarkable in the DCP than in the SCP in preclinical and nonproliferative DR as

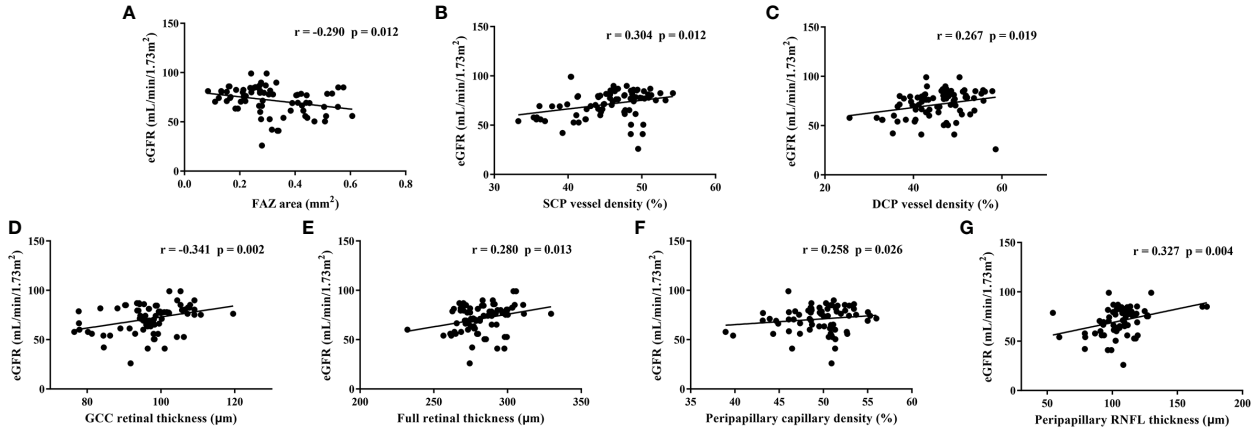

FIGURE 2
Relationships between estimated glomerular filtration rate (eGFR) and each representative optical coherence tomography angiography parameter in all individuals. FAZ: foveal avascular zone, SCP, superficial capillary plexus; DCP, deep capillary plexus; GCC, ganglion cell complex; RNFL, retinal nerve fibre layer; r, Pearson correlation coefficient.

TABLE 6 Correlation analysis between renal function parameters and optical coherence tomography (angiography) parameters in non-diabetic nephropathy individuals.

	eGFR (mL/min/1.73m^2)		Blood urea (mmol/L)		Blood creatinine (μmol/L)		Blood uric acid (μmol/L)		Urinary protein (g/L)		Urinary microalbumin (mg/L)	
	r	p	r	p	r	p	r	p	r	p	r	P
FAZ area (mm^2)	-0.389	**0.016**	0.024	0.887	0.330	**0.043**	-0.097	0.584	-0.194	0.312	-0.222	0.286
SCP vessel density												
Whole area (%)	0.420	**0.008**	-0.074	0.655	-0.491	**0.002**	0.201	0.247	0.557	**0.002**	0.018	0.931
Foveal (%)	0.182	0.268	0.107	0.519	-0.318	**0.049**	0.026	0.884	0.257	0.178	0.036	0.863
Parafoveal (%)	0.509	**<0.001**	-0.066	0.691	-0.288	0.076	0.212	0.223	0.441	**0.017**	0.200	0.338
Perifoveal (%)	0.429	**0.006**	-0.109	0.508	-0.509	**0.001**	0.239	0.167	0.522	**0.004**	0.0003	0.998
DCP vessel density												
Whole area (%)	0.244	0.135	-0.253	0.12	-0.218	0.182	-0.028	0.873	0.368	**0.049**	-0.117	0.579
Foveal (%)	0.329	**0.041**	0.009	0.956	-0.304	0.06	0.060	0.732	0.295	0.12	0.166	0.427
Parafoveal (%)	0.112	0.496	-0.307	0.057	-0.199	0.224	-0.078	0.657	0.28	0.142	-0.157	0.453
Perifoveal (%)	0.291	0.072	-0.256	0.116	-0.232	0.156	0.010	0.955	0.339	0.072	-0.072	0.731
GCC retinal thickness												
Whole area (μm)	0.207	0.200	0.238	0.139	-0.265	0.099	-0.031	0.859	0.226	0.238	0.026	0.901
Foveal (μm)	0.18	0.265	0.097	0.552	-0.147	0.366	0.035	0.844	-0.017	0.932	-0.094	0.653
Parafoveal (μm)	0.419	**0.007**	0.278	0.083	-0.008	0.963	0.144	0.411	0.012	0.95	-0.006	0.978
Perifoveal (μm)	0.080	0.623	0.194	0.23	-0.346	**0.029**	-0.111	0.525	0.305	0.107	0.045	0.832
Full retinal thickness												
Whole area (μm)	0.181	0.264	0.339	**0.032**	-0.074	0.651	-0.090	0.609	0.067	0.729	-0.086	0.683
Foveal (μm)	0.116	0.477	0.249	0.121	-0.148	0.362	-0.023	0.895	-0.067	0.73	-0.409	**0.042**
Parafoveal (μm)	0.277	0.083	0.322	**0.043**	0.023	0.887	-0.019	0.912	-0.018	0.925	-0.206	0.323
Perifoveal (μm)	0.130	0.425	0.327	**0.039**	-0.104	0.524	-0.120	0.491	0.105	0.589	-0.009	0.965

(Continued)

TABLE 6 Continued

	eGFR (mL/min/1.73m^2)		Blood urea (mmol/L)		Blood creatinine (μmol/L)		Blood uric acid (μmol/L)		Urinary protein (g/L)		Urinary microalbumin (mg/L)	
	r	p	r	p	r	p	r	p	r	p	r	P
Peripapillary capillary density (μm)	0.438	**0.007**	-0.217	0.204	0.035	0.840	0.100	0.580	0.138	0.500	-0.153	0.486
Peripapillary RNFL thickness (μm)	0.153	0.372	-0.12	0.484	-0.067	0.699	-0.037	0.839	0.256	0.206	0.368	0.084

eGFR, estimated glomerular filtration rate; FAZ, foveal avascular zone; SCP, superficial capillary plexus; DCP, deep capillary plexus; GCC, ganglion cell complex; RNFL, retinal nerve fibre layer; r, Pearson correlation coefficient; p value in bold style, p<0.05.

TABLE 7 Included Optical coherence tomography angiography (OCTA) variables and variables with significance in multivariate linear regression analyses for different renal function variables.

Group	Renal function variable	Included OCTA variable in multivariate analysis	r	p	OCTA variable with significance in multivariate analysis*	β	p
All	eGFR	FAZ area	-0.29	0.012	FAZ area	-16.43	0.039
		SCP vessel density (whole area)	0.304	0.007	Peripapillary RNFL thickness	0.169	0.025
		DCP vessel density (whole area)	0.267	0.019			
		GCC retinal thickness (whole area)	0.341	0.002			
		Full retinal thickness (whole area)	0.28	0.013			
		Peripapillary capillary density	0.258	0.026			
		Peripapillary RNFL thickness	0.327	0.004			
NDN	eGFR	FAZ area	-0.389	0.016	FAZ area	-18.746	0.048
		SCP vessel density (whole area)	0.42	0.008	SCP vessel density (whole area)	0.58	0.036
		DCP vessel density (foveal)	0.329	0.041			
		GCC retinal thickness (parafoveal)	0.419	0.007			
		Peripapillary capillary density	0.438	0.007			
	Blood urea	Full retinal thickness (whole area)	0.339	0.032	Full retinal thickness (whole area)	0.033	0.032
	Blood creatinine	FAZ area	0.33	0.043	SCP vessel density (whole area)	-1.024	0.003
		SCP vessel density (whole area)	-0.491	0.002			
		GCC retinal thickness (perifoveal)	-0.346	0.029			
	Urinary protein	SCP vessel density (whole area)	0.557	0.002	SCP vessel density (whole area)	0.004	0.002
		DCP vessel density (whole area)	0.368	0.049			
	Urinary microalbumin	Full retinal thickness (foveal)	-0.409	0.042	NA		
DN	Blood uric acid	GCC retinal thickness (perifoveal)	0.359	0.043	Peripapillary RNFL thickness	2.692	0.009
		Peripapillary RNFL thickness	0.442	0.009			

The included OCTA variables in multivariate linear regression analyses were those variables with statistical significance in previous univariate analyses. eGFR, estimated glomerular filtration rate; FAZ, foveal avascular zone; SCP, superficial capillary plexus; RNFL, retinal nerve fibre layer; DCP, deep capillary plexus; GCC, ganglion cell complex; NDN, non- diabetic nephropathy; DN, diabetic nephropathy; r, Pearson correlation coefficient; β, regression coefficient; *adjusted for sex; age and DM duration.

the disease develops (17, 18). Histologically, the SCP is a network supplying and connecting other capillary plexuses, whereas the DCP is composed of lobular configurations without abundant capillary connections (19). The SCP may have stronger self-regulatory ability than the DCP. In this sense, the DCP may be more vulnerable than the SCP and may serve as an initial marker in early-stage DR. However, our study revealed that SCP vessels seem to reduce more obviously than DCP vessels in DN individuals, which was quite an interesting finding. This may suggest that DN patients have more pronounced and advanced capillary dropout than NDN patients, even when they

only have "preclinical DR". The explanation for such advanced capillary dropout may be attributed to the complicated mechanisms of DN and its complications. The renin-angiotensin-aldosterone system exerts a strong vasoconstrictive effect and possibly induces haemodynamic disturbances in the retinal microvasculature (20). Oxidative stress and inflammation occurring in DN might also accelerate the process of retinal vascular endothelial cell impairment (21). Furthermore, anaemia in DN secondary to erythropoietin reduction, uraemic toxin accumulation and dialysis might be responsible for capillary impairment, as stated in previous studies (22, 23).

Another interesting finding in our study was that the peripapillary capillary density was reduced in DN. The radial peripapillary capillary plexus (RPCP) and the SCP are closely related and components of the superficial vascular complex. The RPCP is nourished by precapillary arterioles from the SCP and is driven by postcapillary venules into the SCP (19). Hence, it may be understandable that SCP vessel density and peripapillary capillary density simultaneously decrease. However, peripapillary capillary data were recorded based on limited resources, and the standard was different; thus, comparisons cannot be fully performed. Cankurtaran's study suggested that preclinical DR patients with microalbuminuria have a higher peripapillary capillary density than those with normal albuminuria, which was similar to our result (24). The major difference was that the population was classified based on the level of albuminuria in Cankurtaran's study but that patients were classified based on the diagnosis of DN in our study.

Compared to capillary density, a more pronounced alteration in DN individuals was reduced macular retinal thickness. This was a novel finding, as no previous study has reported similar results. Macular retinal thickness was not altered as CKD or albuminuria progressed in previous DN-related studies (15, 24). One possible explanation for the difference between these results is the DR stage variation in the included population, as stated above. Another possible explanation is the controversial mechanism of DN. Classically speaking, proteinuria is followed by decline in renal function. However, some DM patients have progressive reduction in eGFR with microalbuminuria regression or even without proteinuria, which may suggest that alteration of eGFR occurs independently of the presence of albuminuria (25, 26). Microalbuminuria and decreased eGFR can be present simultaneously or separately in DN. This may pose a challenge for the definition of DN, as an abnormal level of eGFR or urinary albumin may be regarded as DN. The group division standard is not uniform in all studies. According to our results, we speculate that the diffuse shrinkage of retinal thickness observed was secondary to capillary dropout. Uraemic toxins might also be a crucial factor. A recent study showed that accumulation of uraemic toxins such as parathyroid hormone and β2-microglobulin correlates closely with GCC impairment in CKD patients without diabetes or dialysis (27). Moreover, dialysis is a potential reason. A Japanese study revealed that haemodialysis not only contributes to relieving DME but also helps to decrease retinal thickness after a one-year follow-up (28). However, this study mainly included DME patients rather than preclinical DR, the mechanism might be partially different in these individuals. Haemodialysis may to some degree accelerate the flow of the retinal/subretinal fluid as well as eliminate toxins and inflammatory particles (29).

For all individuals, eGFR was closely related to most OCTA parameters. Even after multivariate linear regression analysis adjusted for age and sex, the level of eGFR still showed a significantly negative correlation with the FAZ area. In the NDN group, the level of eGFR was associated with the FAZ/SCP vessel density. These results in our study suggest that eGFR may be a good indicator for microvascular impairment in all preclinical DR individuals and NDN individuals. Similar to our study, Vadalà's and Wang's studies showed that eGRF correlated positively with macular vessel density in T2DM patients with CDK (16, 30). In contrast, no association between eGFR and FAZ area/vessel density in DM patients was reported in Cheung's study, while this study showed that large intercapillary area is associated with eGFR (31).These contradictions among studies may be related to a variation in DR stage, a different adoption of the eGFR equation, various measurement methods of OCTA parameters and a relatively small sample. In addition, it may be affected by complicated systemic confounding factors among different study groups. In the NDN group, the urinary protein level was positively associated with the SCP vessel density, but no association between the urinary microalbumin level and each OCTA parameter was noted. This finding is at odds with some publications. In a Turkish study, urinary microalbumin levels correlated negatively with DCP vessel density in T2DM patients with and without DN (32). Yao's study revealed that macular vessel density correlated negatively with urinary protein levels in adults with primary nephrotic syndrome (33). The analysed subgroup in our study had NDN rather than NDN combined with DN or other kinds of nephropathy, and thus the differences among individuals may be indistinctive. Moreover, in the NDN group, proteinuria may be physiological or very mild, and its correlation with OCTA parameters might be less meaningful. In the DN group, most OCTA parameters lacked correlation with renal function parameters. A potential explanation for this is that the process of DN had actually initiated and progressively worsened the retinal microvasculature when DN was not diagnosed in preclinical DR individuals. At this stage, renal function and OCTA parameters change in parallel. However, as DN develops, retinal impairment may not only be affected by renal functions but also be influenced by secondary systemic alterations, such as electrolyte imbalance, anaemia, hypertension, uraemic toxin accumulation and dialysis (34). These factors may cause an unparallel relationship between OCTA parameters and renal function parameters in the DN group.

We noticed that NDN group has better BCVA when compared to DN group. Cataract severity may mainly account for the variation. In addition, DM duration seemed to be longer in DN group than in NDN group. Though the difference didn't reach statistical significance, the effect of DM duration should be considered. However, the subsequent multivariate linear regression analyses adjusted for sex, age and DM duration may partially avoid the effect of DM duration.

The major limitation of our study was the small sample and its retrospective nature. Another limitation was that the included individuals were Chinese, which cannot represent the entire population of T2DM individuals. The topic deserves further

exploration using a well-designed prospective study with a large sample size.

In conclusion, in preclinical DR, DN patients have reduced retinal vessel density and thickness compared to NDN patients. Preclinical DR may be more severe in DN individuals than in NDN individuals with regard to microvascular and microstructural impairment. Moreover, eGFR may be a good indicator for retinal microvascular impairment.

Data availability statement

The original contributions presented in the study are included in the article/supplementary material. Further inquiries can be directed to the corresponding author.

Ethics statement

The studies involving human participants were reviewed and approved by Sun Yat-sen Memorial Hospital, Sun Yat-sen University. Written informed consent for participation was not required for this study in accordance with the national legislation and the institutional requirements.

Author contributions

All authors contributed to the study conception and design. Material preparation, data collection and analysis were performed by ZL and HY. The first draft of the manuscript was written by ZL and HY, and all authors commented on previous versions of the manuscript. All authors contributed to the article and approved the submitted version.

Funding

This research was supported by the Project of Administration of Traditional Chinese Medicine of Guangdong Province, China (20221077).

Conflict of interest

The authors declare that the research was conducted in the absence of any commercial or financial relationships that could be construed as a potential conflict of interest.

Publisher's note

All claims expressed in this article are solely those of the authors and do not necessarily represent those of their affiliated organizations, or those of the publisher, the editors and the reviewers. Any product that may be evaluated in this article, or claim that may be made by its manufacturer, is not guaranteed or endorsed by the publisher.

References

1. Vujosevic S, Aldington SJ, Silva P, Hernández C, Scanlon P, Peto T, et al. Screening for diabetic retinopathy: new perspectives and challenges. *Lancet Diabetes Endocrinol* (2020) 8(4):337–47. doi: 10.1016/S2213-8587(19)30411-5

2. Flyvbjerg A. The role of the complement system in diabetic nephropathy. *Nat Rev Nephrol* (2017) 13(5):311–8. doi: 10.1038/nrneph.2017.31

3. Yang J, Liu Z. Mechanistic pathogenesis of endothelial dysfunction in diabetic nephropathy and retinopathy. *Front Endocrinol (Lausanne)* (2022) 13:816400. doi: 10.3389/fendo.2022.816400

4. Saini DC, Kochar A, Poonia R. Clinical correlation of diabetic retinopathy with nephropathy and neuropathy. *Indian J Ophthalmol* (2021) 69(11):3364–8. doi: 10.4103/ijo.IJO_1237_21

5. Zhang J, Wang Y, Li L, Zhang R, Guo R, Li H, et al. Diabetic retinopathy may predict the renal outcomes of patients with diabetic nephropathy. *Ren Fail* (2018) 40 (1):243–51. doi: 10.1080/0886022X.2018.1456453

6. Li Z, Wen X, Zeng P, Liao Y, Fan S, Zhang Y, et al. Do microvascular changes occur preceding neural impairment in early-stage diabetic retinopathy? evidence based on the optic nerve head using optical coherence tomography angiography. *Acta Diabetol* (2019) 56(5):531–9. doi: 10.1007/s00592-019-01288-8

7. Sun Z, Yang D, Tang Z, Ng DS, Cheung CY. Optical coherence tomography angiography in diabetic retinopathy: an updated review. *Eye (Lond)* (2021) 35(1):149–61. doi: 10.1038/s41433-020-01233-y

8. 2. Classification and Diagnosis of Diabetes. Standards of medical care in diabetes-2018. *Diabetes Care* (2018) 41(Suppl 1):S13–s27. doi: 10.2337/dc18-S002

9. Solomon SD, Chew E, Duh EJ, Sobrin L, Sun JK, VanderBeek BL, et al. Diabetic retinopathy: A position statement by the American diabetes association. *Diabetes Care* (2017) 40(3):412–8. doi: 10.2337/dc16-2641

10. Tuttle KR, Bakris GL, Bilous RW, Chiang JL, de Boer IH, Goldstein-Fuchs J, et al. Diabetic kidney disease: a report from an ADA consensus conference. *Diabetes Care* (2014) 37(10):2864–83. doi: 10.2337/dc14-1296

11. Li DY, Yin WJ, Yi YH, Zhang BK, Zhao J, Zhu CN, et al. Development and validation of a more accurate estimating equation for glomerular filtration rate in a Chinese population. *Kidney Int* (2019) 95(3):636–46. doi: 10.1016/j.kint.2018.10.019

12. Oumer KS, Liu Y, Charkos TG, Yang S. Association between urine albumin to creatinine ratio and bone mineral density: a cross-sectional study. *Ir J Med Sci* (2022) 191(1):427–32. doi: 10.1007/s11845-021-02551-0

13. Whelton PK, Carey RM, Aronow WS, Casey DE Jr., Collins KJ, Dennison Himmelfarb C, et al. 2017 ACC/AHA/AAPA/ABC/ACPM/AGS/APhA/ASH/ASPC/NMA/PCNA guideline for the prevention, detection, evaluation, and management of high blood pressure in adults: Executive summary: A report of the American college of Cardiology/American heart association task force on clinical practice guidelines. *Hypertension* (2018) 71(6):1269–324. doi: 10.1161/HYP.0000000000000066

14. Li Z, Alzogool M, Xiao J, Zhang S, Zeng P, Lan Y, et al. Optical coherence tomography angiography findings of neurovascular changes in type 2 diabetes mellitus patients without clinical diabetic retinopathy. *Acta Diabetol* (2018) 55(10):1075–82. doi: 10.1007/s00592-018-1202-3

15. Zhuang X, Cao D, Zeng Y, Yang D, Yao J, Kuang J, et al. Associations between retinal microvasculature/microstructure and renal function in type 2 diabetes patients with early chronic kidney disease. *Diabetes Res Clin Pract* (2020) 168:108373. doi: 10.1016/j.diabres.2020.108373

16. Wang W, He M, Gong X, Wang L, Meng J, Li Y, et al. Association of renal function with retinal vessel density in patients with type 2 diabetes by using swept-source optical coherence tomographic angiography. *Br J Ophthalmol* (2020) 104 (12):1768–73. doi: 10.1136/bjophthalmol-2019-315450

17. Sandhu HS, Eladawi N, Elmogy M, Keynton R, Helmy O, Schaal S, et al. Automated diabetic retinopathy detection using optical coherence tomography angiography: a pilot study. *Br J Ophthalmol* (2018) 102(11):1564–9. doi: 10.1136/bjophthalmol-2017-311489

18. Zeng Y, Cao D, Yu H, Yang D, Zhuang X, Hu Y, et al. Early retinal neurovascular impairment in patients with diabetes without clinically detectable retinopathy. *Br J Ophthalmol* (2019) 103(12):1747–52. doi: 10.1136/bjophthalmol-2018-313582

19. Campbell JP, Zhang M, Hwang TS, Bailey ST, Wilson DJ, Jia Y, et al. Detailed vascular anatomy of the human retina by projection-resolved optical coherence tomography angiography. *Sci Rep* (2017) 7:42201. doi: 10.1038/srep42201

20. Wennmann DO, Hsu HH, Pavenstädt H. The renin-angiotensin-aldosterone system in podocytes. *Semin Nephrol* (2012) 32(4):377–84. doi: 10.1016/j.semnephrol.2012.06.009

21. Samsu N. Diabetic nephropathy: Challenges in pathogenesis, diagnosis, and treatment. *BioMed Res Int* (2021) 2021:1497449. doi: 10.1155/2021/1497449

22. Düzgün E, Demir N, Alkan AA, Uslu Doğan C, Çakır A. Retinochoroidal vascular plexuses in patients with iron deficiency anaemia. *Clin Exp Optom* (2022) 105 (3):326–32. doi: 10.1080/08164622.2021.1916387

23. Koca S, Bozkurt E, Eroğul Ö, Yavaşoğlu F, Doğan M, Akdoğan M, et al. Evaluation of macular and optic disc radial peripapillary vessel density with optical coherence tomography angiography in iron deficiency anemia. *Photodiagnosis Photodyn Ther* (2022) 38:102744. doi: 10.1016/j.pdpdt.2022.102744

24. Cankurtaran V, Inanc M, Tekin K, Turgut F. Retinal microcirculation in predicting diabetic nephropathy in type 2 diabetic patients without retinopathy. *Ophthalmologica* (2020) 243(4):271–9. doi: 10.1159/000504943

25. Robles NR, Villa J, Felix FJ, Fernandez-Berges D, Lozano L. Non-proteinuric diabetic nephropathy is the main cause of chronic kidney disease: Results of a general population survey in Spain. *Diabetes Metab Syndr* (2017) 11 Suppl 2:S777–s781. doi: 10.1016/j.dsx.2017.05.016

26. Kume S, Araki SI, Ugi S, Morino K, Koya D, Nishio Y, et al. Secular changes in clinical manifestations of kidney disease among Japanese adults with type 2 diabetes from 1996 to 2014. *J Diabetes Investig* (2019) 10(4):1032–40. doi: 10.1111/jdi.12977

27. Zeng X, Hu Y, Chen Y, Lin Z, Liang Y, Liu B, et al. Retinal neurovascular impairment in non-diabetic and non-dialytic chronic kidney disease patients. *Front Neurosci* (2021) 15:703898. doi: 10.3389/fnins.2021.703898

28. Takamura Y, Matsumura T, Ohkoshi K, Takei T, Ishikawa K, Shimura M, et al. Functional and anatomical changes in diabetic macular edema after hemodialysis initiation: One-year follow-up multicenter study. *Sci Rep* (2020) 10(1):7788. doi: 10.1038/s41598-020-64798-4

29. Himmelfarb J, Ikizler TA. Hemodialysis. *N Engl J Med* (2010) 363(19):1833–45. doi: 10.1056/NEJMra0902710

30. Vadalà M, Castellucci M, Guarrasi G, Terrasi M, La Blasca T, Mulè G. Retinal and choroidal vasculature changes associated with chronic kidney disease. *Graefes Arch Clin Exp Ophthalmol* (2019) 257(8):1687–98. doi: 10.1007/s00417-019-04358-3

31. Cheung CY, Tang F, Ng DS, Wong R, Lok J, Sun Z, et al. The relationship of quantitative retinal capillary network to kidney function in type 2 diabetes. *Am J Kidney Dis* (2018) 71(6):916–8. doi: 10.1053/j.ajkd.2017.12.010

32. Ucgul Atilgan C, Atilgan KG, Kosekahya P, Goker YS, Karatepe MS, Caglayan M, et al. Retinal microcirculation alterations in microalbuminuric diabetic patients with and without retinopathy. *Semin Ophthalmol* (2021) 36(5-6):406–12. doi: 10.1080/08820538.2021.1896745

33. Yao T, He Y, Huang L, Chen J, Zhang Z, Yang W, et al. Quantitative vessel density analysis of macular and peripapillary areas by optical coherence tomography angiography in adults with primary nephrotic syndrome. *Microvasc Res* (2022) 144:104407. doi: 10.1016/j.mvr.2022.104407

34. John S. Complication in diabetic nephropathy. *Diabetes Metab Syndr* (2016) 10 (4):247–9. doi: 10.1016/j.dsx.2016.06.005

frontiers | Frontiers in Endocrinology

TYPE Systematic Review
PUBLISHED 03 April 2023
DOI 10.3389/fendo.2023.1144290

OPEN ACCESS

EDITED BY
Mohd Imtiaz Nawaz,
Department of Ophthalmology, King Saud University, Saudi Arabia

REVIEWED BY
Sudhanshu Kumar Bharti,
Patna University, India
Xuedong An,
Guang'anmen Hospital, China Academy of Chinese Medical Sciences, China
Ming Jin,
China-Japan Friendship Hospital, China

*CORRESPONDENCE
Chuanhong Jie
jiechuanhong@163.com

†These authors have contributed equally to this work and share first authorship

SPECIALTY SECTION
This article was submitted to Clinical Diabetes, a section of the journal Frontiers in Endocrinology

RECEIVED 14 January 2023
ACCEPTED 17 March 2023
PUBLISHED 03 April 2023

CITATION
Liu Z, Chen Y, Jie C, Wang J, Deng Y, Hou X, Li Y and Cai W (2023) The comparative effects of oral Chinese patent medicines in non-proliferative diabetic retinopathy: A Bayesian network meta-analysis of randomized controlled trials. *Front. Endocrinol.* 14:1144290. doi: 10.3389/fendo.2023.1144290

The comparative effects of oral Chinese patent medicines in non-proliferative diabetic retinopathy: A Bayesian network meta-analysis of randomized controlled trials

Ziqiang Liu[1†], Yunru Chen[2†], Chuanhong Jie[1*], Jianwei Wang[1], Yu Deng[1], Xiaoyu Hou[1], Yuanyuan Li[1] and Wenjing Cai[1]

[1]Ophthalmology Department, Eye Hospital China Academy of Chinese Medical Sciences, Beijing, China, [2]Centre for Evidence-based Chinese Medicine, School of Traditional Chinese Medicine, Beijing University of Chinese Medicine, Beijing, China

Background: Non-proliferative diabetic retinopathy (NPDR), a common diabetic complication with high morbidity, is featured by impaired visual function and fundus lesions. It has been reported that oral Chinese patent medicines (OCPMs) may improve visual acuity and fund signs. However, the best possible OCPMs for NPDR remain questionable and merit further investigation.

Methods: From inception to October 20, 2022, seven databases were searched for eligible randomized controlled trials (RCTs). The outcomes were clinical effective rate, visual acuity, visual field gray value, microaneurysm volume, hemorrhage area, macular thickness, and adverse events rate. The revised Cochrane risk-of-bias tool (ROB 2) was used to assess the quality of the included studies. Network meta-analysis was performed using R 4.1.3 and STATA 15.0 software.

Results: We included 42 RCTs with 4,858 patients (5,978 eyes). The Compound Danshen Dripping Pill (CDDP) combined with calcium dobesilate (CD) had the most improvement in clinical efficacy rate (SUCRA, 88.58%). The Compound Xueshuantong Capsule (CXC) combined with CD may be the best intervention (SUCRA, 98.51%) for the improvement of visual acuity. CDDP alone may be the most effective treatment option (SUCRA, 91.83%) for improving visual field gray value. The Hexuemingmu Tablet (HXMMT) and Shuangdan Mingmu Capsule (SDMMC) combined with CD may be the most effective treatment for reducing microaneurysm volume and hemorrhage area (SUCRA, 94.48%, and 86.24%), respectively. Referring to reducing macular thickness, CXC combined with CD ranked first (SUCRA, 86.23%). Moreover, all OCPMs did not cause serious adverse reactions.

Conclusion: OCPMs are effective and safe for NPDR. CDDP alone, and combined with CD, may be the most effective in improving visual field gray value and clinical efficacy rate, respectively; CXC combined with CD may be the best in enhancing

BCVA and reducing macular thickness; HXMMT and SDMMC combined with CD, maybe the most effective regarding microaneurysm volume and hemorrhage area, respectively. However, the reporting of methodology in the primary study is poor, potential biases may exist when synthesizing evidence and interpreting the results. The current findings need to be confirmed by more large-sample, double-blind, multi-center RCTs of rigorous design and robust methods in the future.

Systematic review registration: https://www.crd.york.ac.uk/prospero/, identifier CRD42022367867.

KEYWORDS

oral Chinese patent medicines, non-proliferative diabetic retinopathy, calcium dobesilate, network meta-analysis, SUCRA

1 Introduction

The prevalence of diabetes in individuals aged 20 to 79 years increased to 537 million worldwide in 2021 and is expected to rise to 783 million in 2045 (1). Diabetic retinopathy (DR) is one of the most common microvascular and neurological complications of diabetes, with a prevalence of 24.7-37.5% in the diabetic population, and is the leading cause of blindness in people of working age (2). According to the international clinical DR severity grading criteria, DR can be divided into non-proliferative diabetic retinopathy (NPDR) and proliferative diabetic retinopathy (PDR). NPDR is characterized by fundus microaneurysms, retinal hemorrhage, cotton wool spots, hard exudate, and intraretinal microvascular abnormality (IRMA) formation. Moreover, retinal neovascularization formation implies a transition to the PDR stage, which can further cause vitreous hemorrhage, retinal detachment, and neovascular glaucoma, leading to severe vision loss and even blindness (3).

Therefore, controlling the progression of DR and maximizing the restoration of visual acuity in patients has become a focus of clinical research. Currently, the main treatment strategies for NPDR are controlling risk factors, such as blood glucose and blood pressure, and improving microcirculation. Retinal laser photocoagulation, intravitreous drug injection, and vitrectomy are mainly applied to patients with PDR, and all have some limitations (4). Calcium dobesilate (CD) is a well-established vasoactive and vasoprotective drug that can reduce retinal capillary permeability and stabilize blood-retinal barrier function, as well as antagonize platelet aggregation and improve local blood circulation, and is widely used clinically in patients with NPDR (5, 6). A meta-analysis involving 221 studies showed that CD might improve fundus bleeding and exudation in patients with DR (5). However, not all NPDR patients benefit (7).

In addition to the above methods, Chinese clinicians have achieved better clinical efficacy by combining oral Chinese patent medicines (OCPMs). OCPMs are traditional Chinese medicine products processed as per the prescription and preparation technology based on Chinese herbal medicine as raw material (8). Several recent basic studies have shown that the active ingredients of OCPMs can reduce retinal ischemia and hypoxia, and improve retinal structure and function through various pathways, such as reducing pericyte loss, attenuating oxidative stress and inflammatory responses (9, 10). Moreover, a growing body of clinical evidence suggested that OCPMs alone or combined with CD for treating NPDR patients could effectively improve patients' visual function and fundus signs (11). However, there is still debate about which OCPM is most effective in treating NPDR. Therefore, our study aimed to systematically assess the effects of different OCPMs on outcome indicators of NPDR using network meta-analysis (NMA).

2 Methods

The study followed the Preferred Reporting Items for Systematic Reviews and Meta-Analyses (PRISMA) Extension Statement for systematic reviews and meta-analyses (12). The PRISMA checklist is detailed in Supplementary File S1.

2.1 Search strategy

Seven academic databases were searched for published research from inception to October 20, 2022, including PubMed, Embase, Cochrane Library, China National Knowledge Infrastructure, Wanfang Database, Weipu Journal Database, and Chinese Biomedical Literature Database. Only Chinese and English articles were retrieved. The detailed search strategies are provided in Supplementary File S2.

2.2 Inclusion and exclusion criteria

1) Patients diagnosed with NPDR according to international or Chinese diagnostic criteria (relying on fundus fluorescein angiography and fundus signs) (3, 13).

2) The interventions of the experimental group were OCPMs with or without CD. Besides, the OCPMs must belong to the seven kinds of OCPMs recommended by the National Healthcare Security Administration (NHSA) (http://www.nhsa.gov.cn/) and National Medical Products Administration (NMPA) (https://www.nmpa.gov.cn/) of the People's Republic of China.

3) The interventions of the control group were treated with CD alone.

4) Outcomes included clinical effective rate (percentage of patients whose visual acuity and fund signs improved after treatment), visual acuity (standard logarithm visual acuity chart), visual field gray value, microaneurysm volume, hemorrhage area, macular thickness, and adverse drug reactions (ADRs).

5) The types of studies were randomized controlled trials (RCTs).

2.3 Data collection and quality assessment

Two authors independently extracted the relevant information. The details included basic trial information, population, detailed inventions, outcomes, and study type. According to Version 2 of the Cochrane risk-of-bias tool (RoB 2) for randomized trials, Two authors independently assessed the risk of bias of the RCTs from five submissions, including randomization process, deviations from intended interventions, missing outcome data, measurement of the outcome, and selection of the reported results (14). All trials were regarded as "low risk", "some concerns", or "high risk". Disagreements were resolved through consensus or third-party adjudication.

2.4 Data analysis

We used STATA 15.0 software to conduct a traditional pairwise meta-analysis and R 4.1.3 software with the "BUGSnet" and "rjags" packages for a Bayesian NMA (15). A random-effects model was analyzed. We ran the Markov chain Monte Carlo (MCMC) simulation with four Markov chains for 200,000 iterations (burn-in iterations=5000, thinning factor=1) (16). The Gelman-Rubin convergence diagnostic was tested. The potential scale reduction factor (PSRF) value close to 1 indicates convergence. We estimated the odds ratio (OR) for dichotomous outcomes and mean difference (MD) for continuous outcomes, with a corresponding 95% credible interval (CrI). The network plot was presented to visualize multiple comparisons. The evaluation of inconsistency was not applicable because there were no "closed loops" in the network plot. The probability values of the surface under the cumulative ranking curve (SUCRA) were estimated for treatment rankings. The SUCRA values ranged from 0-100%. A higher value indicates a higher likelihood that therapy is the best among the interventions being compared (17). Heterogeneity was assessed using the I^2 test. If there was substantial heterogeneity (I^2 > 50%), subgroup analysis and sensitivity analysis were considered. Publication bias was examined by the comparison-adjusted funnel plot.

3 Results

3.1 Search results

We retrieved 12,591 records in total. After removing duplicates, 8,105 records remained for screening. Of which, 7,968 records were excluded by reading the title and abstract, and 95 by reading the full text. Finally, 42 two-arm RCTs with 4,858 patients (5,978 eyes) were included in our study. The Flowchart of the search is shown in Figure 1.

3.2 Characteristics of included studies

In total, 4,858 patients (5,978 eyes) and 7 kinds of OCPMs were involved in the 42 RCTs. Concerning treatment, 2,334 patients (2,790 eyes) used CD alone, 846 patients (1,351 eyes) treated only OCPMs, and 1,678 patients (1,837 eyes) received with OCPMs combined with CD. Regarding outcomes, 36 studies (85.71%), 8 studies (19.05%), 19 studies (45.24%), 14 studies (33.33%), 18 studies (42.86%), 18 studies (42.86%), and 22 studies (52.38%) assessed the clinical efficacy rate, visual acuity, visual field gray value, microaneurysm volume, hemorrhage area, macular thickness, and ADRs, respectively. The detailed characteristics of the studies are demonstrated in Table 1.

All 42 included RCTs were two-arm studies. The interventions of the experimental group were either OCMPs alone or OCMPs combined with CD, and the control group was CD alone. There were six different types of OCMPs among the combined therapies, including the Compound Xueshuantong Capsule (CXC) combined

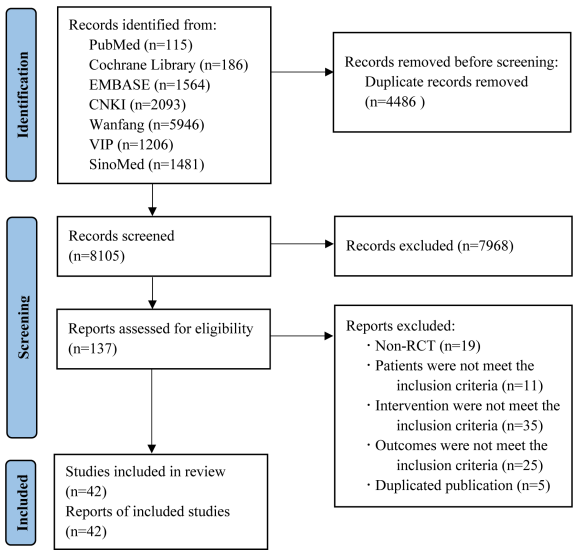

FIGURE 1
Flowchart of the search for eligible studies.

10.3389/fendo.2023.1144290

TABLE 1 Characteristics of the included studies.

Study ID	Sample Size (E/C)	Sex (M/F)	Age (Year, E/C)	Intervention of experimental group	Intervention of control group	Course (Months)	Outcomes
Du JH 2018 (18)	48/48	(29/19)/(30/18)	(64.2 ± 4.3)/(62.7 ± 4.0)	CXC	CD	1	①
Huang W 2021 (19)	30/30	(17/13)/(18/12)	(52.85 ± 6.38)/(51.86 ± 6.16)	CXC+CD	CD	5	① ③ ④ ⑤ ⑥ ⑦
An LN 2020 (20)	35/35	(19/16)/(20/15)	(51.17 ± 17.83)/(52.12 ± 15.76)	CXC+CD	CD	3	① ④ ⑥ ⑦
Wang J 2020 (21)	44/42	(26/19)/(23/19)	(69.52 ± 7.11)/(68.35 ± 6.82)	CXC+CD	CD	5	① ③ ④ ⑤ ⑥ ⑦
Yan H 2020 (22)	46/46	(27/19)/(25/21)	(48.5 ± 4.9)/(47.4 ± 4.6)	CXC+CD	CD	3	① ⑦
Chai F 2018 (23)	54/53	(32/22)/(30/23)	(61.11 ± 6.01)/(61.19 ± 6.03)	CXC+CD	CD	3	① ③ ⑤ ⑥
Wang Q 2018 (24)	50/50	(26/24)/(27/23)	(55.02 ± 2.58)/(54.80 ± 2.61)	CXC+CD	CD	6	① ③ ④ ⑤ ⑥
Ma JP 2018 (25)	27/27	(16/11)/(15/12)	(53.02 ± 4.13)/(53.08 ± 4.25)	CXC+CD	CD	5	① ③ ④ ⑤ ⑥ ⑦
Yu W 2017 (26)	34/34	(19/15)/(17/17)	(57.4 ± 8.3)/(58.1 ± 7.9)	CXC+CD	CD	3	① ③ ⑤ ⑥
Rao XJ 2017 (27)	110/125	(61/49)/(68/57)	(49.5 ± 5.9)/(50.2 ± 6.4)	CXC+CD	CD	3	①
Men LB 2020 (28)	40/40	(21/19)/(22/18)	(66.97 ± 2.86)/(67.46 ± 2.52)	CXC+CD	CD	2	① ② ③ ⑤ ⑥
Li Y 2019 (29)	49/49	(28/21)/(27/22)	(66.82 ± 4.03)/(66.41 ± 4.11)	CXC+CD	CD	3	① ③
Pei R 2015 (30)	32/32	(17/15)/(16/16)	(56.4 ± 2.1)/(55.3 ± 1.2)	CXC+CD	CD	5	① ③ ④ ⑤ ⑥ ⑦
Zhou YD 2022 (31)	63/63	(34/29)/(35/28)	(51.14 ± 8.1)/(52.04 ± 2.2)	CXC+CD	CD	3	① ③ ④ ⑤ ⑥ ⑦
Luo D 2015 (32)	28/29	(18/10)/(19/10)	(59.54 ± 7.46)/(57.86 ± 10.03)	CDDP	CD	3	③
Jin M 2009 (33)	30/28	NR	(62.78 ± 7.69)/(61.11 ± 7.27)	CDDP	CD	3	② ③ ⑤
Chen Y 2006 (34)	31/32	(17/14)/(15/17)	(54.60 ± 10.40)/(58.12 ± 9.31)	CDDP	CD	3	①
Xu HT 2019 (35)	43/43	(24/19)/(25/18)	(53.11 ± 4.41)/(53.06 ± 4.39)	CDDP+CD	CD	4	① ③ ④ ⑤ ⑥ ⑦
Li Y 2017 (36)	89/89	(31/58)/(28/61)	(56.5 ± 7.2)/(55.8 ± 6.8)	CDDP+CD	CD	2	①
Wang HM 2016 (37)	45/45	(23/22)/(24/21)	(57.15 ± 6.68)/(57.06 ± 6.72)	CDDP+CD	CD	2	①
Bai YX 2017 (38)	38/38	(20/18)/(21/17)	(40-72)/(39-71)	CDDP+CD	CD	4	① ② ③ ④ ⑤ ⑦
Ruan YX 2017 (39)	35/35	(18/17)/(20/15)	(52.5 ± 1.1)/(52.8 ± 1.7)	CDDP+CD	CD	4	① ③ ④ ⑤ ⑥ ⑦
Huang YX 2021 (40)	45/45	(28/17)/(29/16)	(67.5 ± 5.3)/(67.3 ± 5.1)	CDDP+CD	CD	6	② ③ ④ ⑦

(Continued)

10.3389/fendo.2023.1144290

TABLE 1 Continued

Study ID	Sample Size (E/C)	Sex (M/F)	Age (Year, E/C)	Intervention of experimental group	Intervention of control group	Course (Months)	Outcomes
Qin YH 2010 (41)	414/221	NR	NR	SDMUC	CD	4	① ⑦
Ji XD 2022 (42)	52/52	(29/23)/(28/24)	(56.63 ± 4.02)/(56.53 ± 4.09)	SDMUC+CD	CD	3	① ⑤ ⑥ ⑦
Liu JP 2019 (43)	60/60	(33/27)/(32/28)	(57.54 ± 8.11)/(57.10 ± 9.26)	SDMUC+CD	CD	4	① ⑤ ⑥ ⑦
Jin L 2019 (44)	72/71	(44/28)/(43/28)	(63.07 ± 8.08)/(62.39 ± 8.34)	SDMUC+CD	CD	4	⑦
Pang YH 2015 (45)	40/40	(18/22)/(16/24)	(49.4 ± 5.7)/(49.6 ± 5.3)	SDMUC+CD	CD	4	①
Zhang DX 2015 (46)	60/59	(24/36)/(24/35)	(60.03 ± 6.11)/(60.79 ± 642)	QG	CD	3	①
Fang J 2022 (47)	51/51	(27/24)/(26/25)	(45.5 ± 1.3)/(50.0 ± 1.4)	QG	CD	6	① ⑦
Duan JG 2006 (48)	107/105	NR	NR	QG	CD	3	⑦
Fan YP 2018 (49)	47/47	(26/21)/(27/20)	(48.6 ± 5.1)/(47.5 ± 4.9)	QG	CD	6	① ⑥ ⑦
Feng JL 2016 (50)	42/41	(29/13)/(27/14)	(55.26 ± 6.29)/(55.89 ± 6.13)	QG+CD	CD	3	① ②
Wang ZQ 2019 (51)	52/48	(31/21)/(29/19)	(66.7 ± 6.2)/(66.8 ± 6.3)	QG+CD	CD	6	①
Wang ZZ 2017 (52)	47/47	(29/18)/(26/21)	(54.5 ± 4.8)/(54.3 ± 4.9)	QG+CD	CD	3	⑦
Sui HL 2014 (53)	43/43	(22/21)/(23/20)	(50.22 ± 14.82)/(50.53 ± 11.28)	QG+CD	CD	6	① ②
Yan JH 2020 (54)	41/41	(24/17)/(25/16)	(56.65 ± 4.02)/(56.96 ± 4.59)	QG+CD	CD	2	① ② ⑦
Ye XL 2019 (55)	88/88	(46/42)/(50/38)	(60.5 ± 13.4)/(60.9 ± 12.7)	HXMMT+CD	CD	3	①
Gao L 2020 (56)	128/128	(75/53)/(72/56)	(58.14 ± 7.63)/(57.65 ± 7.82)	HXMMT+CD	CD	3	① ③ ④ ⑤ ⑥ ⑦
Zhu HM 2013 (57)	30/30	(13/17)/(14/16)	(61.5 ± 13.1)/(61.6 ± 12.7)	DHHYK	CD	3	① ②
Li JB 2019 (58)	54/54	(29/25)/(28/26)	(55.4 ± 3.1)/(56.1 ± 3.7)	MMDHP+CD	CD	5	① ③ ④ ⑤ ⑥ ⑦
A YN 2019 (59)	50/50	(20/30)/(22/28)	(52.61 ± 5.39)/(53.02 ± 5.41)	MMDHP+CD	CD	1	③ ④ ⑤ ⑥

E/C, experimental group/control group; M/F, male/female; OCPMs, oral Chinese patent medicines; NR, Not Reported; CD, calcium dobesilate; CXC, Compound Xueshuantong Capsule; CDDP, Compound Danshen Dripping Pill; SDMUC, Shuangdan Mingmu Capsule; QG, Qiming Granule; HXMMT, Hexuemingmu Tablet; DHHYK, Danhong Huayu Koufuye; MMDHP, Mingmu Dihuang Pill; ①Clinical effective rate; ②Visual acuity; ③visual field gray value; ④microaneurysm volume; ⑤hemorrhage area; ⑥macular thickness; ⑦adverse events rate

with CD [13 RCTs (19–31)], the Compound Danshen Dripping Pill (CDDP) combined with CD [6 RCTs (35–40)], the Shuangdan Mingmu Capsule (SDMUC) combined with CD [4 RCTs (42–45)], the Qiming Granule (QG) combined with CD [5 RCTs (50–54)], the Hexuemingmu Tablet (HXMMT) combined with CD [2 RCTs (55, 56)], and the Mingmu Dihuang Pill (MMDHP) combined with CD [2 RCTs (58, 59)]. There were five different kinds of OCMPs among using OCMPs alone, including CXC [only 1 RCT (18)], CDDP [3 RCTs (32–34)], SDMUC [1 RCT (41)], QG [4 RCTs (46–49)] and Danhong Huayu Koufuye (DHHYK) [only 1 RCT (57)]. Detailed information OCMPs is described in Supplementary File S3. Furthermore, a network graph depicted the relationship between various interventions and each outcome, which is shown in Figure 2.

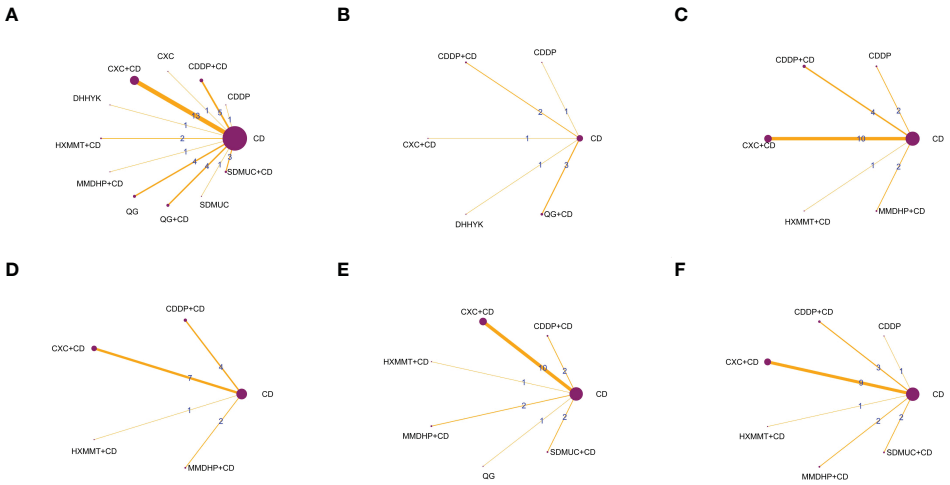

FIGURE 2
The network graphs comparing OCPMs for NPDR. **(A)** Clinical effective rate; **(B)** Visual acuity; **(C)** Visual field gray value; **(D)** Microaneurysm volume; **(E)** Hemorrhage area; **(F)** Macular thickness. CD, calcium dobesilate; CXC, Compound Xueshuantong Capsule; CDDP, Compound Danshen Dripping Pill; SDMUC, Shuangdan Mingmu Capsule; QG, Qiming Granule; HXMMT, Hexuemingmu Tablet; DHHYK, Danhong Huayu Koufuye; MMDHP, Mingmu Dihuang Pill.

3.3 Risk of bias assessment

All 42 selected RCTs reported specific randomization methods, including 18 RCTs (19, 21, 22, 24–26, 28, 29, 31, 35, 38, 40, 43, 48, 49, 55–57) using a simple random number Table 1 RCT (52) using the stratified randomization, and 1 RCT (41) using random parallel control method. Two RCTs were regarded as "low risk" in the "randomization process" due to reporting allocation concealment. Two RCTs (27, 39) were classified as high-risk because they were randomized by order of visit and admission number. In terms of deviations from intended interventions, three RCTs (32, 41, 48) adopted double-blind methods, and were thus considered as "low risk", and all the other RCTs were rated as "some concerns". All studies were evaluated as "low risk" in the missing outcome data due to there were complete data in all studies; In terms of measurement of the outcome, all studies were rated as "low risk" because the two groups were consistent and objective; In addition, there were no details of registration reported or any previously published study protocols, so all RCTs were rated as "some concerns". Thus, apart from two RCTs (27, 39), all RCTs were rated as "some concerns". The details of the risk of bias assessment are depicted in Figure 3.

3.4 Pairwise meta-analysis

We performed the pairwise meta-analysis in the seven outcomes with different OCMPs with or without CD versus CD in NPDR patients. The results (forest plots and heterogeneity analysis) are shown in Supplementary File S4. Overall, the heterogeneity of direct comparisons was moderate (I^2 < 50% for most comparisons), except QG compared to CD for the clinical efficacy rate (I^2 = 83.0%), CXC+CD compared to CD for the ray value of the visual field (I^2 = 96.2%), CXC+CD compared to CD for macular thickness (I^2 = 96.2%). Therefore, we used the fixed-effects model. Since the patients with DR included in this study were all staged as NPDR, which was consistent and had no obvious clinical heterogeneity, different courses of treatment may be substantial sources of clinical heterogeneity. Through different courses of OCMPs, we conducted subgroup analysis to find the source of heterogeneity. Meanwhile, after changing the effect model and eliminating the literature effect size one by one, the original results remained unchanged, indicating that the sensitivity analysis results were negative and the results were relatively reliable. The details are shown in Supplementary Files S5–S7.

3.5 Network meta-analysis

3.5.1 Clinical efficacy clinical rate

Thirty-six studies reported the clinical efficacy rate. We found that all the included OCPMs, apart from CXC, DHHYK, and MMDHP+CD had higher clinical efficacy than CD alone (Table 2A). Based on the ranking probability of SUCRA, CDDP+CD had the highest efficacy rate (88.58%), followed by CDDP (69.27%) and QG+CD (66.98%), whereas CD alone obtained

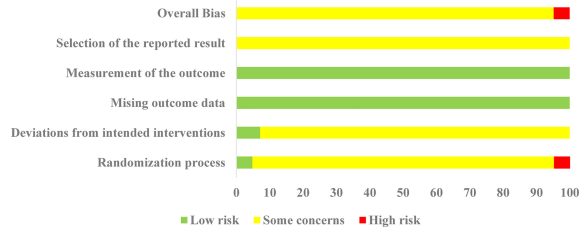

FIGURE 3
Summary of risk of bias assessment based on revised Cochrane RoB 2 tool.

TABLE 2 League table of NMA estimations.

(A) Network meta-analysis comparisons for clinical effective rate											
CD											
0.16 (0.03,0.69)	**CDDP**										
0.11 (0.04,0.26)	**0.66 (0.11,4.09)**	**CDDP+CD**									
0.33 (0.07,1.43)	2.05 (0.24,17.82)	3.11 (0.53,18.86)	**CXC**								
0.24 (0.15,0.36)	1.45 (0.31,7.62)	2.20 (0.82,6.73)	0.71 (0.15,3.51)	**CXC+CD**							
0.41 (0.11,1.47)	2.53 (0.36,19.87)	3.85 (0.81,20.21)	1.24 (0.17,9.20)	1.73 (0.45,6.89)	**DHHYK**						
0.31 (0.13,0.70)	1.88 (0.35,11.58)	2.85 (0.86,10.97)	0.92 (0.17,5.29)	1.29 (0.51,3.40)	0.74 (0.16,3.50)	**HXMMT+CD**					
0.31 (0.05,1.63)	1.92 (0.18,19.29)	2.92 (0.37,20.89)	0.93 (0.09,9.07)	1.32 (0.20,7.41)	0.75 (0.08,6.25)	1.01 (0.13,6.54)	**MMDHP +CD**				
0.23 (0.10,0.42)	1.38 (0.26,7.58)	2.09 (0.66,6.94)	0.68 (0.13,3.50)	0.95 (0.41,2.04)	0.55 (0.12,2.24)	0.74 (0.23,2.03)	0.72 (0.11,5.00)	**QG**			
0.19 (0.08,0.42)	1.15 (0.21,6.93)	1.74 (0.50,6.53)	0.56 (0.10,3.20)	0.79 (0.30,2.00)	0.45 (0.10,2.10)	0.61 (0.18,1.94)	0.60 (0.09,4.53)	0.83 (0.29,2.54)	**QG+CD**		
0.27 (0.09,0.77)	1.66 (0.27,11.24)	2.50 (0.66,11.20)	0.81 (0.13,5.18)	1.13 (0.38,3.66)	0.65 (0.12,3.49)	0.88 (0.23,3.39)	0.86 (0.12,7.22)	1.18 (0.37,4.59)	1.44 (0.39,5.65)	**SDMUC**	
0.21 (0.07,0.56)	1.28 (0.21,8.48)	1.95 (0.47,8.20)	0.62 (0.10,3.91)	0.88 (0.27,2.65)	0.50 (0.09,2.59)	0.68 (0.17,2.50)	0.67 (0.09,5.43)	0.93 (0.27,3.25)	1.12 (0.28,4.22)	0.77 (0.17,3.25)	**SDMUC +CD**
(B) Network meta-analysis comparisons for visual acuity											
CD											
-0.19 (-0.41,0.03)	**CDDP**										
-0.09 (-0.25,0.05)	0.10 (-0.17,0.36)	**CDDP+CD**									
-0.46 (-0.68,-0.24)	-0.27 (-0.58,0.04)	**-0.37 (-0.62,-0.10)**	**CXC+CD**								
-0.07 (-0.29,0.15)	0.12 (-0.19,0.43)	0.02 (-0.23,0.29)	**0.39 (0.08,0.70)**	**DHHYK**							
-0.11 (-0.24,0.02)	0.08 (-0.17,0.33)	-0.02 (-0.21,0.18)	**0.35 (0.10,0.60)**	-0.04 (-0.29,0.21)	**QG+CD**						

(Continued)

10.3389/fendo.2023.1144290

TABLE 2 Continued

(C) Network meta-analysis comparisons for visual field gray value											
CD											
1.29 (0.73,1.81)	**CDDP**										
0.93 (0.67,1.19)	-0.36 (-0.93,0.27)	**CDDP+CD**									
0.92 (0.75,1.08)	-0.37 (-0.91,0.21)	-0.02 (-0.32,0.29)	**CXC+CD**								
0.51 (-0.00,1.02)	**-0.78 (-1.50,-0.01)**	-0.42 (-1.00,0.15)	-0.41 (-0.95,0.13)	**HXMMT +CD**							
0.99 (0.63,1.35)	-0.30 (-0.92,0.37)	0.06 (-0.39,0.50)	0.07 (-0.33,0.47)	0.48 (-0.15,1.11)	**MMDHP+CD**						
(D) Network meta-analysis comparisons for microaneurysm volume											
CD											
3.05 (2.56,3.51)	**CDDP+CD**										
3.52 (3.05,3.99)	0.47 (-0.19,1.15)	**CXC+CD**									
4.04 (3.14,4.95)	0.99 (-0.01,2.03)	0.53 (-0.49,1.54)	**HXMMT +CD**								
3.17 (2.66,3.65)	0.12 (-0.56,0.81)	-0.35 (-1.05,0.33)	-0.87 (-1.92,0.14)	**MMDHP +CD**							
(E) Network meta-analysis comparisons for hemorrhage area											
CD											
0.80 (0.50,1.10)	**CDDP**										
0.81 (0.69,0.96)	0.01 (-0.31,0.35)	**CDDP+CD**									
0.81 (0.73,0.90)	0.01 (-0.30,0.32)	-0.01 (-0.17,0.15)	**CXC+CD**								
0.56 (0.38,0.74)	-0.24 (-0.59,0.11)	**-0.25 (-0.50,-0.04)**	**-0.25 (-0.46,-0.05)**	**HXMMT +CD**							
0.85 (0.73,0.99)	0.05 (-0.27,0.38)	0.04 (-0.16,0.22)	0.05 (-0.11,0.20)	**0.29 (0.07,0.53)**	**MMDHP +CD**						
0.91 (0.76,1.05)	0.10 (-0.23,0.44)	0.09 (-0.12,0.28)	0.10 (-0.07,0.26)	**0.35 (0.11,0.58)**	0.05 (-0.15,0.24)	**SDMUC+CD**					

(Continued)

10.3389/fendo.2023.1144290

TABLE 2 Continued

(F) Network meta-analysis comparisons for macular thickness									
CD									
68.87 (36.48,101.20)	**CDDP+CD**								
70.76 (55.83,85.51)	1.88 (-33.73,37.47)	**CXC+CD**							
45.19 (-0.48,90.77)	-23.67 (-79.56,32.22)	-25.57 (-73.48,22.60)	**HXMMT +CD**						
52.16 (19.76,84.49)	-16.71 (-62.45,29.08)	-18.60 (-54.01,17.02)	6.98 (-49.01,62.74)	**MMDHP +CD**					
22.01 (-23.93,67.98)	-46.85 (-102.96,9.49)	-48.75 (-97.01,-0.34)	-23.23 (-87.96,41.40)	-30.15 (-86.36,26.06)	**QG**				
47.06 (14.64,79.50)	-21.85 (-67.65,24.15)	-23.69 (-59.28,12.00)	1.85 (-54.22,57.84)	-5.09 (-50.87,40.55)	25.04 (-31.22,81.28)	**SDMUC +CD**			

The differences between the compared groups were deemed as significant when the 95% CrI of the OR did not contain 1.00 or the MD did not contain 0.00, which is marked as bold font. The data are the OR (95% CrI) of the column intervention compared to the row intervention, i.e., for the clinical effective rate, CD alone was significantly less effective than CDDP alone (OR 0.16, 95% CrI 0.03,0.69). CD, calcium dobesilate; CXC, Compound Xueshuantong Capsule; CDDP, Compound Danshen Dripping Pill; SDMUC, Shuangdan Mingmu Capsule; QG, Qiming Granule; HXMMT, Hexueming mu Tablet; DHHYK, Danhong Huayu Koufuye; MMDHP, Mingmu Dihuang Pill.

the worst effect (2.27%). The detail is shown in Figure 4A and Table 3.

3.5.2 Visual acuity

Eight studies informed the improvement of visual acuity. CXC+CD obtained a better effect than CDDP+CD, QG+CD, DHHYK, and CD alone (Table 2B). Based on the ranking probability of SUCRA, CXC+CD ranked first (98.51%), followed by CDDP (70.34%) and QG+CD (49.27%), whereas CD alone obtained the worst effect (6.25%). The detail is shown in Figure 4B and Table 3.

3.5.3 Visual field gray value

The assessment of the visual field gray value included six interventions. Four interventions (CDDP, CDDP+CD, CXC+CD, and MMDHP+CD) could improve the visual field gray value compared to CD alone (Table 2C). According to the ranking probability of SUCRA, CDDP had the highest SUCRA value (91.83%), followed by MMDHP+CD (67.47%) and CDDP+CD (59.74%), whereas CD alone obtained the worst effect (0.51%). The detail is shown in Figure 4C and Table 3.

3.5.4 Microaneurysm volume

Fourteen studies involving five interventions reported microaneurysm volume. Four treatment types (CDDP+CD, CXC+CD, HXMMT+CD, and MMDHP+CD) showed the ability to reduce microaneurysm volume more than CD alone, while other treatments did not show significant differences. Based on the ranking probability of SUCRA, HXMMT+CD might have the highest possibility (94.48%), while CD alone might be the least improved treatment (0.0%). The detail is shown in Figure 4D and Table 3.

3.5.5 Hemorrhage area

Eighteen studies informed the decrease of hemorrhage area. We found that all the included OCPMs, including CDDP, CDDP+CD, CXC+CD, HXMMT+CD, MMDHP+CD, and SDMUC+CD, reduced hemorrhage area more than CD alone (Table 2E). Based on the ranking probability of SUCRA, SDMUC+CD ranked first (86.24%), followed by MMDHP+CD (72.29%) and CDDP+CD (59.2%), whereas CD alone obtained the worst effect (0.0%). The detail is shown in Figure 4E and Table 3.

3.5.6 Macular thickness

Eighteen studies involving 7 interventions reported macular thickness. Network comparisons suggested that four treatment types (CDDP+CD, CXC+CD, MMDHP+CD, and SDMUC+CD) were better than CD alone in reducing macular thickness (Table 2F). According to SUCRA, CXC+CD had the highest SUCRA value (86.23%), followed by CDDP+CD (80.94%) and MMDHP+CD (57.05%), whereas CD alone obtained the worst effect (3.11%). The detail is shown in Figure 4F, and Table 3.

3.5.7 Adverse drug reactions

In this study, The NMA for ADRs was difficult because 8 of the 22 included studies reported no adverse reactions in the

10.3389/fendo.2023.1144290

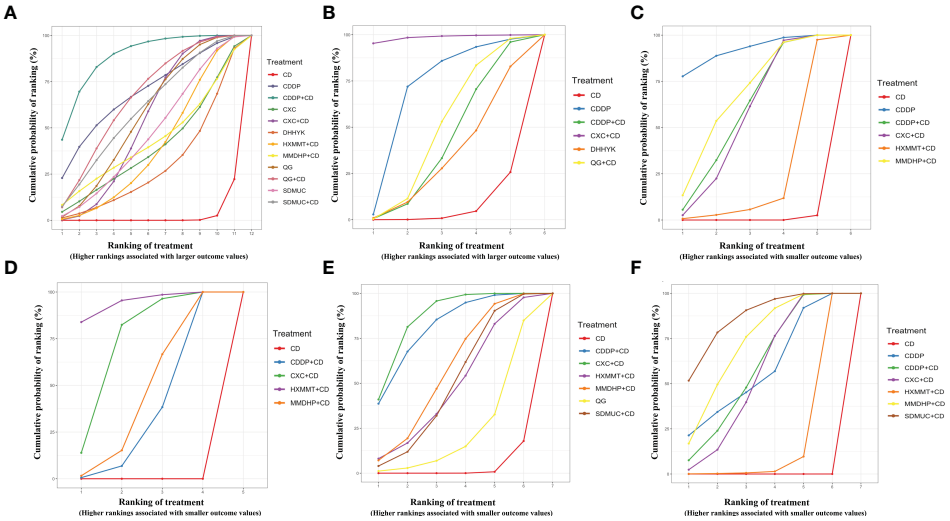

FIGURE 4
Surface under the cumulative ranking curve (SUCRA) probabilities of different interventions for six outcomes. **(A)** Clinical effective rate; **(B)** Visual acuity; **(C)** Visual field gray value; **(D)** Microaneurysm volume; **(E)** Hemorrhage area; **(F)** Macular thickness. CD, calcium dobesilate; CXC, Compound Xueshuantong Capsule; CDDP, Compound Danshen Dripping Pill; SDMUC, Shuangdan Mingmu Capsule; QG, Qiming Granule; HXMMT, Hexuemingmu Tablet; DHHYK, Danhong Huayu Koufuye; MMDHP, Mingmu Dihuang Pill.

TABLE 3 Ranking probability of interventions.

Intervention	Clinical effective rate		Visual acuity		Visual field gray value		Microaneurysm volume		Hemorrhage area		Macular thickness	
	SUCRA (%)	Rank	SUCRA (%)	Rank	SUCRA (%)	Rank	SUCRA (%)	Rank	SUCRA (%)	Rank	SUCRA (%)	Rank
CXC+CD	54.02	6	98.51	1	56.74	4	73.19	2	55.29	5	86.23	1
CDDP+CD	88.58	1	41.8	4	59.74	3	36.45	4	59.2	3	80.94	2
QG+CD	66.98	3	49.27	3	–	–	–	–	–	–	–	–
SDMUC+CD	60.63	4	–	–	–	–	–	–	86.24	1	49.94	4
MMDHP+CD	43.56	8	–	–	67.47	2	45.87	3	72.29	2	57.05	3
HXMMT+CD	40.01	9	–	–	23.7	5	94.48	1	18.67	6	48.82	5
CXC	39.97	10	–	–	–	–	–	–	–	–	–	–
CDDP	69.27	2	70.34	2	91.83	1	–	–	58.3	4	–	–
QG	57.18	5	–	–	–	–	–	–	–	–	23.91	6
SDMUC	47.47	7	–	–	–	–	–	–	–	–	–	–
DHHYK	30.04	11	33.85	5	–	–	–	–	–	–	–	–
CD	2.27	12	6.25	6	0.51	6	0	5	0	7	3.11	7

CD, calcium dobesilate; CXC, Compound Xueshuantong Capsule; CDDP, Compound Danshen Dripping Pill; SDMUC, Shuangdan Mingmu Capsule; QG, Qiming Granule; HXMMT, Hexuemingmu Tablet; DHHYK, Danhong Huayu Koufuye; MMDHP, Mingmu Dihuang Pill, -: no value.

experimental and control groups. The other 14 studies reported 160 cases of adverse drug reactions, including 2 studies that did not identify specific ADRs. According to the results of the pairwise meta-analysis, there were no adverse reactions in the experimental and control groups, apart from QG, in which those of the OCPMs were lower than those of CD alone (Supplementary File S5).

3.6 Sensitivity analysis

For sensitivity analysis, we excluded RCTs with high risk of bias (2 studies) and RCTs with short treatment courses of 1-2 months (6 studies), respectively. The NMA results were re-evaluated. We found that both the effect size and direction did not change significantly, only the confidence

intervals have gotten a little bit wider. The ranking probabilities were also not changed substantially. These suggested that the NMA results are robust to a certain extent. The details are shown in Supplementary Files S8.

3.7 Publication bias

Figure 5 depicts the comparison-adjusted funnel plot for six outcomes to assess publication bias. It can be seen that the calibration auxiliary line was not completely perpendicular to the centerline, suggesting that the NMA may have potential publication bias.

4 Discussion

In recent decades, diabetes has progressed from a disease occurring mainly in populations of developed countries to a worldwide epidemic. DR, which is a major cause of visual impairment in a continuously increasing number of diabetic patients, is a common complication of diabetes (4). Once patients reach the PDR stage, they may progress to more serious diseases such as retinal neovascularization, vitreous hemorrhage, and retinal detachment, which can severely disrupt the visual function of patients even with interventions such as laser and vitrectomy (60). Therefore, early treatment and prevention at the stage of NPDR have become an urgent clinical problem to be solved. In China, clinicians often apply OCPMs for the treatment of NPDR with good clinical efficacy (11). DR belongs to the category of "thirsty eye disease" according to traditional Chinese medicine, and its pathogenesis is mainly attributed to the deficiency of both qi and yin and the stasis of ocular collateral (61). Based on this etiology and pathogenesis, the clinical treatment of DR can be based on Chinese herbal medicines that benefit Qi, nourish Yin, invigorate blood, and disperse blood stasis, and the OCMPs selected for this NMA all belong to this category.

4.1 Main findings

This NMA systematically evaluated the efficacy and safety of 7 commonly used OCPMs (CXC, CDDP, QG, SDMUC, MMDHP, HXMMT, and DHHYK) alone or combined with CD in patients with NPDR based on information from 42 studies involving 7 categories of outcomes. Our results showed that OCPMs alone or combined with CD were superior to CD alone in terms of an improved clinical efficacy rate, improved visual acuity and visual field gray value, reduced fundus hemorrhage and exudation, and better drug safety, which is consistent with the results of a published pairwise meta-analysis (11). More so, by comparing different types of proprietary Chinese medicines, the NMA also suggests that more attention should be given to CDDP, CXC, HXMMT, and SDMMC in the clinical treatment of NPDR.

The NMA results suggested that CDDP+CD and CDDP alone might be the best treatment options for increasing clinical efficacy rate and improving visual field gray value. CDDP is a herbal compound used for the treatment of cardiovascular diseases, made from *Salvia miltiorrhiza* Bunge [Lamiaceae], *Panax notoginseng* (Burkill) F.H.Chen [Araliaceae] and a small number of Borneolum Syntheticum, and contain active ingredients such as tanshinone, protocatechuic acid, ginsenoside, and Panax ginsenoside (62). Due to its vascular protective effects (63), CDDP is often used clinically in patients with DR. A Meta-analysis that included eight RCTs involving 524 patients found that CDDP combined with western drugs was effective in improving patients' visual function (64), which is consistent with our present NMA results. Meanwhile, basic studies have shown that CDDP can improve retinal vascular and neurological function by inhibiting inflammation, oxidative stress, and apoptosis, reducing vascular endothelial cell damage, and increasing retinal thickness (65, 66), which may explain the superiority of CDDP over other OCPMs in improving visual function.

We found that CXC+CD might be the best choice for improving visual acuity and reducing macular thickness. CXC is composed of four

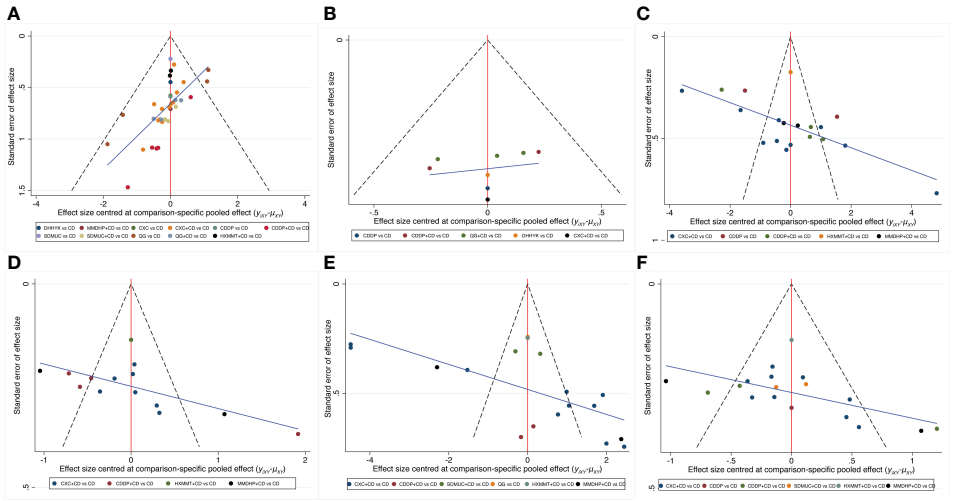

FIGURE 5
Comparison-adjusted funnel plot for six outcomes. **(A)** Clinical effective rate; **(B)** Visual acuity; **(C)** Visual field gray value; **(D)** Microaneurysm volume; **(E)** Hemorrhage area; **(F)** Macular thickness. CD, calcium dobesilate; CXC, Compound Xueshuantong Capsule; CDDP, Compound Danshen Dripping Pill; SDMUC, Shuangdan Mingmu Capsule; QG, Qiming Granule; HXMMT, Hexuemingmu Tablet; DHHYK, Danhong Huayu Koufuye; MMDHP, Mingmu Dihuang Pill.

herbal medicines, *Panax notoginseng* (Burkill) F.H.Chen [Araliaceae], *Astragalus mongholicus* Bunge [Fabaceae], *Salvia miltiorrhiza* Bunge [Lamiaceae], and *Scrophularia ningpoensis* Hemsl. [Scrophulariaceae], and its active ingredients are mainly quercetin, luteolin, kaempferol, and tanshinone Iia, which may be related to the tumor necrosis factor (TNF) signal pathway, hypoxia-inducible factor-1 signal pathway, and vascular endothelial growth factor (VEGF) signal pathway in DR (67). Modern pharmacological studies have shown that CXC can reduce retinal damage by reducing erythrocyte aggregation and lowering plasma viscosity, as well as inhibiting aldose reductase activity, controlling high expression of VEGF, and intercellular cell adhesion molecule-1 (68, 69). In addition, research has also revealed that CXC protects against high glucose-damaged retinal vascular endothelial cells, thereby reducing the blood-retinal intra-retinal barrier damage and decreasing retinal leakage (9). Compared with other OCPMs, CXC contains *Astragalus mongholicus* Bunge [Fabaceae], which could replenish Qi, lift Yang, promote water, and reduce swelling. These may explain why CXC is superior to other OCPMs in improving visual acuity and reducing macular thickness.

The NMA showed that HXMMT+CD had the best effect of reducing the microaneurysm volume. HXMMT is composed of 18 herbs. Modern pharmacological studies have shown that HXMMT can effectively inhibit platelet aggregation and adhesion and improve blood rheology (70, 71). In addition, several clinical studies have shown that HXMMT can effectively improve fundus hemorrhage and exudation, and stabilize lesion efficacy in patients with NPDR (72, 73). *In vitro* experiments, HXMMT can effectively reduce retinal damage through antioxidant, anti-inflammatory, and anti-angiogenic properties (74). While there are fewer *in vivo* studies on HXMMT in DR, they only study applied HXMMT to rats with branch retinal vein obstruction and found that it could improve retinal edema and enhance retinal function by improving retinal microcirculation and regulating VEGF-α expression (75). Compared with other OCPMs, HXMMT contains Typha angustifolia L and salvia, which are commonly used clinically to stop bleeding and resolve blood stasis. Meanwhile, HXMMT has more therapeutic targets shared by different active ingredients and more signaling pathways, such as neuroactive ligand-receptor interaction and chemokine signaling pathway (71), which may be the reason why HXMMT has the best efficacy in reducing the microaneurysm volume.

SDMMC+CD may be the best intervention in reducing retinal hemorrhage area, which is consistent with the previously existing pairwise Meta-analysis results (76). Published studies have confirmed that SDMMC can improve glucose dyslipidemia and blood rheology, reduce oxidative stress, and can effectively improve fundus signs, protect the retinal structure, and reduce retinal hemorrhage in patients with DR (77, 78). Experimental studies have shown that SDMMC can improve the blood rheological status of DR rats, dilate retinal arteries, and improve retinal blood supply (79). Compared with other OCPMs, SDMMC contains more blood-cooling herbs such as *Ligustrum lucidum* W.T.Aiton [Oleaceae], *Eclipta prostrata* (L.) L. [Asteraceae], has been proven to reduce the inflammatory response and inhibit neovascularization by decreasing the expression of VEGFA and TNF-α (80). It may explain the better effect of SDMMC in reducing the retinal hemorrhage area than other OCPMs.

ADRs also deserve our attention apart from efficacy. However, the NMA showed that the OCPMs selected in this study did not cause serious adverse reactions. To use OCPMs in a manner that will limit ADRs, we suggest that clinicians applying OCPMs should give different types of OCPMs according to the actual situation of the patients and patients should avoid taking OCPMs on an empty stomach.

4.2 Strengths and limitations

To our knowledge, this is the first comprehensive evaluation of different types of OCPMs alone or in combination with CD for NPDR using a reticulated meta-analysis, and the recommended ranking order based on efficacy and safety provides a usable basis for clinicians. Our study has the following strengths: (1) The screening criteria were strict, with the study population limited to patients with NPDR and CD as a fixed control, which ensured the uniformity of disease and interventions, thus reducing heterogeneity to some extent; (2) The OCPMs selected are those recommended in the NHSA and NMPA catalogs to ensure consistency with the actual clinic. (3) This NMA not only focuses on efficacy indicators such as the clinical efficiency rate, visual acuity, visual field gray value, microaneurysm volume, hemorrhage area, and macular thickness, but also the incidence of ADRs; (4) This NMA projects the optimal treatment for each outcome indicator according to SUCRA, which can be used as a reference for the clinic.

Although the current NMA may fill the gap in the efficacy of different types of OCPMs for NPDR, there are still some limitations: (1) The overall risk of the vast majority of studies was rated as “some concern”. And the criteria for clinical efficacy of included studies were not completely consistent, though all studies were based on the improvement of visual acuity and fund signs, so the NMA results should be interpreted cautiously; (2) The number of studies included in some interventions was limited, with only two, one, and two RCTs that included HXMMT, DHHYK, and MMDHP, respectively; (3) The studies included in the current NMA are all from China, so the NMA results may not apply to other countries; (4) Some of the OCPMs contain the same monomers which may exert similar therapeutic effects and may not fully explain the conclusions reached in our study. The current data extracted from clinical trials are incapable of exploring interactive effects of integrative therapies and combination of multiple herbal substances, further studies focusing on pharmacological features of OCPMs are needed.

4.3 Implications for future RCTs of OCPMs

A large number of RCTs on OCPMs have been published, but issues regarding poor reporting and the high potential of bias have attracted widespread attention (81). We believe that the reasons for the poor quality of RCTs on OCPMs may include the following: (1) In terms of policy, the regulatory system for OCPMs is not robust enough. Reports of phase I, II, and III trials for OCPMs are hardly available in public; (2) Most RCTs for OCPMs do not have pre-specified study protocols and prospective registration, and thus lack detailed information on sample size calculation, randomization procedure, blinding, etc. (3) Most of the trials did not follow RCT reporting guidelines such as SPIRIT and

CONSORT (82, 83); (4) Although these OPCMs are currently in regular clinical use in China, most of the published RCTs are single-center studies with an early publication year and lack data updates (84).

In order to enhance the reporting and conducting of RCTs for OCPMs, the following four efforts are needed: (1) The regulatory system for Chinese patent medicines should be strengthened, and publication of trial results conducted by pharmaceutical companies and relevant affiliations should be encouraged by the authority to improve transparency; (2) Investigators should develop detailed study protocols in advance and register their trial in the clinical trial registration platform (https://www.chictr.org.cn/index.aspx); (3) Protocol of RCTs should be reported according to SPIRIT and final report should be reported according to the CONSORT statement. (4) Multicenter and large-sample RCTs for OCPMs are recommended. Moreover, future research should pay more attention on key methodological issues and the quality of conducting.

5 Conclusions

This NMA evaluated the efficacy and safety of OCMPs alone or combined with CD for the treatment of patients with NPDR. The results showed that OCMPs combined with CD or alone were efficient in improving visual function and fundus signs in NPDR patients. In terms of improving the clinical efficacy rate and visual field gray value, CDDP combined with CD and CDDP alone may be the best intervention. Regarding improving visual acuity and reducing macular thickness, CXC combined with CD may be the most effective treatment option. In terms of reducing microaneurysm volume and hemorrhage area, HXMMT and SDMMC combined with CD may be the most effective. The OCPMs could increase clinical efficacy, and neither had a significantly increased risk of ADRs. However, regarding the limitations in methodology and potential risk of bias, more RCTs with high quality are needed to confirm the evidence of the NMA results. OCPMs should be used with more caution in clinical practice. Besides, RCTs of OCPMs should pay more attention on key methodological issues and the quality of conducting in the future.

Data availability statement

The original contributions presented in the study are included in the article/Supplementary Material. Further inquiries can be directed to the corresponding author.

Author contributions

ZL and YC: conceptualization, methodology, formal analysis, and writing the original draft. YD and XH: methodology and supervision. YL and WC: visualization and review editing. JW: language editing and supervision. CJ: conceptualization, funding, and project administration. All authors contributed to the article and approved the submitted version.

Funding

This work was supported by grants from the National Natural Science Foundation of China (general program No. 81874494), the Natural Science Foundation of Beijing Municipality (No. 7182187), the Science and Technology Innovation Project of China Academy of Chinese Medical Sciences (No. CI2021A02604), and the Capital Foundation of Medical Development (No. 2020-2-4182 and 2020-3-4184).

Conflict of interest

The authors declare that the research was conducted in the absence of any commercial or financial relationships that could be construed as a potential conflict of interest.

Publisher's note

Supplementary material

The Supplementary Material for this article can be found online at: https://www.frontiersin.org/articles/10.3389/fendo.2023.1144290/full#supplementary-material

References

1. Sun H, Saeedi P, Karuranga S, Pinkepank M, Ogurtsova K, Duncan BB, et al. IDF diabetes atlas: Global, regional and country-level diabetes prevalence estimates for 2021 and projections for 2045. *Diabetes Res Clin Pract* (2022) 183:109119. doi: 10.1016/j.diabres.2021.109119

2. Li Y, Teng D, Shi X, Qin G, Qin Y, Quan H, et al. Prevalence of diabetes recorded in mainland China using 2018 diagnostic criteria from the American diabetes association: national cross sectional study. *BMJ (Clinical Res ed.)* (2020) 369:m997. doi: 10.1136/bmj.m997

3. Wilkinson CP, Ferris FL, Klein RE, Lee PP, Agardh CD, Davis M, et al. Proposed international clinical diabetic retinopathy and diabetic macular edema disease severity scales. *Ophthalmology* (2003) 110(9):1677–82. doi: 10.1016/S0161-6420(03)00475-5

4. Cheung N, Mitchell P, Wong TY. Diabetic retinopathy. *Lancet (London England)* (2010) 376(9735):124–36. doi: 10.1016/S0140-6736(09)62124-3

5. Zhang X, Liu W, Wu S, Jin J, Li W, Wang N. Calcium dobesilate for diabetic retinopathy: A systematic review and meta-analysis. *Sci China Life Sci* (2015) 58 (1):101–7. doi: 10.1007/s11427-014-4792-1

6. Liu J, Li S, Sun D. Calcium dobesilate and micro-vascular diseases. *Life Sci* (2019) 221:348–53. doi: 10.1016/j.lfs.2019.02.023

7. Stamper RL, Smith ME, Aronson SB, Cavender JC, Cleasby GW, Fung WE, et al. The effect of calcium dobesilate on nonproliferative diabetic retinopathy: a controlled study. *Ophthalmology* (1978) 85(6):594–606. doi: 10.1016/s0161-6420(78)35643-8

8. Jia Y, Sun J, Zhao Y, Tang K, Zhu R, Zhao W, et al. Chinese Patent medicine for osteoporosis: A systematic review and meta-analysis. *Bioengineered* (2022) 13(3):5581–97. doi: 10.1080/21655979.2022.2038941

9. Xing W, Song Y, Li H, Wang Z, Wu Y, Li C, et al. Fufang xueshuantong protects retinal vascular endothelial cells from high glucose by targeting YAP. *Biomed. Pharmacother. = Biomed. Pharmacotherapie* (2019) 120:109470. doi: 10.1016/j.biopha.2019.109470

10. Nie F, Yan J, Ling Y, Liu Z, Fu C, Li X, et al. Effect of shuangdan mingmu capsule, a Chinese herbal formula, on oxidative stress-induced apoptosis of pericytes through PARP/GAPDH pathway. *BMC Complementary Med Therapies* (2021) 21 (1):118. doi: 10.1186/s12906-021-03238-w

11. Zhang Y, An X, Duan L, Jin D, Duan Y, Zhou R, et al. Effect of Chinese patent medicines on ocular fundus signs and vision in calcium dobesilate-treated persons with non-proliferative diabetic retinopathy: A systematic review and meta-analysis. *Front Endocrinol* (2022) 13:799337. doi: 10.3389/fendo.2022.799337

12. Hutton B, Salanti G, Caldwell DM, Chaimani A, Schmid CH, Cameron C, et al. The PRISMA extension statement for reporting of systematic reviews incorporating network meta-analyses of health care interventions: checklist and explanations. *Ann Internal Med* (2015) 162(11):777–84. doi: 10.7326/M14-2385

13. Fundus Disease Group, O.S.o.C.M.A. Guidelines for clinical diagnosis and treatment of diabetic retinopathy, (2014). *Chin J Ophthalmol* (2014) 50(11):851–65. doi: 10.3760/cma.j.issn.0412-4081.2014.11.014

14. Cumpston M, Li T, Page MJ, Chandler J, Welch VA, Higgins JP, et al. Updated guidance for trusted systematic reviews: A new edition of the cochrane handbook for systematic reviews of interventions. *Cochrane Database Systematic Rev* (2019) 10: ED000142. doi: 10.1002/14651858.ED000142

15. Béliveau AA-O, Boyne DJ, Slater J, Brenner D, Arora P. BUGSnet: an r package to facilitate the conduct and reporting of Bayesian network meta-analyses. *BMC Med Res Methodol* (2019) 19:196. doi: 10.1186/s12874-019-0829-2

16. Salanti G. Indirect and mixed-treatment comparison, network, or multiple-treatments meta-analysis: Many names, many benefits, many concerns for the next generation evidence synthesis tool. *Res synthesis Methods* (2012) 3(2):80–97. doi: 10.1002/jrsm.1037

17. Dias S, Sutton AJ, Ades AE, Welton NJ. Evidence synthesis for decision making 2: a generalized linear modeling framework for pairwise and network meta-analysis of randomized controlled trials. *Med Decis Making* (2013) 33(5):607–17. doi: 10.1177/0272989X12458724

18. Du JH, Zhang Z, Li JQ, Zhu XR, Chai XH, Gong L, et al. Effect of compound xueshuantong on blood lipid and fundus microaneurysm in diabetic retinopathy. *Modern J Integrated Traditional Chin Western Med* (2018) 27(06):663–5. doi: CNKI:SUN:XDJH.0.2018-06-030

19. Huang W, Tang XD, Liu J. Analysis of the therapeutic effect of calcium dobesilate combined with compound xueshuantong capsules on diabetic retinopathy. *Contemp Med* (2021) 27(31):162–4. doi: 10.3969/j.issn.1009-4393.2021.31.066

20. An LN. Clinical study of compound xueshuantong combined with calcium dobesilate in the treatment of diabetic retinopathy. *Pract Clin J Integrated Traditional Chin Western Med* (2020) 20(14):69–71. doi: 10.13638/j.issn.1671-4040.2020.14.034

21. Wang J, Du W, Li Y. Effect of calcium oxybenzenesulfate combined with compound xueshuantong capsule on senile diabetic retinopathy and hemorheology. *Chin J Gerontol.* (2020) 40(08):1603–6. doi: 10.3969/j.issn.1005-9202.2020.08.010

22. Yan H, Song JH. Effect of compound xueshuantong capsule in the adjuvant treatment of non proliferative diabetic retinopathy and its influence on the hemodynamics of patients with OA. *Strait Pharm J* (2020) 32(05):141–2. doi: 10.3969/j.issn.1006-3765.2020.05.060

23. Chai F, Wang Y, Huang Q. Effects of compound xueshuantong capsule combined with calcium dobesilate on IGF-1, VEGF and hemodynamic indexes in early diabetic retinopathy. *J Pract Traditional Chin Med* (2018) 34(11):1360–2. doi: 10.3969/j.issn.1004-2814.2018.11.068

24. Wang Q. Clinical efficacy of compound xueshuantong capsule combined with calcium oxybenesulfate in the treatment of early diabetic retinopathy and its influence on hs-CRP and IGF-1 levels. *Pract Clin J Integrated Traditional Chin Western Med* (2018) 18(06):16–17+53. doi: 10.13638/j.issn.1671-4040.2018.06.008

25. Ma JP. Curative effect evaluation of compound xueshuantong capsule combined with calcium dobesilate for patients with early diabetic retinopathy. *Int Eye Sci* (2018) 18(02):305–8. doi: 10.3980/j.issn.1672-5123.2018.2.25

26. Yu W, Lin BS, Ma SF, Zhang WW, Wu QL. Effect of calcium oxybenesulfate combined with compound xueshuantong capsule on early diabetic retinopathy and serum IGF-1 and VEGF levels. *Chin J Gerontol.* (2017) 37(21):5311–3. doi: 10.3969/j.issn.1005-9202.2017.21.041

27. Rao XJ, Wu YM, Wei LJ, Ma Y. Comparison of efficacy between traditional Chinese medicine combined with western medicine and simple western medicine for patients with NPDR. *Int Eye Sci* (2017) 17(01):148–50. doi: 10.3980/j.issn.1672-5123.2017.1.41

28. Men LB. Effects of relapse-xueshuantong combined with calcium oxybenesulfate on visual acuity and levels of inflammatory factors in patients with diabetic retinopathy. *Clin Med* (2020) 40(01):124–5. doi: 10.19528/j.issn.1003-3548.2020.01.051

29. Li Y. Effects of compound xueshuantong combined with calcium oxybenesulfate on vascular growth factor levels and visual acuity in patients with diabetic retinopathy. *Diabetes New World* (2019) 22(07):180–1. doi: 10.16658/j.cnki.1672-4062.2019.07.180

30. Pei D, Gao H. Clinical effects and hs-CRP,VEGF and IGF-1 levels of xueshuantong capsule combined with calcium dobesilate in treatment of early diabetic retinopathy. *Modern J Integrated Traditional Chin Western Med* (2015) 24 (35):3896–3898,3907. doi: 10.3969/j.issn.1008-8849.2015.35.007

31. Zhou YD, Zheng MR, Wang FF. Clinical studv of calcium dobesilate combined with compound xueshuantong in the treatment of diabetic retinopathy. *Sichuan J Anat* (2022) 30(1):62–4. doi: 10.3969/j.issn.1005-1457.2022.01.021

32. Luo D, Qin Y, Yuan W, Deng H, Zhang Y, Jin M. Compound danshen dripping pill for treating early diabetic retinopathy: A randomized, double-dummy, double-blind study. *Evidence-Based Complementary Altern Med* (2015) 2015:1-7. doi: 10.1155/2015/539185

33. Jin M, Deng H, Yuan W, Yang G. Clinical observation of compound salvia miltiorrhiza dripping pills in the treatment of early diabetic retinopathy. *Chin Community Doctors* (2009) 25(16):32–3. doi: CNKI:SUN:XCYS.0.2009-16-033

34. Chen Y, Zhong JY. Clinical study of compound salvia miltiorrhiza dripping pills in the treatment of simple diabetic retinopathy. *Chin Community Doctors* (2006) 23):75. doi: 10.3969/j.issn.1672-5085.2011.35.124

35. Xu HT. Effect of compound salvia miltiorrhiza dripping pills combined with calcium oxybenzenesulfate in the treatment of diabetic retinopathy. *Chin J Convalescent Med* (2019) 28(08):884–6. doi: 10.13517/j.cnki.ccm.2019.08.041

36. Li Y. Clinical efficacy evaluation of the combination regimen of calcium oxybenesulfate capsules and compound danshen dripping pills in the treatment of diabetic retinopathy. *J Aerospace Med* (2017) 28(10):1229–31. doi: 10.3969/j.issn.2095-1434.2017.10.037

37. Wang HM, Tian DZ, Han XY. Effect of compound salvia miltiorrhiza dripping pills on non-proliferative diabetic retinopathy. *Chin J Clin Rational Drug Use* (2016) 9 (23):49–50. doi: 10.15887/j.cnki.13-1389/r.2016.23.035

38. Bai YX. Effect of calcium dobesilate combined with compound danshen dripping pills on diabetic retinopathy and serum inflammatory factors. *J Qiqihar Med Univ* (2017) 38(22):2641–3. doi: 10.3969/j.issn.1002-1256.2017.22.014

39. Ruan YX, Chen M, Liu ZQ, Wang ZL, Sun N, Huang X, et al. Clinical study on the treatment of diabetic retinopathy by oral compoundDanshen dripping pill combined with calcium dobesilate. *Med Sci J Cent South China* (2017) 45(01):18–20 +23. doi: 10.15972/j.cnki.43-1509/r.2017.01.004

40. Huang YX, Sun HP, Tang YQ, Chen X. Effects of compound danshen dripping pills on inflammatory mediators, cytokines and visual function in patients with diabetic retinopathy. *Chin J Integr Med Cardio-Cerebrovascular Dis* (2021) 19(08):1364–1366 +1408. doi: 10.12102/j.issn.1672-1349.2021.08.030

41. Qin YH, Li F, Tu LY, Qiu B, Zhang ML, Cao JH, et al. Multicentric clinical study of shuangdan mingmu capsule on diabetic retinopathy. *J Hunan Univ Chin Med* (2010) 1):46–51. doi: 10.3969/j.issn.1674-070X.2010.01.015

42. Ji XD, Liu WT. Safety and efficacy of shuangdan mingmu capsule combined with calcium dobesilate dispersible tablets in the treatment of diabetic retinopathy. *Clin Res Pract* (2022) 7(11):85–7. doi: 10.19347/j.cnki.2096-1413.202211024

43. Liu JP, Kong YH, Wang L. Clinical efficacy of shuangdan mingmu capsules combined with calcium dobesilate in the treatment of diabetic retinopathy and its effects on serum levels of vascular endothelial growth factor, platelet-derived growth factor and interleukin-1. *Eval Anal Drug-Use Hospitals* (2019) 19(11):1332–1334+1338. doi: 10.14009/j.issn.1672-2124.2019.11.015

44. Jin L, Zhang LJ. Clinical study on shuangdan mingmu capsules combined with calcium dobesilate in treatment of diabetic retinopathy. *Drugs Clinic* (2019) 34 (01):159–63. doi: 10.7501/j.issn.1674-5515.2019.01.035

45. Pang YH. Clinical observation of shuangdanmingmu capsule in treating diabetic retinopathy. *Diabetes New World* (2015) 35(3):39–9. doi: 10.16658/j.cnki.1672-4062.2015.03.013

46. Zhang DX. Randomized controlled study of qiming granule and dishengming capsule in the treatment of diabetic retinopathy. *Pharmacol Clinics Chin Materia Med* (2015) 31(3):151–2. doi: 10.13412/j.cnki.zyyl.2015.03.050

47. Fang J, Lv H, Zhang XD, Liu F, Yang LN. Clinical study on qiming granules for non-proliferative diabetic retinopathy. *New Chin Med* (2022) 54(08):97–9. doi: 10.13457/j.cnki.jncm.2022.08.022

48. Duan JG, Liao PZ, Wu L, Li SM, Yu YG, Qiu B, et al. Randomized controlled double-blind multicentric clinical trail on non-proliferative DiabeticRetinopathy treated by qi-ming granule. *J Chengdu Univ Traditional Chin Med* (2006) 29(2):1–5. doi: CNKI:SUN:CDZY.0.2006-02-000

49. Fan YP, Li YL, Chen GL, Wang HH, Lin YJ. Effect and safety evaluation of qiming granule on the treatment of nonproliferative diabetic retinonathy. *Int Eye Sci* (2018) 18(12):2260–3. doi: 10.3980/j.issn.1672-5123.2018.12.34

50. Feng JL, Zhou P, Wu QL, Chen YN, Tian J. Effect of qiming granule combined with calcium dobesilate on diabetic retinopathy in the third stage. *Hebei Med J* (2016) 38(22):3430–3. doi: 10.3969/j.issn.1002-7386.2016.22.018

51. Wang ZQ, Lei Y, Zhang R. Improvement of qiming granule combined with calcium dobesilate on fundus microcirculation in the treatment of patients with non-proliferative diabetic retinopathy. *Clin Res Pract* (2019) 4(31):117–8. doi: 10.19347/j.cnki.2096-1413.201931049

52. Wang ZZ. Qi Ming granule combined with calcium dobesilate in treatment of nonproliferative diabetic retinopathy. *Int Eye Sci* (2017) 17(04):702–5. doi: 10.3980/j.issn.1672-5123.2017.4.28

53. Sui HL, Yu CY, Xue HM, Wang RN. The clinical curative observation on qiming granule combined with calcium dobesilate capsules in treatment of patients with nonproliferative diabetic retinopathy. *Med Innovation China* (2014) 11(20):99–102. doi: 10.3969/j.issn.1674-4985.2014.20.036

54. Yan JH. Effect of qiming granule combined with calcium dobesilate in the treatment of non-proliferative diabetic retinopathy. *Henan Med Res* (2020) 29 (34):6477–9. doi: 10.3969/j.issn.1004-437X.2020.34.055

55. Ye XL, Guo XN, Xiong F. Clinical observation of oral calcium dobesilate combined with HeXueMingMu tablet in the treatment of nonproliferative diabetic retinopathy. *J North Sichuan Med Coll* (2019) 34(2):223–5. doi: 10.3969/j.issn.1005-3697.2019.02.16

56. Gao L, Qi T, Xu WB, Wan L. Hexuemingmu tablets combined with calcium dobesilate on early DiabeticRetinopathy. *China Pharm* (2020) 29(10):133–5. doi: 10.3969/j.issn.1006-4931.2020.10.040

57. Zhu HM, Jiang Y, Li L, Yu S. Efficacy of danhong huayu in treatment of diabetic retinopathy. *Chin J Exp Traditional Med Formulae* (2013) 19(17):320–3. doi: 10.11653/syfj2013170320

58. Li JB, Wei XY. Clinical study on mingmu dihuang pills combined with calcium dobesilate in treatment of early diabetic retinopathy. *Drugs Clinic* (2019) 34(04):1197–201. doi: CNKI:SUN:GWZW.0.2019-04-069

59. Ayinu-Nulahou, Wang YH, Bu Q, Zhao Y. Clinical efficacy of calcium dobesilate dispersible tablets combined withMingmu dihuang pills in treatment of NPDR. *Int Eye Sci* (2019) 19(6):992–6. doi: 10.3980/j.issn.1672-5123.2019.6.23

60. Kollias AN, Ulbig MW. Diabetic retinopathy: Early diagnosis and effective treatment. *Deutsches Arzteblatt Int* (2010) 107(5):75–83; quiz 84. doi: 10.3238/arztebl.2010.0075

61. Jie CH. Constructing the thinking of syndrome differentiation and treatment of diabetic retinopathy under the mode of combination of disease-syndrome symptom. *China J Chin Ophthalmol* (2022) 32(11):841–5. doi: 10.13444/j.cnki.zgzyykzz.2022.11.001

62. Liao W, Ma X, Li J, Li X, Guo Z, Zhou S, et al. A review of the mechanism of action of dantonic® for the treatment of chronic stable angina. *Biomed. Pharmacother. = Biomed. Pharmacotherapie* (2019) 109:690–700. doi: 10.1016/j.biopha.2018.10.013

63. Hu Y, Sun J, Wang T, Wang H, Zhao C, Wang W, et al. Compound danshen dripping pill inhibits high altitude-induced hypoxic damage by suppressing oxidative stress and inflammatory responses. *Pharm Biol* (2021) 59(1):1585–93. doi: 10.1080/13880209.2021.1998139

64. Huang H, Li Y, Huang Q, Lei R, Zou W, Zheng Y. Efficacy of compound danshen dripping pills combined with western medicine in the treatment of diabetic retinopathy: a systematic review and meta-analysis of randomized controlled trials. *Ann Palliative Med* (2021) 10(10):10954–62. doi: 10.21037/apm-21-2563

65. Zhang Q, Xiao X, Zheng J, Li M, Yu M, Ping F, et al. Compound danshen dripping pill inhibits retina cell apoptosis in diabetic rats. *Front Physiol* (2018) 9:1501. doi: 10.3389/fphys.2018.01501

66. Liu L, Li X, Cai W, Guo K, Shi X, Tan L, et al. Coadministration of compound danshen dripping pills and bezafibrate has a protective effect against diabetic retinopathy. *Front Pharmacol* (2022) 13:1014991. doi: 10.3389/fphar.2022.1014991

67. Li H, Li B, Zheng Y. Exploring the mechanism of action compound-xueshuantong capsule in diabetic retinopathy treatment based on network pharmacology. *Evidence-Based Complementary Altern Medicine: eCAM* (2020) 2020:8467046. doi: 10.1155/2020/8467046

68. Jian W, Yu S, Tang M, Duan H, Huang J. A combination of the main constituents of fufang xueshuantong capsules shows protective effects against streptozotocin-induced retinal lesions in rats. *J Ethnopharmacol* (2016) 182:50–6. doi: 10.1016/j.jep.2015.11.021

69. Hao GM, Lv TT, Wu Y, Wang HL, Xing W, Wang Y, et al. The hippo signaling pathway: A potential therapeutic target is reversed by a Chinese patent drug in rats with diabetic retinopathy. *BMC Complementary Altern Med* (2017) 17(1):187. doi: 10.1186/s12906-017-1678-3

70. Fei YX, Wang SQ, Yang LJ, Qiu YY, Li YZ, Liu WY, et al. Salvia miltiorrhiza bunge (Danshen) extract attenuates permanent cerebral ischemia through inhibiting platelet activation in rats. *J Ethnopharmacol.* (2017) 207:57–66. doi: 10.1016/j.jep.2017.06.023

71. Yao H, Xin D, Zhan Z, Li Z. Network pharmacology-based approach to comparatively predict the active ingredients and molecular targets of compound xueshuantong capsule and hexuemingmu tablet in the treatment of proliferative diabetic retinopathy. *Evidence-Based Complementary Altern Medicine: eCAM* (2021) 2021:6642600. doi: 10.1155/2021/6642600

72. Hua YF. Effect of retinal photocoagulation combined with hexue mingmu tablet on diabetic retinopathy of stage II and IV. *J Chin Pract Diagnosis Ther* (2012) 26 (01):29–30. doi: CNKI:41-1400/R.20120110.1036.012

73. Chen XL, Tao LM. Clinical observation of calcium dobesilate and hexuemingmu tablets in treatment of nonproliferative diabetic retinopathy. *Int Eye Sci* (2013) 13 (01):101–3. doi: 10.3980/j.issn.1672-5123.2013.01.27

74. Xi YJ. Exploration ofthe major pharmacological effect and clinical positioning of hexuemingmu tablets against retinal degenerative diseases based on the integration strategy. [master's thesis]. Tianjin (IL): Tianjin University of Chinese Medicine (2022).

75. Long P, Yan W, Liu J, Li M, Chen T, Zhang Z, et al. Therapeutic effect of traditional Chinese medicine on a rat model of branch retinal vein occlusion. *J Ophthalmol* (2019) 2019:9521379. doi: 10.1155/2019/9521379

76. Liu WN, Su Y, Xia YT, Yan XL, Li L, Xiao YP, et al. Efficacy and safety evaluation of shuangdan mingmu capsule in the treatment of type 2 diabetic retinopathy. *China J Chin Ophthalmol* (2022) 32(05):348–53. doi: 10.13444/j.cnki.zgzyykzz.2022.05.003

77. Peng J, Pan K, Liu ZR, Qin YH, Peng QH. Effects of shuangdan mingmu capsule on the expressions of VEGF in the retina of diabetic rat models. *Int Eye Sci* (2018) 18 (11):1958–62. doi: 10.3980/j.issn.1672-5123.2018.11.03

78. Zhao HQ, Fu CJ, Meng P, Wang YH, Qin YH, Zhang XL. Study on screening of effective components in shuangdan mingmu capsules inInhibiting proliferation of human umbilical vein endothelial cells. *Chin J Inf Traditional Chin Med* (2019) 26 (07):48–51. doi: 10.3969/j.issn.1005-5304.2019.07.012

79. Zhao YW, Fu CJ, Yan JC, Nie FJ, Chen JY, Zheng XB, et al. Effects of shuangdan mingmu capsules on blood rheology and retinal microvasculature in rats with diabetic retinopathy. *Recent Adv Ophthalmol* (2022) 42(05):342–6. doi: 10.13389/j.cnki.rao.2022.0069

80. Wang J, Han X, Li L, Han S, Zhao Y, Cui ZL, et al. Treating different disease with same method in traditional Chinese medicine:mechanisms of eclipta albaglossy privet fruit medicinal pair in treating diabetic nephropathy and diabetic retinopathy based on network pharmacology. *J Tianjin Univ Traditional Chin Med* (2021) 40(03):374–83. doi: 10.11656/j.issn.1673-9043.2021.03.21

81. Lin S, Shi Q, Ge Z, Liu Y, Cao Y, Yang Y, et al. Efficacy and safety of traditional Chinese medicine injections for heart failure with reduced ejection fraction: A Bayesian network meta-analysis of randomized controlled trials. *Front Pharmacol* (2021) 12:659707. doi: 10.3389/fphar.2021.659707

82. Moher D, Hopewell S, Schulz KF, Montori V, Gøtzsche PC, Devereaux PJ, et al. CONSORT 2010 explanation and elaboration: updated guidelines for reporting parallel group randomised trials. *Int J Surg* (2010) 10(1):28–55. doi: 10.1016/j.ijsu.2011.10.001

83. Chan AW, Tetzlaff JM, Altman DG, Laupacis A, Gøtzsche PC, Krleža-Jerić K, et al. SPIRIT 2013 statement: defining standard protocol items for clinical trials. *Ann Internal Med* (2013) 158(3):200–7. doi: 10.7326/0003-4819-158-3-201302050-00583

84. Cheng CW, Wu TX, Shang HC, Li YP, Altman DG, Moher D, et al. CONSORT extension for Chinese herbal medicine formulas 2017: Recommendations, explanation, and elaboration. *Ann Internal Med* (2017) 167(2):112–21. doi: 10.7326/M16-2977

frontiers | Frontiers in Endocrinology

TYPE Review
PUBLISHED 17 April 2023
DOI 10.3389/fendo.2023.1116136

OPEN ACCESS

EDITED BY
Rajashekhar Gangaraju,
University of Tennessee Health Science Center (UTHSC), United States

REVIEWED BY
Vicente Bermúdez,
Instituto de Investigaciones Bioquímicas de Bahía Blanca (INIBIBB), Argentina
Gao Guoquan,
Zhongshan School of Medicine,
Sun Yat-sen University, China

*CORRESPONDENCE
Xiaorong Li
lixiaorong@tmu.edu.cn

†These authors have contributed equally to this work

SPECIALTY SECTION
This article was submitted to Cellular Endocrinology, a section of the journal Frontiers in Endocrinology

RECEIVED 07 December 2022
ACCEPTED 04 April 2023
PUBLISHED 17 April 2023

CITATION
Xu M, Chen X, Yu Z and Li X (2023) Receptors that bind to PEDF and their therapeutic roles in retinal diseases. *Front. Endocrinol.* 14:1116136. doi: 10.3389/fendo.2023.1116136

Receptors that bind to PEDF and their therapeutic roles in retinal diseases

Manhong Xu†, Xin Chen†, Zihao Yu† and Xiaorong Li*

Tianjin Key Laboratory of Retinal Functions and Diseases, Tianjin Branch of National Clinical Research Center for Ocular Disease, Eye Institute and School of Optometry, Tianjin Medical University Eye Hospital, Tianjin, China

Retinal neovascular, neurodegenerative, and inflammatory diseases represented by diabetic retinopathy are the main types of blinding eye disorders that continually cause the increased burden worldwide. Pigment epithelium-derived factor (PEDF) is an endogenous factor with multiple effects including neurotrophic activity, anti-angiogenesis, anti-tumorigenesis, and anti-inflammatory activity. PEDF activity depends on the interaction with the proteins on the cell surface. At present, seven independent receptors, including adipose triglyceride lipase, laminin receptor, lipoprotein receptor-related protein, plexin domain-containing 1, plexin domain-containing 2, F1-ATP synthase, and vascular endothelial growth factor receptor 2, have been demonstrated and confirmed to be high affinity receptors for PEDF. Understanding the interactions between PEDF and PEDF receptors, their roles in normal cellular metabolism and the response the initiate in disease will be accommodating for elucidating the ways in which inflammation, angiogenesis, and neurodegeneration exacerbate disease pathology. In this review, we firstly introduce PEDF receptors comprehensively, focusing particularly on their expression pattern, ligands, related diseases, and signal transduction pathways, respectively. We also discuss the interactive ways of PEDF and receptors to expand the prospective understanding of PEDF receptors in the diagnosis and treatment of retinal diseases.

KEYWORDS

pigment epithelium-derived factor (PEDF), receptor, adipose triglyceride lipase (ATGL), laminin receptor (LR), lipoprotein receptor-related protein 6 (LRP6), plexin domain-containing (PLXDC), F1-ATP synthase, vascular endothelial growth factor receptor 2 (VEGFR2)

1 Introduction

Pigment epithelium-derived factor (PEDF), also known as serpin family F member 1 (SERPINF1), is a 50 kDa protein encoded by the SERPINE1 gene (1). The human gene encoding PEDF is located on chromosome 17p13.3 and comprises 9 exons encoding a 418 amino acid protein (NCBI Reference Sequence: NG_028180.1). PEDF belongs to the serine

protease inhibitor superfamily (SERPINS), the members of which share a common structural element, a reactive center loop (RCL) (2). Most SERPINS members are serine protease inhibitors, including plasmin inhibitors, antichymotrypsin, and antitrypsin (3). However, PEDF is considered to be a noninhibitory serpin as it is activated after chymotrypsin RCL cleavage and lacks protease activity (4).

In 1991, Joyce Tombran-Tink et al. first discovered that medium from retinal pigment epithelial (RPE) cells induced Y79 retinoblastoma tumor cell differentiation and increased tumor cell neurite outgrowth. Considering these findings, they identified the protein with the neurotrophic function induced by RPE cell-conditioned medium and termed it PEDF (1, 5). In addition to exerting as a neurotrophic factor, PEDF was recognized for its other functions. One decade after its discovery, PEDF was shown to protect motor neurons from chronic glutamate-mediated neurodegeneration (6) and protect photoreceptors from light damage (7, 8). In addition, PEDF is considered to be a potent angiogenesis inhibitor, which contributes to its important role in both antiangiogenesis and antitumorigenesis (9, 10). This discovery initiated a new era of PEDF function and mechanism exploration in angiogenic and degenerative diseases, especially in diabetes and diabetic complications.

An increasing number of studies have shown that the PEDF mechanism of action and related molecular pathways are involved in mediating or inducing signal transduction. PEDF activity depends on the high affinity of PEDF for interacting proteins, namely PEDF receptors on the cell surface (11). Understanding the interactions between PEDF and PEDF receptors, their roles in normal cellular metabolism and the response the initiate in disease may help elucidate the ways in which inflammation, angiogenesis, and neurodegeneration exacerbate disease pathology. In this review, we introduce these PEDF receptors to readers in a comprehensive way and suggest the potential underlying mechanisms for diseases characterized by multipathological changes, including angiogenesis, neurodegeneration, and inflammation. This increase in understanding may lead to new approaches to combat these diseases.

2 PEDF distribution and expression

The mRNA encoding PEDF (SERPINF1 mRNA) has been identified in several kinds of normal human tissues and organs, including blood cells, plasma, lymph nodes, brain, spinal cord, heart, arteries, muscle, lung, eye, bone, colon, kidney, liver, spleen, breast, thyroid, prostate, and pancreas (12). SERPINF1 mRNA is also expressed in embryonic ocular tissues. PEDF has been found in developing cones, RPE granules, neuroblasts and the ganglion cell layer (GCL) of developing human retinas (13). PEDF can also be found in the human amniotic membrane (14). In embryonic mouse eyes, PEDF is first detected on embryonic day (E) 14.5 in RPE cells, initially in the inner plexiform layer and subsequently, on E18.5, in the GCL layer, inner nuclear layer, choroid and ciliary body (15). In mouse embryonic livers, PEDF is found on E12.5, and gradually increases and maintains high expression in the liver (16). In addition, PEDF is highly expressed in murine primary long-term hematopoietic stem cells (HSCs) (17).

PEDF levels have been shown to be decreased in angiogenic tissues or organs, such as the retinas from patients with proliferative diabetic retinopathy (PDR) (18–24). PEDF exerts antiangiogenic effects by inducing endothelial cell apoptosis (25, 26), which contributes to its antitumor effects. On the other hand, PEDF directly promotes differentiation, inhibits proliferation, mediates tumor cell apoptosis, and ultimately abrogates tumors (12), such as melanomas (27, 28), pancreatic carcinomas (29), prostate tumors (30) and ovarian tumors (31). An increasing number of studies on PEDF have shown that this protein maintains the growth and development of important organs and supports important organ functions. For example, PEDF played cardioprotective roles by increasing glucose uptake in the ischemic myocardium, an effect mediated through PI3K/AKT signaling and GLUT4 translocation (32) and enhanced cardiac function by reducing hypoxia-induced cell injury (33). Pulmonary PEDF expression was increased in idiopathic pulmonary fibrosis and inversely correlated with pulmonary microvascular density and vascular endothelial growth factor (VEGF) levels (34). Plasma PEDF levels in chronic kidney disease patients were found to be significantly increased compared with those in patients without chronic kidney disease (35). In addition, renal PEDF levels were significantly decreased in a diabetic rat model (36). Exogenously overexpressed PEDF in mice resulted in the inhibition of retinal neovascularization (RNV) in an oxygen-induced retinopathy (OIR) model (37). However, PEDF deficiency caused severe vessel loss in the retinas of the OIR model mice (38).

The PEDF receptors discovered to date include patatin-like phospholipase domain-containing protein 2 (PNPLA2)/adipose triglyceride lipase (ATGL) (39), laminin receptor (25), lipoprotein receptor-related protein 6 (LRP6) (40), plexin domain-containing 1 (PLXDC1), PLXDC2 (41), F1-ATP synthase (42), and vascular endothelial growth factor receptor 2 (VEGFR2) (43). In this review, we expound on the distribution and function of each PEDF receptor, as well as the molecular signaling pathways in which they are involved (see Table 1).

3 Receptors that bind to PEDF

3.1 Adipose triglyceride lipase

The dynamic balance between energy intake and consumption is critical for maintaining the integrity of an organism. When calorie intake exceeds energy expenditure, the remaining energy is converted into fatty acids (FAs) and stored as triglycerides (TGs). However, when energy expenditure (EE) surpasses caloric intake, TG is hydrolyzed and FAs are released (80). Dysregulated lipolysis leads to an overabundance of circulating FAs, which leads to several destructive, lipotoxic pathologic changes, such as insulin resistance, type 2 diabetes, fatty liver, nonalcoholic fatty liver disease, and inflammation (44–47). In 2004, three independent institutes identified ATGL, the main enzyme critical for the initial step of TG degradation, and named it ATGL (81), iPLA2ζ (82), and desnutrin (83). To prevent confusion, we use ATGL in the following discussion. The human gene encoding ATGL is located

TABLE 1 PEDF receptor summary.

PEDF Receptors	Other Names	Chr	Expression in Tissues	Expression in Cells	Ligands	Related Diseases	Reference
ATGL	PNPL2 iPLA2ζ Desnutrin	11	adipose tissue, bone marrow, colon, and small intestine	human Y-79 cell, mouse photoreceptor cells (661W), rat photoreceptor cell line (R28), and bovine retinal RPE cells	PEDF, LC3, ABHD5, UBXD8, G0S2, HIG2, TNF-α, insulin, PPAR-γ, PKA, AMPK, and Fsp27	Insulin resistance Fatty liver Inflammation	(44–47)
LRP6	ADCAD2 STHAG7	12	heart, brain, placenta, spleen, testes, and ovaries	human hippocampus, rental tubular cells, hepatocytes, intestinal epithelial cells, osteoblasts, osteoclasts, and developing embryo cells	PEDF, Wnt ligands, and Fzd	Brain defects Posterior truncation Abnormal limb patterning Alzheimer's disease Atherosclerosis Diabetes Hyperlipidemia Hypertension Coronary artery disease	(48–55)
PLXDC1	TEM3 TEM7	7	gall bladder, endometrium, ovary, heart, esophagus	endothelial cells and rodent ganglion cells	PEDF, LRP1, and Nidogen	Glioblastoma Ovarian cancer Gastric cancer Renal cell carcinoma Colorectal cancer Lung cancer Breast cancer Osteosarcoma	(56–64)
PLXDC2	TEM7R	10	gall bladder, lung, skin, endometrium, kidney	human tumor vascular endothelial cells, neural progenitor cells, pluripotent stem cells, and hepatocytes	PEDF, Wnt3a, Wnt5a, Wnt8a, and ADGRD1	Coronary artery disease Ovarian cancer Diabetic mellitus Diabetic retinopathy Testicular germ cell tumors Sotos syndrome Ischemic stroke Laryngeal squamous cell Carcinoma Breast carcinoma Breast cancer Colorectal tumor	(56, 65–74)
LR	LAMR RPSA	3	ovary, lymph node, bone marrow, appendix, esophagus	tumor cells and blood cells	PEDF	Breast cancer Lung cancer Ovarian cancer Prostate cancer Gastric cancer Thyroid cancer Leukemia Lymphoma	(75, 76)
F1-ATP Synthase	ATP5F1	18 5	heart, kidney, duodenum, colon, adrenal	endothelial cells, hepatocytes, adipocytes, and keratinocytes	PEDF and F0-ATP Synthase	Angiogenesis diseases Lipoprotein metabolism diseases	(77)

(Continued)

TABLE 1 Continued

PEDF Receptors	Other Names	Chr	Expression in Tissues	Expression in Cells	Ligands	Related Diseases	Reference
						Innate immunity diseases Hypertension Food intake dysregulation	
VEGFR2	Flk-1 KDR CD309	4	lacenta, thyroid, fat, lung, endometrium	endothelial cells, hematopoietic cells, macrophages, and smooth muscle cells	PEDF and VEGFA	Tumor angiogenesis	(78, 79)

Chr, Chromosome; PNPL2, Patatin-Like Phospholipase Domain Containing 2; iPLA2ζ, Independent Phospholipase A2-ζ; ADCAD2, Coronary Artery Disease, Autosomal Dominant 2; STHAG7, Selective Tooth Agenesis 7; TEM3, Tumor Endothelial Marker 3; TEM7, Tumor Endothelial Marker 7; TEM7R, Tumor Endothelial Marker 7-Related Protein; LAMR, Laminin Receptor; RPSA, Ribosomal Protein SA; Flk-1, Fetal Liver Kinase 1; KDR, Kinase Insert Domain Receptor; CD309, Cluster of Differentiation 309; ATP5F1; ATP Synthase F1; LC3, Light Chain 3; ABHD5, α/β Hydrolase Domain-Containing 5; UBXD8, UBX Domain-Containing Protein 8; G0S2, G0/G1 Switch 2; HIG2, Hypoxia-induced Gene 2; TNF-α, Tumor Necrosis Factor-α; PPAR-γ, Peroxisome Proliferators-Activated Receptors-γ; PKA, Protein Kinase A; AMPK, Adenosine 5'-Monophosphate Activated Protein Kinase; Fsp27, Fat Specific Protein 27; Fzd, Frizzled; LRP1, Laminin Receptor Protein 1; ADGRD1, Adhesion G Protein-Coupled Receptor D1; VEGFA, Vascular Endothelial Growth Factor 1; F0-ATPase, F0-ATP Synthase 3 Receptors that bind to PEDF.

on chromosome 11p15.5 and includes 10 exons encoding a 504 amino acid protein (NCBI Reference Sequence: NG_023394.1). As a key participant in lipid catabolism, ATGL is highly expressed in brown adipose tissue (BAT) and white adipose tissue (WAT). However, in nonadipose tissues such as skeletal muscle (84), heart (85), liver (86), lung (87), and ocular tissues, and especially in the neural retina and RPE cells (ARPE-19 and hTERT) (39), ATGL mRNA is highly expressed, although at a lower level than in adipose tissues. In addition, researchers found that ATGL was also expressed in human Y-79 cells (11), mouse photoreceptor (661W) cells (88), a rat photoreceptor precursor (R28) cell line (39) and bovine RPE cells (89). ATGL is mainly localized in TG-rich intracellular lipid droplets (LDs), and the catalytic site in human and murine ATGL comprises a dyad consisting of serine 47 and aspartate 166 at the N-terminus of the protein (81, 90). Notably, the following factors may affect ATGL localization: the C-terminal portion includes a hydrophobic LD-binding region, and mutation in the ATGL C-terminus can negatively affect AGTL-LD binding (44). In addition, ATGL binds LC3, an autophagosome marker that promotes ATGL recruitment to LDs (47).

ATGL and hormone-sensitive lipase (HSL) are the major lipases in adipocytes in humans and mice. Several factors are involved in the regulation of ATGL activity. During catecholamine-stimulated lipolysis, for example, PKA phosphorylates α/β hydrolase domain-containing 5 (ABHD5) and promotes ATGL release from the LD surface. The direct interaction of ABHD5 with ATGL promotes the hydrolysis of triacylglycerols (TAG) (91) and broadens region-specificity of ATGL, because as it no longer exclusively engages in sn-2 reactions and engages in more sn-1 and sn-2 reactions (92). Notably, in adipocytes, the combination of an adipocyte- or FA-binding protein with ABHD5 induces ATGL activity, probably by preventing the inhibition of ATGL protease activity (93). In nonadipocytes, ubiquitin regulatory X domain-containing protein 8 (UBXD8) interacts with ATGL and causes the dissociation of CGI-58, resulting in a decrease in ATGL activity (94). ATGL activity is activated by ABHD5 and inhibited by the G0S2 protein in a noncompetitive manner (95). Specifically, G0S2 engages in direct protein-protein interactions and thus impedes substrate accessibility (96). Hypoxia-inducible gene 2 (HIG2), a HIF-1 target, has recently been identified as an inhibitor of ATGL that directly interacts with the AT GL patatin-like phospholipase domain (97, 98).

PEDF is also involved in regulating ATGL (see Figure 1). As a secreted protein, PEDF binds to ATGL on the RPE cell membrane, mediating the first step in its biological effects (33). PEDF regulates lipid metabolic functions through a concomitant elevation in the scavenger receptor CD36. The crucial roles played by PEDF are thought to be mediated through ATGL activation (99). For example, PEDF enhances the nuclear import of the predominantly cytosolic ATGL protein to promote its subsequent proteasomal degradation in the nucleus, thus diminishing ATGL protein stability in a COP1-dependent manner (99). During the development of inflammation-associated hepatic steatosis, endogenous PEDF directly interacted with ATGL and was neutralized by TNF-α, possibly in a PPARα-dependent manner (100). Endothelial damage is critical to vascular leakage and the subsequent shock in sepsis patients. Elevated serum PEDF levels in patients with sepsis induced increased extravasation, which was induced by the abnormal expression of ATGL (101). In addition, both PEDF and the PEDF-derived peptide 44mer promoted cardiac triglyceride degeneration by binding to ATGL (33).

ATGL is regulated by many factors at the transcriptional and post-transcriptional levels. In mice, ATGL controls energy supply and systemically hydrolyzes FAs, thereby influencing mitochondrial β-oxidation and the activation of peroxisome proliferator-activated receptors (PPARs) (102). ATGL decreases PPAR-γ signaling in the brain and suppresses appetite. Additionally, ATGL-deficient humans typically have obesity (103). At the transcriptional level, tumor necrosis factor-α (TNF-α) and insulin decrease ATGL expression, respectively. In this process, PPAR-γ interacts with the ATGL promoter and induces ATGL mRNA expression (104). Under starvation conditions, forkhead box protein O1 (FoxO1) showed increased affinity for the ATGL promoter (105), and this affinity was decreased by an increase in insulin level (106). Regarding the posttranscriptional phosphorylation of ATGL, studies with mice have shown that ATGL phosphorylation at Ser406 either by protein kinase A (PKA) or adenosine 5'-monophosphate-activated protein7 kinase (AMPK) increased ATGL activity (107, 108). In

addition, fat-specific protein 27 (Fsp27) reduced ATGL transcript levels by regulating the affinity of early growth response proteins for the ATGL promoter in human adipocytes and thus decreased ATGL-mediated lipolysis (109, 110) (see Figure 1).

3.2 Lipoprotein receptor-related protein 6

Lipoprotein receptor-related protein 6 (LRP6) was first isolated by Sheryl D. Brown et al., who reported the chromosomal location of LRP6 on human chromosome 12 in 1998 (111). The low-density lipoprotein receptor (LDLR) family comprises cell surface receptors, and several members are involved in numerous signaling pathways and are expressed in various target organs (112). LRP6 is a unique member of the LDL receptor gene family, as indicated by sequence comparisons, and exhibits the closest relationship to the LRP5 gene, a possible therapeutic target for type 1 diabetes (113). Both LRP5 and LRP6 function as coreceptors in the Wnt/β-catenin pathway (111); nevertheless, studies have indicated that LRP5 and LRP6 act distinctly owing to differences in their tissue distribution and affinity for individual Wnt ligands (114). LRP5 and LRP6 are structurally related, exhibiting approximately 71% homology at the nucleotide level, and are broadly expressed in humans, including the hippocampus, renal tubular cells, hepatocytes, intestinal epithelial cells, osteoblasts, and osteoclasts (115). Although LRP5 and LRP6 are functionally and structurally similar, LRP6 is more closely related to glucose and lipid metabolism signaling pathways and plays a more crucial role in developmental processes than LRP5 (116–118).

The human LRP6 (hLRP6) gene is located on chromosome 12p13.2, is 150 kb long and consists of 23 exons. hLRP6 is highly evolutionarily conserved, with negligible differences observed among Drosophila, Xenopus and Mus (119). LRP6 is highly expressed in the heart, brain, placenta, spleen, testes and ovaries but is expressed at low levels in the liver, skeletal muscle, prostate and colon mucosa (111). Mice show LRP6 expression levels in the heart, brain, lungs and kidneys similar to those in humans (111). According to a βgeo reporter activity assay, LRP6 is an endogenous gene and has been detected in all types of developing embryo cells (120).

In mice, LRP6 is essential to the canonical and noncanonical Wnt signaling pathways. When the LRP6 gene carries an insertion mutation and an individual Wnt gene is mutated, *Lrp6*$^{-/-}$ homozygous embryos present developmental defects (120). Mice that lack LRP6 genes typically exhibit mid-/hindbrain defects, posterior limb truncations, and abnormal limb patterning, similar to Wnt7a-mutant mice (48). In addition, LRP6 plays an important role in the mouse forebrain (121). In Alzheimer's disease (AD), a neurodegenerative disorder characterized by deficient cognitive processes and the accumulation of amyloid precursor protein (APP) and amyloid-β, LRP6 mutations are considered to be pathogenic factors. Notably, the conditional deletion of the LRP6 gene in mouse forebrain neuronal cells led to the destruction of synaptic integrity and memory loss in an age-dependent manner, potentially due to increased processing of APP in to amyloid-β (51). In addition, De Ferrari GV et al. showed that in two brain bank data series, a single nucleotide polymorphism (SNP) in exon 18 of LRP6 was associated with Alzheimer's disease (49).

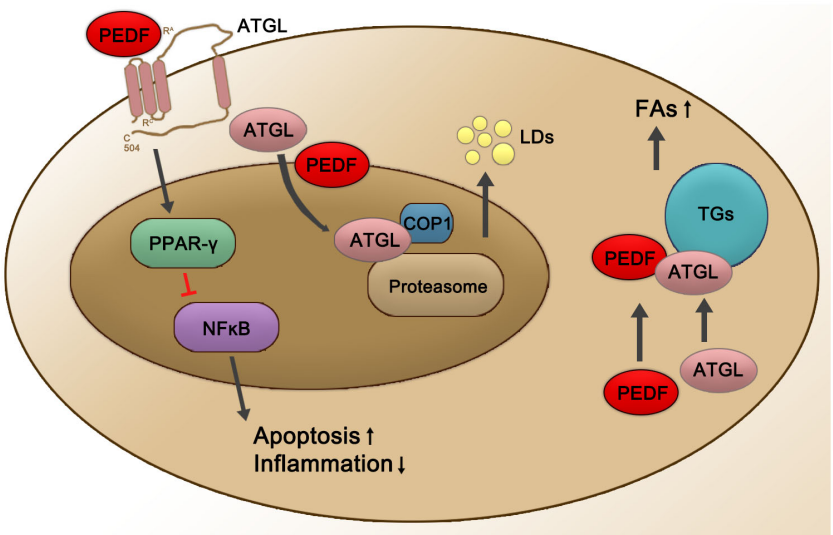

FIGURE 1
Schematic representation of PEDF-activated ATGL signaling. PEDF binds to the cell surface membrane receptor ATGL, which leads to the upregulation of PPARγ and then suppresses NFκB at the transcriptional level, subsequently leading to decreased inflammation and an increased apoptosis rates. PEDF also enhances nuclear import of +predominantly cytosolic ATGL protein for its subsequent proteasomal degradation in the nucleus, thereby diminishing ATGL protein stability in a COP1-dependent manner, which enhances the release of LDs. In addition, the PEDF-ATGL interaction promotes the hydrolysis of TGs and the release of FAs. Red lines represent inhibited pathways, and black arrows show activated pathways. PPAR-γ, peroxisome proliferator-activated receptor γ; NFκB, nuclear factor κB; COP1, constitutive photomorphogenic 1; LDs, lipid droplets; TGs, triglycerides; FAs, fatty acids.

Recently, a reduction in Wnt-mediated transcription resulting from mutations in LRP6 has been confirmed to lead to several features of metabolic syndrome, including atherosclerosis (50), diabetes (55), hyperlipidemia (50, 53), and hypertension (54), but not obesity. Coronary artery disease (CAD) is usually caused by several risk factors of metabolic syndrome. In 2007, Mani et al. reported on a family with autosomal dominant early CAD, characterized by the features of hyperlipidemia, hypertension, and osteoporosis, which were found to be associated with a short piece of chromosome 12p; specifically, the group identified a mutation in LPR6 that encoded a coreceptor in the Wnt signaling pathway (52). The identified mutation damaged the Wnt signaling pathway *in vitro* because an arginine residue in the epidermal growth factor-like (EGF-like) domain was replaced with a cysteine residue. This finding encouraged the investigators to focus on the relationships between LRP6 and various human diseases, especially atherosclerosis (51).

After the binding of the Wnt ligand, the Fzd/LRP6 receptor and the scaffold protein Dishevelled (Dvl) form a signaling body that is endocytosed. The signaling body induced glycogen synthase kinase 3 (GSK3)-mediated phosphorylation of LRP6 on the PPPSP motif, which initiated the phosphorylation of adjacent S/T clusters through casein kinase 1γ (CK1γ) (122, 123). In addition to GSK3, other kinases phosphorylate the LRP6-PPPSP motif in a Wnt-independent manner. For example, due to the initiation of phosphorylation of cyclin-dependent kinase 14 (CDK14/PFTK1) and its regulators, mitotic cyclin Y and cyclin Y-like 1 (CCNY/CCNYL1), the ability of LRP6 to respond to Wnt ligands is greatest during the G2/M period (123–127). Phosphorylated LRP6 recruits a polyprotein called the "destruction complex", which includes the scaffold protein Axin and Adenomatous Polyposis Coli(APC) tumor suppressors, the kinases CK1α and GSK3, and the protein E3 ubiquitin ligase β-transduction protein repeat sequence (β-TrCP). In the absence of Wnt ligands, CK1α and GSK3 in the destruction complex phosphorylate β-catenin, inducing β-TrCP-mediated degradation by the proteasome. Wnt/LRP6 signaling inhibits destruction complex activity through at least two mechanisms. First, GSK3 is the product of inhibited LRP6 phosphorylation. Second, the signaling body matures into a multivesicular body, in which the destruction complex is isolated with LRP6. Wnt/LRP6 signaling is enhanced by members of the R-sponge protein (RSPO) family of secreted proteins, which bind to the LGR4/5 receptor and the E3 protein ligase RNF43/ZNRF3 to stabilize the Wnt receptor on the cell surface (54, 128–133).

The canonical Wnt signaling pathway is a conservative intracellular signaling pathway. When the receptor complex on the cell surface, specifically, the Wnt-Fzd-LRP5/6 complex, binds to a Wnt ligand, the canonical Wnt pathway is rapidly activated. Then, Wnt phosphorylation of the cytoplasmic tail of the Fzd-LRP5/6 complex triggers the recruitment and phosphorylation of disheveled protein (also known as Dishevelled, Dvl) in the cytoplasm (134, 135). Subsequently, Axin is recruited to the receptor complex to inhibit its decomposition and the phosphorylation of β-catenin. The stable nuclear translocation of soluble β-catenin in the cytoplasm promotes the activation of the downstream Wnt/β-catenin signaling pathway *via* the transcription and translation of target genes (134, 135). In the absence of Wnt ligands or in the presence of Wnt receptor inhibitors, β-catenin is bound by Axin, Axin and casein kinase Ia (CKIa) and glycogen synthase kinase 3β (GSK3β); moreover, two APC protein kinases combine to form a destruction complex (134). CKIa and GSK3β mediate the phosphorylation of β-catenin in the cytoplasm. Phosphorylated β-catenin is recognized by b-TrCP and induces ubiquitination, which ultimately leads to the degradation of β-catenin (136). Many inhibitors of the Wnt signaling pathway, including Dickkopf WNT Signaling Pathway Inhibitor 1, DKK-1 (137), R-spondins (138), Norrin (139), endostatin (140), PEDF (40), and very low-density lipoprotein receptor, have been identified (141, 142). These negative regulatory molecules of the Wnt signaling pathway ultimately lead to the transcription of target genes, inducing cell proliferation, differentiation, or apoptosis (see Figure 2).

3.3 Plexin domain-containing 1 and plexin domain-containing 2

Plexin domain-containing 1 (PLXDC1), also known as tumor endothelial marker 7, is a member of the tumor vascular endothelial marker family (143). The genes encoding PLXDC1 are highly expressed during tumor angiogenesis and enriched in many types of tumor endothelial cells (144), including glioblastoma endothelium (57, 63), ovarian cancer (62), gastric cancer (60), renal cell carcinoma (61), colorectal cancer (64), lung cancer (58), breast cancer (56), and osteosarcoma (59). PLXDC1 has been found to be highly expressed in the endothelial cells in the ocular disease DR context and is highly specific to diseased blood vessels (145). PLXDC1 has also been shown to be expressed in rodent retinal ganglion cells (RGCs) (145). Transmission electron microscopy has revealed that PLXDC1 was mainly expressed at tight junctions between endothelial cells, and some PLXDC1 expression was detected on the surface of the blood vessel lumen (146).

PLXDC1 is a novel LRP1-regulated cell-signaling protein. Regulation of PLXDC1 activity by LRP1 was confirmed in CHO cells, and in extracts of RAW264.7 cells and mouse liver, PLXDC1 coimmunoprecipitated with LRP1 (147). The Nidogen/PLXDC1 interaction enhanced cell spreading in PLXDC1-transfected 293T cells, suggesting that Nidogen is a candidate ligand for PLXDC1 (148). Akash Nanda et al. identified cortactin as a protein candidate for binding to the extracellular region of both PLXDC1 and its closest homolog, which were all expressed in the tumor endothelium (146).

Plexin domain-containing 2 (PLXDC2) is a largely uncharacterized transmembrane protein with a homologous nidogen region and a plexin repeat in its extracellular domain. In mice, PLXDC2-betageo expression is prominent in the brain, including in the cortical hem, midbrain-hindbrain boundary, and midbrain floorplate, during midembryonic stages (E9.5-E11.5). On E15.5, PLXDC2 expression was apparent in a large number of discrete nuclei and structures throughout the brain, including the glial wedge and derivatives of the cortical hem. PLXDC2 was also found to be expressed in other tissues, most notably the limbs, lung buds and developing heart, as well as in the spinal cord and dorsal

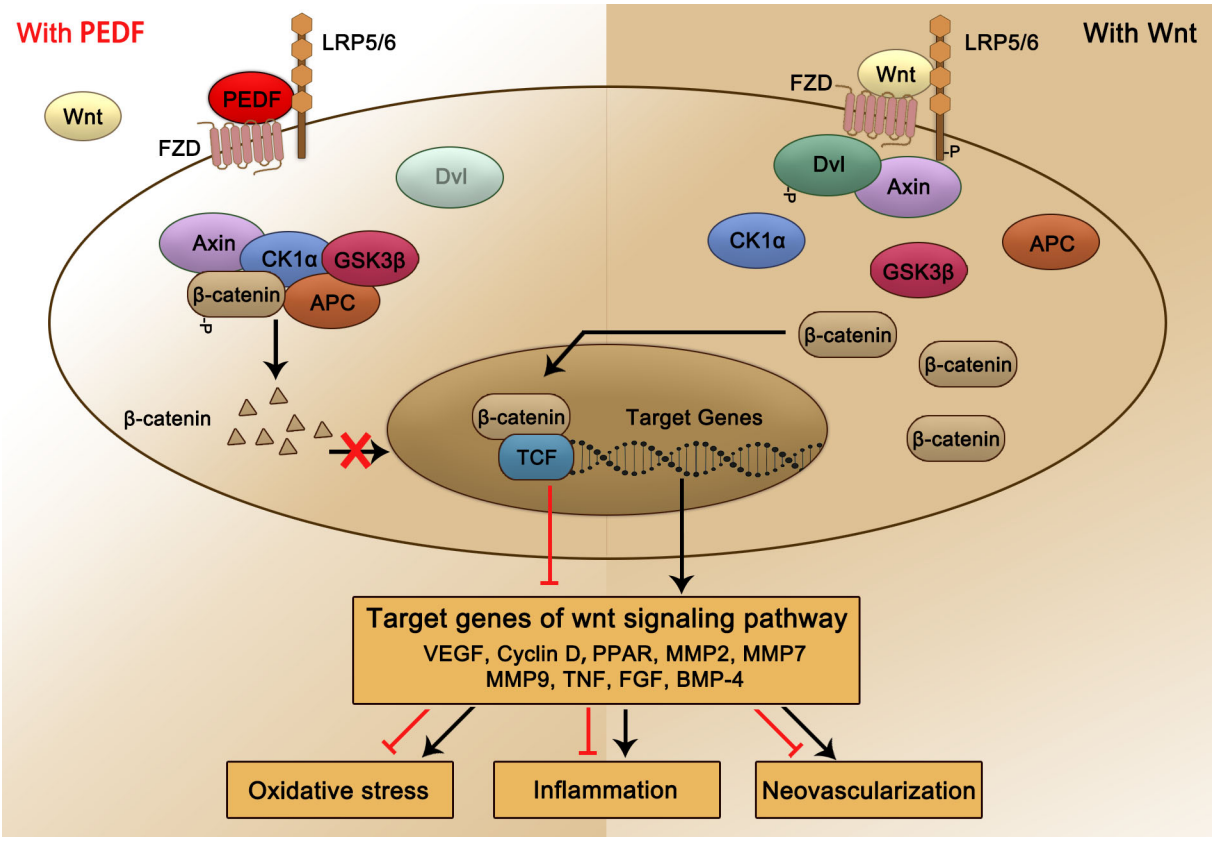

FIGURE 2
Schematic representation of PEDF-activated LRP6 signaling. PEDF binds to the Fzd-LRP5/6 complex and activates the canonical Wnt/β-catenin pathway. The key protein Dvl is recruited and phosphorylated, subsequently forming a destruction complex that also includes Axin, CKIa, GSK3β, and APC tumor suppressors and inhibiting the phosphorylation and nuclear translocation of β-catenin, which is bound. This process leads to changes in target gene transcription and expression, which reduce the occurrence of relevant pathological consequences, such as oxidative stress, inflammation, and NV. Dvl, dishevelled; CKIa, casein kinase Ia; GSK3β, glycogen synthase kinase 3β.

root ganglia (149). In humans, PLXDC2 has been found to be expressed in endothelial cells of the tumor stroma, neural progenitor cells, and pluripotent stem cells and in human hepatocellular carcinoma (HCC) tissues, including HCC cells, tumor vascular endothelial cells, and some infiltrating cells (150).

The PLXDC2 level is elevated during tumor angiogenesis (143). PLXDC2, a mitogen for neural progenitors, has been shown to be a novel regulator of the development of different brain regions involved in the coordinated control of cell proliferation and cell fate along and across the neuraxis (151). PLXDC2 expression increases during cellular senescence and is a marker of adult stem cells (152). In addition, PLXDC2 has been associated with CAD (72), ovarian cancer (73), diabetes mellitus (71), DR (68), testicular germ cell tumors (74), Sotos syndrome (66), ischemic stroke (70), laryngeal squamous cell carcinoma (69), breast cancer (56), and colorectal tumors (65, 67).

In 2014, Guo Cheng et al. identified PEDF binding to PLXDC1 and PLXDC2 on the surface of 293T cells (see Figure 3). PEDF interacted with PLXDC1 to promote the secretion of interleukin-10 by macrophages, which exerted neuroprotective effects on rat RGCs, and PEDF combined with PLXDC2 promoted apoptosis in endothelial cells (41). With few reports on the role or mechanism of PEDF and PLXDC in DR or neovascular fundus diseases, PLXDC1 has been shown to inhibit cell proliferation and invasion in tumor cells, promote endothelial cell separation in mice. With a protective effect on RGCs, PLXDC1 is likely to be an important receptor for PEDF, particularly in fundus diseases. In addition to PEDF, other molecules are ligands of PLXDC1 or PLXDC2. Moreover, members of the Wnt family (Wnt3a, Wnt5a and Wnt8b) show a striking overlap with PLXDC2 expression in certain areas (69). Cortactin can bind to the extracellular terminus of PLXDC2 (152). PLXDC2 has also been shown to be an activating ligand for ADGRD1 on cumulus cells (153).

3.4 Laminin receptor

The laminin receptor (LR) is a laminin-binding protein with a molecular weight of approximately 67 kDa and is a nonintegrin cell surface receptor of the extracellular matrix (154). LR contributes to laminin binding, ribosome biosynthesis, cytoskeletal organization, and nuclear function, and it controls key cellular processes, including cell adhesion, migration, proliferation and survival, protein synthesis, development, and differentiation (76). Research on LR is mainly focused on its role on the development of tumors, specifically its promotion of tumor cell adhesion to the basement

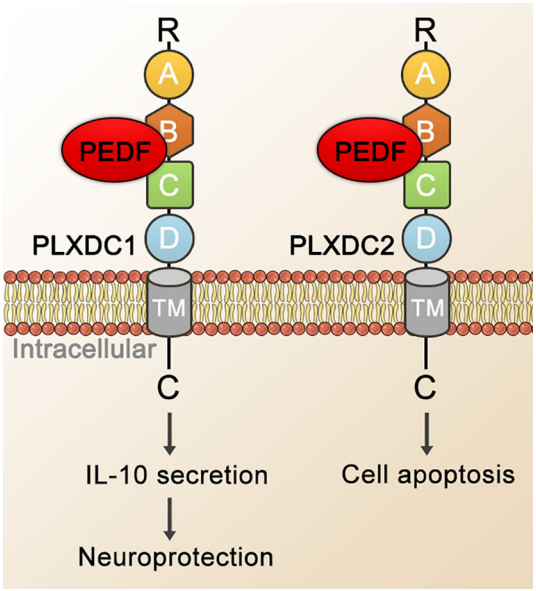

FIGURE 3
Schematic representation of PEDF-activated PLXDC1 or PLXDC2 signaling. PEDF binds to the cell-surface homologous membrane proteins PLXDC1 and PLXDC2 through their extracellular domains. Domain B plays an important role in binding PEDF. The TM and the C-terminus of these receptors mediate downstream signaling. Ultimately, this signal transduction mechanism stimulates the PLXDC1-dependent secretion of IL-10, which exerts neuroprotective and apoptosis-promoting effects in combination with PLXDC2. TM, transmembrane domain; IL-10, interleukin-10.

membrane, which is the first step in the tumor cell invasion and metastasis. Therefore, compared with normal cells, LR in tumor cells is overexpressed, and its overexpression is considered to be a molecular marker of cancer metastasis and aggressiveness, including breast cancer, lung cancer, ovarian cancer, prostate cancer, gastric cancer, thyroid cancer, leukemia and lymphoma (75, 76).

In vitro yeast two-hybrid screening experiments confirmed that LR is a cell membrane surface receptor of PEDF. Researchers have also determined that the PEDF isoform that interacts with LR consists of 34 peptides. Surface plasmon resonance analysis showed that PEDF interacts with LR, and PEDF also interacts with endothelial cells. LR-plasma membrane binding induces endothelial cell apoptosis and inhibits endothelial cell migration and the formation of vascular networks *in vitro* (25). The combination of the PEDF 34mer and LR may also mediate endothelial cell apoptosis through the LR-JNK-PPAR-γ-FasL-caspase 8 pathway, thereby exerting an anti-NV effect in the retina. In apoptotic cells, the PEDF 34mer binds to LR to phosphorylate JNK/MAPK, which then activates the transcription factor PPARγ through PPARγ ligand binding and nuclear translocation. In the nucleus, PPAR-γ and RXR combine in the form of heterodimers and recruit specific nuclear coactivators that activate the transcription of target FasL genes in a ligand-dependent manner. Both PPAR-γ and RXR promote the transcription mechanism initiated at FasL gene promoters, ultimately inducing the expression of FasL protein (155) (see Figure 4).

3.5 VEGFR2

Three VEGFR subtypes are encoded by different genes: VEGFR1 (Flt-1 in mice) and VEGFR2 (Flk-1; KDR) are structurally similar, while VEGFR3 (Flt-4) carries proteolytically cleaved extracellular domains (156–158). VEGF receptors are highly expressed in endothelial cells, hematopoietic cells,

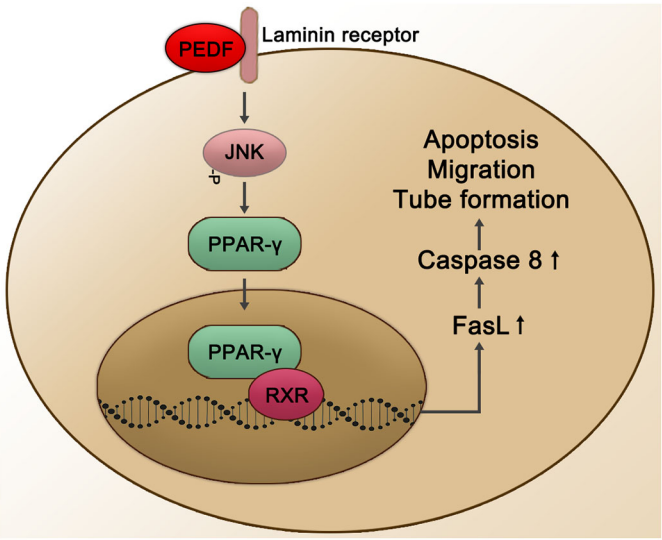

FIGURE 4
Schematic representation of the PEDF-activated laminin receptor. The PEDF 34mer binds to LR to activate the JNK-PPAR-γ-dependent signal transduction pathway. Subsequently, the combination of PPAR-γ and RXR is activated in the nucleus, promoting the transcription mechanism of FasL gene promoters and affecting biological processes through the upregulation of Caspase 8, such as cell apoptosis, migration, and tube formation. JNK, Jun N-terminal kinase; RXR, retinoid X receptor.

macrophages, and smooth muscle cells (159–161). VEGF-A isoforms drive physiological and pathophysiological angiogenesis *via* VEGFR1 and VEGFR2 signaling, while lymphatic angiogenesis is mediated by VEGF-C/D isoforms *via* VEGFR3 (162). VEGFR2 is a large membrane protein consisting of seven extracellular immunoglobulin (Ig)-like domains, a single transmembrane helix, and a split intracellular kinase domain. VEGF-A is an endogenous agonist of VEGFR2 that binds to ligand binding sites in Ig-like domain 2 (D2) and D3 on the basis of the stoichiometry of one VEGF-A dimer to one VEGFR dimer (163, 164).

VEGF-A, VEGFR1, and VEGFR2 play important roles in physiological and pathological angiogenesis, including tumor angiogenesis. Although VEGF-A isoforms exhibit similar VEGFR2-binding properties, activation of VEGFR2 is a complex multistep process. The VEGFR2 signaling pathway is critical for controlling vascular endothelial cell activity, migration, and permeability (165, 166). In cancer cells, transcription factors induced by hypoxia-inducible factors rapidly increase gene transcription rates, resulting in elevated levels of VEGF gene expression while enhancing the stability of VEGF mRNA (78, 79). The direct result of VEGF-VEGFR binding is endothelial cell budding, increased vascular permeability, and increased expression of tissue matrix metalloproteinases, resulting in extracellular matrix digestion. These processes lead to the movement of endothelial and pericyte cells, eventually leading to vasodilation and the formation of pathological vascular networks.

In 2006, Jianxing Ma demonstrated that PEDF inhibited VEGFR2 (167). PEDF inhibits VEGF expression at the transcriptional level by inhibiting hypoxia-induced increases in VEGF promoter activity, HIF-1 nuclear translocation, and mitogen-activated protein kinase phosphorylation. Other investigators have reported that PEDF exerts the anti-VEGF actions by binding to its key angiogenic receptor, VEGF-R2 (43). This binding inhibits receptor activation and ultimately reverses critical downstream VEGF-A signaling by reducing VEGF-R2 tyrosine kinase activity and inhibiting two phosphorylation sites in VEGF-induced HUVECs (Y951 is critical for cell migration and pathological angiogenesis, and Y1175 phosphorylates downstream signaling). Inhibition of VEGF angiogenesis signaling molecules such as PI3K, PLC-γ, FAK and Src may regulate many aspects of endothelial cell biology, including cell proliferation, migration, and survival. Behzad Shahbazi et al. also showed that PEDF binds to the VEGFR2, as well as laminin receptor much stronger than ATP synthase β-subunit, VEGFR1, and LRP6 using molecular docking, molecular dynamics (MD) simulation, and Molecular mechanics/Poisson-Boltzmann surface area (MM/PBSA) approach. Besides, the N-terminal of PEDF owns the most important enactment in the interaction with its receptors (168).

3.6 F1-ATP synthase

F-ATP is an ATP synthase in the bacterial plasma membrane, the eukaryotic mitochondrial inner membrane and chloroplast thylakoid membrane. F-ATPase leverages the membrane proton gradient to drive ATP synthesis, passing the passive proton flux through the membrane along its electrochemical gradient, and releasing newly formed ATP from the active site of F-ATP synthase using the energy released by transport reaction (169). F-ATP synthase is composed of two domains, F0-ATP synthase and F1-ATP synthase. In previous studies on angiogenesis, lipoprotein metabolism, innate immunity, hypertension or food intake regulation, F1-ATP synthase was found to be expressed only in cell mitochondria and was used to synthesize ATP that was needed by cells(77). Luigi Notari et al. demonstrated for the first time that PEDF binds F1 ATP synthase b subunit on the endothelial cell surface and inhibits endothelial extracellular ATP synthesis (170). In addition, F1-ATP synthase can inhibit cell growth, proliferation, and migration and directly induce multiple forms of cell death (171).

4 Therapeutic roles of PEDF and its receptors in ocular fundus diseases

Millions of people worldwide are affected by ocular fundus diseases such as DR, age-related macular degeneration (AMD), retinal vein occlusion (RVO), retinal artery occlusion (RAO), and fundus tumors. Inflammation, oxidative stress, neurodegeneration, and neovascularization (NV) are involved in the development of these diseases. As an endogenous multifunctional factor, defects or deficiencies that alter PEDF expression have been shown to be closely related to the progression of some of the abovementioned diseases. Related studies have shown that PEDF levels are markedly decreased in the vitreous, retinas and aqueous humors of diabetic patients with proliferative DR compared with those of either nondiabetic individuals or diabetic patients with nonproliferative DR (18, 24, 172). The high-glucose environment in diabetic patients directly downregulates the expression of PEDF in RPE cells, resulting in the loss of its inhibitory effect on angiogenesis. Other studies have shown that the early postnatal retinal vascularization occurs at a faster rate in PEDF-deficient mice, and NV has been observed in the OIR model (26, 38). Injection of exogenous PEDF into the vitreous can significantly inhibit this pathological change (173). These studies have shown that an increase or decrease in PEDF expression is likely important to the development of retinopathy of prematurity (ROP) lesions and abnormal vascular changes. Notably, Holekamp et al. and Park et al., studying neovascular age-related macular degeneration (nAMD) patients and an argon laser-induced choroidal neovascularization (CNV) model in BN rats confirmed that decreased PEDF expression levels were associated with oxidative damage to RPE cells and may lead to CNV formation, which is a key factor in AMD pathological changes (37, 174). Moreover, studies with proliferative vitreoretinopathy (PVR) patients have shown increased levels of PEDF in the vitreous (175), suggesting that PEDF may act through a positive regulatory feedback loop to counteract the angiogenic response and inhibit the activity of fibrotic factors. The dynamic changes in PEDF levels in the abovementioned case studies suggested its potential therapeutic role in related fundus diseases. Clarifying the mechanism and molecular pathway of signal transduction mediated or induced by the membrane surface receptor of PEDF will contribute to the in-

depth understanding of the pathological mechanism of fundus lesions and provide new ideas for disease intervention and treatment.

There are extensive reports on the role of PEDF and ATGL in ophthalmology. As mentioned above, ATGL is expressed in a variety of cells in the eye. In the natural retina, ATGL is distributed in the RPE, the inner segments of photoreceptors, and inner nuclear and RGC layers (39). Western blots of ARPE-19 cells and R28 cells membrane fractions yield a single 83-kDa band representing an immunoreactive protein. Specific biotinylation of cell-surface proteins enables ATGL labeling in ARPE-19 cells, and kinetic experiments have shown that fluorescein-labeled human recombinant PEDF binds to cell-surface proteins with a structure similar to that of ATGL. Based on these findings, ATGL is considered to be a plasma membrane protein that interacts with PEDF in these retinal cells (39). ATGL shows phospholipase A2 (PLA2) activity, which is enhanced after binding to PEDF, resulting in the release of active nonesterified fatty acids (NEFAs) and lysophosphatidic acid (LPA), which can be a second messenger or interact with C protein-coupled receptors (107). PEDF increases the PLA activity of ATGL, which plays a potential role in regulating the survival-promoting effect of PEDF on R28 cells (39). Retinal NV is a factor in a variety of eye-blinding diseases, such as DR and ROP. PEDF possibly exerts its antiangiogenic effects by interacting with ATGL in endothelial cells, as indicated by PEDF upregulation of FasL expression by regulating NF-κB in a PNPLA2-dependent manner (102, 103). Ocular neurodegenerative diseases such as glaucoma, hypertensive and ischemic retinopathies are results of the death of RGCs. Müller cells endow neonatal RGCs with trophic properties, and Müller cell-derived PEDF is secreted to support the regeneration of damaged RGCs. Researchers have shown that PEDF secreted by Müller cells promoted RGC survival through the engagement of ATGL (104). R28 cells express neuronal genes and carry functional cell-surface ATGL. PEDF specifically binds to the L4 region in ATGL, which is between Ile193 and Leu249, and thus protects R28 cells from undergoing apoptosis. In other words, ATGL, especially its L4 ectodomain, is essential to the anti-apoptotic and survival effects of PEDF on retinal cells (105).

LRP6 is one of the most widely studied receptors of PEDF, and it plays an important role in the occurrence and progression of DR. Notably, compared with that in nondiabetic controls, the activation of the Fzd-LRP5/6 coreceptor complex in the retina of patients with nonproliferative DR was significantly increased. Studies have shown that in two different recently developed ocular vessel models: OIR mice, which develop ischemia-induced retinal NV, or *Vldlr*$^{-/-}$ mice, which develop subretinal NV, the Wnt signaling pathway was activated, and β-catenin was translocated into the nucleus and negatively correlated with the retinal PEDF level (40). Intravitreal injection of PEDF significantly inhibited Wnt signaling pathway activation in this mouse model retina by binding to LRP6 with high affinity and subsequently regulating the expression of downstream target genes, including VEGF, PPAR, MMP2, MMP9, TNF, FGF and BMP-4. As a result, the increase in the oxidative stress response, the increase in the inflammatory response level and the formation of retinal NV in the pathogenesis of DR were attenuated, demonstrating a therapeutic role in DR.

The function and mechanism of PEDF action in fundus diseases mediated through other receptors have not been fully studied. Recent studies, however, have shown that in animal models of retinal NV (an OIR model and a laser-induced CNV model), both the PEDF 34mer and PEDF polypeptide 336 (PEDF 336) exhibit high affinity for LR (176). In a CNV model, PEDF 34mer spot treatment significantly inhibited the formation of CNV through its interaction with LR. In the OIR model, PEDF 336 bound LR with high affinity and inhibited retinal NV (176). In choroidal and retinal endothelial cells, VEGF induced LR expression, which can be inhibited by PEDF 336 (177). In addition, although the roles and mechanisms of PEDF and PLXDC in the eye have rarely been reported, considering that PEDF-activated PLXDC1 protected rat RGCs and that the combination of PEDF and PLXDC2 induced apoptosis of endothelial cells (41), these two membrane receptors may be important to PEDF effects on fundus diseases. They are therefore worthy of further study by researchers. The correlation between VEGFR2 activation and NV has been widely recognized. Zhang et al. proposed that the competitive blockade of VEGF-VEGFR-2 binding by PEDF may be crucial for PEDF effects on VEGF-induced permeability and angiogenesis in retinal capillary endothelial cells (167). Besides, PEDF bound specifically to the extracellular domain of VEGF-R2 and prevented activation of an intrinsic tyrosine kinase, disrupting the flow of VEGF-A downstream signals in primate retinal vascular endothelial cells (43). Furthermore, F1-ATP synthase inhibited cell growth, proliferation, and migration by inhibiting extracellular ATP synthesis and directly induced death in several cell types (19). Therefore, the interaction between PEDF and F1-ATP synthase may reasonably explain for the inhibitory effect of PEDF on NV (42).

5 Conclusion

PEDF receptors are widely expressed in ocular tissues and exhibit important physiological and pathological significance. These characteristics implicate the importance of basic research and clinical application of PEDF in the diagnosis, pathogenesis and drug development of DR. DR is a preventable but incurable type of blindness. At present, intravitreal injection of anti-VEGF drugs is an effective treatment method to control retinal NV in patients with DR. Among the many types of anti-VEGF drugs, monoclonal antibody anti-VEGF drugs (such as bevacizumab and ranibizumab) target VEGFR2 and have been designed to antagonize the binding of VEGF and VEGFR2. However, these anti-VEGF treatments still present certain limitations. A number of clinical studies have shown that the effect of anti-VEGF treatment in the clinic was clearly inferior to that obtained in Phase III clinical trials. After intravitreal injection, vision initially improved compared with that at the baseline, but it continued to decrease, not maintaining the initial benefits. Moreover, not all patients responded to anti-VEGF treatment. Exploring new treatments for retinal NV, reducing the number of intravitreal injections by optimizing treatment methods, and administering sustained-release preparations/eye drops have

always been the research focus of ophthalmologists and scientific researchers.

Since it was discovered in 1989, PEDF has shown great potential as a drug target for the treatment of DR due to its antiangiogenic, anti-inflammatory, neuroprotective, and neurotrophic effects. With increasing attention on PEDF and the gradual deepening of relevant exploration, an increasing number of researchers have focused on mechanistic research, drug development and clinical transformation of PEDF-specific peptides with biological effects and have clarified the high-affinity structure of PEDF and PEDF receptors. Domains and specific amino acid sequences are helpful to locate PEDF-derived peptides that can truly perform a certain biological function. The therapeutic effect of PEDF-derived peptides is clear and focused, and as a therapeutic drug, its administration method is more adaptable and efficient. For example, drug loaded exosomes or nanomaterials exert therapeutic effects of the PEDF polypeptide to a greater extent than other methods. Therefore, it is important to accelerate the clinical translation and application of PEDF peptides.

Regarding the study of PEDF receptors alone, the roles of LRP6, ATGL and LR in the pathogenesis of DR are relatively clear. For example, the expression levels of LRP6 and ATGL are clearly related to DR pathogenesis, the severity of the disease, and the VEGF expression level. Therefore, the PEDF receptor may be used as a predictive biomarker for the development and progression of DR, which can help in the diagnosis of the disease. In addition, PEDF receptors are expressed not only in eye tissues but also in various tissues of the body, such as heart, bone marrow, kidney and so on. The study of the mechanism of PEDF receptors in nonocular diseases can broaden the horizons of researchers and help their exploration into DR pathogenesis more comprehensively.

There are still certain limitations to the development of treatments that target PEDF receptors. PEDF binds to different receptors and may exert the same effect. For example, by binding to ATGL or LRP6, PEDF exerts anti-inflammatory effects. If ATGL is blocked, LRP6 may continue to compensate and have the inflammatory functions. In addition, most PEDF receptors are not specific receptors and blocking these receptors will affect the physiological functions of other ligands bound to them.

Besides, although PEDF has shown strong therapeutic potential in the ophthalmology field, only one Phase I clinical study has shown that an adenovirus carrying PEDF exerted a therapeutic effect in patients with advanced neovascular age-related macular degeneration. To mediate a biological effect, PEDF must first be ligated to its cell membrane surface receptor. Moreover, PEDF binds to a specific domain of the PEDF receptor or a regulatory site to mediate its biological function. Through the identification of these binding sites, the true value of receptor research in the development of corresponding DR treatments can be demonstrated.

Author contributions

MX designed this study. MX and XC collected the data and wrote the manuscript. ZY collected the details of tables, figures, generated the tables, figures, figure legends, and wrote the first draft of the manuscript. XL reviewed and revised the manuscript and was also involved with the manuscript development, proofreading and approved the final version of the manuscript. All authors contributed to the article and approved the submitted version.

Funding

This work is supported by National Natural Science Foundation of China (82171085), National Natural Science Foundation of China (81900891) and Tianjin Research Innovation Project for Postgraduate Students (2021YJSB271).

Acknowledgments

All authors would like to thank Professor Joyce Tombran-Tink for her guidance on the structure and logic of the manuscript.

Conflict of interest

The authors declare that the research was conducted in the absence of any commercial or financial relationships that could be construed as a potential conflict of interest.

Publisher's note

References

1. Tombran-Tink J, Chader GG, Johnson LV. PEDF: a pigment epithelium-derived factor with potent neuronal differentiative activity. *Exp Eye Res* (1991) 53:411–4. doi: 10.1016/0014-4835(91)90248-D

2. Lucas A, Yaron JR, Zhang L, Ambadapadi S. Overview of serpins and their roles in biological systems. *Methods In Mol Biol (Clifton N.J.)* (2018) 1826:1–7. doi: 10.1007/978-1-4939-8645-3_1

3. Sanrattana W, Maas C, De Maat S. SERPINs-from trap to treatment. *Front Med (Lausanne)* (2019) 6:25. doi: 10.3389/fmed.2019.00025

4. Tombran-Tink J. The neuroprotective and angiogenesis inhibitory serpin, PEDF: new insights into phylogeny, function, and signaling. *Front Biosci* (2005) 10:2131–49. doi: 10.2741/1686

5. Steele FR, Chader GJ, Johnson LV, Tombran-Tink J. Pigment epithelium-derived factor: neurotrophic activity and identification as a member of the serine protease inhibitor gene family. *Proc Natl Acad Sci USA* (1993) 90:1526–30. doi: 10.1073/pnas.90.4.1526

6. Bilak MM, Corse AM, Bilak SR, Lehar M, Tombran-Tink J, Kuncl RW. Pigment epithelium-derived factor (PEDF) protects motor neurons from chronic glutamate-mediated neurodegeneration. *J Neuropathol Exp Neurol* (1999) 58:719–28. doi: 10.1097/00005072-199907000-00006

7. Cayouette M, Smith SB, Becerra SP, Gravel C. Pigment epithelium-derived factor delays the death of photoreceptors in mouse models of inherited retinal degenerations. *Neurobiol Dis* (1999) 6:523–32. doi: 10.1006/nbdi.1999.0263

8. Cao W, Tombran-Tink J, Elias R, Sezate S, Mrazek D, Mcginnis JF. *In Vivo* Protection of photoreceptors from light damage by pigment epithelium-derived factor. *Invest Ophthalmol Vis Sci* (2001) 42:1646–52. doi: 10.1007/978-1-4615-1355-1_14

9. Dawson DW, Volpert OV, Gillis P, Crawford SE, Xu H, Benedict W, et al. Pigment epithelium-derived factor: a potent inhibitor of angiogenesis. *Science* (1999) 285:245–8. doi: 10.1126/science.285.5425.245

10. Franco-Chuaire ML, Ramirez-Clavijo S, Chuaire-Noack L. Pigment epithelium-derived factor: clinical significance in estrogen-dependent tissues and its potential in cancer therapy. *Iran J Basic Med Sci* (2015) 18:837–55. doi: 10.1016/j.mce.2009.12.001

11. Alberdi E, Aymerich MS, Becerra SP. Binding of pigment epithelium-derived factor (PEDF) to retinoblastoma cells and cerebellar granule neurons. evidence for a PEDF receptor. *J Biol Chem* (1999) 274:31605–12. doi: 10.1074/jbc.274.44.31605

12. Broadhead ML, Dass CR, Choong PF. Cancer cell apoptotic pathways mediated by PEDF: prospects for therapy. *Trends Mol Med* (2009) 15:461–7. doi: 10.1016/j.molmed.2009.08.003

13. Karakousis PC, John SK, Behling KC, Surace EM, Smith JE, Hendrickson A, et al. Localization of pigment epithelium derived factor (PEDF) in developing and adult human ocular tissues. *Mol Vis* (2001) 7:154–63. doi: 10.1017/S0952523801184166

14. Niknejad H, Yazdanpanah G, Kakavand M. Extract of fetal membrane would inhibit thrombosis and hemolysis. *Med Hypotheses* (2015) 85:197–202. doi: 10.1016/j.mehy.2015.04.030

15. Behling KC, Surace EM, Bennett J. Pigment epithelium-derived factor expression in the developing mouse eye. *Mol Vis* (2002) 8:449–54. doi: 10.1016/S0960-9822(02)01286-1

16. Sawant S, Aparicio S, Tink AR, Lara N, Barnstable CJ, Tombran-Tink J. Regulation of factors controlling angiogenesis in liver development: a role for PEDF in the formation and maintenance of normal vasculature. *Biochem Biophys Res Commun* (2004) 325:408–13. doi: 10.1016/j.bbrc.2004.10.041

17. Rörby E, Billing M, Dahl M, Warsi S, Andradottir S, Miharada K, et al. The stem cell regulator PEDF is dispensable for maintenance and function of hematopoietic stem cells. *Sci Rep* (2017) 7:10134. doi: 10.1038/s41598-017-09452-2

18. Spranger J, Osterhoff M, Reimann M, Mohlig M, Ristow M, Francis MK, et al. Loss of the antiangiogenic pigment epithelium-derived factor in patients with angiogenic eye disease. *Diabetes* (2001) 50:2641–5. doi: 10.2337/diabetes.50.12.2641

19. Ogata N, Nishikawa M, Nishimura T, Mitsuma Y, Matsumura M. Inverse levels of pigment epithelium-derived factor and vascular endothelial growth factor in the vitreous of eyes with rhegmatogenous retinal detachment and proliferative vitreoretinopathy. *Am J Ophthalmol* (2002) 133:851–2. doi: 10.1016/S0002-9394(02)01406-X

20. Ogata N, Nishikawa M, Nishimura T, Mitsuma Y, Matsumura M. Unbalanced vitreous levels of pigment epithelium-derived factor and vascular endothelial growth factor in diabetic retinopathy. *Am J Ophthalmol* (2002) 134:348–53. doi: 10.1016/S0002-9394(02)01568-4

21. Guan M, Yam HF, Su B, Chan KP, Pang CP, Liu WW, et al. Loss of pigment epithelium derived factor expression in glioma progression. *J Clin Pathol* (2003) 56:277–82. doi: 10.1136/jcp.56.4.277

22. Boehm BO, Lang G, Feldmann B, Kurkhaus A, Rosinger S, Volpert O, et al. Proliferative diabetic retinopathy is associated with a low level of the natural ocular anti-angiogenic agent pigment epithelium-derived factor (PEDF) in aqueous humor. a pilot study. *Horm Metab Res* (2003) 35:382–6. doi: 10.1055/s-2003-41362

23. Boehm BO, Lang G, Volpert O, Jehle PM, Kurkhaus A, Rosinger S, et al. Low content of the natural ocular anti-angiogenic agent pigment epithelium-derived factor (PEDF) in aqueous humor predicts progression of diabetic retinopathy. *Diabetologia* (2003) 46:394–400. doi: 10.1007/s00125-003-1040-9

24. Yokoi M, Yamagishi S, Saito A, Yoshida Y, Matsui T, Saito W, et al. Positive association of pigment epithelium-derived factor with total antioxidant capacity in the vitreous fluid of patients with proliferative diabetic retinopathy. *Br J Ophthalmol* (2007) 91:885–7. doi: 10.1136/bjo.2006.110890

25. Bernard A, Gao-LI J, Franco CA, Bouceba T, Huet A, Li Z. Laminin receptor involvement in the anti-angiogenic activity of pigment epithelium-derived factor. *J Biol Chem* (2009) 284:10480–90. doi: 10.1074/jbc.M809259200

26. He X, Cheng R, Benyajati S, Ma JX. PEDF and its roles in physiological and pathological conditions: implication in diabetic and hypoxia-induced angiogenic diseases. *Clin Sci (Lond)* (2015) 128:805–23. doi: 10.1042/CS20130463

27. Garcia M, Fernandez-Garcia NI, Rivas V, Carretero M, Escamez MJ, Gonzalez-Martin A, et al. Inhibition of xenografted human melanoma growth and prevention of metastasis development by dual antiangiogenic/antitumor activities of pigment epithelium-derived factor. *Cancer Res* (2004) 64:5632–42. doi: 10.1158/0008-5472.CAN-04-0230

28. Yang H, Xu Z, Iuvone PM, Grossniklaus HE. Angiostatin decreases cell migration and vascular endothelium growth factor (VEGF) to pigment epithelium derived factor (PEDF) RNA ratio *in vitro* and in a murine ocular melanoma model. *Mol Vis* (2006) 12:511–7. doi: 10.1016/j.visres.2005.12.018

29. Uehara H, Miyamoto M, Kato K, Ebihara Y, Kaneko H, Hashimoto H, et al. Expression of pigment epithelium-derived factor decreases liver metastasis and correlates with favorable prognosis for patients with ductal pancreatic adenocarcinoma. *Cancer Res* (2004) 64:3533–7. doi: 10.1158/0008-5472.CAN-03-3725

30. Guan M, Jiang H, Xu C, Xu R, Chen Z, Lu Y. Adenovirus-mediated PEDF expression inhibits prostate cancer cell growth and results in augmented expression of PAI-2. *Cancer Biol Ther* (2007) 6:419–25. doi: 10.4161/cbt.6.3.3757

31. Cheung LW, Au SC, Cheung AN, Ngan HY, Tombran-Tink J, Auersperg N, et al. Pigment epithelium-derived factor is estrogen sensitive and inhibits the growth of human ovarian cancer and ovarian surface epithelial cells. *Endocrinology* (2006) 147:4179–91. doi: 10.1210/en.2006-0168

32. Yuan Y, Liu X, Miao H, Huang B, Liu Z, Chen J, et al. PEDF increases GLUT4-mediated glucose uptake in rat ischemic myocardium *via* PI3K/AKT pathway in a PEDFR-dependent manner. *Int J Cardiol* (2019) 283:136–43. doi: 10.1016/j.ijcard.2019.02.035

33. Zhang H, Sun T, Jiang X, Yu H, Wang M, Wei T, et al. PEDF and PEDF-derived peptide 44mer stimulate cardiac triglyceride degradation *via* ATGL. *J Transl Med* (2015) 13:68. doi: 10.1186/s12967-015-0432-1

34. Cosgrove GP, Brown KK, Schiemann WP, Serls AE, Parr JE, Geraci MW, et al. Pigment epithelium-derived factor in idiopathic pulmonary fibrosis: a role in aberrant angiogenesis. *Am J Respir Crit Care Med* (2004) 170:242–51. doi: 10.1164/rccm.200308-1151OC

35. Shiga Y, Miura S, Mitsutake R, Yamagishi S, Saku K. Significance of plasma levels of pigment epithelium-derived factor as determined by multidetector row computed tomography in patients with mild chronic kidney disease and/or coronary artery disease. *J Int Med Res* (2011) 39:880–90. doi: 10.1177/147323001103900322

36. Wang JJ, Zhang SX, Lu K, Chen Y, Mott R, Sato S, et al. Decreased expression of pigment epithelium-derived factor is involved in the pathogenesis of diabetic nephropathy. *Diabetes* (2005) 54:243–50. doi: 10.2337/diabetes.54.1.243

37. Park K, Jin J, Hu Y, Zhou K, Ma JX. Overexpression of pigment epithelium-derived factor inhibits retinal inflammation and neovascularization. *Am J Pathol* (2011) 178:688–98. doi: 10.1016/j.ajpath.2010.10.014

38. Huang Q, Wang S, Sorenson CM, Sheibani N. PEDF-deficient mice exhibit an enhanced rate of retinal vascular expansion and are more sensitive to hyperoxia-mediated vessel obliteration. *Exp Eye Res* (2008) 87:226–41. doi: 10.1016/j.exer.2008.06.003

39. Notari L, Baladron V, Aroca-Aguilar JD, Balko N, Heredia R, Meyer C, et al. Identification of a lipase-linked cell membrane receptor for pigment epithelium-derived factor. *J Biol Chem* (2006) 281:38022–37. doi: 10.1074/jbc.M600353200

40. Park K, Lee K, Zhang B, Zhou T, He X, Gao G, et al. Identification of a novel inhibitor of the canonical wnt pathway. *Mol Cell Biol* (2011) 31:3038–51. doi: 10.1128/MCB.01211-10

41. Cheng G, Zhong M, Kawaguchi R, Kassai M, Al-Ubaidi M, Deng J, et al. Identification of PLXDC1 and PLXDC2 as the transmembrane receptors for the multifunctional factor PEDF. *Elife* (2014) 3:e05401. doi: 10.7554/eLife.05401

42. Deshpande M, Notari L, Subramanian P, Notario V, Becerra SP. Inhibition of tumor cell surface ATP synthesis by pigment epithelium-derived factor: implications for antitumor activity. *Int J Oncol* (2012) 41:219–27. doi: 10.3892/ijo.2012.1431

43. Zhang M, Tombran-Tink J, Yang S, Zhang X, Li X, Barnstable CJ. PEDF is an endogenous inhibitor of VEGF-R2 angiogenesis signaling in endothelial cells. *Exp Eye Res* (2021) 213:108828. doi: 10.1016/j.exer.2021.108828

44. Schweiger M, Schoiswohl G, Lass A, Radner FP, Haemmerle G, Malli R, et al. The c-terminal region of human adipose triglyceride lipase affects enzyme activity and lipid droplet binding. *J Biol Chem* (2008) 283:17211–20. doi: 10.1074/jbc.M710566200

45. Soni KG, Mardones GA, Sougrat R, Smirnova E, Jackson CL, Bonifacino JS. Coatomer-dependent protein delivery to lipid droplets. *J Cell Sci* (2009) 122:1834–41. doi: 10.1242/jcs.045849

46. Ellong EN, Soni KG, Bui QT, Sougrat R, Golinelli-Cohen MP, Jackson CL. Interaction between the triglyceride lipase ATGL and the Arf1 activator GBF1. *PloS One* (2011) 6:e21889. doi: 10.1371/journal.pone.0021889

47. Martinez-Lopez N, Garcia-Macia M, Sahu S, Athonvarangkul D, Liebling E, Merlo P, et al. Autophagy in the CNS and periphery coordinate lipophagy and lipolysis in the brown adipose tissue and liver. *Cell Metab* (2016) 23:113–27. doi: 10.1016/j.cmet.2015.10.008

48. Yang Y, Niswander L. Interaction between the signaling molecules WNT7a and SHH during vertebrate limb development: dorsal signals regulate anteroposterior patterning. *Cell* (1995) 80:939–47. doi: 10.1016/0092-8674(95)90297-X

49. De Ferrari GV, Papassotiropoulos A, Biechele T, Wavrant De-Vrieze ,F, Avila ME, Major MB, et al. Common genetic variation within the low-density lipoprotein receptor-related protein 6 and late-onset alzheimer's disease. *Proc Natl Acad Sci U.S.A.* (2007) 104:9434–9. doi: 10.1073/pnas.0603523104

50. Sarzani R, Salvi F, Bordicchia M, Guerra F, Battistoni I, Pagliariccio G, et al. Carotid artery atherosclerosis in hypertensive patients with a functional LDL receptor-related protein 6 gene variant. *Nutr Metab Cardiovasc Dis* (2011) 21:150–6. doi: 10.1016/j.numecd.2009.08.004

51. Go GW. Low-density lipoprotein receptor-related protein 6 (LRP6) is a novel nutritional therapeutic target for hyperlipidemia, non-alcoholic fatty liver disease, and atherosclerosis. *Nutrients* (2015) 7:4453–64. doi: 10.3390/nu7064453

52. Mani A, Radhakrishnan J, Wang H, Mani A, Mani MA, Nelson-Williams C, et al. LRP6 mutation in a family with early coronary disease and metabolic risk factors. *Science* (2007) 315:1278–82. doi: 10.1126/science.1136370

53. Huertas-Vazquez A, Plaisier C, Weissglas-Volkov D, Sinsheimer J, Canizales-Quinteros S, Cruz-Bautista I, et al. TCF7L2 is associated with high serum triacylglycerol and differentially expressed in adipose tissue in families with familial combined hyperlipidaemia. *Diabetologia* (2008) 51:62–9. doi: 10.1007/s00125-007-0850-6

54. Piao S, Lee SH, Kim H, Yum S, Stamos JL, Xu Y, et al. Direct inhibition of GSK3beta by the phosphorylated cytoplasmic domain of LRP6 in wnt/beta-catenin signaling. *PloS One* (2008) 3:e4046. doi: 10.1371/journal.pone.0004046

55. Liu PH, Chang YC, Jiang YD, Chen WJ, Chang TJ, Kuo SS, et al. Genetic variants of TCF7L2 are associated with insulin resistance and related metabolic phenotypes in Taiwanese adolescents and Caucasian young adults. *J Clin Endocrinol Metab* (2009) 94:3575–82. doi: 10.1210/jc.2009-0609

56. Davies G, Cunnick GH, Mansel RE, Mason MD, Jiang WG. Levels of expression of endothelial markers specific to tumour-associated endothelial cells and their correlation with prognosis in patients with breast cancer. *Clin Exp Metastasis* (2004) 21:31–7. doi: 10.1023/B:CLIN.0000017168.83616.d0

57. Beaty RM, Edwards JB, Boon K, Siu IM, Conway JE, Riggins GJ. PLXDC1 (TEM7) is identified in a genome-wide expression screen of glioblastoma endothelium. *J Neurooncol* (2007) 81:241–8. doi: 10.1007/s11060-006-9227-9

58. Pierce A, Barron N, Linehan R, Ryan E, O'driscoll L, Daly C, et al. Identification of a novel, functional role for S100A13 in invasive lung cancer cell lines. *Eur J Cancer* (2008) 44:151–9. doi: 10.1016/j.ejca.2007.10.017

59. Halder C, Ossendorf C, Maran A, Yaszemski M, Bolander ME, Fuchs B, et al. Preferential expression of the secreted and membrane forms of tumor endothelial marker 7 transcripts in osteosarcoma. *Anticancer Res* (2009) 29:4317–22. doi: 10.1007/978-3-642-72707-8_4

60. Zhang ZZ, Hua R, Zhang JF, Zhao WY, Zhao EH, Tu L, et al. TEM7 (PLXDC1), a key prognostic predictor for resectable gastric cancer, promotes cancer cell migration and invasion. *Am J Cancer Res* (2015) 5:772–81.

61. Li XH, Yang CZ, Wang J. Network spatio-temporal analysis predicts disease stage-related genes and pathways in renal cell carcinoma. *Genet Mol Res* (2016) 15. doi: 10.4238/gmr.15028061

62. Kim GH, Won JE, Byeon Y, Kim MG, Wi TI, Lee JM, et al. Selective delivery of PLXDC1 small interfering RNA to endothelial cells for anti-angiogenesis tumor therapy using CD44-targeted chitosan nanoparticles for epithelial ovarian cancer. *Drug Delivery* (2018) 25:1394–402. doi: 10.1080/10717544.2018.1480672

63. Falchetti ML, D'alessandris QG, Pacioni S, Buccarelli M, Morgante L, Giannetti S, et al. Glioblastoma endothelium drives bevacizumab-induced infiltrative growth *via* modulation of PLXDC1. *Int J Cancer* (2019) 144:1331–44. doi: 10.1002/ijc.31983

64. Pietrzyk L, Wdowiak P. Serum TEM5 and TEM7 concentrations correlate with clinicopathologic features and poor prognosis of colorectal cancer patients. *Adv Med Sci* (2019) 64:402–8. doi: 10.1016/j.advms.2019.07.001

65. Rmali KA, Puntis MC, Jiang WG. Prognostic values of tumor endothelial markers in patients with colorectal cancer. *World J Gastroenterol* (2005) 11:1283–6. doi: 10.3748/wjg.v11.i9.1283

66. Visser R, Gijsbers A, Ruivenkamp C, Karperien M, Reeser HM, Breuning MH, et al. Genome-wide SNP array analysis in patients with features of sotos syndrome. *Horm Res Paediatr* (2010) 73:265–74. doi: 10.1159/000284391

67. Greening DW, Kapp EA, Ji H, Speed TP, Simpson RJ. Colon tumour secretopeptidome: insights into endogenous proteolytic cleavage events in the colon tumour microenvironment. *Biochim Biophys Acta* (2013) 1834:2396–407. doi: 10.1016/j.bbapap.2013.05.006

68. Hosseini SM, Boright AP, Sun L, Canty AJ, Bull SB, Klein BE, et al. The association of previously reported polymorphisms for microvascular complications in a meta-analysis of diabetic retinopathy. *Hum Genet* (2015) 134:247–57. doi: 10.1007/s00439-014-1517-2

69. Kim JS, Kim SY, Lee M, Kim SH, Kim SM, Kim EJ. Radioresistance in a human laryngeal squamous cell carcinoma cell line is associated with DNA methylation changes and topoisomerase II alpha. *Cancer Biol Ther* (2015) 16:558–66. doi: 10.1080/15384047.2015.1017154

70. O'connell GC, Petrone AB, Treadway MB, Tennant CS, Lucke-Wold N, Chantler PD, et al. Machine-learning approach identifies a pattern of gene expression in peripheral blood that can accurately detect ischaemic stroke. *NPJ Genom Med* (2016) 1:16038. doi: 10.1038/npjgenmed.2016.38

71. Li J, Wei J, Xu P, Yan M, Li J, Chen Z, et al. Impact of diabetes-related gene polymorphisms on the clinical characteristics of type 2 diabetes Chinese han population. *Oncotarget* (2016) 7:85464–71. doi: 10.18632/oncotarget.13399

72. Azzam SK, Osman WM, Lee S, Khalaf K, Khandoker AH, Almahmeed W, et al. Genetic associations with diabetic retinopathy and coronary artery disease in emirati patients with type-2 diabetes mellitus. *Front Endocrinol (Lausanne)* (2019) 10:283. doi: 10.3389/fendo.2019.00283

73. Bates M, Spillane CD, Gallagher MF, Mccann A, Martin C, Blackshields G, et al. The role of the MAD2-TLR4-MyD88 axis in paclitaxel resistance in ovarian cancer. *PloS One* (2020) 15:e0243715. doi: 10.1371/journal.pone.0243715

74. Qin G, Mallik S, Mitra R, Li A, Jia P, Eischen CM, et al. MicroRNA and transcription factor co-regulatory networks and subtype classification of seminoma and non-seminoma in testicular germ cell tumors. *Sci Rep* (2020) 10:852. doi: 10.1038/s41598-020-57834-w

75. Pesapane A, Di Giovanni C, Rossi FW, Alfano D, Formisano L, Ragno P, et al. Discovery of new small molecules inhibiting 67 kDa laminin receptor interaction with laminin and cancer cell invasion. *Oncotarget* (2015) 6:18116–33. doi: 10.18632/oncotarget.4016

76. Pesapane A, Ragno P, Selleri C, Montuori N. Recent advances in the function of the 67 kDa laminin receptor and its targeting for personalized therapy in cancer. *Curr Pharm Des* (2017) 23:4745–57. doi: 10.2174/1381612823666170710125332

77. Champagne E, Martinez LO, Collet X, Barbaras R. Ecto-F1Fo ATP synthase/F1 ATPase: metabolic and immunological functions. *Curr Opin Lipidol* (2006) 17:279–84. doi: 10.1097/01.mol.0000226120.27931.76

78. Ikeda E, Achen MG, Breier G, Risau W. Hypoxia-induced transcriptional activation and increased mRNA stability of vascular endothelial growth factor in C6 glioma cells. *J Biol Chem* (1995) 270:19761–6. doi: 10.1074/jbc.270.34.19761

79. Forsythe JA, Jiang BH, Iyer NV, Agani F, Leung SW, Koos RD, et al. Activation of vascular endothelial growth factor gene transcription by hypoxia-inducible factor 1. *Mol Cell Biol* (1996) 16:4604–13. doi: 10.1128/MCB.16.9.4604

80. Schreiber R, Xie H, Schweiger M. Of mice and men: the physiological role of adipose triglyceride lipase (ATGL). *Biochim Biophys Acta Mol Cell Biol Lipids* (2019) 1864:880–99. doi: 10.1016/j.bbalip.2018.10.008

81. Zimmermann R, Strauss JG, Haemmerle G, Schoiswohl G, Birner-Gruenberger R, Riederer M, et al. Fat mobilization in adipose tissue is promoted by adipose triglyceride lipase. *Science* (2004) 306:1383–6. doi: 10.1126/science.1100747

82. Jenkins CM, Mancuso DJ, Yan W, Sims HF, Gibson B, Gross RW. Identification, cloning, expression, and purification of three novel human calcium-independent phospholipase A2 family members possessing triacylglycerol lipase and acylglycerol transacylase activities. *J Biol Chem* (2004) 279:48968–75. doi: 10.1074/jbc.M407841200

83. Villena JA, Roy S, Sarkadi-Nagy E, Kim KH, Sul HS. Desnutrin, an adipocyte gene encoding a novel patatin domain-containing protein, is induced by fasting and glucocorticoids: ectopic expression of desnutrin increases triglyceride hydrolysis. *J Biol Chem* (2004) 279:47066–75. doi: 10.1074/jbc.M403855200

84. Jocken JW, Smit E, Goossens GH, Essers YP, Van Baak MA , Mensink M, et al. Adipose triglyceride lipase (ATGL) expression in human skeletal muscle istype I (oxidative) fiber specific. *Histochem Cell Biol* (2008) 129:535–8. doi: 10.1007/s00418-008-0386-y

85. Kienesberger PC, Pulinilkunnil T, Sung MM, Nagendran J, Haemmerle G, Kershaw EE, et al. Myocardial ATGL overexpression decreases the reliance on fatty acid oxidation and protects against pressure overload-induced cardiac dysfunction. *Mol Cell Biol* (2012) 32:740–50. doi: 10.1128/MCB.06470-11

86. Ong KT, Mashek MT, Bu SY, Greenberg AS, Mashek DG. Adipose triglyceride lipase is a major hepatic lipase that regulates triacylglycerol turnover and fatty acid signaling and partitioning. *Hepatology* (2011) 53:116–26. doi: 10.1002/hep.24006

87. Al-Zoughbi W, Pichler M, Gorkiewicz G, Guertl-Lackner B, Haybaeck J, Jahn SW, et al. Loss of adipose triglyceride lipase is associated with human cancer and induces mouse pulmonary neoplasia. *Oncotarget* (2016) 7:33832–40. doi: 10.18632/oncotarget.9418

88. Desjardin JT, Becerra SP, Subramanian P. Searching for alternatively spliced variants of phospholipase domain-containing 2 (Pnpla2), a novel gene in the retina. *J Clin Exp Ophthalmol* (2013) 4:295. doi: 10.4172/2155-9570.1000295

89. Subramanian P, Notario PM, Becerra SP. Pigment epithelium-derived factor receptor (PEDF-r): a plasma membrane-linked phospholipase with PEDF binding affinity. *Adv Exp Med Biol* (2010) 664:29–37. doi: 10.1007/978-1-4419-1399-9_4

90. Rydel TJ, Williams JM, Krieger E, Moshiri F, Stallings WC, Brown SM, et al. The crystal structure, mutagenesis, and activity studies reveal that patatin is a lipid acyl hydrolase with a ser-asp catalytic dyad. *Biochemistry* (2003) 42:6696–708. doi: 10.1021/bi027156r

91. Yamaguchi T, Omatsu N, Morimoto E, Nakashima H, Ueno K, Tanaka T, et al. CGI-58 facilitates lipolysis on lipid droplets but is not involved in the vesiculation of lipid droplets caused by hormonal stimulation. *J Lipid Res* (2007) 48:1078–89. doi: 10.1194/jlr.M600493-JLR200

92. Eichmann TO, Kumari M, Haas JT, Farese RV, Jr., Zimmermann, R., Lass A, et al. Studies on the substrate and stereo/regioselectivity of adipose triglyceride lipase, hormone-sensitive lipase, and diacylglycerol-o-acyltransferases. *J Biol Chem* (2012) 287:41446–57. doi: 10.1074/jbc.M112.400416

93. Hofer P, Boeszoermenyi A, Jaeger D, Feiler U, Arthanari H, Mayer N, et al. Fatty acid-binding proteins interact with comparative gene identification-58 linking lipolysis with lipid ligand shuttling. *J Biol Chem* (2015) 290:18438–53. doi: 10.1074/jbc.M114.628958

94. Olzmann JA, Richter CM, Kopito RR. Spatial regulation of UBXD8 and p97/VCP controls ATGL-mediated lipid droplet turnover. *Proc Natl Acad Sci U.S.A.* (2013) 110:1345–50. doi: 10.1073/pnas.1213738110

95. Cornaciu I, Boeszoermenyi A, Lindermuth H, Nagy HM, Cerk IK, Ebner C, et al. The minimal domain of adipose triglyceride lipase (ATGL) ranges until leucine 254 and can be activated and inhibited by CGI-58 and G0S2, respectively. *PloS One* (2011) 6: e26349. doi: 10.1371/journal.pone.0026349

96. Yang X, Lu X, Lombes M, Rha GB, Chi YI, Guerin TM, et al. The G(0)/G(1) switch gene 2 regulates adipose lipolysis through association with adipose triglyceride lipase. *Cell Metab* (2010) 11:194–205. doi: 10.1016/j.cmet.2010.02.003

97. Zhang X, Saarinen AM, Hitosugi T, Wang Z, Wang L, Ho TH, et al. Inhibition of intracellular lipolysis promotes human cancer cell adaptation to hypoxia. *Elife* (2017) 6. doi: 10.7554/eLife.31132

98. Padmanabha Das KM, Wechselberger L, Liziczai M, De La Rosa Rodriguez M, Grabner GF, Heier C, et al. Hypoxia-inducible lipid droplet-associated protein inhibits adipose triglyceride lipase. *J Lipid Res* (2018) 59:531–41. doi: 10.1194/jlr.M082388

99. Niyogi S, Ghosh M, Adak M, Chakrabarti P. PEDF promotes nuclear degradation of ATGL through COP1. *Biochem Biophys Res Commun* (2019) 512:806–11. doi: 10.1016/j.bbrc.2019.03.111

100. Yang Z, Sun J, Ji H, Shi XC, Li Y, Du ZY, et al. Pigment epithelium-derived factor improves TNFalpha-induced hepatic steatosis in grass carp (Ctenopharyngodon idella). *Dev Comp Immunol* (2017) 71:8–17. doi: 10.1016/j.dci.2017.01.016

101. He T, Hu J, Yan G, Li L, Zhang D, Zhang Q, et al. Pigment epithelium-derived factor regulates microvascular permeability through adipose triglyceride lipase in sepsis. *Clin Sci (Lond)* (2015) 129:49–61. doi: 10.1042/CS20140631

102. Schweiger M, Paar M, Eder C, Brandis J, Moser E, Gorkiewicz G, et al. G0/G1 switch gene-2 regulates human adipocyte lipolysis by affecting activity and localization of adipose triglyceride lipase. *J Lipid Res* (2012) 53:2307–17. doi: 10.1194/jlr.M027409

103. Albert JS, Yerges-Armstrong LM, Horenstein RB, Pollin TI, Sreenivasan UT, Chai S, et al. Null mutation in hormone-sensitive lipase gene and risk of type 2 diabetes. *N Engl J Med* (2014) 370:2307–15. doi: 10.1056/NEJMoa1315496

104. Kim JY, Tillison K, Lee JH, Rearick DA, Smas CM. The adipose tissue triglyceride lipase ATGL/PNPLA2 is downregulated by insulin and TNF-alpha in 3T3-L1 adipocytes and is a target for transactivation by PPARgamma. *Am J Physiol Endocrinol Metab* (2006) 291:E115–27. doi: 10.1152/ajpendo.00317.2005

105. Chakrabarti P, English T, Karki S, Qiang L, Tao R, Kim J, et al. SIRT1 controls lipolysis in adipocytes *via* FOXO1-mediated expression of ATGL. *J Lipid Res* (2011) 52:1693–701. doi: 10.1194/jlr.M014647

106. Chakrabarti P, Kandror KV. FoxO1 controls insulin-dependent adipose triglyceride lipase (ATGL) expression and lipolysis in adipocytes. *J Biol Chem* (2009) 284:13296–300. doi: 10.1074/jbc.C800241200

107. Pagnon J, Matzaris M, Stark R, Meex RC, Macaulay SL, Brown W, et al. Identification and functional characterization of protein kinase a phosphorylation sites in the major lipolytic protein, adipose triglyceride lipase. *Endocrinology* (2012) 153:4278–89. doi: 10.1210/en.2012-1127

108. Kim SJ, Tang T, Abbott M, Viscarra JA, Wang Y, Sul HS. AMPK phosphorylates Desnutrin/ATGL and hormone-sensitive lipase to regulate lipolysis and fatty acid oxidation within adipose tissue. *Mol Cell Biol* (2016) 36:1961–76. doi: 10.1128/MCB.00244-16

109. Grahn THM, Kaur R, Yin J, Schweiger M, Sharma VM, Lee MJ, et al. Fat-specific protein 27 (FSP27) interacts with adipose triglyceride lipase (ATGL) to regulate lipolysis and insulin sensitivity in human adipocytes. *J Biol Chem* (2014) 289:12029–39. doi: 10.1074/jbc.M113.539890

110. Singh M, Kaur R, Lee MJ, Pickering RT, Sharma VM, Puri V, et al. Fat-specific protein 27 inhibits lipolysis by facilitating the inhibitory effect of transcription factor Egr1 on transcription of adipose triglyceride lipase. *J Biol Chem* (2014) 289:14481–7. doi: 10.1074/jbc.C114.563080

111. Brown SD, Twells RC, Hey PJ, Cox RD, Levy ER, Soderman AR, et al. Isolation and characterization of LRP6, a novel member of the low density lipoprotein receptor gene family. *Biochem Biophys Res Commun* (1998) 248:879–88. doi: 10.1006/bbrc.1998.9061

112. Dieckmann M, Dietrich MF, Herz J. Lipoprotein receptors–an evolutionarily ancient multifunctional receptor family. *Biol Chem* (2010) 391:1341–63. doi: 10.1515/bc.2010.129

113. Hey PJ, Twells RC, Phillips MS, Yusuke N, Brown SD, Kawaguchi Y, et al. Cloning of a novel member of the low-density lipoprotein receptor family. *Gene* (1998) 216:103–11. doi: 10.1016/S0378-1119(98)00311-4

114. Kelly OG, Pinson KI, Skarnes WC. The wnt co-receptors Lrp5 and Lrp6 are essential for gastrulation in mice. *Development* (2004) 131:2803–15. doi: 10.1242/dev.01137

115. Wang ZM, Luo JQ, Xu LY, Zhou HH, Zhang W. Harnessing low-density lipoprotein receptor protein 6 (LRP6) genetic variation and wnt signaling for innovative diagnostics in complex diseases. *Pharmacogenomics J* (2018) 18:351–8. doi: 10.1038/tpj.2017.28

116. Macdonald BT, Tamai K, He X. Wnt/beta-catenin signaling: components, mechanisms, and diseases. *Dev Cell* (2009) 17:9–26. doi: 10.1016/j.devcel.2009.06.016

117. Zhong Z, Baker JJ, Zylstra-Diegel CR, Williams BO. Lrp5 and Lrp6 play compensatory roles in mouse intestinal development. *J Cell Biochem* (2012) 113:31–8. doi: 10.1002/jcb.23324

118. Joiner DM, Ke J, Zhong Z, Xu HE, Williams BO. LRP5 and LRP6 in development and disease. *Trends Endocrinol Metab* (2013) 24:31–9. doi: 10.1016/j.tem.2012.10.003

119. Cheng Z, Biechele T, Wei Z, Morrone S, Moon RT, Wang L, et al. Crystal structures of the extracellular domain of LRP6 and its complex with DKK1. *Nat Struct Mol Biol* (2011) 18:1204–10. doi: 10.1038/nsmb.2139

120. Pinson KI, Brennan J, Monkley S, Avery BJ, Skarnes WC. An LDL-receptor-related protein mediates wnt signalling in mice. *Nature* (2000) 407:535–8. doi: 10.1038/35035124

121. Liu CC, Tsai CW, Deak F, Rogers J, Penuliar M, Sung YM, et al. Deficiency in LRP6-mediated wnt signaling contributes to synaptic abnormalities and amyloid pathology in alzheimer's disease. *Neuron* (2014) 84:63–77. doi: 10.1016/j.neuron.2014.08.048

122. Davidson G, Wu W, Shen J, Bilic J, Fenger U, Stannek P, et al. Casein kinase 1 gamma couples wnt receptor activation to cytoplasmic signal transduction. *Nature* (2005) 438:867–72. doi: 10.1038/nature04170

123. Niehrs C, Shen J. Regulation of Lrp6 phosphorylation. *Cell Mol Life Sci* (2010) 67:2551–62. doi: 10.1007/s00018-010-0329-3

124. Davidson G, Shen J, Huang YL, Su Y, Karaulanov E, Bartscherer K, et al. Cell cycle control of wnt receptor activation. *Dev Cell* (2009) 17:788–99. doi: 10.1016/j.devcel.2009.11.006

125. Niehrs C, Acebron SP. Mitotic and mitogenic wnt signalling. *EMBO J* (2012) 31:2705–13. doi: 10.1038/emboj.2012.124

126. Huang YL, Anvarian Z, Doderlein G, Acebron SP, Niehrs C. Maternal Wnt/STOP signaling promotes cell division during early xenopus embryogenesis. *Proc Natl Acad Sci USA* (2015) 112:5732–7. doi: 10.1073/pnas.1423533112

127. Koch S, Acebron SP, Herbst J, Hatiboglu G, Niehrs C. Post-transcriptional wnt signaling governs epididymal sperm maturation. *Cell* (2015) 163:1225–36. doi: 10.1016/j.cell.2015.10.029

128. Aberle H, Bauer A, Stappert J, Kispert A, Kemler R. Beta-catenin is a target for the ubiquitin-proteasome pathway. *EMBO J* (1997) 16:3797–804. doi: 10.1093/emboj/16.13.3797

129. Niehrs C, Acebron SP. Wnt signaling: multivesicular bodies hold GSK3 captive. *Cell* (2010) 143:1044–6. doi: 10.1016/j.cell.2010.12.003

130. Taelman VF, Dobrowolski R, Plouhinec JL, Fuentealba LC, Vorwald PP, Gumper I, et al. Wnt signaling requires sequestration of glycogen synthase kinase 3 inside multivesicular endosomes. *Cell* (2010) 143:1136–48. doi: 10.1016/j.cell.2010.11.034

131. Stamos JL, Weis WI. The beta-catenin destruction complex. *Cold Spring Harb Perspect Biol* (2013) 5:a007898. doi: 10.1101/cshperspect.a007898

132. Vinyoles M, Del Valle-Perez B, Curto J, Vinas-Castells R, Alba-Castellon L, Garcia, et al. Multivesicular GSK3 sequestration upon wnt signaling is controlled by p120-catenin/cadherin interaction with LRP5/6. *Mol Cell* (2014) 53:444–57. doi: 10.1016/j.molcel.2013.12.010

133. Acebron SP, Niehrs C. Beta-Catenin-Independent roles of Wnt/LRP6 signaling. *Trends Cell Biol* (2016) 26:956–67. doi: 10.1016/j.tcb.2016.07.009

134. Logan CY, Nusse R. The wnt signaling pathway in development and disease. *Annu Rev Cell Dev Biol* (2004) 20:781–810. doi: 10.1146/annurev.cellbio.20.010403.113126

135. Bilic J, Huang YL, Davidson G, Zimmermann T, Cruciat CM, Bienz M, et al. Wnt induces LRP6 signalosomes and promotes dishevelled-dependent LRP6 phosphorylation. *Science* (2007) 316:1619–22. doi: 10.1126/science.1137065

136. Zeng X, Tamai K, Doble B, Li S, Huang H, Habas R, et al. A dual-kinase mechanism for wnt co-receptor phosphorylation and activation. *Nature* (2005) 438:873–7. doi: 10.1038/nature04185

137. Mao B, Wu W, Li Y, Hoppe D, Stannek P, Glinka A, et al. LDL-receptor-related protein 6 is a receptor for dickkopf proteins. *Nature* (2001) 411:321–5. doi: 10.1038/35077108

138. Kim KA, Zhao J, Andarmani S, Kakitani M, Oshima T, Binnerts ME, et al. R-spondin proteins: a novel link to beta-catenin activation. *Cell Cycle* (2006) 5:23–6. doi: 10.4161/cc.5.1.2305

139. Ye X, Wang Y, Cahill H, Yu M, Badea TC, Smallwood PM, et al. Norrin, frizzled-4, and Lrp5 signaling in endothelial cells controls a genetic program for retinal vascularization. *Cell* (2009) 139:285–98. doi: 10.1016/j.cell.2009.07.047

140. Hanai J, Gloy J, Karumanchi SA, Kale S, Tang J, Hu G, et al. Endostatin is a potential inhibitor of wnt signaling. *J Cell Biol* (2002) 158:529–39. doi: 10.1083/jcb.200203064

141. Chen Y, Hu Y, Lu K, Flannery JG, Ma JX. Very low density lipoprotein receptor, a negative regulator of the wnt signaling pathway and choroidal neovascularization. *J Biol Chem* (2007) 282:34420–8. doi: 10.1074/jbc.M611289200

142. Lee K, Shin Y, Cheng R, Park K, Hu Y, Mcbride J, et al. Receptor heterodimerization as a novel mechanism for the regulation of wnt/beta-catenin signaling. *J Cell Sci* (2014) 127:4857–69. doi: 10.1242/jcs.149302

143. Carson-Walter EB, Watkins DN, Nanda A, Vogelstein B, Kinzler KW, St Croix B. Cell surface tumor endothelial markers are conserved in mice and humans. *Cancer Res* (2001) 61:6649–55.

144. Bagley RG, Rouleau C, Weber W, Mehraein K, Smale R, Curiel M, et al. Tumor endothelial marker 7 (TEM-7): a novel target for antiangiogenic therapy. *Microvasc Res* (2011) 82:253–62. doi: 10.1016/j.mvr.2011.09.004

145. Yamaji Y, Yoshida S, Ishikawa K, Sengoku A, Sato K, Yoshida A, et al. TEM7 (PLXDC1) in neovascular endothelial cells of fibrovascular membranes from patients with proliferative diabetic retinopathy. *Invest Ophthalmol Vis Sci* (2008) 49:3151–7. doi: 10.1167/iovs.07-1249

146. Nanda A, Buckhaults P, Seaman S, Agrawal N, Boutin P, Shankara S, et al. Identification of a binding partner for the endothelial cell surface proteins TEM7 and TEM7R. *Cancer Res* (2004) 64:8507–11. doi: 10.1158/0008-5472.CAN-04-2716

147. Gaultier A, Simon G, Niessen S, Dix M, Takimoto S, 3rd Cravatt BF, et al. LDL receptor-related protein 1 regulates the abundance of diverse cell-signaling proteins in the plasma membrane proteome. *J Proteome Res* (2010) 9:6689–95. doi: 10.1021/pr1008288

148. Lee HK, Seo IA, Park HK, Park HT. Identification of the basement membrane protein nidogen as a candidate ligand for tumor endothelial marker 7 *in vitro* and *in vivo*. *FEBS Lett* (2006) 580:2253–7. doi: 10.1016/j.febslet.2006.03.033

149. Miller SF, Summerhurst K, Runker AE, Kerjan G, Friedel RH, Chedotal A, et al. Expression of Plxdc2/TEM7R in the developing nervous system of the mouse. *Gene Expr Patterns* (2007) 7:635–44. doi: 10.1016/j.modgep.2006.12.002

150. Yamamoto N, Eguchi A, Hirokawa Y, Ogura S, Sugimoto K, Iwasa M, et al. Expression pattern of plexin domain containing 2 in human hepatocellular carcinoma. *Monoclon Antib Immunodiagn Immunother* (2020) 39:57–60. doi: 10.1089/mab.2019.0050

151. Miller-Delaney SF, Lieberam I, Murphy P, Mitchell KJ. Plxdc2 is a mitogen for neural progenitors. *PloS One* (2011) 6:e14565. doi: 10.1371/journal.pone.0014565

152. Schwarze SR, Fu VX, Desotelle JA, Kenowski ML, Jarrard DF. The identification of senescence-specific genes during the induction of senescence in prostate cancer cells. *Neoplasia* (2005) 7:816–23. doi: 10.1593/neo.05250

153. Bianchi E, Sun Y, Almansa-Ordonez A, Woods M, Goulding D, Martinez-Martin N, et al. Control of oviductal fluid flow by the G-protein coupled receptor Adgrd1 is essential for murine embryo transit. *Nat Commun* (2021) 12:1251. doi: 10.1038/s41467-021-21512-w

154. Digiacomo V, Meruelo D. Looking into laminin receptor: critical discussion regarding the non-integrin 37/67-kDa laminin receptor/RPSA protein. *Biol Rev Camb Philos Soc* (2016) 91:288–310. doi: 10.1111/brv.12170

155. Gong Q, Qiu S, Li S, Ma Y, Chen M, Yao Y, et al. Proapoptotic PEDF functional peptides inhibit prostate tumor growth–a mechanistic study. *Biochem Pharmacol* (2014) 92:425–37. doi: 10.1016/j.bcp.2014.09.012

156. Koch S, Claesson-Welsh L. Signal transduction by vascular endothelial growth factor receptors. *Cold Spring Harb Perspect Med* (2012) 2:a006502. doi: 10.1101/cshperspect.a006502

157. Smith GA, Fearnley GW, Tomlinson DC, Harrison MA, Ponnambalam S. The cellular response to vascular endothelial growth factors requires co-ordinated signal transduction, trafficking and proteolysis. *Biosci Rep* (2015) 35. doi: 10.1042/BSR20150171

158. Peach CJ, Mignone VW, Arruda MA, Alcobia DC, Hill SJ, Kilpatrick LE, et al. Molecular pharmacology of VEGF-a isoforms: binding and signalling at VEGFR2. *Int J Mol Sci* (2018) 19. doi: 10.3390/ijms19041264

159. Kabrun N, Buhring HJ, Choi K, Ullrich A, Risau W, Keller G. Flk-1 expression defines a population of early embryonic hematopoietic precursors. *Development* (1997) 124:2039–48. doi: 10.1242/dev.124.10.2039

160. Ishida A, Murray J, Saito Y, Kanthou C, Benzakour O, Shibuya M, et al. Expression of vascular endothelial growth factor receptors in smooth muscle cells. *J Cell Physiol* (2001) 188:359–68. doi: 10.1002/jcp.1121

161. Witmer AN, Dai J, Weich HA, Vrensen GF, Schlingemann RO. Expression of vascular endothelial growth factor receptors 1, 2, and 3 in quiescent endothelia. *J Histochem Cytochem* (2002) 50:767–77. doi: 10.1177/002215540205000603

162. Simons M, Gordon E, Claesson-Welsh L. Mechanisms and regulation of endothelial VEGF receptor signalling. *Nat Rev Mol Cell Biol* (2016) 17:611–25. doi: 10.1038/nrm.2016.87

163. Leppanen VM, Prota AE, Jeltsch M, Anisimov A, Kalkkinen N, Strandin T, et al. Structural determinants of growth factor binding and specificity by VEGF receptor 2. *Proc Natl Acad Sci USA* (2010) 107:2425–30. doi: 10.1073/pnas.0914318107

164. Brozzo MS, Bjelic S, Kisko K, Schleier T, Leppanen VM, Alitalo K, et al. Thermodynamic and structural description of allosterically regulated VEGFR-2 dimerization. *Blood* (2012) 119:1781–8. doi: 10.1182/blood-2011-11-390922

165. Shweiki D, Itin A, Soffer D, Keshet E. Vascular endothelial growth factor induced by hypoxia may mediate hypoxia-initiated angiogenesis. *Nature* (1992) 359:843–5. doi: 10.1038/359843a0

166. Mcmahon G. VEGF receptor signaling in tumor angiogenesis. *Oncologist* (2000) 5 Suppl 1:3–10. doi: 10.1634/theoncologist.5-suppl_1-3

167. Zhang SX, Wang JJ, Gao G, Parke K, Ma JX. Pigment epithelium-derived factor downregulates vascular endothelial growth factor (VEGF) expression and inhibits VEGF-VEGF receptor 2 binding in diabetic retinopathy. *J Mol Endocrinol* (2006) 37:1–12. doi: 10.1677/jme.1.02008

168. Shahbazi B, Arab SS, Mafakher L, Azadmansh K, Teimoori-Toolabi L. Computational assessment of pigment epithelium-derived factor as an anti-cancer protein during its interaction with the receptors. *J Biomol Struct Dyn* (2022), 1–17. doi: 10.1080/07391102.2022.2069863

169. Nirody JA, Budin I, Rangamani P. ATP synthase: evolution, energetics, and membrane interactions. *J Gen Physiol* (2020) 152. doi: 10.1085/jgp.201912475

170. Notari L, Arakaki N, Mueller D, Meier S, Amaral J, Becerra SP. Pigment epithelium-derived factor binds to cell-surface F(1)-ATP synthase. *FEBS J* (2010) 277:2192–205. doi: 10.1111/j.1742-4658.2010.07641.x

171. Qiu F, Zhang H, Yuan Y, Liu Z, Huang B, Miao H, et al. A decrease of ATP production steered by PEDF in cardiomyocytes with oxygen-glucose deprivation is associated with an AMPK-dependent degradation pathway. *Int J Cardiol* (2018) 257:262–71. doi: 10.1016/j.ijcard.2018.01.034

172. Zheng B, Li T, Chen H, Xu X, Zheng Z. Correlation between ficolin-3 and vascular endothelial growth factor-to-pigment epithelium-derived factor ratio in the vitreous of eyes with proliferative diabetic retinopathy. *Am J Ophthalmol* (2011) 152:1039–43. doi: 10.1016/j.ajo.2011.05.022

173. Wang Y, Lu Q, Gao S, Zhu Y, Gao Y, Xie B, et al. Pigment epithelium-derived factor regulates glutamine synthetase and l-glutamate/l-aspartate transporter in retinas with oxygen-induced retinopathy. *Curr Eye Res* (2015) 40:1232–44. doi: 10.3109/02713683.2014.990639

174. Holekamp NM, Bouck N, Volpert O. Pigment epithelium-derived factor is deficient in the vitreous of patients with choroidal neovascularization due to age-related macular degeneration. *Am J Ophthalmol* (2002) 134:220–7. doi: 10.1016/S0002-9394(02)01549-0

175. Abu El-Asrar AM, Imtiaz Nawaz M, Kangave D, Siddiquei MM, Geboes K. Osteopontin and other regulators of angiogenesis and fibrogenesis in the vitreous from patients with proliferative vitreoretinal disorders. *Mediators Inflammation* (2012) 2012:493043. doi: 10.1155/2012/493043

176. Sheibani N, Wang S, Darjatmoko SR, Fisk DL, Shahi PK, Pattnaik BR, et al. Novel anti-angiogenic PEDF-derived small peptides mitigate choroidal neovascularization. *Exp Eye Res* (2019) 188:107798. doi: 10.1016/j.exer.2019.107798

177. Sheibani N, Zaitoun IS, Wang S, Darjatmoko SR, Suscha A, Song YS, et al. Inhibition of retinal neovascularization by a PEDF-derived nonapeptide in newborn mice subjected to oxygen-induced ischemic retinopathy. *Exp Eye Res* (2020) 195:108030. doi: 10.1016/j.exer.2020.108030

10.3389/fendo.2023.1116136

Glossary

ABHD5	α/β hydrolase domain-containing 5
AD	Alzheimer's disease
ADCAD2	Coronary Artery Disease, Autosomal Dominant 2
ADGRD1	Adhesion G-protein coupled receptor D1
AMPK	Adenosine 5'-monophosphate-activated protein kinase
APC	Adenomatous Polyposis Coli
APP	Amyloid precursor protein
ATGL	Adipose triglyceride lipase
ATP5F1	ATP Synthase F1
BAT	Brown adipose tissue
BMP-4	Bone morphogenesis protein 4
CAD	Coronary artery disease
CCNY/CCNYL1	Cyclin Y and cyclin Y-like 1
CD309	Cluster of Differentiation 309
CDK14	Cyclin-dependent kinase 14
CHO	Chinese hamster ovary
Chr	Chromosome
CK1γ	Casein kinase 1γ
CKIa	Casein kinase Ia
CNV	Choroidal neovascularization
COP1	Constitutive photomorphogenic 1
D2	Domains 2
DKK-1	Dickkopf-1
Dvl	Dishevelled
E	Embryonic day
EE	Energy expenditure
EGF-like	Epidermal growth factor-like
F0-ATPase	F0-ATP Synthase
FAs	Fatty acids
FGF	Fibroblast growth factor
Flk-1	Fetal Liver Kinase 1
FoxO1	Forkhead box protein O1
Fsp27	Fat specific protein 27
Fzd	Frizzled
G0S2	G0/G1 Switch 2
GCL	Ganglion cell layer
GSK3	Glycogen synthase kinase 3
HCC	Human hepatocellular carcinoma

(Continued)

Continued

HIG2	Hypoxia-induced Gene 2
HIG2	Hypoxia-inducible gene 2
hLRP6	human LRP6
HSCs	Hematopoietic stem cells
HSL	Hormone-sensitive lipase
Ig	Immunoglobulin
IL-10	interleukin-10
iPLA2ζ	Independent Phospholipase A2-ζ
JNK	Jun N-terminal kinase
KDR	Kinase Insert Domain Receptor
LAMR	Laminin Receptor
LC3	Light Chain 3
LDLR	Low-density lipoprotein receptor
LDs	Lipid droplets
LPA	Lysophosphatidic acid
LR	Laminin receptor
LRP1	Laminin Receptor Protein 1
LRP6	Lipoprotein receptor-related protein 6
MD	Molecular dynamics
MM	Molecular mechanics
MMP2	Matrix metallopeptidase 2
nAMD	neovascular age-related macular degeneration
NEFA	Non-esterified fatty acids
NFκB	Nuclear factor κB
NV	neovascularization
OIR	Oxygen-induced retinopathy
PBSA	Poisson-Boltzmann surface area
PEDF	Pigment epithelium-derived factor
PKA	Protein kinase A
PLA2	Phospholipase A2
PLXDC	Plexin domain containing
PNPL2	Patatin-Like Phospholipase Domain Containing 2
PNPLA2	Patatin-like phospholipase domain-containing protein 2
PPARs	Peroxisome proliferators-activated receptors
PPAR-γ	Proliferator-activated receptor-γ
PVR	Proliferative vitreoretinopathy
RAO	Retinal artery occlusion
RCL	Reactive center loop
RGCs	Retinal ganglion cells
RNV	Retinal neovascularization

(Continued)

Continued

ROP	Retinopathy of prematurity
RPE	Retinal pigment epithelial
RPSA	Ribosomal Protein SA
RSPO	R-sponge protein
RVO	Retinal vein occlusion
RXR	Retinoid X receptor
SERPINF1	Serpin family F member 1
SERPINS	Serine protease inhibitor superfamily
SNP	Single nucleotide polymorphism
STHAG7	Selective Tooth Agenesis 7
TAG	Triacylglycerols
TEM3	Tumor Endothelial Marker 3
TEM7	Tumor Endothelial Marker 7
TEM7R	Tumor Endothelial Marker 7-Related Protein
TGs	Triglycerides
TNF-α	Tumor necrosis factor-α
UBXD8	Ubiquitin regulatory X domain-containing protein 8
VEGF	Vascular endothelial growth factor
VEGFA	Vascular Endothelial Growth Factor 1
VEGFR2	Vascular endothelial growth factor receptor 2
WAT	White adipose tissue
β-TrCP	β-transducin repeat-containing protein

frontiers | Frontiers in Endocrinology

TYPE Original Research
PUBLISHED 08 May 2023
DOI 10.3389/fendo.2023.1143535

OPEN ACCESS

EDITED BY
Mohd Imtiaz Nawaz,
King Saud University, Saudi Arabia

REVIEWED BY
Sudhanshu Kumar Bharti,
Patna University, India
Juan Wang,
Tongji University, China

*CORRESPONDENCE
Wentao Dong
stef.dongwentao@126.com
Jie Li
doctorjacklee@163.com
Jie Zhong
zhongjie@med.uestc.edu.cn

†These authors have contributed equally to this work and share first authorship

RECEIVED 13 January 2023
ACCEPTED 12 April 2023
PUBLISHED 08 May 2023

CITATION
Zeng Y, Liu M, Li M, Wei D, Mao M, Liu X, Chen S, Liu Y, Chen B, Yang L, Liu S, Qiao L, Zhang R, Li J, Dong W and Zhong J (2023) Early changes to retinal structure in patients with diabetic retinopathy as determined by ultrawide swept-source optical coherence tomography-angiography. *Front. Endocrinol.* 14:1143535. doi: 10.3389/fendo.2023.1143535

Early changes to retinal structure in patients with diabetic retinopathy as determined by ultrawide swept-source optical coherence tomography-angiography

Yong Zeng[1,2†], Miao Liu[1,2†], Mengyu Li[1,2], Dinyang Wei[1,2], Mingzhu Mao[1,2], Xinyue Liu[1,2], Sizhu Chen[1,2], Yang Liu[3], Bo Chen[1,2], Lei Yang[4], Sanmei Liu[1,2], Lifeng Qiao[1,2], Ruifan Zhang[1,2], Jie Li[1,2*], Wentao Dong[1,2*] and Jie Zhong[1,2*]

[1]Department of Ophthalmology, Sichuan Provincial People's Hospital, University of Electronic Science and Technology of China, Chengdu, China, [2]Department of Ophthalmology, Chinese Academy of Sciences Sichuan Translational Medicine Research Hospital, Chengdu, China, [3]Jinniu Maternity and Child Health Hospital of Chengdu, Department of Child Healthcare, Chengdu, China, [4]Department of Pulmonary and Critical Care Medicine, Enyang District People's Hospital of Bazhong, Bazhong, Sichuan, China

Purpose: To investigate retinal vascular changes in patients with diabetic retinopathy (DR) using the newly developed ultrawide rapid scanning swept-source optical coherence tomography angiography (SS-OCTA) device.

Methods: This cross-sectional, observational study enrolled 24 patients (47 eyes) with DR, 45 patients (87 eyes) with diabetes mellitus (DM) without DR, and 36 control subjects (71 eyes). All subjects underwent 24 × 20 mm SS-OCTA examination. Vascular density (VD) and the thickness of the central macula (CM; 1 mm diameter) and temporal fan-shaped areas of 1–3 mm (T3), 3–6 mm (T6), 6–11 mm (T11), 11–16 mm (T16), and 16–21 mm (T21) were compared among groups. The VD and the thicknesses of the superficial vascular complex (SVC) and deep vascular complex (DVC) were analyzed separately. The predictive values of VD and thickness changes in DM and DR patients were evaluated by receiver operating characteristic (ROC) curve analysis.

Results: The average VDs of the SVC in the CM and the T3, T6, T11, T16, and T21 areas were significantly lower in the DR than in the control group, whereas only the average VD of the SVC in the T21 area was significantly lower in the DM group. The average VD of the DVC in the CM was significantly increased in the DR group, whereas the average VDs of the DVC in the CM and T21 area were significantly decreased in the DM group. Evaluation of the DR group showed significant increases in the thicknesses of SVC-nourishing segments in the CM and T3, T6, and T11 areas and significant increases in the thicknesses of DVC-nourishing segments in the CM and T3 and T6 areas. In contrast, none of these parameters showed significant changes in the DM group. ROC curve analysis showed that the average VD of the SVC in the CM, T3, and T21 had better ability

10.3389/fendo.2023.1143535

to predict DR, with areas under the ROC curves (AUCs) of 0.8608, 0.8505, and 0.8353, respectively. The average VD of the DVC in the CM was also predictive of DR, with an AUC of 0.8407.

Conclusions: The newly developed ultrawide SS-OCTA device was better able to reveal early peripheral retinal vascular changes than traditional devices.

KEYWORDS

vascular density (VD), thickness, diabetes mellitus, diabetic retinopathy, SS-OCTA, peripheral retina

1 Introduction

Diabetes mellitus (DM) is a common and frequently occurring disease worldwide that was estimated to affect 536.6 million adults aged 20-79 years in 2021 (1). Diabetic retinopathy (DR) is a frequent ocular complication of DM, characterized by neurovascular injury and vision impairment (2). Early screening and therapies for DR are now considered effective for preventing blindness or vision loss (3). Although patients have been screened for DR using dilated and seven-field fundus photography techniques (4, 5), these methods cannot analyze blood flow or deep retinal changes. Microaneurysms, venous beading, vascular leakage, and nonperfused areas can be visualized by fundus fluorescein angiography, but this method is invasive, time-consuming, and not quantitative, and is associated with a risk of allergy (6, 7). Optical coherence tomography (OCT) is a type of ocular fundus examination that can obtain information on retinal layers *via* tomography scans. This method is widely used in the diagnosis and follow-up of patients with diabetic macular edema and other macular diseases (8–10), although it cannot determine blood flow.

OCT angiography (OCTA) is a rapid, noninvasive, and high-resolution ocular fundus examination that can simultaneously perform tomography scans and obtain blood flow information (11, 12). The high resolution of OCTA can determine the occurrence of preclinical retinopathy, by, for example, identifying changes in the foveal avascular zone, as well as alterations in vessel density and retinal thickness (11, 13). Although imaging by OCTA was previously limited to a 3 × 3 mm or 6 × 6 mm area in the center of the macula, this method can acquire high-resolution tomography and angiography images of 12 × 12 mm and even 24 × 20 mm areas of the retina and choroid using a single capture (Figure 1) (14, 15). These types of wide-field OCTA can provide considerable information on the retina and choroid, broadening knowledge of DR and other ocular fundus diseases.

The TowardPi swept-source (SS) OCT and OCTA system (BMizar, TowardPi Medical Technology, Beijing, China) is a newly developed high-resolution and wide-field tomographic and angiography imaging system with an A-scan rate as high as 400 KHz and an axial scan depth of 6 mm. This system can acquire 24-mm-wide tomography and 24 × 20 mm angiography information in about 15 seconds in a single capture (16). The present study utilized this system to analyze baseline parameters in patients with DR, patients with DM without DR, and normal controls, including vascular density and thickness of various areas of the superficial and deep layers of the retina. Use of this system may help determine changes in the peripheral retina of patients with DR, suggesting its usefulness in early screening for this condition.

2 Materials and methods

2.1 Participants

This cross-sectional, observational study enrolled 24 patients (47 eyes) with DR, 45 patients (87 eyes) with DM without DR, and 36 control subjects (71 eyes) who visited the Department of Ophthalmology at Sichuan Provincial People's Hospital in

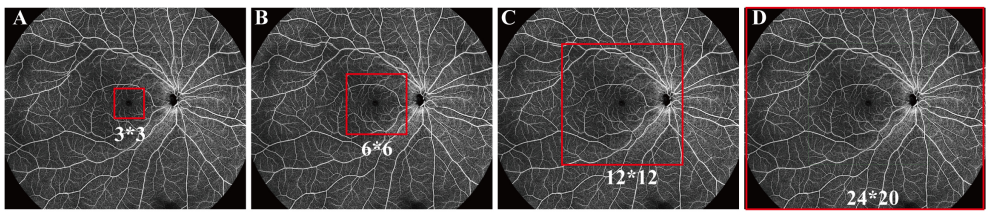

FIGURE 1
Fields detected by optical coherence tomography angiography (OCTA). **(A)** 3 × 3 mm, **(B)** 6 × 6 mm, **(C)** 12 × 12 mm, and **(D)** 24 × 20 mm.

Chengdu, Sichuan, China between January and July 2022. The study was conducted in accordance with the Declaration of Helsinki and was approved by the Ethics Committee of Sichuan Provincial People's Hospital (permit number 2022–258). All participants provided written informed consent prior to enrollment.

2.2 Inclusion and exclusion criteria

DR was diagnosed according to the criteria Early Treatment Diabetic Retinopathy Study. DM was diagnosed according to the criteria set by the World Health Organization (WHO) (17). Patients were included if they (1) were aged >18 years, (2) had been definitively diagnosed with type 2 DM, (3) did not have an unknown cause of vision loss, and (4) had an OCTA image quality index >8. Patients were excluded if they had (1) severe opacity of the cornea, lens, or vitreous; (2) glaucoma, high myopia, or other ocular diseases that might influence blood flow in the retina; (3) a history of nondiabetic chorioretinopathy or ocular fundus surgery or photocoagulation; or (4) insufficient medical data (e.g., DM history, current treatment protocol, or glycemic control). The participants were then divided into the DR, DM, and normal control (NC) groups based on their diagnosis.

2.3 Demographic data and ophthalmic examinations

Demographic and clinical characteristics of all subjects were recorded, including their age, gender, height, weight, past medical history, duration of diabetes, type of diabetes, and treatment. All subjects underwent ophthalmic examinations, including optometry, and measurements of intraocular pressure (IOP) and axial eye length (AL). Other factors recorded included best corrected visual acuity (BCVA) and refractive error. Anterior segments were examined by slit-lamp biomicroscopy. Following full dilation of the pupil, all eyes underwent fundus examination through indirect ophthalmoscopy and photography (Daytona, Optos, United Kingdom). DR and other types of chorioretinopathy were diagnosed by two experienced licensed doctors based on the results of fundus examinations and assessments of all retinas images. Glycosylated hemoglobin A1c (HbA1c) and fasting blood glucose (FBG) concentrations were measured in all patients diagnosed with DR and DM.

2.4 OCT and OCTA data

All subjects underwent SS-OCT and SS-OCTA (TowardPi BMizar, TowardPi Medical Technology, Beijing, China) examinations while their pupils were still dilated. This newly developed SS-OCT/SS-OCTA system has an A-scan rate of 400 KHz, an axial scan depth of 6 mm, a B-scan length of 24 mm, and OCTA area of 24 × 20 mm. This system has an axial optical resolution of 3.8-μm and a transverse resolution of 10-μm, enabling the capture of high-resolution fundus images. The ability of this system to acquire OCT images 24-mm in width and 6-mm in depth, as well as ultrawide OCTA images of 24 × 20 mm, enabled the determination of information on chorioretinal vascular density (VD) and thickness at 24 × 20 mm in a single capture. Images were subsequently graded 1–10 by the SS-OCTA platform, with only images graded ≥8 utilized in the present study.

All the primary data were acquired and exported by the built-in software of the SS-OCT and SS-OCTA platform. The built-in Early Treatment Diabetic Retinopathy Study rings of the platform were applied to compare the different areas of the retina. The VD and thickness of the central macula (CM) (1 mm diameter) and of the temporal fan-shaped areas at 1–3 mm (T3), 3–6 mm (T6), 6–11 mm (T11), 11–16 mm (T16), and 16–21 mm (T21) (Figure 2) were compared in the DR, DM, and NC groups, as were the deep vascular complex (DVC), superficial vascular complex (SVC), and average thicknesses of the SVC and DVC nourishing segments. A flow diagram of the experimental design is shown in Figure 3.

2.5 Statistical analysis

All statistical analyses were performed using IBM SPSS software (version 26.0). The normal distribution of data was assessed using the Kolmogorov–Smirnov test. Data are presented as the mean ± standard deviation. Differences in age, right or left eye, AL, and other characteristics were analyzed by independent sample t-tests or analysis of variance (ANOVA). Differences in gender were evaluated by crosstabs analysis. Pairwise correlations among VD, thickness, and DR were analyzed by receiver operating characteristic (ROC) curve analysis. Areas under the ROC curve (AUC) >0.8 were considered significant. A p-value < 0.05 was regarded as statistically significant.

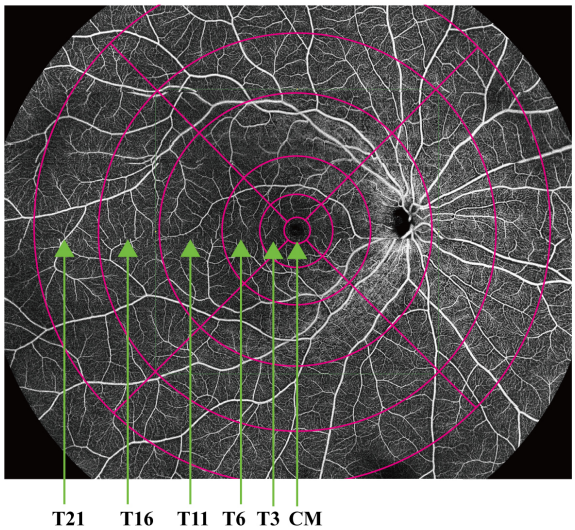

FIGURE 2
Vascular density and thickness of the central macula (CM) (1 mm diameter) and temporal fan-shaped areas of 1–3 mm (T3), 3–6 mm (T6), 6–11 mm (T11), 11–16 mm (T16), and 16–21 mm (T21).

10.3389/fendo.2023.1143535

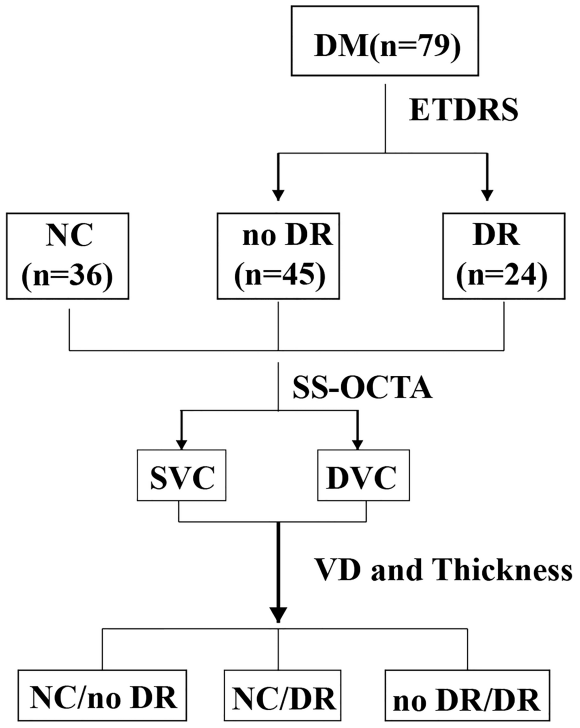

FIGURE 3
Flow diagram of the experimental design. DM, diabetes mellitus; ETDRS, Early Treatment Diabetic Retinopathy study; NC, normal control; DR, diabetic retinopathy; SS-OCTA, swept-source optic coherence tomography angiography; SVC, superficial vascular complex; DVC, deep vascular complex; VD, vascular density.

3 Results

3.1 Baseline data

This study enrolled 47 eyes from 24 patients with, 87 eyes from 45 patients with DM without DR, and 71 eyes of 36 age- and gender-matched control subjects. The baseline demographic and clinical characteristics of these three groups are shown in Table 1. The three groups showed no significant differences in numbers of subjects (p = 0.181), age (p = 0.083), FBG (0.059), AL (p = 0.087), and Hypertension (p = 0.859).

3.2 VD and thickness analysis of the SVC and DVC

The average VDs of the SVC in the CM, T3, T6, T11, T16, and T21 areas were significantly lower in the DR than in the NC and DM groups, whereas only the average VD of SVC in the T21 area was significantly lower in the DM than in the NC group (Figure 4A). The average VDs of the DVC in the CM and T21 area were significantly lower in the DM than in the NC group (Figure 4B). Compared with the DM group, the average VDs of the DVC in the CM and T3, T6, T11, T16, and T21 areas were higher in the DR group, but only the CM difference was statistically significant (Figure 4B). The average thicknesses of SVC nourishing segments in the CM and in the T3, T6, and T11 areas were significantly higher in the DR than in the DM group, whereas the average thicknesses of SVC nourishing segments in the T16 and T21 areas did not differ significantly in the three groups (Figure 4C). The average thicknesses of DVC nourishing segments in the CM and the T3, and T6 areas were significantly higher in the DR than in the DM group, whereas the average thicknesses of DVC nourishing segments in the T11, T16 and T21 areas did not differ significantly in the three groups (Figure 4D). The average thicknesses of SVC and DVC nourishing segments did not differ significantly in the DM and NC groups (Figures 4C, D). All of these findings are summarized in Table 2.

3.3 ROC curves of VD in the DM and DR groups

ROC curve analysis of the average VDs of the SVC showed that the AUCs were 0.8608 (95% CI 0.7982–0.9235, p < 0.0001) for the CM, 0.8506 (95% CI 0.7852–0.9159, p < 0.0001) for the T3 area, and 0.8353 (95% CI 0.7641–0.9065, p < 0.0001) for the T21 area,

TABLE 1 Baseline demographic and clinical characteristics of DR patients, DM patients and healthy controls.

	Normal Control	DM	DR	P Values
Patients (Female)	36 (23)	45 (20)	24 (8)	0.181
Age, yr	54.00 ± 9.83	58.20 ± 10.22	53.88 ± 7.96	0.083
Eyes	71	87	47	0.999
Type of DM	N/A	2	2	N/A
Duration of DM, yr	N/A	7.02 ± 6.17	11.38 ± 7.10	0.010
FBG, mmol/L	N/A	7.82 ± 2.36	9.24 ± 3.45	0.059
HbA1c, %	N/A	7.42 ± 1.48	9.12 ± 2.09	0.000
AL, mm	23.33 ± 0.69	23.60 ± 0.85	23.51 ± 0.79	0.087
Hypertension	36 (10)	45 (14)	24 (6)	0.859

Values are shown as means ± SD. A P value less than 0.05 was considered statistically significant.
DM, diabetes mellitus; DR, diabetic retinopathy; FBG, fasting blood-glucose; HbA1c, hemoglobin A1C; AL, axial lengths; N/A, not applicable.

10.3389/fendo.2023.1143535

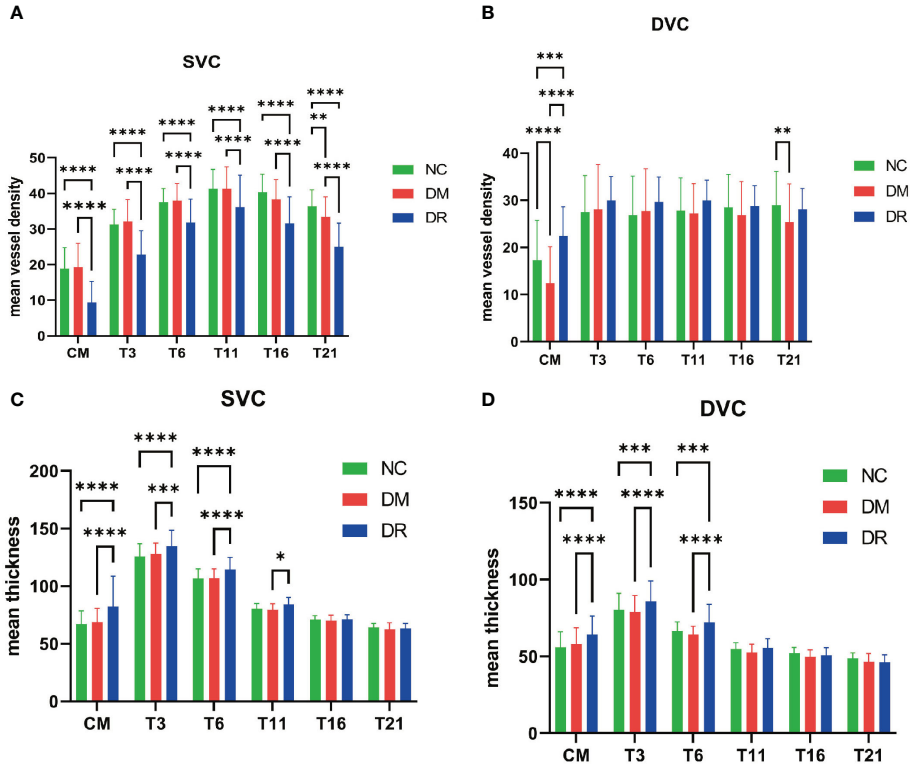

FIGURE 4
Vascular density (VD) and thickness analysis of the superficial vascular complex (SVC) and deep vascular complex (DVC). **(A)** Compared with the normal control (NC) group, **the** average VDs of the SVC were significantly lower in all retinal areas of patients with diabetic retinopathy (DR), as well as being significantly lower in the temporal fan-shaped area of 16–21 mm (T21) in patients with diabetes mellitus (DM). **(B)** The average VDs of the DVC in the central macula (CM) and T21 were lower in DM patients; although the average VDs of the DVC in all areas were higher in DR patients, only the changes in the CM were statistically significant. **(C)** The average thicknesses of SVC nourishing segments did not differ significantly in the NC and DM groups. The average thicknesses of these segments in the CM and temporal fan-shaped areas of 1–3 mm (T3), 3–6 mm (T6), and 6–11 mm (T11) were significantly greater in the DR than in the DM group. **(D)** The average thicknesses of DVC nourishing segments did not differ significantly in the NC and DM groups. The average thicknesses of these segments in the CM, T3, and T6 were significantly greater in the DR than in the DM group. *p < 0.05, **p < 0.01, ***p < 0.001, and ****p < 0.0001.

showing that these parameters were predictive of DR development (Figure 5B). The optimal CM cut-off value predicting DR was 15.50, with a sensitivity of 85.11%, a specificity of 80.46%, and a Youden Index of 0.66. The optimal T3 cut-off value predicting DR was 29.50, with a sensitivity of 85.11%, a specificity of 73.56%, and a Youden Index of 0.59. The optimal T21 cut-off value predicting DR was 28.50, with a sensitivity of 76.60%, a specificity of 82.76%, and a Youden Index of 0.59. In the DVC, only the average VD in the CM was predictive of DR (Figure 5D), with an AUC of 0.8407 (95% CI 0.7735–0.9078, p < 0.0001). The optimal CM cut-off value predicting DR was 17.50, with a sensitivity of 80.85%, a specificity of 81.61%, and a Youden Index was 0.62. The average VDs of the SVC and DVC were not predictive of DM (Figures 5A, C), and the average thicknesses of the SVC and DVC were not predictive of either DM or DR (Supplementary Figure 1).

4 Discussion

This cross-sectional, observational study analyzed the average VD of the SVC and DVC and the average thicknesses of SVC and DVC nourishing segments in patients among the NC, DM, and DR groups. Using the newly developed SS-OCT and SS-OCTA system, this study analyzed changes to the peripheral retina (21 mm) in the three groups. The average VDs of the SVC in all observed areas were significantly lower in the DR than in the NC group, whereas only the T21 area showed a significant decrease in the DM compared with the NC group. The average VDs of the DVC in the CM and T21 area were significantly lower in the DM than in the NC group. No significant changes in the thicknesses of SVC or DVC nourishing segments were observed in the peripheral retina (21 mm). ROC curve analysis showed that the average VDs of the SVC in the CM and in the T3 and T21 areas revealed were predictive of DR development, whereas only the average VD of the DVC in the CM was predictive of DR.

Recent developments in ultrawide OCT and OCTA equipment has resulted in the ability to image areas measuring 24 × 20 mm, the maximum range currently available among all OCTA devices (18, 19). Use of this advanced equipment has shown that the density of the choroidal vessels and the thicknesses of the inner retina segments at the periphery were significantly lower in nonpathological myopic fundi (16). This equipment was also

10.3389/fendo.2023.1143535

TABLE 2 Comparisons of superficial and deep complex vessel densities and thickness among the NC, DM, and DR groups data.

		NC	DM	DR	p1 (NC vs DM)	p2 (NC vs DR)	p3 (DM vs DR)
Superficial Vascular Complex Vessel Densities	CM	18.90 ± 5.92	19.33 ± 6.66	9.40 ± 5.89	0.8907	<0.0001	<0.0001
	T3	31.31 ± 4.20	32.13 ± 6.12	22.85 ± 6.70	0.6578	<0.0001	<0.0001
	T6	37.54 ± 3.82	37.97 ± 4.80	31.83 ± 6.58	0.8895	<0.0001	<0.0001
	T11	41.25 ± 5.49	41.25 ± 6.17	36.15 ± 8.97	0.9999	<0.0001	<0.0001
	T16	40.34 ± 5.01	38.30 ± 5.55	31.60 ± 7.42	0.0739	<0.0001	<0.0001
	T21	36.41 ± 4.62	33.45 ± 5.59	25.02 ± 6.61	0.0046	<0.0001	<0.0001
Deep Vascular Complex Vessel Densities	CM	17.27 ± 8.52	12.43 ± 7.74	22.43 ± 6.18	<0.0001	0.0005	<0.0001
	T3	27.49 ± 7.74	28.13 ± 9.46	29.96 ± 5.09	0.8495	0.17	0.3449
	T6	26.89 ± 8.24	27.72 ± 8.97	29.66 ± 5.26	0.7556	0.1067	0.3021
	T11	27.86 ± 6.93	27.22 ± 6.34	30.00 ± 4.27	0.8445	0.2619	0.0869
	T16	28.55 ± 6.94	26.85 ± 7.09	28.83 ± 4.27	0.3102	0.9771	0.2897
	T21	28.94 ± 7.17	25.42 ± 8.02	28.11 ± 4.37	0.007	0.8139	0.1028
Superficial Vessel Complex Thicknesses	CM	67.11 ± 11.52	68.9 ± 11.78	82.19 ± 26.38	0.4619	<0.0001	<0.0001
	T3	125.76 ± 11.09	128.1 ± 9.33	134.74 ± 13.77	0.2647	<0.0001	0.0003
	T6	106.54 ± 8.34	106.86 ± 8.11	114.38 ± 10.53	0.9743	<0.0001	<0.0001
	T11	80.55 ± 4.43	79.37 ± 5.41	84.28 ± 6.01	0.7121	0.0888	0.0112
	T16	70.92 ± 3.52	70.06 ± 4.91	71.34 ± 3.84	0.836	0.9687	0.7316
	T21	64.23 ± 3.32	62.57 ± 5.71	63.34 ± 4.19	0.516	0.8712	0.8946
Deep Vessel Complex Thicknesses	CM	55.9 ± 10.12	58 ± 10.68	64.34 ± 11.85	0.2138	<0.0001	<0.0001
	T3	80.28 ± 10.82	78.85 ± 10.85	85.96 ± 13.19	0.4868	0.0003	<0.0001
	T6	66.54 ± 5.94	64.34 ± 5.39	72.32 ± 11.57	0.1865	0.0003	<0.0001
	T11	54.93 ± 4.04	52.68 ± 5.29	55.55 ± 5.97	0.1697	0.9056	0.1051
	T16	52.1 ± 3.74	49.64 ± 4.53	50.85 ± 4.86	0.1218	0.6728	0.6699
	T21	48.83 ± 3.45	46.6 ± 5.16	46.3 ± 4.76	0.1746	0.1969	0.9756

All results are shown as means ± SD.
NC, normal control; DM, diabetes mellitus; DR, diabetic retinopathy.

found to clearly delineate choroidal osteomas from the adjacent vessels in the choroidal Sattler's and Haller's layers (16), providing further evidence that the newly developed OCT and OCTA system can simultaneously acquire ultrawide and high-resolution images of the fundus. At present, 3 × 3 mm and 6 × 6 mm OCT and OCTA devices are widely used in clinical practice, with the use of 12 × 12 mm devices increasing, providing additional information about the peripheral retina. Using these 12 × 12 mm OCT and OCTA devices, retinal microvascular abnormalities have been observed in the peripheral retinas of DM patients without DR (15), with the 24 × 20 mm devices providing additional information on the peripheral retina.

Fundus fluorescein angiography (FFA) is a traditional imaging technique for DR, as it can show retinal neovascular and vascular leakage. This method, however, is invasive and expensive, carries a risk of allergy, and can negatively affect the liver and kidneys, thus limiting its widespread use (20, 21). SS-OCTA may be a good alternative, as it can avoid these problems. Although a comparison of 24×20 mm^2 SS-OCTA with FFA in evaluating DR lesions showed good to moderate agreement, SS-OCTA had several advantages, including its noninvasiveness, lower cost, rapid performance, and reproducible results (22). A recent study analyzing the effect of scan area on the detection of DR lesions, by comparing 12 mm × 12 mm central and 24 mm × 20 mm images, found that the ultra-widefield SS-OCTA detected more intra-retinal microvascular and neovascular abnormalities, with higher rates of ischemia in the mid-peripheral than in the posterior retina (23). Another study found that ultra-widefield color fundus photography (UWF CFP) plus SS-OCTA and UWF CFP plus FFA showed good agreement in the rate of detection of DR lesions and DR severity grade (24). Taken together, these findings suggested that ultra-wide SS-OCTA has advantages when compared with FFA or 12 mm × 12 mm

10.3389/fendo.2023.1143535

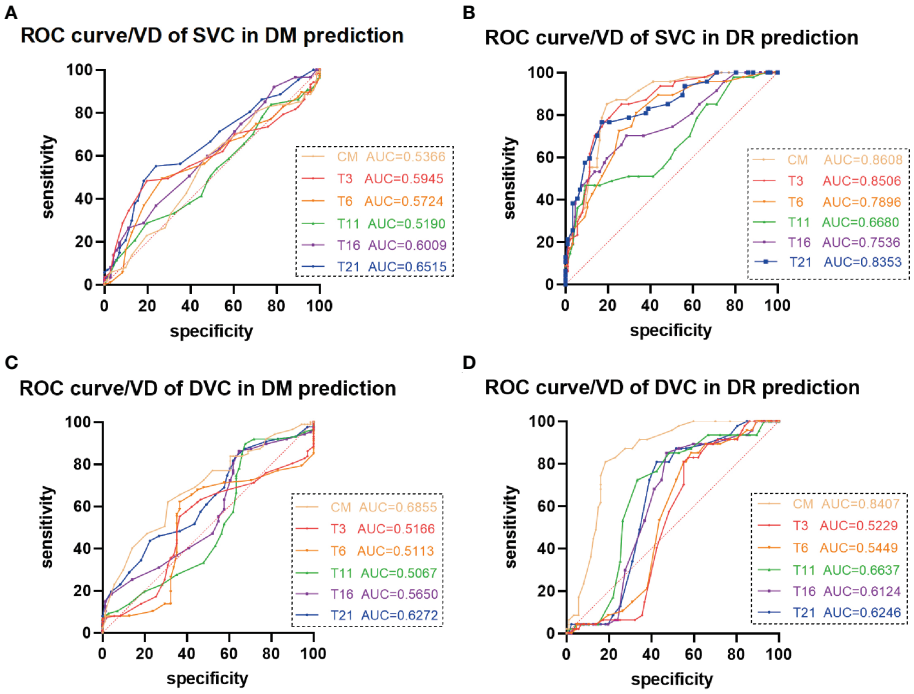

FIGURE 5
Receiver operating characteristic (ROC) curve analysis of vascular density (VD) in patients with diabetes mellitus (DM) and diabetic retinopathy (DR). **(A**, **C)** The average VDs of the **(A)** superficial vascular complex (SVC) and **(C)** deep vascular complex (DVC) showed poor ability to predict DM. **(B)** The average VDs of the SVC in the central macula (CM) and temporal fan-shaped areas of 1–3 mm (T3) and 16–21 mm (T21) revealed better ability to predict DR. **(D)** The average VD of the DVC in the CM revealed ability to predict DR.

OCTA, with the potential to be a rapid, repeatable and noninvasive method for DR screening and follow-up.

Studies using 3 × 3 mm OCT and OCTA devices have found no significant differences in the VD and thickness of the superficial and deep retinal layers between DM and NC groups (25–27), findings partially consistent with the results of the present study. In contrast, other studies have found that the VD and thickness in the parafoveal and/or perifoveal layers are significantly lower in patients with DM than in NCs (28–30). These studies differ from the present study in their inclusion and exclusion criteria. Most previous studies defined DM without DR based on fundus photography, whereas the present study excluded DR based on both 24 × 20 mm OCTA and fundus photography. Microaneurysms and fovea avascular zone changes can be detected by OCTA in DM patients through normal fundus photography (28, 31). These subjects were excluded from the present study based on the results of high-resolution and ultrawide field OCTA.

The present study showed early VD changes of the SVC and DVC in the peripheral retina (21 mm) in patients with DM, as well as in patients with DR. ROC curve analysis found that the VD of the SVC in T21 showed good ability to predict DR. Moreover, the VD of the SVC in T21 was the only significant change in the SVC in patients with DM. These results indicate that the VD of T21 is an early indicator of DR progression and may be a biomarker predictive of DR. The VD of the SVC in all areas was significantly lower in patients with DR, a finding consistent with previous results (15, 29, 32). The newly developed OCTA device expanded the detectable area to T16 and T21, thereby consolidating previous results. The findings in patients with DM also suggested that retinal circulation was affected before clinical manifestations of DR (28, 33). The decreased VD in the SVC in DR results largely from an incremental loss of capillary segments (34), whereas the increased VD in the DVC is regarded as an autoregulatory response to increased metabolic demand in mild to moderate DR. The present study found that SVC nourishing segments in the CM, T3, T6, and T11 and DVC nourishing segments in the CM, T3, and T6 were thicker in patients with DR, a finding consistent with a previous study using another type of OCTA device (35).

The present study had several limitations. First, demographic information, DM duration, and other previous medical history was self-reported by the study subjects. Collecting more data can help avoid potential bias in relation to the duration of diabetes and blood glucose control. Studies using a larger number of patients, as well as measurements of blood pressure, lipids, and other laboratory data, are required to confirm the present findings. Studies should also include patients with progressive DR, thus allowing longitudinal determinations of changes in retinal structure during the progression of DR.

In conclusion, the present study showed that the progression of DR was accompanied by changes in the peripheral retina. The ultrawide and rapid scanning SS-OCT and SS-OCTA system expanded the detectable area to 24 × 20 mm. Prospective studies including larger numbers of patients are needed to confirm these findings and expand the use of the newly developed SS-OCT and SS-OCTA device.

Data availability statement

The raw data supporting the conclusions of this article will be made available by the authors, without undue reservation.

Ethics statement

The studies involving human participants were reviewed and approved by the Ethics Committee of Sichuan Provincial People's Hospital. The patients/participants provided their written informed consent to participate in this study.

Author contributions

JZ, JL, WD, YZ, ML—involved in study conceptualization. MyL, DW, MM, XL—involved in study supervision. ML, SC, YL, BC, LY, LS, LQ, RZ—involved in data acquisition and data analysis. JZ, YZ—involved in data interpretation; YZ, ML—involved in the drafting of the manuscript. JZ, JL, WD, ZY, ML—involved in interpretation of results. JZ, JL, WD, ZY, ML—involved in critical review of the manuscript. All authors contributed to the article and approved the submitted version.

Funding

This study was supported by the Sichuan Province Central Government Guides Local Science and Technology Development Special Project (2021ZYD0108), the Natural Science Foundation of Sichuan Province (2022NSFSC1352), the Science & Technology Department of Sichuan Province (2017YSKY0001, 2021YJ0234), the medical science and technology project of Health and Family Commission of Sichuan Province (16PJ454), the Sichuan Provincial People's Hospital (2021QN13) and the 2021 open project of Sichuan Provincial Key Laboratory for Human Disease Genetics Research (2021kflx008).

Conflict of interest

The authors declare that the research was conducted in the absence of any commercial or financial relationships that could be construed as a potential conflict of interest.

Publisher's note

All claims expressed in this article are solely those of the authors and do not necessarily represent those of their affiliated organizations, or those of the publisher, the editors and the reviewers. Any product that may be evaluated in this article, or claim that may be made by its manufacturer, is not guaranteed or endorsed by the publisher.

Supplementary material

The Supplementary Material for this article can be found online at: https://www.frontiersin.org/articles/10.3389/fendo.2023.1143535/full#supplementary-material

References

1. Sun H, Saeedi P, Karuranga S, Pinkepank M, Ogurtsova K, Duncan BB, et al. IDF diabetes atlas: global, regional and country-level diabetes prevalence estimates for 2021 and projections for 2045. *Diabetes Res Clin Pract* (2022) 183:109119. doi: 10.1016/j.diabres.2021.109119

2. Roy S, Kim D. Retinal capillary basement membrane thickening: role in the pathogenesis of diabetic retinopathy. *Prog Retin Eye Res* (2021) 82:100903. doi: 10.1016/j.preteyeres.2020.100903

3. Purola P, Ojamo M, Gissler M, Uusitalo H. Changes in visual impairment due to diabetic retinopathy during 1980-2019 based on nationwide register data. *Diabetes Care* (2022) 45(9):2020–7. doi: 10.2337/dc21-2369

4. Lawrence MG. The accuracy of digital-video retinal imaging to screen for diabetic retinopathy: an analysis of two digital-video retinal imaging systems using standard stereoscopic seven-field photography and dilated clinical examination as reference standards. *Trans Am Ophthalmol Soc* (2004) 102:321–40.

5. Li H, Yu X, Zheng B, Ding S, Mu Z, Guo L. Early neurovascular changes in the retina in preclinical diabetic retinopathy and its relation with blood glucose. *BMC Ophthalmol* (2021) 21(1):220. doi: 10.1186/s12886-021-01975-7

6. Kylstra JA, Brown JC, Jaffe GJ, Cox TA, Gallemore R, Greven CM, et al. The importance of fluorescein angiography in planning laser treatment of diabetic macular edema. *Ophthalmology* (1999) 106:2068–73. doi: 10.1016/S0161-6420(99)90485-2

7. Goatman KA, Cree MJ, Olson JA, Forrester JV, Sharp PF. Automated measurement of microaneurysm turnover. *Invest Ophthalmol Vis Sci* (2003) 44(12):5335–41. doi: 10.1167/iovs.02-0951

8. Choi MY, Jee D, Kwon JW. Characteristics of diabetic macular edema patients refractory to anti-VEGF treatments and a dexamethasone implant. *PloS One* (2019) 14:e0222364. doi: 10.1371/journal.pone.0222364

9. Udaondo P, Adan A, Arias-Barquet L, Ascaso FJ, Cabrera-López F, Castro-Navarro V, et al. Challenges in diabetic macular edema management: an expert consensus report. *Clin Ophthalmol* (2021) 15:3183–95. doi: 10.2147/OPTH.S320948

10. Munk MR, Somfai GM, de Smet MD, Donati G, Menke MN, Garweg JG, et al. The role of intravitreal corticosteroids in the treatment of DME: predictive OCT biomarkers. *Int J Mol Sci* (2022) 23(14). doi: 10.3390/ijms23147585

11. de Carlo TE, Chin AT, Bonini Filho MA, Adhi M, Branchini L, Salz DA, et al. Detection of microvascular changes in eyes of patients with diabetes but not clinical diabetic retinopathy using optical coherence tomography angiography. *Retina* (2015) 35:2364–70. doi: 10.1097/IAE.0000000000000882

12. Udaondo P, Parravano M, Vujosevic S, Zur D, Chakravarthy U. Update on current and future management for diabetic maculopathy. *Ophthalmol Ther* (2022) 11(2):489–502. doi: 10.1007/s40123-022-00460-8

13. Srinivasan S, Sivaprasad S, Rajalakshmi R, Anjana RM, Malik RA, Kulothungan V, et al. Early retinal functional alteration in relation to diabetes duration in patients with type 2 diabetes without diabetic retinopathy. *Sci Rep* (2022) 12(1):11422. doi: 10.1038/s41598-022-15425-x

14. Xuan Y, Chang Q, Zhang Y, Ye X, Liu W, Li L, et al. Clinical observation of choroidal osteoma using swept-source optical coherence tomography and optical coherence tomography angiography. *Appl Sci* (2022) 12:4472. doi: 10.3390/app12094472

15. Xu F, Li Z, Gao Y, Yang X, Huang Z, Li Z, et al. Retinal microvascular signs in pre- and early-stage diabetic retinopathy detected using wide-field swept-source optical coherence tomographic angiography. *J Clin Med* (2022) 11(15). doi: 10.3390/jcm11154332

16. Zhang W, Li C, Gong Y, Liu N, Cao Y, Li Z, et al. Advanced ultrawide-field optical coherence tomography angiography identifies previously undetectable changes

in biomechanics-related parameters in nonpathological myopic fundus. *Front Bioeng Biotechnol* (2022) 10:920197. doi: 10.3389/fbioe.2022.920197

17. Alberti KG, Zimmet PZ. Definition, diagnosis and classification of diabetes mellitus and its complications. part 1: diagnosis and classification of diabetes mellitus provisional report of a WHO consultation. *Diabetes Med* (1998) 15:539–53. doi: 10.1002/(SICI)1096-9136(199807)15:7<539::AID-DIA668<3.0.CO;2-S

18. Chiku Y, Hirano T, Takahashi Y, Tuchiya A, Nakamura M, Murata T. Evaluating posterior vitreous detachment by widefield 23-mm swept-source optical coherence tomography imaging in healthy subjects. *Sci Rep* (2021) 11:19754. doi: 10.1038/s41598-021-99372-z

19. Horie S, Ohno-Matsui K. Progress of imaging in diabetic retinopathy-from the past to the present. *Diagnostics (Basel)* (2022) 12(7). doi: 10.3390/diagnostics12071684

20. Tan A, Tan GS, Denniston AK, Keane PA, Ang M, Milea D, et al. An overview of the clinical applications of optical coherence tomography angiography. *Eye (Lond)* (2018) 32:262–86. doi: 10.1038/eye.2017.181

21. Spaide RF, Klancnik JMJr, Cooney MJ. Retinal vascular layers imaged by fluorescein angiography and optical coherence tomography angiography. *JAMA Ophthalmol* (2015) 133:45–50. doi: 10.1001/jamaophthalmol.2014.3616

22. Zeng QZ, Li SY, Yao YO, Jin EZ, Qu JF, Zhao MW. Comparison of 24×20 mm2 swept-source OCTA and fluorescein angiography for the evaluation of lesions in diabetic retinopathy. *Int J Ophthalmol* (2022) 15:1798–805. doi: 10.18240/ijo.2022.11.10

23. Li M, Mao M, Wei D, Liu M, Liu X, Leng H, et al. Different scan areas affect the detection rates of diabetic retinopathy lesions by high-speed ultra-widefield swept-source optical coherence tomography angiography. *Front Endocrinol (Lausanne)* (2023) 14:1111360. doi: 10.3389/fendo.2023.1111360

24. Li J, Wei D, Mao M, Li M, Liu S, Li F, et al. Ultra-widefield color fundus photography combined with high-speed ultra-widefield swept-source optical coherence tomography angiography for non-invasive detection of lesions in diabetic retinopathy. *Front Public Health* (2022) 10:1047608. doi: 10.3389/fpubh.2022.1047608

25. Dai Y, Zhou H, Chu Z, Zhang Q, Chao JR, Rezaei KA, et al. Microvascular changes in the choriocapillaris of diabetic patients without retinopathy investigated by swept-source OCT angiography. *Invest Ophthalmol Vis Sci* (2020) 61:50. doi: 10.1167/iovs.61.3.50

26. Qiu B, Zhao L, Zhang X, Wang Y, Wang Q, Nie Y, et al. Associations between diabetic retinal microvasculopathy and neuronal degeneration assessed by swept-source OCT and OCT angiography. *Front Med (Lausanne)* (2021) 8:778283. doi: 10.3389/fmed.2021.778283

27. Han Y, Wang X, Sun G, Luo J, Cao X, Yin P, et al. Quantitative evaluation of retinal microvascular abnormalities in patients with type 2 diabetes mellitus without clinical sign of diabetic retinopathy. *Transl Vis Sci Technol* (2022) 11(4):20. doi: 10.1167/tvst.11.4.20

28. Cao D, Yang D, Huang Z, Zeng Y, Wang J, Hu Y, et al. Optical coherence tomography angiography discerns preclinical diabetic retinopathy in eyes of patients with type 2 diabetes without clinical diabetic retinopathy. *Acta Diabetol* (2018) 55:469–77. doi: 10.1007/s00592-018-1115-1

29. Li L, Almansoob S, Zhang P, Zhou YD, Tan Y, Gao L. Quantitative analysis of retinal and choroid capillary ischaemia using optical coherence tomography angiography in type 2 diabetes. *Acta Ophthalmol* (2019) 97:240–6. doi: 10.1111/aos.14076

30. Zeng Y, Cao D, Yu H, Yang D, Zhuang X, Hu Y, et al. Early retinal neurovascular impairment in patients with diabetes without clinically detectable retinopathy. *Br J Ophthalmol* (2019) 103(12):1747–52. doi: 10.1136/bjophthalmol-2018-313582

31. Vujosevic S, Muraca A, Alkabes M, Villani E, Cavarzeran F, Rossetti L, et al. Early microvascular and neural changes in patients with type 1 and type 2 diabetes mellitus without clinical signs of diabetic retinopathy. *Retina* (2019) 39(3):435–45. doi: 10.1097/IAE.0000000000001990

32. Attia Ali Ahmed M, Shawkat Abdelhaleem A. Evaluation of microvascular and visual acuity changes in patients with early diabetic retinopathy: optical coherence tomography angiography study. *Clin Ophthalmol* (2022) 16:429–40. doi: 10.2147/OPTH.S353426

33. Palma F, Camacho P. The role of optical coherence tomography angiography to detect early microvascular changes in diabetic retinopathy: a systematic review. *J Diabetes Metab Disord* (2021) 20:1957–74. doi: 10.1007/s40200-021-00886-0

34. Rosen RB, Andrade Romo JS, Krawitz BD, Mo S, Fawzi AA, Linderman RE, et al. Earliest evidence of preclinical diabetic retinopathy revealed using optical coherence tomography angiography perfused capillary density. *Am J Ophthalmol* (2019) 203:103–15. doi: 10.1016/j.ajo.2019.01.012

35. Liu T, Lin W, Shi G, Wang W, Feng M, Xie X, et al. Retinal and choroidal vascular perfusion and thickness measurement in diabetic retinopathy patients by the swept-source optical coherence tomography angiography. *Front Med (Lausanne)* (2022) 9:786708. doi: 10.3389/fmed.2022.786708

frontiers | Frontiers in Endocrinology

TYPE Original Research
PUBLISHED 10 May 2023
DOI 10.3389/fendo.2023.1138676

OPEN ACCESS

EDITED BY
Mohd Imtiaz Nawaz,
King Saud University, Saudi Arabia

REVIEWED BY
Sungjae Kim,
Kyungbok University, Republic of Korea
Peng Jin,
Virginia Tech, United States

*CORRESPONDENCE
Jun-Kyu Byun
jkbyun@knu.ac.kr
Jang-Hyuk Yun
yunjh@kangwon.ac.kr

†These authors have contributed equally to this work

RECEIVED 18 January 2023
ACCEPTED 19 April 2023
PUBLISHED 10 May 2023

CITATION
Kim I, Seo J, Lee DH, Kim Y-H, Kim J-H, Wie M-B, Byun J-K and Yun J-H (2023) *Ulmus davidiana* 60% edible ethanolic extract for prevention of pericyte apoptosis in diabetic retinopathy.
Front. Endocrinol. 14:1138676.
doi: 10.3389/fendo.2023.1138676

Ulmus davidiana 60% edible ethanolic extract for prevention of pericyte apoptosis in diabetic retinopathy

Iljin Kim[1†], Jieun Seo[2†], Dong Hyun Lee[3†], Yo-Han Kim[4], Jun-Hyung Kim[4], Myung-Bok Wie[4], Jun-Kyu Byun[5*] and Jang-Hyuk Yun[4*]

[1]Department of Pharmacology, Inha University College of Medicine, Incheon, Republic of Korea, [2]Faculty of Engineering, Yokohama National University, Yokohama, Japan, [3]Department of Ophthalmology, Inha University Hospital, Inha University College of Medicine, Incheon, Republic of Korea, [4]College of Veterinary Medicine and Institute of Veterinary Science, Kangwon National University, Chuncheon, Gangwon, Republic of Korea, [5]Research Institute of Pharmaceutical Sciences, College of Pharmacy, Kyungpook National University, Daegu, Republic of Korea

Diabetic retinopathy (DR) is a disease that causes visual deficiency owing to vascular leakage or abnormal angiogenesis. Pericyte apoptosis is considered one of the main causes of vascular leakage in diabetic retina, but there are few known therapeutic agents that prevent it. *Ulmus davidiana* is a safe natural product that has been used in traditional medicine and is attracting attention as a potential treatment for various diseases, but its effect on pericyte loss or vascular leakage in DR is not known at all. In the present study, we investigated on the effects of 60% edible ethanolic extract of *U. davidiana* (U60E) and catechin 7-O-β-D-apiofuranoside (C7A), a compound of *U. davidiana*, on pericyte survival and endothelial permeability. U60E and C7A prevented pericyte apoptosis by inhibiting the activation of p38 and JNK induced by increased glucose and tumor necrosis factor alpha (TNF-α) levels in diabetic retina. Moreover, U60E and C7A reduced endothelial permeability by preventing pericyte apoptosis in co-cultures of pericytes and endothelial cells. These results suggest that U60E and C7A could be a potential therapeutic agent for reducing vascular leakage by preventing pericyte apoptosis in DR.

KEYWORDS

diabetic retinopathy, pericyte apoptosis, endothelial permeability, *Ulmus davidiana*, catechin 7-O-β-D-apiofuranoside

1 Introduction

Diabetic retinopathy (DR) is a disease that causes visual impairment in middle-aged people and is the most common microvascular complication in patients with diabetes (1–3). One of the main causes of DR is an increase in endothelial permeability in the retina, resulting in macular edema, which causes serious visual impairment (2, 4). Pericyte loss is closely related to increased endothelial permeability in DR.

Pericytes surround endothelial cells and play an important role in maintaining the integrity of blood vessels (5, 6). In particular, pericytes interact with endothelial cells to increase the expression of tight junction proteins in endothelial cells, thereby preventing increase in endothelial permeability (7–10). Pericyte loss occurs in the early stages of DR (11–13), therefore, inhibiting pericyte loss may prevent increased endothelial permeability, thereby avoiding serious visual damage such as macular edema. Recently, we confirmed that tumor necrosis factor alpha (TNF-α), which is an important protein that induces pericyte loss *via* apoptosis, is elevated in diabetic retina (8, 14). Additionally, previous studies reveal that high glucose increases apoptosis in retinal pericytes (15); however, few treatments are known to prevent pericyte apoptosis induced by high glucose or TNF-α levels.

Ulmus davidiana is a deciduous broad-leaf tree, widely distributed in the east and is a safe natural product used in traditional medicine. *U. davidiana* is known to exhibit pharmacological properties such as antioxidant, anti-inflammatory, anticancer effects (16–18), and its stem or root has long been used for the treatment of various diseases such as edema, mastitis, cancer, inflammation, and rheumatoid arthritis (19–21). Interestingly, *U. davidiana* was known to play a role in preventing apoptosis in various cells such as mouse embryonic fibroblast cells, mouse embryonic liver cells, and rat pheochromocytoma cells [10-12]. However, it is not known how *U. davidiana* extract and compound isolated therefrom affect pericyte apoptosis and endothelial permeability; hence, this was investigated in the present study.

In this study, using a 60% edible ethanolic extract of *U. davidiana* (U60E) and the compound catechin 7-O-β-D-apiofuranoside (C7A) known as the main bioactive component of *U. davidiana* extract (22, 23), the effects and related mechanisms of *U. davidiana* on the increase in pericyte apoptosis and endothelial permeability induced by high glucose and TNF-α were investigated. We demonstrated that U60E and C7A prevent pericyte apoptosis by blocking the activities of p38 and JNK, which are increased by high glucose and TNF-α levels. Additionally, U60E and C7A restored the decreased ZO-1 expression and increased permeability in endothelial cells caused by pericyte apoptosis induced by high glucose and TNF-α when pericytes and endothelial cells were co-cultured. Taken together, these results suggest a potential therapeutic benefit of U60E and C7A in preventing pericyte apoptosis in DR.

2 Materials and methods

2.1 Cell cultures

Human placental pericytes (PromoCell, Heidelberg, Germany) and human retinal microvascular endothelial cells (HRMECs; ACBRI, Kirkland, WA, USA) were maintained in pericytes medium including growth factors (PromoCell) and M199 medium (HyClone, Logan, UT, USA) with 20% fetal bovine serum (FBS), respectively. In an incubator with a humidified environment containing 5% CO_2, the cells were cultured at 37°C.

2.2 Reagents and antibodies

R&D Systems (Minneapolis, MA, USA) provided the recombinant human TNF-α, whereas Millipore (St. Louis, MO, USA) provided the p38 and JNK activator anisomycin, p38 inhibitor SB203580, JNK inhibitor SP600125, glucose, and mannitol, respectively. Cell Signaling Technology (Danvers, MA, USA) provided the primary anti-phospho-p38, anti-p38, anti-phospho-JNK, anti-JNK, anti-phospho-Erk1/2, anti-Erk1/2, and anti-cleaved caspase-3 antibodies. Thermo Fisher Scientific (Waltham, MA) provided the anti-ZO-1 and anti-occludin antibodies. Santa Cruz Biotechnology (Dallas, TX, USA) provided the anti-β-tubulin and peroxidase-conjugated secondary antibodies. ChemFaces (Wuhan, Hubei, China) provided the C7A.

2.3 Preparation of U60E extracts

U. davidiana (branches with barks) was officially collected in June 2020 in Dolsan-eup, Yeosu-si, Jeollanam-do, Republic of Korea. A voucher specimen (UDB2020-06) was placed in the herbarium of the Kangwon National University College of Forest & Environmental Sciences. *U. davidiana* was used as experimental materials by removing impurities, washing, and shading. Once, 10 kg of *U. davidiana* were extracted at room temperature using 60% edible ethanol. After that, the extract was concentrated by eliminating 60% edible ethanol while under vacuum, producing 570 g (U60E) (Supplementary Figure 1). Dimethyl sulfoxide (DMSO) was used to dissolved the dried 60% edible ethanol extract before it was diluted in a cell culture medium.

2.4 Cell viability assay

The 3-(4,5-di methylthiazol-2-yl)-2,5-diphenyltetrazolium bromide (MTT) labeling kit (Millipore Sigma) was used to assess the cell viability. Briefly, U60E and/or TNF-α were applied to 5×10^3 cells planted into 96-well plates for 72 h. After 3 h, the cells were treated with MTT reagent (5 mg/mL), and the formazan product produced was assessed by measuring the intensity of the absorbance at 570 nm.

2.5 FACS analysis

5×10^5 cells were exposed to the indicated reagents for 72 h in order to identify apoptosis. The cells were harvested and given two PBS washes. After that, the cells were labelled with FITC Annexin V and PI (BD Biosciences, Franklin Lakes, NJ, USA) for 15 min, and

staining was measured by flow cytometry on a FACSCalibur (BD Biosciences, Franklin Lakes, NJ, USA). Data were examined using the FlowJo program. Cells that were positive for Annexin V were considered to be apoptotic.

2.6 Western blot analysis

A solution comprising 20 mM Tris (pH 7.5), 150 mM sodium chloride (NaCl), 1% Triton X-100, and a cocktail of protease inhibitors was used to lyse the cells. Proteins from cell lysates were put into nitrocellulose membranes after being electrophoretically separated on 7–10% sodium dodecyl sulfate-polyacrylamide gel electrophoresis gels. The blots were incubated with the indicated primary antibodies (1:1000) at 4°C overnight, and then probed with secondary antibodies (1:5000) at room temperature for 1 h. The blots were subsequently exposed to a film after being treated with an enhanced chemiluminescence substrate (Thermo Fisher Scientific).

2.7 Bromodeoxyuridine enzyme-linked immunosorbent assay for cell proliferation estimation

The manufacturer's instructions were followed while measuring cell proliferation with the Cell Proliferation BrdU ELISA kit (Roche Diagnostics, Indianapolis, IN, USA). Cells treated with the indicated reagents for 72 h were labelled with 10 μM BrdU for 1 h and then incubated with an anti-BrdU peroxidase-conjugated antibody for 90 min. After washing, the substrate reaction, which was gauged using an ELISA plate reader at 450 nm, was used to identify the bound peroxidase.

2.8 Endothelial permeability assay

By measuring the flux of Evans blue (MilliporeSigma)-labeled bovine serum albumin (BSA; MilliporeSigma) through the cell monolayers using a Transwell plate, endothelial permeability was determined (8). Briefly, HRMECs or pericytes were plated on the top or bottom sides of the Transwell filter (Costar, Washington, DC, USA) and cultured in normal or high glucose conditions with U60E and/or TNF-α for an additional 72 h on each side. Evans blue dye was used in the culture medium to measure endothelial permeability. The optical properties of the medium in the bottom chamber were assessed spectrophotometrically at 650 nm (Tecan Infinite M200PRO).

2.9 Statistics analysis

A standard two-tailed Student's *t*-test was used to conduct statistical analyses, and statistical significance was set at $p < 0.05$. Mean ± standard deviation (SD) was used to present quantitative data and figures.

3 Results

3.1 U60E and C7A prevent decrease in cell viability in the pericytes

The effect of U60E on the viability of pericytes and endothelial cells was investigated using an MTT assay. Treatment with U60E alone did not affect the viability of pericytes and HRMECs at any of the indicated concentrations (Figures 1A, B). However, when exposed to high levels of glucose or TNF-α, U60E prevented the decrease in cell viability among pericytes, but not in HRMECs (Figures 1C–F). Next, we tried to find out which compound in U60E plays this role. In a previous study, we confirmed that C7A (Supplementary Figure 2) is an important bioactive compound related to cell survival isolated from *U. davidiana* extract, and U60E also contains abundant C7A (24). Therefore, we hypothesized that C7A contained in U60E is an important compound in preventing the decrease in cell viability of pericytes. Like U60E, when exposed to high levels of glucose or TNF-α, C7A prevented the decrease in cell viability among pericytes, but not in HRMECs (Supplementary Figures 3A–D). These results indicate that C7A contained in U60E prevents the decrease in pericyte cell viability in DR.

3.2 U60E and C7A prevent pericyte apoptosis

Cell apoptosis and proliferation were measured using annexin-V/PI flow cytometric analysis, western blot analysis, and BrdU proliferation ELISA assays, to determine how U60E prevents the decrease in pericyte cell viability in DR. Interestingly, U60E effectively prevented pericyte apoptosis induced by high glucose and TNF-α (Figures 2A, B), however, there was no effect on HRMEC apoptosis (Figures 2C, D). U60E also effectively prevented increased level of apoptosis-associated protein (cleaved caspase-3) by high glucose and TNF-α in pericytes, but had no effect on HRMECs (Figure 2E). In addition, U60E did not affect the proliferation of pericytes or HRMECs exposed to high glucose and TNF-α (Figures 2F–I). C7A also effectively prevented pericyte apoptosis induced by high glucose and TNF-α (Supplementary Figure 4A), but had no effect on HRMEC apoptosis (Supplementary Figure 4B). Additionally, C7A effectively prevented high glucose- and TNF-α-induced increased expression of cleaved caspase-3 in pericytes, but did not affect HRMECs (Supplementary Figure 4C). C7A also did not affect the proliferation of pericytes or HRMECs exposed to high glucose and TNF-α (Supplementary Figures 4D, E). These results indicated that C7A contained in U60E prevents pericyte apoptosis in DR.

3.3 U60E and C7A prevent pericyte apoptosis by reducing the increase in p38 and JNK activity in the diabetic retina

The mechanism by which U60E and C7A prevent pericyte apoptosis was determined. High glucose and TNF-α levels

10.3389/fendo.2023.1138676

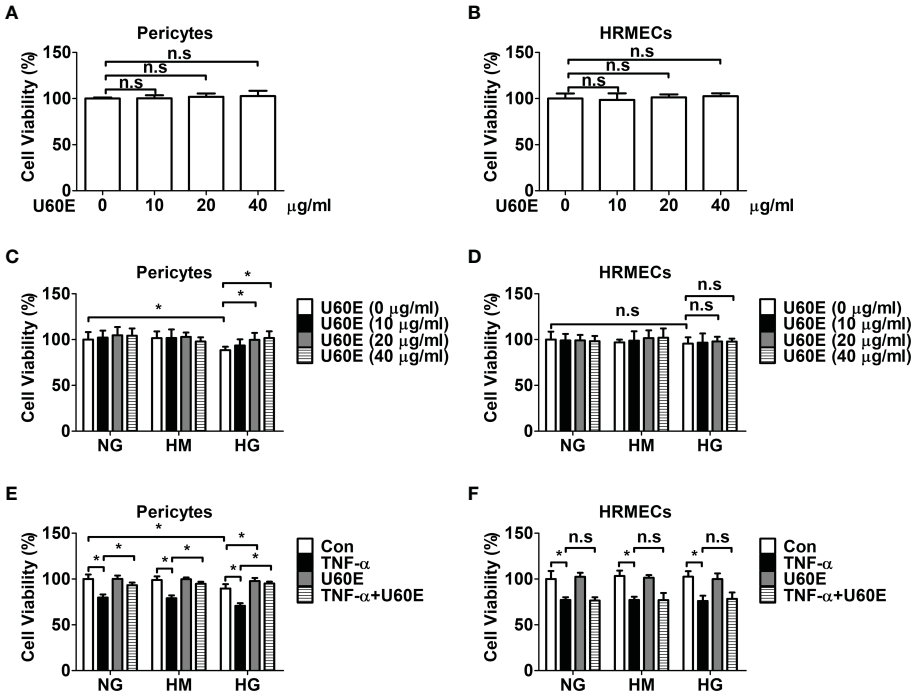

FIGURE 1
Effect of U60E on cell viability of pericytes and human retinal microvascular endothelial cells (HRMECs). Pericytes **(A)** and HRMECs **(B)** were treated with U60E for 72 h at indicated doses. The cell viability was determined by the MTT assay. The bar graph represents the means ± standard deviation (SD) (n = 5). Pericytes **(C)** and HRMECs **(D)** were treated with U60E for 72 h at indicated doses under the conditions of high glucose (HG; 30 mM glucose). Normal glucose (NG; 5 mM glucose) and high mannitol (HM; 5 mM glucose and 25 mM mannitol) were used as controls. The cell viability was determined by the MTT assay. The bar graph represents the means ± SD (n = 5). *P < 0.05. Pericytes **(E)** and HRMECs **(F)** were treated with U60E (20 μg/ml) for 72 h under the conditions of HG, with or without tumor necrosis factor α (TNF-α) (100 ng/ml). The cell viability was determined by the MTT assay. The bar graph represents the means ± SD (n = 5). No significance (n.s.) indicates P > 0.05, *P < 0.05.

increased the phosphorylation of p38 and JNK, but not Erk1/2, in a time-dependent manner in pericytes (Supplementary Figures 5A, B). However, U60E played a role in reducing the phosphorylation of p38 and JNK, which was increased by high glucose and TNF-α levels (Figures 3A, B). To further evaluate the role of p38 and JNK in pericyte apoptosis, we used the p38 inhibitor SB203580, JNK inhibitor SP600125, and p38 and JNK activator anisomycin. SB203580 completely blocked p38 phosphorylation, but not JNK, while SP600125 completely blocked JNK phosphorylation, but not p38 (Supplementary Figures 6A, B). However, both SB203580 and SP600125 played a role in reducing pericyte apoptosis induced by high glucose and TNF-α levels (Supplementary Figures 6C, D). In addition, anisomycin completely prevented the inhibition of high glucose- and TNF-α-induced phosphorylation of p38 and JNK and apoptosis by U60E in pericytes (Figures 3C–F). Like U60E, C7A also played a role in reducing the phosphorylation of p38 and JNK, which was increased by high glucose and TNF-α levels (Supplementary Figures 7A, B). In addition, anisomycin also completely prevented the inhibition of high glucose- and TNF-α-induced phosphorylation of p38 and JNK and apoptosis by C7A in pericytes (Supplementary Figures 7A–D). These results indicated that C7A contained in U60E inhibited apoptosis by blocking the activation of p38 and JNK in the pericytes of DR.

3.4 U60E and C7A prevent endothelial permeability by blocking pericyte apoptosis

Since it was previously confirmed that pericyte survival prevents endothelial permeability by increasing the tight junction protein ZO-1, but not occludin (8), we hypothesized that U60E and C7A would also prevent endothelial permeability by increasing the tight junction protein ZO-1. When pericytes and HRMECs were co-cultured on both sides of the Transwell membrane, the permeability was lower than that of HRMECs cultured on both sides of the Transwell (Figure 4A). In addition, when pericytes and HRMECs were co-cultured, endothelial permeability was increased in both high glucose and TNF-α, conditions that induce pericyte apoptosis (Figure 4A). However, when only HRMECs were co-cultured on both sides of the Transwell, endothelial permeability increased only when treated with TNF-α and not high glucose (Figure 4A). Similarly, when pericytes and HRMECs were co-cultured, the expression level of ZO-1 protein in HRMECs on the top side of the Transwell was higher than that in HRMECs cultured alone, but there was no change in occludin protein levels (Figures 4B, C). In addition, when pericytes and HRMECs were co-cultured, both high glucose and TNF-α, decreased the expression level of ZO-1 (Figures 4B, C). However, when only HRMECs were co-cultured

10.3389/fendo.2023.1138676

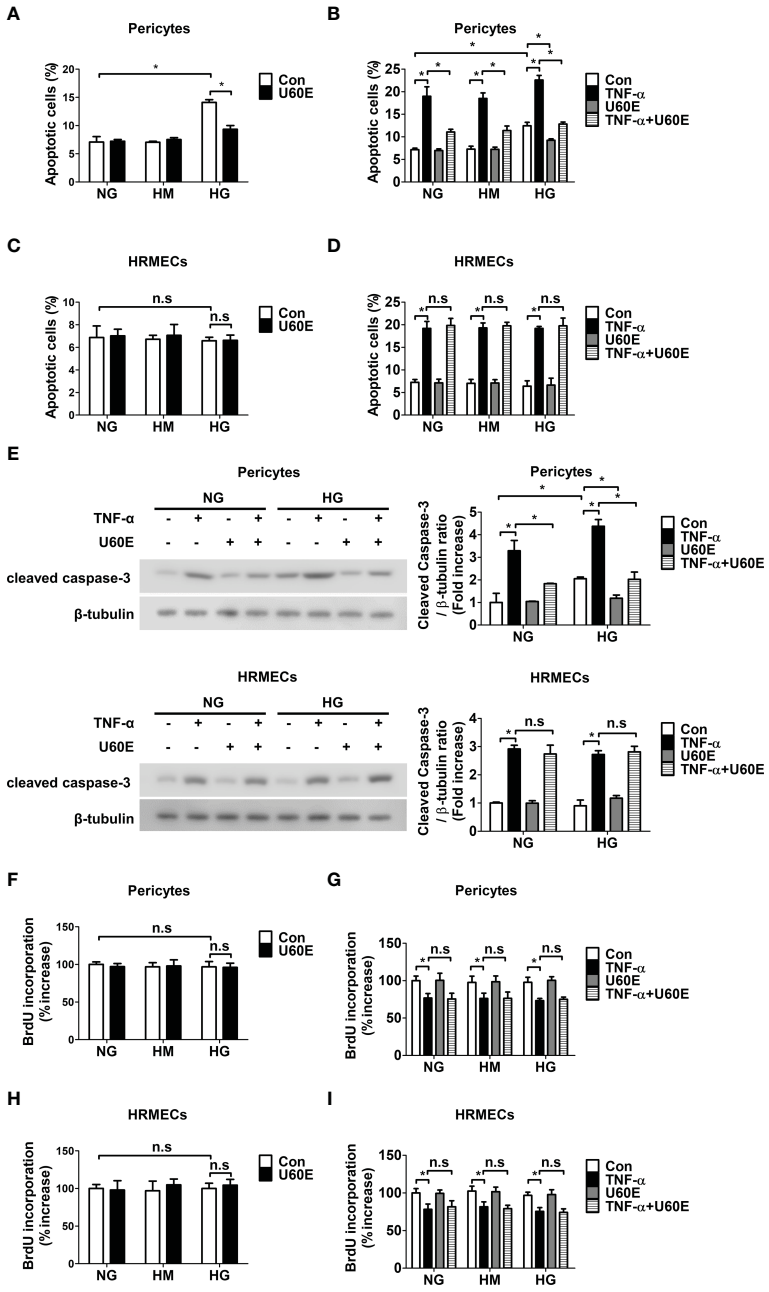

FIGURE 2
Effect of U60E on survival and proliferation in pericytes and human retinal microvascular endothelial cells (HRMECs). **(A-I)** Pericytes and HRMECs were treated with U60E (20 μg/ml) for 72 h under the conditions of high glucose (HG; 30 mM glucose), with or without tumor necrosis factor α (TNF-α) (100 ng/ml). Normal glucose (NG; 5 mM glucose) and high mannitol (HM; 5 mM glucose and 25 mM mannitol) were used as controls. Cell apoptosis of pericytes **(A, B)** and HRMECs **(C, D)** was determined by Annexin V/PI staining and flow cytometric analysis. The apoptotic cells were expressed as a percentage of apoptotic cells in the total cell population. The bar graph represents the means ± standard deviation (SD) (n = 3). **(E)** The cleaved caspase-3 expression was determined by western blot analysis. β-tubulin were used as controls. The right histogram showed quantitative densitometric analysis. The bar graph represents the means ± standard deviation (SD) (n = 3). Cell proliferation of pericytes **(F, G)** and HRMECs **(H, I)** was determined by 5′-bromodeoxy-2′-uridine (BrdU) proliferation ELISA. The bar graph represents the means ± SD (n = 5). No significance (n.s.) indicates $P > 0.05$, $^*P < 0.05$.

on both sides of the Transwell, the expression level of ZO-1 decreased only when treated with TNF-α and not high glucose (Figures 4B, C). Furthermore, when pericytes and HRMECs were co-cultured as well as when only HRMECs were cultured, the expression level of occludin was decreased only when treated with TNF-α, not high glucose (Figures 4B, C). These results indicate that pericyte apoptosis induced by high glucose and TNF-α increases endothelial permeability by reducing the expression of ZO-1 in endothelial cells, and TNF-α not only induces pericyte apoptosis, but also increases endothelial permeability by directly decreasing the expression of ZO-1 and occludin in endothelial cells. On the other hand, high glucose did not directly affect permeability or tight

10.3389/fendo.2023.1138676

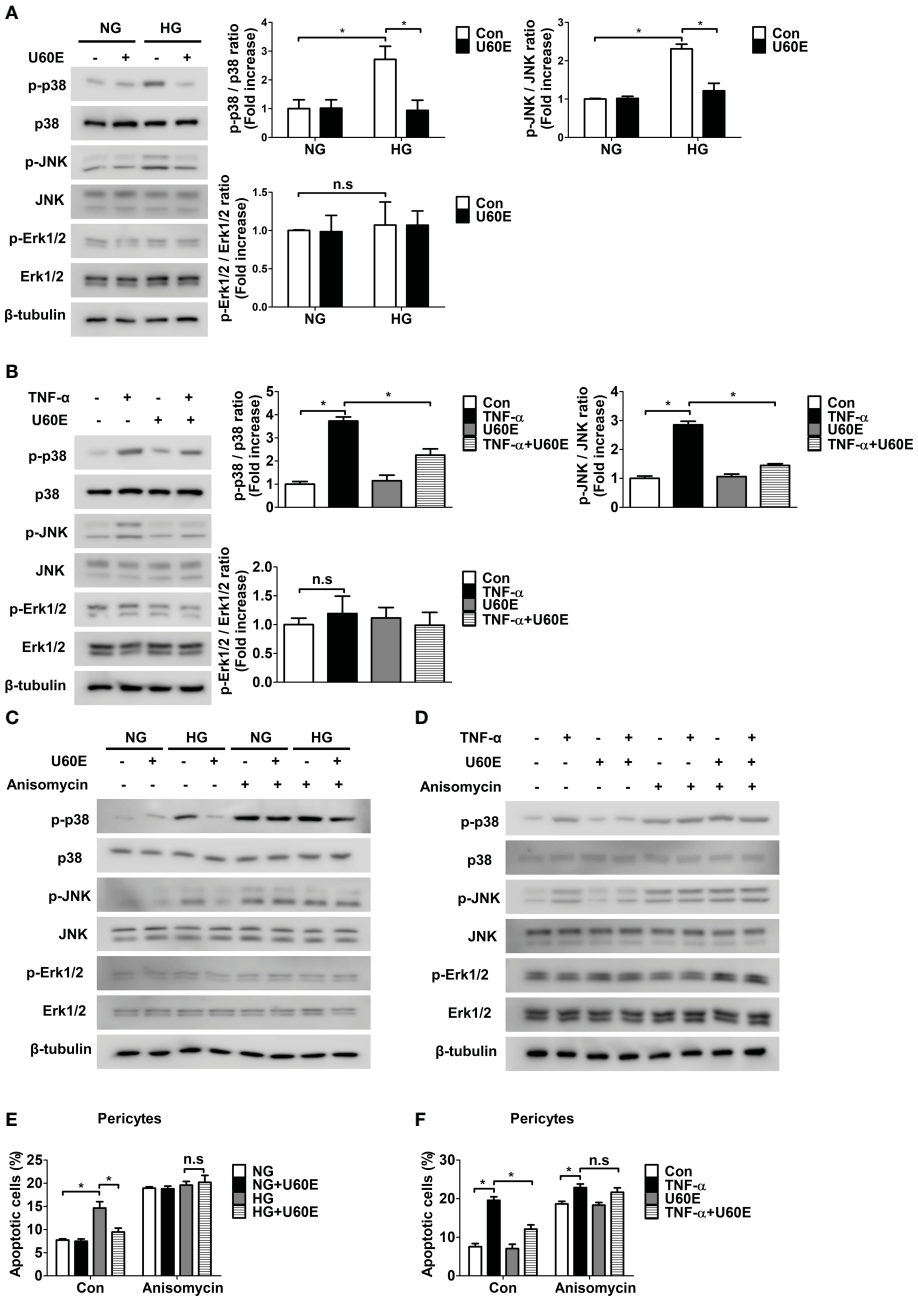

FIGURE 3
Involvement of p38 and JNK signaling in U60E-induced pericyte survival. **(A–D)** Pericytes were treated with U60E (20 μg/mL), tumor necrosis factor α (TNF-α) (100 ng/ml), and/or anisomycin (100 ng/ml) for 30 min under conditions exposed to normal glucose (NG; 5 mM glucose) or high glucose (HG, 30 mM glucose) for 24 h. The phosphorylation of p38 (p-p38), JNK (p-JNK), and Erk1/2 (p-Erk1/2) was determined by western blot analysis. p38, JNK, Erk1/2, and β-tubulin were used as controls. **(A, B)** The right histogram showed quantitative densitometric analysis. The bar graph represents the means ± standard deviation (SD) (n = 3). **(E, F)** Pericytes were treated with U60E (20 μg/mL), TNF-α (100 ng/ml), and/or anisomycin (100 ng/ml) for 72 h under NG or HG conditions. Cell apoptosis was determined by Annexin V/PI staining and flow cytometric analysis. The apoptotic cells were expressed as a percentage of apoptotic cells in the total cell population. The bar graph represents the means ± SD (n = 3). No significance (n.s.) indicates $P > 0.05$, $^*P < 0.05$.

junction protein levels in endothelial cells. Next, we investigated the effect of U60E and C7A on endothelial permeability. U60E prevented endothelial permeability only when pericytes and HRMECs were co-cultured, not when only HRMECs were cultured (Figure 4D). Similarly, U60E restored the ZO-1 expression level decreased by high glucose or TNF-α only when pericytes and HRMECs were co-cultured (Figures 4E, F), but not when only HRMECs were cultured (Figures 4G, H). In addition, U60E did not affect occludin expression levels when co-cultured with pericytes and HRMECs, or when only HRMECs were cultured (Figures 4E–H). Like U60E, C7A also prevented endothelial permeability only when pericytes and HRMECs were co-cultured,

10.3389/fendo.2023.1138676

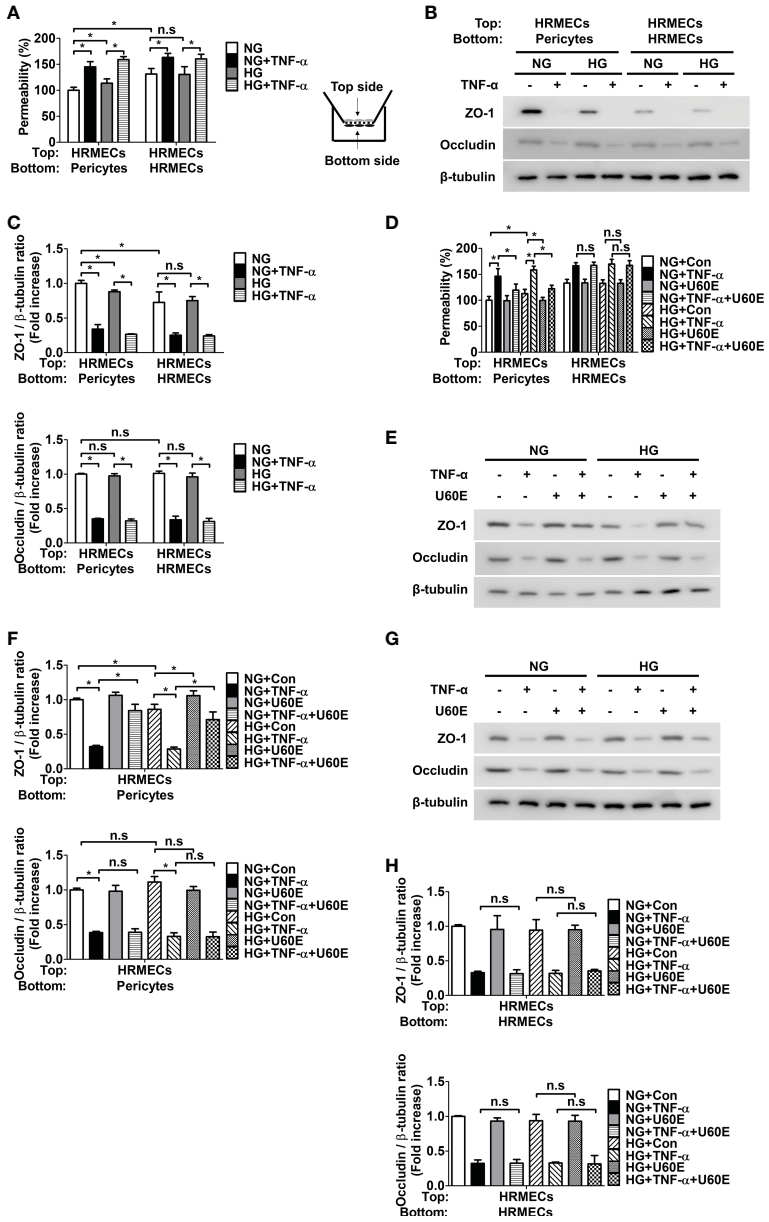

FIGURE 4
Effect of U60E on the *in vitro* permeability in co-cultures of pericytes and human retinal microvascular endothelial cells (HRMECs) and the tight junction protein expression in HRMECs. **(A)** Pericytes and HRMECs incubated on the indicated side of the Transwells as depicted at right. Pericytes and HRMECs were treated with tumor necrosis factor α (TNF-α) (100 ng/ml) under normal glucose (NG; 5 mM glucose) or high glucose (HG, 30 mM glucose) for 72 h. The permeability was measured using Evans blue dye (*n* = 5). **(B)** The tight junction protein expression of ZO-1 and occludin was measured from the top side HRMECs lysates obtained by **(A)**. **(C)** Quantitative densitometric analysis in **(B)** to calculate the ratio of each protein to β-tubulin. The bar graph represents the means ± standard deviation (SD) (*n* = 3). **(D)** Pericytes and HRMECs were incubated on the indicated side of the Transwells and then treated with U60E (20 μg/mL) and/or TNF-α under conditions exposed to NG or HG for 72 h. The permeability was measured using Evans blue dye (*n* = 5). **(E–H)** The tight junction protein expression of ZO-1 and occludin was measured from the top side HRMECs lysates under conditions for co-culture of pericytes and HRMECs **(E, F)** or conditions for culturing only HRMECs **(G, H)** obtained by **(D)**. Quantitative densitometric analysis was performed to calculate the ratio of each protein to β-tubulin **(F, H)**. The bar graph represents the means ± SD (*n* = 3). No significance (n.s.) indicates $P > 0.05$, $^*P < 0.05$.

not when only HRMECs were cultured (Supplementary Figure 8A). C7A also restored the ZO-1 expression level decreased by high glucose or TNF-α only when pericytes and HRMECs were co-cultured (Supplementary Figures 8B, C), but not when only HRMECs were cultured (Supplementary Figures 8D, E). In addition, C7A also did not affect occludin expression levels when co-cultured with pericytes and HRMECs, or when only HRMECs were cultured (Supplementary Figures 8B–E). These results suggest that C7A contained in U60E is not directly involved in permeability of endothelial cells, but prevents pericyte apoptosis induced by high glucose and TNF-α levels, thereby preventing an increase in endothelial permeability.

4 Discussion

In this study, we investigated the effect of U60E on endothelial permeability in DR. In our previous studies, we confirmed that U60E prevents VEGF-induced endothelial cell proliferation, tube formation, and migration; therefore, we hypothesized that U60E could be an effective treatment for retinopathy caused by abnormal angiogenesis, such as proliferative DR (25). However, the effect of U60E on endothelial permeability, another major cause of DR, is unknown. In the present study, U60E did not directly affect endothelial permeability when HRMECs were cultured alone (Figure 4D), but we confirmed that U60E prevented the increase in endothelial permeability induced by high glucose and TNF-α when HRMECs and pericytes were co-cultured (Figure 4D). Therefore, U60E may prevent endothelial permeability through pericytes.

Pericyte loss occurs in the early stage of DR (11–13) and is closely related to an increase in endothelial permeability (8, 10). According to our previous study, we confirmed that increased TNF-α in the diabetic retina induces pericyte apoptosis, leading to pericyte loss, thereby reducing ZO-1 expression in endothelial cells and increasing endothelial permeability (14). In addition, high glucose levels are known to induce rat retinal pericyte apoptosis (15), and we previously confirmed that high glucose induces pericyte apoptosis (26). *U. davidiana* extract also prevents apoptosis in various cells, such as mouse embryonic fibroblast cells, mouse embryonic liver cells, and rat pheochromocytoma cells [10–12]. In addition, in a previous study, we confirmed that the C7A compound contained in *U. davidiana* extract had bioactivity related to cell survival, and U60E also contained C7A (24). In addition, C7A is known as a representative bioactive compound of *U. davidiana* extract (22, 23). Therefore, we hypothesized that C7A contained in *U. davidiana* extract could prevent endothelial permeability by preventing pericyte apoptosis induced by high glucose or TNF-α in DR. In the present study, we confirmed that U60E and C7A prevent pericyte apoptosis induced by high glucose and TNF-α (Figures 2A–E, Supplementary Figures 4A–C). In addition, when HRMECs and pericytes were co-cultured, we confirmed that U60E and C7A restored the decrease in the expression of ZO-1 and the increase in permeability induced by high glucose and TNF-α in endothelial cells (Figures 4D–F, Supplementary Figures 8A–C). These results suggest that C7A contained in U60E prevents endothelial permeability by inhibiting pericyte apoptosis induced by high glucose and TNF-α levels.

DR is the most common microvascular complication in diabetic patients and is the leading cause of blindness between the ages of 20 and 64 (27). The two main causes of DR are retinal vascular leakage and abnormal retinal angiogenesis (27). Interestingly, through previous study (25) and this study, almost all *in vitro* experiments confirmed that U60E or C7A prevent both retinal vascular leakage and retinal angiogenesis in the condition of DR. These are interesting results that U60E or C7A can block both major causes of DR. However, in the case of our studies, there is a limitation that only *in vitro* experiments were conducted. Through *in vivo* experiments, it seems necessary to confirm whether U60E and C7A actually prevent retinal vascular leakage and abnormal retinal angiogenesis in DR. Furthermore, it seems necessary to confirm whether U60E and C7A are actually effective in DR patients through clinical trials. In addition, although U60E and C7A are extract and compound of the *U. davidiana*, which is safe natural product used in traditional medicine, respectively, additional confirmation of the side effects of U60E or C7A seems necessary to safely use the agents in clinical practice. Although more research is needed for these agents to be commercialized in clinical practice, the discovery of potential disease treatment agents at the cell level, such as this study, is thought to be a basic stepping stone for the development of actual clinical treatments in the future.

In this study, we investigated the mechanisms by which U60E and C7A prevent pericyte apoptosis induced by high glucose and TNF-α levels. Previously, we confirmed that high glucose and TNF-α induce pericyte apoptosis by decreasing the expression level of Bcl-2, a pro-survival protein, and increasing the expression level of Bax, a pro-apoptotic protein (14). However, the mechanism by which high glucose and TNF-α induce pericyte apoptosis is unclear. TNF-α and high levels of glucose have been shown to increase the activation of p38, JNK, and ERK1/2 in various cells (28–32). It is also well known that p38, JNK, and ERK1/2 activation is closely related to the apoptotic pathway (33). Recent studies revealed a component of *U. davidiana* extract was known to inhibit TNF-α-induced activation of p38, JNK, and ERK1/2 in human dermal fibroblasts (34). Therefore, we hypothesized that U60E and C7A might prevent pericyte apoptosis by blocking the activation of p38, JNK, or ERK1/2. We confirmed that high glucose and TNF-α induce pericyte apoptosis by activating p38 and JNK (Supplementary Figures 6A–D). However, high levels of glucose and TNF-α did not activate ERK1/2 in the pericytes (Supplementary Figures 5A, B). In addition, we confirmed that U60E and C7A prevented pericyte apoptosis by blocking the activation of p38 and JNK, but were not involved in ERK1/2 (Figures 3C–F, Supplementary Figures 7A–D). These results suggest that C7A contained in U60E prevents apoptosis by blocking the activation of p38 and JNK in pericytes caused by high glucose and TNF-α in DR.

5 Conclusions

DR is the leading cause of vision damage in working-aged people and is currently the most common microvascular complication despite treating DR through glycemic control and photocoagulation. One of the main causes of DR is vascular leakage in the retina, and when vascular leakage occurs in the retina, it causes serious vision damage. Pericytes play a role in interacting with endothelial cells to increase the tight junction protein ZO-1 of the endothelial cells, thereby reducing endothelial permeability. Therefore, when pericyte loss occurs, vascular leakage is more likely to occur. Interestingly, pericyte loss is one of the most characteristic and earliest changes in DR. In addition, pericyte

apoptosis occurs in DR, resulting in pericyte loss. Therefore, if a substance capable of preventing apoptosis of pericytes is found, it may be used as a therapeutic agent for DR by preventing retinal vascular leakage. *U. davidiana* is a safe natural product that has been used in traditional medicine and is attracting attention as a potential treatment for various diseases, but its effect on pericyte loss or vascular leakage in DR is not known at all.

In this study, we confirmed that C7A, a major compound of *U. davidiana* and U60E, prevented the reduction of pericyte cell viability in DR. In addition, U60E and C7A prevented pericyte apoptosis by blocking the activity of p38 and JNK induced by high glucose and TNF-α in DR. U60E and C7A also prevented the increase in endothelial permeability caused by pericyte apoptosis in DR. These results suggest that U60E and C7A may be a potential therapeutic agents in DR by preventing pericyte apoptosis.

Data availability statement

The original contributions presented in the study are included in the article/Supplementary Material, further inquiries can be directed to the corresponding authors.

Author contributions

IK, JS, and DL wrote the manuscript and performed experiments. Y-HK, J-HK, and M-BW analyzed the data and reviewed the manuscript. J-HY and J-KB designed the study and wrote/edited the manuscript. All authors have read and agreed to the published version of the manuscript.

Funding

This study was supported by 2021 Research Grant from Kangwon National University (520210059) and a National Research Foundation of Korea grants funded by the Korean government (NRF-2020R1I1A3071928 to J-HY, NRF-2021R1C1C2003405 to J-KB, and NRF-2021R1A5A2031612 to IK).

Conflict of interest

The authors declare that the research was conducted in the absence of any commercial or financial relationships that could be construed as a potential conflict of interest.

Publisher's note

All claims expressed in this article are solely those of the authors and do not necessarily represent those of their affiliated organizations, or those of the publisher, the editors and the reviewers. Any product that may be evaluated in this article, or claim that may be made by its manufacturer, is not guaranteed or endorsed by the publisher.

Supplementary material

The Supplementary Material for this article can be found online at: https://www.frontiersin.org/articles/10.3389/fendo.2023.1138676/full#supplementary-material

References

1. Antonetti DA, Klein R, Gardner TW. Diabetic retinopathy. *N Engl J Med* (2012) 366(13):1227–39. doi: 10.1056/NEJMra1005073

2. Duh EJ, Sun JK, Stitt AW. Diabetic retinopathy: current understanding, mechanisms, and treatment strategies. *JCI Insight* (2017) 2(14):e93751. doi: 10.1172/jci.insight.93751

3. Shah CA. Diabetic retinopathy: a comprehensive review. *Indian J Med Sci* (2008) 62(12):500–19.

4. Moss SE, Klein R, Klein BE. The incidence of vision loss in a diabetic population. *Ophthalmology* (1988) 95(10):1340–8. doi: 10.1016/s0161-6420(88)32991-x

5. Shepro D, Morel NM. Pericyte physiology. *FASEB J* (1993) 7(11):1031–8. doi: 10.1096/fasebj.7.11.8370472

6. Armulik A, Abramsson A, Betsholtz C. Endothelial/pericyte interactions. *Circ Res* (2005) 97(6):512–23. doi: 10.1161/01.RES.0000182903.16652.d7

7. Hori S, Ohtsuki S, Hosoya K, Nakashima E, Terasaki T. A pericyte-derived angiopoietin-1 multimeric complex induces occludin gene expression in brain capillary endothelial cells through tie-2 activation *in vitro*. *J Neurochem* (2004) 89(2):503–13. doi: 10.1111/j.1471-4159.2004.02343.x

8. Yun JH, Jeong HS, Kim KJ, Han MH, Lee EH, Lee K, et al. Beta-adrenergic receptor agonists attenuate pericyte loss in diabetic retinas through akt activation. *FASEB J* (2018) 32(5):2324–38. doi: 10.1096/fj.201700570RR

9. Yun JH, Koh YJ, Jeong HS, Lee DH, Lee EH, Cho CH. Propranolol increases vascular permeability through pericyte apoptosis and exacerbates oxygen-induced retinopathy. *Biochem Biophys Res Commun* (2018) 503(4):2792–9. doi: 10.1016/j.bbrc.2018.08.041

10. Yun JH. Interleukin-1beta induces pericyte apoptosis *via* the NF-kappaB pathway in diabetic retinopathy. *Biochem Biophys Res Commun* (2021) 546:46–53. doi: 10.1016/j.bbrc.2021.01.108

11. Cogan DG, Toussaint D, Kuwabara T. Retinal vascular patterns. IV. diabetic retinopathy. *Arch Ophthalmol* (1961) 66:366–78. doi: 10.1001/archopht.1961.00960010368014

12. Hall AP. Review of the pericyte during angiogenesis and its role in cancer and diabetic retinopathy. *Toxicol Pathol* (2006) 34(6):763–75. doi: 10.1080/01926230600936290

13. Beltramo E, Porta M. Pericyte loss in diabetic retinopathy: mechanisms and consequences. *Curr Med Chem* (2013) 20(26):3218–25. doi: 10.2174/09298673113209990022

14. Yun JH. Hepatocyte growth factor prevents pericyte loss in diabetic retinopathy. *Microvasc Res* (2021) 133:104103. doi: 10.1016/j.mvr.2020.104103

15. Wang W, Zhao H, Chen B. DJ-1 protects retinal pericytes against high glucose-induced oxidative stress through the Nrf2 signaling pathway. *Sci Rep* (2020) 10(1):2477. doi: 10.1038/s41598-020-59408-2

16. Lee S-E, Kim Y-S, Kim J-E, Bang J-K, Seong N-S. Antioxidant activity of ulmus davidiana var. japonica n. and hemipteleae davidii p. *Korean J Med Crop Sci* (2004) 12 (4):321–7.

17. Choi SY, Lee S, Choi WH, Lee Y, Jo YO, Ha TY. Isolation and anti-inflammatory activity of bakuchiol from ulmus davidiana var. japonica. *J Med Food* (2010) 13 (4):1019–23. doi: 10.1089/jmf.2009.1207

18. Ahn J, Lee JS, Yang KM. Ultrafine particles of ulmus davidiana var. japonica induce apoptosis of gastric cancer cells *via* activation of caspase and endoplasmic reticulum stress. *Arch Pharm Res* (2014) 37(6):783–92. doi: 10.1007/s12272-013-0312-2

19. Hong N-D, Rho Y-S, Kim N-J, Kim J-S. A study on efficacy of ulmi cortex. *Korean J Pharmacognosy* (1990) 21(3):217–22.

20. Lee S. (1996) 39.

21. Kim E-J, Jang M-K, Yoon E-H, Jung C-Y, Nam D-W, Lee S-D, et al. Efficacy of pharmacopuncture using root bark of ulmus davidiana planch in patients with knee osteoarthritis: a double-blind randomized controlled trial. *J Acupuncture Meridian Stud* (2010) 3(1):16–23. doi: 10.1016/S2005-2901(10)60003-9

22. Jung MJ, Heo S-I, Wang M-H. HPLC analysis and antioxidant activity of ulmus davidiana and some flavonoids. *Food Chem* (2010) 120(1):313–8. doi: 10.1016/j.foodchem.2009.09.085

23. Park YJ, Kim DM, Jeong MH, Yu JS, So HM, Bang IJ, et al. (-)-Catechin-7-O-beta-d-Apiofuranoside inhibits hepatic stellate cell activation by suppressing the STAT3 signaling pathway. *Cells* (2019) 9(1):30. doi: 10.3390/cells9010030

24. Yun JH, Kim HO, Jeong JH, Min Y, Park KH, Si CL, et al. Ulmus davidiana var. japonica extracts suppress lipopolysaccharide-induced apoptosis through intracellular calcium modulation in U937 macrophages. *Front Energy Res* (2022) 10. doi: 10.3389/fenrg.2022.820330

25. Park J, Kim HO, Park KH, Wie MB, Choi SE, Yun JH. A 60% edible ethanolic extract of ulmus davidiana inhibits vascular endothelial growth factor-induced angiogenesis. *Molecules* (2021) 26(4):781. doi: 10.3390/molecules26040781

26. Park SW, Yun JH, Kim JH, Kim KW, Cho CH, Kim JH. Angiopoietin 2 induces pericyte apoptosis *via* alpha3beta1 integrin signaling in diabetic retinopathy. *Diabetes* (2014) 63(9):3057–68. doi: 10.2337/db13-1942

27. Crawford TN, Alfaro DV3rd, Kerrison JB, Jablon EP. Diabetic retinopathy and angiogenesis. *Curr Diabetes Rev* (2009) 5(1):8–13. doi: 10.2174/157339909787314149

28. Hoshi S, Nomoto K, Kuromitsu J, Tomari S, Nagata M. High glucose induced VEGF expression *via* PKC and ERK in glomerular podocytes. *Biochem Biophys Res Commun* (2002) 290(1):177–84. doi: 10.1006/bbrc.2001.6138

29. Xu ZG, Kim KS, Park HC, Choi KH, Lee HY, Han DS, et al. High glucose activates the p38 MAPK pathway in cultured human peritoneal mesothelial cells. *Kidney Int* (2003) 63(3):958–68. doi: 10.1046/j.1523-1755.2003.00836.x

30. Takata F, Dohgu S, Matsumoto J, Takahashi H, Machida T, Wakigawa T, et al. Brain pericytes among cells constituting the blood-brain barrier are highly sensitive to tumor necrosis factor-alpha, releasing matrix metalloproteinase-9 and migrating *in vitro*. *J Neuroinflamm* (2011) 8:106. doi: 10.1186/1742-2094-8-106

31. Sabio G, Davis RJ. TNF and MAP kinase signalling pathways. *Semin Immunol* (2014) 26(3):237–45. doi: 10.1016/j.smim.2014.02.009

32. Shan L, Yang D, Zhu D, Feng F, Li X. High glucose promotes annulus fibrosus cell apoptosis through activating the JNK and p38 MAPK pathways. *Biosci Rep* (2019) 39(7):BSR20190853. doi: 10.1042/BSR20190853

33. Wada T, Penninger JM. Mitogen-activated protein kinases in apoptosis regulation. *Oncogene* (2004) 23(16):2838–49. doi: 10.1038/sj.onc.1207556

34. Lee S, Yu JS, Phung HM, Lee JG, Kim KH, Kang KS. Potential anti-skin aging effect of (-)-Catechin isolated from the root bark of ulmus davidiana var. japonica in tumor necrosis factor-alpha-Stimulated normal human dermal fibroblasts. *Antioxidants (Basel)* (2020) 9(10):981. doi: 10.3390/antiox9100981

frontiers | Frontiers in Endocrinology

TYPE Original Research
PUBLISHED 17 May 2023
DOI 10.3389/fendo.2023.1108097

OPEN ACCESS

EDITED BY
Rajashekhar Gangaraju,
University of Tennessee Health Science Center (UTHSC), United States

REVIEWED BY
Guoqiang Zeng,
Shenzhen University General Hospital, China
Carmen Clapp,
National Autonomous University of Mexico, Mexico

*CORRESPONDENCE
Ming-Shan He
mingshanher@gmail.com

RECEIVED 25 November 2022
ACCEPTED 08 May 2023
PUBLISHED 17 May 2023

CITATION
Hsieh T-C, Deng G-H, Chang Y-C, Chang F-L and He M-S (2023) A real-world study for timely assessing the diabetic macular edema refractory to intravitreal anti-VEGF treatment. *Front. Endocrinol.* 14:1108097. doi: 10.3389/fendo.2023.1108097

A real-world study for timely assessing the diabetic macular edema refractory to intravitreal anti-VEGF treatment

Tsung-Cheng Hsieh[1], Guang-Hong Deng[2], Yung-Ching Chang[3], Fang-Ling Chang[3] and Ming-Shan He[3,4]*

[1]Institute of Medical Sciences, Tzu Chi University, Hualien, Taiwan, [2]Tzu Chi University Research Center for Big Data Teaching, Research and Statistic Consultation, Hualien, Taiwan, [3]Department of Ophthalmology, Buddhist Tzu Chi General Hospital, Hualien, Taiwan, [4]Department of Ophthalmology and Visual Science, Tzu Chi University, Hualien, Taiwan

Background: Early Identifying and characterizing patients with diabetic macular edema (DME) is essential for individualized treatment and outcome optimization. This study aimed to timely investigate optical coherence tomography (OCT) biomarkers of DME refractory to intravitreal anti-vascular endothelial growth factor (VEGF) therapy.

Methods: We retrospective reviewed 72 eyes from 44 treatment-naïve patients who were treated with intravitreal anti-VEGF for DME. OCT scans prior to anti-VEGF were evaluated for serous retinal detachment (SRD), size of outer nuclear layer cystoid changes, diffuse retinal thickening, integrity of the inner segment-outer segment (IS-OS) junction, quantity and location of hyperreflective foci, vitreomacular interface abnormalities, and epiretinal membrane (ERM). The Baseline best-corrected visual acuity (BCVA) and central macular thickness was recorded at baseline and 4 months after treatment with anti-VEGF. The main outcome measure was the correlation between spectral-domain OCT measurements and BCVA response at baseline and after anti-VEGF treatment (mean change from baseline; ≥ 10 Early Treatment Diabetic Retinopathy Study letters in BCVA).

Results: Partially continuous IS-OS layers (partially vs. completely continuous: β, -0.138; Wald chi-square, 16.392; P<0.001) was predictor of better response to anti-VEGF treatment. In contrast, ERM (present vs. absent ERM: β, 0.215; Wald chi-square, 5.921; P=0.015) and vitreomacular traction (vitreomacular traction vs. posterior vitreous detachment: β=0.259; Wald chi-square=5.938; P=0.015) were the predictors of poor response. The improvement of BCVA trended toward the OCT predictive value of central macular thickness reduction; however, this was not significant.

Conclusion: Partially continuous IS-OS layers is predictive of better response to anti-VEGF therapy in DME. Meanwhile, ERM is a significant predictor of poor response.

KEYWORDS

diabetic macular edema, anti-vegf, optical coherence tomography, epiretinal membrane, diabetic retinopathy

Introduction

Vision loss associated with diabetic retinopathy (DR) is most commonly caused by diabetic macular edema (DME) (1). The Diabetes Control and Complications Trial (DCCT) reported that 27% of patients with type 1 diabetes developed macular edema within 9 years of diabetes onset (2). Other studies indicate that in type 2 diabetes patients, the prevalence increases from 3% within 5 years of diagnosis to 28% after 20 years (3). Although several treatment options are available, no consensus on DME treatment based on patient status has been achieved.

Vascular endothelial growth factor (VEGF) is an important mediator of abnormal vascular permeability in eyes with DME (4). Anti-VEGF injections are generally proposed as first-line therapy for center-involved DME and are effective in improving visual acuity (VA), with 10%–40% of patients achieving significant improvement in VA after 1 year of treatment (5, 6). However, a considerable proportion have unsatisfactory response to anti-VEGF agents; 40% of eyes with DME do not or have suboptimal response to anti-VEGF treatment (7, 8). Nonetheless, there is little information to date about the prognostic factors of poor responders.

Optical coherence tomography (OCT) images are readily available to physicians and provide detailed information. Structural changes presumably reflect part of the complex pathophysiologic processes occurring in DME. Furthermore, anatomical measures on spectral-domain (SD) OCT can predict treatment success or failure of various therapies (9). Distinct structural changes identifiable on SD-OCT could reflect part of the intraocular pathophysiologic process change after anti-VEGF treatments and help predict the treatment response.

Among patients with DME refractory to anti-VEGF therapy after a loading dose of three consecutive monthly injections, those who were switched to other treatment modalities (e.g., corticosteroids) had better visual and anatomical outcomes at 12 months than did those who continued with anti-VEGF therapy (10). *Post hoc* analysis from the DRCR.net Protocol I study also indicates that early central macular thickness (CMT) response to anti-VEGF is a significant prognostic indicator of medium to long-term anatomical outcomes in DME (11). Accordingly, the early identification of patients who would not benefit from first-line treatment with anti-VEGF therapy is critical. Real-world studies have become increasingly important in providing evidence of treatment effectiveness in clinical practice. They can therefore provide information on the long-term safety, particularly of rare events, and efficacy of drugs in large heterogeneous populations, as well as information on utilization patterns and health and economic outcomes (12). We aimed to investigate whether the characteristics identified on SD-OCT could be predictive markers of treatment response after three monthly anti-VEGF therapies in DME patients.

Research design and methods

Study design and setting

This retrospective study was approved by the Institutional Review Board of the Research Ethics Committee of Hualien Tzu-Chi Hospital and Buddhist Tzu-Chi Medical Foundation (IRB110-188-B) and was conducted in accordance with the guidelines of the Declaration of Helsinki. Data were obtained from Hualien Tzu Chi Hospital Medical Center. Data of patients with DME treated with intravitreal anti-VEGF between April 1, 2013 and April 1, 2021 were reviewed. Written informed consent was obtained from all patients.

Study participants

The inclusion criteria were as follows (1): age≥ 20 years; (2) type 1 or 2 diabetes mellitus; (3) treatment-naïve DME causing visual loss macular edema defined clinically and as retinal thickness of >300 μm in the central subfield and intraretinal or subretinal fluid seen on SD-OCT; and (4) treatment with anti-VEGF agents. The exclusion criteria were (1) another concomitant ocular disease that causes macular edema (i.e., neovascular age-related macular degeneration or choroidal neovascularization due to other reasons, retinal vein occlusion, uveitis, and recent intraocular surgery possibly causing postsurgical macular edema or influence drug absorption, such as cataract surgery or vitrectomy); (2) previous treatment with intraocular corticosteroids or pan-retinal photocoagulation within 6 months before treatment with anti-VEGF agents. For patients who received bilateral treatment, both the eyes were included. Refractory DME was defined as a reduction of less than 10% in retinal thickness on SD-OCT measured 1 month after at least three monthly anti-VEGF injections. Data on demographic data, age, sex, and type of retinopathy (non-proliferative or proliferative) were collected from patient charts.

Optical coherence tomography analysis

Qualitative and quantitative evaluations of SD-OCT images encompassing the fovea were performed at baseline and 4 months after treatment to assess the presence of several morphologic features, including (1) SRD (height at the fovea was measured); (2) cystoid changes in the outer nuclear layer (ONL) and maximal cyst size (small <100μm, large 100-200μm, giant >200μm); (3) continuity of the inner segment-outer segment (IS-OS) layer (completely continuous, partly disrupted, completely disrupted); (4) presence of hyperreflective foci (HRF), as well as quantity (few, 2–10; many >11) and location (between the internal limiting membrane and the inner nuclear layer; between the outer plexiform layer and external limiting membrane; in all retinal layers); (5) status of the vitreomacular interface (detached, vitreomacular adhesion [VMA], vitreomacular traction[VMT]); (6) presence of an epiretinal membrane (ERM); (7) CMT; and (8) presence of diffuse retinal thickening (DRT), as well as the width (≦1, 1–3, 3–6 mm). OCT scans were obtained using SD-OCT (Heidelberg Spectralis, Heidelberg, Germany). The listed features were evaluated using a horizontal b-scan encompassing the fovea. The OCT images were evaluated by two experienced retina specialists (MS He and YC Chang) blinded to the outcome. CMT was recorded at baseline and at 1, 2, 3, and 4 months.

10.3389/fendo.2023.1108097

Statistical analysis

Continuous variables and categorical variables were expressed as the mean with standard deviation and as the frequency with proportion, respectively. Both eyes of the patients were included in the analysis. Considering the correlation between eyes, the generalized estimate equation (GEE) was employed for assessing the baseline predictors for the continuous outcome of central macular thickness reduction and central macular thickness reduction <10%. All statistical analyses were performed using SPSS for Windows (version 21.0; IBM, Armonk, NY, USA). All p values were two-sided, and $p<0.05$ was considered statistically significant.

Results

Study participants

A total of 72 eyes from 44 patients were included in the analysis. The demographic patient characteristics are shown in Table 1. All eyes with DME had no history of anti-VEGF treatment and were treated with three consecutive monthly intravitreal injections of anti-VEGF. Three main types of anti-VEGF drugs were used in our cohort, the most common of which was ranibizumab (n=60 eyes, 83.3%), followed by aflibercept (n=10, 13.9%) and bevacizumab (n=2, 2.8%). A total of 24 eyes (33.3%) had proliferative diabetic retinopathy (PDR), 43 eyes (59.7%) had severe non-proliferative diabetic retinopathy (NPDR), and 5 eyes (6.9%) had moderate NPDR.

Anatomic baseline characteristics

The baseline OCT characteristics are shown in Table 1. With respect to the DME morphology, DRT was the most common presentation (n=59 eyes, 81.9%), followed by cystoid macular edema (CME) (n=33 eyes, 45.8%) and SRD (n=16 eyes, 22.2%). Furthermore, eyes with DME were more commonly to present with complete continuous IS-OS continuity (52.8%), HRF (86.1%), and VMA (88.9%) in the baseline.

Optical coherence tomography predictors for treatment response

Eyes with partially continuous IS-OS layers had a better treatment response after 4 months (partially vs. completely continuous: β=-0.138; Wald chi-square=16.392; P<0.001). Baseline VMT was a predictor of poor functional treatment response after 4 months (VMT vs. posterior vitreous detachment: β=0.259; Wald chi-square=5.938; P=0.015). Moreover, eyes with ERM at baseline were more likely to have poor response at 4 months (present vs. absent ERM: β=0.215; Wald chi-square=5.921; P=0.015). Figure 1 shows the OCT biomarkers that were

TABLE 1 Descriptive statistics: demographic data and optical coherence tomography baseline measures.

Variables are based on number of subjects		
Sex	N (%)	
Female	25 (56.8%)	
Male	19 (43.2%)	
Age (yrs), Mean (SD)	62.64 (9.75)	
HbA1c (%), Mean (SD)	8.34 (2.09)	
Variables are based on number of eyes		
Baseline Measures	Left eye N=37	Right eye N=35
Diffuse retinal thickening		
3-6mm	15 (40.5%)	17 (48.6%)
1-3mm	17 (45.9%)	6 (17.1%)
≤1mm	3 (8.1%)	1 (2.9%)
0mm (ref.)	2 (5.4%)	11 (31.4%)
ONL cyst size		
Giant	1 (2.7%)	2 (5.7%)
Large	8 (21.6%)	11 (31.4%)
Small	4 (10.8%)	7 (20.0%)
No (ref.)	24 (64.9%)	15 (42.9%)
IS-OS continuity		
Completely disrupted	2 (5.6%)	2 (5.7%)
Partially continuous	13 (36.1%)	16 (45.7%)
Completely continuous	21 (58.3%)	17 (48.6%)
HRF foci-quantity & foci-location		
Many (≥11) & all layers	9 (24.3%)	14 (40.0%)
Many (≥11) & OPL-ELM	1 (2.7%)	0 (0.0%)
Many (≥11) & ILM-INL	1 (2.7%)	3 (8.6%)
Few (2-10) & all layers	8 (21.6%)	5 (14.3%)
Few (2-10) & OPL-ELM	2 (5.4%)	2 (5.7%)
Few (2-10) & ILM-INL	11 (29.7%)	6 (17.1%)
Absent	5 (13.5%)	5 (14.3%)
Vitreomacular interface		
VMT	1 (2.8%)	0 (0.0%)
VMA	30 (83.3%)	34 (90.1%)
PVD	5 (13.9%)	1 (2.9%)
ERM		
Yes	7 (18.9%)	8 (22.9%)
No (ref.)	30 (81.1%)	27 (77.1%)

(Continued)

10.3389/fendo.2023.1108097

TABLE 1 Continued

Variables are based on number of eyes		
Baseline Measures	Left eye N=37	Right eye N=35
SRD		
Yes	5 (13.5%)	11 (31.4%)
No	32 (86.5%)	24 (68.6%)
DR type		
PDR	13 (35.1%)	11 (31.4%)
Severe NPDR	22 (59.5%)	21 (60.0%)
Moderate NPDR	2 (5.4%)	3 (8.6%)

ELM, external limiting membrane; ERM, epiretinal membrane; ref, reference; HRF, hyperreflective foci; ILM, internal limiting membrane; IS-OS, inner segment-outer segment; NPDR, non- proliferative diabetic retinopathy; ONL, outer nuclear layer; OPL, outer plexiform layer; PDR, proliferative diabetic retinopathy; PVD, posterior vitreous detachment; SD, standard deviation; SRD, serous retinal detachment; VMA, vitreomacular adhesion; VMT, vitreomacular traction.

predictive of treatment response after 4 months. The predictive values of all OCT measures examined are shown in Table 2. Baseline predictors of mean CMT reduction are shown in Figure 2. Furthermore, the odds of gaining BCVA ≥10 letters at 4 months trended toward the OCT predictive value of CMT reduction; however, this was not significant (Table 3). All OCT biomarkers that were predictive of good BCVA response are shown in Figure 3.

In a subanalysis, eyes with CMT reduction of less than 10% after 4 months were designated to the refractory group (Table 4). The results showed that ERM at baseline predicted highly increased odds of poor response at 4 months (OR, 12.469; 95% CI, 2.012–77.259; P=0.007). In contrast, large ONL cyst sizes at baseline (OR, 0.096; 95% CI, 0.015–0.62; P=0.014) and partially continuous IS-OS layers (OR, 0.139; 95% CI, 0.026–0.742; P=0.021) were less likely to be refractory group after 4 months (Figure 4).

In the univariate analysis, SRD at baseline was significantly associated with treatment response to anti-VEGF agents (MD, -188.69 μm; 95% CI, -128.95 to -248.43; P<0.001) (Table 5). However, in multivariate survival analysis, treatment response to anti-VEGF regimens was not a significant influencing factor in patients with SRD (present vs. absent: β, 0.01; Wald chi-square, 0.005; P=0.945) (Table 2).

Discussion

In this real-world evidence-based study, we identified partially continuous IS-OS layers as biomarkers that predict better response to anti-VEGF therapy in DME. In contrast, ERM is a significant predictor of poor response. DME has a complex pathogenesis, with multiple factors contributing to its pathophysiology, including angiogenic, inflammatory, hypoxic, and hemodynamic processes that lead to the breakdown of the blood-retinal barrier (BRB) and leakage of intraretinal fluid (13). Anti-VEGF injections are generally

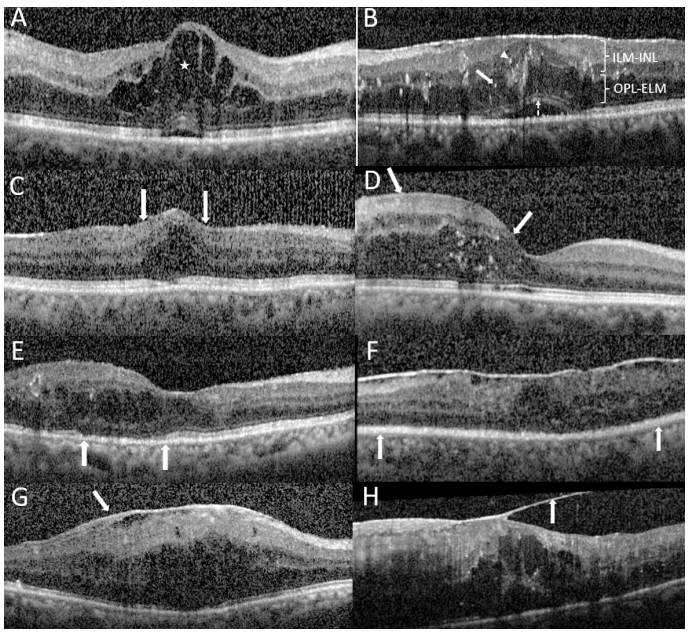

FIGURE 1
OCT measures. **(A)**, Grading of outer nuclear layer (ONL) cysts: Cystoid diabetic macular edema (DME) with a giant ONL cyst (★). **(B)**, Serous retinal detachment (SRD) with diffuse retinal thickening (DRT, width of 3–6mm) showing retinal elevation between the sensory retina and the retinal pigment epithelium (dashed arrow); the height of SRD is measured. Grading of hyperreflective foci (HRF): A high number of HRF (≥11) are distributed in all layers (located between the ILM and INL [arrowhead] and between OPL and ELM [arrow]). **(C, D)**, Grading of DRT: **(C)**, DME associated with focal DRT (width ≦1 mm, between arrows). **(D)**, DME related to localized DRT (width within 1–3 mm, between arrows). **(E, F)**, Grading of the inner segment-outer segment (IS-OS) integrity. **(E)**, Partially disrupted continuity of the IS-OS layer (between arrows). **(F)**, Complete discontinuity of the IS-OS layer (between arrows). **(G)**, DME associated with epiretinal membrane (arrow). **(H)**, DME associated with vitreomacular traction (arrow). ELM, external limiting membrane; ILM, internal limiting membrane; INL, inner nuclear layer; OPL, outer plexiform layer.

10.3389/fendo.2023.1108097

TABLE 2 Baseline predictors for the mean reduction (improvement) of central macular thickness.

Variable	β	Wald Chi-Square	P-value
Sex			
Female	-0.068	0.465	0.495
Male (ref.)	–		
Age	0.006	2.053	0.152
Diffuse retinal thickening			
3-6mm	0.104	0.756	0.384
1-3mm	0.149	1.864	0.172
≤1mm	-0.108	3.542	0.060
0mm (ref.)	–		
ONL cyst size			
Giant	0.069	1.080	0.299
Large	0.035	0.381	0.537
Small	-0.165	1.908	0.167
No (ref.)	–		
IS-OS continuity			
Completely disrupted	-0.396	2.034	0.154
Partially continuous	-0.138	16.392	<0.001
Completely continuous (ref.)	–		
HRF foci-quantity			
Many (≥11) & all layers	0.102	1.130	0.288
Many (≥11) & OPL-ELM	-0.076	0.037	0.847
Many (≥11) & ILM-INL	0.013	0.037	0.848
Few (2-10) & all layers	0.140	2.062	0.151
Few (2-10) & OPL-ELM	0.227	0.348	0.555
Few (2-10) & ILM-INL	0.072	1.666	0.197
Absent (ref.)	–		
Vitreomacular interface			
VMT	0.259	5.938	0.015
VMA	0.083	0.845	0.358
PVD (ref.)	–		
ERM			
Yes	0.215	5.921	0.015
No (ref.)	–		
DR type			
PDR	-0.216	1.631	0.202
Severe NPDR	-0.121	0.555	0.456
Moderate NPDR (ref.)	–		

(Continued)

10.3389/fendo.2023.1108097

TABLE 2 Continued

Variable	β	Wald Chi-Square	P-value
SRD			
Yes	0.010	0.005	0.945
No (ref.)	–		

ELM, external limiting membrane; ERM, epiretinal membrane; ref, reference; HRF, hyperreflective foci; ILM, internal limiting membrane; IS-OS, inner segment-outer segment; NPDR, non-proliferative diabetic retinopathy; ONL, outer nuclear layer; OPL, outer plexiform layer; PDR, proliferative diabetic retinopathy; PVD, posterior vitreous detachment; SRD, serous retinal detachment; VMA, vitreomacular adhesion; VMT, vitreomacular traction; β, beta coefficient.

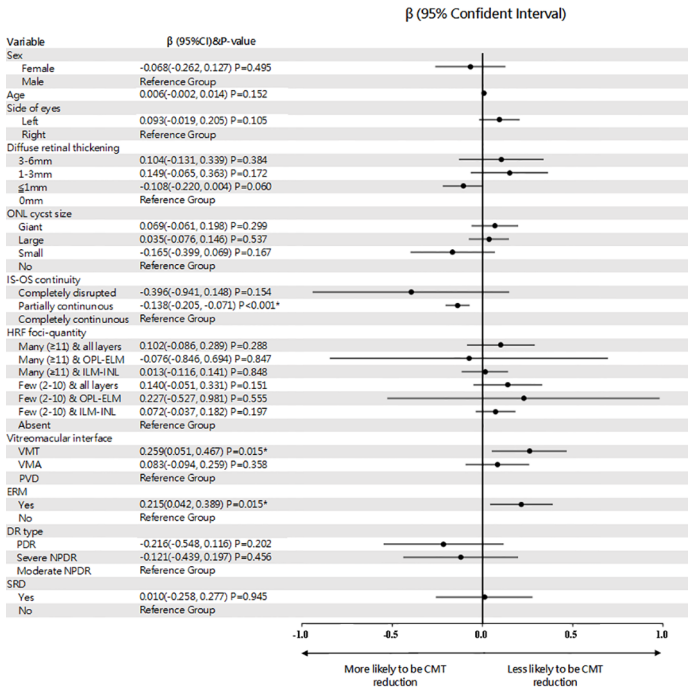

FIGURE 2
Forest plot of baseline predictors of CMT reduction, using generalized estimate equation model. CMT, central macular thickness; ONL, outer nuclear layer; IS-OS, inner segment-outer segment; HRF, hyperreflective foci; OPL, outer plexiform layer; ELM, external limiting membrane; ILM, internal limiting membrane; VMA, vitreomacular adhesion; VMT, vitreomacular traction; PVD, posterior vitreous detachment; ERM, epiretinal membrane; PDR, proliferative diabetic retinopathy; NPDR, non-proliferative diabetic retinopathy; SRD, serous retinal detachment; β, beta coefficient.
* Statistically significant at p<0.05.

recommended as the first-line therapy for DME; however, refractory cases are not uncommon. A *post-hoc* analysis of the DRCR.net Protocol I reported an approximately 40% prevalence of refractory DME after 2 years of monthly intravitreal ranibizumab treatment (7). Combined data from the RIDE/RISE trial found that 23% of eyes receiving intravitreal ranibizumab had persistent macular edema at the end of the study period (14). The real-world prevalence of refractory DME may be higher than estimated in these studies, as rigorous enrolment and follow-up protocols in clinical trials are unlikely to be fully replicated in everyday practice (15). An important issue is the possibility of early identification of patients who would not benefit from first-line anti-VEGF therapy.

VEGF is significantly higher in all types of DME than that in the eyes of non-diabetes patients, indicating that VEGF is equally important for any morphological changes in eyes with DME (16). However, evidence indicates that bioactive factors such as cytokines are also released into the retina. The proposed pathophysiology of each type is quite different; thus, each DME type has its own morphological and topographic characteristics (17). interleukin (IL)-6, a pro-inflammatory cytokine, intraocular levels of IL-6 were significantly higher in eyes with SRD than in eyes with DRT or CME, implying active inflammation. A recent study showed a better response to dexamethasone implants in eyes with SRD (9). The predictive value of SRD at baseline for the treatment response to anti-VEGF agents in DME remains controversial. Although some studies reported a significant improvement in VA in patients with SRD at baseline (18, 19), others found no difference or even worse functional results (20, 21). Univariate analysis to assess whether SRD is responsive to anti-VEGF agents in the current study showed that SRD significantly responded to anti-VEGF agents. However, in the multivariate survival analysis, treatment response to anti-VEGF regimens was not a significant influencing factor in patients with SRD. This can happen when SRD and other covariates are highly correlated. Furthermore, additional variables (ex. ERM) may

10.3389/fendo.2023.1108097

TABLE 3 Baseline predictors of a ≥10 letter gain in best-corrected visual acuity.

Variable	OR	95% CI		P-value
		Upper	Lower	
Sex				
Female	0.243	0.041	1.430	0.118
Male (ref.)	1	.	.	
Age	1.033	0.945	1.128	0.477
Diffuse retinal thickening				
3-6mm	6.030	0.941	38.656	0.058
1-3mm	0.450	0.041	4.933	0.513
≤1mm	0.996	0.014	69.310	0.998
0mm (ref.)	1			
ONL cyst size				
Giant	0.003	0.001	10.015	0.996
Large	2.126	0.541	8.633	0.275
Small	0.839	0.156	4.508	0.938
No (ref.)	1			
IS-OS continuity				
Completely disrupted	0.005	0.011	12.021	0.996
Partially continuous	1.052	0.343	3.224	0.929
Completely continuous (ref.)	1			
HRF foci-quantity				
Many (≥11)	0.166	0.021	1.324	0.090
Few (2-10)	0.250	0.035	1.765	0.164
Absent (ref.)	1			
ERM				
Yes	0.346	0.061	1.976	0.233
No (ref.)	1			
DR type				
PDR	0.602	0.112	3.237	0.555
Severe NPDR	0.799	0.165	3.879	0.781
Moderate NPDR (ref.)	1			
SRD				
Yes	1.366	0.293	6.098	0.708
No (ref.)	1			

CI, confidence interval; ERM, epiretinal membrane; ref, reference; HRF, hyperreflective foci; IS-OS, inner segment-outer segment; NPDR, non- proliferative diabetic retinopathy; ONL, outer nuclear layer; OR,Odds ratio; PDR, proliferative diabetic retinopathy; PVD, posterior vitreous detachment; SRD, serous retinal detachment; VMA, vitreomacular adhesion; VMT, vitreomacular traction.

explain more of the variance in the outcome variable, and thus reduce the impact of the initially significant of SRD.

In DME, the concentration of intraocular VEGF is significantly correlated with IL-6 levels (16). Anti-VEGF therapy reduces intraocular subclinical inflammation, and the aqueous humor concentration of IL-6 is decreased after anti-VEGF treatment (22). This could explain the response to anti-VEGF therapy in eyes with SRD in the current study. Our result was also consistent with that in the study by Sophie et al. (18) who reported that suppression of VEGF effectively eliminated subretinal fluid. Future prospective comparative investigations of the efficacy of anti-VEGF and of dexamethasone implants in eyes with SRD are required to optimize patient management.

10.3389/fendo.2023.1108097

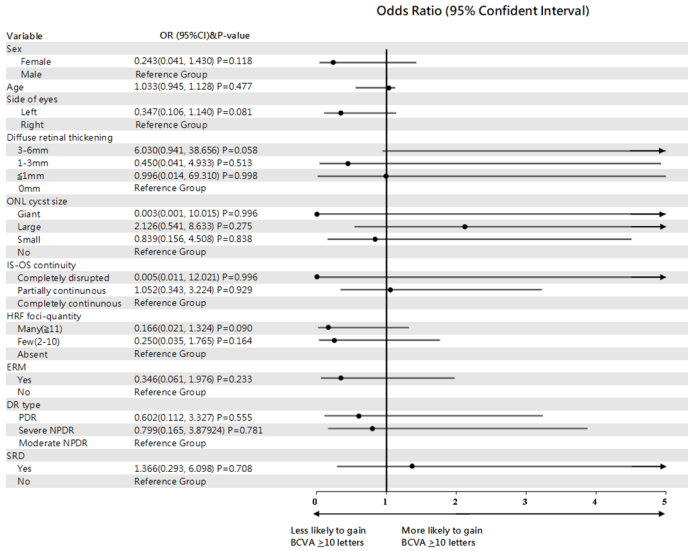

FIGURE 3
Forest plot of baseline predictors of a ≥10 letter gain in BCVA, using generalized estimate equation model. BCVA, best-corrected visual acuity; ONL, outer nuclear layer; IS-OS, inner segment-outer segment; HRF, hyperreflective foci; ERM, epiretinal membrane; SRD, serous retinal detachment.

In the current study, 45.8% of all patients presented with ONL cysts, and the majority had large ONL cysts (100–200 μm), mainly occurring at a relatively late stage of the disease. We found that large ONL cysts at baseline are less likely to be refractory group after anti-VEGF treatment at 4 months. Previous studies have reported that large ONL cysts negatively affect macular function and are predictive of worse VA outcomes after anti-VEGF therapy (23, 24). Elevated VEGF levels in DR affect the inner BRB, leading to increased vascular permeability, decreased osmotic gradient, extracellular fluid accumulation, and cyst formation (25). Furthermore, liquefaction necrosis of Müller cells and related inflammatory factors result in fluid accumulation in the cystic space (17). However, unlike SRD, IL-6 and IL-8 levels were not significantly increased in eyes with cystic changes (16). This indicated that the eye may not be in an active inflammatory state; rather, it could be a remnant of a previous inflammatory reaction (16). Anti-VEGF agents have been shown to decrease permeability and improve inner BRB by interacting with junctional proteins in the vascular endothelium (23). Our results support this finding and are consistent with a recent report that throughout anti-VEGF treatment, significant regression of ONL cysts accompanied notable improvement of macular function with a substantial decrease in their size (23). Nevertheless, we could not find an association between large ONL cysts and a mean reduction of CMT after anti-VEGF treatment at four months. Furthermore, only 3 eyes presented with giant ONL cysts (>200 μm), and we were unable to find an association between treatment outcomes and anti-VEGF agents in patients with giant ONL cysts.

The pathogenesis of DRT involves the persistent breakdown of the inner BRB and impairment of fluid absorption by Müller cells (17). DRT can be localized or more diffusely encompass the macula. Previous studies have reported that intravitreal anti-VEGF therapy is more effective for the DRT type than for the other types of DME (20, 26). Nevertheless, no study assessed whether the degree of the DRT would interfere with the treatment response or not. To clarify the relationship between DRT and response to anti-VEGF treatment, we first qualitatively evaluated the width of the DRT on a standard horizontal 6-mm B-scan OCT centered through the fovea and further stratified it into three subgroups (≤ 1, 1–3, and 3–6 mm). The results showed that the width of DRT was inversely proportional to the odds of poor response. Specifically, there was a trend indicating that the degree of DRT was proportionally associated with better response, although this was not significant in multivariate analysis.

There is a high incidence of vitreomacular interface abnormality (VMIA) among DME patients (27). The current study found a 20.8% incidence of ERM in our cohort. Although DR and its severity are risk factors for developing secondary ERM (27, 28), cases of VMIA are excluded from major clinical trials, even though DME is associated with this condition in 25% of patients (29). Nevertheless, knowledge regarding the effect of VMIA on the response to anti-VEGF treatment in patients with DME has not been thoroughly investigated. Ercalik et al. retrospectively evaluated 56 eyes with or without ERM and found a negative effect of ERM on intravitreal anti-VEGF treatment (30). Wong et al. conducted a prospective study of 104 eyes with DME treated with anti-VEGF and found that ERM was associated with a worsened visual and anatomic response (31). Notably, neither study considered other OCT biomarkers; thus, the findings might not completely represent the true impact of ERM in eyes with DME.

Considering the diversity of OCT morphology in DME, we included various OCT biomarker characteristics and considered ERM as a variable in eyes with refractory DME, despite anti-VEGF therapy. Furthermore, we used a multivariate statistical model to analyze the association between treatment response and each OCT biomarker. Our results showed that ERM significantly increased the

10.3389/fendo.2023.1108097

TABLE 4 Baseline predictors of central macular thickness reduction <10%.

Variable	OR	95% CI		P-value
		Upper	Lower	
Sex				
Female	1.044	0.264	4.134	0.951
Male (ref.)	1			
Age	0.907	0.629	1.313	0.411
Diffuse retinal thickening				
3-6mm	0.208	0.017	2.547	0.219
1-3mm	0.321	0.024	4.285	0.390
≤1mm	0.403	0.008	20.297	0.649
0mm (ref.)	1			
ONL cyst size				
Giant	1.229	0.106	14.216	0.869
Large	0.096	0.015	0.620	0.014
Small	0.398	0.033	4.790	0.468
No (ref.)	1			
IS-OS continuity				
Completely disrupted	0.151	0.013	1.730	0.129
Partially continuous	0.139	0.026	0.742	0.021
Completely continuous (ref.)	1			
HRF foci-quantity				
Many (≥11)	4.566	0.222	93.953	0.325
Few (2-10)	0.733	0.047	11.381	0.824
Absent (ref.)	1			
ERM				
Yes	12.469	2.012	77.259	0.007
No (ref.)	1			
DR type				
PDR	1.753	0.258	11.936	0.566
Severe NPDR	2.489	0.305	20.288	0.394
Moderate NPDR (ref.)	1			
SRD				
Yes	0.221	0.034	1.414	0.111
No (ref.)	1			

CI, confidence interval; ERM, epiretinal membrane; ref, reference; HRF, hyperreflective foci; IS-OS, inner segment-outer segment; NPDR, non- proliferative diabetic retinopathy; ONL, outer nuclear layer; OR, Odds ratio; PDR, proliferative diabetic retinopathy; PVD, posterior vitreous detachment; SRD, serous retinal detachment; VMA, vitreomacular adhesion; VMT, vitreomacular traction.

odds of poor response. According to previous study on ERM pathology in diffuse DME, multilayered membranes are mainly composed of hyalocytes and myofibroblasts. Hyalocytes were shown to produce VEGF and can transdifferentiate into myofibroblasts, known for their contractive properties (32). Furthermore, contraction of the ERM may cause perifoveal capillary leakage and aggravate macular edema. It has also been demonstrated that glial cells in ERM produce various cytokines and growth factors. VEGF and its receptors, as well as IL-6, are localized to cells in the ERM of patients with DR, thus further increasing inflammation and possibly promoting DME persistence (30, 33). Furthermore, ERM may act as a physical barrier and decrease drug

10.3389/fendo.2023.1108097

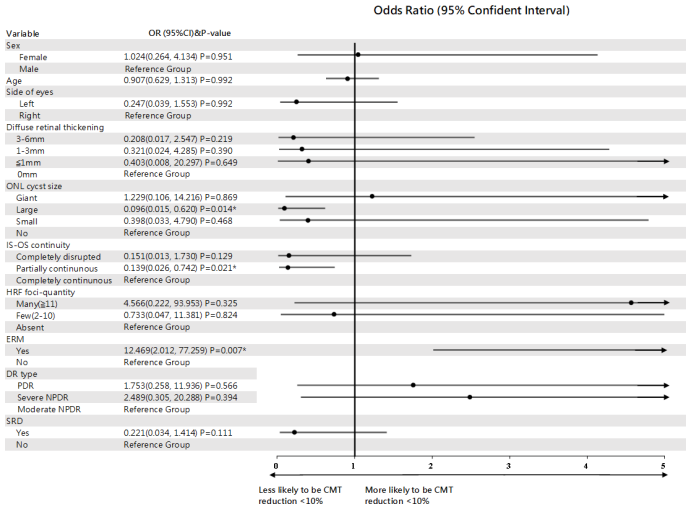

FIGURE 4
Forest plot of baseline predictors of CMT reduction <10%, using generalized estimate equation model. CMT, central macular thickness; ONL, outer nuclear layer; IS-OS, inner segment-outer segment; HRF, hyperreflective foci; ERM, epiretinal membrane; SRD, serous retinal detachment. *Statistically significant at p<0.05.

penetration after intravitreal injections of anti-VEGF in DME treatment (34).

The connective tissue growth factor (CTGF) is one of the most potent profibrotic factors. It can stimulate fibroblast proliferation and collagen deposition, resulting in fibrosis (35). Anti-VEGF has been reported to cause hypoxia in vascular endothelial cells and increase CTGF expression, which plays an important role in ERM formation (36). As a result, anti-VEGF therapy may potentially aggravate ERM contractions and interfere with the resolution of macular edema in diabetes. These results may explain the increased likelihood of poor response in this group. Nevertheless, consistent with the guidelines for DME management by retinal specialists, PPV is currently recommended as a therapeutic option in cases of DME associated with VMT (37). In the absence of traction formation, there is no consensus on the role of PPV in the actual treatment of diabetic eyes. Our results call for further comparative studies and treatment modalities other than anti-VEGF in DME patients presenting with ERM-impaired visual and anatomic outcomes.

HRF represents subclinical lipoproteins that extravasate after inner BRB breakdown. It is initially present in the inner retinal layers and subsequently migrates to the outer retinal layers (38). HRF is an important imaging marker for retinal inflammation (39). However, the predictive value of HRF for visual outcomes after anti-VEGF treatment in DME is unclear (9). In our study, we did not find that the presence of HRF was associated with treatment response after anti-VEGF therapy. The integrity of outer retinal layers is a direct indicator of the health of the retinal photoreceptors and retinal pigment epithelium. IS-OS integrities is an important factor for predicting VA after treatment. Subjects with long-standing DME may demonstrate focal or diffuse loss of integrity of the IS-OS junction. Previous studies have reported that IS-OS integrity can be expected to recover after anti-VEGF therapy (17, 23). Our results support this finding and show a better response to anti-VEGF therapy in eyes with partially continuous IS-OS layers.

Our study has some limitations. First, its retrospective and non-randomized design precluded a well-matched control enrollment. Second, the sample size was small, which may have hindered the significance of the results. Third, we prescribed three anti-VEGF agents to treat DME in the real-world clinical practice setting. Although most eyes were treated with ranizucimumab (83.3%), we did not assess each anti-VEGF regimen separately, and thus, the different efficacy between each agent may not have been accounted. Fourth, in our study, despite the odds of gaining BCVA ≥10 letters trended toward the OCT predictive value of CMT reduction, no OCT biomarkers showed significant predictive value for good BCVA response at 4 months. We found that the OCT predictive value of CMT reduction cannot fully translate into the change of VA, which was consistent with the study of a *post hoc* analysis of the protocol T randomized clinical trial (40). They found changes in CMT appear to account for only a small proportion of the total variation in changes in BCVA, and concluded that changes in CMT cannot support as a surrogate for changes in VA in evaluating anti-VEGF for DME. Despite these limitations, an important strength of

TABLE 5 Analysis for mean change of subfoveal serous retinal detachment (μm) at 4 months.

	N	Mean	SD	MD	95%CI	P-value
SRD (baseline)	32	207.06	139.37	-188.69	-248.43, -128.95	<0.001
SRD (at 4 months)		18.38	51.90			

CI, confidence interval; MD, mean difference; SD, standard deviation; SRD, serous retinal detachment.

our study is that we included various common OCT markers in patients with DME, which yielded ample information and helped us tailor timely and individualized treatment during daily practice.

In conclusion, partial IS-OS continuity is the marker that predicts better response to anti-VEGF treatment in eyes with DME. In contrast, the presence of ERM is a significant predictor of poor response. Our results raise the pertinent issue that DME patients with ERM are significant poor responders to anti-VEGF therapy and may benefit more from other therapeutic approaches.

Data availability statement

The original contributions presented in the study are included in the article/supplementary material. Further inquiries can be directed to the corresponding author.

Ethics statement

The studies involving human participants were reviewed and approved by Institutional Review Board of the Research Ethics Committee of Hualien Tzu-Chi Hospital and Buddhist Tzu-Chi Medical Foundation. The patients/participants provided their written informed consent to participate in this study.

Author contributions

T-CH and M-SH had full access to all of the data in the study and take responsibility for the integrity of the data and the accuracy of the data analysis. Concept and design: M-SH. Acquisition, analysis, or interpretation of data: T-CH, G-HD, Y-CC, and M-SH. Drafting of the manuscript: T-CH, G-HD, and M-SH. Critical revision of the manuscript for important intellectual content: T-CH, F-LC, and M-SH. Statistical analysis: T-CH and G-HD. Administrative, technical, or material support: G-HD, M-SH, and Y-CC. Supervision: T-CH, M-SH. All authors contributed to the article and approved the submitted version.

Acknowledgments

The authors thank the Tzu Chi University (TCU) Research Center for Big Data Teaching, Research and Statistic Consultation for providing statistic consultation assistance.

Conflict of interest

The authors declare that the research was conducted in the absence of any commercial or financial relationships that could be construed as a potential conflict of interest.

Publisher's note

All claims expressed in this article are solely those of the authors and do not necessarily represent those of their affiliated organizations, or those of the publisher, the editors and the reviewers. Any product that may be evaluated in this article, or claim that may be made by its manufacturer, is not guaranteed or endorsed by the publisher.

References

1. Kempen JH, O'Colmain BJ, Leske MC, Haffner SM, Klein R, Moss SE, et al. The prevalence of diabetic retinopathy among adults in the united states. *Arch Ophthalmol (Chicago Ill: 1960).* (2004) 122(4):552–63. doi: 10.1001/archopht.122.4.552

2. White NH, Sun W, Cleary PA, Tamborlane WV, Danis RP, Hainsworth DP, et al. Effect of prior intensive therapy in type 1 diabetes on 10-year progression of retinopathy in the DCCT/EDIC: comparison of adults and adolescents. *Diabetes* (2010) 59(5):1244–53. doi: 10.2337/db09-1216

3. Klein R, Klein BE, Moss SE, Cruickshanks KJ. The Wisconsin epidemiologic study of diabetic retinopathy. XV. the long-term incidence of macular edema. *Ophthalmology* (1995) 102(1):7–16. doi: 10.1016/s0161-6420(95)31052-4

4. Aiello LP, Avery RL, Arrigg PG, Keyt BA, Jampel HD, Shah ST, et al. Vascular endothelial growth factor in ocular fluid of patients with diabetic retinopathy and other retinal disorders. *New Engl J Med* (1994) 331(22):1480–7. doi: 10.1056/NEJM199412013312203

5. Massin P, Bandello F, Garweg JG, Hansen LL, Harding SP, Larsen M, et al. Safety and efficacy of ranibizumab in diabetic macular edema (RESOLVE study): a 12-month, randomized, controlled, double-masked, multicenter phase II study. *Diabetes Care* (2010) 33(11):2399–405. doi: 10.2337/dc10-0493

6. Mitchell P, Bandello F, Schmidt-Erfurth U, Lang GE, Massin P, Schlingemann RO, et al. The RESTORE study: ranibizumab monotherapy or combined with laser versus laser monotherapy for diabetic macular edema. *Ophthalmology* (2011) 118 (4):615–25. doi: 10.1016/j.ophtha.2011.01.031

7. Bressler SB, Ayala AR, Bressler NM, Melia M, Qin H, Ferris FL3rd, et al. Persistent macular thickening after ranibizumab treatment for diabetic macular edema with vision impairment. *JAMA ophthalmol* (2016) 134(3):278–85. doi: 10.1001/jamaophthalmol.2015.5346

8. Gonzalez VH, Campbell J, Holekamp NM, Kiss S, Loewenstein A, Augustin AJ, et al. Early and long-term responses to anti-vascular endothelial growth factor therapy in diabetic macular edema: analysis of protocol I data. *Am J ophthalmol* (2016) 172:72–9. doi: 10.1016/j.ajo.2016.09.012

9. Zur D, Iglicki M, Busch C, Invernizzi A, Mariussi M, Loewenstein A. OCT biomarkers as functional outcome predictors in diabetic macular edema treated with dexamethasone implant. *Ophthalmology* (2018) 125(2):267–75. doi: 10.1016/j.ophtha.2017.08.031

10. Busch C, Zur D, Fraser-Bell S, Laíns I, Santos AR, Lupidi M, et al. Shall we stay, or shall we switch? continued anti-VEGF therapy versus early switch to dexamethasone implant in refractory diabetic macular edema. *Acta Diabetol* (2018) 55(8):789–96. doi: 10.1007/s00592-018-1151-x

11. Dugel PU, Campbell JH, Kiss S, Loewenstein A, Shih V, Xu X, et al. ASSOCIATION BETWEEN EARLY ANATOMIC RESPONSE TO ANTI-VASCULAR ENDOTHELIAL GROWTH FACTOR THERAPY AND LONG-TERM OUTCOME IN DIABETIC MACULAR EDEMA: an independent analysis of protocol i study data. *Retina (Philadelphia Pa)* (2019) 39(1):88–97. doi: 10.1097/IAE.0000000000002110

12. Blonde L, Khunti K, Harris SB, Meizinger C, Skolnik NS. Interpretation and impact of real-world clinical data for the practicing clinician. *Adv Ther* (2018) 35 (11):1763–74. doi: 10.1007/s12325-018-0805-y

13. Das A, McGuire PG, Rangasamy S. Diabetic macular edema: pathophysiology and novel therapeutic targets. *Ophthalmology* (2015) 122(7):1375–94. doi: 10.1016/j.ophtha.2015.03.024

14. Brown DM, Nguyen QD, Marcus DM, Boyer DS, Patel S, Feiner L, et al. Long-term outcomes of ranibizumab therapy for diabetic macular edema: the 36-month

results from two phase III trials: RISE and RIDE. *Ophthalmology* (2013) 120(10):2013–22. doi: 10.1016/j.ophtha.2013.02.034

15. Egan C, Zhu H, Lee A, Sim D, Mitry D, Bailey C, et al. The united kingdom diabetic retinopathy electronic medical record users group, report 1: baseline characteristics and visual acuity outcomes in eyes treated with intravitreal injections of ranibizumab for diabetic macular oedema. *Br J ophthalmol* (2017) 101(1):75–80. doi: 10.1136/bjophthalmol-2016-309313

16. Sonoda S, Sakamoto T, Yamashita T, Shirasawa M, Otsuka H, Sonoda Y. Retinal morphologic changes and concentrations of cytokines in eyes with diabetic macular edema. *Retina (Philadelphia Pa)* (2014) 34(4):741–8. doi: 10.1097/IAE.0b013e3182a48917

17. Seo KH, Yu SY, Kim M, Kwak HW. Visual and morphologic outcomes of intravitreal ranibizumab for diabetic macular edema based on optical coherence tomography patterns. *Retina (Philadelphia Pa).* (2016) 36(3):588–95. doi: 10.1097/IAE.0000000000000770

18. Sophie R, Lu N, Campochiaro PA. Predictors of functional and anatomic outcomes in patients with diabetic macular edema treated with ranibizumab. *Ophthalmology* (2015) 122(7):1395–401. doi: 10.1016/j.ophtha.2015.02.036

19. Fickweiler W, Schauwvlieghe AME, Schlingemann RO, Maria Hooymans JM, Los LI, Verbraak FD. Predictive value of optical coherence tomographic features in the bevacizumab and ranibizumab in patients with diabetic macular edema (brdme) study. *Retina (Philadelphia Pa).* (2018) 38(4):812–9. doi: 10.1097/IAE.0000000000001626

20. Shimura M, Yasuda K, Yasuda M, Nakazawa T. Visual outcome after intravitreal bevacizumab depends on the optical coherence tomographic patterns of patients with diffuse diabetic macular edema. *Retina (Philadelphia Pa)* (2013) 33(4):740–7. doi: 10.1097/IAE.0b013e31826b6763

21. Giocanti-Aurégan A, Hrarat L, Qu LM, Sarda V, Boubaya M, Levy V, et al. Functional and anatomical outcomes in patients with serous retinal detachment in diabetic macular edema treated with ranibizumab. *Invest Ophthalmol Visual sci* (2017) 58(2):797–800. doi: 10.1167/iovs.16-20855

22. Sakamoto S, Takahashi H, Tan X, Inoue Y, Nomura Y, Arai Y, et al. Changes in multiple cytokine concentrations in the aqueous humour of neovascular age-related macular degeneration after 2 months of ranibizumab therapy. *Br J Ophthalmol* (2018) 102(4):448–54. doi: 10.1136/bjophthalmol-2017-310284

23. Reznicek L, Cserhati S, Seidensticker F, Liegl R, Kampik A, Ulbig M, et al. Functional and morphological changes in diabetic macular edema over the course of anti-vascular endothelial growth factor treatment. *Acta ophthalmol* (2013) 91(7):e529–36. doi: 10.1111/aos.12153

24. Deák GG, Bolz M, Ritter M, Prager S, Benesch T, Schmidt-Erfurth U. A systematic correlation between morphology and functional alterations in diabetic macular edema. *Invest Ophthalmol Visual sci* (2010) 51(12):6710–4. doi: 10.1167/iovs.09-5064

25. Fine BS, Brucker AJ. Macular edema and cystoid macular edema. *Am J Ophthalmol* (1981) 92(4):466–81. doi: 10.1016/0002-9394(81)90638-3

26. Usui-Ouchi A, Tamaki A, Sakanishi Y, Tamaki K, Mashimo K, Sakuma T, et al. Factors affecting a short-term response to anti-VEGF therapy in diabetic macular edema. *Life (Basel Switzerland)* (2021) 11(2). doi: 10.3390/life11020083

27. Ghazi NG, Ciralsky JB, Shah SM, Campochiaro PA, Haller JA. Optical coherence tomography findings in persistent diabetic macular edema: the vitreomacular interface. *Am J Ophthalmol* (2007) 144(5):747–54. doi: 10.1016/j.ajo.2007.07.012

28. Cheung N, Tan SP, Lee SY, Cheung GCM, Tan G, Kumar N, et al. Prevalence and risk factors for epiretinal membrane: the Singapore epidemiology of eye disease study. *Br J Ophthalmol* (2017) 101(3):371–6. doi: 10.1136/bjophthalmol-2016-308563

29. Akbar Khan I, Mohamed MD, Mann SS, Hysi PG, Laidlaw DA. Prevalence of vitreomacular interface abnormalities on spectral domain optical coherence tomography of patients undergoing macular photocoagulation for centre involving diabetic macular oedema. *Br J Ophthalmol* (2015) 99(8):1078–81. doi: 10.1136/bjophthalmol-2014-305966

30. Ercalik NY, Imamoglu S, Kumral ET, Yenerel NM, Bardak H, Bardak Y. Influence of the epiretinal membrane on ranibizumab therapy outcomes in patients with diabetic macular edema. *Arquivos brasileiros oftalmol* (2016) 79(6):373–5. doi: 10.5935/0004-2749.20160106

31. Wong Y, Steel DHW, Habib MS, Stubbing-Moore A, Bajwa D, Avery PJ, et al. Vitreoretinal interface abnormalities in patients treatedwith ranibizumab for diabetic macular oedema. *Graefe's Arch Clin Exp Ophthalmol* (2017) 255(4):733–42. doi: 10.1007/s00417-016-3562-0

32. Hagenau F, Vogt D, Ziada J, Guenther SR, Haritoglou C, Wolf A, et al. Vitrectomy for diabetic macular edema: optical coherence tomography criteria and pathology of the vitreomacular interface. *Am J Ophthalmol* (2019) 200:34–46. doi: 10.1016/j.ajo.2018.12.004

33. Harada C, Mitamura Y, Harada T. The role of cytokines and trophic factors in epiretinal membranes: involvement of signal transduction in glial cells. *Prog retinal eye Res* (2006) 25(2):149–64. doi: 10.1016/j.preteyeres.2005.09.001

34. Namba R, Kaneko H, Suzumura A, Shimizu H, Kataoka K, Takayama K, et al. *In vitro* epiretinal membrane model and antibody permeability: relationship with anti-VEGF resistance in diabetic macular edema. *Invest Ophthalmol Visual sci* (2019) 60 (8):2942–9. doi: 10.1167/iovs.19-26788

35. Kita T, Hata Y, Kano K, Miura M, Nakao S, Noda Y, et al. Transforming growth factor-β2 and connective tissue growth factor in proliferative vitreoretinal diseases: possible involvement of hyalocytes and therapeutic potential of rho kinase inhibitor. *Diabetes* (2007) 56(1):231–8. doi: 10.2337/db06-0581

36. Marticorena J, Romano MR, Heimann H, Stappler T, Gibran K, Groenewald C, et al. Intravitreal bevacizumab for retinal vein occlusion and early growth of epiretinal membrane: a possible secondary effect? *Br J Ophthalmol* (2011) 95(3):391. doi: 10.1136/bjo.2009.177287

37. Schmidt-Erfurth U, Garcia-Arumi J, Bandello F, Berg K, Chakravarthy U, Gerendas BS, et al. Guidelines for the management of diabetic macular edema by the European society of retina specialists (EURETINA). *Ophthalmol J Int d'ophtalmol Int J Ophthalmol Z fur Augenheilkunde* (2017) 237(4):185–222. doi: 10.1159/000458539

38. Markan A, Agarwal A, Arora A, Bazgain K, Rana V, Gupta V. Novel imaging biomarkers in diabetic retinopathy and diabetic macular edema. *Ther Adv ophthalmol* (2020) 12:2515841420950513. doi: 10.1177/2515841420950513

39. Midena E, Pilotto E, Bini S. Hyperreflective intraretinal foci as an OCT biomarker of retinal inflammation in diabetic macular edema. *Invest Ophthalmol Visual sci* (2018) 59(13):5366. doi: 10.1167/iovs.18-25611

40. Bressler NM, Odia I, Maguire M, Glassman AR, Jampol LM, MacCumber MW, et al. Association between change in visual acuity and change in central subfield thickness during treatment of diabetic macular edema in participants randomized to aflibercept, bevacizumab, or ranibizumab: a *Post hoc* analysis of the protocol T randomized clinical trial. *JAMA Ophthalmol* (2019) 137(9):977–85. doi: 10.1001/jamaophthalmol.2019.1963

frontiers | Frontiers in Endocrinology

TYPE Review
PUBLISHED 18 May 2023
DOI 10.3389/fendo.2023.1157189

OPEN ACCESS

EDITED BY
Mohd Imtiaz Nawaz,
King Saud University, Saudi Arabia

REVIEWED BY
Haiping Duan,
Qingdao Municipal Center for Disease Control and Prevention, China
Mashhood Uz Zafar Farooq,
Karachi Institute of Medical Sciences, Pakistan

*CORRESPONDENCE
Tao Xin
xintao@sdfmu.edu.cn
Deshan Liu
liudeshan@sdu.edu.cn

†These authors have contributed equally to this work and share first authorship

RECEIVED 02 February 2023
ACCEPTED 04 May 2023
PUBLISHED 18 May 2023

CITATION
Huai B, Huai B, Su Z, Song M, Li C, Cao Y, Xin T and Liu D (2023) Systematic evaluation of combined herbal adjuvant therapy for proliferative diabetic retinopathy.
Front. Endocrinol. 14:1157189.
doi: 10.3389/fendo.2023.1157189

Systematic evaluation of combined herbal adjuvant therapy for proliferative diabetic retinopathy

Baogeng Huai[1,2†], Baosha Huai[3†], Zhenghua Su[1], Min Song[1], Changling Li[2], Yingjuan Cao[4], Tao Xin[5*] and Deshan Liu[2*]

[1]First Clinical Medical College, Shandong University of Traditional Chinese Medicine, Jinan, China, [2]Department of Traditional Chinese Medicine, Qilu Hospital, Cheeloo College of Medicine, Shandong University, Jinan, China, [3]Department of Ophthalmology, Qilu Hospital, Cheeloo College of Medicine, Shandong University, Jinan, China, [4]Department of Nursing, Qilu Hospital, Cheeloo College of Medicine, Shandong University, Jinan, China, [5]Department of Neurosurgery, The First Affiliated Hospital of Shandong First Medical University & Shandong Provincial Qianfoshan Hospital, Jinan, China

Objective: To evaluate the efficacy and safety of combined traditional Chinese medicine in the adjuvant treatment of proliferative diabetic retinopathy (PDR) by Meta-analysis.

Methods: PubMed, Embase, Web of Science, Cochrane Library, China National Knowledge Infrastructure (CNKI), Wanfang databases were searched by computer. Random controlled clinical trials (RCTS) using traditional Chinese medicine as adjuvant therapy for proliferative diabetic retinopathy were screened, and Stata16.0 software was used to perform meta-analysis on the final included literatures.

Results: A total of 18 studies involving 1392 patients were included. Meta-analysis showed that the clinical effective rate OR=2.99 (*CI*: 2.18-4.10, I^2 = 42.7%, *P*<0.05); Visual acuity MD=0.10(*CI*: 0.06-0.13, I^2 = 0%, *P*<0.05); Fundus efficacy OR=5.47 (*CI*: 1.33-22.51, I^2 = 71.4%, *P*<0.05); Neovascularisation regression rate OR=8 (*CI*: 3.83-16.71, I^2 = 30.1%, *P*<0.05); Macular foveal thickness MD=-44.24 (*CI*: -84.55–3.93, I^2 = 95.6%, *P*<0.05); Absorption of vitreous hemorrhage OR=4.7 (*CI*: 2.26-9.77, I^2 = 0%, *P*<0.05); Fasting blood glucose MD=-0.23, (*CI*: -0.38–0.07, I^2 = 0%, *P*<0.05); 2h postprandial blood glucose MD=-0.19 (*CI*: -0.52-0.14, I^2 = 0%, *P*=0.25). From the results, the combined Chinese medicine adjuvant therapy showed better efficacy than the control group. A total of 69 kinds of traditional Chinese medicine were involved in 18 studies, among which the top four applied frequencies were Panax notoginseng, Rehmannia rehmannii, Astragalus membranaceus and Poria cocos. Most of the medicines were sweet and bitter in taste, the qi tended to be slight cold and cold, and the meridian tropism belongs to the liver meridian.

Conclusion: The combination of traditional Chinese medicine adjuvant therapy has a good curative effect on PDR patients. However, the relevant clinical trials are few and more high-quality clinical trials are still needed, what's more the attention should be paid to the exploration of its safety.

KEYWORDS

traditional Chinese medicine, proliferative diabetic retinopathy, meta analysis, diabetic complications, Chinese medicinal herb

1 Introduction

Diabetic retinopathy (DR) is one of the most common clinical complications of diabetes mellitus (DM). Of the 537 million diabetic patients worldwide, DR accounts for about 22.27% and has become the leading cause of blindness in middle-aged and older adults (1). As a disease with a large potential patient population base and a high probability of blindness and disability, DR brings serious life hindrances and mental suffering to patients while adding heavy economic pressure and burden to society. As the world's largest diabetes population, China has a staggering 140.9 million people with diabetes, with the number of diabetic retinopathy patients estimated to be between 34 and 53 million (2). The search for clinical drugs that can effectively treat diabetic retinopathy is an urgent problem worldwide, especially in China.

Chinese medicine has been handed down in China for thousands of years. A large amount of research evidence shows that it has excellent therapeutic effects on diabetes and its complications by reducing blood glucose, lipid profile and improving other metabolic indicators (3). At the same time, many studies have also proved that Chinese herbal therapy has a better intervention effect on DR (4, 5). In China's extensive clinical practice, not only traditional Chinese medicine practitioners commonly utilize herbal remedies to treat DR, while Western medical practitioners also frequently incorporate certain Chinese patent medicines to complement their treatment regimens for DR.

However, it is worth noting that DR can be divided into two types: Non-proliferative diabetic retinopathy (NPDR) and Proliferative diabetic retinopathy (PDR) based on the presence of neovascularization, and the two have distinct pathological features (6). Currently, research on TCM treatment for DR in China focuses mostly on the NPDR stage, where clinical manifestations include blood stasis lesions such as retinal microaneurysms and venous beading, and herbal remedies are often used to improve retinal microcirculation, with their efficacy widely recognized (7). However, the effectiveness and safety of TCM treatment for PDR, in which new blood vessels grow in the retina, are still debated. High-level research evidence is urgently needed to determine whether TCM treatment can help improve clinical symptoms in PDR patients and whether it is safe to use in this stage. To this end, we conducted this study with the aim of addressing this controversy. Additionally, to better guide the selection and subsequent research of TCM treatments, we summarized the frequency, four natures and five flavors, and meridian tropism of the herbal medicines included in the studies, aiming to explore the laws of TCM treatment for PDR.

2 Methods

2.1 Literature search

This study searched PubMed, Web of Science, Cochrane Library, Embase database, China Knowledge Network, Wanfang to include randomized clinical controlled trials of combination treatment of PDR with Chinese herbs since the establishment of the database until October 8, 2022.

2.2 Inclusion criteria

(1) Study type: a randomized controlled trial of Chinese herbal medicine for treating PDR, language not limited.

(2) Study subjects: all included cases must meet the pathological diagnostic criteria for PDR.

(3) Interventions: The interventions in the control group can be conventional Western medical treatment, such as drugs, photocoagulation or surgery, or blank; the interventions in the trial group should be based on conventional Western medical treatment combined with the use of Chinese herbal medicine as an adjunct, which can be herbal medicine, compound prescriptions, Chinese patent medicines, injections, ion introduction.

(4) Outcome indicators: Assess post-treatment outcomes involving at least one clinical efficacy, visual acuity, blood glucose, fundus efficacy, regression of neovascularisation, macular central recess thickness, and absorption of vitreous blood accumulation.

2.3 Exclusion criteria

(1) Type of literature is a review, animal test, or another non-clinical trial article.

(2) Non-simultaneous randomized controlled clinical trials, lack of randomization of groupings.

(3) The treatment method does not include herbal medicine as an adjunctive treatment.

(4) Lack of observation on relevant indicators.

(5) Inappropriate statistical methods or severe errors in the data.

2.4 Data extraction

Two researchers (Baogeng Huai and Baosha Huai) independently screened the literature according to the above criteria using EndNote X9 software, cross-checked, and controversial literature was decided by a third party (Changling Li) in consultation. Judgments were made based on whether the study population belonged to PDR patients, whether the intervention method involved TCM treatment, and whether there were any logical loopholes or data errors in the research. An Excel sheet was used to prepare an information extraction form based on the study content, and the data were extracted as follows.

(1) Basic information about the literature: first author, date of publication.

(2) Trial subjects: sample size of the trial and control groups.

(3) Interventions: type, dosage form, a dose of Chinese herbal medicine and control drugs, and duration of intervention.

(4) Outcome indicators: clinical efficacy, visual acuity, fundus efficacy criteria, neovascularization regression rate, central macular recess thickness.

2.5 Evaluation of literature quality and risk of bias

The risk of bias assessment tool of the Cochrane Systematic Reviews was used to evaluate the included studies, including randomization, allocation concealment, whether blinding was used, completeness of outcome indicators, whether study results were reported selectively, and other biases. The evaluation results were categorized into three risk levels: "high risk," "low risk," and "uncertain."

2.6 Statistical methods

The study was analyzed using Stata16.0 software. The mean difference (MD) was selected for the analysis of the effect of measures, and the odds ratio (OR) was selected as the effect size for dichotomous variables, both using a 95% confidence interval (CI). *P*-values and I^2 were calculated to determine whether heterogeneity existed among the included studies, and if heterogeneity was observed ($P<0.05$, or $I^2>50\%$), a random-effects model was selected; if no heterogeneity was observed ($P>0.05$, and $I^2\leq50\%$), a fixed-effects model was selected. $\alpha = 0.05$ was used as the meta-analysis test level. Publication bias was evaluated using the funnel plot, Begg's test, and Egger's test.

3 Results

3.1 Basic process for inclusion in the literature

As of October 2022, a total of 547 studies in the literature that could be potentially relevant were retrieved. After title and abstract screening, 47 articles were reviewed in total, and 18 RCT studies (8–25) were finally included for Meta-analysis based on the inclusion criteria (Figure 1). There are 1392 patients altogether in the sample size of the 18 studies. The intervention group and the control group had equivalent pre-treatment data (Table 1).

3.2 Evaluation of the quality of the included literature

The 18 pieces of literature were divided into six items to explore the quality of the studies. All 18 papers were organized for randomized sequence generation using the randomized order principle. 11 datasets (9–11, 13–16, 19, 20, 23, 25) used either the random number table or the coin flip method, so the bias judgment was assessed as low risk. Only one study (10) used a single-blind design, and the remaining studies did not involve blinding, so the risk of bias was assessed as high. While the remaining four were not mentioned. (There was no mention of concealment of assignment order, insufficient result data, selective reporting, or other biases.)

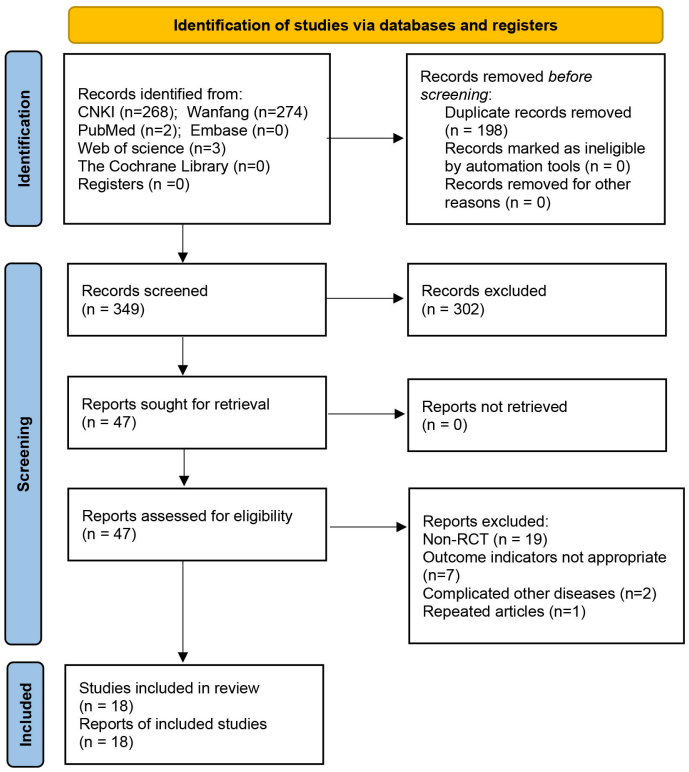

FIGURE 1
Flow chart of literature retrieval.

10.3389/fendo.2023.1157189

TABLE 1 Basic information about the included literature.

Study	Average Age		Treatment Group		Control Group		Intervention		Treatment Duration	Outcomes
	Treatment Group	Control Group	Male	Female	Male	Female	Treatment Group	Control Group		
Lv 2017	51.2 ± 12.3	50.9 ± 11.4	–	–	–	–	DaMing Decoction	Calcium Dobesilate	12 W	3
Fan 2016	64.3 ± 10.3	65.4 ± 11.2	16	14	15	15	Compound XueShuanTong Capsule	Diabetic Basal Treatment	12W	3, 5
Sun 2016	–	–	–	–	–	–	HuaYuMingMu Decoction	Calcium Dobesilate	24 W	1, 2
Li 2016	41.55 ± 6.51	40.57 ± 6.48	22	21	20	22	Photocoagulation+ Lycium Rehmannia Pills	Photocoagulation	12 W	1, 2, 7
Ji 2010	–	–	–	–	–	–	TangWangZengShi Decoction	Basal Treatment	24 W	1
Niu 2010	55.97 ± 6.35	56.82 ± 7.56	8	8	9	7	DaMing Decoction	Calcium Dobesilate	4 W	1,2,3
Han 2019	54.57 ± 11.47	51.13 ± 11.84	8	9	9	6	SanQi Powder	Basal Treatment	2 W	6
Yuan 2012	–	–	–	–	–	–	Photocoagulation +Discriminated Chinese Medicne	Photocoagulation	8 W	1
Teng 2012	–	–	–	–	–	–	Argon Laser+ DaMing Decoction	Argon Laser	8 W	1, 3
Di 2007	58.6	61.2	18	32	16	15	Photocoagulation +ZiYinLiangXueSanYu Decoction	Photocoagulation	48 W	4
Wang 2012	55.47 ± 8.74	56.1 ± 8.89	18	12	19	11	Photocoagulation+ Lycium Rehmannia Pills+ XueSaiTong capsule	Photocoagulation	12 W	1, 2, 7
Zhang 2019	61.5 ± 4.6	60.7 ± 4.4	27	23	28	22	Calcium Dobesilate+ Photocoagulation+ HuoXueMingMu Tablets	Calcium Dobesilate+ Photocoagulation	12~24 W	1, 4
Wang 2020	58.24 ± 4.88	59.33 ± 5.04	59	41	60	40	Discriminated Chinese Medicne	Basal Treatment	24 W	1, 4
Li 2015	58.5	60.1	10	8	9	9	Chinese Medicine Ion Introduction	Iodized Lecithin Tablets	4 W	6
Wu 2017	56.45 ± 7.28	55.89 ± 8.34	20	21	22	19	Chinese Medicine Ion Introduction	Iodized Lecithin Tablets	4 W	6
Sha 2019	47.1 ± 7.8	48.1 ± 6.9	17	18	15	20	Minimally Invasive Vitrectomy+ ZiYinHuaYuTongLuo Prescription	Minimally Invasive Vitrectomy	4 W	5
Ma 2016	–	–	–	–	–	–	Modified BuYangHuanWu Decoction	Calcium Dobesilate	24 W	1
Zhao 2021	53.7 ± 6.7	54.5 ± 7.1	27	15	25	17	Ranibizumab Combined with PPV +Five Ling Powder and Ba Zhen Decoction	Ranibizumab Combined with PPV	12 W	1, 5

Clinical Efficacy; 2. Visual Acuity Level; 3. Fundus Efficacy; 4. Neovascularisation Regression Rate; 5. Macular Central Recess Thickness; 6. Absorption of Vitreous Hemorrhage; 7. Absorption of Vitreous Hemorrhage; "-" indicates that the data was not mentioned in the included study.

3.3 Results of meta-analysis

3.3.1 Clinical efficacy

A total of 9 articles (10–13, 15, 18–20, 25) reported the clinical efficacy of combined herbal treatments for patients with PDR, including 827 patients. The meta results showed that combined herbal treatments effectively improved the clinical outcomes of patients with PDR (9 studies, 827 patients, OR=2.99, *CI*: 2.18-4.10, I^2 = 42.7%, *P*<0.05) (Figure 2).

3.3.2 Visual acuity level

A total of 3 articles (11, 13, 18) reported the effect of combined herbal treatment on visual acuity in patients with PDR. 177 patients were included, and the meta results showed that combined herbal treatment could improve the visual acuity level of patients to some extent (3 studies, 177 patients, MD=0.10, *CI*: 0.06-0.13, I^2 = 0%, *P*<0.05) (Figure 3).

3.3.3 Fundus efficacy

A total of 3 articles (8, 9, 13) reported the fundus efficacy of combined herbal treatment in patients with PDR. 202 patients were included, and the meta results showed that combined herbal treatment significantly improved the fundus efficacy in patients with PDR (3 studies, 202 patients, OR=5.47, *CI*: 1.33-22.51, I^2 = 71.4%, *p*<0.05) (Figure 4).

3.3.4 Neovascularisation regression rate

A total of 4 articles (17–20) reported the effect of herbal combination therapy on the regression of neovascularisation. 424 patients were included and the meta results showed that herbal combination therapy was effective in helping the regression of retinal neovascularisation in patients with PDR (4 studies, 424 cases, OR=8, *CI*: 3.83-16.71, I^2 = 30.1%, *P*<0.05) (Figure 5).

3.3.5 Macular central recess thickness

A total of 3 articles (9, 23, 25) reported on the effect of herbal combination therapy on macular central recess thickness, including 214 patients, and the meta results showed that herbal combination therapy was effective in reducing macular central recess thickness in patients with PDR (3 studies, 214 patients, MD=-44.24, *CI*:-84.55–3.93, I^2 = 95.6%, *p*<0.05) (Figure 6).

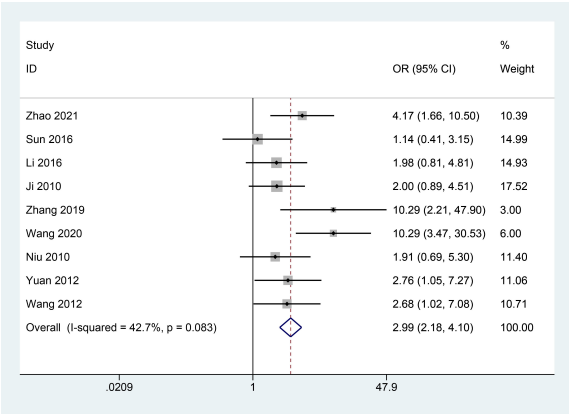

FIGURE 2
Forest plot of clinical efficacy.

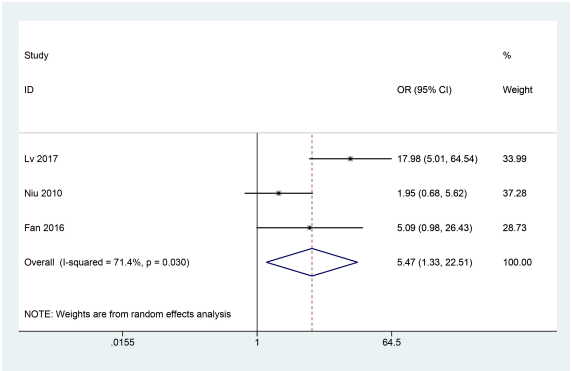

FIGURE 4
Forest plot of fundus efficacy.

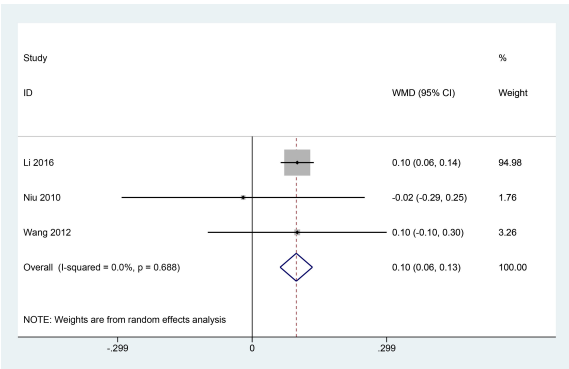

FIGURE 3
Forest plot of visual acuity level.

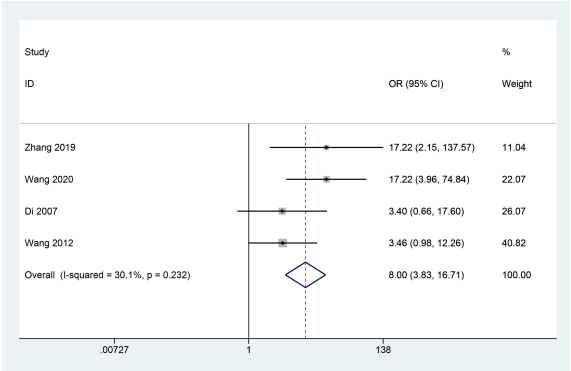

FIGURE 5
Forest plot of neovascularisation regression rate.

3.3.6 Absorption of vitreous hemorrhage

A total of 3 articles (14, 21, 22) reported the effect of herbal combination therapy on vitreous blood accumulation in patients with PDR. 183 patients were included and the meta results showed that herbal combination therapy was effective in helping vitreous blood accumulation absorption in patients with PDR (3 studies, 183 cases, OR=4.7, *CI*: 2.26-9.77, I^2 = 0%, *P*<0.05) (Figure 7).

3.3.7 Fasting blood glucose and postprandial 2h blood glucose levels

A total of 2 articles (11, 18) reported the effect of herbal combination therapy on fasting blood glucose and postprandial 2h blood glucose in patients with PDR. 145 patients were included, and the meta results showed that herbal combination therapy was effective in reducing fasting blood glucose in patients with PDR (2 studies, 145 patients, fasting blood glucose: MD=-0.23, *CI*: -0.38-0.07, I^2 = 0%. *P*<0.05; postprandial 2h glucose, MD=-0.19, *CI*: -0.52-0.14, I^2 = 0%, *P*=0.25) (Figures 8, 9).

3.4 Publication bias

The clinical efficiency was tested for publication bias. The funnel plot showed that the symmetry was acceptable. Further quantitative analysis was performed using Begg 's and Egger 's tests. The results showed that there was no publication bias in the outcome index (*P* = 0.251, *P* = 0.112, respectively) (Figure 10).

3.5 Inclusion of Chinese herbal medicines

In all 18 studies, a total of 69 herbal medicines were applied. After counting the frequency of repetition, it was found that the top four herbal medicines in terms of frequency were Panax notoginseng, Rehmanniae Radix, Astragali Radix and Poria, with their efficacy categories of resolving blood stasis and stopping bleeding, clearing heat and cooling the blood, tonifying Qi, promoting water retention and reducing swelling, respectively (Table 2).

3.6 Analysis of the odour and meridian orientation of the included herbs

By analysing the nature, taste and meridian orientation information of the 69 herbs intervening in the PDR, the results showed that sweet and bitter herbs accounted for the highest

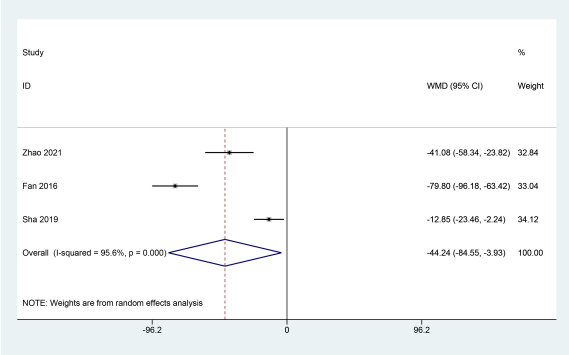

FIGURE 6
Forest plot of macular central recess thickness.

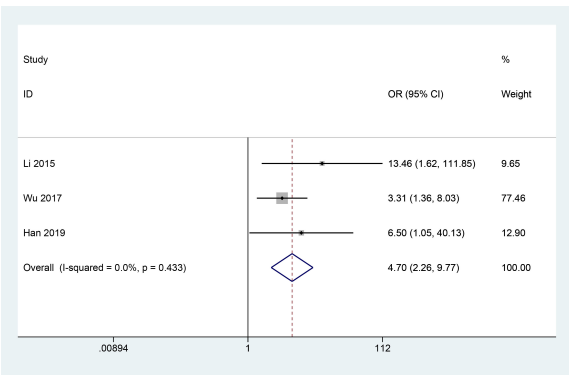

FIGURE 7
Forest plot of absorption of vitreous hemorrhage.

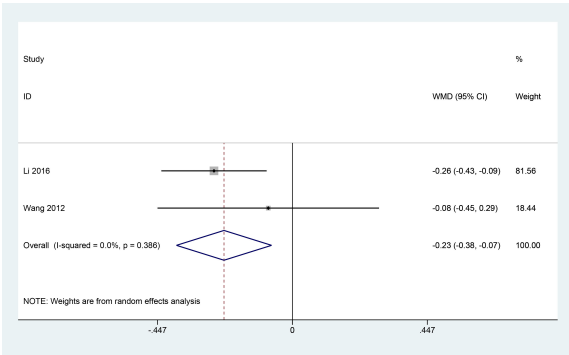

FIGURE 8
Forest plot of fasting blood glucose levels.

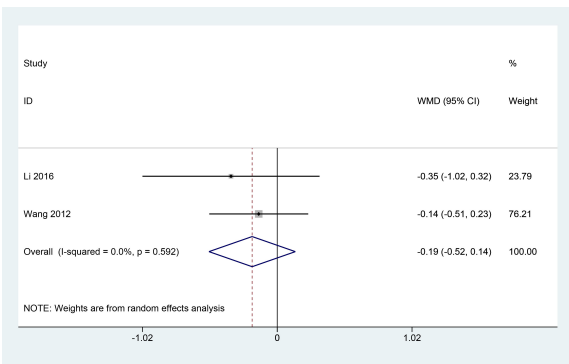

FIGURE 9
Forest plot of postprandial 2h blood glucose levels.

frequency, with the two together accounting for 68.47%; most herbs were on the cold side. In terms of meridian orientation, herbs belonging to the liver meridian accounted for the highest proportion of the 69 species, at 69.57%, which may be related to the theory that the liver opening into the eye in traditional Chinese medicine thinking (Table 3) (Figure 11).

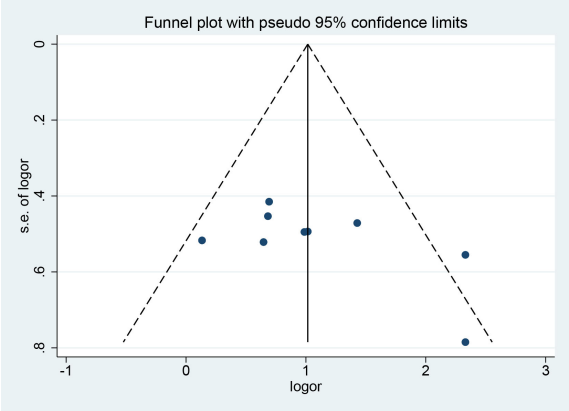

FIGURE 10
The funnel plot of clinical efficacy.

4 Discussion

4.1 Summary of main results

Our study included a total of 18 research articles, involving 1,392 patients with PDR. The results show that TCM therapy as an adjunctive treatment effectively improves the clinical outcome and visual acuity of PDR patients and the extent of their fundus lesions.

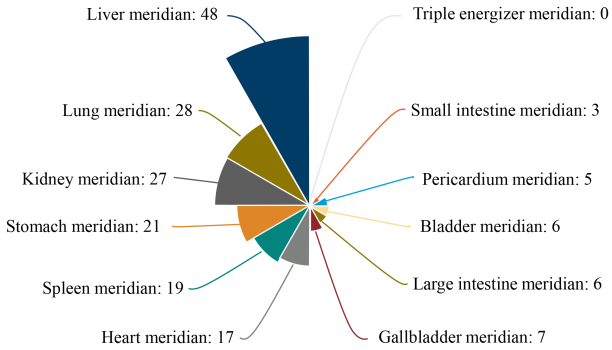

FIGURE 11
Rose diagram of herbal meridian analysis.

TABLE 2 Top 10 Chinese Medicines in Frequency.

Herbs	Frequency	Main Efficacy
Panax Notoginseng	12	Blood Hemostasis
Rehmanniae Radix	10	Heat and Cool Blood
Astragali Radix	9	Energen-Invigorating
Poria	9	Anti-Water Swelling
Alismatis Rhizoma	6	Anti-Water Swelling
Typhae Pollen	6	Blood Hemostasis
Lycii Fructus	6	Invigorating Yin
Salviae Miltiorrhizae Radix Et Rhizoma	6	Activating Blood
Chrysanthemi Flos	5	Diverging Wind Heat
Angelicae Sinensis Radix	5	Hematic

TABLE 3 Odor and Taste Analysis.

Taste	Frequency	Proportion (%)	Nature	Frequency	Proportion (%)
Sweet	39	35.14	Slight cold	17	26.15
Bitter	37	33.33	Cold	16	24.62
Acrid	17	15.32	Balanced	13	20
Salty	10	9.01	Warm	10	15.38
Sour	4	3.6	Cool	5	7.69
Light	2	1.8	Slight warm	4	6.15
Astringent	2	1.8	Hot	0	0

It also has multiple therapeutic effects, such as lowering blood glucose, promoting capillary regression, and accelerating absorption of vitreous hemorrhage, which has multiple positive clinical implications for PDR. The results of publication bias test showed that there was no publication bias in the main indicator, which proved that the results were reliable.

4.2 Advantages and limitations of research

The main advantage of this meta-analysis is that it is the first systematic evaluation of the effectiveness of traditional Chinese medicine (TCM) in treating PDR, which preliminary answer the controversial issue of whether TCM is appropriate for PDR treatment. This is of great significance for guiding clinical PDR treatment. Throughout the study, we strictly followed the systematic review method, included almost all relevant and standard RCT studies available online, and the conclusions drawn were comprehensive and robust. Additionally, we conducted bias tests to confirm the reliability of our findings.

However, our study also has some limitations. Firstly, only one of the included studies mentioned the absence of complications and adverse reactions, while the remaining studies did not explore the safety of Chinese herbal medicine in treating PDR. Moreover, most of the studies did not use allocation concealment and blinding methods, nor did they design a placebo group, which may lead to bias in the study results. Finally, as all the literature included in our study came from China, the results we obtained may be more applicable to Chinese PDR patients, and whether TCM is effective for PDR patients in other countries still requires further research.

4.3 Analysis of Chinese herbal medicine

The study counted the Chinese medicines used in each study, and the results showed that the top four in terms of replication rate were Panax notoginseng, Rehmanniae Radix, Astragali Radix, and Poria. Panax notoginseng, the root and rhizome of Panax notoginseng, is usually used as a powder in amounts of 1.5-6 g. It is considered by Chinese medicine practitioners to be a critical medicine in the treatment of blood disorders, with the characteristics of "stopping bleeding and activating blood, stopping bleeding without leaving stasis." Studies have shown that Panax notoginseng can effectively increase the concentration of thrombin and the number of platelets to shorten the clotting time and play a hemostatic role (26). Panax notoginseng contains various types of compounds such as cyclic terpenes and their glycosides, phenolic compounds, sugars, amino acids, and organic acids. These drugs have a variety of pharmacological effects including anti-ageing, hypoglycaemic, anti-inflammatory and immune system boosting (27).

There are relatively few studies on treating DR and PDR with Rehmanniae Radix. However, interestingly, a study from China showed that when the cases of effective treatment of diabetic retinopathy with Chinese herbs in the Chinese Journal Full Text Database (CNKI) were aggregated, Rehmanniae Radix ranked first in the frequency of administration, with 48 times (28), suggesting that Rehmanniae Radix has excellent potential for the treatment of DR and PDR. Its specific mechanisms need to be further explored. Astragalus is the dried root of Astragalus mongolica or Astragalus membranaceus, a leguminous plant, first published in Shen nong Ben Cao Jing and used medicinally in China for more than 2,000 years. It is a sacred tonic for the qi and is one of the most widely used Chinese herbs in China today. Studies have shown that the main anti-diabetic chemicals contained in Astragalus are astragalus polysaccharides, astragalosides, and astragalus flavonoids (29). These drug components can alleviate structural damage and apoptosis of retinal cells caused by the high glucose environment through multiple mechanisms such as hypoglycaemia, anti-oxidative stress, increased free radical scavenging activity, anti-inflammatory response, and inhibition of endoplasmic reticulum stress (30–32). Poria cocos, the dried nucleus of a porous fungus, is a particular herbal medicine that can be used for both medicinal and food purposes. In ancient times, Chinese medicine practitioners believed that regular Poria cocos could strengthen the spleen, promote hydration, tonify the qi and calm the mind, and prolong life, placing it alongside nine other drugs such as ginseng and Ganoderma lucidum as "immortal herbs". However, there are relatively few records and studies on the use of Poria as a treatment for DR. It ranks highly among the therapeutic drugs for PDR due to its unique effect of promoting the body's water metabolism (33). In addition to retinal microaneurysms, haemorrhages, and neovascularization, DR often results in diabetic macular oedema (DME) due to the disruption of the blood-retinal barrier and altered hemodynamics, causing extracellular fluid accumulation (34). PDR patients whose disease has progressed to the late stages of DR are usually associated with severe DME with exudative symptoms. Unfortunately, similar to Rehmanniae Radix, there is almost a gap in research exploring Poria alone for treating DME. However, a computer search of the Chinese Journal Full Text Database (CNKI) and Wanfang database for clinical cases related to the treatment of macular oedema ranked Poria first with a frequency of 60 recurrences (35), suggesting that TCM community generally recognizes the efficacy of Poria in the treatment of DME. At the same time, its specific mechanism of action needs to be further explored.

5 Conclusion

In summary, our study preliminarily proved that Chinese herbal medicine can effectively improve the clinical outcomes, visual acuity, and degree of retinopathy in patients with proliferative diabetic retinopathy (PDR), as well as reducing blood glucose levels, aiding capillary regression, and alleviating vitreous hemorrhage. These conclusions have significant implications for resolving controversies surrounding the application of traditional Chinese medicine (TCM) in the field of PDR. In addition, data mining of herbal medicines included in the literature reveals that researchers prefer to use herbs with sweet or bitter taste and slight cold or cold properties that belong to the liver meridian to treat PDR. In future studies, we need a larger sample of high-quality,

multi-centre RCT studies to provide evidence for treating PDR with Chinese herbs. These studies should also focus on exploring safety.

Author contributions

This review was created by BGH, BSH, ZS, MS, DL, TX, CL and YC. The First drafts of the article were written by BGH and BSH, and further revisions were contributed to by the other co-authors. The final version of the work was approved by all authors. DL obtained funding for this study. All authors contributed to the article and approved the submitted version.

Funding

Project of National Natural Science Foundation of China: Construction and Empirical Study of Rural Elderly Type 2 Diabetes Mellitus with MCI Management Model Based on Complex Adaptive System Theory (72274110). Project of Shandong Provincial Natural Science Foundation: Study on the Role and Mechanism of Salvianolic Acid in Promoting IGFBP3 Methylation to Regulate Microcirculation Disorder in Diabetic Cardiomyopathy (ZR2022QH163). Qilu Geriatric Diseases Chinese and Western Academic School Inheritance Workshop Project (No.2022-93-1-10).

Conflict of interest

The authors declare that the research was conducted in the absence of any commercial or financial relationships that could be construed as a potential conflict of interest.

Publisher's note

References

1. Teo ZL, Tham Y, Yu M, Chee ML, Rim TH, Cheung N, et al. Global prevalence of diabetic retinopathy and projection of burden through 2045. *Ophthalmology* (2021) 128:1580–91. doi: 10.1016/j.ophtha.2021.04.027

2. Group NATG. Technical scheme of grading diagnosis and treatment service for diabetic retinopathy. *Chin J Gen Practitioners* (2017) 16:589–93. doi: 10.3760/cma.j.issn.1671-7368.2017.08.005

3. Tian J, Jin D, Bao Q, Ding Q, Zhang H, Gao Z, et al. Evidence and potential mechanisms of traditional Chinese medicine for the treatment of type 2 diabetes: a systematic review and meta-analysis. *Diabet Obes Metab* (2019) 21:1801–16. doi: 10.1111/dom.13760

4. Ai X, Yu P, Hou Y, Song X, Luo J, Li N, et al. A review of traditional Chinese medicine on treatment of diabetic retinopathy and involved mechanisms. *BioMed Pharmacother* (2020) 132:110852. doi: 10.1016/j.biopha.2020.110852

5. Chen Q, Ni Q, Liu Y. Guidelines for diagnosis and treatment of diabetic retinopathy (2021-09-24). *World Tradition Chin Med* (2021) 16:3270–77. doi: 10.3969/j.issn.1673-7202.2021.22.002

6. Wilkinson CP, Ferris FL, Klein RE, Lee PP, Agardh CD, Davis M, et al. Proposed international clinical diabetic retinopathy and diabetic macular edema disease severity scales. *Ophthalmology* (2003) 110:1677–82. doi: 10.1016/S0161-6420(03)00475-5

7. Chen Z, Xie L, Hao X. Research progress of traditional Chinese medicine in the treatment of diabetic retinopathy. *J Tradition Chin Ophthalmol* (2023) 33:84–7. doi: 10.13444/j.cnki.zgzyykzz.2023.01.021

8. Lu XD, Cao J. Study on the mechanism of PD1 /PDL1 signaling pathway in proliferative diabetic retinopathy treated by Chinese traditional study on the mechanism of PD1 /PDL1 signaling pathway in proliferative diabetic retinopathy treated by Chinese traditional medicine. *Pharmacol Clinics Chin Materia Med* (2017) 33:136–40. doi: 10.13412/j.cnki.zyyl.2017.06.035

9. Fan XJ, Zhang GF. Effect of compound xueshuantong capsule in treatment patients of cataract with proliferative diabetic retinopathy. *Chin J Biochem Pharm* (2016) 36:121–23. doi: 10.3969/j.issn.1005-1678.2016.12.034

10. Sun R, Hui SY. In different periods of diabetic retinopathy in the observation of the curative effect of treatment of HuaYuMingMu decoction and its influence on VEGF. *World Chin Med* (2016) 11:75–8. doi: 10.3969/j.issn.1673-7202.2016.01.018

11. Li JL, Dong JG. Effect of qiju dihuang pill combined with photocoagulation on proliferative stage of diabetic retinopathy. *J Pract Diabetol* (2016) 12:18–20. doi: CNKI:SUN:LNSY.0.2016-06-013

12. Ji LP. Tangwang zengshi decoction in the treatment of 126 cases of diabetic retinopathy. *Chin Med Mod Dis Educ China* (2010) 8:27–8. doi: 10.3969/j.issn.1672-2779.2010.13.020

13. Niu SY. *The clinical study on proiferative diabetic retinopathy with chinses traditional medicine-DaMingYin*. Heilongjiang University of Chinese Medicine (2010). Available at: https://kns.cnki.net/kcms/detail/detail.aspx?FileName=1011037812.nh&DbName=CMFD2012.

14. Han MY. *Clinical observation and mechanism study of sanqi combined with vitrectomy on patients with proliferative diabetic retinopathy*. Beijing University of Chinese Medicine (2018). Available at: https://kns.cnki.net/kcms/detail/detail.aspx?FileName=1018205351.nh&DbName=CMFD2018.

15. Yuan CY. Efficiency of Chinese herbal medicine combined with laser photocoagulation on proliferation diabetic retinopathy. *Clin Med Eng* (2012) 19:819–20. doi: 10.3969/j.issn.1674-4659.2012.05.0819

16. Teng XM, Sun H. Clinical experience of traditional Chinese medicine combined with retinal laser in treatment of proliferative diabetic retinopathy. *Heilongjiang Univ Chin Med* (2009) 38:22–3. doi: 10.3969/j.issn.1000-9906.2012.04.013

17. Di PH, Zhao N, Sun RX, Wang JC. The effect of Chinese traditional medicine combine with laser on the treatment of new vessels of diabetic retinopathy. *Hebei J Tradition Chin Med* (2007), 29:543–45. doi: 10.3969/j.issn.1002-2619.2007.06.044

18. Wang RJ. *Traditional Chinese medicine combined with retinal photocoagulation in treatment of diabetic retinopathy(gan shen yin xu and xue yu xing) clinical study abstract*. Yunnan University of Chinese Medicine (2012). Available at: https://kns.cnki.net/kcms/detail/detail.aspx?FileName=1013132859.nh&DbName=CMFD2013.

19. Zhang L. Clinical observation of Chinese and Western medicine combined with retinal laser treatment in proliferative diabetic retinopathy complicated with vitreous hemorrhage. *Diabetes New World* (2019) 22:189–91. doi: 10.16658/j.cnki.1672-4062.2019.11.189

20. Wang SJ. *Data from: the effect of combined treatment of Chinese and Western medicine in proliferative diabetic retinopathy complicated with vitreous hemorrhage*. CNKI (2020). Available at: https://kns.cnki.net/kcms/detail/detail.aspx?FileName=CXCM202004003033&DbName=CPFD2020.

21. Li J, Li XH, Wang Q. Clinical observation on treating stage IV vitreous hemorrhage of diabetic retinopathy by Chinese medicine combined with iontophoresis. *J Sichuan Tradition Chin Med* (2015) 33:141–42. doi: CNKI:SUN:SCZY.0.2015-10-067

22. Wu YY. Clinical observation on Chinese herbs combined with iontophoresis in the treatment of stage IV vitreous hemorrhage of diabetic retinopathy. *Guangming J Chin Med* (2017) 32:1482–84. doi: 10.3969/j.issn.1003-8914.2017.10.048

23. Sha YF, Duan SL, Du DJ. Clinical study on ziyin huayu tongluo prescription in adjuvant treatment for proliferative diabetic retinopathy. *New Chin Med* (2019) 51:166–68. doi: 10.13457/j.cnki.jncm.2019.06.049

24. Ma WQ, Li ZH, Jiang WL. The observation of efficacy of traditional Chinese medicine combined with vitrectomy in the treatment of; proliferative diabetic retinopathy. *J Chin Ophthalmol Otorhinolaryngol* (2016) 6:5. doi: 10.3969/j.issn.1674-9006.2016.02.011

25. Zhao YX, Wang S, Ju JJ. Influence of addition and subtraction of bazhen decoction and five drugs with poria combined with leizhumab on conscious symptoms and retinal function recovery in patients with proliferative diabet-ic retinopathy after vitrectomy. *J Aerospace Med* (2021) 32:385–88. doi: 10.3969/j.issn.2095-1434.2021.04.002

26. Xie Y, Wang C. Herb–drug interactions between panax notoginseng or its biologically active compounds and therapeutic drugs: a comprehensive pharmacodynamic and pharmacokinetic review. *J Ethnopharmacol* (2023) 307:116156. doi: 10.1016/j.jep.2023.116156

27. Wang T, Guo R, Zhou G, Zhou X, Kou Z, Sui F, et al. Traditional uses, botany, phytochemistry, pharmacology and toxicology of panax notoginseng (Burk.) F.H. Chen: a review. *J Ethnopharmacol* (2016) 188:234–58. doi: 10.1016/j.jep.2016.05.005

28. Gu Z, Yang Y, Shi Y. Analysis of the medication rule of contemporary medical doctors for treating diabetic retinitis based on the TCM inheritance auxiliary platform. *J Liaoning Univ Tradition Chin Med* (2022) 24:130–34. doi: 10.13194/j.issn.1673-842x.2022.01.029

29. Salehi B, Carneiro JNP, Rocha JE, Coutinho HDM, Morais Braga MFB, Sharifi Rad J, et al. Astragalus species: insights on its chemical composition toward pharmacological applications. *Phytother Res* (2021) 35:2445–76. doi: 10.1002/ptr.6974

30. Peng Q, Tong P, Gu L, Li W. Astragalus polysaccharide attenuates metabolic memory-triggered ER stress and apoptosis *via* regulation of miR-204/SIRT1 axis in retinal pigment epithelial cells. *Biosci Rep* (2020) 40(1):BSR20192121. doi: 10.1042/BSR20192121

31. You L, Lin Y, Fang Z, Shen G, Zhao J, Wang T. Research advances on astragaloside-IV in treatment of diabetes mellitus and its complications pharmacological effects. *Zhongguo zhongyao zazhi* (2017) 42:4700–06. doi: 10.19540/j.cnki.cjcmm.20171010.007

32. Zhang K, Pugliese M, Pugliese A, Passantino A. Biological active ingredients of traditional Chinese herb astragalus membranaceus on treatment of diabetes: a systematic review. *Mini Rev medicinal Chem* (2015) 15:315. doi: 10.2174/1389557515666150227113431

33. Hu G, Huang C, Zhang Y, Xiao W, Jia J. Accumulation of biomass and four triterpenoids in two-stage cultured poria cocos mycelia and diuretic activity in rats. *Chin J Nat Med* (2017) 15:265–70. doi: 10.1016/S1875-5364(17)30043-2

34. Zhang J, Zhang J, Zhang C, Zhang J, Gu L, Luo D, et al. Diabetic macular edema: current understanding, molecular mechanisms and therapeutic implications. *Cells* (2022) 11:3362. doi: 10.3390/cells11213362

35. Liang JH, Chen YB, Qu N, Zhang Y, Zeng DX, Hu S. Medication rule of macular edema treated by traditional Chinese medicine. *Guangxi Med J* (2019) 41:1514–1517+1531. doi: 10.11675/j.issn.0253-4304.2019.12.11

frontiers | Frontiers in Endocrinology

TYPE Original Research
PUBLISHED 24 May 2023
DOI 10.3389/fendo.2023.1184717

OPEN ACCESS

EDITED BY
Mohd Imtiaz Nawaz,
King Saud University, Saudi Arabia

REVIEWED BY
Xuefei Song,
Shanghai Ninth People's Hospital, China
Chang Won Jeong,
Wonkwang University, Republic of Korea

*CORRESPONDENCE
Yan Cui
qlcyteam@163.com

†These authors have contributed equally to this work

RECEIVED 12 March 2023
ACCEPTED 11 May 2023
PUBLISHED 24 May 2023

CITATION
Qi Z, Si Y, Feng F, Zhu J, Yang X, Wang W, Zhang Y and Cui Y (2023) Analysis of retinal and choroidal characteristics in patients with early diabetic retinopathy using WSS-OCTA. *Front. Endocrinol.* 14:1184717. doi: 10.3389/fendo.2023.1184717

Analysis of retinal and choroidal characteristics in patients with early diabetic retinopathy using WSS-OCTA

Zhihao Qi[1,2†], Yuanyuan Si[1,2†], Feng Feng[2,3], Jing Zhu[1], Xuepeng Yang[1,2], Wenjuan Wang[1], Yuting Zhang[1] and Yan Cui[1*]

[1]Department of Ophthalmology, Qilu Hospital of Shandong University, Jinan, China, [2]Cheeloo College of Medicine, Shandong University, Jinan, China, [3]Department of Nephrology, Qilu Hospital of Shandong University, Jinan, China

Introduction: Diabetic retinopathy (DR) is one of the most common and destructive microvascular complications of DM, and has become a major cause of irreversible visual impairment. The purpose of this study was to evaluate the changes in fundus microcirculation in non-diabetic retinopathy (NDR) and mild non-proliferative diabetic retinopathy (NPDR) in patients with type 2 diabetic mellitus (T2DM) using widefield swept-source optical coherence tomography angiography (WSSOCTA), and to investigate the correlation with laboratory indices of T2DM.

Methods: Eighty nine, 58 and 28 eyes were included in the NDR, NPDR and Control groups, respectively, were enrolled in this study. The 12mm×12mm fundus images obtained by WSS-OCTA were divided into 9 regions (supratemporal, ST; temporal, T; inferotemporal, IT; superior, S; central macular area, C; inferior, I; supranasal, SN; nasal, N; inferonasal, IN) to evaluate changes in vessel density (VD) of the superficial capillary plexus (SCP), deep capillary plexus (DCP), choriocapillaris, and mid-large choroidal vessel (MLCV), as well as changes in inner retinal thickness (IRT), outer retinal thickness (ORT), and choroidal thickness (CT). Results: Compared with control group, MLCV VD (I, N, IN) was significantly decreased in NDR group, SCP VD (IT, C, I) and DCP VD (T, IT, I) were significantly decreased in NPDR group. In NPDR group, DCP VD (IT) was significantly decreased compared with that in NDR group. Compared with control group, CT (ST, T, IT, S, SN, IN) was significantly declined in NDR group, and IRT (ST, IT) and ORT (ST, N) were significantly increased in NPDR group. In NPDR group, IRT (ST) and ORT (T, S) were significantly increased compared with NDR group. Correlation analysis showed that age, body mass index, fasting blood glucose, fasting insulin, fasting C-peptide, and estimated glomerular filtration rate in T2DM patients were statistically correlated with retinal and choroidal thickness/VD.

Discussion: Structural and blood flow changes in the choroid occur before the onset of DR and precede changes in the retinal microcirculation, and MLCV thickness/VD is a more sensitive imaging biomarker for the clinical detection of DR. WSS-OCTA enables large-scale non-invasive visual screening and follow-up of the retinal and choroidal vasculature in DR patients, providing a new strategy for the prevention and monitoring of DR in patients with T2DM.

KEYWORDS

type 2 diabetes mellitus, early-diabetic retinopathy, widefield swept-source optical coherence tomography angiography, mid-large choroidal vessel, physiological indices, midperipheral fundus

Introduction

Diabetes mellitus (DM), a metabolic disease characterized by chronic elevated blood glucose levels, can cause progressive damage to microvasculature, large vessels and nerves throughout the body (1, 2). Diabetic retinopathy (DR) is one of the most common and destructive microvascular complications of DM, and has become a major cause of irreversible visual impairment (3–5). Clinically, DR can be divided into two main stages: non-proliferative diabetic retinopathy (NPDR) and proliferative diabetic retinopathy (PDR). Damage to the retinal capillaries worsens as the disease progresses (6).

DM-induced vascular dysfunction eventually leads to tissue injury and degeneration, and thus the retinal changes in DR have always been of interest. It seems logical to conclude that DM also affects the choroidal vasculature (7). Retinal capillary abnormalities can be detected in many ways, but few detection devices can directly quantify the status of the mid-large choroidal vasculature (MLCV). Previous studies have used pulsatile ocular blood flow (POBF), choroidal vascularity index (CVI), and other indirect indicators of choroidal blood flow (8, 9). However, studies on MLCV in DR patients are still limited. Therefore, to investigate the relationship between choroidal blood flow changes and DR, an ancillary test that is non-invasive, visual, and directly measures choroidal perfusion may be helpful.

As an imaging technique with the advantages of speed, safety, high resolution and non-invasiveness, optical coherence tomography angiography (OCTA) has been widely used in clinical practice in recent years. It has a built-in quantitative analysis index to measure vessel morphology and density (10, 11). In addition, swept-source OCTA (SS-OCTA) can scan and generate 12mm×12mm images of the superficial, deep and choroidal retinal capillary layers, allowing perfusion studies of the choroidal matrix and lumen (12, 13). This study directly quantifies MLCV using widefield SS-OCTA (WSS-OCTA). With its unique built-in algorithm, WSS-OCTA has the ability to evaluate fundus abnormalities over a larger area, which may provide new insight into DR by correlating the vascular arc region in the central and mid-peripheral fundus.

PDR with severe visual impairment has generally received more attention from researchers than NPDR, which has seen little intervention. Recent studies have shown that about 50% of people with DM have mild visual problems (14). A more in-depth study of the fundus of diabetic patients is essential to monitor preclinical and early DR. Previous studies of DR using OCTA were limited to a 3mm×3mm or 6mm×6mm fundus area. However, most of the histopathologic changes in diabetic chorioretinopathy (DC) were found in the midperipheral area (7), so there was an urgent need to study DR on a larger scale (15–17). By performing thickness/vessel density (VD) analyses with a scan area of 12mm×12mm, we systematically described the circulatory and structural characteristics of the central and midperipheral retina and choroid in preclinical/early-stage DR. On this basis, the correlation between VD/thickness of each fundus layer and clinical-physiological indices in T2DM patients was also investigated. The aim of this study is to detect fundus changes and damage in T2DM patients earlier and to provide guidance for clinical prevention and monitoring.

Materials and methods

Study participants

According to the diagnostic criteria of T2DM in the *Clinical guidelines for prevention and treatment of type 2 diabetes mellitus in the elderly in China* (2022 edition) (18), 93 patients with T2DM and 20 healthy subjects of similar age were enrolled in Qilu Hospital of Shandong University from November 2021 to March 2022. All subjects underwent comprehensive ophthalmologic examinations, including best corrected visual acuity (BCVA), axial length (AL), spherical equivalent, intraocular pressure (IOP), slit lamp, high resolution optical coherence tomography (OCT), fundus color photography and WSS-OCTA. And we collected subjects' demographic data (sex, age, body mass index (BMI), history of T2DM) and clinical laboratory indices (fasting blood glucose, FBG; fasting insulin, FINS; fasting C-peptide, FCP; glycosylated hemoglobin type A1c, HbA1c; estimated glomerular filtration rate, eGFR).

Inclusion criteria for subjects were as follows: 1) age ≥ 18 years old; 2) BCVA ≥ z1.0log-MAR, spherical equivalent ≤ ± 1.50D, IOP ≤ 21.00 mmHg; 3) clear optical media. Exclusion criteria were as follows: 1) AL ≥ 26mm or AL ≤ 21mm; 2) ocular trauma or ocular surgery; 3) treatment history of panretinal laser photocoagulation or anti-vascular endothelial growth factor therapy; 4) ocular complications, such as keratitis, conjunctivitis, glaucoma, vitreous opacity, retinal detachment, macular edema, anterior macular membrane, pigmented retinitis, retinal arteriovenous occlusion and etc.; 5) the low quality of binocular WSS-OCTA image and the patients with poor compliance; 6) medication history of anticoagulant, lipid-lowering and antioxidant drugs; 7) infectious diseases; 8) pregnant. According to the *Clinical Practice Guidelines on the Management of Nonproliferative and Proliferative Diabetic Retinopathy without Diabetic Macular Edema* proposed by the American Society of Retina Specialists in 2020 (19), the patients with T2DM were divided into NDR group and NPDR group. Due to the inconsistency of binocular clinical manifestations in some individuals with T2DM, we only included eyes with more severe clinical diagnosis in these individuals. Finally, 89, 58 and 28 eyes were included in the NDR, NPDR and control groups, respectively. Written informed consent was obtained before examinations (version 1.0 dint 20210605001). This study adhered to the tenets of the Declaration of Helsinki and was approved by the Ethics Committee of Qilu Hospital (KYLL-202111-024-1).

WSS-OCTA device parameters and observation indicators

The WSS-OCTA device (YG100K Yalkaid, TowardPi Medical Technology Co., Ltd., Beijing, China) uses a wide-field laser source

for imaging with a scan frequency of 100 kHz, a depth of 6 mm, an area of 24 mm × 20 mm, and an image resolution of 3.8 μm (Figure 1A).

The device has real-time high-frequency eye-tracking technology and motion correction algorithms to avoid image artifacts caused by eye movements. Scanning the fundus in B-scan mode, we selected images in the range of 12 mm × 12 mm area (Figure 1B), and the device automatically identified four vascular layers (Figures 1C–F), including the SCP from the internal limiting membrane (ILM) to 9 μm above the inner plexiform layer (IPL), the DCP from the interface of 9 μm above the IPL to 9μm below the outer plexiform layer (OPL), the CC 29 μm below the Bruch's membrane (BM), and the MLCV 29 μm beneath the BM to the choroid-sclera interface (CSI) (Figures 1G–J). VD, the ratio of the vascularized area to the total image area, was automatically quantified by a high-order moment amplitude decorrelation angiography algorithm. And from the 24 mm × 20 mm area of the Enface images (Figure 2A), the 12 mm × 12 mm area was selected for thickness analysis (Figure 2B). The built-in software automatically generated topographic maps of the thickness of the inner retinal layer (IRL), the outer retinal layer (ORL) and the choroidal layer (Figures 2C–E). The inner retinal thickness (IRT) is the distance from the ILM to the IPL, the outer retinal thickness (ORT) is the distance from the IPL to the BM, and the choroidal thickness (CT) is the distance from the BM to the CSI (Figures 2F–H).

The 12mm × 12mm images of each layer of the fundus were automatically divided into nine 4mm × 4mm regions: supratemporal (ST), temporal (T), inferotemporal (IT), superior (S), central macular area (C), inferior (I), supranasal (SN), nasal (N), inferonasal (IN). The VD/thickness of each region at each layer was quantified. Each eye was scanned twice and the results were averaged. All WSS-OCTA examinations were performed by one trained operator.

Statistical analysis

In this study, we mainly used binocular data, which do not satisfy the assumption of data independence due to the existence of hierarchical structure in individuals, eye categories, layers and regions, and the strong correlation of binocular data in the same individual. Therefore, we used a generalized linear mixed-effects model for the between-group variability analysis of retinal and choroidal thickness/VD data. This analysis was performed using the lmer and glmmTMB functions in R. Statistical significance was considered at $P<0.05$. Analysis of the correlation between laboratory indices and fundus indicators in T2DM subjects was performed by a linear mixed-effects model, and this analysis was implemented by the glmer function in R. Statistical significance was considered at $P<0.05$.

Results

Demographics characteristics and clinical laboratory indices

Demographic and laboratory characteristics of the study population are shown in Table 1. A total of 175 eyes were included in our study; 89, 58 and 28 eyes were included in the NDR, NPDR, and control groups, respectively. There were no significant differences in age, BMI and FCP among the three groups. Compared with the control group, the NDR and NPDR groups showed statistically significant differences in FBG, FINS, HbA1c and eGFR.

Thickness analysis of retina and choroid

In the total area of 12mm×12mm fundus, there was no significant difference in IRT and ORT among the three groups

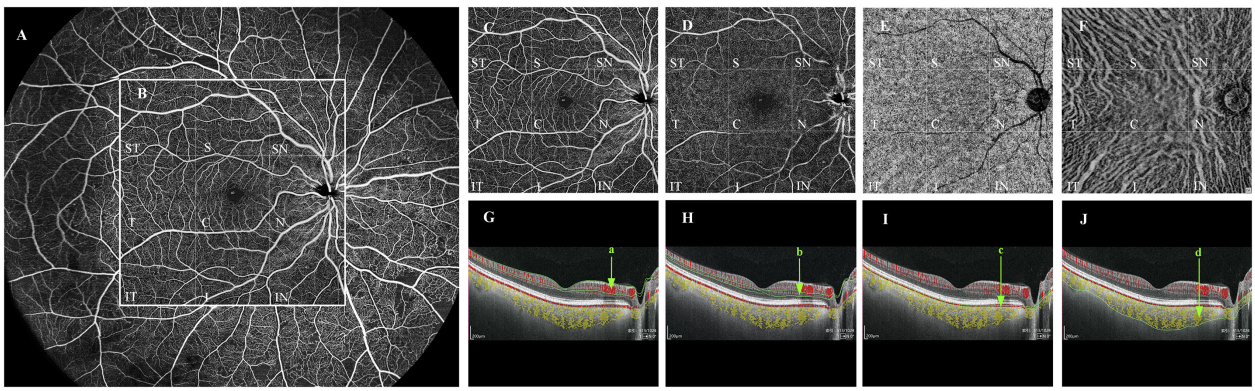

FIGURE 1
Quantification of vessel density in each vascular layer of the fundus by WSS-OCTA. Taking the right fundus vascular image obtained by WSS-OCTA in the 24 mm × 20 mm region as an example **(A)**, we selected the binarized images of the fundus in the 12mm×12mm area for VD quantitative analysis, and divided them by the built-in software into nine 4mm×4mm regions (ST, T, IT, S, C, I, SN, N, and IN **(B)**). Each cross-sectional image obtained by WSS-OCTA scanning was automatically sectioned by the built-in software into four vascular layers, namely, SCP, DCP, CC, and MLCV **(C–F)**, and divided into the above nine 4mm×4mm regions, the VD of each region in each vascular layer was quantified. **(G–J)** are imaging tomography at the level of the macular fovea; the areas within the green line (a–d) are SCP **(C)**, DCP **(D)**, CC **(E)**, and MLCV **(F)**, respectively. VD, vessel density; ST, supratemporal; T, temporal; IT, inferotemporal; S, superior; C, central macular area; I, inferior; SN, supranasal; N, nasal; IN, inferonasal; SCP, superficial capillary plexus; DCP, deep capillary plexus; CC, choriocapillary; MLCV, mid-to-large choroidal vessel.

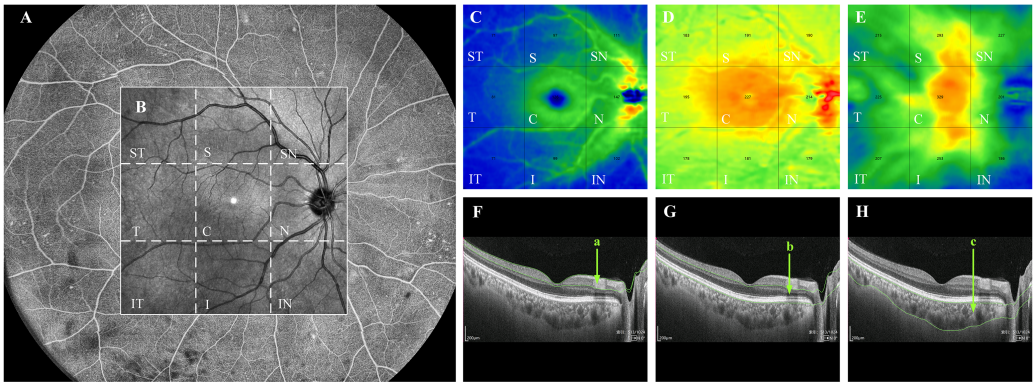

FIGURE 2
Quantification of thickness in each layer of the fundus by WSS-OCTA. WSS-OCTA can scan fundus images in the range of 24mm×20mm **(A)**. In this study, fundus image data in the range of 12mm×12mm were selected for quantitative thickness analysis **(B)**. Each cross-sectional image obtained by WSS-OCTA scanning was automatically sectioned by the built-in software into three thickness topographic maps, namely, IRL, ORL and choroid **(C–E)**, each image is divided by the built-in software into nine regions, namely, ST, S, SN, T, C, N, IT, I, and IN regions. The thickness of each region in each layer is quantified. **(F–H)** are the imaging tomography at the level of the macular fovea, where the distance between the green lines in (a–c) indicate the IRT, ORT, and CT, respectively. IRL, inner retinal layer; ORL outer retinal layer; ST, supratemporal; T, temporal; IT, inferotemporal; S, superior; C, central macular area; I, inferior; SN, supranasal; N, nasal; IN, inferonasal; IRT, inner retinal thickness; ORT, outer retinal thickness; CT, choroidal thickness.

(Figures 3A, B). And compared with the control group, a significant decrease in CT was observed in the NDR group (Figure 3C). Further analysis showed that there was no significant difference in IRT and ORT between the control and NDR groups in all 4mm×4mm regions. However, IRT was significantly increased in ST and IT regions in the NPDR group compared to the control group (Figure 3A). ORT in NPDR group was significantly increased in ST and N regions compared with control (Figure 3B). Furthermore, the NPDR group showed significantly increased IRT in ST region, ORT in T and S regions compared to the NDR group (Figures 3A, B). Compared with the control group, CT in ST, T, IT, S, I, SN, and IN regions was significantly decreased in the NDR group, and CT in IN region was significantly decreased in the NPDR group (Figure 3C). Details of thickness changes in each area of each group are shown in Table 2; Figure 4.

VD analysis of retina and choroid

In the total area of 12mm×12mm fundus, the VD of SCP and DCP in NPDR group was significantly lower than that in control group (Figures 5A, B). In addition, decreased VD of MLCV was observed in the NDR group compared with control group (Figure 5D).

In all 4mm×4mm regions, VD of SCP and DCP was not significantly different in the NDR group compared with the control group. Compared with the control group, the VD of IT, C, I regions in SCP and T, IT, I regions in DCP were significantly reduced in the NPDR group (Figures 5A, B). In addition, VD in the IT region of the DCP was significantly declined in NPDR group compared to the NDR group.

There was no significant difference in VD of the CC layer between the three groups (Figure 5C).

TABLE 1 Demographics characteristics and clinical physiological indexes of each group.

	Control	NDR	NPDR	P_1	P_2	P_3
Patients (male)	20 (9)	53 (28)	40 (24)	/	/	/
Eyes	28	89	58	/	/	/
Age (years)	59.70 ± 6.95	58.55 ± 10.38	58.00 ± 10.15	0.80	0.97	0.85
BMI (kg/m^2)	24.90 ± 2.93	25.63 ± 3.71	25.99 ± 3.25	0.45	0.21	0.48
FBG (mmol/L)	5.00 ± 0.66	8.58 ± 3.04	9.24 ± 3.30	<0.01**	<0.01**	0.94
FINS (μ IU/mL)	5.16 ± 2.84	14.49 ± 14.61	15.75 ± 13.98	<0.01**	<0.01**	0.93
FCP (ng/mL)	1.28 ± 0.96	1.24 ± 0.91	1.20 ± 0.80	0.69	0.67	0.48
HbA1c (%)	5.98 ± 0.60	8.83 ± 1.83	8.69 ± 1.53	<0.01**	<0.01**	0.31
eGFR (mL/min/1.73m^2)	95.31 ± 15.16	115.55 ± 44.43	109.75 ± 31.01	<0.01**	0.02*	0.97

Statistically significant values are shown with */**P<0.05 is marked by *P<0.01 is marked by **P_1: Control vs. NDR; P_2: Control vs. NPDR; P_3: NDR vs. NPDR.
Control, healthy subjects; NDR, non-diabetic retinopathy; NPDR, non-proliferative diabetic retinopathy; FBG, fasting blood-glucose; FINS, fasting insulin; FCP, fasting C-peptide; HbA1c, glycosylated hemoglobin type A1c; eGFR, estimated glomerular filtration rate.

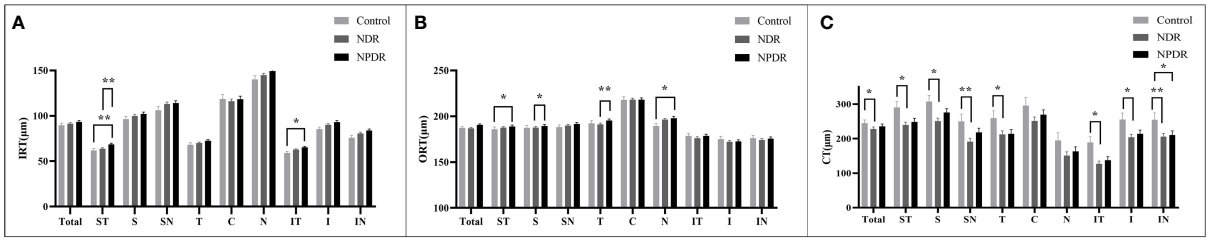

FIGURE 3
Thickness of retina and choroid in nine 4mm×4mm regions. IRT **(A)**, ORT **(B)** and CT **(C)** are quantified and compared between groups. Statistically significant values are indicated with *, *P< 0.05, **P< 0.01. Control, healthy subjects; NDR, non-diabetic retinopathy; NPDR, non-proliferative diabetic retinopathy; IRT, inner retinal thickness; ORT, outer retinal thickness; CT, choroidal thickness.

TABLE 2 Thickness differences of fundus in each layer and region between groups.

Layer	Region	Control	NDR	NPDR	P_1	P_2	P_3
IRT	Total	92.00 ± 30.97	92.75 ± 28.48	95.32 ± 27.91	0.691	0.174	0.191
	ST	61.71 ± 6.13	62.92 ± 7.24	68.22 ± 9.12	0.337	0.001**	0.000**
	S	96.86 ± 9.93	97.90 ± 12.07	101.33 ± 13.75	0.525	0.197	0.217
	SN	109.61 ± 12.17	111.04 ± 14.94	113.50 ± 15.75	0.736	0.934	0.518
	T	68.36 ± 7.77	69.38 ± 7.14	72.47 ± 10.03	0.348	0.057	0.137
	C	119.43 ± 36.51	116.88 ± 10.98	118.12 ± 12.02	0.601	0.817	0.845
	N	145.04 ± 15.71	145.29 ± 16.28	144.29 ± 16.65	0.889	0.760	0.477
	IT	60.50 ± 4.93	62.17 ± 5.64	64.83 ± 8.87	0.198	0.015*	0.090
	I	87.79 ± 8.92	89.27 ± 8.31	91.91 ± 13.18	0.438	0.113	0.181
	IN	78.75 ± 9.25	79.87 ± 9.44	83.22 ± 9.81	0.202	0.298	0.114
ORT	Total	187.15 ± 17.12	187.08 ± 16.64	190.94 ± 17.40	0.893	0.116	0.312
	ST	184.46 ± 9.69	186.69 ± 9.39	189.22 ± 8.75	0.275	0.048*	0.103
	S	187.04 ± 7.87	186.11 ± 8.83	190.7 ± 29.95	0.867	0.051	0.048*
	SN	187.93 ± 8.11	188.93 ± 8.89	192.93 ± 11.03	0.424	0.063	0.090
	T	191.32 ± 11.31	190.62 ± 10.53	197.07 ± 11.73	0.868	0.058	0.014*
	C	217.75 ± 11.32	217.03 ± 10.85	220.95 ± 11.36	0.835	0.550	0.547
	N	193.82 ± 8.08	196.25 ± 11.64	199.83 ± 14.14	0.368	0.043*	0.131
	IT	175.93 ± 15.88	175.78 ± 9.54	178.10 ± 9.02	0.852	0.495	0.208
	I	172.32 ± 13.24	170.62 ± 8.72	173.88 ± 9.22	0.544	0.896	0.277
	IN	173.75 ± 12.89	171.71 ± 9.38	175.72 ± 9.71	0.359	0.935	0.166
CT	Total	241.04 ± 96.81	207.81 ± 90.36	214.84 ± 75.26	0.015*	0.084	0.365
	ST	274.07 ± 68.13	237.02 ± 75.85	249.26 ± 63.45	0.032*	0.118	0.433
	S	294.93 ± 71.99	255.15 ± 92.76	270.05 ± 66.82	0.026*	0.192	0.252
	SN	240.79 ± 80.01	197.96 ± 87.52	208.00 ± 59.45	0.008**	0.113	0.158
	T	248.14 ± 85.95	213.47 ± 77.05	217.90 ± 61.80	0.040*	0.088	0.809
	C	281.89 ± 94.50	255.64 ± 98.00	269.69 ± 78.26	0.094	0.357	0.406
	N	178.00 ± 95.57	154.53 ± 83.20	160.69 ± 64.81	0.085	0.219	0.675

(Continued)

TABLE 2 Continued

Layer	Region	Control	NDR	NPDR	P_1	P_2	P_3
	IT	243.86 ± 99.50	213.66 ± 74.18	214.12 ± 58.45	0.049*	0.131	0.644
	I	238.11 ± 97.68	210.08 ± 77.94	212.45 ± 53.54	0.032*	0.083	0.791
	IN	169.57 ± 103.18	132.80 ± 63.21	131.45 ± 42.81	0.009**	0.025*	0.694

Statistically significant values are shown with */**P<0.05 is marked by* P<0.01 is marked by**. P_1:Control vs. NDR; P_2:Control vs. NPDR; P_3:NDR vs. NPDR. Control, healthy subjects; NDR, non-diabetic retinopathy; NPDR, non-proliferative diabetic retinopathy; IRT, inner retinal thickness; ORT, outer retinal thickness; CT, choroidal thickness; ST, supratemporal; T, temporal; IT, inferotemporal; S, superior; C, central macular area; I, inferior; SN, supranasal; N, nasal; IN, inferonasal.

Compared to the control group, VD in MLCV layer was significantly decreased in the I, N, and IN regions in the NDR group, but did not differ in all regions in the NPDR group (Figure 5D). Details of VD changes in each area of each group are shown in Table 3 and Figure 4.

Correlation analysis between laboratory indexes and thickness/VD in T2DM patients

We analyzed the correlations between thickness in each region at each layer of the fundus and laboratory indices in patients with T2DM. FBG was positively correlated with ORT in Total, ST, T, SN, and N regions. BMI had positive correlation with ORT in Total, ST, S, C, SN, and IN regions, as well as CT in ST region. eGFR was positively related with IRT in Total, S, C, and I regions, as well as CT in Total, I, N and IN regions. In addition, we found that age was negatively correlated with the thickness of all regions in each layer. FINS was related with CT of the Total area negatively. And FCP and HbA1c were not correlated with the thickness of each area of each layer. See Table 4 for details.

The correlations between VD in different regions of each layer and laboratory indices in T2DM patients were also analyzed. FBG was negatively correlated with VD of Total, S, SN, and N regions in DCP layer. BMI was related with VD of the C region in MLCV layer positively, but had negative relationship with VD of ST, S, and SN regions in SCP layer, Total, ST, S, and SN regions in DCP layer, and VD of S region in CC layer. eGFR was negatively correlated with VD of both N region in DCP layer and ST region in MLCV layer. FINS was positively correlated with VD of N region in SCP layer and negatively correlated with VD of regions containing I in DCP layer, ST in CC layer and S in MLCV layer. VD of SN in SCP layer, Total, ST, S and SN in DCP layer, S and SN in CC layer had negative relationship with FCP. Age was negatively correlated with VD of most regions in MLCV layer, while HbA1c was not related with VD in each region of each layer. See Table 5 for details.

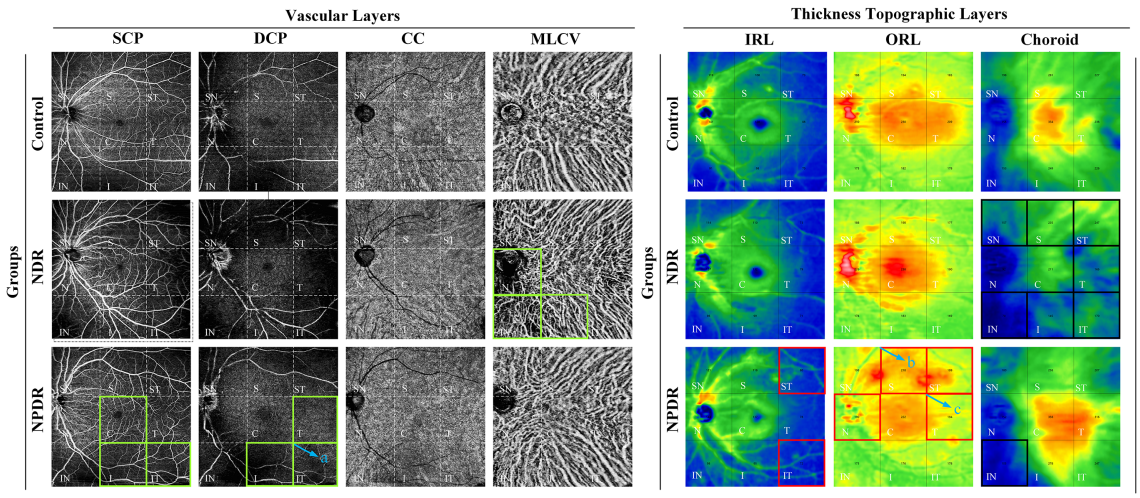

FIGURE 4
Summary of VD/thickness differences in 9 regions of each layer of retina and choroid. Regions with decreased VD are indicated by the green boxes. NPDR vs. control: SCP VD in C, I, and IT regions, DCP VD in T, I, and IT regions decreased in the NPDR group. NDR vs. control: MLCV VD decreased in N, IN, and I regions in the NDR group. The IT region where DCP VD was decreased in the NPDR group compared to the NDR group is shown in the green box in **(a)**. Regions of increased thickness are indicated by the red boxes. NPDR vs. control: IRT in ST and IT regions, ORT in N and ST regions increased in NPDR group. NPDR vs NDR: ORT in S **(b)** and T **(c)** regions increased in the NPDR group. Regions with decreased thickness are indicated by the black boxes, which CT decreased in ST, T, IT, S, SN, and IN regions decreased in the NDR group and IN regions decreased in the NPDR group compared to control. Control, healthy subjects; NDR, non-diabetic retinopathy; NPDR, non-proliferative diabetic retinopathy; VD, vessel density; SCP, superficial capillary plexus; DCP, deep capillary plexus; CC, choriocapillaris; MLCV, mid-to-large choroidal vessel; IRL, inner rtinal layer, ORL, outer retinal layer, IRT, inner retinal thickness; ORT, outer retinal thickness; CT, choroidal thickness, ST, supratemporal; T, temporal; IT, inferotemporal; S, superior; C, central macular area; I, inferior; SN, supranasal; N, nasal; IN, inferonasal.

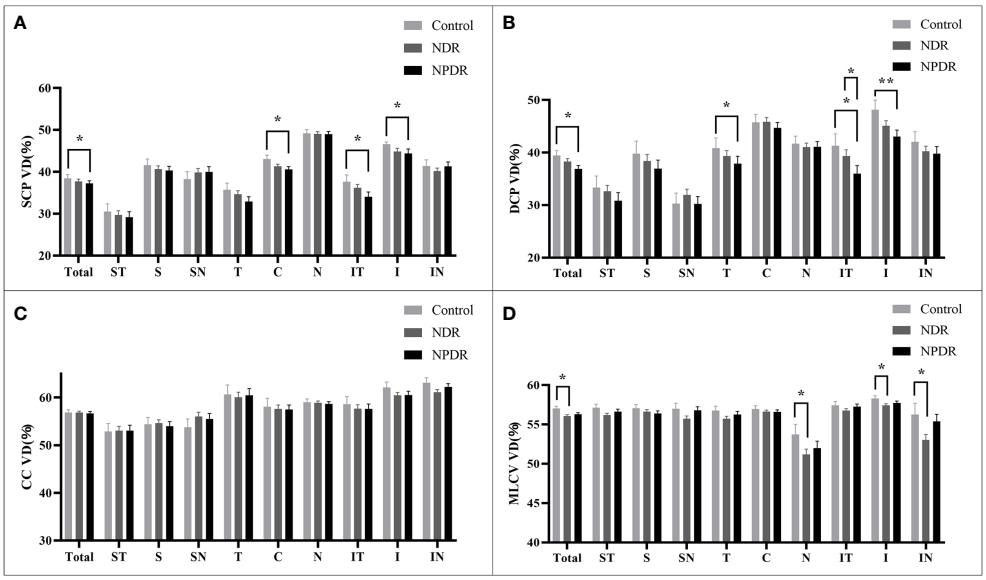

FIGURE 5
VD of retina and choroid in nine 4mm×4mm regions. SCP VD **(A)**, DCP VD **(B)**, CC VD **(C)** and MLCV VD **(D)** are quantified and compared between groups. Statistically significant values are indicated with *, *P< 0.05, **P< 0.01. Control, healthy subjects; NDR, non-diabetic retinopathy; NPDR, non-proliferative diabetic retinopathy, VD, vessel density; SCP, superficial capillary plexus; DCP, deep capillary plexus; CC, choriocapillaris; MLCV, mid-to-large choroidal vessel.

TABLE 3 VD differences of fundus in each layer and region between groups.

Layer	Region	Control	NDR	NPDR	P_1	P_2	P_3
SCP	Total	40.41 ± 8.03	39.60 ± 8.14	39.08 ± 8.06	0.181	0.037*	0.600
	ST	30.50 ± 7.63	29.73 ± 8.12	29.19 ± 6.91	0.591	0.465	0.724
	S	41.54 ± 6.65	40.65 ± 5.74	40.31 ± 5.69	0.727	0.576	0.809
	SN	38.21 ± 9.34	39.83 ± 6.78	39.97 ± 7.50	0.254	0.283	0.952
	T	35.71 ± 6.15	34.63 ± 7.03	32.93 ± 5.34	0.427	0.069	0.187
	C	43.00 ± 2.93	41.33 ± 4.30	40.55 ± 4.41	0.092	0.023*	0.434
	N	49.18 ± 2.72	49.09 ± 4.18	49.02 ± 3.17	0.895	0.845	0.869
	IT	37.61 ± 6.83	36.13 ± 6.93	34.05 ± 6.35	0.355	0.031*	0.085
	I	46.54 ± 4.31	44.87 ± 4.77	44.34 ± 5.27	0.121	0.044*	0.573
	IN	41.39 ± 4.94	40.13 ± 6.49	41.33 ± 5.34	0.287	0.939	0.208
DCP	Total	40.39 ± 9.79	39.24 ± 9.39	37.63 ± 9.32	0.428	0.045*	0.142
	ST	33.32 ± 9.45	32.60 ± 8.85	30.84 ± 9.54	0.746	0.207	0.191
	S	39.75 ± 9.59	38.39 ± 9.07	36.93 ± 9.94	0.647	0.329	0.497
	SN	30.29 ± 12.26	31.93 ± 10.23	30.43 ± 10.12	0.372	0.794	0.347
	T	40.43 ± 8.94	39.21 ± 7.98	36.67 ± 7.74	0.587	0.036*	0.080
	C	46.64 ± 6.34	45.35 ± 6.12	43.84 ± 6.16	0.393	0.108	0.271
	N	41.68 ± 3.94	41.03 ± 6.90	41.09 ± 5.66	0.589	0.726	0.765
	IT	41.25 ± 8.94	39.34 ± 8.68	35.98 ± 8.18	0.390	0.022*	0.034*
	I	48.14 ± 6.37	45.12 ± 7.40	43.07 ± 8.19	0.070	0.003**	0.136
	IN	42.04 ± 6.06	40.21 ± 9.03	39.79 ± 6.91	0.227	0.208	0.755

(Continued)

TABLE 3 Continued

Layer	Region	Control	NDR	NPDR	P_1	P_2	P_3
CC	Total	58.06 ± 6.15	57.83 ± 5.71	57.70 ± 6.37	0.653	0.527	0.737
	ST	52.86 ± 6.28	53.06 ± 6.59	53.03 ± 7.20	0.843	0.943	0.870
	S	54.39 ± 5.59	54.60 ± 4.98	53.98 ± 6.01	0.737	0.927	0.599
	SN	53.75 ± 9.16	56.00 ± 5.28	55.47 ± 7.02	0.451	0.869	0.627
	T	60.64 ± 3.53	60.06 ± 3.48	60.47 ± 5.70	0.561	0.587	0.955
	C	58.04 ± 2.74	57.61 ± 6.81	57.45 ± 4.22	0.674	0.786	0.775
	N	59.00 ± 2.61	58.89 ± 3.11	58.64 ± 3.14	0.854	0.702	0.971
	IT	58.61 ± 5.92	57.66 ± 5.61	57.57 ± 6.34	0.462	0.438	0.913
	I	62.11 ± 3.38	60.46 ± 4.08	60.53 ± 5.20	0.071	0.098	0.861
	IN	63.11 ± 3.34	61.12 ± 3.96	62.19 ± 5.21	0.637	0.992	0.815
MLCV	Total	56.73 ± 2.31	55.48 ± 4.44	56.12 ± 2.95	0.018*	0.158	0.342
	ST	57.14 ± 1.48	56.20 ± 2.23	56.64 ± 1.51	0.051	0.239	0.361
	S	57.07 ± 1.41	56.65 ± 1.45	56.40 ± 2.71	0.332	0.152	0.228
	SN	57.00 ± 1.59	55.72 ± 3.73	56.81 ± 1.76	0.123	0.602	0.208
	T	56.75 ± 2.01	55.73 ± 3.24	56.26 ± 1.93	0.105	0.361	0.545
	C	56.96 ± 1.69	56.62 ± 1.43	56.59 ± 1.62	0.326	0.469	0.406
	N	53.71 ± 3.61	51.17 ± 6.50	51.98 ± 4.22	0.047*	0.190	0.601
	IT	57.43 ± 1.73	56.76 ± 2.40	57.26 ± 1.54	0.133	0.496	0.363
	I	58.29 ± 1.33	57.43 ± 1.85	57.72 ± 1.29	0.017*	0.100	0.665
	IN	56.25 ± 2.25	53.01 ± 7.75	55.41 ± 3.96	0.045*	0.441	0.064

Statistically significant values are shown with */**P<0.05 is marked by *P<0.01 is marked by **P_1: Control vs. NDR; P_2: Control vs. NPDR; P_3: NDR vs. NPDR. The unit of VD is percentage (%). Control, healthy subjects; NDR, non-diabetic retinopathy; NPDR, non-proliferative diabetic retinopathy; VD, vessel density; SCP, superficial capillary plexus; DCP, deep capillary plexus; CC, choriocapillary; MLCV, mid-to-large choroidal vessel; ST, supratemporal; T, temporal; IT, inferotemporal; S, superior; C, central macular area; I, inferior; SN, supranasal; N, nasal; IN, inferonasal.

TABLE 4 Correlation analysis between thickness and clinical physiological indexes in T2DM.

Layer	Region	Age		BMI		FBG		FINS		FCP		HbA1c		eGFR	
		ES	P	ES	P	ES	P	ES	P	ES	P	ES	P	ES	P
IRT	**Total**	-.263	.005**	-.199	.488	.212	.519	-.060	.390	-.471	.695	.572	.358	.068	.008**
	ST	-.119	.125	.187	.400	.220	.393	-.002	.978	.033	.969	.451	.354	.028	.163
	T	-.097	.228	.245	.280	.257	.984	-.034	.559	.004	.996	.163	.742	.028	.179
	IT	-.103	.082	-.008	.961	.296	.111	.021	.635	-.374	.574	.482	.482	.028	.075
	S	-.359	.002**	.453	.178	.380	.328	-.121	.157	.660	.639	.802	.275	.079	.010**
	C	-.298	.005**	.533	.077	.463	.178	-.065	.401	.510	.684	.796	.223	.093	.001**
	I	-.261	.003**	.166	.528	.233	.448	-.011	.866	.200	.860	.365	.533	.059	.012*
	SN	-.364	.009**	.255	.529	.186	.692	-.195	.055	-1.453	.396	.453	.609	.055	.137
	N	-.575	.000**	.063	.886	.450	.366	-.141	.202	-1.264	.493	.909	.336	.121	.002**
	IN	-.111	.245	.209	.436	.133	.665	.051	.457	-.157	.888	.719	.214	.036	.146
ORT	**Total**	-.244	.000**	.519	.004	.593	.003**	-.074	.089	.832	.276	.048	.903	.020	.219
	ST	-.290	.000**	.608	.012	.598	.034*	-.067	.285	1.648	.116	.204	.705	.014	.545

(Continued)

TABLE 4 Continued

Layer	Region	Age		BMI		FBG		FINS		FCP		HbA1c		eGFR	
		ES	P	ES	P	ES	P	ES	P	ES	P	ES	P	ES	P
	T	-.295	.007**	.578	.065	.836	.020*	-.073	.363	1.830	.171	.664	.332	.028	.331
	IT	-.126	.207	.317	.250	.535	.078	-.047	.515	-1.083	.340	.451	.395	.039	.139
	S	-.177	.070	.582	.026	.388	.187	-.119	.076	1.264	.244	-.266	.640	.010	.699
	C	-.170	.142	.738	.015	.266	.427	-.034	.666	1.670	.184	-.214	.745	.036	.236
	I	-.224	.009**	.299	.220	.342	.221	-.084	.178	-.413	.691	.186	.727	.044	.049
	SN	-.240	.011*	.671	.012	.745	.015*	-.093	.175	.371	.749	.427	.471	.013	.610
	N	-.261	.015*	.481	.124	1.326	.000**	-.117	.146	.679	.617	1.037	.141	.030	.292
	IN	-.252	.008**	.610	.022	.460	.130	-.037	.592	-.170	.881	.316	.588	.030	.236
CT	**Total**	-3.060	.000**	2.403	.079	.381	.803	-.646	.023*	9.162	.095	.576	.833	.454	.000**
	ST	-2.486	.000**	3.767	.041*	1.492	.486	.100	.835	13.483	.087	-.345	.932	-.053	.762
	T	-2.187	.001**	2.170	.258	.341	.877	-.311	.528	11.195	.166	.728	.862	.124	.491
	IT	-1.869	.007**	2.547	.180	-.539	.797	-.736	.142	3.596	.646	-3.351	.360	.097	.602
	S	-3.338	.000**	2.895	.188	.264	.917	-.199	.726	9.647	.301	-1.152	.820	.133	.523
	C	-3.146	.000**	.743	.716	-1.063	.703	-.546	.380	9.808	.340	1.625	.759	.365	.107
	I	-3.061	.000**	2.871	.117	1.402	.506	-.264	.578	9.198	.238	2.766	.490	.406	.018
	SN	-2.327	.001**	3.709	.074	-1.950	.414	-.190	.723	14.913	.090	-1.512	.740	.210	.286
	N	-1.916	.008**	.853	.678	-2.228	.343	-.472	.370	12.394	.153	1.881	.674	.422	.026
	IN	-1.811	.000**	1.781	.230	-2.069	.226	-.174	.647	6.891	.277	.598	.584	.349	.010

Statistically significant values are shown with */**P<0.05 is marked by *P<0.01 is marked by **. ES: effect size (um). FBG, fasting blood-glucose; FINS, fasting insulin; FCP, fasting C-peptide; HbA1c, glycosylated hemoglobin type A1c; eGFR, estimated glomerular filtration rate; IRT, inner retinal thickness; ORT, outer retinal thickness; CT, choroidal thickness.

Discussion

DR is one of the most common and damaging microvascular complications of diabetes and a common eye disease leading to blindness, that will eventually develop in almost all patients with diabetes (20). Previous studies have shown that the fundus changes in DR and DC occur first in the midperipheral region (7, 21). Therefore, in this study, 12 mm×12 mm midperipheral fundus images were scanned by WSS-OCTA and the changes in fundus thickness/VD in preclinical and early DR and their correlation with laboratory indices were investigated by quantitative data.

Traditional OCTA is insensitive to imaging blood flow in the choroidal Sattler and Haller layers. TowardPi has a broader scanning range and has developed a three-dimensional spatial recognition algorithm, which identifies OCT signals with differences between large vessels and the stroma by a threshold segmentation algorithm, and then achieved the morphological reconstruction of MLCV (22). As it is supplemented with various signal enhancement and pseudo-signal elimination techniques, the retinal vessels cast less shadow, which in turn results in clearer MLCV layer images and more stable data. Compared with the control group, the decrease in MLCV VD in the NDR group was present in the N, IN, and I regions of the midperiphery of the fundus, whereas no significant difference in MLCV VD was observed in the patients of the NPDR group. Tan et al. showed that the CVI was significantly lower in NDR group than that in control group, which is consistent with the results of the present study, suggesting that the choroidal VD in T2DM patients was reduced before the onset of DR (23). The retinal vasculature lacks autonomic innervation, whereas the choroidal circulation is innervated by sympathetic and parasympathetic nerves (24, 25). We speculate that the decrease in choroidal blood flow in NDR patients may be due to diabetes-induced neurological disorders and vasculopathy, or both. Although choroidal blood flow was normalized in patients with mild NPDR with their own neuromodulation, this does not mean that the choroidal vasculature is not pathologically altered. Improving choroidal blood flow and its adaptive regulation may be a viable therapeutic strategy (26).

Grunwald et al. showed that hemodynamic changes were an early marker of diabetic retinopathy (27). We found that SCP VD (IT, C, I) and DCP VD (T, IT,I) was significantly decreased in the NPDR group compared with the control group, which is consistent with the results of previous studies (27). Of particular note are the IT and I regions, where superficial and deep retinal VD co-varies, and which may be the regions primarily affected in retinal lesions. A study showed that in the peripheral region of the diabetic cohort fundus, the temporal area of the SCP had the lowest perfusion and the inferior sector of the DCP had less perfusion, which may be related to the presence of the temporal watershed of the major temporal vascular arcades (28). In the clinical practice of performing fluorescein fundus angiography, we found that the

10.3389/fendo.2023.1184717

TABLE 5 Correlation analysis between VD and clinical physiological indexes in T2DM.

Layer	Region	Age		BMI		FBG		FINS		FCP		HbA1c		eGFR	
		ES	P	ES	P	ES	P	ES	P	ES	P	ES	P	ES	P
SCP	**Total**	-.007	.853	-.193	.087	-.123	.332	-.015	.554	-.756	.101	-.103	.663	.008	.438
	ST	.012	.844	-.508	.003**	-.320	.144	-.062	.157	-1.615	.033*	-.446	.258	.021	.170
	T	.069	.167	-.073	.615	-.151	.378	.027	.459	-.405	.529	-.062	.853	.000	.975
	IT	-.019	.703	.046	.751	-.041	.800	-.007	.860	.780	.211	-.205	.474	.001	.946
	S	-.001	.988	-.391	.004**	-.195	.233	-.047	.185	-1.729	.004	.098	.753	.014	.281
	C	.038	.307	-.044	.681	-.127	.309	-.005	.856	-.451	.329	.029	.902	-.010	.318
	I	-.053	.228	-.002	.986	.020	.892	-.051	.108	-.364	.504	-.111	.693	.003	.821
	SN	.027	.625	-.498	.002**	-.291	.119	-.017	.668	-1.642	.018*	-.026	.943	.009	.522
	N	.026	.379	-.039	.654	-.040	.695	.052	.015*	-.125	.741	.104	.595	-.005	.541
	IN	-.052	.264	.207	.131	.211	.190	-.012	.735	.172	.776	.213	.497	-.007	.583
DCP	**Total**	.017	.694	-.279	.021*	-.327	.017*	-.026	.354	-1.196	.017*	-.109	.669	.002	.835
	ST	-.007	.921	-.515	.012*	-.411	.089	-.093	.075	-2.001	.027*	-.266	.573	.025	.188
	T	-.001	.990	-.041	.818	-.186	.380	.011	.813	-.593	.454	.263	.522	.010	.555
	IT	-.082	.248	.093	.641	-.120	.593	-.030	.569	1.112	.191	-.194	.622	.001	.947
	S	.054	.507	-.631	.007**	-.538	.048*	-.038	.520	-2.521	.011*	-.092	.860	.001	.955
	C	-.038	.473	-.153	.315	-.280	.115	-.019	.628	-.697	.291	.218	.522	-.001	.943
	I	.007	.920	-.163	.432	-.211	.373	-.109	.031	-.770	.376	-.522	.243	-.011	.548
	SN	.109	.167	-.685	.003**	-.582	.030*	.022	.706	-2.221	.027*	-.125	.812	-.002	.910
	N	.152	.113	-.184	.234	-.406	.024*	.045	.256	-.555	.411	-.429	.218	-.030	.028*
	IN	-.057	.375	.155	.405	.134	.540	-.064	.177	.118	.886	-.165	.698	-.015	.361
CC	**Total**	-.041	.132	-.052	.512	.009	.921	-.024	.193	-.071	.827	-.006	.969	.009	.208
	ST	-.053	.358	-.261	.111	-.201	.303	-.100	.015*	-.835	.248	-.304	.417	.021	.167
	T	-.104	.014*	.191	.113	.135	.341	.026	.407	.678	.190	.306	.253	.015	.170
	IT	-.091	.037*	.136	.275	.169	.225	.019	.555	1.210	.240	.239	.335	.018	.132
	S	.047	.315	-.316	.017*	-.217	.166	-.027	.435	-1.149	.047*	-.078	.796	-.003	.805
	C	-.024	.721	-.153	.537	-.230	.246	-.038	.402	1.092	.137	-.601	.118	-.024	.165
	I	-.004	.919	-.074	.511	-.035	.788	-.026	.358	-.109	.824	-.286	.252	.004	.705
	SN	.052	.284	-.380	.005	-.234	.151	-.016	.654	-1.534	.010**	.226	.479	-.004	.776
	N	.013	.613	-.066	.384	.058	.517	.028	.140	-.323	.328	.030	.860	-.008	.275
	IN	-.020	.572	.170	.092	.244	.369	-.010	.710	.572	.199	.014	.950	-.007	.474
MLCV	**Total**	-.037	.000**	.029	.552	-.050	.368	-.009	.445	.168	.404	.012	.904	.004	.374
	ST	-.033	.056	.031	.526	.029	.621	-.011	.370	.048	.823	-.158	.151	-.009	.046*
	T	-.080	.000**	.035	.617	.066	.419	-.003	.881	.183	.544	-.081	.603	-.002	.717
	IT	-.058	.001**	.035	.477	-.034	.538	-.017	.178	.279	.177	-.087	.366	-.003	.539
	S	-.027	.096	.001	.982	-.009	.869	-.026	.028*	-.027	.899	.134	.217	.003	.428
	C	-.032	.012*	.088	.015*	.016	.718	-.012	.214	.296	.063	.059	.479	-.003	.389
	I	-.027	.048*	.040	.329	-.001	.985	-.008	.440	.004	.982	-.029	.747	-.003	.435
	SN	-.064	.027*	.026	.784	-.080	.390	-.005	.826	.318	.356	.039	.825	.004	.583

(Continued)

TABLE 5 Continued

Layer	Region	Age		BMI		FBG		FINS		FCP		HbA1c		eGFR	
		ES	P	ES	P	ES	P	ES	P	ES	P	ES	P	ES	P
	N	-.166	.000**	.056	.695	-.205	.219	.004	.918	1.133	.063	.240	.450	.014	.273
	IN	-.237	.000**	.081	.645	-.150	.450	-.008	.850	.707	.340	.299	.432	.029	.075

Statistically significant values are shown with */**P<0.05 is marked by *P<0.01 is marked by **. ES: effect size (%). FBG, fasting blood-glucose; FINS, fasting insulin; FCP, fasting C-peptide; HbA1c, glycosylated hemoglobin type A1c; eGFR, estimated glomerular filtration rate; VD, vessel density; SCP, superficial capillary plexus; DCP, deep capillary plexus; CC, choriocapillaris; MLCV, mid-to-large choroidal vessel.

infra-temporal retinal artery was the first to fill and the last to empty, which corresponds to the IT and I areas in this study. Therefore, we hypothesize that hyperglycemia may cause the inferior temporal retinal artery to be the first to decrease in perfusion.

In addition, we did not find a decrease in VD of SCP or DCP in the NDR group, nor did the VD of CC appear statistically different between groups. However, Cao and colleagues reported that they found changes in SCP, DCP, and CC within a 6-mm × 6-mm area centered on the orbit in NDR patients, which contributed to the detection of preclinical DR (29). Another study found that the VD of the SCP was significantly higher in the NDR group than that in control group (30). Results that are inconsistent with previous studies need to be confirmed in further scientific studies in the future.

In the present study, IRT (ST, IT) and ORT (ST, N) were found increased in the NPDR group compared with controls. Hirotaka et al. found that the retinal capillary perfusion zone (PA-NPDR) was significantly thicker in DR compared with that in non-diabetic retinopathy perfusion zone (PA-NDR), which may be due to leakage of vascular tissue in retinal layers (31). In addition, significantly reduced CT was observed in seven mid-peripheral regions (ST, T, IT, S, I, SN, IN) in NDR patients, but most of these regions were not significantly different in the NPDR group compared with the normal group. A cross-sectional study of 100 NDR eyes by Gupta et al. showed a significant reduction in CT in the central fovea and peripheral area of the macula compared to controls, which is consistent with our findings (32). CT changes may be associated with MLCV filling. As choroidal vasodilation and leakage lead to tissue edema, vascular stiffness increases (33), which may explain the CT rebound in the NPDR group.

We performed a correlation analysis between thickness/VD and laboratory indices. FBG was positively correlated with ORT of the mid-peripheral regions and negatively correlated with VD of part regions in the DCP layer. A number of reports suggested that FBG is an independent risk factor for the occurrence of DR (34). Elevated FBG in diabetic patients increases hemoglobin glycosylation and increased glycosylation of hemoglobin increases its affinity for oxygen, therefore, preventing its release at the tissue inducing hypoxia and oxidative stress (OS), which further leads to a decrease in VD (35).

In patients with T2DM, BMI was positively correlated with ORT and CT in some regions, and negatively correlated with VD in mid-peripheral regions in all layers. Hammes et al. found a significantly increased risk of retinopathy in the obese subgroup by univariate analysis (36). Another study similarly showed a higher incidence of ocular complications in T2DM patients with higher BMI (37). These studies support our results. Therefore, controlling BMI of T2DM patients to normal levels is important to protect retinal structure and blood flow.

In the present study, eGFR was positively correlated with IRT and CT in some regions, and negatively correlated with VD of DCP and MLCV layers in mid-peripheral regions. However, some studies had shown that the occurrence of DR is associated with a decrease in eGFR, which might be that a large numbers of severe NPDR or PDR patients were included in their studies (38, 39). Another study showed an increased trend of eGFR in patients with early T2DM (40), which is consistent with the trend of our research. In the early stage of diabetes, glomerular perfusion pressure increases with the dilatation of renal afferent glomerular arterioles, resulting in the decrease of creatinine and the increase of eGFR. We hypothesized that the increased renal blood may affect the distribution of blood throughout the body and lead to the decrease of blood in the fundus, which may be one of the reasons for the decrease of fundus VD.

The research is limited in several ways: 1) This study collected outpatients and inpatients with T2DM, most of whom were between 40 and 60 years old, hence there was a lack of observation of younger or older diabetics. Small sample size and single-center study design were also limitations. 2) We gathered binocular data from several participants. And generalized linear mixed model was used to diminish the binocular interaction. Subsequent prospective studies with strictly monocular data could further validate our results. 3) No abnormalities were found in the central macular area and no further partitioning study was conducted. This study focused on the midperipheral fundus.

Conclusion

Structural and blood flow changes in the choroid appear before the onset of DR and precede changes in the retinal microcirculation, and MLCV thickness/VD is a more sensitive imaging biomarker for clinical detection of DR. Choriocapillaris are not affected in preclinical DR and early DR, therefore more attention could be paid to the MLCV. FBG, BMI and eGFR levels have relationship with thickness/VD in fundus of T2DM patients, which may be associated with the occurrence and development of DR. WSS-OCTA enables large-scale non-invasive visual screening and follow-up of the retinal and choroidal vasculature in DR patients, which provides a new strategy for the prevention and monitoring of DR in patients with T2DM.

Data availability statement

The original contributions presented in the study are included in the article/Supplementary Material. Further inquiries can be directed to the corresponding author.

Ethics statement

The studies involving human participants were reviewed and approved by Ethics Committee of Qilu Hospital of Shandong University. The patients/participants provided their written informed consent to participate in this study.

Author contributions

ZQ and YS: study concept and design; ZQ, JZ, XY, and WW: biological material collection and data acquisition; FF and YS: data analysis and interpretation; ZQ and YZ: overall study supervision; and ZQ and YS: drafting of the manuscript. ZQ, YS, and FF also reviewed the underlying data. All authors contributed to the article and approved the submitted version.

Funding

We thank the Natural Science Foundation of Shandong Province, China (grant numbers: ZR2020MH174) and Qilu Hygiene andHealth Leading Personnel Project for their support.

Acknowledgments

The authors sincerely thank the healthy subjects and patients with T2DM who participated in this study, and sincerely thank Drs. Xuemiao Wang, Hailian Wang, Lin Tian, and Chunhong Liu from the Department of Endocrinology, Qilu Hospital, Shandong University. We thank the Natural Science Foundation of Shandong Province, China (grant numbers: ZR2020MH174) and Qilu Hygiene andHealth Leading Personnel Project for their support.

Conflict of interest

The authors declare that the research was conducted in the absence of any commercial or financial relationships that could be construed as a potential conflict of interest.

Publisher's note

All claims expressed in this article are solely those of the authors and do not necessarily represent those of their affiliated organizations, or those of the publisher, the editors and the reviewers. Any product that may be evaluated in this article, or claim that may be made by its manufacturer, is not guaranteed or endorsed by the publisher.

Supplementary material

The Supplementary Material for this article can be found online at: https://www.frontiersin.org/articles/10.3389/fendo.2023.1184717/full#supplementary-material

References

1. Zimmet PZ. Diabetes and its drivers: the largest epidemic in human history? *Clin Diabetes Endocrinol* (2017) 3:1–. doi: 10.1186/s40842-016-0039-3

2. Wong TY, Cheung CMG, Larsen M, Sharma S, Simo R. Diabetic retinopathy. *Nat Rev Dis Primers.* (2016) 2. doi: 10.1038/nrdp.2016.12

3. Lin T, Gubitosi-Klug RA, Channa R, Wolf RM. Pediatric diabetic retinopathy: updates in prevalence, risk factors, screening, and management. *Curr Diabetes Rep* (2021) 21(12). doi: 10.1007/s11892-021-01436-x

4. Cheung N, Mitchell P, Wong TY. Diabetic retinopathy. *Lancet* (2010) 376 (9735):124–36. doi: 10.1016/S0140-6736(09)62124-3

5. Lin K-Y, Hsih W-H, Lin Y-B, Wen C-Y, Chang T-J. Update in the epidemiology, risk factors, screening, and treatment of diabetic retinopathy. *J Diabetes Invest* (2021) 12(8):1322–5. doi: 10.1111/jdi.13480

6. Gonzalez VH, Campbell J, Holekamp NM, Kiss S, Loewenstein A, Augustin AJ, et al. Early and long-term responses to anti vascular endothelial growth factor therapy in diabetic macular edema: analysis of protocol I data. *Am J Ophthalmology.* (2016) 172:72–9. doi: 10.1016/j.ajo.2016.09.012

7. Lutty GA. Diabetic choroidopathy. *Vision Res* (2017) 139:161–7. doi: 10.1016/j.visres.2017.04.011

8. Kase S, Endo H, Yokoi M, Kotani M, Katsuta S, Takahashi M, et al. Choroidal thickness in diabetic retinopathy in relation to long-term systemic treatments for diabetes mellitus. *Eur J Ophthalmology.* (2016) 26(2):158–62. doi: 10.5301/ejo.5000676

9. Wu H, Zhang G, Shen M, Xu R, Wang P, Guan Z, et al. Assessment of choroidal vascularity and choriocapillaris blood perfusion in anisomyopic adults by SS-OCT/OCTA. *Invest Ophthalmol Visual Sci* (2021) 62(1). doi: 10.1167/iovs.62.1.8

10. Bakirci S, Celik E, Acikgoz SB, Erturk Z, Tocoglu AG, Imga NN, et al. The evaluation of nailfold videocapillaroscopy findings in patients with type 2 diabetes with and without diabetic retinopathy. *Northern Clinics Istanbul.* (2019) 6(2):146–50. doi: 10.14744/nci.2018.02222

11. Spaide RF, Klancnik JMJr., Cooney MJ. Retinal vascular layers imaged by fluorescein angiography and optical coherence tomography angiography. *JAMA Ophthalmology.* (2015) 133(1):45–50. doi: 10.1001/jamaophthalmol.2014.3616

12. Borrelli E, Parravano M, Sacconi R, Costanzo E, Querques L, Vella G, et al. Guidelines on optical coherence tomography angiography imaging: 2020 focused update. *Ophthalmol Ther* (2020) 9(4):697–707. doi: 10.1007/s40123-020-00286-2

13. Yau JWY, Rogers SL, Kawasaki R, Lamoureux EL, Kowalski JW, Bek T, et al. Global prevalence and major risk factors of diabetic retinopathy. *Diabetes Care* (2012) 35(3):556–64. doi: 10.2337/dc11-1909

14. Yau JWY, Rogers SL, Kawasaki R, Lamoureux EL, Kowalski JW, Bek T. Global Prevalence and Major Risk Factors of Diabetic Retinopathy. *Diabetes Care* (2012) 35 (3):556–64. doi: 10.2337/dc11-1909

15. Sun Z, Yang D, Tang Z, Ng DS, Cheung CY. Optical coherence tomography angiography in diabetic retinopathy: an updated review. *Eye* (2021) 35(1):149–61. doi: 10.1038/s41433-020-01233-y

16. Safi H, Safi S, Hafezi-Moghadam A, Ahmadieh H. Early detection of diabetic retinopathy. *Survey Ophthalmology*. (2018) 63(5):601–8. doi: 10.1016/j.survophthal.2018.04.003

17. Qian Y, Yang J, Liang A, Zhao C, Gao F, Zhang M. Widefield swept-source optical coherence tomography angiography assessment of choroidal changes in vogt-Koyanagi-Harada disease. *Front Med* (2021) 8. doi: 10.3389/fmed.2021.698644

18. Chinese Diabetes S. Guideline for the prevention and treatment of type 2 diabetes mellitus in China(2020 edition). *Chin J Endocrinol Metab* (2021) 37(4):311–98. doi: 10.3760/cma.j.cn311282-20210304-00142

19. Yonekawa Y, Modi YS, Kim LA, Skondra D, Kim JE, Wykoff CC. American Society of retina specialists clinical practice guidelines: management of nonproliferative and proliferative diabetic retinopathy without diabetic macular edema. *J Vitreoretinal Diseases.* (2020) 4(2):125–35. doi: 10.1177/2474126419893829

20. Antonetti DA, Klein R, Gardner TW. Mechanisms of disease diabetic retinopathy. *New Engl J Med* (2012) 366(13):1227–39. doi: 10.1056/NEJMra1005073

21. Xu F, Li Z, Gao Y, Yang X, Huang Z, Li Z, et al. Retinal microvascular signs in pre- and early-stage diabetic retinopathy detected using wide-field swept-source optical coherence tomographic angiography. *J Clin Med* (2022) 11(15). doi: 10.3390/jcm11154332

22. Zhou N, Xu X, Liu Y, Wei W, Peng X. Appearance of tumor vessels in patients with choroidal osteoma using swept-source optical coherence tomographic angiography. *Front Oncol* (2021) 11. doi: 10.3389/fonc.2021.762394

23. Tan K-A, Laude A, Yip V, Loo E, Wong EP, Agrawal R. Choroidal vascularity index - a novel optical coherence tomography parameter for disease monitoring in diabetes mellitus? *Acta Ophthalmologica* (2016) 94(7):E612–E6. doi: 10.1111/aos.13044

24. Kastelan S, Oreskovic I, Biscan F, Kastelan H, Antunica AG. Inflammatory and angiogenic biomarkers in diabetic retinopathy. *Biochemia Medica.* (2020) 30(3). doi: 10.11613/BM.2020.030502

25. Joussen AM, Poulaki V, Le ML, Koizumi K, Esser C, Janicki H, et al. A central role for inflammation in the pathogenesis of diabetic retinopathy. *FASEB J* (2004) 18 (10):1450–+. doi: 10.1096/fj.03-1476fje

26. Lawrence MB, Smith CW, Eskin SG, McIntire LV. EFFECT OF VENOUS SHEAR-STRESS ON CD18-MEDIATED NEUTROPHIL ADHESION TO CULTURED ENDOTHELIUM. *Blood* (1990) 75(1):227–37. doi: 10.1182/blood.V75.1.227.227

27. Grunwald JE, Alexander J, Ying G-S, Maguire M, Daniel E, Whittock-Martin R, et al. Retinopathy and chronic kidney disease in the chronic renal insufficiency cohort (CRIC) study. *Arch Ophthalmology.* (2012) 130(9):1136–44. doi: 10.1001/archophthalmol.2012.1800

28. Amato A, Nadin F, Borghesan F, Cicinelli MV, Chatziralli I, Sadiq S, et al. Widefield optical coherence tomography angiography in diabetic retinopathy. *J Diabetes Res* (2020) 2020. doi: 10.1155/2020/8855709

29. Cao D, Yang D, Huang Z, Zeng Y, Wang J, Hu Y, et al. Optical coherence tomography angiography discerns preclinical diabetic retinopathy in eyes of patients with type 2 diabetes without clinical diabetic retinopathy. *Acta Diabetologica.* (2018) 55 (5):469–77. doi: 10.1007/s00592-018-1115-1

30. Nesper PL, Roberts PK, Onishi AC, Chai H, Liu L, Jampol LM, et al. Quantifying microvascular abnormalities with increasing severity of diabetic retinopathy using optical coherence tomography angiography. *Invest Ophthalmol Visual Science.* (2017) 58(6):307–15. doi: 10.1167/iovs.17-21787

31. Ito H, Ito Y, Kataoka K, Ueno S, Takeuchi J, Nakano Y, et al. Association between retinal layer thickness and perfusion status in extramacular areas in diabetic retinopathy. *Am J Ophthalmology.* (2020) 215:25–36. doi: 10.1016/j.ajo.2020.03.019

32. Gupta P, Thakku SG, Sabanayagam C, Tan G, Cheung CMG, Lamoureux EL, et al. Characterisation of choroidal morphological and vascular features in diabetes and diabetic retinopathy. *Br J Ophthalmology.* (2017) 101(8):1038–44. doi: 10.1136/bjophthalmol-2016-309366

33. Ferreira JT, Proenca R, Alves M, Dias-Santos A, Santos BO, Cunha JP, et al. Retina and choroid of diabetic patients without observed retinal vascular changes: a longitudinal study. *Am J Ophthalmology.* (2017) 176:15–25. doi: 10.1016/j.ajo.2016.12.023

34. Hsieh Y-T, Hsieh M-C. Fasting plasma glucose variability is an independent risk factor for diabetic retinopathy and diabetic macular oedema in type 2 diabetes: an 8-year prospective cohort study. *Clin Exp Ophthalmology.* (2020) 48(4):470–6. doi: 10.1111/ceo.13728

35. Reddy VS, Agrawal P, Sethi S, Gupta N, Garg R, Madaan H, et al. Associations of FPG, A1C and disease duration with protein markers of oxidative damage and antioxidative defense in type 2 diabetes and diabetic retinopathy. *Eye* (2015) 29 (12):1585–93. doi: 10.1038/eye.2015.177

36. Hammes H-P, Welp R, Kempe H-P, Wagner C, Siegel E, Holl RW, et al. Risk factors for retinopathy and DME in type 2 diabetes-results from the German/Austrian DPV database. *PloS One* (2015) 10(7). doi: 10.1371/journal.pone.0132492

37. Gray N, Picone G, Sloan F, Yashkin A. Relation between BMI and diabetes mellitus and its complications among US older adults. *South Med J* (2015) 108(1):29–36. doi: 10.14423/SMJ.0000000000000214

38. Rodriguez-Poncelas A, Mundet-Tuduri X, Miravet-Jimenez S, Casellas A, Barrot-De la Puente JF, Franch-Nadal J, et al. Chronic kidney disease and diabetic retinopathy in patients with type 2 diabetes. *PloS One* (2016) 11(2). doi: 10.1371/journal.pone.0149448

39. Yamamoto M, Fujihara K, Ishizawa M, Osawa T, Kaneko M, Ishiguro H, et al. Overt proteinuria, moderately reduced eGFR and their combination are predictive of severe diabetic retinopathy or diabetic macular edema in diabetes. *Invest Ophthalmol Visual Science.* (2019) 60(7):2685–9. doi: 10.1167/iovs.19-26749

40. Schroijen MA, de Mutsert R, Dekker FW, de Vries APJ, de Koning EJP, Rabelink TJ, et al. The association of glucose metabolism and kidney function in middle-aged adults. *Clin Kidney J* (2021) 14(11):2383–90. doi: 10.1093/ckj/sfab074

frontiers | Frontiers in Endocrinology

TYPE Original Research
PUBLISHED 26 May 2023
DOI 10.3389/fendo.2023.1171628

OPEN ACCESS

EDITED BY
Mohd Imtiaz Nawaz,
King Saud University, Saudi Arabia

REVIEWED BY
Robert Charles Andrew Symons,
University of Melbourne, Australia
Guangming Wan,
First Affiliated Hospital of Zhengzhou University, China
Taiji Nagaoka,
Nihon University, Japan

*CORRESPONDENCE
Junjie Ye
yejunjie_xh@163.com

†These authors have contributed equally to this work and share first authorship

RECEIVED 22 February 2023
ACCEPTED 10 May 2023
PUBLISHED 26 May 2023

CITATION
Yang Z, Di Y, Ye J, Yu W and Guo Z (2023) Comparison of the adjuvant effect of conbercept intravitreal injection at different times before vitrectomy for proliferative diabetic retinopathy.
Front. Endocrinol. 14:1171628.
doi: 10.3389/fendo.2023.1171628

Comparison of the adjuvant effect of conbercept intravitreal injection at different times before vitrectomy for proliferative diabetic retinopathy

Zhikun Yang[1,2†], Yu Di[1,2†], Junjie Ye[1,2*], Weihong Yu[1,2] and Zijian Guo[3]

[1]Department of Ophthalmology, Peking Union Medical College Hospital, Chinese Academy of Medical Sciences, Beijing, China, [2]Key Laboratory of Ocular Fundus Disease, Chinese Academy of Medical Sciences and Peking Union Medical College, Beijing, China, [3]Department of Clinical Laboratory, Peking Union Medical College Hospital, Chinese Academy of Medical Sciences, Beijing, China

Purpose: To assess the optimal time of intravitreal conbercept (IVC) treatment prior to pars plana vitrectomy (PPV) in patients with severe proliferative diabetic retinopathy (PDR).

Method: This study was exploratory in nature. Forty-eight consecutive patients (48 eyes) with PDR were divided into four groups according to different IVC times (0.5 mg/0.05 mL) before PPV: group A (3 days), group B (7 days), group C (14 days), and group D (non-IVC). Intraoperative and postoperative effectiveness were assessed, and vitreous VEGF concentrations were detected.

Result: For intraoperative effectiveness, groups A and D had a higher incidence of intraoperative bleeding than groups B and C ($P = 0.041$). Furthermore, groups A-C required less surgical time than group D ($P < 0.05$). For postoperative effectiveness, group B had a significantly higher proportion of visual acuity that improved or remained unchanged than group D ($P = 0.014$), and groups A-C had lower proportions of postoperative bleeding than group D. The vitreous VEGF concentration of group B (67.04 $\pm$ 47.24 pg/mL) was significantly lower than that of group D (178.29 $\pm$ 110.50 pg/mL) ($P = 0.005$).

Conclusion: IVC treatment that was administered 7 days preoperatively was associated with better effectiveness and a lower vitreous VEGF concentration than its administration at other time points.

KEYWORDS

conbercept, proliferative diabetic retinopathy, pars plana vitrectomy, vascular endothelial growth factor, adjuvant effect

1 Introduction

Diabetes mellitus (DM) is a chronic, noncommunicable, multisystem disease that has reached epidemic proportions. By 2040, the proportion of the world's adult population with DM is expected to increase to 10.4%, translating to 642 million patients with diabetes (1). Diabetic retinopathy (DR) is an ocular microvascular complication of DM, and it is the most common cause of blindness worldwide (2). The severe stage of DR is proliferative diabetic retinopathy (PDR), defining characteristic of which is neovascularization, and tractional retinal detachment (TRD) are common complications (3). Pars plana vitrectomy (PPV) is an established management method for advanced complications of PDR (4–6). However, intraoperative bleeding generally occurs during epiretinal neovascular membrane peeling, which may necessitate more surgical maneuvers, increase instrument replacement frequency, and lengthen surgical time. Therefore, many researchers have used anti-vascular endothelial growth factor (VEGF) as an adjuvant treatment before PPV in patients with severe PDR and found that it can reduce the incidence of intraoperative bleeding and the total surgical time (7–10)

Conbercept (KH902; Chengdu Kanghong Biotech Co., Sichuan, China) is a novel recombinant fusion protein that can specifically bind to VEGF-A, VEGF-B, and placental growth factor (PLGF) (11). It has been widely used in treating retinal vascular diseases, such as neovascular age-related degeneration, diabetic macular edema, and retinal vein occlusion (12–14). The effect of conbercept on vitrectomy for PDR was initially reported in 2016, when it was proposed that intravitreal conbercept injection (IVC) before PPV could minimize the risk of intraoperative bleeding (15). In most studies, the researchers have performed IVC 3 to 14 days before PPV in patients with PDR, but the optimal time-point for IVC remains controversial (8, 16–19). This lack of clarity may decrease the effect of IVC application in some cases. Furthermore, most studies have evaluated intraoperative and postoperative effectiveness without investigating the mechanism at the molecular level.

The present study was performed to compare the adjuvant effect of IVC at different times before vitrectomy for PDR and to determine the optimal time for injection. Furthermore, we investigated the changes in VEGF concentration in the vitreous humor of patients with severe PDR after IVC to better understand the mechanisms at the molecular level.

2 Methods

2.1 Patients

This study was exploratory in nature. Forty-eight consecutive patients (48 eyes) with PDR were diagnosed at the Peking Union Medical College Hospital (PUMCH) Department of Ophthalmology and assigned to four groups by sortation randomization method. Data were collected between February 2016 and April 2022. The study was approved by the hospital's institutional review board (NO. HS-1035) and complied with the Declaration of Helsinki. The inclusion criteria were (1) aged 18 years or older; (2) diagnosed with type 2 DM; (3) diagnosed with severe PDR (presence of VH with proliferation or TRD) and requiring surgical intervention; and (4) pan-retinal photocoagulation (PRP) was not applicable or could not be completed because of non-absorbable VH or retinal detachment by neovascularized fibrovascular membrane. The exclusion criteria were (1) received an intravitreal injection of any anti-VEGF within 3 months; (2) received an intravitreal dexamethasone implant within 6 months or an intravitreal injection of steroids within 3 months; (3) a history of vitrectomy; (4) existence of diseases other than DR, e.g., retinal vein occlusion and choroidal neovascularization; (5) existence of eye infection and intraocular inflammation; or (6) existence of severe systemic diseases, such as uncontrolled diabetes, uncontrolled hypertension, recent myocardial infarction or cerebral vascular accident.

2.2 Ocular examinations and laboratory assessment

Before IVC and after PPV, all patients received comprehensive ophthalmic examinations, including best-corrected visual acuity (BCVA) measurement, intraocular pressure (IOP) evaluation, anterior segment slit-lamp examination, and fundus examination. In addition, axial length, corneal curvature, and corneal endothelial cell count were assessed before PPV. B-scan ultrasonography was used to observe the degree of VH, vitreous proliferation, and retinal detachment. Fasting blood glucose (FBG) and 2-h postprandial blood glucose (2 h-PBG) data were also collected at the time of enrollment.

2.3 Treatment procedures

Patients were divided into four groups according to the time of IVC (0.5 mg/0.05 mL) before PPV: group A (3 days), group B (7 days), group C (14 days), and group D (non-IVC). All the patients signed an informed consent form prior to each IVC and PPV.

For IVC, all patients received levofloxacin eye drops four times a day for 3 days before the injection. Following topical anesthesia and sterilization of the operating field, a 30-gauge needle was inserted into the superior temporal pars plana (4 mm posterior to the limbus), and 0.5 mg (0.05 mL) of conbercept was injected. Then, ofloxacin eye ointment was administered after the IOP returned to normal. All patients were followed up 1 day after IVC, and levofloxacin eye drops were applied for another 3 days.

For PPV, all surgeries were performed by the same experienced retina surgeon (Junjie Ye) using a 23G vitrectomy system. After vitrectomy, posterior vitreous detachment, fibrovascular membrane delamination, and retinal photocoagulation were performed as needed. Intraoperative hemostasis was obtained by increasing the perfusion pressure, fluid/air exchange, or endodiathermy. Silicone oil or perfluoropropane (C3F8) tamponade was employed when necessary.

To ensure the comparability of all the indicators between the groups, we used the "VH grading system" to assess the severity of VH after IVC and the "complexity score" to evaluate the difficulty of PPV. The grading criteria for VH were as follows: Grade 0, no VH; Grade 1, mild VH with visible fundus details, but with difficulty observing the retina nerve fiber layer or small vessels; Grade 2, moderate VH with visible optic disc and large vessels; Grade 3, severe VH with faint fundus reflex, only optic disc visible; Grade 4, very severe VH with no fundus reflex and no view of the fundus (20). The complexity score was graded by quantifying (1) the fibrovascular proliferation number (each quadrant involved corresponds to one point); (2) the fibrovascular proliferation location: posterior to the equator (zero points), anterior to the equator (one point), both anterior and posterior (two points); (3) TRD (one point), tractional rhegmatogenous retinal detachment (two points); and (4) the absence of posterior vitreous detachment (one point) (21).

2.4 Vitreous humor collection and testing

We collected 1.0 mL of undiluted vitreous humor at the beginning of surgeries (cataract or PPV) into a 1.5 mL sterile Eppendorf tube; then, it was frozen at −80°C until testing. The vitreous humor samples were thawed at room temperature, and VEGF was measured by an enzyme-linked immunosorbent assay kit (R&D Systems, Minneapolis, MN, USA) according to the manufacturer's protocol.

2.5 Intraoperative and postoperative effectiveness assessment

Intraoperative effectiveness was assessed using the following parameters: intraoperative bleeding (macroscopic bleeding in the surgery especially during the process of fibrotic membrane dissection), hemostatic techniques (increasing the perfusion pressure, fluid/air exchange, or endodiathermy), intraocular tamponade (silicone oil, C3F8, or intraocular irrigation solution), and total surgical time (the time from the first incision to the time of final surgical closure). Additionally, BCVA, IOP, anterior inflammation, and postoperative bleeding (including vitreous hemorrhage, retinal hemorrhage, and early postoperative hyphema) at 3 days after PPV were used to assess early postoperative effectiveness.

2.6 Statistical analysis

Statistical analyses were conducted using SPSS statistical software version 26.0 (IBM, Armonk, NY, USA). Continuous variables are presented as the mean ± standard deviation (SD) or median (quartile range, QR), and categorical variables are presented as numbers and percentages. A Kolmogorov-Smirnova test was used to test the parameter distribution. For continuous variables, the one-way analysis of variance or the Kruskal-Wallis test was used to compare parameters between different groups, and the paired t-test or nonparametric Wilcoxon signed-rank test was used to compare parameters between the initial (before IVC) and final (3 days after PPV) visits. In addition, Pearson's chi-squared test or Fisher's exact test was performed to compare categorical variables. The differences in the data are reported with 95% confidence intervals (CIs). A two-tailed P value of ≤0.05 was considered statistically significant for all analyses.

3 Results

3.1 Demographics and clinical characteristics

Forty-eight patients (48 eyes) with type 2 DM were included in the study, of which 25 were male and 23 were female, and their mean age was 51.5 ± 9.8 years (range, 27-69 years). The mean duration of DM was 12.84 ± 6.58 years (range, 0.3-26 years). At the time of enrollment, the FBG and 2 h-PBG were 7.12 ± 2.16 mmol/L and 9.40 ± 2.76 mmol/L, respectively.

Among the 48 eyes with severe PDR, there were 26 right eyes and 22 left eyes. The median value of BCVA was 1.85 LogMAR, and the mean value of IOP was 14.02 mmHg. The severity of VH after IVC was as follows: Grade 0, two eyes; Grade 1, thirteen eyes; Grade 2, five eyes; Grade 3, eleven eyes; and Grade 4, seventeen eyes. The PPV complexity score was 5.21 ± 2.43. One eye, 1 eye, 4 eyes, and 5 eyes underwent lensectomy in groups A, B, C, and D, respectively.

There were 12 patients (12 eyes) in each group (groups A-D). We found no statistically significant differences in age, duration of DM, FBG, 2 h-PBG, BCVA, IOP, VH grade, or PPV complexity score among the subgroups (Table 1).

3.2 Intraoperative effectiveness assessment

There was a statistically significant difference in the proportion of patients who experienced intraoperative bleeding among the subgroups (P = 0.039) (Table 2). Group A (nine eyes, 75%) and group D (nine eyes, 75%) had a higher proportion of patients with intraoperative bleeding than group B (four eyes, 33.33%) and group C (three eyes, 33.33%) (P = 0.041). There was no statistically significant difference in the utilization of different hemostatic techniques among the subgroups (P = 0.095, 0.600, 0.737) (Table 2). There was a statistically significant difference in the proportion of patients who achieved spontaneous hemostasis among the subgroups (P = 0.016) (Table 2), and more patients in group A (six eyes, 50%) achieved spontaneous hemostasis than in group D (0 eyes, 0%) (P = 0.014) (Table 3).

There was a statistically significant difference in the total surgical time among the subgroups (P = 0.001) (Table 2), and group D (87.33 ± 21.13 min) had a statistical longer total surgical time than groups B (51.83 ± 12.63 min), and C (55.75 ± 20.00 min) (P = 0.001, 0.005). However, there was no statistically significant difference between groups A, B, and C (P > 0.05) (Table 4).

10.3389/fendo.2023.1171628

TABLE 1 Demographic characteristics and initial ocular manifestations of patients with proliferative diabetic retinopathy.

	Group A	Group B	Group C	Group D	F/H	P -value
Ages (years)	44.50 ± 11.77	51.17 ± 10.44	54.92 ± 6.82	55.33 ± 5.65	3.704#	0.018
Gender						
Male	2 (16.67%)	3 (25%)	7 (58.33%)	5 (41.67%)	5.132	0.184
Female	10 (83.33%)	9 (75%)	5 (41.67%)	7 (58.33%)		
Duration of DM	11.94 ± 7.35	9.50 ± 4.62	14.67 ± 7.62	15.25 ± 5.33	2.087#	0.116
FBG (mmol/L)	5.85 (2.38)	6.65 (4.15)	7.70 (3.10)	6.90 (4.07)	3.669	0.300
2h-PBG (mmol/L)	8.86 ± 2.95	10.03 ± 2.64	10.57 ± 3.22	8.13 ± 1.60	2.050#	0.121
BCVA (LogMAR)	1.85 (1.28)	2.08 (0.45)	1.85 (0.56)	1.15 (1.0)	5.702	0.127
IOP (mmHg)	14.83 ± 3.51	13.67 ± 2.96	14.08 ± 3.37	13.51 ± 2.88	1.360#	0.715
Grading of VH						
Grade 0	0 (0.00%)	1 (8.33%)	1 (8.33%)	0 (0.00%)	2.197	1.000
Grade 1	4 (33.33%)	4 (33.33%)	1 (8.33%)	4 (33.33%)	3.058	0.406
Grade 2	2 (16.67%)	0 (0.00%)	2 (16.67%)	1 (8.33%)	2.512	0.734
Grade 3	3 (25.00%)	2 (16.67%)	3 (25.00%)	3 (25.00%)	0.560	1.000
Grade 4	3 (25.00%)	5 (41.67%)	5 (41.67%)	4 (33.33%)	1.102	0.909
Complexity score of PPV	5.17 ± 2.29	4.92 ± 2.50	5.50 ± 2.61	5.25 ± 2.60	0.111#	0.953

DM, diabetes mellitus; FBG, fasting blood-glucose; PBG, posprandial blood glucose; VH, vitreous. hemorrhage; PPV, pars plana vitrectomy. # means F value: one-way analysis of variance test, *P-value < 0.05.

TABLE 2 Intraoperative and postoperative effectiveness assessment of preoperative IVC treatment of patients with proliferative diabetic retinopathy.

	Group A	Group B	Group C	Group D	F/H	P -value
Intraoperative bleeding	9 (75%)	4 (33.33%)	4 (33.33%)	9 (75%)	8.392	0.039*
Hemostatic techniques						
Increasing the infusion bottle height	0 (0.00%)	2 (16.67%)	2 (16.67%)	5 (41.67%)	6.436	0.095
Fluid/air exchange	1 (8.33%)	0 (0.00%)	0 (0.00%)	2 (16.67%)	3.097	0.600
Endodiathermy	2 (16.67%)	0 (0.00%)	1 (8.33%)	2 (16.67%)	2.290	0.737
Spontaneous. hemostasis	6 (50.00%)	2 (16.67%)	1 (8.33%)	0 (0.00%)	9.537	0.016*
Intraocular tamponade						
Silicon oil	8 (66.67%)	8 (66.67%)	8 (66.67%)	9 (75%)	7.024	0.057
C3F8	3 (25.00%)	0 (0.00%)	0 (0.00%)	2 (16.67%)	6.932	0.200
Intraocular irrigation	1 (8.33%)	4 (33.33%)	2 (16.67%)	3 (25.00%)	7.415	1.000
Total surgical time (minutes)	67.5 ± 29.43	51.83 ± 12.63	55.75 ± 20.00	87.33 ± 21.13	6.518# F	0.001*
BCVA						
Improved or remained unchanged	9 (75.00%)	12 (100.00%)	10 (83.33%)	6(50.00%)	8.845	0.031*
Decreased	3 (25.00%)	0 (0.00%)	2 (16.67%)	6 (50.00%)		
IOP (mmHg)	15.25 ± 2.93	14.92 ± 4.29	16.00 ± 5.94	15.17 ± 2.86	0.148#	0.930
Intraocular inflammation	6 (50.00%)	5 (41.67%)	5 (41.67%)	5 (41.67%)	1.797	0.701
Postoperative bleeding	5 (41.67%)	5 (41.67%)	6 (50.00%)	8 (66.67%)	2.000	0.705

BCVA, best corrected visual acuity. #means F value: one-way analysis of variance test, *P-value < 0.05.

TABLE 3 The differences between groups in intraoperative bleeding and spontaneous hemostasis.

	Intraoperative bleeding			Spontaneous hemostasis		
	Group A	Group B	Group C	Group A	Group B	Group C
Group B	0.041*			0.193		
Group C	0.041*	1.000		0.069	1.000	
Group D	1.000	0.041*	0.041*	0.014*	0.478	1.000

*P-value < 0.05.

3.3 Early postoperative effectiveness assessment

Compared with the initial BCVAs in the patients, the proportion of patients with a visual acuity that improved or remained unchanged in group B was significantly higher than those in group D (P = 0.014) (Table 4). There was no statistically significant difference in IOP between the subgroups (P = 0.930). Only one eye had an elevated IOP (29 mmHg) in group C, which could be controlled by hypotensive eye drops. Although there was no statistically significant difference in the proportion of patients with postoperative bleeding among the subgroups (P = 0.705), groups A, B, and C had lower proportions than group D (Table 2).

3.4 VEGF concentration in vitreous humor

The mean VEGF concentrations in the vitreous humor were 125.34 ± 76.89 pg/mL, 67.04 ± 47.24 pg/mL, 93.81 ± 63.57 pg/mL, and 178.29 ± 110.50 pg/mL in groups A-D, respectively. There was a statistically significant difference among the subgroups (P = 0.032). The VEGF concentrations in the vitreous humor in group B were significantly lower than those in group D (P = 0.005). However, there were no significant differences between groups A, C, and D (P > 0.05) (Figure 1).

3.5 Adverse events

No ocular or systemic adverse events were observed after IVC and PPV.

4 Discussion

In this study, we compared the adjuvant effect of IVC at different times before vitrectomy for PDR and investigated the vitreous VEGF concentrations in the patients with severe PDR. In terms of intraoperative effectiveness, we found that group with IVC 3 days prior to vitrectomy and group with non-IVC had a higher incidence of intraoperative bleeding than groups with IVC 7 days and 14 days preoperatively. However, group with IVC 3 days prior to vitrectomy had a higher proportion of patients who achieved spontaneous hemostasis than group with non-IVC. Furthermore, groups with 3 days, 7 days, and 14 days prior to vitrectomy required less total surgical time than group with non-IVC. In terms of postoperative effectiveness, group with 3 days prior to vitrectomy had a significantly higher proportion of patients with a visual acuity that improved or remained unchanged than group with non-IVC, and groups with 3 days, 7 days, and 14 days prior to vitrectomy had lower a proportion of patients who experienced postoperative bleeding than group with non-IVC. Group with 3 days prior to vitrectomy had a significantly lower concentration vitreous VEGF concentration (67.04 ± 47.24 pg/mL) than group with non-IVC (178.29 ± 110.50 pg/mL).

Anti-VEGF treatment has been used preoperatively to reduce vascular proliferation and the vascularity of neovascular tissue. Several studies have investigated the efficiency of anti-VEGF treatment before PPV in patients with PDR (7–9, 15, 19). Hattori et al. (22) found better adjunct effect on PDR patients with intravitreal bevacizumab (IVB) at 3 days before PPV than non-IVB before PPV. Furthermore, Castillo et al. (7) performed a study to assess the optimal interval of intravitreal bevacizumab (IVB) administration in diabetic patients undergoing PPV for severe PDR. They found better postoperative outcomes at 6 months when subjects received preoperative IVB at 5 to 10 days before PPV compared to 1-3 days for the treatment of PDR-related complications. In addition, Wang et al. (23) performed a meta-analysis to compare the efficiency of different perioperative time points of anti-VEGF treatment in patients who underwent PPV for severe PDR. They reported that anti-VEGF treatment at 6 to 14 days before PPV could significantly improve post-operative BCVA, decrease the incidence of recurrent vitreous hemorrhage, as well as

TABLE 4 The differences between groups in total surgical time and improved or remained unchanged BCVA.

	Total surgical time			Improved or remained unchanged BCVA		
	Group A	Group B	Group C	Group A	Group B	Group C
Group B	0.299			0.217		
Group C	0.549	0.971		1.000	0.478	
Group D	0.127	0.001*	0.005*	0.400	0.014*	0.193

*P-value < 0.05.

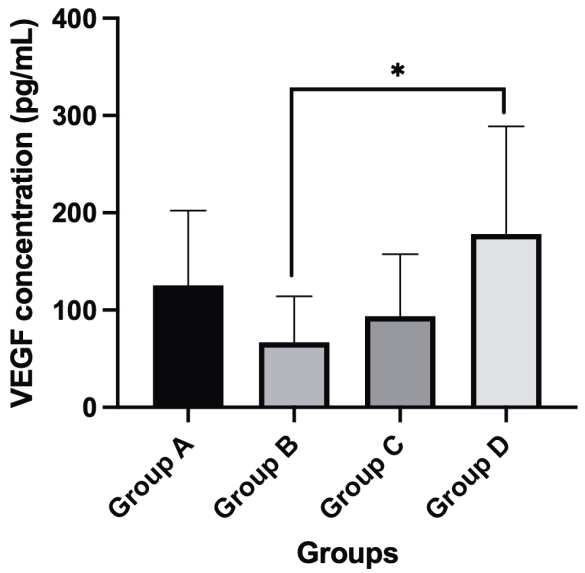

FIGURE 1
Comparison of VEGF concentrations (mean value) in different subgroups after IVC treatment. *P-value < 0.05.

reduce the duration of surgery. In our study, we found the administration of IVC treatment at 7 days preoperatively was more effective than the administration of the treatment at other time points in reducing the incidence of intraoperative and postoperative bleeding, shortening the surgical time, improving early postoperative BCVA, and decreasing vitreous VEGF concentration.

In terms of intraoperative bleeding, Simunovic et al. (24) performed a meta-analysis of 22 randomized control trials and reported that the use of anti-VEGF treatment before PPV results in less intraoperative bleeding. Furthermore, Wang et al. (23) reported that anti-VEGF treatment at 1 to 5 days, 6 to 14 days, and more than 14 days before PPV significantly reduced the incidence of intraoperative bleeding. In our study, we found that the incidence of intraoperative bleeding after receiving IVC at 7 days and 14 days was lower than that of receiving IVC at 3 days and in the control group. The results might be related to the time conbercept reached the peak concentration. Li et al. (25) investigated the ocular pharmacokinetics of rabbits following a single dose of IVC (0.5 mg) and found that the vitreous half-life of conbercept was 4.24 days. Moreover, Du et al. (26) observed total VEGF levels in hyperglycemic mouse eyes and reported that the conbercept concentration remained at high levels for 4 days. Thus, we speculated that preoperative IVC treatment at 3 days may not provide enough time for neovascular regression. Although Mao et al. (27) proposed that administering IVC 3 to 7 days before PPV to manage PDR could reduce the incidence of intraoperative bleeding, and the mean time (4.95 days) of IVC administration before PPV was longer than the half-life (4.24 days) of conbercept.

The reduction in surgical time after preoperative IVC was similar to that after other anti-VEGF agents. Li et al. (16) performed a prospective randomized study to assess the clinical efficiency of preoperative IVC treatment for severe PDR patients. The results demonstrated that IVC treatment at 7 days and 14 days significantly reduced the total surgery time when compared to the control group. Furthermore, Gao et al. (19) found that preoperative IVC treatment at 3 to 5 days also reduced the duration of surgery. Likewise, we found that the patients who received IVC treatment at 3 days, 7 days, and 14 days had shorter total surgery times than the control group. The surgical time reduction was mainly because anti-VEGF agents can cause fibrovascular proliferative membrane retraction and shrinkage, which makes manipulative techniques and visualization easier during surgery. In addition, we were able to manage most membrane dissections in IVC patients without the use of endodiathermy or blood aspiration, thereby reducing the need for tool exchange and shortening the surgical time.

Wakabayashi et al. (28) proposed that high vitreous levels of VEGF prior to vitrectomy are associated with high neovascular activity and may cause extensive proliferative changes. Therefore, such patients may be more susceptible to postoperative bleeding after PPV. Conbercept is a fully humanized, soluble, VEGF receptor protein. The most notable characteristic of conbercept is that it binds not only to VEGF-A but also to VEGF-B and PIGF (11). Some studies have reported that preoperative IVC treatment caused less postoperative bleeding (10, 19, 26). In our study, we found that the VEGF concentrations of groups A-C (125.34 ± 76.89 pg/mL, 67.04 ± 47.24 pg/mL, 93.81 ± 63.57 pg/mL, respectively) were lower than those of group D (178.29 ± 110.50 pg/mL), and the incidence of postoperative bleeding in groups A-C was lower than that of group D. Thus, we speculated that postoperative bleeding might be related to the vitreous VEGF concentration. Furthermore, Nistic et al. (29) suggested that intraoperative bleeding increases the risk of postoperative bleeding. In our study, the incidence of intraoperative bleeding was not significantly different between group A and group D, but group A had a higher proportion of patients who achieved spontaneous hemostasis than group D. Therefore, this could explain why group A had less patients with postoperative bleeding than group D.

Numerous factors might be associated with postoperative BCVA, such as a history of TRD, surgical trauma, postoperative bleeding, and silicone oil tamponade. Chen et al. (30) performed a meta-analysis and proposed that preoperative IVC achieved better BCVA outcomes. Furthermore, Castillo et al. (7) reported better postoperative BCVA at 6 months when subjects received preoperative anti-VEGF 5-10 days before PPV for PDR as opposed to 1-3 days. Wang et al. (23) also found that preoperative anti-VEGF treatment at 6 to 14 days significantly improved postoperative BCVA when compared with that of the sham group. Similarly, we found that group B had a significantly higher proportion of patients with a visual acuity that improved or remained unchanged than group D. This might be related to significantly less intraoperative and postoperative bleeding, shorter total surgical times, and fewer intraoperative manipulations in group B than in group D.

Zhang et al. (31) reported that concentrations of VEGF-A and VEGF-B decreased significantly in the vitreous humor of patients with PDR after IVC. Furthermore, Hu et al. (17) detected intraocular proangiogenic profibrotic cytokine profiles within 7 days after IVC in patients with PDR. They reported that the vitreous VEGF-A concentration decreased ten-fold at day 2 and

remained at a low level at 3 days, 4 days, 5 days, 6 days, and 7 days. Nevertheless, our results showed that the vitreous VEGF concentration in group B (7 days, 67.04 ± 47.24 pg/mL) was lower than that in group A (3 days, 125.34 ± 76.89 pg/mL) and in group C (14 days, 93.81 ± 63.57 pg/mL). This might be attributed to the fact that our study detected all VEGF family members, including not only VEGF-A and VEGF-B but also VEGF-C and VEGF-D. VEGF-C and VEGF-D also play a role in ocular angiogenesis. Hu et al. (17) identified that the expression levels of VEGF-C and VEGF-D were upregulated with the remarkable inhibition of VEGF-A by IVC. VEGF-A, VEGF-C, and VEGF-D share a common receptor, namely, VEGFR2; thus, with the downregulation of VEGF-A by anti-VEGF drugs, VEGF-C and VEGF-D might be upregulated in a feedback manner. In the study by Hu et al. (17), they found that the total concentrations of VEGF-A, VEGF-B, and VEGF-C at 7 days were also lower than those at 2 days, 3 days, 4 days, 5 days, and 6 days.

The present study has several limitations. First, the small sample size is the major limitation and may lead to an overestimation of the preoperative IVC effect in our study. Additional multicenter studies with larger samples may be needed. Second, the follow-up time was short in our study. Yang et al. (15) proposed that preoperative IVC may reduce the incidence of early postoperative bleeding in patients undergoing diabetic vitrectomy. However, it did not significantly reduce the incidence of late postoperative bleeding. Therefore, we only performed short-term follow-ups on patients to evaluate early postoperative effects. Third, Hu et al. (17) found that the vitreous VEGF-A concentration decreased ten-fold at day 2 and remained at a low level at 3 days, 4 days, 5 days, 6 days, and 7 days. Thus, we should measure the VEGF concentration at 1 day or two days after IVC. Finally, we detected only the VEGF concentration in this study. Zhang et al. (30) proposed that PIGF may be an attractive molecular target in the prevention of pathological angiogenesis in PDR. Furthermore, the PIGF concentration must be detected to investigate the preoperative IVC effect in PDR patients at a deeper molecular level.

In conclusion, our study revealed that IVC treatment was a potentially effective adjunctive therapy prior to PPV for severe PDR. Additionally, the administration of IVC treatment at 7 days preoperatively was more effective than the administration of the treatment at other time points in reducing the incidence of intraoperative and postoperative bleeding, shortening the surgical time, improving early postoperative BCVA, and decreasing vitreous VEGF concentration.

Data availability statement

The raw data supporting the conclusions of this article will be made available by the authors, without undue reservation.

Ethics statement

The studies involving human participants were reviewed and approved by the Ethics Committee of Peking Union Medical Hospital (NO. HS-1035). The patients/participants provided their written informed consent to participate in this study.

Author contributions

(I)Conception and design: JY. (II) Provision of study materials or patients: JY and ZY. (III) Collection and assembly of data: YD, JY, WY, and ZG; Data analysis and interpretation: YD and. ZY. All authors contributed to the article and approved the submitted version.

Conflict of interest

The authors declare that the research was conducted in the absence of any commercial or financial relationships that could be construed as a potential conflict of interest.

Publisher's note

References

1. Ogurtsova K, da Rocha Fernandes JD, Huang Y, Linnenkamp U, Guariguata L, Cho NH, et al. IDF diabetes atlas: global estimates for the prevalence of diabetes for 2015 and 2040. *Diabetes Res Clin Pract* (2017) 128:40–50. doi: 10.1016/j.diabres.2017.03.024

2. Faselis C, Katsimardou A, Imprialos K, Deligkaris P, Kallistratos M, Dimitriadis K. Microvascular complications of type 2 diabetes mellitus. *Curr Vasc Pharmacol* (2020) 18(2):117–24. doi: 10.2174/1570161117666190502103733

3. Chaudhary S, Zaveri J, Becker N. Proliferative diabetic retinopathy (PDR). *Dis Mon* (2021) 67(5):101140. doi: 10.1016/j.disamonth.2021.101140

4. Altan T, Acar N, Kapran Z, Unver YB, Ozdogan S. Transconjunctival 25-gauge sutureless vitrectomy and silicone oil injection in diabetic tractional retinal detachment. *Retina* (2008) 28(9):1201–6. doi: 10.1097/IAE.0b013e3181853d3c

5. Gupta B, Wong R, Sivaprasad S, Williamson TH. Surgical and visual outcome following 20-gauge vitrectomy in proliferative diabetic retinopathy over a 10-year period, evidence for change in practice. *Eye (Lond)* (2012) 26(4):576–82. doi: 10.1038/eye.2011.348

6. Storey PP, Ter-Zakarian A, Philander SA, Olmos de Koo L, George M, Humayun MS, et al. VISUAL AND ANATOMICAL OUTCOMES AFTER DIABETIC TRACTION AND TRACTION-RHEGMATOGENOUS RETINAL DETACHMENT REPAIR. *Retina* (2018) 38(10):1913–9. doi: 10.1097/iae.0000000000001793

7. Castillo J, Aleman I, Rush SW, Rush RB. Preoperative bevacizumab administration in proliferative diabetic retinopathy patients undergoing vitrectomy: a randomized and controlled trial comparing interval variation. *Am J Ophthalmol* (2017) 183:1–10. doi: 10.1016/j.ajo.2017.08.013

8. Cui J, Chen H, Lu H, Dong F, Wei D, Jiao Y, et al. Efficacy and safety of intravitreal conbercept, ranibizumab, and triamcinolone on 23-gauge vitrectomy for patients with proliferative diabetic retinopathy. *J Ophthalmol* (2018) 2018:4927259. doi: 10.1155/2018/4927259

9. Pakzad-Vaezi K, Albiani DA, Kirker AW, Merkur AB, Kertes PJ, Eng KT, et al. A randomized study comparing the efficacy of bevacizumab and ranibizumab as pre-treatment for pars plana vitrectomy in proliferative diabetic retinopathy. *Ophthalmic Surg Lasers Imaging Retina* (2014) 45(6):521–4. doi: 10.3928/23258160-20141118-06

10. Wang Q, Cai H, Xu D, Cui L, Zhang Y, Chen M. Pars plana vitrectomy assisted by intravitreal injection of conbercept enhances the therapeutic effect and quality of life in patients with severe proliferative diabetic retinopathy. *Am J Transl Res* (2022) 14 (2):1324–31.

11. Chen X, Li J, Li M, Zeng M, Li T, Xiao W, et al. KH902 suppresses high glucose-induced migration and sprouting of human retinal endothelial cells by blocking VEGF and PIGF. *Diabetes Obes Metab* (2013) 15(3):224–33. doi: 10.1111/dom.12008

12. Liu K, Wang H, He W, Ye J, Song Y, Wang Y, et al. Intravitreal conbercept for diabetic macular oedema: 2-year results from a randomised controlled trial and open-label extension study. *Br J Ophthalmol* (2022) 106(10):1436–43. doi: 10.1136/bjophthalmol-2020-318690

13. Cui J, Sun D, Lu H, Dai R, Xing L, Dong H, et al. Comparison of effectiveness and safety between conbercept and ranibizumab for treatment of neovascular age-related macular degeneration. a retrospective case-controlled non-inferiority multiple center study. *Eye (Lond)* (2018) 32(2):391–9. doi: 10.1038/eye.2017.187

14. Sun Z, Zhou H, Lin B, Jiao X, Luo Y, Zhang F, et al. EFFICACY AND SAFETY OF INTRAVITREAL CONBERCEPT INJECTIONS IN MACULAR EDEMA SECONDARY TO RETINAL VEIN OCCLUSION. *Retina* (2017) 37(9):1723–30. doi: 10.1097/iae.0000000000001404

15. Yang X, Xu J, Wang R, Mei Y, Lei H, Liu J, et al. A randomized controlled trial of conbercept pretreatment before vitrectomy in proliferative diabetic retinopathy. *J Ophthalmol* (2016) 2016:2473234. doi: 10.1155/2016/2473234

16. Li B, Li MD, Ye JJ, Chen Z, Guo ZJ, Di Y. Vascular endothelial growth factor concentration in vitreous humor of patients with severe proliferative diabetic retinopathy after intravitreal injection of conbercept as an adjunctive therapy for vitrectomy. *Chin Med J (Engl)* (2020) 133(6):664–9. doi: 10.1097/cm9.0000000000000687

17. Hu Z, Cao X, Chen L, Su Y, Ji J, Yuan S, et al. Monitoring intraocular proangiogenic and profibrotic cytokines within 7 days after adjunctive anti-vascular endothelial growth factor therapy for proliferative diabetic retinopathy. *Acta Ophthalmol* (2022) 100(3):e726–36. doi: 10.1111/aos.14957

18. Su L, Ren X, Wei H, Zhao L, Zhang X, Liu J, et al. INTRAVITREAL CONBERCEPT (KH902) FOR SURGICAL TREATMENT OF SEVERE PROLIFERATIVE DIABETIC RETINOPATHY. *Retina* (2016) 36(5):938–43. doi: 10.1097/iae.0000000000000900

19. Gao S, Lin Z, Chen Y, Xu J, Zhang Q, Chen J, et al. Intravitreal conbercept injection as an adjuvant in vitrectomy with silicone oil infusion for severe proliferative diabetic retinopathy. *J Ocul Pharmacol Ther* (2020) 36(5):304–10. doi: 10.1089/jop.2019.0149

20. Ahn J, Woo SJ, Chung H, Park KH. The effect of adjunctive intravitreal bevacizumab for preventing postvitrectomy hemorrhage in proliferative diabetic retinopathy. *Ophthalmology* (2011) 118(11):2218–26. doi: 10.1016/j.ophtha.2011.03.036

21. Grigorian RA, Castellarin A, Fegan R, Seery C, Del Priore LV, Von Hagen S, et al. Epiretinal membrane removal in diabetic eyes: comparison of viscodissection with conventional methods of membrane peeling. *Br J Ophthalmol* (2003) 87(6):737–41. doi: 10.1136/bjo.87.6.737

22. Hattori T, Shimada H, Nakashizuka H, Mizutani Y, Mori R, Yuzawa M. Dose of intravitreal bevacizumab (Avastin) used as preoperative adjunct therapy for proliferative diabetic rtinopathy. *Retina* (2010) 30(5):761–4. doi: 10.1097/iae.0b013e3181c70168

23. Wang DY, Zhao XY, Zhang WF, Meng LH, Chen YX. Perioperative anti-vascular endothelial growth factor agents treatment in patients undergoing vitrectomy for complicated proliferative diabetic retinopathy: a network meta-analysis. *Sci Rep* (2020) 10(1):18880. doi: 10.1038/s41598-020-75896-8

24. Simunovic MP, Maberley DA ANTI-VASCULAR. ENDOTHELIAL GROWTH FACTOR THERAPY FOR PROLIFERATIVE DIABETIC RETINOPATHY: a systematic review and meta-analysis. *Retina* (2015) 35(10):1931–42. doi: 10.1097/iae.0000000000000723

25. Li H, Lei N, Zhang M, Li Y, Xiao H, Hao X. Pharmacokinetics of a long-lasting anti-VEGF fusion protein in rabbit. *Exp Eye Res* (2012) 97(1):154–9. doi: 10.1016/j.exer.2011.09.002

26. Du L, Peng H, Wu Q, Zhu M, Luo D, Ke X, et al. Observation of total VEGF level in hyperglycemic mouse eyes after intravitreal injection of the novel anti-VEGF drug conbercept. *Mol Vis* (2015) 21:185–93.

27. Mao JB, Wu HF, Chen YQ, Zhao SX, Tao JW, Zhang Y, et al. Effect of intravitreal conbercept treatment before vitrectomy in proliferative diabetic retinopathy. *Int J Ophthalmol* (2018) 11(7):1217–21. doi: 10.18240/ijo.2018.07.23

28. Wakabayashi Y, Usui Y, Okunuki Y, Ueda S, Kimura K, Muramatsu D, et al. Intraocular VEGF level as a risk factor for postoperative complications after vitrectomy for proliferative diabetic retinopathy. *Invest Ophthalmol Vis Sci* (2012) 53(10):6403–10. doi: 10.1167/iovs.12-10367

29. Nisic F, Jovanovic N, Mavija M, Alimanovic-Halilovic E, Nisic A, Lepara O, et al. Vitreous concentrations of vascular endothelial growth factor as a potential biomarker for postoperative complications following pars plana vitrectomy. *Arch Med Sci* (2019) 15(2):449–56. doi: 10.5114/aoms.2018.73208

30. Chen GH, Tzekov R, Mao SH, Tong YH, Jiang FZ, Li WS. Intravitreal conbercept as an adjuvant in vitrectomy for proliferative diabetic retinopathy: a meta-analysis of randomised controlled trials. *Eye (Lond)* (2022) 36(3):619–26. doi: 10.1038/s41433-021-01474-5

31. Zhang Y, Gao Z, Zhang X, Yuan Z, Ma T, Li G, et al. Effect of intravitreal conbercept injection on VEGF-a and -b levels in the aqueous and vitreous humor of patients with proliferative diabetic retinopathy. *Exp Ther Med* (2021) 21(4):332. doi: 10.3892/etm.2021.9763

frontiers | Frontiers in Endocrinology

TYPE Original Research
PUBLISHED 02 June 2023
DOI 10.3389/fendo.2023.1131993

OPEN ACCESS

EDITED BY
Mohd Imtiaz Nawaz,
King Saud University, Saudi Arabia

REVIEWED BY
Mairaj Mohammad Siddiquei,
King Saud University, Saudi Arabia
Yana Sirman,
Kyiv Eye Microsurgery Center, Ukraine

*CORRESPONDENCE
Hai-Dong Zou
zouhaidong@sjtu.edu.cn

RECEIVED 26 December 2022
ACCEPTED 15 May 2023
PUBLISHED 02 June 2023

CITATION
Xiang ZY, Chen SL, Qin XR, Lin SL, Xu Y, Lu LN and Zou HD (2023) Changes and related factors of blood CCN1 levels in diabetic patients.
Front. Endocrinol. 14:1131993.
doi: 10.3389/fendo.2023.1131993

Changes and related factors of blood CCN1 levels in diabetic patients

Zhao-Yu Xiang[1,2], Shu-Li Chen[1,2], Xin-Ran Qin[1,2], Sen-Lin Lin[2], Yi Xu[2], Li-Na Lu[2] and Hai-Dong Zou[1,2]*

[1]National Clinical Research Center for Eye Diseases, Department of Ophthalmology, Shanghai General Hospital, School of Medicine, Shanghai Jiao Tong University, Shanghai, China, [2]Shanghai Engineering Center for Precise Diagnosis and Treatment of Eye Diseases, Shanghai Eye Diseases Prevention & Treatment Center, Shanghai Eye Hospital, Shanghai, China

Objective: To study the differences in blood cellular communication network factor 1 (CCN1) levels between patients with diabetes mellitus (DM) and healthy individuals and to explore the relationship between CCN1 and diabetic retinopathy (DR).

Methods: Plasma CCN1 levels were detected using ELISA in 50 healthy controls, 74 patients with diabetes without diabetic retinopathy (DM group), and 69 patients with diabetic retinopathy (DR group). Correlations between CCN1 levels and age, body mass index, mean arterial pressure, hemoglobin A1c, and other factors were analyzed. The relationship between CCN1 expression and DR was explored using logistic regression after adjusting for confounding factors. Blood mRNA sequencing analysis was performed for all subjects, and the molecular changes that may be related to CCN1 were explored. The retinal vasculature of streptozotocin-induced diabetic rats was examined using fundus fluorescein angiography; in addition, retinal protein expression was examined using western blotting.

Results: Plasma CCN1 levels in patients with DR were significantly higher than in the control and DM groups; however, no significant differences were observed between healthy controls and patients with DM. CCN1 levels negatively correlated with body mass index and positively correlated with the duration of diabetes and urea levels. It was observed that high (OR 4.72, 95% CI: 1.10–20.25) and very high (OR 8.54, 95% CI: 2.00–36.51) levels of CCN1 were risk factors for DR. Blood mRNA sequencing analysis revealed that CCN1-related pathways were significantly altered in the DR group. The expression of hypoxia-, oxidative stress-, and dephosphorylation-related proteins were elevated, while that of tight junction proteins were reduced in the retinas of diabetic rats.

Conclusion: Blood CCN1 levels are significantly elevated in patients with DR. High and very high levels of plasma CCN1 are risk factors for DR. Blood CCN1 level may be a potential biomarker for diagnosis of DR. The effects of CCN1 on DR may be related to hypoxia, oxidative stress, and dephosphorylation.

KEYWORDS

diabetic Retinopathy, CCN1/Cyr61, diabetic complications, blood-retinal barrier, blood biomarker

1 Introduction

Diabetes is a metabolic disease characterized by hyperglycemia. Long-standing hyperglycemia chronically damages various organs, particularly the eyes, kidneys, heart, blood vessels, and nerves, leading to serious complications. Diabetic retinopathy (DR) is one of the most common microvascular complications of diabetes and one of the leading causes of incident blindness in working-age adults (1).

Cellular communication network factor 1 (CCN1) is a dynamically expressed extracellular matrix protein (2). CCN1, which is primarily secreted by endothelial cells, binds to the extracellular matrix and cell surface and controls the signal transduction between them (3). CCN1 is rapidly upregulated in response to various stimuli (e.g., mechanical/shear stress, hypoxia, and inflammation) and plays a key role in wound repair, cell growth, differentiation, adhesion, and angiogenesis (4). CCN1 is an essential regulator of vascular development and an important component of pathological neovascularization.

CCN1 is closely associated with diabetic microangiopathy (5–8), particularly diabetic retinopathy (5). You et al. reported the occurrence of higher levels of CCN1 in the vitreous humor of patients with proliferative diabetic retinopathy (PDR) compared to patients without diabetes (5). This observation has been consistently confirmed by Zhang et al. (9), Choi et al. (10), and Zhou et al. (11). Additionally, it was observed that the vascular activity in patients with PDR significantly affected the vitreous levels of CCN1 (11, 12). Zhou et al. observed that CCN1 levels were significantly higher in patients with active PDR than in patients with quiescent PDR (11); additionally, Zhang et al. found that vitreous CCN1 levels were higher in patients with PDR who had extensive neovascularization in the retina than in those with limited neovascularization (9). However, CCN1 levels were higher in the PDR group than in the control group, regardless of the PDR status (11, 12). Furthermore, CCN1 was upregulated in the neovascularized membranes of patients with PDR (12, 13) and was mostly expressed in endothelial cells and myofibroblasts (12). Additionally, the anti-vascular endothelial growth factor (VEGF) vitreous injection was able to reduce VEGF levels in the vitreous; however, it was unable to reduce CCN1 levels (12).

Animal and in vitro experiments have demonstrated the key role of CCN1 in DR (3–5, 9, 10, 13, 14). In animal models with streptozotocin (STZ)-induced diabetes, retinal CCN1 protein levels were significantly elevated (4, 9, 13, 15); additionally, Zhang et al. found that CCN1 was substantially concentrated in the ganglion cell and inner plexiform layers (9). Vitreous injections of exogenous advanced glycation end products and VEGF increased retinal CCN1 levels (4, 14). Depletion or knockdown of CCN1 significantly inhibited retinal neovascularization in mouse models with oxygen-induced retinopathy (3, 5, 10, 16, 17). Lee et al. reported that CCN1 produced by pericytes was capable of promoting choroidal neovascularization through Wnt5a (3). Di et al. found that the neoangiogenic effect of CCN1 was mediated by the PI3K/Akt-VEGF pathway (16, 17).

DR is a common microvascular complication of diabetes that can lead to vision loss and blindness; thus, the early detection and treatment of DR are crucial. The study of DR biomarkers is conducive to the early detection of DR and the exploration of its mechanism, as blood samples are easier to obtain than vitreous humor samples. Although CCN1 is closely associated with DR, there are few studies on blood CCN1 levels in patients with diabetes. Studies on the comparison of the blood CCN1 levels in patients with diabetes and healthy individuals and the relation between blood CCN1 levels and DR have not been reported. Additionally, the study of blood CCN1 levels, as a DR biomarker, could be a potential diagnostic tool. In this study, we analyzed plasma CCN1 levels and mRNA sequencing results in 50 healthy controls and 143 patients with type 2 diabetes (74 without DR and 69 with DR) to explore the predictive potential of plasma CCN1 in the diabetic population and the plausible mechanism through which systemic CCN1 affects DR.

2 Materials and methods

2.1 Subjects and examination

The participants included in this study were recruited from the Shanghai Cohort Study of Diabetic Eye Disease (SCODE; clinicaltrials.gov identifier: NCT03665090). This study adhered to the ethical principles of the Declaration of Helsinki and was approved by the Ethics Committee of Shanghai First People's Hospital (2013KY023). In 2003, SCODE established a health record for diabetic residents and began conducting annual assessments (18). In 2008, SCODE built a community remote DR screening system that combined digital fundus photography with Internet technology, which improved the efficiency of DR diagnosis (19). This study selected cross-sectional data from the SCODE study conducted between 2017–2018.

The examination methods for the SCODE study have been previously described (20). The inclusion criteria for this study were as follows: (1) diabetes mellitus (DM) diagnosed in the endocrinology department and (2) intraocular pressure in both eyes in the range of 10–21 mmHg. The exclusion criteria were as follows: (1) history of eye diseases other than DR, such as glaucoma, optic neuropathy, and hereditary eye diseases, among others; (2) history of eye surgery; (3) severe systemic diseases; (4) inability to cooperate with the examination; and (5) fundus images of poor quality. The diagnoses of type 1 and type 2 diabetes in this study were based on the diagnostic criteria for diabetes proposed by the WHO in 1999 (21). The diagnosis of DR was based on the International Clinical Classification of DR proposed at the 2002 International Ophthalmology Conference (22).

The researchers recorded basic information such as the date of birth, sex, height, weight, diabetes type, diagnosis time, and medical history of the research subjects. Venous blood samples were drawn from each subject, and tested for the levels of blood glucose, hemoglobin A1c (HbA1c), total blood cholesterol, and blood urea, among others. The best-corrected visual acuity was measured using an international standard visual acuity chart. The eyelids, conjunctiva, cornea, anterior chamber, iris, pupil, and lens were examined using slit-lamp biomicroscopy (SL130, Zeiss, Germany). Body Mass Index and Mean Arterial Pressure were

calculated using the following equations:

$$Body\ Mass\ Index\ (BMI, kg/m^2) = weight\ (kg) \div height^2(m^2)$$

$$Mean\ Arterial\ Pressure\ (MAP, mmHg) = systolic\ blood\ pressure\ (mmHg) \times \frac{1}{3} + diastolic\ blood\ pressure\ (mmHg) \times \frac{2}{3}$$

2.2 Plasma CCN1

CCN1 concentrations in human plasma samples were determined using a commercially available ELISA kit (DCYR10, R&D Systems, USA) according to the manufacturer's instructions (mean minimum detectable dose: 1.54 pg/mL, intra-assay precision: 2.3%, inter-assay precision: 6.4%).

2.3 mRNA sequencing

Total white blood cell RNA was isolated using the RNeasy Mini Kit (Qiagen, Germany). Paired-end libraries were synthesized using the TruSeq™ RNA Sample Preparation Kit (Illumina, USA) following the TruSeq™ RNA Sample Preparation Guide and sequenced on an Illumina NovaSeq 6000 (Illumina, USA). Library construction and sequencing were performed by Sinotech Genomics Co. Ltd. (Shanghai, China).

Paired-end sequence files (FASTQ) were mapped to the reference genome (GRCh38.100) using Hisat2 (Hierarchical Indexing for Spliced Alignment of Transcripts, version 2.0.5). The output SAM (sequencing alignment/map) files were converted to BAM (binary alignment/map) files and sorted using SAMtools (version 1.3.1).

Gene abundance was expressed as fragments per kilobase of exons per million reads mapped (FPKM). StringTie software was used to count the fragments within each gene and the TMM algorithm was used for normalization.

Differential mRNA expression was analyzed using the edgeR package. Differentially expressed RNAs with |log1.5(FC)| values > 1 and q-value< 0.05, were considered significantly different and retained for further analysis. In this study, we specifically analyzed genes that differed in both DR vs. DM and DR vs. control comparisons that changed in the same direction.

2.4 Animals

Animals were handled in accordance with the Association for Research in Vision and Ophthalmology Statement for the Use of Animals in Ophthalmic and Vision Research. A single intraperitoneal injection (40 mg/kg) of STZ was used to induce type 1 diabetes in adult Brown Norway rats weighing >200 g. Rats were fasted for 12 h prior to intraperitoneal injection. Rats of similar age and weight (n = 6) were used as the control group and were injected with equal amounts of sodium citrate buffer (0.1 mol/L). Body weight and blood glucose levels were measured before the injection and at 3, 4, and 8 weeks after the injection. Rats were considered diabetic if their blood glucose levels were >300 mg/dL three days after STZ injection (n = 6). Nine weeks after the injection, the control and STZ rats were sacrificed, and retinal tissue samples were collected from each eye (Supplementary Figure 1). Tissue samples were placed in liquid nitrogen and subsequently stored at −80°C for further experiments.

2.5 Fundus fluorescein angiography

The rats in each group were subjected to fluorescein fundus angiography (FFA) using Micron IV (Phoenix Research Labs, USA) 8 weeks after the induction of DM. The rats were intraperitoneally injected with sodium pentobarbital (40 mg/kg) for anesthesia, pupil dilation was performed with one drop of tropicamide (Santen Pharmaceutical Corporation, Japan), and the corneal surface was coated with methyl cellulose to keep it moist. During the FFA examination, the rats were intraperitoneally injected with 10% sodium fluorescein (0.001 mL/g, Fluorescite, Alcon, USA) for a quick examination.

2.6 Western blot analysis

Proteins were extracted from tissue homogenates. For Western blot analysis, protein samples were fractionated in 4–20% SurePAGE™ Precast Gels (M00657, GenScript Biotech Corporation, China) and transferred to nitrocellulose membranes. The analysis was performed with anti-CCN1 (ab228592, Abcam, UK), anti-CDC42 (2466T, Cell Signaling Technology, USA), anti-Claudin5 (4C3C2, Invitrogen, USA), anti-COX6c (ab150422, Abcam, UK), anti-CREB1 (R23983, ZEN- BIOSCIENCE, China), anti-HIF1α (ab179483, Abcam, UK), anti-NDUFα1 (15561-1-AP, Proteintech Group, USA), anti- SEPN1 (55333-1-AP, Proteintech Group, USA), anti-SHP1 (ab32559, Abcam, UK, anti-VEGFa (NB100-664, Novus Biologicals, USA), and anti-β-tubulin (2146S, Cell Signaling Technology, USA) antibodies. Immunoassays were performed using enhanced chemiluminescence (17046; ZEN-BIOSCIENCE, China), in accordance with the manufacturer's instructions. Protein levels were determined by densitometric scanning of protein bands. Six retinas were used in each group, and the results for each retina were averaged from three replicates.

2.7 Statistical analysis

The Kolmogorov–Smirnov U test was used to test the normality of all variables. Normally distributed descriptive data were

10.3389/fendo.2023.1131993

represented as the mean ± standard deviation, and non-normally distributed descriptive data were represented as the median (quartile 1, quartile 3). One-way analysis of variance was used to compare the between-group differences in normally distributed data. The Kruskal-Wallis test was used to compare the between-group differences for non-normally distributed data. The Mann-Whitney U test was used to compare differences in non-normally distributed data between the two groups. Spearman's correlation test was used to analyze the correlation between parameters when the data were normally distributed. A binary logistic regression model was established with DR as the dependent variable (DR = 1, without DR = 0) to evaluate the relationship between the variables and CCN1. CCN1 was stratified according to its quartiles (low CCN1< 127.72 pg/mL, 127.72 pg/mL ≤ moderate CCN1< 173.85 pg/mL, 173.85 pg/mL ≤ high CCN1< 250.32 pg/mL, very high CCN1 ≥ 250.32 pg/mL). Age, sex (male = 1, female = 0), BMI, duration of diabetes, urea, MAP, fasting glucose, HbA1c, low-density lipoprotein, and total cholesterol levels were included in the multivariate model for confounding factor correction. The Bonferroni correction was performed for multiple uncorrected comparisons. Differences were considered statistically significant at P< 0.05. Statistical analysis was performed using SPSS 22 software (International Business Machines Corporation, America).

3 Results

3.1 Characteristics of the participants

A total of 193 participants (95 female, 98 male) were included in the analysis. No significant differences (all p > 0.05) in age, BMI, MAP, low-density lipoprotein, and total cholesterol levels were observed between the groups (control, DM, and DR). However, levels of fasting glucose (H = 66.62, p< 0.001), HbA1c (H = 64.47, p< 0.001), high-density lipoprotein (F = 3.28, p = 0.04), and urea (F = 9.73, p = 0.008) were significantly different in the three groups. The levels of fasting glucose (H = 24.39, p = 0.027) and HbA1c (H = 31.48, p = 0.001) of the DR group were significantly higher than those of the DM group, whereas the levels of fasting glucose (H = 59.21, p< 0.001) and HbA1c (H = 52.34, p< 0.001) of the DM group were significantly higher than those of the control group. Levels of high-density lipoprotein were significantly higher in the control group than in the DM group (p = 0.036). Urea levels were significantly higher in the DR group than in the control group (H = 32.33, p = 0.005). Furthermore, the duration of diabetes was significantly longer in the DR group than in the DM group (H = 13.28, p< 0.001; Table 1).

3.2 Plasma CCN1

Blood CCN1 levels were significantly different in the three groups (H = 23.67, p< 0.001). CCN1 levels in the DR group were significantly higher than those in the DM (H = 38.44, p< 0.001) and control (H = 43.75, p< 0.001) groups. However, no significant difference in CCN1 expression was observed between the control

TABLE 1 Characteristics of the participants.

	CCN1, pg/mL†	Age, y†	Duration of diabetes, y†	Fasting glucose, mmol/L†	HbA1c, %†	Urea, mmol/L†	BMI, kg/m²‡	MAP, mmHg‡	High-density lipoprotein, mmol/L‡	Low-density lipoprotein, mmol/L‡	Total cholesterol, mmol/L‡
Control	152.7 (104.9, 193.7)	69 (67, 74)	N/A	5.35 (5.15, 5.94)	5.80 (5.70, 6.15)	5.41 (4.31, 6.26)	24.74 ± 3.62	96 ± 9	1.42 ± 0.39	3.05 ± 0.89	5.25 ± 1.02
DM	164.0 (99.3, 218.0)	69 (66, 73)	11.0 (4.0, 21.5)	6.93 (6.05, 8.31)	6.80 (6.25, 7.40)	5.74 (4.93, 6.84)	24.71 ± 3.56	95 ± 7	1.25 ± 0.33	2.90 ± 1.10	4.95 ± 1.26
DR	235.4 (157.4, 291.6)	71 (66, 75)	18.0 (11.6, 22.4)	8.19 (7.11, 9.60)	7.70 (6.90, 8.65)	6.10 (4.98, 8.00)	24.43 ± 2.47	97 ± 8	1.34 ± 0.35	2.90 ± 0.96	4.88 ± 1.05
H/F	23.67	2.35	13.28	66.62	64.47	9.73	0.18	0.97	3.28	0.4	1.73
p-value	<0.001*	0.31	<0.001*	<0.001*	<0.001*	0.008*	0.83	0.38	0.04*	0.67	0.18

CCN1, Cellular Communication Network Factor 1; BMI, Body Mass Index; MAP, Mean Arterial Pressure; HbA1c, Hemoglobin A1c; DM, Diabetes mellitus; DR, Diabetic Retinopathy; N/A, not applicable.
†skewed data analyzed using Kruskal-Wallis test; ‡ normal distributed data analyzed using one-way analysis of variance; * significant difference among groups, p< 0.05.

and DM groups (H = 5.32, p > 0.05; Table 1). In addition, similar levels of CCN1 were observed in both male and female subgroups (Supplementary Materials).

3.3 Influencing factors of CCN1

There were no sex differences in the CCN1 levels in the control (U = 304, p = 0.630), DM (U = 768, p = 0.201), or DR groups (U = 605, p = 0.895). CCN1 levels negatively correlated with BMI (r = –0.359, p< 0.001) and positively correlated with the duration of diabetes (r = 0.370, p< 0.001) and urea levels (r = 0.206, p = 0.041). CCN1 levels were not significantly correlated (all p > 0.05) with age (r = 0.103), MAP (r = –0.112), fasting glucose (r = 0.189), HbA1c (r = 0.190), high-density lipoprotein (r = 0.132), low-density lipoprotein (r = 0.141), or total cholesterol (r = 0.091) (Supplementary Figure 2).

3.4 DR and CCN1

The areas under the receiver operating characteristic curves for DR were 0.730 (95% CI: 0.644–0.817), 0.713 (95% CI: 0.625–0.802), and 0.684 (95% CI: 0.593–0.775) for CCN1 levels, HbA1c levels, and duration of diabetes, respectively, whereas no significant differences were observed for age, urea, and BMI (all p > 0.05; Table 2; Figure 1).

In patients with diabetes, very high blood CCN1 levels were associated with an increased risk of DR (OR 5.91, 95% CI: 2.12–16.49). Furthermore, after multifactorial correction, both high and very high blood CCN1 levels were found to be associated with an increased risk of DR (high: OR 4.72, 95% CI: 1.10–20.25; very high: OR 8.54, 95% CI: 2.00–36.51).

3.5 Changes in blood mRNA Associated with CCN1

Pairwise comparisons (DR vs. DM, DR vs. control) of genes obtained by mRNA sequencing analysis yielded 237 differentially expressed genes, of which 219 genes were upregulated and 18 genes were downregulated in the DR group. All the genes obtained from the screening met the |FC| value >1.5 and q-value<0.05. Among the 237 differential genes obtained by sequencing, those associated with CCN1 included *HIF1A-AS3, SELENON, MIF, CDC42-IT1, SRCAP, AC009927.1, AC116348.2, CDC42EP1, COX6CP1, AC112191.1, AL117336.1, NOG*, and *AL157871.3*.

Moreover, *HIF1A-AS3, SELENON, MIF, CDC42-IT1, SRCAP, AC009927.1, AC116348.2, CDC42EP1, COX6CP1, AC112191.1*, and *AL157871.3* were upregulated, while *AL117336.1* and *NOG* were downregulated in the DR group (Supplementary Tables 1, 2).

3.6 Animal examination of FFA

To analyze the changes in the retinal vascular system in diabetic rats, an FFA examination was performed. The optic disc is located at the center of the retina, and the retinal vessels radiate around it. Rats in the control group showed a clear fundus and fluorescence. However, eight weeks after DM induction, rats in the diabetic group exhibited retinal vascular tortuosity, dilation, filling defects, and leakage, which were consistent with DR (Figure 2A).

3.7 Changes in retinal protein associated with CCN1

Protein expression of CCN1 (U = 35, p = 0.004), as well as CCN1-related proteins (CDC42: U = 36, p = 0.002; COX6c: U = 34, p = 0.009; CREB1: U = 36, p = 0.002; HIF1α: U = 36, p = 0.002; NDUFα1: U = 36, p = 0.002; SEPN1: U = 34, p = 0.009; SHP1: U = 32, p = 0.026) were significantly upregulated in the retina of diabetic rats (all p value< 0.05). Additionally, the protein expression of VEGF was upregulated (U = 35, p = 0.004), while Claudin5 was downregulated (U = 34, p = 0.009) in the retina of diabetic rats (Figures 2B, C).

4 Discussion

DR is the leading cause of blindness in working-age adults (1). CCN1 is upregulated by various stimuli and exerts various biological effects by interacting with the extracellular matrix and cell surface. CCN1 has been shown to be closely related to DR. Moreover, CCN1 in the vitreous humor and neovascular membrane has received considerable attention; however, research on blood

TABLE 2 Association between CCN1 and DR: Binary and multivariable logistic regression analysis.

	Unadjusted model	Adjusted model 1†	Adjusted model 2‡	Adjusted model 3§
CCN1 low	Reference	Reference	Reference	Reference
CCN1 moderate	1.47 (0.51, 4.21)	1.49 (0.51, 4.30)	1.98 (0.53, 7.41)	2.28 (0.56, 9.34)
CCN1 high*	2.32 (0.86, 6.30)	2.41 (0.87, 6.63)	4.22 (1.10, 16.11) *	4.72 (1.10, 20.25) *
CCN1 very high*	5.91 (2.12, 16.49) *	5.96 (2.11, 16.79) *	8.99 (2.33, 34.62) *	8.54 (2.00, 36.51) *

CCN1, Cellular Communication Network Factor 1; OR, Odds Ratio; DR, Diabetic Retinopathy.
CCN1 was stratified according to its quartiles, low CCN1< 127.72 pg/mL, 127.72 pg/mL ≤ moderate CCN1< 173.85 pg/mL, 173.85 pg/mL ≤ high CCN1< 250.32 pg/mL, very high CCN1 ≥ 250.32 pg/mL
†adjusted for age and sex (male = 1, female = 0); ‡ adjusted for age, sex, BMI, duration of diabetes, and urea; §adjusted for age, sex, BMI, duration of diabetes, urea, MAP, fasting glucose, HbA1c, high-density lipoprotein, low-density lipoprotein, and total cholesterol; *significance of the logistic regression model, p< 0.05.

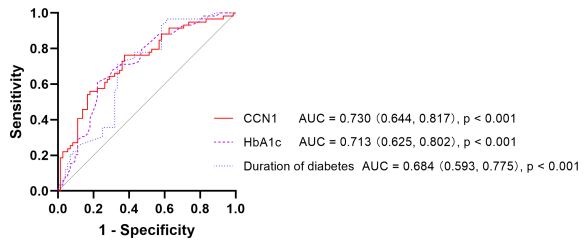

FIGURE 1
Receiver operating characteristic curve of DR DR, Diabetic Retinopathy; CCN1, Cellular Communication Network Factor 1; HbA1c, Hemoglobin A1c; AUC, Area Under Curve.

levels of CCN1 is limited. Since blood is a more accessible biological sample, the study of blood CCN1 levels could help us further understand the relationship between CCN1 and DR and its potential clinical application. We report, for the first time, the comparison of the blood CCN1 levels between patients with type 2 diabetes and healthy individuals. We observed that plasma CCN1 levels in patients with DR were significantly higher than those in diabetic patients without DR and healthy subjects. This finding is consistent with previous conclusions drawn from studies on vitreous humor.

Winzap et al. analyzed blood CCN1 levels in patients with acute coronary syndrome and established that diabetes does not affect CCN1 levels (23). This observation is consistent with our results, which revealed a non-significant difference in the CCN1 levels of the DM and control groups. HbA1c is an important indicator of long-term glycemic control. Neither the study conducted by Winzap et al. (23) nor our study showed a significant correlation between HbA1c and CCN1 levels. However, Winzap et al. found that baseline blood glucose levels were correlated with CCN1 levels (23), which was not observed in our study. This difference may be due to the inclusion of patients with acute coronary syndrome in their study; additionally, the blood glucose levels may have partially reflected the stress level in the body (23). However, the blood glucose level in our study reflected the subjects' glycemic control status.

We found that BMI, duration of diabetes, and urea levels were associated with CCN1 expression, but these correlations were weak. Considering the relation between CCN1 and DR, we believe that the correlation between CCN1 and these parameters may be due to their association with DR. CCN1 is closely associated with vascular injury. Feng et al. reported that blood CCN1 levels in diabetic subjects were positively correlated with severity of peripheral arterial disease (6). CCN1 levels is significantly elevated in patients with ST-segment elevation myocardial infarction compared to that in patients with non-ST-segment elevation myocardial infarction (24), and high levels of CCN1 can potentially predict the occurrence of cardiovascular risk events (23–25). We believe that the elevation of CCN1 levels may reflect the impairment of organ function, especially the function of blood vessels. DR is characterized by a series of fundus lesions caused by leakage and occlusion of retinal microvessels. CCN1 may be involved in the development and progression of DR through its effects on the blood vessels.

As an early response gene, CCN1 is induced by various factors, such as inflammation, hypoxia, and mechanical stimulation (2). Changes in *HIF1A-AS3, CDC42-IT1, SRCAP, AC116348.2, CDC42EP1*, and *AL117336.1* in blood mRNA sequencing analysis may reflect the induction of CCN1. Previous studies have shown that hypoxia significantly induced CCN1 expression in endothelial cells (5, 26) and HIF-1α promoted CCN1 transcription under hypoxia (26, 27). In our study, *HIF1A-AS3* was found to be upregulated in DR. Previous studies have revealed that *HIF1A-AS1* and *HIF1A-AS2* regulate the expression of HIF-1α mRNA (28, 29). We observed an increase in HIF1α in diabetic rats, which reflects the hypoxic state of the retina. In addition, changes in the expression of *CDC42-IT1, SRCAP, CDC42EP1*, and *AL117336.1* may indicate changes in CREB and small GTPase-related pathways, which have been shown to play a key role in the regulation of CCN1 (30–32). The phosphorylation of CREB and its kinases play a vital role in RhoA-mediated regulation (30, 31, 33). The *SRCAP*, which is upregulated in the DR group, is a transcriptional activator of CREB-mediated transcription (34). *CDC42EP1* is a CDC42-binding protein that promotes angiogenesis through cytoskeletal regulation (35). Additionally, *CDC42-IT1* and *AL117336.1* may be involved in the regulation of CREB-related pathways; however, their specific roles remain unclear. CDC42 and CREB1 levels were higher in the retina of diabetic rats. CREB regulates the transcription of CCN1 by directly binding to its promoter (30, 31). *AC116348.2* encodes an integrin-related molecule, and it has been reported that secreted CCN1 exerts its biological effects by binding to integrins (36).

High plasma levels of CCN1 in patients might indicate an impaired blood-retinal barrier. Changes in *SELENON, MIF, AC009927.1, COX6CP1, AC112191.1, NOG*, and *AL157871.3* in blood mRNA sequencing analysis indicated changes in systemic oxidative stress or phosphorylation levels, suggesting the possibility of blood-retinal barrier injury. Diabetic rats showed vascular tortuosity and leakage upon FFA examination. VEGF expression increased in the retinas of diabetic rats, while Claudin5 expression decreased. The retinal vessels of diabetic rats were damaged and the blood-retinal barrier was compromised. CCN1 is mainly expressed in endothelial cells and mediates angiogenic effects (36). Previous studies have suggested that increased CCN1 expression stimulates oxidative stress and disrupts tight junction integrity in endothelial cells (13). In our study, alterations in the expression of *SELENON, COX6CP1, NOG*, and *AL157871.3* suggest elevated levels of oxidative stress. We examined the relevant target molecules and found that the target molecules COX6c, NDUFα1, and SEPN1 levels were elevated in the retinas of diabetic rats. In addition, CCN1 can inhibit pericyte adhesion and cause anoikis by regulating the phosphorylation of focal adhesions (37). *AC009927.1* and *AC112191.1* are associated with the regulation of phosphorylation, particularly tyrosine phosphorylation. We examined the levels of SHP1, which promotes dephosphorylation,

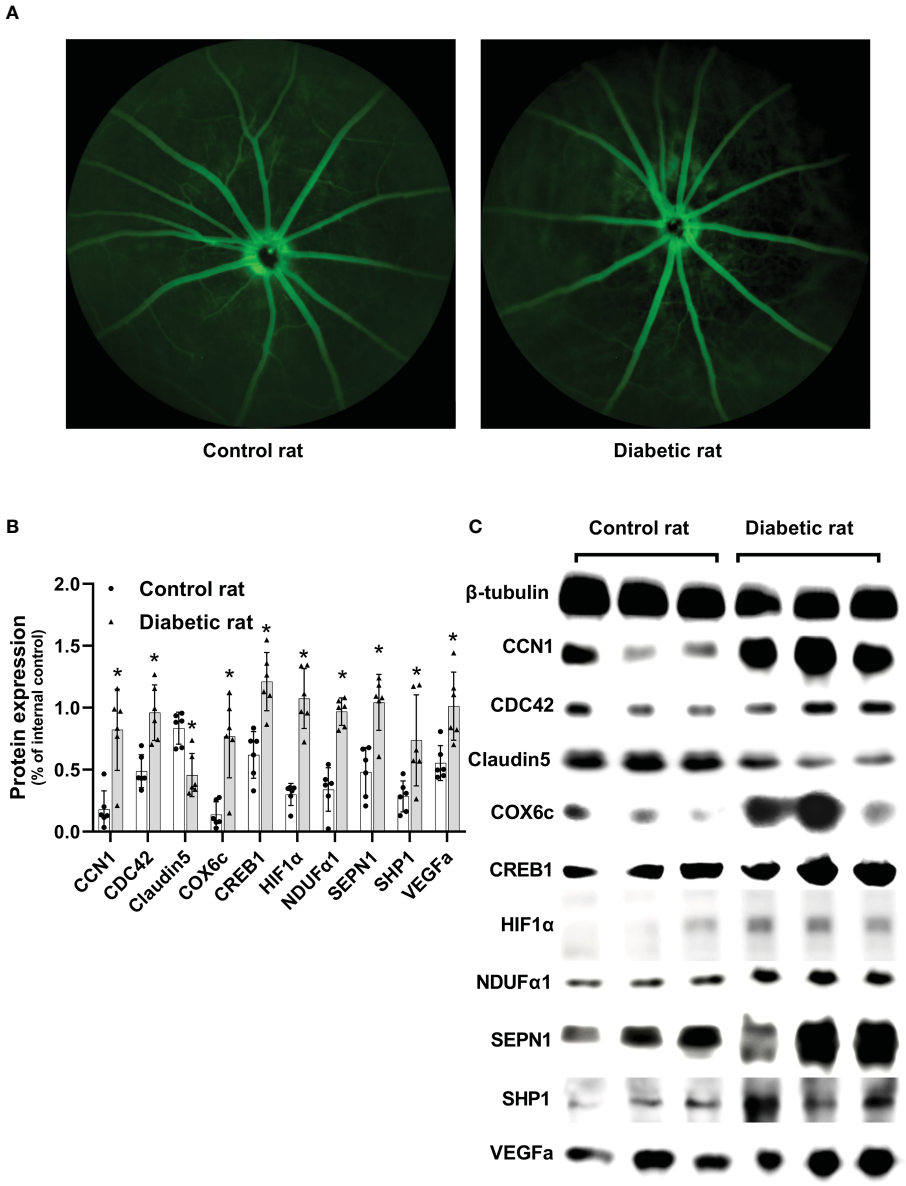

FIGURE 2
Differences in the retina between diabetic and non-diabetic rats. **(A)** Fundus fluorescein angiography of diabetic and non-diabetic rats. **(B)** Differences in protein expression levels between diabetic and non-diabetic rats. **(C)** Western blotting strip images of diabetic and non-diabetic rats. CCN1, Cellular Communication Network Factor 1; COX6c, cytochrome c oxidase subunit 6c; CREB1, Cyclic AMP-responsive element-binding protein1; HIF1α, Hypoxia-inducible factor 1α; NDUFα1, NADH dehydrogenase 1 alpha subcomplex; SEPN1, Selenoprotein N 1; SHP1, Protein-tyrosine phosphatase 1C; VEGFa, vascular endothelial growth factor a; Differences between control and diabetic rats were compared using the Mann–Whitney test, and the values of protein expression were analyzed using β-tubulin as the internal control; *p< 0.05, compared with controls.

in the retina and found that SHP1 was upregulated in diabetic rats, consistent with previous studies (37).

This study has some limitations. First, this was a cross-sectional study, and longitudinal cohorts are needed to demonstrate the predictive effect of CCN1 on DR. Second, we did not differentiate the severity of DR and, therefore, could not clarify the relation between CCN1 levels and the severity of DR. Third, our study included only subjects from Shanghai, China, and the generalizability of the findings remains to be proven. Fourth, we discussed the mechanism of CCN1 based only on sequencing and retinal protein results, which provides information for subsequent mechanistic studies that need to be verified in the future. Fifth, we did not test the level of CCN1 in the vitreous fluid and could not analyze the relationship between CCN1 vitreous levels and CCN1 blood levels.

In conclusion, we measured plasma CCN1 levels in the healthy controls, DM, and DR groups and found that CCN1 expression was significantly elevated in patients with DR, whereas there was no difference between healthy controls and DM groups. Additionally, it was observed that elevated CCN1 levels were risk factors for DR,

even after multifactorial correction. CCN1 was negatively correlated with BMI and positively correlated with the duration of diabetes and urea levels. Thus, CCN1 levels may reflect vascular damage caused by chronic hyperglycemia, rather than glycemic control. The results of mRNA sequencing analysis suggested that CCN1 levels in the blood could be upregulated due to hypoxia and may damage the blood-retinal barrier through oxidative stress and phosphorylation after interaction with integrin. Blood CCN1 levels may be a potential biomarker for DR and may be involved in the occurrence and development of DR.

Data availability statement

The datasets presented in this study can be found in online repositories. The names of the repository/repositories and accession number(s) can be found below: https://www.ncbi.nlm.nih.gov/geo/, GSE221521.

Ethics statement

The studies involving human participants were reviewed and approved by the Ethics Committee of Shanghai First People's Hospital. The patients/participants provided their written informed consent to participate in this study. The animal study was reviewed and approved by Shanghai First People's Hospital Animal Ethics Committee.

Author contributions

ZX contributes to the acquisition of data, analysis, and interpretation of data, and drafting the manuscript. SC, XQ, SL, YX and LL contributes to the acquisition of data and interpretation of data. HZ contributes to the conception, design, and final approval. All authors read and approved the manuscript.

Funding

This study was funded by Chinese National key research and development program (Project number 2021YFC2702100); Shanghai engineering research center of precise diagnosis and treatment of eye diseases, Shanghai, China (Project No. 19DZ2250100)

Acknowledgments

We would like to thank Editage (www.editage.cn) for English language editing.

Conflict of interest

The authors declare that the research was conducted in the absence of any commercial or financial relationships that could be construed as a potential conflict of interest.

Publisher's note

Supplementary material

The Supplementary Material for this article can be found online at: https://www.frontiersin.org/articles/10.3389/fendo.2023.1131993/full#supplementary-material

References

1. Zheng Y, He M, Congdon N. The worldwide epidemic of diabetic retinopathy. *Indian J Ophthalmol* (2012) 60(5):428–31. doi: 10.4103/0301-4738.100542

2. Kim KH, Won JH, Cheng N, Lau LF. The matricellular protein Ccn1 in tissue injury repair. *J Cell Commun Signal* (2018) 12(1):273–9. doi: 10.1007/s12079-018-0450-x

3. Lee S, Elaskandrany M, Lau LF, Lazzaro D, Grant MB, Chaqour B. Interplay between Ccn1 and Wnt5a in endothelial cells and pericytes determines the angiogenic outcome in a model of ischemic retinopathy. *Sci Rep* (2017) 7(1):1405. doi: 10.1038/s41598-017-01585-8

4. Hughes JM, Kuiper EJ, Klaassen I, Canning P, Stitt AW, Van Bezu J, et al. Advanced glycation end products cause increased ccn family and extracellular matrix gene expression in the diabetic rodent retina. *Diabetologia* (2007) 50(5):1089–98. doi: 10.1007/s00125-007-0621-4

5. You JJ, Yang CH, Chen MS, Yang CM. Cysteine-rich 61, a member of the ccn family, as a factor involved in the pathogenesis of proliferative diabetic retinopathy. *Invest Ophthalmol Vis Sci* (2009) 50(7):3447–55. doi: 10.1167/iovs.08-2603

6. Feng B, Xu G, Sun K, Duan K, Shi B, Zhang N. Association of serum Cyr61 levels with peripheral arterial disease in subjects with type 2 diabetes. *Cardiovasc Diabetol* (2020) 19(1):194. doi: 10.1186/s12933-020-01171-9

7. Ge K, Wu JJ, Qian L, Wu MJ, Wang FL, Xu B, et al. Bioinformatic analysis of the effect of type ii diabetes on skin wound healing. *Genet Mol Res* (2015) 14(2):4802–11. doi: 10.4238/2015.May.11.12

8. Sawai K, Mukoyama M, Mori K, Kasahara M, Koshikawa M, Yokoi H, et al. Expression of Ccn1 (Cyr61) in developing, normal, and diseased human kidney. *Am J Physiol Renal Physiol* (2007) 293(4):F1363–72. doi: 10.1152/ajprenal.00205.2007

9. Zhang X, Yu W, Dong F. Cysteine-rich 61 (Cyr61) is up-regulated in proliferative diabetic retinopathy. *Graefes Arch Clin Exp Ophthalmol* (2012) 250(5):661–8. doi: 10.1007/s00417-011-1882-7

10. Choi J, Lin A, Shrier E, Lau LF, Grant MB, Chaqour B. Degradome products of the matricellular protein Ccn1 as modulators of pathological angiogenesis in the retina. *J Biol Chem* (2013) 288(32):23075–89. doi: 10.1074/jbc.M113.475418

11. Zhou F, Zhang Y, Chen D, Su Z, Jin L, Wang L, et al. Potential role of Cyr61 induced degeneration of human Muller cells in diabetic retinopathy. *PloS One* (2014) 9 (10):e109418. doi: 10.1371/journal.pone.0109418

12. You JJ, Yang CM, Chen MS, Yang CH. Elevation of angiogenic factor cysteine-rich 61 levels in vitreous of patients with proliferative diabetic retinopathy. *Retina* (2012) 32(1):103–11. doi: 10.1097/IAE.0b013e318219e4ad

13. Li H, Li T, Wang H, He X, Li Y, Wen S, et al. Diabetes promotes retinal vascular endothelial cell injury by inducing Ccn1 expression. *Front Cardiovasc Med* (2021) 8:689318. doi: 10.3389/fcvm.2021.689318

14. Kuiper EJ, Hughes JM, Van Geest RJ, Vogels IM, Goldschmeding R, Van Noorden CJ, et al. Effect of vegf-a on expression of profibrotic growth factor and extracellular matrix genes in the retina. *Invest Ophthalmol Vis Sci* (2007) 48(9):4267–76. doi: 10.1167/iovs.06-0804

15. Sun L, Huang T, Xu W, Sun J, Lv Y, Wang Y. Advanced glycation end products promote vegf expression and thus choroidal neovascularization *Via* Cyr61-Pi3k/Akt signaling pathway. *Sci Rep* (2017) 7(1):14925. doi: 10.1038/s41598-017-14015-6

16. Di Y, Zhang Y, Nie Q, Chen X. Ccn1/Cyr61-Pi3k/Akt signaling promotes retinal neovascularization in oxygen-induced retinopathy. *Int J Mol Med* (2015) 36(6):1507–18. doi: 10.3892/ijmm.2015.2371

17. Di Y, Zhang Y, Yang H, Wang A, Chen X. The mechanism of Ccn1-enhanced retinal neovascularization in oxygen-induced retinopathy through Pi3k/Akt-vegf signaling pathway. *Drug Des Devel Ther* (2015) 9:2463–73. doi: 10.2147/DDDT.S79782

18. Wang N, Xu X, Zou H, Zhu J, Wang W, Ho PC. The status of diabetic retinopathy and diabetic macular edema in patients with type 2 diabetes: a survey from beixinjing district of shanghai city in China. *Ophthalmologica* (2008) 222(1):32–6. doi: 10.1159/000109276

19. Peng J, Zou H, Wang W, Fu J, Shen B, Bai X, et al. Implementation and first-year screening results of an ocular telehealth system for diabetic retinopathy in China. *BMC Health Serv Res* (2011) 11:250. doi: 10.1186/1472-6963-11-250

20. Lin Q, Jia Y, Li T, Wang S, Xu X, Xu Y, et al. Optic disc morphology and peripapillary atrophic changes in diabetic children and adults without diabetic retinopathy or visual impairment. *Acta Ophthalmol* (2022) 100(1):e157–e66. doi: 10.1111/aos.14885

21. Kuzuya T. Early diagnosis, early treatment and the new diagnostic criteria of diabetes mellitus. *Br J Nutr* (2000) 84 Suppl 2:S177–81. doi: 10.1079/096582197388644

22. Wilkinson CP, Ferris FL3rd, Klein RE, Lee PP, Agardh CD, Davis M, et al. Proposed international clinical diabetic retinopathy and diabetic macular edema disease severity scales. *Ophthalmology* (2003) 110(9):1677–82. doi: 10.1016/s0161-6420(03)00475-5

23. Winzap P, Davies A, Klingenberg R, Obeid S, Roffi M, Mach F, et al. Diabetes and baseline glucose are associated with inflammation, left ventricular function and short- and long-term outcome in acute coronary syndromes: role of the novel biomarker cyr 61. *Cardiovasc Diabetol* (2019) 18(1):142. doi: 10.1186/s12933-019-0946-6

24. Klingenberg R, Aghlmandi S, Liebetrau C, Räber L, Gencer B, Nanchen D, et al. Cysteine-rich angiogenic inducer 61 (Cyr61): a novel soluble biomarker of acute myocardial injury improves risk stratification after acute coronary syndromes. *Eur Heart J* (2017) 38(47):3493–502. doi: 10.1093/eurheartj/ehx640

25. Liu C, Cao Y, He X, Zhang C, Liu J, Zhang L, et al. Association of Cyr61-Cysteine-Rich protein 61 and short-term mortality in patients with acute heart failure and coronary heart disease. *biomark Med* (2019) 13(18):1589–97. doi: 10.2217/bmm-2019-0111

26. You JJ, Yang CM, Chen MS, Yang CH. Regulation of Cyr61/Ccn1 expression by hypoxia through cooperation of c-Jun/Ap-1 and hif-1alpha in retinal vascular endothelial cells. *Exp Eye Res* (2010) 91(6):825–36. doi: 10.1016/j.exer.2010.10.006

27. Kunz M, Moeller S, Koczan D, Lorenz P, Wenger RH, Glocker MO, et al. Mechanisms of hypoxic gene regulation of angiogenesis factor Cyr61 in melanoma cells. *J Biol Chem* (2003) 278(46):45651–60. doi: 10.1074/jbc.M301373200

28. Li L, Wang M, Mei Z, Cao W, Yang Y, Wang Y, et al. Lncrnas Hif1a-As2 facilitates the up-regulation of hif-1α by sponging to mir-153-3p, whereby promoting angiogenesis in huvecs in hypoxia. *BioMed Pharmacother* (2017) 96:165–72. doi: 10.1016/j.biopha.2017.09.113

29. Chen D, Wu L, Liu L, Gong Q, Zheng J, Peng C, et al. Comparison of Hif1a–As1 and Hif1a–As2 in regulating Hif–1α and the osteogenic differentiation of pdlcs under hypoxia. *Int J Mol Med* (2017) 40(5):1529–36. doi: 10.3892/ijmm.2017.3138

30. Hanna M, Liu H, Amir J, Sun Y, Morris SW, Siddiqui MA, et al. Mechanical regulation of the proangiogenic factor Ccn1/Cyr61 gene requires the combined activities of mrtf-a and creb-binding protein histone acetyltransferase. *J Biol Chem* (2009) 284(34):23125–36. doi: 10.1074/jbc.M109.019059

31. Han JS, Macarak E, Rosenbloom J, Chung KC, Chaqour B. Regulation of Cyr61/Ccn1 gene expression through rhoa gtpase and P38mapk signaling pathways. *Eur J Biochem* (2003) 270(16):3408–21. doi: 10.1046/j.1432-1033.2003.03723.x

32. Walsh CT, Radeff-Huang J, Matteo R, Hsiao A, Subramaniam S, Stupack D, et al. Thrombin receptor and rhoa mediate cell proliferation through integrins and cysteine-rich protein 61. *FASEB J* (2008) 22(11):4011–21. doi: 10.1096/fj.08-113266

33. Dobroff AS, Wang H, Melnikova VO, Villares GJ, Zigler M, Huang L, et al. Silencing camp-response element-binding protein (Creb) identifies Cyr61 as a tumor suppressor gene in melanoma. *J Biol Chem* (2009) 284(38):26194–206. doi: 10.1074/jbc.M109.019836

34. Johnston H, Kneer J, Chackalaparampil I, Yaciuk P, Chrivia J. Identification of a novel Snf2/Swi2 protein family member, srcap, which interacts with creb-binding protein. *J Biol Chem* (1999) 274(23):16370–6. doi: 10.1074/jbc.274.23.16370

35. Liu Z, Vong QP, Liu C, Zheng Y. Borg5 is required for angiogenesis by regulating persistent directional migration of the cardiac microvascular endothelial cells. *Mol Biol Cell* (2014) 25(6):841–51. doi: 10.1091/mbc.E13-09-0543

36. Leu SJ, Lam SC, Lau LF. Pro-angiogenic activities of Cyr61 (Ccn1) mediated through integrins Alphavbeta3 and Alpha6beta1 in human umbilical vein endothelial cells. *J Biol Chem* (2002) 277(48):46248–55. doi: 10.1074/jbc.M209288200

37. Liu H, Yang R, Tinner B, Choudhry A, Schutze N, Chaqour B. Cysteine-rich protein 61 and connective tissue growth factor induce deadhesion and anoikis of retinal pericytes. *Endocrinology* (2008) 149(4):1666–77. doi: 10.1210/en.2007-1415

frontiers | Frontiers in Endocrinology

TYPE Original Research
PUBLISHED 03 July 2023
DOI 10.3389/fendo.2023.1160615

OPEN ACCESS

EDITED BY
Rajashekhar Gangaraju,
University of Tennessee Health Science Center (UTHSC), United States

REVIEWED BY
Du Shaolin,
Dongguan Tungwah Hospital, China
Salvatore Di Lauro,
Hospital Clínico Universitario de Valladolid, Spain

*CORRESPONDENCE
Xu Mingchao
xumingchao036@163.com

RECEIVED 07 February 2023
ACCEPTED 13 June 2023
PUBLISHED 03 July 2023

CITATION
Xiaodong L, Xuejun X, Xiaojuan S, Yu H and Mingchao X (2023) Characterization of peripheral blood inflammatory indicators and OCT imaging biological markers in diabetic retinopathy with or without nephropathy.
Front. Endocrinol. 14:1160615.
doi: 10.3389/fendo.2023.1160615

Characterization of peripheral blood inflammatory indicators and OCT imaging biological markers in diabetic retinopathy with or without nephropathy

Li Xiaodong[1,2,3], Xie Xuejun[2], Su Xiaojuan[3], He Yu[4] and Xu Mingchao[5]*

[1]Department of Ophthalmology, The First Affiliated Hospital of Guizhou University of Chinese Medicine, Chengdu, China, [2]Department of Ophthalmology, Hospital of Chengdu University of Traditional Chinese Medicine, Chengdu, China, [3]Chengdu University of Traditional Chinese Medicine, Chengdu, China, [4]Department of Ophthalmology, Chengdu First People's Hospital, Chengdu, China, [5]Traditional Chinese Medicine Hospital of Meishan, Meishan, China

Objective: To observe the distribution characteristics of peripheral blood inflammatory indexes and retinal macular area optical coherence tomography (OCT) imaging biomarkers in patients with diabetic retinopathy (DR) with or without diabetic nephropathy (DN), in order to seek clinical biomarkers that can predict the development of DR and DN.

Methods: A total of 169 inpatients with DR who visited the ophthalmology department of the Affiliated Hospital of Chengdu University of Traditional Chinese Medicine from October 2020 to June 2022 and had complete clinical data were collected, and the patients with DR were divided into two major groups, DR and DR/DN, according to whether they had DN, and then further divided into four subgroups, Non-proliferative DR(NPDR), proliferative DR(PDR), NPDR/DN and PDR/DN, according to the stage of DR. The distribution characteristics of peripheral blood inflammatory indexes [Neutrophil to lymphocyte ratio(NLR) and Platelet to neutrophil ratio(PLR)], renal function indexes [Cystatin-C(CYS-C), Creatinine(Crea), Uric acid(UA)and Urinary albumin to creatinine ratio(UACR)] and OCT imaging indexes [Hyperreflective foci(HRF), Disorgnization of retinal inner layers(DRIL), Outer retinal tubulations(ORTs), Central retinal thickness(CRT), Retinal nerve fiber layer(RNFL) and Ganglion cell layer(GCL)] were analyzed between the above subgroups.

Results: There was no difference between DR and DR/DN groups in terms of gender, family history of diabetes, duration of diabetes and Body mass index(BMI) (P>0.05), the mean age of the DR/DN group was significantly lower than that of the DR group (P<0.05), and the proportion of the DR/DN group with a history of hypertension was significantly higher than that of the DR group (P<0.05); there was no significant difference in hemoglobin A1C(HbA1c) between DR and DR/DN groups (P>0.05). (P>0.05), Hemoglobin(HGB) was significantly higher in the DR group than in the DR/DN group (P <0.05), NLR, PLR, Crea, UA and CYS-C were significantly higher in the DR/DN group than in the DR group (P<0.05); there was no significant difference in the comparison of HRF, DRIL, ORTs positive rate and

CRT between the DR and DR/DN groups (P>0.05). RNFL and GCL thickness were significantly lower in the DR/DN group than in the DR group (P<0.05); history of hypertension (OR=2.759), NLR (OR=1.316), PLR (OR=1.009), Crea (OR=1.018), UA (OR=1.004), CYS-C (OR=3.742) were the independent (OR=0.951), age (OR=0.951), HGB (OR=0.976), RNFL (OR=0.909) and GCL (OR=0.945) were independent protective factors for DR/DN; RNFL (OR=0.899) and GCL (OR=0.935) were independent protective factors for NPDR/DN, RNFL (OR=0.852) and GCL (OR=0.928) were independent protective factors for PDR/DN. ROC curve analysis showed that the area under the curve (AUC) for CYS-C, PLR, Crea, UA and the combination of the four indicators to predict DR/DN were 0.717, 0.625, 0.647, 0.616 and 0.717, respectively.

Conclusions: (1) Low age combined with hypertension HGB, NLR, PLR, CYS-C, Crea and UA may be serum biological markers for predicting DN in DR; meanwhile, PLR, CYS-C, Crea, UA and the combination of the four indicators can be used for risk assessment and adjunctive diagnosis of DN in DR combined with hypertension. (2) The RNFL and GCL thickness in the temporal aspect of the central macular sulcus may be imaging biological markers for predicting DN in DR; meanwhile, GCL thickness may have important value for risk prediction and diagnosis of DN in combination with DR.

KEYWORDS

diabetic retinopathy, diabetic nephropathy, neutrophil-to-lymphocyte ratio (NLR), platelet-to-lymphocyte ratio (PLR), optical coherence tomography (OCT), inflammation

1 Introduction

Diabetic retinopathy (DR) and diabetic nephropathy (DN) are common diabetic microangiopathies, and their similar pathogenesis and physiological characteristics determine their insidious onset, and they are prone to progression to irreversible visual damage and end-stage renal organopathy. Therefore, early diagnosis and timely intervention are crucial for the treatment outcome and prognosis of DR and DN. The gold standard for clinical DN diagnosis is “renal tissue biopsy”. In contrast, the diagnosis of clinical DR can be accomplished by non-invasive and simple fundus examination such as optical coherence tomography (OCT), OCT Angiography(OCTA) and fundus photography combined with clinical laboratory indicators. Studies have shown that about 26.7% of patients with type 2 diabetes have both DR and DN (1). At present, some studies have confirmed the feasibility and reliability of DR in combination with relevant clinical examinations to assist in the diagnosis of DN, such as retinal vessel curvature, diameter, branching angle and coefficient, and vascular geometry parameters such as aspect ratio (2). In addition, clinical indicators including blood lipids (3), blood bilirubin (4) and urine microalbumin (5). and urinary haptoglobin (6). and other laboratory tests. In this clinical study, we analyzed the clinical characteristics of peripheral blood inflammatory indexes, renal function indexes and retinal macular OCT biological indexes in patients with DR and DR combined with DN, explored the risk factors and protective factors of DR combined with DN, and evaluated the predictive value of DR combined with the above influencing factors for DN, in order to provide a new reference basis for the early clinical diagnosis and treatment of DN.

2 Research materials and methods

2.1 Source

this retrospective study was conducted on outpatients or inpatients with type 2 diabetes who attended the ophthalmology department of the Affiliated Hospital of Chengdu University of Chinese Medicine from October 2020 to June 2022 and had complete clinical information.

2.2 Inclusion criteria

(1). inpatients over 18 years of age with confirmed type 2 diabetic retinopathy with or without diabetic nephropathy.

(2). Information on the clinical consultation process, relevant laboratory tests and specialist findings of all included patients must be complete.

(3). Patients who met all the above criteria were included in this clinical study.

2.3 Exclusion criteria

(1). Patients with other special types of diabetes such as type 1 diabetes and gestational diabetes.

(2). Combined with severe acute complications of diabetes, such as diabetic ketoacidosis and hyperosmolar hyperglycemic states.

(3). Combined with severe organic liver and lung pathologies, cardiovascular and cerebrovascular complications, malignant tumors and hematologic diseases.

(4). Primary organic renal disease secondary to other immune, infection or drug toxicity related renal diseases, such as systemic lupus erythematosus nephritis.

(5). History of surgery in the last three months, history of acute infection or stress trauma, history of taking antibiotics, antivirals, hormones and immunosuppressive drugs that affect the laboratory results of peripheral venous blood.

(6). Combined with other ocular diseases, such as keratoconjunctivitis, glaucoma, uveitis, retinal arteriovenous obstruction, and other diseases.

(7). Those meeting any of the above may not be included in this clinical study.

(8). Ocular diseases that affect the discrimination and measurement of retinal structure levels in the macula in OCT, such as severe nuclear cataract.

(9). Extensive vitreous hemorrhage, proliferative vitreoretinal lesions in the macula anterior and macular regions of the retina, etc. (Note: This criterion is applicable to the determination and measurement of OCT biomarkers)

(10). Received vitreoretinal-related ophthalmic treatment, surgery such as vitrectomy + peel + silicone oil filling, total retinal laser photocoagulation and anti-VEGF drug vitreous cavity drug injection in the 3-6 months prior to admission. (Note: This criterion applies to the determination and measurement of OCT biomarkers)

2.4 Diagnostic criteria

(1). Diagnostic criteria for type 2 diabetes mellitus: according to the diagnostic criteria published by WHO (2019), the diagnosis is made by meeting any one of the following three: I. Typical diabetic symptoms (such as the presence of polyuria, polydipsia, polyphagia and unexplained weight loss) + random venous plasma glucose concentration ≥ 11.1 mmol/l; II. Fasting glucose concentration ≥7.0mmol/l (whole blood ≥6.1mmol/l); III. Two-hour glucose concentration ≥11.1mmol/l in OGTT test.

(2). Diagnostic criteria for diabetic retinopathy: I. Meet the above diagnostic criteria for type 2 diabetes and have a clear history of type 2 diabetes; II. Fundus signs refer to the international clinical grading criteria for diabetic retinopathy (as shown in Table 1).

(3). Diagnostic criteria for diabetic nephropathy: I. Meet the above diagnostic criteria for type 2 diabetes mellitus with a clear history of type 2 diabetes mellitus; II. According to Urinary albumin to creatinine ratio(UACR)>30mg/g and/or eGFR<60ml-min-1-(1.732)-1, and ask the nephrologist to consult to exclude other factors causing renal disease.

3 Research methodology

The clinical data of all patients were collected independently by two trained ophthalmology residents through our electronic medical record system, and the fundus imaging data were collected through the database stored in Spectralis HRA+OCT by two trained ophthalmology residents who read and measured the films, and the controversial part of the data was discussed and decided with the third supervising physician.

TABLE 1 International clinical grading criteria for diabetic retinopathy (7).

Grading	Disease severity	Lesions seen in the fundus after pupil dilatation
Level 1	No obvious retinal lesions	No abnormalities
Level 2	Mild NPDR	Microaneurysm only
Level 3	Moderate NPDR	Presence of milder than severe non-proliferative diabetic retinopathy except for microaneurysms
Level 4	Heavy NPDR	Presence of any of the following, but not yet proliferative diabetic retinopathy. a. More than 20 intraretinal hemorrhages in all four quadrants b. Venous bead-like changes in more than two quadrants c. Significant intraretinal microvascular abnormalities in more than one quadrant (IRMA sign)
Level 5	PDR	Any of the following changes occur. a. Neovascularization b. Vitreous, retinal hemorrhage or preretinal hemorrhage

3.1 General information of patients

including age, sex, weight, height, duration of diabetes and family history, history of hypertension and other general information. BMI was obtained by calculating the formula weight/height^2 in kg/m^2.

3.2 Laboratory test indexes

Hemoglobin A1C(HbA1c), Hemoglobin(HGB), Neutrophil to lymphocyte ratio(NLR), Platelet to neutrophil ratio(PLR), Cystatin-C(CYS-C), Creatinine(Crea), Uric acid(UA)and Urinary albumin to creatinine ratio(UACR). The above laboratory test results were provided by the Laboratory Department of our hospital.

3.3 OCT fundus imaging indexes

All patients were examined by Spectralis HRA+OCT completed by Heidelberg, Germany. Horizontal axial and vertical axial scans were performed *via* the macula centrale, and Hyperreflective foci (HRF), Disorgnization of retinal inner layers(DRIL), Outer retinal tubulations(ORTs), Central retinal thickness(CRT), and Ganglion cell layer(GCL) thickness indexes within 2000 μm from the macula centrale in the OCT images of the horizontal axial scans were selected and measured for recording. Retinal nerve fiber layer (RNFL) and GCL thickness indicators. All OCT examinations and reporting operations were performed by our attending ophthalmologist or associate ophthalmologist.

(1) HRF: isolated and well-defined borders with reflective intensity stronger than or equal to that of the RPE layer, without artifacts and with a diameter of 20-50 μm round or oval highly reflective particles are visible in each retinal layer in macular OCT (8); manual counting of HRF within 2000 μm from the central macular recess.

(2) DRIL: structural disorder or blurred borders at all levels of the inner retina visible in macular OCT (9); manual measurement of DRIL within 2000 μm from the central macular recess was determined.

(3) ORTs: the ring-shaped or oval-shaped border of highly reflective signal around the low-reflective signal located in the outer nuclear layer of the retina is visible in macular OCT (10) (2) The ORTs were identified by human measurement within 2000 μm from the central macular recess

(4) CRT: the thickness of the inner retinal boundary membrane to the RPE layer at the central recess in macular OCT; determined by the machine's own software measurement.

(5) RNFL: the second layer of retinal hyperreflective band in macular OCT, the thickness of macular nasal hyperreflective band is thicker the closer to the optic disc, the thickness of macular temporal hyperreflective band is significantly lower than the nasal side, and the closer to the periphery, the thinner it is; RNFL thickness is determined by the machine's own software measurement, and the thickness value at 2000 μm from the temporal side of the central macula is selected for manual correction measurement according to the specific situation.

(6) GCL: the low reflection signal band under RNFL in macular OCT; GCL thickness was determined by the machine's own software measurement, and the manual correction measurement was performed according to the specific situation, and the thickness value at 2000 μm from the temporal side of the central macular concavity was selected.

3.4 Fluorescein fundus angiography examination index

FFA examination of all patients was completed by Spectralis HRA+OCT from Heidelberg, Germany, and the specific staging of DR in both eyes of patients was determined according to FFA images and reports. All patients' FFA reports were confirmed by professors of our ophthalmology department.

3.5 Study grouping

All patients meeting the criteria of this study were divided into 2 major groups, DR and DR/DN, with DR group as the control group and DR/DN as the observation group; on this basis, they were further subdivided into 4 subgroups, NPDR, PDR, NPDR/DN and PDR/DN, according to the stage of DR, with NPDR as the control group and PDR, NPDR/DN and PDR/DN groups as the observation group.

3.6 Statistical analysis

IBM SPSS26.0 was applied for data analysis. Count data conforming to normal distribution were expressed by ($x \pm s$), statistics by independent samples t-test, one-way ANOVA, multiple comparisons between groups by LSD method, data not conforming to normal distribution were expressed by M(Q1,Q2), multi-group statistics by Kruskal-wallis H-test, two-group and between-group Mann-Whitney was used for comparison; measurement data were statistically analyzed by chi-square test and Fisher exact test. The risk factors were analyzed by multi-factor logistic regression analysis; the ROC curves were used to analyze the critical value of each factor in predicting the level of diagnosed disease; the correlation between the factors was analyzed by Pearson correlation and Spearman correlation analysis, and $P<0.05$ indicated that the difference was statistically significant.

4 Results

4.1 Basic data

A total of 169 patients were included in this study, including 119 patients with DR and 50 patients with DR combined with DN, with an age range of 26-82 years and a mean age of 56.16 ± 10.80 years, and 96 males, accounting for 56.8% of the cases.

4.2 The results of peripheral blood laboratory tests in patients with DR and DR/DN in this study

4.2.1 General information

As shown in Table 2, the proportion of hypertension history in the DR/DN group was significantly higher than that in the DR group, and the difference was statistically significant (P<0.05), and the mean age in the DR/DN group was significantly lower than that in the DR group, and the difference was statistically significant (P<0.01); although the proportion of family history of diabetes in the DR/DN group was also significantly higher than that in the DR group, the difference was not statistically significant (P<0.05). In addition, the differences in gender, duration of diabetes and BMI between the DR group and the DR/DN group were not statistically significant (P>0.05). As shown in Table 3, after re-grouping according to DR staging, the mean age showed a significant trend of NPDR > PDR > NPDR/DN > PDR/DN, and the difference was statistically significant (P< 0.01), and the proportion of hypertension history showed a trend of PDR/DN > NPDR/DN > PDR > NPDR, but the difference was not statistically significant (P 0.01). Their differences in gender, family history of diabetes, duration of diabetes, and BMI were not statistically significant (P>0.05).

4.2.2 Laboratory indices

The results of HbA1c, HGB, NLR, PLR, Crea, UA and CYS-C in the DR and DR/DN groups are shown in Table 4, the level of HbA1c in the DR group was slightly higher than that in the DR/DN group, the difference was not statistically significant (P>0.05), the level of HGB in the DR group was significantly higher than that in the DR/DN group, the difference was statistically The differences were statistically significant (P<0.05), and the peripheral blood inflammatory indexes NLR and PLR and renal function indexes Crea, UA and CYS-C in the DR group were significantly lower than those in the DR/DN group, and the differences were statistically significant (P<0.05), as shown in Figure 1.

The results of laboratory test indexes in the four groups of NPDR, PDR, NPDR/DN and PDR/DN are shown in Table 5, and the differences in HGB, PLR, Crea and CYS-C levels among the four groups were statistically significant (P<0.05). The differences between the first 3 groups and the PDR/DN group were statistically significant (P<0.05); PLR levels increased in the order of PDR<NPDR<NPDR< NPDR/DN<PDR/DN, and the differences between the first 2 groups and the PDR/DN group were statistically significant (P < 0.05); Crea and CYS-C levels increased in the order of NPDR< PDR < NPDR/DN < PDR/DN, and the differences between the first 2 groups and the PDR/DN group were statistically significant (P<0.05). The differences between the first two groups and the PDR/DN group were statistically significant (P<0.05); the levels of CYS-C increased in the order of NPDR< PDR < NPDR < NPDR/DN < PDR/DN, and the differences between the NPDR group and the other three groups and the PDR group and the PDR/DN group were statistically significant (P<0.05)The differences in HbA1c, NLR and UA levels between the four groups were not statistically significant (P>0.05), with HbA1c levels decreasing in the order of NPDR/DN > PDR > NPDR > PDR/DN, and the differences between the four groups were statistically significant (P> 0.05). In addition, the levels of NLR and UA increased in the order of PDR < NPDR < NPDR/DN < PDR/DN, and the differences between the first two groups were statistically significant (P<0.05) compared with the PDR/DN group, as shown in Figure 2.

4.2.3 Factors influencing DR/DN

With DR/DN as the dependent variable and age, history of HBP, HGB, NLR, PLR, Crea, UA and CYS-C with statistically significant differences (P<0.05) as independent variables, the results of multifactorial logistic regression analysis showed that age and HGB were independent protective factors for DR/DN, while history of HBP, NLR, PLR, Crea, UA and CYS-C were independent risk factors for DR/DN (P<0.05). See Table 6.

TABLE 2 Comparison of general information between DR and DR/DN groups.

	DR	DR/DN	χ2/T	P
Male/Female (example)	63/56	33/17	2.03	0.15
Family history of DM (%)	25.21%	38%	4.83	0.18
History of HBP (%)	33.61%	52%	4.15	0.04
Duration of DM disease (years)	10 (7,18)	10 (7,16)	-0.16	0.87
BMI(Kg/m)^2	24.27 ± 3.34	23.58 ± 2.96	1.35	0.18
Age (years)	57.8 ± 10.52	52.2 ± 10.51	3.17	0.002

TABLE 3 Comparison of general information between subgroups.

	NPDR	PDR	NPDR/DN	PDR/DN	χ2/T	P
Male/Female (example)	41/29	22/27	22/9	11/8	5.46	0.14
Family history of DM (%)	27.14%	22.45%	38.71%	36.84%	3.13	0.37
History of HBP (%)	31.43%	36.73%	45.16%	63.16%	6.95	0.07
Duration of DM disease (years)	10(6.5,18)	10 (7.5,17.5)	13 (10,20)	8 (6,13)	4.58	0.21
BMI(Kg/m)^2	24.15 ± 2.78	24.44 ± 4.03	23.19 ± 2.63	24.23 ± 3.41	1.01	0.39
Age (years)	58.67 ± 10.66	56.57 ± 10.32	55.48 ± 9.82	46.95 ± 9.62	6.52	<0.001

4.2.4 Factors influencing PDR, NPDR/DN and PDR/DN

PDR, NPDR/DN and PDR/DN were used as dependent variables, age, history of HBP, HGB, NLR, PLR, Crea, UA and CYS-C were used as independent variables, and the results of multifactorial logistic regression showed that CYS-C was an independent risk factor for PDR, NPDR/DN and PDR/DN independent risk factors, and UACR was a PDR/DN independent risk factor. As shown in Table 7.

4.2.5 Laboratory tests with predictive value for DR/DN

CYS-C, PLR, Crea, and UA are meaningful for the diagnosis of DR/DN, among which the best diagnostic efficacy is CYS-C. When the value of CYS-C is greater than 1.17, the risk level of DR complicating DN increases significantly. In addition, CYS-C, Crea and UACR were significant for the diagnosis of PDR with DN, among which the best diagnostic efficacy was still CYS-C, and when the CYS-C value was greater than 1.335, the risk level of PDR with DN increased significantly. As shown in Table 8.

4.2.6 Correlation analysis of laboratory test indicators with DR and DN staging

The results of correlation analysis showed that CYS-C, UACR, and DN staging were significantly positively correlated with DR staging (P<0.05), age and HGB were significantly negatively correlated with DN staging (P<0.05), and NLR, PLR, Crea, UA, UACR, and CYS-C were significantly positively correlated with DN staging (P< 0.05). In addition, the correlations between each laboratory test index are shown in Table 9.

4.3 Study the predictive value of DR for DN based on macular OCT imaging index

A total of 213 eyes of 128 patients with DR and DR/DN were included in this part, including 152 eyes with DR and 61 eyes with DR/DN, with a mean age of 55.27 ± 10.30 years and 58.59% of males.

4.3.1 Comparison of OCT imaging indexes between DR and DR/DN groups

As shown in Table 10, the positive rates of HRF, DRIL, ORTs and CRT were higher in the DR/DN group than in the DR group, but the comparative differences were not statistically significant (P>0.05), and the thicknesses of RNFL and GCL in the temporal aspect of the central macular sulcus were significantly lower in the DR/DN group than in the DR group, and the comparative differences were statistically significant (P<0.05). As shown in Table 11, the HRF, DRIL positivity rate and GCL thickness were significantly different between the four groups of NPDR, PDR, NPDR/DN, and PDR/DN (P<0.05). See Figure 3 for details.

4.3.2 Fundus imaging indices of DR/DN

Multi-factor Logistic regression analysis was performed successively with DR/DN as the dependent variable and RNFL and GCL thickness as the independent variables, and the results showed that RNFL and GCL thickness were independent protective factors for DR/DN. Subgroup analysis studies were conducted with PDR, NPDR/DN and PDR/DN as dependent variables and HRF, DRIL, RNFL and GCL thickness as independent variables in multifactorial logistic regression analysis, respectively, and the

TABLE 4 Comparison of laboratory test indices between DR and DR/DN groups.

	DR	DR/DN	T/H/Z	P
HbA1c	8.0 (7.0,9.3)	7.5 (6.5,9.7)	-0.87	0.38
HGB	128.73 ± 18.43	120.14 ± 20.60	0.91	0.02
NLR	2.12 (1.65,2.83)	2.63 (1.64,3.88)	-1.93	0.04
PLR	115.27 ± 46.27	145.45 ± 75.02	10.134	0.002
Crea	67.60 (55.90,80.50)	84.10 (60.38,117.78)	-2.89	0.004
UA	354.03 ± 89.79	389.96 ± 99.89	-2.32	0.02
CYS-C	1.11 (0.88,1.29)	1.34 (1.14,2.01)	-4.44	<0.001

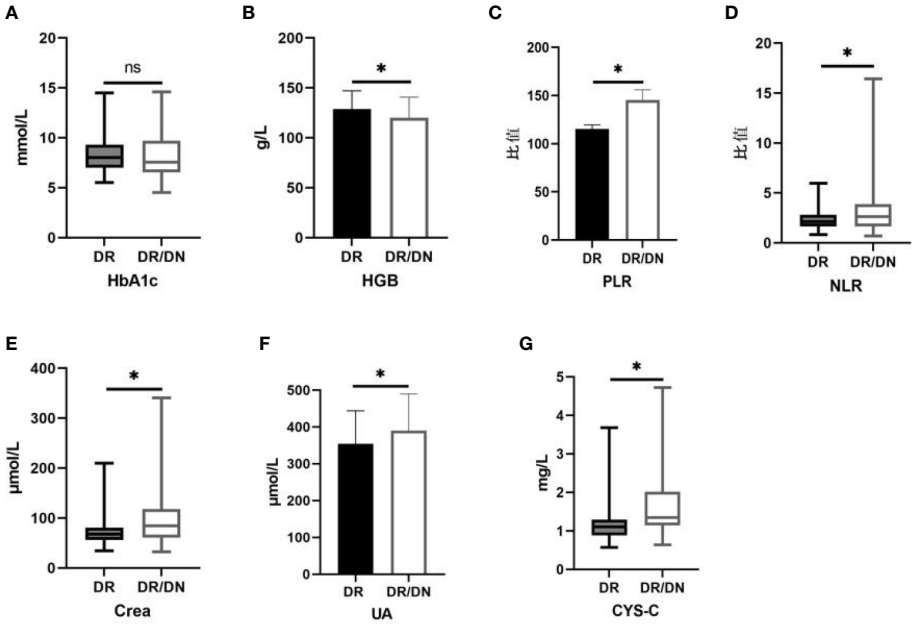

FIGURE 1
Histogram comparing laboratory test indicators between DR and DR/DN groups. (*represents $p<0.05$, indicating statistical significance). **(A-G)** Comparison of HbA1c, HGB, PLR, NLR, Crea, UA, and CYS-C results between the DR And DR/DN groups.

results showed that HRF and DRIL were independent risk factors for PDR, while RNFL and GCL thickness were independent protective factors for NPDR/DN and PDR/DN. factors. The results are shown in Table 12.

4.3.3 Diagnostic value of RNFL and GCL thickness for DR/DN

GCL thickness reduction has value for the diagnosis of DR/DN, and when the GCL thickness is below 41.5 μm, the risk of DR with concurrent DN is higher; further study found that when the GCL thickness is below 42.5 μm, the risk of NPDR with concurrent DN is higher, and when the GCL thickness is below 40.5 μm, then the risk of PDR with concurrent DN is higher. RNFL thickness reduction has value for the diagnosis of PDR/DN diagnosis has some value, when RNFL thickness is lower than 20.5 μm, then PDR and found DN risk is higher. See Table 13.

4.3.4 Correlation between OCT imaging indices and DR and DN staging

The results of correlation analysis showed that HRF, ORTs, DRIL, and DN staging were significantly positively correlated with DR staging ($P<0.05$), and no significant correlation was seen between each imaging index and DN staging ($P>0.05$), and the correlation between each imaging index is shown in Table 14.

5 Discussion

5.1 Young age and hypertension are risk factors for DR Complicated with DN

This study showed that the mean age of patients in the DR/DN group was significantly lower than that of the DR group, and

TABLE 5 Comparison of laboratory test indicators between subgroups.

	NPDR	PDR	NPDR/DN	PDR/DN	T/H/Z	*P*
HbA1c	7.8 (6.8,10.3)	8.1 (7.0,8.8)	8.3 (7.0,10.6)	7.0 (5.2,8.6)	4.46	0.22
HGB	129.84 ± 21.12	127.14 ± 13.77	126.16 ± 18.35	110.32 ± 20.74	5.50	<0.001
NLR	2.25 (1.58, 3.23)	1.90 (1.67,2.76)	2.33(1.84,3.23)	3.23 (1.64,4.26)	4.93	0.18
PLR	116.62 ± 48.77	113.34 ± 42.87	134.29 ± 61.17	163.65 ± 92.31	4.52	0.005
Crea	66.60 (54.8,79.1)	72.40 (56.95,83.60)	75.60 (54.70,105.6)	106.1 (61.4,132.0)	13.78	0.01
UA	356.67 ± 101.96	350.24 ± 69.64	378.39 ± 89.74	408.84 ± 114.59	2.22	0.08
CYS-C	1.01 (0.84, 1.22)	1.16 (1.01,1.40)	1.25 (1.10,1.59)	1.47 (1.23,2.68)	31.09	<0.001
UACR			655.8 (143.3,871.3)	1717 (670,2805.35)	-2.57	0.01

10.3389/fendo.2023.1160615

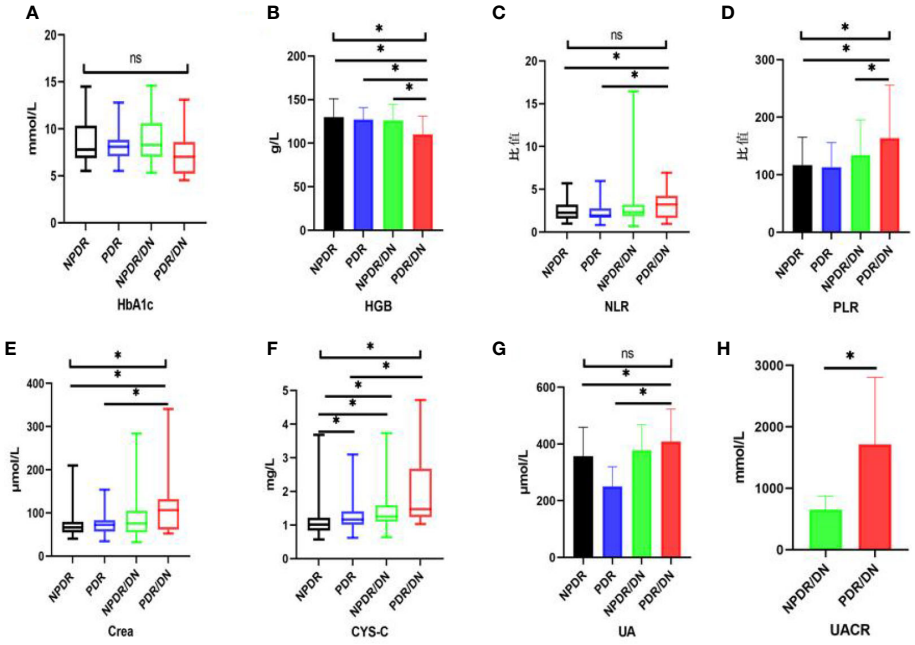

FIGURE 2
Histogram comparing laboratory test indicators between subgroups. (*represents p<0.05, indicating statistical significance). **(A-G)** Comparison of HbA1c, HGB, NLR, PLR, Crea, CYS-C and UA results between NPDR, PDR, NPDR/DN and PDR/DN groups; **(H)** Comparison of UACR results between NPDR/DN and PDR/DN groups.

subgroup analysis showed that the mean age of the PDR/DN group was below 50 years old, and the age of the PDR, NPDR/DN and PDR/DN groups showed a significant trend toward younger age compared with the NPDR group, and the results of multifactorial analysis indicated that age was a protective factor for DR/DN. A national study (11) also found that the age of the PDR patient group was significantly younger than that of the NPDR patient group, In the study of Cheng Haihai (12), it was shown that younger DN patients were more likely to have DR complications (12), which is also consistent with the results of the present study. The above findings suggest that older DR patients have a lower risk of DN complications and younger DR patients have a higher risk of DN complications. Although age is an uncontrollable factor, it also suggests that more clinical caution should be taken in younger DR patients, and more frequent outpatient follow-up is needed to intervene in time for the possible onset or progression of DN. In addition, the proportion of the DR/DN group with a history of hypertension was found to be significantly higher than that of the DR group in this study, and the history of hypertension was an independent risk factor for DR/DN, which is basically consistent with domestic and international studies, in which Pu Danfeng 's (13) study found that the duration of hypertension and systolic blood pressure were independent risk factors for DR/DN, and the other study (14) also confirmed that hypertension is indeed closely associated with the progression of DR and DN. Therefore, strict control of hypertension can significantly reduce the risk of DR and DN development.

TABLE 6 Risk factors and protective factors for DR/DN.

Factors	β	S.E	Waldχ2	df	*P*	OR	95% CI	
							Lower limit	Upper limit
Age	-0.50	0.017	8.861	1	0.003	0.951	0.920	0.983
History of HBP	1.015	0.369	7.556	1	0.006	2.759	1.338	5.687
CYS-C	1.320	0.350	14.213	1	<0.001	3.742	1.884	7.431
PLR	0.009	0.003	8.824	1	0.004	1.009	1.003	1.015
HGB	-0.024	0.009	6.587	1	0.010	0.976	0.959	0.994
Crea	0.018	0.005	11.220	1	0.001	1.018	1.007	1.028
UA	0.004	0.002	4.947	1	0.026	1.004	1.000	1.008
NLR	0.275	0.118	5.387	1	0.020	1.316	1.044	1.660

TABLE 7 Risk factors for PDR, NPDR/DN and PDR/DN.

Diagnosis	Influencing Factors	β	S.E	Waldχ2	df	*P*	OR	95% CI	
								Lower limit	Upper limit
PDR	CYS-C	1.755	0.764	5.271	1	0.022	5.781	1.293	25.850
NPDR/DN	CYS-C	1.829	0.806	5.144	1	0.023	6.227	1.282	30.248
PDR/DN	CYS-C	1.662	0.836	3.951	1	0.047	5.272	1.023	27.160
	UACR	0.001	0.000	9.515	1	0.002	1.001	1.000	1.002

5.2 High HGB level is a protective factor for DR Concurrent DN

Hyperglycemia is a controllable risk factor for diabetic complications. Chinese Guidelines for the Prevention and Treatment of Type 2 Diabetes (15) HbA1c has become a new criterion for the diagnosis of diabetes and an important indicator for predicting chronic microvascular complications of diabetes. When HbA1c is greater than 7%, the risk of developing DR and DN is significantly higher, and the HbA1c in both the DR and DR/DN groups in this study was significantly greater than 7%. It has also been confirmed in previous studies that HbA1c is an important indicator of DR (11) and DN (16). In the present study, HbA1c was lower in the DR/DN group than in the DR group and was significantly lower in the PDR/DN group than in the NPDR/DN group, but the difference between the groups was not statistically significant. We speculate that it may be related to the fact that patients with DR/DN, especially PDR/DN, strictly control their blood glucose level after the symptoms of renal dysfunction or after the obvious loss of vision, while patients with NPDR alone tend to ignore their ocular symptoms and do not pay attention to them or do not take regular glucose-lowering treatment, so the level of blood glucose control is poor; meanwhile, HbA1c is a product of HGB binding to glucose in red blood cells, so its At the same time, HbA1c is the product of HGB binding to glucose in erythrocytes, so its decrease is not only related to blood glucose but may also be closely related to the change of HGB concentration in the same period. The HGB in the DR/DN group in this study was significantly lower than that in the DR group, and the mean HGB values between subgroups still differed significantly, and the mean HGB values in the PDR/DN group were significantly lower than those in the other 3 groups, which is also basically in line with the trend of HbA1c result changes in this study. In addition, the results of this study found that HGB was a protective factor for DR/DN. Results of a Korean cross-sectional study based on 2123 patients with diabetes mellitus (17) showed that high HGB levels significantly reduced the risk of DR prevalence; in addition there are also scholars (18) found a significant negative association between HGB levels and the index and severity of retinal ischemia in DR; Previous studies (19) have also confirmed that anemia is an independent risk factor for DR and DN; combined with the above studies, high HGB levels have been shown to delay the development of DR and DN. Therefore, we speculate that HbA1c and HGB are mutually influential factors, suggesting that the HGB of patients with DR and DN should be closely monitored in clinical practice, and combined with fasting and postprandial glucose, the true glycemic control level of patients should be comprehensively evaluated.

5.3 PLR and NLR may be peripheral blood inflammatory biomarkers of DN predicted by DR

NLR and PLR are novel non-specific inflammatory markers that have received more attention in recent years. elevated levels of NLR

TABLE 8 Laboratory test indicators for predicting DR/DN and PDR/DN.

	Indicators	AUC	Sensitivity	Specificity	Yoden Index	Threshold value	*P*	95% CI	
								Lower limit	Upper limit
DR/DN	CYS-C	0.717	72%	65.5%	0.375	1.17	<0.001	0.628	0.805
	PLR	0.625	74%	52.2%	0.253	103.73	0.010	0.534	0.716
	Crea	0.647	52%	79%	0.31	83.55	0.003	0.546	0.767
	UA	0.616	42%	79%	0.21	406.5	0.017	0.524	0.709
	United 1	0.717	64%	72.4%	0.354		<0.001	0.629	0.804
PDR/DN	CYS-C	0.787	68.4%	76.3%	0.437	1.34	<0.001	0.687	0.866
	Crea	0.683	63.2%	71%	0.342	88.25	0.021	0.528	0.837
	UACR	0.783	57.9%	88.1%	0.43	1362.3	<0.001	0.652	0.913
	United 2	0.795	78.9%	71%	0.499		0.001	0.667	0.922

10.3389/fendo.2023.1160615

TABLE 9 Correlation distribution of laboratory test indicators with DR and DN staging.

	HBP	Age	HGB	NLR	PLR	Crea	UA	UACR	CYS-C	DR	DN
HBP	1										
Age	0.142	1									
HGB	-0.140	-0.019	1								
NLR	0.214*	-0.083	-0.017	1							
PLR	0.084	-0.185	0.023	0.474*	1						
Crea	0.344*	0.137	-0.188*	0.254*	0.087	1					
UA	0.189*	0.023	-0.007	0.221*	0.018	0.498*	1				
UACR	0.485*	0.485 *	-0.466*	0.367*	0.334*	0.674*	0.432*	1			
CYS-C	0.352*	0.352 *	-0.354*	0.227*	0.161*	0.709*	0.415*	0.687*	1		
DR	0.038	-0.159*	-0.148	0.025	0.069	0.129	0.012	0.432*	0.285*	1	
DN	0.064	-0.286*	-0.324*	0.334*	0.375*	0.430*	0.297*	0.529*	0.501*	0.371*	1

*represents $p < 0.05$, indicating statistical significance.

and PLR represent an increase in neutrophils and platelets, which release large amounts of inflammatory cytokines that inhibit lymphocyte inflammatory regulation and protection, and the immune balance between neutrophils and lymphocytes is disrupted (20), with tumors (21), cardiovascular and cerebrovascular complications (19), respiratory diseases (22), diabetes mellitus (23) and other systemic chronic inflammatory diseases are closely related, NLR value is independently associated with neovascular Age-related macular degeneration (24). Moreover, Higher PLR could reduce the risk of Type 2 Diabetes Mellitus. Larger increase of NLR could increase Type 2 Diabetes Mellitus risk (25). And an increasing number of scholars are now studying their relationship with diabetic microvascular complications. One study showed that (26) Platelets and neutrophils interact with each other, and under inflammatory stimulation neutrophils produce platelet chemokines and activating factors, and activated platelets release large amounts of pro-inflammatory and pro-angiogenic factors that damage vascular endothelial cells, leading to increased vascular permeability, edema, and exudation, which further activate neutrophils to release more inflammatory mediators and induce chronic microangiopathy and inflammatory responses (26), promoting DN (27) and DR (28) of progression. Recent findings suggest that Lymphocyte percentage can be used as an inflammatory marker for the development of DME in patients with severe DR (29).The NLR and PLR in the DR/DN group in this study were significantly higher than those in the DR group, suggesting a more severe inflammatory response in DR/DN; previous studies also found that NLR predicted DN progression (30) and the severity of DR (31); a recent study (32) demonstrated that NLR and PLR are risk factors for DN and may be predictors of early DN patients (33); another study (34) also showed that NLR was an independent risk factor for DR, DN, and DR/DN, Latest Research suggest that PLR may be an independent risk factor for evaluating DR in type 2 diabetes patients (35).The present study found that both NLR and PLR were independent risk factors for DR/DN, and the risk of DR complicated by DN was significantly increased when PLR > 103.73. Previous studies found that PLR also predicted diabetes-related lower extremity vascular disease (36), atherosclerosis and diabetic foot ulcers (37). This suggests that platelets are not only involved in thrombosis, but also play an important role in regulating the immune inflammatory response, especially in the intravascular one. Meanwhile, correlation analysis showed that PLR was significantly positively correlated with NLR, and both PLR and NLR were significantly positively correlated with DN stage; Furthermore, The systemic immune-inflammation index (SII) is a novel and integrated inflammatory biomarker, SII was

TABLE 10 Comparison of OCT imaging indexes between DR and DR/DN groups.

	DR	DR/DN	χ2/F	*P*
HRF	102 (67.1%)	43 (70.5%)	0.23	0.63
DRIL	106 (69.7%)	47 (77%)	1.15	0.28
ORTs	39 (25.7%)	18 (29.5%)	0.33	0.57
CRT	270.81 ± 86.31	299.00 ± 136.43	3.53	0.07
RNFL	19.26 ± 4.91	17.64 ± 3.64	5.42	0.02
GCL	39.68 ± 10.69	34.97 ± 6.97	10.53	0.001

TABLE 11 Comparison table of OCT imaging indices between subgroups.

	NPDR	PDR	NPDR/DN	PDR/DN	χ2/F	P-value
HRF	63 (59.4%)	39 (84.8%)	27 (71.7%)	16 (69.6%)	9.73	0.02
DRIL	66 (62.3%)	40 (87.0%)	26 (68.4%)	21 (91.3%)	14.53	0.002
ORTs	23 (21.7%)	16 (34.8%)	9 (23.7%)	9 (39.1%)	4.88	0.18
CRT	273.72 ± 95.11	264.11 ± 61.83	291.89 ± 95.43	310.74 ± 187.67	1.33	0.27
RNFL	19.51 ± 4.55	18.67 ± 5.67	18.08 ± 4.16	16.91 ± 2.47	2.47	0.06
GCL	39.98 ± 10.23	38.98 ± 11.76	35.42± 6.94	33.96 ± 7.07	3.70	0.01

calculated as the platelet count × neutrophil count/lymphocyte count. New research results indicate that the higher SII level is associated with DN in Type 2 Diabetes Mellitus patients. The SII could be a cost-effective and straightforward approach to detecting DN (38). In conclusion, we speculate that PLR and NLR are important inflammatory biomarkers for predicting DN in DR, and are closely related to DN severity.

5.4 CYS-C, UA and Crea may be peripheral blood biomarkers of DN predicted by DR

2. Serum CYS-C, an endogenous marker of glomerular filtration rate, is associated with diabetic macroangiopathy (39) and microangiopathy (40) both have relevance. In the present study, CYS-C was significantly higher in the DR/DN group than in the DR group, and CYS-C was an independent risk factor not only for DR/DN but also for PDR, NPDR/DN and PDR/DN, respectively. Previous clinical studies (41) found that Cys C was an independent risk factor for DN complicated by DR; the present study confirmed that CYS-C had predictive value for DR/DN and PDR/DN, and the likelihood of DR complicated by DN was higher when CYS-C> 1.17 mg/L, and the risk of PDR complicated by DN was higher when CYS-C was elevated to 1.335 mg/L. Other clinical studies (42)have found a significantly increased risk of renal insufficiency in PDR patients with CYS-C above 1.315 mg/L. The most recent Meta-analysis (43) The results showed that CYS-C has significant diagnostic value for DN, and the abnormal rate of CYS-C in the urine of patients gradually increased with the aggravation of DN, and the abnormal rate of CYS-C in the urine of patients with stage 3 DN was 100% (44); and our study showed a significant positive correlation between serum CYS-C and DN stage. One study

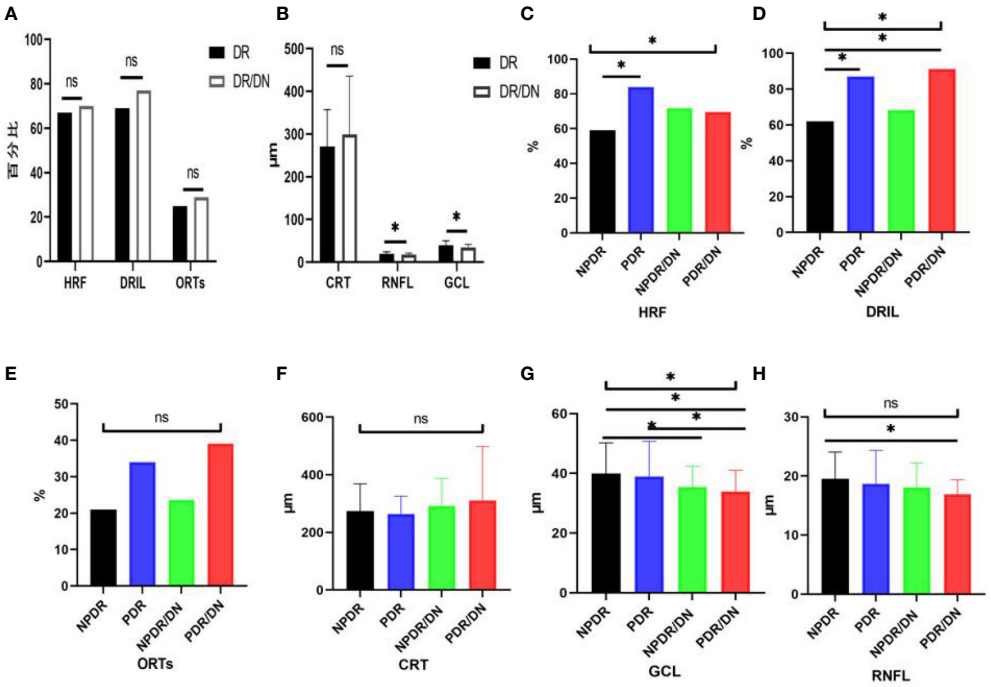

FIGURE 3
Histogram comparing DR with DR/DN and subgroup analysis of fundus imaging indices. (*represents $p<0.05$, indicating statistical significance). **(A, B)** Results of comparison of OCT indexes between DR And DN; **(C–H)** Comparison results of four OCT indexes: NPDR, PDR, NPDR/DN and PDR/DN.

TABLE 12 Results of multi-factor logistic regression analysis for DR/DN, PDR, NPDR/DN and PDR/DN.

Diagnosis	Markers	B	S.E	Waldχ2	df	*P*	OR	95% CI	
								Lower limit	Upper limit
DR/DN	RNFL	-0.095	0.037	6.753	1	0.009	0.909	0.846	0.977
	GCL	-0.056	0.017	10.580	1	0.001	0.945	0.914	0.978
PDR	HRF	1.134	0.508	4.995	1	0.025	1.322	0.119	0.870
	DRIL	1.180	0.528	4.995	1	0.025	1.307	0.109	0.865
NPDR/DN	RNFL	-0.107	0.046	5.503	1	0.019	0.899	0.821	0.983
	GCL	-0.067	0.022	9.033	1	0.003	0.935	0.896	0.977
PDR/DN	RNFL	-0.161	0.059	7.500	1	0.006	0.852	0.759	0.955
	GCL	-0.075	0.027	7.991	1	0.005	0.928	0.881	0.977

showed that CYS-C could be an early predictor of tubular injury in T2DM diabetic patients (45).A domestic study (34) found that CYS-C was only associated with DN and weakly correlated with DR, which may be related to the fact that the study did not group the severity of DR.Recent research has discovered that CYS-C was a risk factor for DN independent of BMI and SBP in diabetes mellitus patients (46). Zheng Yanhui et al (47) found that CYS-C was an independent risk factor for DR and positively correlated with the severity of DR, while the present study also found that CYS-C was an independent risk factor for PDR and significantly and positively correlated with the stage of DR. A Meta (48) analyzed the correlation between CYS-C and DR in 4354 Chinese patients with type 2 diabetes and confirmed that CYS-C was strongly associated with DR progression, which is consistent with the results of the present study. In addition, one study found that CYS-C promotes increased VEGF levels to induce angiogenesis (49) and was closely associated with the expression of various inflammatory factors CRP, IL-6 and TNF-α (50), CYS-C levels were significantly positively correlated with PLR and NLR in the present study, suggesting that CYS-C levels may be related to the degree of inflammatory response *in vivo*. Therefore, CYS-C can be used as an important serum indicator for predicting the development of DN in DR.

Serum UA is the end product of purine degradation and has antioxidant and pro-oxidant properties, UA can decrease glucose-stimulated insulin secretion and cause β-cell death. The mechanisms underlying these effects are UA-induced oxidative stress and inflammation within the β-cells. UA also stimulates inducible nitric oxide (NO) synthase (iNOS) gene expression leading to NO-induced β-cell dysfunction. Thus hyperuricemia may potentially cause β-cell dysfunction, leading to diabetes (51). High levels of UA stimulate proliferation of human vascular smooth muscle cells, increase the expression of endothelin-1 and CRP, increase ROS production, and damage vascular endothelial cells (52), leading to macrovascular and microangiopathy. Therefore, excessive UA is strongly associated with diabetic microangiopathy (53). In this study, UA was significantly higher in the DR/DN group than in the DR group, and UA was an independent risk factor for DR/DN, and the risk of DR complicating DN increased when UA was >406.5 μmol/L; Lai Na's study (54) showed that the risk of DR occurred significantly increased when UA exceeded 304.75 μmol/L, while the risk of DN occurred significantly increased when UA > 379.05 μmol/L (54). The above studies suggest that high UA can be a better predictor of the development of DR and DN. In the correlation analysis, UA levels were significantly and positively correlated with DN staging, which is consistent with previous studies (55). In addition, scholars (56) found that UA levels increased with increasing DR severity and could be used as a clinical indicator to assess the severity of DR, and that men with high UA had a significantly higher risk of developing DR (57). However, the results of this study showed no significant correlation between UA and DR staging, and the difference in UA comparison between the DR and PDR groups in the subgroup analysis was not

TABLE 13 Prediction data table of RNFL and GCL for DR/DN, NPDR/DN, PDR/DN.

	Indicators	AUC	Sensitivity	Specificity	Yoden Index	Threshold value	*P*	95% CI	
								Lower limit	Upper limit
DR/DN	RNFL	0.579	80.3%	36.8%	0.171	20.5	0.07	0.500	0.659
	GCL	0.642	85.2%	48.0%	0.332	41.5	0.001	0.569	0.716
NPDR/DN	RNFL	0.522	97.4%	56.0%	0.134	24.5	0.678	0.423	0.620
	GCL	0.605	86.8%	40.4%	0.262	42.5	0.043	0.521	0.689
PDR/DN	RNFL	0.636	95.7%	36.3%	0.31	20.5	0.034	0.546	0.725
	GCL	0.642	91.3%	45.3%	0.366	40.5	0.026	0.546	0.738

TABLE 14 Correlation distribution of OCT imaging indices with DR and DN staging.

	HRF	CRT	ORTs	RNFL	GCL	DRIL	DR	DN
HRF	1							
CRT	0.361*	1						
ORTs	0.391*	0.427*	1					
RNFL	-0.041	0.034	-0.096	1				
GCL	0.047	0.005	-0.128	-0.149*	1			
DRIL	0.467*	0.237*	0.331*	0.018	0.063	1		
DR	0.315*	0.091	0.228*	-0.090	-0.031	0.438*	1	
DN	0.116	-0.184	0.102	0.011	-0.205	0.047	0.334*	1

*represents p<0.05, indicating statistical significance.

statistically significant, which may be related to the small sample size included in this study. There is a relevant study found that higher UA levels are associated with various stages of the onset and progression of DN, including metabolic, cardiovascular and kidney function abnormalities (58).Therefore, serum UA may be a marker for DR to predict DN and assess the severity of DN.

Currently, although Crea is affected by various factors such as age, gender and weight, it is also one of the most direct markers for clinicians to determine renal function, and an increase in Crea indicates a decrease in glomerular filtration. The present study found that Crea is an independent risk factor for DR/DN, and the likelihood of DN complicating DR increases when Crea>83.55μmol/L, and the risk of DN complicating PDR increases when Crea rises to 88.25 μmol/L. The significant positive correlation between Crea level and DN stage suggests that Crea can be a serum marker for assessing the severity of DN and predicting DN by DR. This suggests that Crea can be a serum marker to assess the severity of DN and to predict DN in DR. Previous studies have also confirmed that regular monitoring of Crea levels is useful in assessing the progression and prognosis of DN (59, 60). In addition, the Crea levels in the PDR group were found to be more than adequate. In addition, Crea levels were higher in the PDR group than in the DR group, but the difference was not statistically significant and did not correlate with DR staging, suggesting that Crea has limited value in assessing DR severity. According to the results of this study, Crea is a helpful serum marker for predicting DN in DR.

5.5 UACR may be a biomarker of DN predicted by DR

UACR is an effective indicator for monitoring early proteinuria and chronic renal impairment. In this study, we found that UACR is an independent risk factor for PDR/DN and has diagnostic significance for PDR/DN, and when the combination of UACR, CYS-C and Crea can improve the predictive value of PDR/DN, and all of them are higher than the diagnostic value of each individual index. Gao Jun et al. (61) found that the combination of UACR, serum Cys-C and amyloid A had a higher diagnostic value for early DN than each individual index, and could be used as a clinical index for monitoring early DN. In this study, UACR was significantly and positively correlated with DN staging, and we hypothesized that UACR could be used to assess the severity of DN. In addition, UACR is also a risk factor for the development of DR (62)., study (63) suggests that high values of UACR within the normal range may be a risk factor for the onset of DR, and the likelihood of DR onset is higher when UACR reaches 16.79 mmol/L. In this study, the UACR index was not collected from patients with DR alone, so it could not be verified whether UACR was a risk factor for DR onset, but correlation analysis found that it was closely related to the staging of DR, indicating that the higher the UACR, the more severe the DR. In conclusion, UACR may be a clinical marker for DR to predict the progression of DN with the aid of diagnosing DN complicated by PDR.

5.6 HRF, DRIL, ORTs and CRT have limited value for DR Prediction DN

At present, macular OCT biological markers such as HRF, DRIL, ORTs and CRT are mainly used to evaluate and monitor the changes of DME condition, treatment effect and visual prognosis. This study mainly analyzed the distribution characteristics of the above OCT biological markers in DR and DR/DN patients. The presence of HRF in all layers of the retina suggests active inflammation of the retina and even the choroid, and more scholars believe that its formation may be related to the activation of microglia and the accumulation of pro-inflammatory factors released, among others (64). DRIL represents a signal disruption and disruption of the second level neurons of the visual transmission pathway and may be closely related to retinal ischemia and hypoxia, previous studies (65) found a significant correlation between DRIL and the area of the retinal nonperfused area, and also studies (66) DRIL and its length are also important biological predictors of DR prognosis The DRIL and its length are also important biological predictors of DR prognosis (67).We found that the positive rates of HRF and DRIL were higher in the DR/DN group than in the DR group, but not statistically significant, and in the subgroup analysis, the positive rates of HRF and DRIL were

significantly higher in the PDR group than in the NPDR group, and HRF and DRIL were independent risk factors for PDR, and the positive rates of HRF and DRIL were also significantly and positively correlated with DR staging, but they did not correlate with either DN staging; the above The results suggest that HRF and DRIL can be biological markers for predicting PDR and DR staging, but have limited predictive value for DN. ORTs mostly occur in the outer nuclear layer of the retina in the macula, and its formation may be associated with the remodeling of photoreceptor cells after retinal damage, and the progression of retinal lesions to the end stage (10).ORTs are suggestive for the progression and treatment prognosis of a variety of CNV-related and degenerative genetic-related retinal diseases, and are used to predict sensitivity to anti-VEGF drugs and visual prognosis, but not as a basis for assessing CNV activity and retreatment (68). In this study, the positive rate of ORTs was found to be significantly correlated with DR staging and not significantly correlated with DN staging.CRT is a common index to assess the indication, efficacy and prognosis of drug therapy for a variety of macular edema diseases and is widely used in clinical and basic research of various retinal and choroidal diseases. In this study, CRT was significantly higher in the DR/DN group than in the DR group, but it was not statistically significant, and no significant correlation was found between CRT and the staging of DR and DN. This may be because DME can occur in all stages of DR, which affects the variability of CRT between groups, or it may be related to the inclusion of more patients with moderate to severe NPDR and PDR in this study.

5.7 RNFL and GCL thickness in macular area may be biomarkers of OCT image for DR Prediction of DN

The current findings mostly support that neurodegenerative changes in the retina have occurred in DR prior to the development of microangiopathy, leading to neuronal apoptosis and glial cell activation, which mainly affects retinal ganglion cells (RGCs) in the RNFL, GCL, and inner plexiform layer, which contains the axons of RGCs, and the GCL and inner plexiform layer, which consists of the nuclei and dendrites of RGCs (69), so the measurement of RNFL and GCL thickness can provide some reference for neurodegenerative changes in the retina. In this study, RNFL and GCL thicknesses were significantly lower in the DR/DN group than in the DR group, and RNFL and GCL thicknesses were independent protective factors for DR/DN, NPDR/DN, and PDR/DN. When RNFL thickness was <20.5 μm, it was diagnostic for PDR/DN, and GCL thicknesses <41.5 μm, 42.5 μm, and 40.5 μm were diagnostic for DR/DN,The above results suggest that RNFL and GCL thickness can be used as biological markers of DR to predict DN, and also confirm the predictive value of retinal neurodegenerative lesions for DN. In previous domestic and international studies, there are relatively few studies related to the thickness changes of RNFL and GCL in the macula at the same time, and most of them study DR from the changes of RNFL thickness around the optic disc (70), open-angle glaucoma (71), myopia (72) and other early neurodegenerative changes in optic nerve and macular diseases, so these studies are not very comparable to the results of the present study. Wang Lili et al (73) found that the thickness of RNFL in the macula has become significantly thinner in diabetic patients compared with normal subjects, so regular monitoring of thickness changes using OCT can help in the early detection of diabetes and early diagnosis and treatment of DR (74).. In the subgroup analysis of this study, the RNFL thickness in the PDR group was lower than that in the NPDR group, but it was not statistically significant, and no significant correlation was found between RNFL thickness changes and DR staging, which may be related to the fact that a normal control group was not established in this study. In addition, Diao Lili et al (75) found a significant thinning of retinal GCL thickness in the macula of diabetic patients, but there was no significant relationship between its thickness change and DR severity, which is consistent with the result that there was no significant correlation between GCL thickness and DR staging in the present study, and is also consistent with Chhablani et al (69) study conclusions. In conclusion, the temporal RNFL and GCL thickness in the macula may be OCT imaging biological markers of DR to predict DN.

6 Conclude

In this part of the study, we found that low age, hypertension, hyperglycemia, anemia, increased inflammatory response, impaired renal function and retinal neurodegenerative changes were important risk factors for DR complicated by DN from an ophthalmic perspective by analyzing the general data, distribution characteristics of laboratory and fundus OCT imaging indices in patients with DR and DR complicated by DN. Inflammatory indicators PLR and NLR, renal function indicators CYS-C, Crea and UA, and OCT imaging indicators macular temporal RNFL and GCL thickness may be important clinicobiological markers for predicting DN complicated by DR when PLR > 103.73, CYS-C>1.17 mg/L, UA > 406.5 μmol/L, Crea > 83.55 μmol/L, RNFL thickness <20.5 μm and GCL thickness <41.5 μm, the risk of DR complicating DN was significantly increased, and the combination of PLR, CYS-C, UA and Crea did not improve the diagnostic value of DR complicating DN; when CYS-C >1.335 mg/L, Crea >88.25 μmol/L, and The combination of CYS-C, Crea and UACR significantly increased the diagnostic value of PDR with DN. The positive correlation between DR staging and DN staging indicated that DR and DN were closely related, and the two were predictors of each other. We speculate that the consistency of the association and progression of DR and DN may be related to the inflammatory response as their common pathogenesis. The inflammatory response of the renal tissue leads to impaired glomerular filtration function, therefore proteinuria, abnormal elevation of clinical serum inflammatory indexes and renal function indexes; the inflammatory response of the retinal tissue leads to retinal microangiopathy and neurodegenerative changes, and macular OCT reveals HRF, ORTs, and DRIL and thinning of RNFL and GCL thickness were seen on macular OCT.

Data availability statement

The raw data supporting the conclusions of this article will be made available by the authors, without undue reservation.

Ethics statement

Ethical review and approval was not required for the study on human participants in accordance with the local legislation and institutional requirements. Written informed consent for participation was not required for this study in accordance with the national legislation and the institutional requirements.

Author contributions

LX designed the study and drafted the manuscript as the first author. SX and LX carried out the literature search. HY contributed to data extraction and quality assessment. XX and XM supervised the study and XM as the corresponding author. All authors contributed to the article and approved the submitted version.

Funding

This work was supported by National Natural Science Foundation of China (NO: 81473735) and Discipline innovation Team of Chengdu University of Traditional Chinese Medicine – Research on the prevention and treatment of fundus diseases with traditional Chinese Medicine (XKTD2022005). The funders had no role in the study design, data collection, data analysis, interpretation, or writing of the report.

Acknowledgments

We would like to acknowledge all the authors of the research articles used for the analysis.

Conflict of interest

The authors declare that the research was conducted in the absence of any commercial or financial relationships that could be construed as a potential conflict of interest.

Publisher's note

References

1. Park HC, Lee YK, Cho A, Han CH, Noh JW, Shin YJ, et al. Diabetic retinopathy is a prognostic factor for progression of chronic kidney disease in the patients with type 2 diabetes mellitus. *PloS One* (2023) 7:e0220506. doi: 10.1371/journal.pone.0220506

2. Sasongko MB, Wang JJ, Donaghue KC, Cheung N, Benitez-Aguirre P, Jenkins A, et al. Alterations in retinal microvascular geometry in young type 1 diabetes. *Diabetes Care* (2010) 6:1331–6. doi: 10.2337/dc10-0055

3. Tolonen N, Hietala K, Forsblom C, Harjutsalo V, Mäkinen VP, Kytö J, et al. Associations and interactions between lipid profiles, retinopathy and nephropathy in patients with type 1 diabetes: the FinnDiane study. *J Intern Med* (2013) 5:469–79. doi: 10.1111/joim.12111

4. Ren Y, Gao L, Guo X, Huo X, Lu J, Li J, et al. Interactive effect of serum uric acid and total bilirubin for micro-vascular disease of type 2 diabetes in China. *J Diabetes Complications* (2018) 11:1000–5. doi: 10.1016/j.jdiacomp.2018.09.002

5. Moriya T, Matsubara M, Kishihara E, Yoshida Y, Ouchi M. Type 2 diabetic patients with diabetic retinopathy and concomitant microalbuminuria showed typical diabetic glomerulosclerosis and progressive renal dysfunction. *J Diabetes Complications* (2016) 6:1111–6. doi: 10.1016/j.jdiacomp.2016.04.007

6. Yang JK, Wang YY, Liu C, Shi TT, Lu J, Cao X, et al. Urine proteome specific for eye damage can predict kidney damage in patients with type 2 diabetes: a case-control and a 5.3-year prospective cohort study. *Diabetes Care* (2017) 2:253–60. doi: 10.2337/dc16-1529

7. Schorr SG, Hammes HP, Müller UA, Abholz HH, Landgraf R, Bertram B, et al. The prevention and treatment of retinal complications in diabetes. *Dtsch Arztebl Int* (2016) 48:816–23. doi: 10.3238/arztebl.2016.0816

8. Lee H, Jang H, Choi YA, Kim CH, Chung H. Association between soluble CD14 in the aqueous humor and hyperreflective foci on optical coherence tomography in patients with diabetic macular edema. *Invest Ophthalmol Vis Sci* (2018) 2:715–21. doi: 10.1167/iovs.17-23042

9. Grewal DS, Hariprasad SM, Jaffe GJ. Role of disorganization of retinal inner layers as an optical coherence tomography biomarker in diabetic and uveitic macular edema. *Ophthalmic Surg Lasers Imaging Retina* (1970) 4:282–8. doi: 10.3928/23258160-20170329-02

10. Zweifel SA, Engelbert M, Laud K, Margolis R, Spaide RF, Freund KB, et al. Outer retinal tubulation: a novel optical coherence tomography finding. *Arch Ophthalmol* (2009) 12:1596–602. doi: 10.1001/archophthalmol.2009.326

11. Chen YB, Sun K. Study on risk factors associated with type 2 diabetic retinopathy. *Jilin Med Science.* (2022) 43(08):2038–41.

12. Cheng H. *A clinical study on the diagnostic value of diabetic retinopathy in type 2 diabetic nephropathy*. Guangdong Pharmaceutical University (2019). doi: 10.27690/d.cnki.ggdyk.2019.000020

13. Pu DF, Wang XJ, Ma J, Shao YM, Liu GP. Risk factors of diabetic retinopathy combined with diabetic nephropathy and their predictive value. *Chin J senile multi-organ Diseases.* (2019) 18(01):30–5.

14. Hammoudi J, Bouanani NEH, Chelqi EH, Bentata Y, Nouayti H, Legssyer A, et al. Diabetic retinopathy in the Eastern Morocco: different stage frequencies and associated risk factors. *Saudi J Biol Sci* (2021) 1:775–84. doi: 10.1016/j.sjbs.2020.11.010

15. Wang FJ, Wang WQ. Interpretation of the guidelines for prevention and treatment of type 2 diabetes mellitus in China (2020 edition). *J Hebei Med University.* (2021) 42(12):1365–71.

16. Yang CW, Wang T, Zhao YQ, Yang GH, Liu CH, Cao WB, et al. Establishment of individualized diagnosis model for early diabetic nephropathy. *Clin Res China* (2020) 33(06):781–783+787. doi: 10.13429/j.cnki.cjcr.2020.06.013

17. Lee MK, Han KD, Lee JH, Sohn SY, Jeong JS, Kim MK, et al. High hemoglobin levels are associated with decreased risk of diabetic retinopathy in Korean type 2 diabetes. *Sci Rep* (2018) 1:5538. doi: 10.1038/s41598-018-23905-2

18. Traveset A, Rubinat E, Ortega E, Alcubierre E, Vazquez B, Hernández M, et al. Lower hemoglobin concentration is associated with retinal ischemia and the severity of diabetic retinopathy in type 2 diabetes. *J Diabetes Res* (2016) 2016:3674946. doi: 10.1155/2016/3674946

19. Liu Y, Xie Y, Dong Z, Zhang XG, Sun XF, Zhang D, et al. Role of hemoglobin in differentiating diabetic nephropathy from non-diabetic nephropathy. *Chin J Nephropathy Res Electronic* (2018) 7(06):271–6.

20. Khandare SA, Chittawar S, Nahar N, Dubey TN, Qureshi Z. Study of neutrophil-lymphocyte ratio as novel marker for diabetic nephropathy in type 2 diabetes. *Indian J Endocrinol Metab* (1970) 3:387–92. doi: 10.4103/ijem.IJEM_476_16

21. Franzolin G, Tamagnone L. Semaphorin signaling in cancer-associated inflammation. *Int J Mol Sci* (2019) 2. doi: 10.3390/ijms20020377

22. Ren Y, Hu Y, Li Y, Feng Y, Lv T, Wang XB, et al. Relationship between neutrophil/lymphocyte ratio and platelet/lymphocyte ratio and activity of interstitial lung disease associated with connective tissue disease. *J Air Force Med Univ* (2023) 44 (01):1–10. doi: 10.13276/j.issn.2097-1656.2023.01.015

23. Mertoglu C, Gunay M. Neutrophil-lymphocyte ratio and platelet-lymphocyte ratio as useful predictive markers of prediabetes and diabetes mellitus. *Diabetes Metab Syndr* (2017) 11:S127–31. doi: 10.1016/j.dsx.2016.12.021

24. Kurtul BE, Ozer PA. The relationship between neutrophil-to-lymphocyte ratio and age-related macular degeneration. *Korean J Ophthalmol* (2016) 5:377–81. doi: 10.3341/kjo.2016.30.5.377

25. Zhang C, Chen H, Cui S, Lin Y, Liang Y, Zhao P, et al. Platelet-lymphocyte ratio, neutrophil-lymphocyte ratio and their dynamic changes with type 2 diabetes mellitus: a cohort study in China. *Endocr Res* (1970) 3-4:138–52. doi: 10.1080/07435800.2022.2127757

26. Chen C, Xu K. Research progress on the role of platelets in inflammatory response. *Hainan Med Sci* (2017) 28(04):623–6.

27. Liu J, Liu X, Li Y, Quan J, Wei S, An S, et al. The association of neutrophil to lymphocyte ratio, mean platelet volume, and platelet distribution width with diabetic retinopathy and nephropathy: a meta-analysis. *Biosci Rep* (2018) 3:BSR20180172. doi: 10.1042/BSR20180172

28. Wang JR, Chen Z, Yang K, Yang HJ, Tao WY, Li YP, et al. Association between neutrophil-to-lymphocyte ratio, platelet-to-lymphocyte ratio, and diabetic retinopathy among diabetic patients without a related family history. *Diabetol Metab Syndr* (2020) 55. doi: 10.1186/s13098-020-00562-y

29. Zhu Y, Cai Q, Li P, Zhou Y, Xu M, Song Y, et al. The relationship between peripheral blood inflammatory markers and diabetic macular edema in patients with severe diabetic retinopathy. *Ann Palliat Med* (2022) 3:984–92. doi: 10.21037/apm-22-102

30. DiGangi C. Neutrophil-lymphocyte ratio: predicting cardiovascular and renal complications in patients with diabetes. *J Am Assoc Nurse Pract* (2016) 8:410–4. doi: 10.1002/2327-6924.12366

31. Ulu SM, Dogan M, Ahsen A, Altug A, Demir K, Acartürk G, et al. Neutrophil-to-lymphocyte ratio as a quick and reliable predictive marker to diagnose the severity of diabetic retinopathy. *Diabetes Technol Ther* (2013) 11:942–7. doi: 10.1089/dia.2013.0097

32. Gu AD, Wu JL, Xu HZ, Guan J, Xu Y. Correlation between neutrophil/lymphocyte ratio, platelet/lymphocyte ratio and diabetic nephropathy. *Chin primary Med* (2021) 28(12):1767–70. doi: 10.3760/cma.issn1008-6706.2021.12.002

33. Feng R, Liu JQ, Qian L, Li Y, Zhang GL. Effects of neutrophil to lymphocyte ratio and platelet to lymphocyte ratio on early diabetic nephropathy and early intervention effect of calcium oxybenzoate. *J Clin Internal Med* (2022) 39(08):547–9.

34. Zhou F, Zhang L, Zhai XD, Liu C. Relationship between neutrophil/lymphocyte ratio and cystatin c and microvascular complications in type 2 diabetes mellitus. *Chin Med J* (2020) 22(08):1168–71. doi: 10.3760/cma.j.cn431274-20190723-00871

35. Zeng J, Chen M, Feng Q, Wan H, Wang J, Yang F, et al. The platelet-to-Lymphocyte ratio predicts diabetic retinopathy in type 2 diabetes mellitus. *Diabetes Metab Syndr Obes* (2023) 15:3617–26. doi: 10.2147/DMSO.S378284

36. Liu N, Sheng J, Pan T, Wang Y. Neutrophil to lymphocyte ratio and platelet to lymphocyte ratio are associated with lower extremity vascular lesions in Chinese patients with type 2 diabetes. *Clin Lab* (2019) 3. doi: 10.7754/Clin.Lab.2018.180804

37. Mineoka Y, Ishii M, Hashimoto Y, Yamashita A, Nakamura N, Fukui M, et al. Platelet to lymphocyte ratio correlates with diabetic foot risk and foot ulcer in patients with type 2 diabetes. *Endocr J* (2019) 10:905–13. doi: 10.1507/endocrj.EJ18-0477

38. Guo W, Song Y, Sun Y, Du H, Cai Y, You Q, et al. Systemic immune-inflammation index is associated with diabetic kidney disease in type 2 diabetes mellitus patients: evidence from NHANES 2011-2018. *Front Endocrinol (Lausanne)* (2022) 13:1071465. doi: 10.3389/fendo.2022.1071465

39. Jung CH, Kim KJ, Kim BY, Kim CH, Kang SK, Mok JO, et al. Relationship between vitamin d status and vascular complications in patients with type 2 diabetes mellitus. *Nutr Res* (2016) 2:117–24. doi: 10.1016/j.nutres.2015.11.008

40. Chen ZY, He L, Zhang Q. Correlation between homocysteine and cystatin c and microvascular complications in type 2 diabetes mellitus. *Modern instruments Med* (2019) 25(05):75–8.

41. Wu ZD, Wu J, Chen LJ, Wang HQ, Ma M, Lin LL, et al. Correlation between serum cystatin c level and retinal vessel diameter in patients with type 2 diabetes mellitus. *Chin Gen Practice.* (2020) 23(15):1895–903.

42. Bai J, Zhang M, Cao X, Cao JJ. Evaluation value of serum cystatin c in renal function impairment in patients with proliferative diabetic retinopathy. *Chin Med J* (2021) 101(30):2400–4. doi: 10.3760/cma.j.cn112137-20210522-01184

43. Liao X, Zhu Y, Xue C. Diagnostic value of serum cystatin c for diabetic nephropathy: a meta-analysis. *BMC Endocr Disord* (1970) 1:149.

44. Gao JB. Relationship between urea, UAlb, U-β2MG and cys-c levels and severity of diabetic nephropathy patients. *Explor rational Drug Use China* (2019) 16(10):122–124+127.

45. Taha MM, Mahdy-Abdallah H, Shahy EM, Helmy MA, ElLaithy LS. Diagnostic efficacy of cystatin-c in association with different ACE genes predicting renal insufficiency in T2DM. *Sci Rep* (2023) 1:5288. doi: 10.1038/s41598-023-32012-w

46. Feng B, Lu Y, Ye L, Yin L, Zhou Y, Chen A, et al. Mendelian randomization study supports the causal association between serum cystatin c and risk of diabetic nephropathy. *Front Endocrinol (Lausanne)* (2022) 13:1043174. doi: 10.3389/fendo.2022.1043174

47. Zheng YH. Relationship between serum RBP4, cys-c levels and diabetic retinopathy. *Chin sanitary Eng* 2019, 18(04):629–31.

48. Yang N, Lu YF, Yang X, Jiang K, Sang AM, Wu HQ, et al. Association between cystatin c and diabetic retinopathy among type 2 diabetic patients in China: a meta-analysis. *Int J Ophthalmol* (2023) 9:1430–40.

49. Zou J, Chen Z, Wei X, Chen Z, Fu Y, Yang X, et al. Cystatin c as a potential therapeutic mediator against parkinson's disease *via* VEGF-induced angiogenesis and enhanced neuronal autophagy in neurovascular units. *Cell Death Dis* (2017) 6:e2854. doi: 10.1038/cddis.2017.240

50. Shlipak MG, Katz R, Cushman M, Sarnak MJ, Stehman-Breen C, Psaty BM, et al. Cystatin-c and inflammatory markers in the ambulatory elderly. *Am J Med* (2005) 12:1416. doi: 10.1016/j.amjmed.2005.07.060

51. Ghasemi A. Uric acid-induced pancreatic β-cell dysfunction. *BMC Endocr Disord* (1970) 1:24. doi: 10.1186/s12902-021-00698-6

52. Kang DH, Park SK, Lee IK, Johnson RJ. Uric acid-induced c-reactive protein expression: implication on cell proliferation and nitric oxide production of human vascular cells. *J Am Soc Nephrol* (2005) 12:3553–62. doi: 10.1681/ASN.2005050572

53. Altemtam N, Russell J, El Nahas M. A study of the natural history of diabetic kidney disease (DKD). *Nephrol Dial Transplant* (2012) 5:1847–54. doi: 10.1093/ndt/gfr561

54. Lena. *The correlation between serum uric acid level and type 2 diabetic nephropathy and diabetic retinopathy*. Yan A'n University (2021).

55. Zoppini G, Targher G, Chonchol M, Ortalda V, Abaterusso C, Pichiri I, et al. Serum uric acid levels and incident chronic kidney disease in patients with type 2 diabetes and preserved kidney function. *Diabetes Care* (2012) 1:99–104. doi: 10.2337/dc11-1346

56. Lee JJ, Yang IH, Kuo HK, Chung MS, Chen YJ, Chen CH, et al. Serum uric acid concentration is associated with worsening in severity of diabetic retinopathy among type 2 diabetic patients in Taiwan–a 3-year prospective study. *Diabetes Res Clin Pract* (2014) 2:366–72. doi: 10.1016/j.diabres.2014.07.027

57. Guo Y, Liu S, Xu H. Uric acid and diabetic retinopathy: a systematic review and meta-analysis. *Front Public Health* (2023), 906760. doi: 10.3389/fpubh.2022.906760

58. Lytvyn Y, Perkins BA, Cherney DZ. Uric acid as a biomarker and a therapeutic target in diabetes. *Can J Diabetes* (2015) 3:239–46. doi: 10.1016/j.jcjd.2014.10.013

59. Cui Y, He JX, Lin H. The value of serum uric acid and serum creatinine levels in the prognosis of diabetic nephropathy patients. *Chin Community physician.* (2021) 37 (34):95–6.

60. Zhang X, Bai R, Zou L, Zong J, Qin Y, Wang Y, et al. Brachial-ankle pulse wave velocity as a novel modality for detecting early diabetic nephropathy in type 2 diabetes patients. *J Diabetes Res* (2023) 2021:8862573. doi: 10.1155/2021/8862573

61. Gao J. Diagnostic value of serum amyloid a, cystatin c and urinary albumin/creatinine ratio in early diabetic nephropathy. *Jilin Med Science.* (2022) 43 (02):532–4.

62. Chen YH, Chen HS, Tarng DC. More impact of microalbuminuria on retinopathy than moderately reduced GFR among type 2 diabetic patients. *Diabetes Care* (2012) 4:803–8. doi: 10.2337/dc11-1955

63. Wang K, Liu XH, Li TJ, Lou QQ. Relationship between urinary albumin/creatinine ratio and diabetic retinopathy in patients with type 2 diabetes mellitus. *New Prog ophthalmology.* (2022) 42(09):714–8. doi: 10.13389/j.cnki.rao.2022.0146

64. Vujosevic S, Bini S, Midena G, Berton M, Pilotto E, Midena E, et al. Hyperreflective intraretinal spots in diabetics without and with nonproliferative diabetic retinopathy: an in vivo study using spectral domain OCT. *J Diabetes Res* (2013) 2013:491835. doi: 10.1155/2013/491835

65. Ishibashi T, Sakimoto S, Shiraki N, Nishida K, Sakaguchi H, Nishida K, et al. Association between disorganization of retinal inner layers and visual acuity after proliferative diabetic retinopathy surgery. *Sci Rep* (2019) 1:12230. doi: 10.1038/s41598-019-48679-z

66. Nadri G, Saxena S, Stefanickova J, Ziak P, Benacka J, Gilhotra JS, et al. Disorganization of retinal inner layers correlates with ellipsoid zone disruption and retinal nerve fiber layer thinning in diabetic retinopathy. *J Diabetes Complications* (2019) 8:550–3. doi: 10.1016/j.jdiacomp.2019.05.006

67. Xu Y, Fang Y, Xie C. Correlation analysis of inner retinal structure disorder and prognosis of visual acuity after vitrectomy in patients with proliferative diabetic retinopathy. *Chin J fundus ophthalmosis.* (2020) 36(11):867–73.

68. Li B, Chen Y. Research progress of tubular structure of outer retina. *Chin J Ophthalmology.* (2020) 56(02):149–54.

69. Chhablani J, Sharma A, Goud A, Peguda HK, Rao HL, Begum VU, et al. Neurodegeneration in type 2 diabetes: evidence from spectral-domain optical coherence tomography. *Invest Ophthalmol Vis Sci* (2015) 11:6333–8. doi: 10.1167/iovs.15-17334

70. Zhao L, Zhong B, Li L, Zhong W, Ding Y. Value of retinal nerve fiber layer thickness and central arterial hemodynamic index in the diagnosis of early diabetic retinopathy. *Chin foreign Med Res* (2022) 20(05):69–72. doi: 10.14033/j.cnki.cfmr.2022.05.019

71. Lu JM, Wei XD, Liu R. The diagnostic value of optic disc and macular region parameters measured by OCT in early primary open-angle glaucoma. *Int J Ophthalmology.* (2022) 22(10):1678–81.

72. Zhao Y. *Measurement of macular retinal ganglion complex thickness in Chinese myopic population*. Shandong University (2021). doi: 10.27272/d.cnki.gshdu.2021.001671

73. Wang LL, Tan W, Song C, Luo HS, Deng WJ, Gou EJ, et al. Changes in the thickness of nerve fiber layer and ganglion cell-inner plexus layer in macular area of diabetic patients and its significance. *Shandong Med* (2018) 58(47):71–3.

74. Shi Q, Dong XM, Zhang M, Cheng YH, Pei C. Clinical study on the morphological and visual function changes in the macular area of fundus in early diabetes mellitus. *Int J Ophthalmology.* (2020) 20(09):1519–23.

75. Diao L, Shi X, Zhang C, Yao L. Changes of retinal nerve fiber layer, ganglion cell layer and inner plexus layer thickness in different stages of diabetic retinopathy and its significance. *J Clin Ophthalmology* (2020) 28(06):481–486.

Frontiers in Endocrinology

Explores the endocrine system to find new therapies for key health issues

The second most-cited endocrinology and metabolism journal, which advances our understanding of the endocrine system. It uncovers new therapies for prevalent health issues such as obesity, diabetes, reproduction, and aging.

Discover the latest Research Topics

See more →

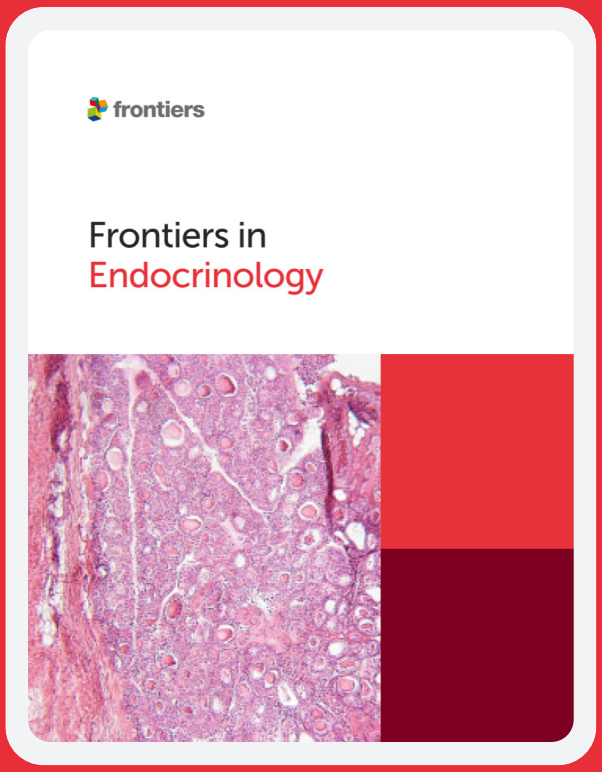

Frontiers

Avenue du Tribunal-Fédéral 34
1005 Lausanne, Switzerland
frontiersin.org

Contact us

+41 (0)21 510 17 00
frontiersin.org/about/contact